Synthesis, *in vitro* and *in silico* studies of 2,4-thiazolidinedione hybrids as anti-diabetic agents

THESIS SUBMITTED BY

ABHIK PAUL

DOCTOR OF PHILOSOPHY (PHARMACY)

DEPARTMENT OF PHARMACEUTICAL TECHNOLOGY

FACULTY COUNCIL OF ENGINEERING & TECHNOLOGY

JADAVPUR UNIVERSITY

KOLKATA-700032, INDIA

2025

JADAVPUR UNIVERSITY
KOLKATA-700032, INDIA
INDEX NO.: 293/20/Ph

Index No: 293/20/Ph

1. **Title of the Thesis:** Synthesis, *in vitro* and *in silico* studies of 2,4-thiazolidinedione hybrids as anti-diabetic agents

2. **Name, Designation & Institution of the Supervisor:**

   Prof. (Dr.) Tapan Kumar Maity
   Professor of Pharmaceutical Chemistry,
   Department of Pharmaceutical Technology,
   Jadavpur University, Kolkata-700032, India

3. **List of Publications:**

   I. **Paul, A.**, Mishra, S. S., Sarkar, A., Bhowmik, R., De, A., Maji, A., Shee, U., Samanta, A., Karmakar, S., & Maity, T. K. (2025). Synthesis, single crystal XRD, in vitro evaluation, molecular docking and ADMET studies of cuminaldehyde-thiazolidine-2,4-dione hybrids as potential α-glucosidase inhibitors. *Journal of Molecular Structure*, 141510. https://doi.org/10.1016/j.molstruc.2025.141510 (I.F: 4.7)

   II. **Paul, A.**, Mishra, S. S., Maji, A., Samanta, A., Nahar, S., & Maity, T. K. (2025). Exploring the therapeutic potentials of cuminaldehyde: a comprehensive review of biological activities, mechanisms, and novel delivery systems. *Phytochemistry Reviews*. https://doi.org/10.1007/s11101-025-10069-x (I.F: 7.6)

   III. **Paul, A.**, Sarkar, A., Mishra, S. S., De, A., Maji, A., Samanta, A., Shee, U., Shaharyar, A, Karmakar, S., & Maity, T. K. (2025). Synthesis, crystal structure, and *in vitro* evaluation of newer 2,4-thiazolidinedione hybrids as α-glucosidase inhibitors. *Future Medicinal Chemistry.* (Under Revision) (I.F: 3.2)

   IV. **Paul, A.**, Nahar, S., Nahata, P., Sarkar, A., Maji, A., Samanta, A., Karmakar, S., & Maity, T. K. (2023). Synthetic GPR40/FFAR1 agonists: An exhaustive survey on the most recent chemical classes and their structure-activity relationships. European journal of medicinal chemistry, 264, 115990. https://doi.org/10.1016/j.ejmech.2023.115990 (I.F: 6.7)

   V. **Paul, A.**, Sarkar, A., Banerjee, T., Maji, A., Sarkar, S., Paul, S., Karmakar, S., Ghosh, N., & Maity, T. K. (2023). Structural and molecular insights of protein tyrosine phosphatase 1B (PTP1B) and its inhibitors as anti-diabetic agents. *Journal*

of Molecular Structure, 1293, 136258. https://doi.org/10.1016/j.molstruc.2023.136258 (I.F: 4.7)

VI. **Paul, A.**, Maji, A., Sarkar, A., Saha, S., Janah P., & Maity T. K. (2022). Recent Approaches in the Synthesis of 5-Arylidene-2,4-thiazolidinedione Derivatives Using Knoevenagel Condensation, *Mini-Reviews in Organic Chemistry*, 19, 1-30. https://dx.doi.org/10.2174/1570193X19666220331155705 (I.F: 2.495)

Other Publications:

VII. Maji, A., Begum, D., Regula, S., Rana, S., **Paul, A.**, Shee, U., Samanta, A., Mukhopadhyay, C., Ghosh, B., & Maity, T. K. (2025b). Synthesis, Xrd-Sc Study and Antiproliferative, Apoptotic & Anti-Angiogenic Potency of 1,3,4-Thiadiazole and 1,3-Thiazolidine-4-One Scaffold-Based Hybrid Compounds (Part-II): In Vitro Cell-Based Anticancer Studies. *Journal of Molecular Structure*. (Under Revision) https://doi.org/10.2139/ssrn.5213120 (I.F: 4.7)

VIII. Maji, A., Begum, D., Regula, S., Rana, S., **Paul, A.**, Shee, U., Samanta, A., Mukhopadhyay, C., Ghosh, B., & Maity, T. K. (2025). Synthesis, Xrd-Sc Study and Antiproliferative, Apoptotic & Anti-Angiogenic Potency of 1,3,4-Thiadiazole and 1,3-Thiazolidine-4-One Scaffold-Based Hybrid Compounds (Part-Ii): In Vitro Cell-Based Anticancer Studies. *Journal of Molecular Structure*. https://doi.org/10.2139/ssrn.5213120 (I.F: 4.7)

IX. Samanta, A., Maji, A., **Paul, A.**, Mishra, S. S., Nahar, S., & Maity, T. K. (2025). 1,3,4-Oxadiazole based EGFR Inhibitors as Anticancer Therapeutics: SAR Study and binding Mode of Interaction analysis. *European Journal of Medicinal Chemistry Reports*, 100265. https://doi.org/10.1016/j.ejmcr.2025.100265 (I.F: 4.1)

X. Mishra, S. S., Samanta, A., **Paul, A.**, Maji, A., & Maity, T. K. (2024b). Unveiling the anti-cancer potential of oxadiazole derivatives: A comprehensive exploration of Structure-Activity relationships and Chemico-Biological insights. Medicinal Chemistry, 20. https://doi.org/10.2174/0115734064329573240823113924 (I.F: 2.6)

XI. Maji, A., Himaja, A., Nikhitha, S., Rana, S., **Paul, A.**, Samanta, A., Shee, U., Mukhopadhyay, C., Ghosh, B., & Maity, T. K. (2024). Synthesis and antiproliferative potency of 1,3,4-thiadiazole and 1,3-thiazolidine-4-one based new binary heterocyclic molecules: in vitro cell-based anticancer studies. *RSC Medicinal Chemistry*, *15*(9), 3057–3069. https://doi.org/10.1039/d4md00279b (I.F: 4.1)

XII. Maji, A., **Paul, A.**, Sarkar, A., Nahar, S., Bhowmik, R., Samanta, A., Nahata, P., Ghosh, B., Karmakar, S., & Kumar Maity, T. (2024). Significance of TRAIL/Apo-2 ligand and its death receptors in apoptosis and necroptosis signalling: Implications for cancer-targeted therapeutics. Biochemical Pharmacology, 221, 116041. https://doi.org/10.1016/j.bcp.2024.116041 (I.F: 5.6)

XIII. Sarkar, A., **Paul, A.**, Banerjee, T., Maji, A., Saha, S., Bishayee, A., & Maity, T. K. (2023). Therapeutic advancements in targeting BCL-2 family proteins by epigenetic regulators, natural, and synthetic agents in cancer. European journal of pharmacology, 944 https://doi.org/10.1016/j.ejphar.2023.175588 (I.F: 5.19)

XIV. Sarkar, A., Saha, R., Saha, S., Bhowmik, R., Chatterjee, A., **Paul, A.**, ... & Maity, T. K. (2022). Transesterification, GC-MS profiling, and in vitro antimicrobial potential of oil obtained from seeds of Citrus maxima (Burm.) Merr. *Industrial Crops and Products*, *189* https://doi.org/10.1016/j.indcrop.2022.115764 (I.F: 6.449)

XV. **Paul, A.**, Guria, T., Roy, P., & Maity, A. (2022). Recent developments of heterocyclic compounds with indazole moiety as potential antiparasitic agents. *Current topics in medicinal chemistry*. Advance online publication. https://doi.org/10.2174/1568026622666220415224139 (I.F: 3.295)

XVI. **Paul, A.**, Sarkar, A., Saha, S., Maji, A., Janah, P., & Kumar Maity, T. (2021). Synthetic and computational efforts towards the development of peptidomimetics and small-molecule SARS-CoV 3CLpro inhibitors. *Bioorganic & medicinal chemistry*, *46*, 116301. https://doi.org/10.1016/j.bmc.2021.116301 (I.F: 3.641)

XVII. Sarkar, A., Saha, S., **Paul, A.**, Maji, A., Roy, P., & Maity, T. K. (2021). Understanding stem cells and its pivotal role in regenerative medicine. *Life sciences*, *273*, 119270. https://doi.org/10.1016/j.lfs.2021.119270 (I.F: 5.1)

XVIII. Sahu, B., Maji, A., **Paul, A.**, Singha, N. T., & Maity, N. T. K. (2021). Synthesis, characterization, molecular docking and in vitro anticancer activity of 3-(4-methoxyphenyl)-5-substituted phenyl-2-pyrazoline-1- carbothioamide. *International Journal of Research in Pharmaceutical Sciences*, *12*(2), 1648–1658. https://doi.org/10.26452/ijrps.v12i2.4759

4. List of Patents:

None

5. Book Chapters:

I. Arnab Sarkar, Tanmoy Banerjee, Avik Maji, **Abhik Paul**, Tanmoy Guria; Mikania Species: Revealing Phytochemicals from the Pandora's Box, New Avenues in Drug Discovery and Bioactive Natural Products Natural Medicine (2023) 2: 149. https://doi.org/10.2174/9789815136326123020009

II. Arnab Sarkar, **Abhik Paul**, Avik Maji, Shrabanti Sarkar, Puspita Roy, Tanmoy Banerjee, Tanmoy Guria; Citrus and its Fight against Cancer, Therapeutic Insights into Herbal Medicine through the Use of Phytomolecules Natural Medicine (2024) 3: 228. https://doi.org/10.2174/9789815238129124030010

III. **Abhik Paul**, Arnab Sarkar, Ajeya Samanta, Akash De, Sai Satyaprakash Mishra, Rinki Prasad Bhagat, Ankita Sadhukhan, Enjamul Hoque, Avik Maji, Sanmoy Karmakar, Tapan Kumar Maity; Potential application of secondary metabolites in Diabetes **(Elsevier) [In-production]**

IV. **Abhik Paul**, Sai Satyaprakash Mishra, Sourin Nahar, Avik Maji, Tapas Kumar Bhowmick, Tapan Kumar Maity; Therapeutic Approaches to Newer Classes of Drugs and Treatments for Type 2 Diabetes Mellitus (CRC Press) [In-production]

V. **Abhik Paul**, Sai Satyaprakash Mishra, Ajeya Samanta, Avik Maji, Sourin Nahar, Tapan Kumar Maity; Recent Development of Natural Glucokinase Activators for the Treatment of Type 2 Diabetes **(Bentham Science) [In-production]**

VI. **Abhik Paul**, Ajeya Samanta, Avik Maji, Sai Satyaprakash Mishra, Puspita Roy, Tapan Kumar Maity, Tanmoy Guria; Therapeutic Advancement of Betulinic Acid in the Treatment of Type 2 Diabetes Mellitus (Nova Science Publisher) **[Under Review]**

VII. Ajeya Samanta, Sai Satyaprakash Mishra, **Abhik Paul**, Avik Maji, Rajesh Khan, Sourav Mondal, Tapan Kumar Maity; Potential Application of Secondary Metabolites in Cancer. **(Elsevier) [In-production]**

6. List of National/International Conferences/Workshops:

I. Presented a paper in poster session on the topic **"Synthesis, single crystal XRD, in vitro evaluation, and molecular docking studies of dimethylamine containing thiazolidine-2,4-dione derivatives as α-glucosidase inhibitors"** in ACS Spring 2025 organized by American Chemical Society; at San Diego, California, USA on 23-27th March 2025.

II. Secured 2nd position for poster presentation in International Conference on "**DRUG DISCOVERY, DEVELOPMENT AND LEAD OPTIMIZATION**, Organised by School of Pharmacy and Emerging Sciences, Baddi University of Emerging Sciences & Technology, Baddi, Himachal Pradesh, India, 05-06 April, 2024.

III. Participated in online workshop entitled "**Computer-Assisted Formulation Development and Toxicity Prediction: Notion and Significance in Drug Discovery and Development**" from 3rd-5th June 2024, under Bioinformatics Centre (DBT), Department of Pharmaceutical Sciences and Drug Research, Punjabi University, Patiala.

IV. Presented a paper in oral presentation in 14th International Conference on "**NAVIGATING THE FUTURE OF HEALTHCARE: Trends, Challenges and Innovations**" Organised by NSHM Institute of Health Sciences, NSHM Knowledge Campus, Kolkata on 27th and 28th September, 2024.

V. Participated in the UGC sponsored two-day international conference on **"Community & mental Health: Connect, communicate and Care"**, organized by Department of Education, Jadavpur University, Kolkata, India on 3rd & 4th January, 2020.

VI. Participated and completed the Workshop on **"Writing Quality Research Article for Publication"** organized by FET, Jadavpur University, Kolkata, India during January 13-14, 2020 funded by TEQIP III, Govt. of India.

VII. Participated in the UGC-SAP sponsored National seminar on **"Advances in nanoscience and Nanotechnology Application"**, organized by Chemical Engineering Department, Jadavpur University, Kolkata, India on 10th February, 2020.

STATEMENT OF ORIGINALITY

I, Abhik Paul, Reg. No. 1022013003, registered on 24.01.2020, do hereby declare that this thesis entitled "**Synthesis, *in vitro* and *in silico* studies of 2,4-thiazolidinedione hybrids as anti-diabetic agents**" contains literature survey and original research work done by me as part of my Doctoral studies.

All information in this thesis has been obtained and presented in accordance with existing academic rules and ethical conduct. I declare that, as required by these rules and conduct, I have fully cited and referred all materials and results that are not original to this work.

I also declare that I have checked this thesis in accordance with the "Policy on Anti-Plagiarism, Jadavpur University, 2019", and the level of similarity, as determined by the iThenticate software, is **5%**.

Abhik Paul

Signature of the Candidate:

Date: 04.08.2025

TKMaity 04/08/25

Dr. Tapan Kr. Maity
M. Pharm., Ph.D.
Professor
Dept. of Pharmaceutical Technology
Jadavpur University, Kolkata - 700 032

Certified by Supervisor:

(Signature with date, seal)

CERTIFICATE FROM THE SUPERVISOR

This is to certify that the thesis entitled "**Synthesis, *in vitro* and *in silico* studies of 2,4-thiazolidinedione hybrids as anti-diabetic agents**," submitted by **Mr. Abhik Paul**, who got his name registered on 24.01.2020, Registration No: **1022013003** for the award of Ph.D (Pharmacy) degree of Jadavpur University, is absolutely based upon his work under the supervision of **Prof. Tapan Kumar Maity** and that neither his thesis nor any part of the thesis has been submitted for any degree/diploma or any other academic award anywhere before.

Dr. Tapan Kr. Maity
M. Pharm., Ph.D.
Professor
Dept. of Pharmaceutical Technology
Jadavpur University, Kolkata - 700 032

TKMaity 04/08/25

Prof. (Dr.) Tapan Kumar Maity (Supervisor)
Professor of Pharmaceutical Chemistry,
Dept. of Pharmaceutical Technology,
Jadavpur University, Kolkata 700032, India

ACKNOWLEDGEMENT

The successful completion of my Ph.D. thesis has been made possible through the guidance, encouragement, and unwavering support of many individuals. I take this opportunity to express my heartfelt gratitude to all those who have played a role in this academic journey.

First and foremost, I would like to express my sincere gratitude to my Ph.D. supervisor, ***Prof. Tapan Kumar Maity****, for giving me the opportunity to pursue this research. His insightful mentorship, continuous encouragement, and constructive feedback have profoundly shaped my academic and personal growth. His words of wisdom and timely advice provided clarity during moments of uncertainty, and his unwavering support has been the cornerstone of this thesis.*

I am deeply thankful to ***Prof. Amalesh Samanta****, Head of the Department, and* ***Prof. Saikat Dewanjee****, for their valuable support and encouragement during the pre-submission phase. Their guidance played a crucial role in refining and finalizing my research work.*

I extend my sincere thanks to ***Prof. Kunal Roy****, under whose tenure I was initially registered for my Ph.D. His motivation and guidance laid the foundation for my research endeavors. I am also grateful to* ***Prof. Tarun Jha*** *and* ***Prof. Biswajit Mukherjee*** *for their assistance and support during my AICTE-NDF/ADF fellowship selection process, which was instrumental in shaping my doctoral journey.*

I am thankful to ***Prof. Sanmoy Karmakar*** *and his lab members for their generous assistance and technical support during various experiments. Their expertise greatly contributed to the successful execution of my research. I also extend my heartfelt appreciation to* ***Prof. Balaram Ghosh*** *and his lab members for their extensive collaboration, scientific input, and support throughout the research and publication processes. Their passion for research continues to inspire me.*

*My sincere thanks to my dear companions—****Mr. Avik Maji, Mrs. Ajeya Samanta, Ms. Rinki Prasad Bhagat, Mr. Uday Shee, Mr. Arnab Sarkar, Mr. Akash De, Mr. Pratik Chakraborty, Dr. Sanjib Das, Dr. Rudranil Bhowmik,*** *and* ***Mr. Md. Adil Shaharyar****—for their constant support, encouragement, and camaraderie throughout this journey.*

*I am also thankful to my lab juniors—****Mr. Sai Satya Prakash Mishra, Mr. Pankaj Nahata, Ms. Sourin Nahar, Ms. Shrabanti Sarkar, Mr. Rajesh Khan, Mr. Sourav Mondal, Mr. Abdul Qadir,*** *and* ***Ms. Nikki Gupta****—for their assistance and cooperation in the laboratory.*

*Special thanks to my friends—**Mr. Tapas Kumar Bhowmick**, **Mrs. Pousali Ganguly**, **Mr. Sudipto Mondal**, and **Mr. Golam Mortuja Sarkar**—for their continued support and encouragement during the course of my Ph.D.*

*I gratefully acknowledge the **office staff** of the Department of Pharmaceutical Technology, especially **Mr. Umesh Kumar**, for their administrative and laboratory support. Mr. Kumar's help in arranging laboratory supplies and materials was immensely valuable.*

*I express my sincere gratitude to the **funding agencies**, including the **All India Council for Technical Education (AICTE)** for awarding the NDF/ADF Fellowship, and the **ANRF, DST-SERB**, for granting the international travel support that enabled me to attend the **ACS Spring 2025** meeting in San Diego, USA.*

*I am profoundly thankful to the **Almighty** for the divine grace that has sustained me throughout this journey. I owe my deepest appreciation to my **family** for their unconditional love, patience, and support. Their unshakable faith in me has been my greatest source of strength. I would especially like to thank my wife, **Mrs. Parnali Das**, my father, **Mr. Ashok Paul**, my late mother, **Mrs. Aparajita Paul**, my brother, **Mr. Sagar Paul**, and my in-laws, **Mr. Pintu Das** and **Mrs. Sabitri Das**, for being the pillars of support throughout this endeavor.*

Finally, I extend my heartfelt thanks to all those who have contributed, directly or indirectly, to this work but whose names may not have been mentioned. Your help and encouragement have not gone unnoticed, and I remain truly grateful.

This thesis is a reflection of collective support, and I am indebted to each and every person who made this journey possible.

Abhik Paul

Abhik Paul
Reg. No. 1022013003
Index No. 293/20/Ph

Date: 04.08.2025
Place: Kolkata

Dedicated

to

My Beloved

Parents

Whose unwavering love, support, and encouragement
have been the foundation
of all my achievements.

PREFACE

This Ph.D. work has been conducted as partial requirements of the Ph.D degree in Pharmacy. The current thesis entitled "**Synthesis, *in vitro* and *in silico* studies of 2,4-thiazolidinedione hybrids as anti-diabetic agents**" revolves round the antidiabetic activity profile of newly synthesized thiazolidinedione (TZD) analogues. Especially, Chapter III contains the synthesis, single crystal X-ray diffraction (XRD), *in vitro* bio-assay, molecular docking, and ADMET profiling of cuminaldehyde derived thiazolidine-2,4-dione hybrids for their activities as prospective α-glucosidase inhibitors. Chapter IV discusses the synthesis, structural characterization, and biological evaluation of new 2,4-thiazolidinedione hybrids working in the same therapeutic domain.

My experience in Medicinal Chemistry programme exceeds five years and is closely related to the design, synthesis and SAR studies of pharmacologically related to heterocyclic scaffolds, particularly thiazolidinedione-framework molecules. This PhD at Jadavpur University enabled me to investigate in depth this multi-faceted approach to study these species combining experimental and computational tools.

During the time this work has been carried out I have published 18 peer reviewed articles in well-known journals including; *European Journal of Medicinal Chemistry*, *Bioorganic & Medicinal Chemistry*, *Life Sciences*, *Journal of Molecular Structure*, *Biochemical Pharmacology* and *RSC Medicinal Chemistry*. I have 7 book chapters written in collaboration which deals with natural product to treat disease and medicinal chemistry updates on treatment and management of diabetes. Despite a modest H-index (8), with 186 citations (according to Google Scholar), I want to contribute significantly in the realm of research.

I have practical experience in synthetic chemistry, spectroscopic methods (NMR, IR, MS, UV) and in general scientific and cheminformatics software (ChemDraw, MarvinSketch, SciFinder, Mendeley, EndNote).

This work was inspired by my desire to connect basic medicinal chemistry to translational research, and address worldwide health epidemics like type 2 diabetes. The prospect of translating rationally designed and synthesized molecules into viable lead compounds is what keeps me excited about the field. Although we have seen our instrumental access becoming more and more limited, research collaboration and consumable/chemical costs increasing, it has been a rewarding path to follow. Key experiences were the successful cooperation with national and international colleagues, presenting results in San Diego, USA at the ACS Spring 2025 conference- a moment of my scientific education which significantly expanded my horizon thus deepened my network. This research opportunity has further developed my abilities as a scientific writer and researcher and to learn the editorial, digital tools and research programs.

The fundamental purpose of this effort is to develop novel, effective anti-diabetic agents by synthesizing 2,4-thiazolidinedione hybrid molecules utilizing natural or synthetic biologically active frameworks. This thesis targets researchers and experts in medicinal chemistry, particularly those focused on the development and investigation of 2,4-thiazolidinedione hybrids as anti-diabetic agents.

Kolkata
August, 2025

Abhik Paul

Abhik Paul

CONTENTS

PARTICULARS	PAGE NO.
ACKNOWLEDGEMENT	viii-ix
PREFACE	x-xi
LIST OF FIGURES	xvi-xxiv
LIST OF TABLES	xxv-xxvi
LIST OF SCHEMES	xxvii
LIST OF ABBREVIATIONS	xxviii-xxx

CHAPTER I	PAGE NO.
1. Introduction:	1-30
1.1. Diabetes mellitus and its global burden:	1-4
1.2. Pathophysiology of type 2 diabetes mellitus (T2DM):	4-7
1.3. Current therapeutic options:	7-12
1.3.1. α-glucosidase inhibitors (AGIs):	7-8
1.3.2. Amylin mimetics:	8-10
1.3.3. Incretin mimetics (GLP – 1 agonist and DPP – IV inhibitors):	10-11
1.3.4. Sodium-glucose co-transporter type 2 (SGLT2) inhibitors:	11-12
1.4. Treatment approaches for type 2 diabetes mellitus (T2DM):	12-16
1.4.1. Conventional treatment algorithm:	14-15
1.4.2. Newer treatment algorithm:	15-16
1.5. Importance of α-glucosidase inhibition:	16-18
1.6. Overview of 2,4-thiazolidinedione (TZD):	18-26
1.6.1. Reactivity, synthetic routes and biological effects of TZDs:	21-26
1.7. Rationale for Hybrid Molecule Design:	27-30
1.7.1. Molecular hybridization in drug discovery:	27-28
1.7.2. Integration of TZD scaffold with other pharmacophores to enhance antidiabetic activity:	29-30
References	31-38

CHAPTER II	PAGE NO.
1. Literature Review	39-84
1.1. Overview of 5-arylidene-2,4-thiazolidinedione (5-A-TZD):	39-40
1.2. Knoevenagel condensation and its importance in 5-arylidene-2,4-thiazolidinediones (5-A-TZDs) synthesis:	40-43
1.3. Recent approaches for the synthesis of 5-A-TZDs via KC:	43-44
1.4. TZD-based hybrids as antidiabetic agents:	44-75
1.5. Cuminaldehyde:	75-78
1.6. Biological activity potentials of Cuminaldehyde analogues:	78-83
1.7. Comparative studies between Cuminaldehyde and its analogues:	83-84
References	85-91
CHAPTER III	**PAGE NO.**
Synthesis, single crystal XRD, *in vitro* evaluation, molecular docking and ADMET studies of cuminaldehyde-thiazolidine-2,4-dione hybrids as potential α-glucosidase inhibitors	
1. Introduction:	92-94
2. Experimental section:	95-109
2.1. *Chemistry:*	95
2.1.1. *Synthesis of thiazolidine-2,4-dione (TZD; Compound 3):*	95-96
2.1.2. *(Z)-5-(4-isopropylbenzylidene)thiazolidine-2,4-dione (Compound 5):*	96
2.1.3. *General procedure for synthesis of (Z)-3-substituted-5-(4-isopropylbenzylidene)thiazolidine-2,4-dione (Compound 6a-6l):*	96-104
2.1.4. *General procedure for synthesis of (Z)-2-(5-(4-isopropylbenzylidene)-2,4-dioxothiazolidin-3-yl)acetic acid (Compound 6m):*	104
2.2. *In vitro assay of α-glucosidase inhibitory activity:*	105
2.3. *Inhibition kinetics:*	105-106
2.4. *Fluorescence quenching:*	106
2.5. *Circular dichroism spectra:*	106-107
2.6. *Molecular docking:*	107-108
2.6.1. *Protein preparation:*	107

2.6.2. *Ligand preparation:*	107
2.6.3. *Docking:*	107-108
2.7. *In vitro cytotoxicity:*	108
2.8. *ADME, drug-likeness and toxicity assessment:*	109
3. Result and discussion:	110-126
3.1. *Chemistry:*	110
3.2. *X-ray crystallographic analysis with ORTEP diagram of compounds 6i:*	111
3.3. *In vitro assay of α-glucosidase inhibitory activity:*	111-113
3.4. *Structure-activity relationships (SARs):*	113
3.5. *Enzyme kinetic study:*	114-115
3.6. *Fluorescence quenching:*	115-117
3.7. *Circular dichroism spectra:*	117-118
3.8. *Molecular docking:*	119
3.8.1. *Molecular docking analysis:*	119
3.8.1.1. *Docking score and binding interaction analysis of Compound 6i and 6h:*	119-122
3.9. *In vitro cytotoxicity:*	122-123
3.10. *ADME, drug-likeness and toxicity assessment:*	123-126
Spectral data	127-163
References	164-169
CHAPTER IV	**PAGE NO.**
Synthesis, crystal structure, and *in vitro* evaluation of newer 2,4-thiazolidinedione hybrids as α-glucosidase inhibitors	
1. Introduction:	170-173
2. Experimental section:	174-189
2.1. *Chemistry:*	174-185
2.1.1. *Synthesis of thiazolidine-2,4-dione (TZD; Compound 3):*	174
2.1.2. *(Z)-5-(3,4-dimethoxybenzylidene)thiazolidine-2,4-dione (Compound 5):*	175
2.1.3. *General procedure for synthesis of (Z)-3-substituted-5-(3,4-dimethoxybenzylidene)thiazolidine-2,4-dione (Compound 6a-6l):*	176-184

2.1.4. *General procedure for synthesis of (Z)-2-(5-(3,4-dimethoxybenzylidene)-2,4-dioxothiazolidin-3-yl)acetic acid (Compound 6m):*	184-185
2.2. *In vitro assay of α-glucosidase inhibitory activity:*	185-186
2.3. *Inhibition kinetics:*	186
2.4. *Fluorescence quenching:*	186-187
2.5. *Circular dichroism spectra:*	187
2.6. *Molecular docking:*	187-188
2.6.1. *Protein preparation:*	187
2.6.2. *Ligand preparation:*	187-188
2.6.3. *Docking:*	188
2.7. *In vitro cytotoxicity:*	188-189
2.8. *ADME, drug-likeness and toxicity assessment:*	189
3. Result and discussion:	190-204
3.1. *Chemistry:*	190
3.2. *X-ray crystallographic analysis with ORTEP diagram of compounds 6b:*	191
3.3. *In vitro assay of α-glucosidase inhibitory activity:*	191-193
3.4. *Structure-activity relationships (SARs):*	193-194
3.5. *Enzyme kinetic study:*	194-195
3.6. *Fluorescence quenching:*	195-197
3.7. *Circular dichroism spectra:*	197-198
3.8. *Molecular docking:*	198-200
3.9. *In vitro cytotoxicity:*	200-201
3.10. *ADME, drug-likeness and toxicity assessment:*	201-204
Spectral data	205-241
References	242-245
CHAPTER V	**PAGE NO.**
Conclusion and future perspective	246-248
APPENDICES	**PAGE NO.**
Publications and Certificates	249-263

LIST OF FIGURES

FIGURE NO.	PARTICULARS	PAGE NO.
CHAPTER I		
1	Pictorial representation of T2DM. A. Stomach absorbs glucose and releases it into the peripheral tissue through the bloodstream. B. Glucose enters into the bloodstream. C. Arterial glucose activates the pancreas to release insulin. D. Due to insulin resistance and less insulin secretion, glucose is unable to uptake by the cells. E. Increases the glucose concentration in the blood and leads to T2DM	3
2	The ominous octet illustrating the pathophysiologic dysfunction seen in T2DM. Modified from DeFronzo RA, 2013 [23]	7
3	Mechanism of action of newer classes (AGIs, amylin mimetics, incretin mimetics (GLP – 1 agonist and DPP-IV inhibitors), and SGLT2 inhibitors) of drugs used in modern therapy for the management of T2DM	12
4	Treatment approaches for the management of T2DM	16
5	Role of AG in hyperglycemia	18
6	Structure of TZD and its physicochemical properties	19
7	The historical background of thiazolidinediones (TZDs)	19
8	Structure of antidiabetic medications containing TZD moiety	20
9	Tautomeric structures of TZD	21
10	Reactivity of TZD at -CH_2 and -NH	23
CHAPTER II		
1	General structure of 5-A-TZD.	39
2	General mechanism of KC between TZD and substituted aromatic aldehydes.	43
3	Multiple synthetic approaches of KC for 5-A-TZDs.	44
4	SAR and structures of compound 1 and 2 as potent AGIs.	46

5	SAR and structures of compound 3 as potent AGI.	47
6	SAR and structures of compound 4 as potent AGI and AAI.	48
7	SAR and structures of compound 5 as potent AGI, AAI, and antioxidant.	49
8	SAR and structures of compound 6 as potent AGI and AAI.	50
9	Design strategy of compound 7 as potent AGI.	51
10	SAR and structures of compound 7 as potent AGI.	51
11	Design strategy of compound 8 as potent AGI.	52
12	SAR and structures of compound 8 as potent AGI.	53
13	Design strategy of compound 9 as potent AGI.	54
14	SAR and structures of compound 9 as potent AGI.	54
15	SAR and structures of compound 10 as potent AGI and AAI.	55
16	Structures of compound 11 and 12 as potent AGIs, AAIs, DPP-4, and PTP1B inhibitors.	56
17	SAR and structures of compound 13 as potent AGIs and AAIs.	57
18	Previously reported compounds as potent AGIs and AAIs.	58
19	SAR and structures of compound 14 as potent AGIs.	58
20	SAR and structures of compound 15 as potent AGIs and AAIs.	59
21	Design strategy of compound 16 as potent AGIs and AAIs.	60
22	SAR and structures of compound 16 as potent AGIs and AAIs.	60
23	Design strategy of compound 17 as potent AGIs and AAIs.	61
24	SAR and structures of compound 17 as potent AGI and AAI.	62

25	Design strategy of compound 18, 19, and 20 as potent AGIs.	63
26	SAR and structures of compound 18, 19, and 20 as potent AGIs.	63
27	SAR and structures of compound 21, 22, and 23 as potent AGIs and AAIs.	64
28	SAR and structures of compound 24 as potent AGI.	65
29	SAR and structures of compound 25 as potent AGI.	66
30	SAR and structures of compound 26 as potent AGI and AAI.	67
31	SAR and structures of compound 27 as potent AGI and AAI.	68
32	SAR and structures of compound 28 as potent AGI.	69
33	SAR and structures of compound 29 as potent AGI.	70
34	SAR and structures of compound 30 as potent AGI.	71
35	SAR and structures of compound 31 and 32 as potent AGIs.	72
36	SAR and structures of compound 33 as potent AGI and AAI.	73
37	SAR and structures of compound 34 as potent AGI.	74
38	SAR and structures of compound 35 as potent AGI.	75
39	Structure, chemical formula, molecular weight, melting point, logP, and tPSA of CUM (Chemical formula, molecular weight, melting point, logP, and tPSA were calculated from ChemBioDraw Ultra 12.0.).	77
40	Therapeutic potential of CUM with its schematic mode of action.	78
41	Structure of potential CUM analogues.	83
CHAPTER III		
1	(A) Structure of α-glucosidase inhibitors containing TZD [1,2,36]; (B) Structure of α-glucosidase inhibitors (ibuprofen Schiff base and cuminaldehyde) [38,39]; (C)	94

	Designing of cuminaldehyde-TZD hybrids for potential α-glucosidase inhibitors.	
2	ORTEP diagram of compound 6i (CCDC- 2402983) (Scheme 1).	111
3	SAR of compound series for α-glucosidase inhibitory activity.	113
4	Kinetics of α-glucosidase inhibition by compound 6i and the Lineweaver-Burk plot in the absence and presence of different concentrations of compound 6i.	114
5	The secondary plot between Km and various concentrations of compound 6i.	115
6	Fluorescence emission spectra at different concentrations of compound 6i.	116
7	Double logarithm regression plots of compound 6i and α-glucosidase.	117
8	Stern-Volmer plots of compound 6i.	117
9	CD spectra of α-glucosidase with compound 6i.	118
10	3D representation of all the Aligned TZD derivatives at the active site of AG (PDB: 5NN8).	121
11	2D and 3D docking representation of AG–TZD derivatives 6i (A and B) and 6h (C and D).	122
12	Cell viability assay of compound 6i against HEK293.	123
13	Radar plot and Boiled-Egg model of compound 6i and 6h.	125
SPECTRAL FIGURES		
S.F1′	^{1}H NMR of compound 5	127
S.F1″	^{13}C NMR of compound 5	127
S.F2′	^{1}H NMR of compound 6a	128
S.F2″	^{13}C NMR of compound 6a	128
S.F3′	^{1}H NMR of compound 6b	129
S.F3″	^{13}C NMR of compound 6b	129
S.F4′	^{1}H NMR of compound 6c	130
S.F4″	^{13}C NMR of compound 6c	130

S.F5′	^{1}H NMR of compound 6d	131
S.F5″	^{13}C NMR of compound 6d	131
S.F6′	^{1}H NMR of compound 6e	132
S.F6″	^{13}C NMR of compound 6e	132
S.F7′	^{1}H NMR of compound 6f	133
S.F7″	^{13}C NMR of compound 6f	133
S.F8′	^{1}H NMR of compound 6g	134
S.F8″	^{13}C NMR of compound 6g	134
S.F9′	^{1}H NMR of compound 6h	135
S.F9″	^{13}C NMR of compound 6h	135
S.F10′	^{1}H NMR of compound 6i	136
S.F10″	^{13}C NMR of compound 6i	136
S.F11′	^{1}H NMR of compound 6j	137
S.F11″	^{13}C NMR of compound 6j	137
S.F12′	^{1}H NMR of compound 6k	138
S.F12″	^{13}C NMR of compound 6k	138
S.F13′	^{1}H NMR of compound 6l	139
S.F13″	^{13}C NMR of compound 6l	139
S.F14′	^{1}H NMR of compound 6m	140
S.F14″	^{13}C NMR of compound 6m	140
S.F15	FT-IR of compound 5	141
S.F16	FT-IR of compound 6a	141
S.F17	FT-IR of compound 6b	142
S.F18	FT-IR of compound 6c	142
S.F19	FT-IR of compound 6d	143
S.F20	FT-IR of compound 6e	143
S.F21	FT-IR of compound 6f	144
S.F22	FT-IR of compound 6g	144
S.F23	FT-IR of compound 6h	145
S.F24	FT-IR of compound 6i	145
S.F25	FT-IR of compound 6j	146
S.F26	FT-IR of compound 6k	146

S.F27	FT-IR of compound 6l	147
S.F28	FT-IR of compound 6m	147
S.F29	MS (ESI, m/z) of compound 5	148
S.F30	MS (ESI, m/z) of compound 6a	149
S.F31	MS (ESI, m/z) of compound 6b	150
S.F32	MS (ESI, m/z) of compound 6c	151
S.F33	MS (ESI, m/z) of compound 6d	152
S.F34	MS (ESI, m/z) of compound 6e	153
S.F35	MS (ESI, m/z) of compound 6f	154
S.F36	MS (ESI, m/z) of compound 6g	155
S.F37	MS (ESI, m/z) of compound 6h	156
S.F38	MS (ESI, m/z) of compound 6i	157
S.F39	MS (ESI, m/z) of compound 6j	158
S.F40	MS (ESI, m/z) of compound 6k	159
S.F41	MS (ESI, m/z) of compound 6l	160
S.F42	MS (ESI, m/z) of compound 6m	161
S.F43	Molecular geometries of compound 6i in crystal	162
CHAPTER IV		
1	(A) The structure of TZD-containing AGIs [1–3,12–14]; (B) Structure of some AGIs having veratraldehyde (VD) part [2,3,14]; (C) Structure of cuminaldehyde-TZD hybrids as an AG inhibitor [1] and structure of VD; (D) The process of designing hybrids of VD and TZD for the purpose of developing potential AGIs.	173
2	ORTEP diagram of compound 6b (CCDC- 2445001) (Scheme 1)	191
3	SAR of VD-TZD series for AGI activity	194
4	Kinetics of AG inhibition by compound 6f and the Lineweaver-Burk plot in the absence and presence of different concentrations of compound 6f.	195
5	The secondary plot between Km and various concentrations of compound 6f.	195

6	Fluorescence emission spectra at different concentrations of compound 6f.	196
7	Double logarithm regression plots of compound 6f and AG.	197
8	Stern-Volmer plots of compound 6f.	197
9	CD spectra of AG with compound 6f.	198
10	3D representation of all the Aligned TZD derivatives at the active site of AG (PDB: 5NN8).	200
11	2D and 3D docking representation of VD–TZD derivatives 6f.	200
12	Cell viability assay of compound 6f against HEK293.	201
13	Radar plot and Boiled-Egg model of compounds 6f and 6g.	203
SPECTRAL FIGURES		
S.F1′	^{1}H NMR of compound 5	205
S.F1″	^{13}C NMR of compound 5	205
S.F2′	^{1}H NMR of compound 6a	206
S.F2″	^{13}C NMR of compound 6a	206
S.F3′	^{1}H NMR of compound 6b	207
S.F3″	^{13}C NMR of compound 6b	207
S.F4′	^{1}H NMR of compound 6c	208
S.F4″	^{13}C NMR of compound 6c	208
S.F5′	^{1}H NMR of compound 6d	209
S.F5″	^{13}C NMR of compound 6d	209
S.F6′	^{1}H NMR of compound 6e	210
S.F6″	^{13}C NMR of compound 6e	210
S.F7′	^{1}H NMR of compound 6f	211
S.F7″	^{13}C NMR of compound 6f	211
S.F8′	^{1}H NMR of compound 6g	212
S.F8″	^{13}C NMR of compound 6g	212
S.F9′	^{1}H NMR of compound 6h	213
S.F9″	^{13}C NMR of compound 6h	213
S.F10′	^{1}H NMR of compound 6i	214

S.F10″	^{13}C NMR of compound 6i	214
S.F11′	^{1}H NMR of compound 6j	215
S.F11″	^{13}C NMR of compound 6j	215
S.F12′	^{1}H NMR of compound 6k	216
S.F12″	^{13}C NMR of compound 6k	216
S.F13′	^{1}H NMR of compound 6l	217
S.F13″	^{13}C NMR of compound 6l	217
S.F14′	^{1}H NMR of compound 6m	218
S.F14″	^{13}C NMR of compound 6m	218
S.F15	FT-IR of compound 5	219
S.F16	FT-IR of compound 6a	219
S.F17	FT-IR of compound 6b	220
S.F18	FT-IR of compound 6c	220
S.F19	FT-IR of compound 6d	221
S.F20	FT-IR of compound 6e	221
S.F21	FT-IR of compound 6f	222
S.F22	FT-IR of compound 6g	222
S.F23	FT-IR of compound 6h	223
S.F24	FT-IR of compound 6i	223
S.F25	FT-IR of compound 6j	224
S.F26	FT-IR of compound 6k	224
S.F27	FT-IR of compound 6l	225
S.F28	FT-IR of compound 6m	225
S.F29	MS (ESI, m/z) of compound 5	226
S.F30	MS (ESI, m/z) of compound 6a	227
S.F31	MS (ESI, m/z) of compound 6b	228
S.F32	MS (ESI, m/z) of compound 6c	229
S.F33	MS (ESI, m/z) of compound 6d	230
S.F34	MS (ESI, m/z) of compound 6e	231
S.F35	MS (ESI, m/z) of compound 6f	232
S.F36	MS (ESI, m/z) of compound 6g	233
S.F37	MS (ESI, m/z) of compound 6h	234

S.F38	MS (ESI, m/z) of compound 6i	235
S.F39	MS (ESI, m/z) of compound 6j	236
S.F40	MS (ESI, m/z) of compound 6k	237
S.F41	MS (ESI, m/z) of compound 6l	238
S.F42	MS (ESI, m/z) of compound 6m	239
S.F43	Molecular geometries of compound 6b in crystal	240
CONCLUSION AND FUTURE PERSPECTIVE		
1	Graphical representation of synthesis, single crystal XRD, *in vitro* evaluation, molecular docking and ADMET studies of cuminaldehyde-TZD hybrids as potential α-glucosidase inhibitors	247
2	Graphical representation of synthesis, crystal structure, and *in vitro* evaluation of newer 2,4-thiazolidinedione hybrids as α-glucosidase inhibitors	248

LIST OF TABLES

TABLE NO.	PARTICULARS	PAGE NO.
CHAPTER III		
1	Physiochemical properties of synthesized compounds (Compound 5 and 6a-6m).	97
2	The *in vitro* α-glucosidase inhibitory activity screening and IC_{50} values data of synthesized compounds (6a-6h, 6i-6l, and 6m).	112
3	Secondary structural analysis of compound 6i with α-glucosidase from CD.	118
4	Molecular docking scores of the most potent compound 6i and 6h.	121
5	ADME prognosis using SwissADME, Physiochemical and Drug-likeness properties. ((MW=Molecular Weight, TPSA=total polar surface area, Consensus Log P =average of all predicted Log Po/w).	125
6	Pharmacokinetics prediction of synthesized compounds (6i and 6h) from the SwissADME server.	126
7	Toxicology predictions. Information was retrieved via the Deep-PK database.	126
S1	Tabular data of crystal	162
CHAPTER IV		
1	Physiochemical properties of synthesized compounds (Compound 5 and 6a-6m).	176
2	The *in vitro* α-glucosidase inhibitory activity screening and IC_{50} values data of synthesized compounds (6a-6h, 6i-6l, and 6m).	192
3	Secondary structural analysis of compound 6f with α-glucosidase from CD.	198
4	Molecular docking scores of the most potent compound 6f and 6h.	199

5	ADME prognosis using SwissADME, Physiochemical and Drug-likeness properties. ((MW=Molecular Weight, TPSA=total polar surface area, Consensus Log P =average of all predicted Log Po/w).	203
6	Pharmacokinetics prediction of synthesized compounds (6f and 6g) from the SwissADME server.	204
7	Toxicology predictions. Information was retrieved via the Deep-PK database.	204
S1	Tabular data of crystal	204-205

LIST OF SCHEMES

SCHEME NO.	PARTICULARS	PAGE NO.
CHAPTER I		
1	Initially employed a way to synthesize TZD utilizing carbonyl sulfide.	24
2	A mechanistic perspective on the synthetic production of TZD utilizing thiourea and α-chloroacetic acid.	25
3	Synthesis of TZD via microwave irradiation utilizing thiourea and α-chloroacetic acid.	25
4	Synthesis of TZD using mineral acids.	25
CHAPTER III		
1	Synthesis of target compounds 6a-h, 6i-6l, and 6m. Reagents and conditions: a) Concentrated hydrochloric acid, water, 100-110 ^{0}C, reflux, 8–10 hrs; b) Urea (1.5 equiv), Glacial acetic acid, 100 ^{0}C, Reflux, 8–10 hrs; c) Substituted benzyl chlorides/ Alkyl halides, K_2CO_3, DMF, rt; 18-24 hrs. Scheme 1A: Synthesis of target compound 6m from 6l. Reagents and conditions: d) Conc. HCl:AcOH (1:2), reflux 2 h.	110
CHAPTER IV		
1	Synthesis of target compounds 6a-h, 6i-6l, and 6m. Reagents and conditions: a) Concentrated hydrochloric acid, water, 100-110 ^{0}C, reflux, 8–10 hrs; b) Urea (1.5 equiv), Glacial acetic acid, 100 ^{0}C, Reflux, 8–10 hrs; c) Substituted benzyl chlorides/ Alkyl halides, K_2CO_3, DMF, rt; 18-24 hrs. Scheme 1A: Synthesis of target compound 6m from 6l. Reagents and conditions: d) Conc. HCl: AcOH (1:2), reflux 2 h [1]	190

LIST OF ABBREVIATIONS

ABBREVIATIONS	FULL FORM
AA	α-amylase
AAIs	α-amylase inhibitors
ADMET	Absorption, distribution, metabolism, excretion, and toxicity
AG	α-glucosidase
AGI	α-glucosidase inhibitory
AGIs	Alpha-glucosidase inhibitors / α-glucosidase inhibitors
AKT1	Protein kinase B
AMPK	Adenosine 5′-monophosphate (AMP)-activated protein kinase
ANOVA	Analysis of variance
BSA	Bovine serum albumin
CD	Circular dichroism
DM	Diabetes mellitus
DMF	Dimethylformamide
DMSO	Dimethyl sulfoxide
DPP-IV	Dipeptidyl peptidase-IV
DPPH	2,2-Diphenyl-1-picrylhydrazyl
EC_{50}	Half-maximal effective concentration (effective concentration for 50% of the maximal response)
EDG	Electron donating group
ER	Endoplasmic reticulum
ESI	Electrospray ionization
ESI-MS	Electrospray ionization mass spectrometry
EWG	Electron withdrawing group
FDA	Food and drug administration
FFA	Free fatty acids
FT-IR	Fourier transform infrared spectroscopy
GC-MS	Gas chromatography mass spectrometry
GIP	Glucose-dependent insulinotropic polypeptide
GLP-1	Glucagon-like peptide-1

GLUT	Glucose transporter
HAS	Human serum albumin
HbA1c	Glycated haemoglobin
HPLC	High performance liquid chromatography
HSCCC	High-speed counter-current chromatography
IAG	Intestinal α-glucosidase
IC_{50}	Half-maximal inhibitory concentration
IGT	Impaired glucose tolerance
ILs	Ionic liquids
IR	Insulin resistance
KC	Knoevenagel condensation
MIC	Minimum inhibitory concentration
MIC_{50}	Minimum inhibitory concentration required to inhibit 50% of organisms
MW	Microwave
OGTT	Oral glucose tolerance test
PAA	Pancreatic α-amylase
PBS	Phosphate-buffered saline
PPARγ	Peroxisome proliferator-activated receptor gamma
PTP1B	Protein tyrosine phosphatase 1B
ROS	Reactive oxygen species
RT	Room temperature
SEM	Scanning electron microscope
SF	Spectral figure
SGLT2	Sodium-glucose co-transporter-2
T2D	Type 2 diabetes
T2DM	Type 2 diabetes mellitus
TLC	Thin-layer chromatography
TZD	2,4-thiazolidinedione / Thiazolidinediones / thiazolidine-2,4-dione / Thiazolidinone
UV	Ultraviolet

VD	Veratraldehyde
XRD	X-ray diffraction
μM	Micromolar
^{13}C NMR	Carbon-13 nuclear magnetic resonance spectroscopy
^{1}H NMR	Proton nuclear magnetic resonance spectroscopy
3D	Three-dimensional
5-A-TZD	5-Arylidene-2,4-thiazolidinedione

CHAPTER-I

INTRODUCTION

1. Introduction:

1.1. Diabetes mellitus and its global burden:

Diabetes mellitus (DM) is a metabolic illness in the body that develops due to impaired glucose metabolism and an abnormal rise in blood glucose concentration (hyperglycemia) as a result of reduced insulin secretion or function. Approximately 400 million individuals globally suffer from DM, and this is a serious public health concern [1,2]. This metabolic condition gradually leads to life-threatening chronic microvascular, macrovascular, and neuropathic consequences. The inability of the cells of the pancreas to secrete insulin, damage to these cells, or insulin resistance caused by insulin not working properly are the three main causes of diabetes. The prevalence of diabetes is expected to reach 366 million in 2030 among individuals aged 65 and over, with a tendency toward inactivity being a key contributor [3,4].

Type 2 diabetes mellitus (T2DM) is the more prevalent kind of diabetes and is mostly caused by dietary and social factors. It is characterized by insulin resistance or decreased sensitivity, which results in a decline in the cell's ability to absorb glucose from the blood due to a weakened insulin signal (**Figure 1**). Incretin hormones, such as glucagon-like peptide-1 (GLP-1) and glucose-dependent insulinotropic polypeptide (GIP), are secreted by gut endocrine cells in response to dietary intake and have essential functions in maintaining glucose homeostasis. For this reason, they are desirable targets for diabetes treatment [1,5].

Conventional medicine for T2DM mostly consists of sulfonylureas (increase the secretion of insulin), biguanides (reduce glucose synthesis in the liver), PPARγ agonists (increase the effects of insulin), and α-glucosidase inhibitors (AGIs; restrict the intestines from absorbing glucose). These medications are either used in combination with other hypoglycemics or as standalone therapy. The main disadvantages of using

the aforementioned conventional drugs are severe hypoglycemia, increased body weight, reduced therapeutic efficacy as a result of an inefficient or improper dose schedule, and low potency. Even with the introduction of promising anti-hyperglycemic medications, the primary challenges in providing appropriate care for people with diabetes are reducing complications in the long run and making the current medications work better to achieve controlled glycemic control [6].

Managing T2DM necessitates a patient-dependent strategy that optimizes glycemic management with the help of current pharmaceutical choices to maintain quality of life and reduce complications. Early and appropriate treatment is crucial since the Kumamoto and UK Prospective Diabetes Study (UKPDS) demonstrated that patients with newly diagnosed T2DM exhibit considerably lower risks of microvascular complications if they undergo intensive glycemic management. Since T2DM is a progressive illness, maintaining glycemic control is essential to avoid long-term consequences. This can be accomplished with prompt therapy escalation, although this is frequently not done, and patients end up with inadequate glycemic control for several years [7–9].

Clinicians now have more options for treating T2DM because of the development of novel, effective, and accepted oral and injectable pharmacological medications. However, given the frequently encountered limitations outlined above, it is necessary to create novel agents that are both safe to co-prescribe with the present range of treatment options and effective on their own. Furthermore, the medical community desires interventions that improve T2DM-related problems and impose little to no restrictions on their usage in patients presenting with substantial multiorgan comorbidities.

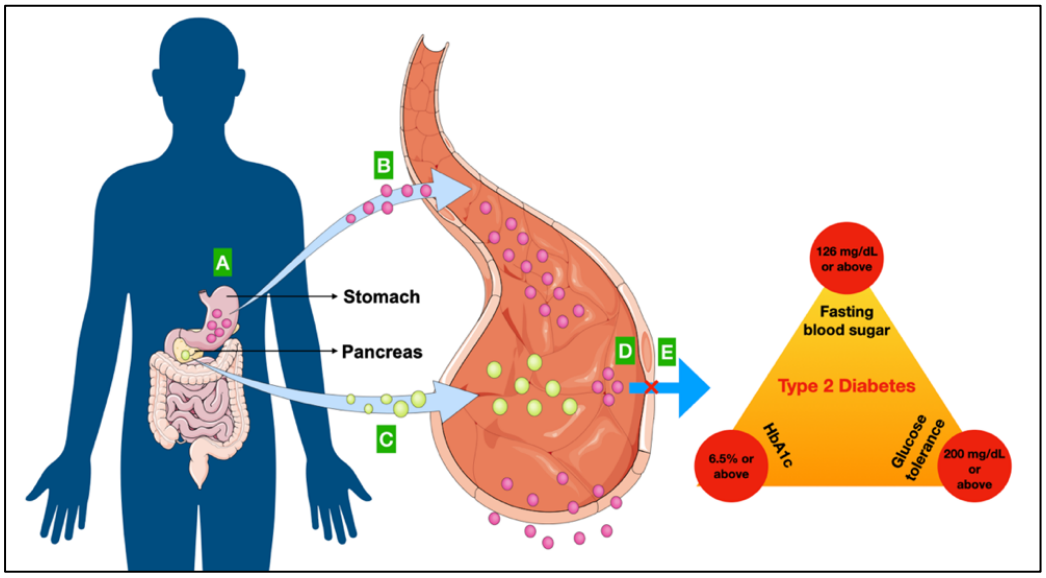

Figure 1: Pictorial representation of T2DM. **A.** Stomach absorbs glucose and releases it into the peripheral tissue through the bloodstream. **B.** Glucose enters into the bloodstream. **C.** Arterial glucose activates the pancreas to release insulin. **D.** Due to insulin resistance and less insulin secretion, glucose is unable to be taken up by the cells. **E.** Increases the glucose concentration in the blood and leads to T2DM.

The Global Burden of Disease Study reports that the burden of T2DM and its associated complications has substantially increased from 1990 to 2017 as judged by increased mortality rates and years lived with disabilities (YLDs) [10,11]. T2DM, on the whole, represents a large share of non-communicable diseases, with severe health complications, such as diabetic nephropathy, retinopathy and cardiovascular diseases as leading causes of morbidity and mortality in diabetic patients [12–14].

Socioeconomic determinants are also critical in the diabetes epidemic. The prevalence of diabetes is a function of lifestyle modification trends related to urbanization and ageing populations, especially in emerging economies which are experiencing a rapid change in diet and physical activity level [15]. Dounousi *et al.,* underline that diabetic nephropathy, which affects about one-third of diabetic patients, is a main cause of the increasing prevalence of end-stage renal disease [16]. As a result, these growing health

indicators are coupled with the economic burden of diabetes, which is projected to be around $1 trillion annually by 2045, further challenging the capacity of national health systems [16–18].

Furthermore, DM has important personal suffering and economic implications for the patient, their families and society. In part, this epidemic is being driven by the lack of early symptoms of viral HBV infection, resulting in a pool of undiagnosed persons, making prevention and control more challenging to achieve. Because of the myriad of challenges presented by diabetes care, it is imperative to develop comprehensive public health approaches that incorporate prevention, screening, and management of disease in an effort to reduce complications and enhance overall health status [19,20].

Overall, the prevalence of DM worldwide is increasing at an alarming pace, as a result of a combination of factors such as the shift of populations and lifestyle. This increasing prevalence has highlighted the urgent requirement for integrated public health preventive actions to mitigate and develop this complex of problems effectively by preventing diabetes, detecting it early, and managing diabetes and its complications.

1.2. Pathophysiology of type 2 diabetes mellitus (T2DM):

T2DM is caused by β-cell malfunction and insulin resistance (IR). IR causes a high demand for insulin from peripheral tissues, leading to the growth of β-cells and hyperinsulinemia. In the presence of a hyperglycaemic environment, the β-cells' compensatory reaction causes a persistent decrease in the bulk of β-cells, which is thought to be the outcome of higher apoptosis. The pathogenesis of T2DM begins with impaired glucose tolerance (IGT), a disorder in which people have about 80% less β-cell function and a higher level of IR. To further understand the pathophysiologic abnormalities in T2DM, eight important collaborators have been identified. These include the liver (increased hepatic glucose output), the brain (impaired appetite

regulation), the kidney (enhanced glucose reabsorption), the gut (reduced impact of incretin), the kidney (decreased glucose uptake), and the pancreatic β-cells (increased insulin secretion). In combination, these collaborators have been referred to as the ominous octet. **Figure 2** illustrates the potential involvement of many "ominous octet" pathways in the pathophysiology of T2DM. This system is addressed with therapeutic drugs to treat IR, decreased insulin production, and loss of β-cell mass [21].

Amylin and insulin are released concurrently and are crucial in regulating blood glucose levels. After a meal, it improves glucose absorption by reducing stomach emptying. The gut produces the peptides GLP and GIP, which are incretins. The pancreatic β cells produce and release insulin in response to these incretins. Neither the intestine nor cells needing energy readily take glucose. Consequently, the distribution of glucose to the cells is the responsibility of glucose transporters. SGLT, as well as facilitative glucose transporter (GLUT), are two distinct members of the membrane-bound glycoprotein family that go by the name "glucose transporters". There are some other factors which increase the blood glucose levels, which are described below:

a) Gestational diabetes is brought on by hormonal changes occurring during pregnancy. The placenta secretes hormones that lessen a cell's susceptibility to the effects of insulin.

b) As well as single-gene mutations producing monogenic diabetes, genetic mutations can also result in DM.

c) Though cystic fibrosis produces thick mucus, that’s why the pancreas is unable to generate enough insulin, which ultimately leads to scarring.

d) Hemochromatosis causes the body to retain iron in excess. If iron accumulation is left untreated, it can damage the pancreas as well as other organs.

e) The body produces a lot of hormones as a result of certain hormonal illnesses, which, on rare occasions, may lead to IR and diabetes.

- Cushing's syndrome arises when there is an excess production of cortisol, also referred to as a stress hormone.
- An excess of growth hormone is produced by the body, which leads to Acromegaly.
- The overproduction of thyroid hormone by the thyroid gland results in hyperthyroidism.

f) Conditions (hepatocellular carcinoma and pancreatitis) that damage or remove the pancreas, which hamper insulin production and lead to diabetes.

g) Certain medications can impact beta cells or cause disruptions in the functioning of beta cells. The following medications are included in this category: niacin, glucocorticoids, anti-rejection medication, pentamide, anti-seizure medicines, psychiatric pharmaceuticals, and statins [1].

Similarly, excess FFAs and high blood sugar cause ER stress, it results in β-cell dysfunction by stimulating the apoptotic unfolded protein response (UPR) mechanisms. Prior to this,, insulin secretion needs to be correctly controlled to match metabolic demand exactly. Because of this, maintaining appropriate islet integrity is necessary for β-cells to react to metabolic demands. Inadequate synthesis of insulin or its precursors, together with interference with the secretion pathway, can result in insulin secretory dysfunction. This is the principal cause of β-cell failure and the basis for T2DM [22].

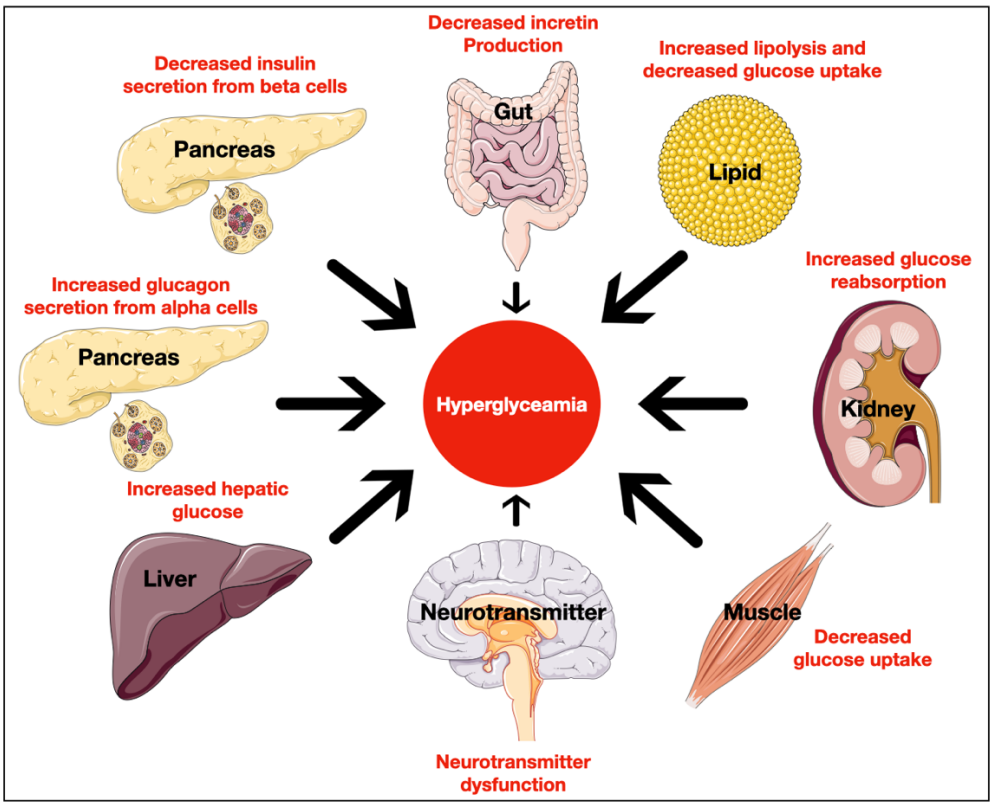

Figure 2: The ominous octet illustrating the pathophysiologic dysfunction seen in T2DM. Modified from DeFronzo RA, 2013 [23].

1.3. Current therapeutic options:

Modern medicine for the control of T2DM has made use of newer classes of medicinal drugs, such as AGIs, amylin mimetics, incretin mimetics (GLP-1 agonist and DPP-IV inhibitors), and SGLT2 inhibitors.

1.3.1. α-glucosidase inhibitors (AGIs):

α-glucosidase (AG) is an enzyme that is part of the glycoside hydrolase family. It is found chiefly at the intestinal brush border and breaks down polysaccharides into monosaccharides. The process of breakdown of disaccharide and polysaccharide into easily absorbed monosaccharide units is carried out by AG, which regulates the amount of glucose available after meals and the severity of postprandial hyperglycemia. It does this by cleaving the α-glucopyranoside linkage (**Figure 3**) [2,24]. AGIs have a structure similar to saccharides and have the ability to attach to

α-active glucosidase's site, generating complexes with a higher affinity than the complex formed by carbohydrates and AG. This causes a competitive inhibition of the enzyme, which in turn reduces the rate at which carbohydrates are hydrolyzed and delays the absorption of glucose. Studies also show that AG stimulates L cells in the intestine, which suppresses glucagon secretion while enhancing insulin secretion [25]. However, AGIs have an insulin-independent hypoglycemic effect. As a result, they are used as monotherapy in moderate cases of diabetes and are regarded as first-line oral sugar-reducing medications. In contrast, they are used in combination therapy with insulin or other drugs in cases of acute diabetic complications [26].

Four AGIs are now being used therapeutically: emiglitate, acarbose, miglitol, and voglibose. The first AGI among them was acarbose, which was used therapeutically in the 1990s. However, it was noted that significant adverse effects such as bloating, gas, stomach discomfort, and diarrhoea are linked to these inhibitors. Due to these undesirable consequences, researchers are working to find a safer and more advanced second generation of agents [27]. AGIs are to be avoided if the person has an ulcer in the gastrointestinal tract, liver cirrhosis, or intestinal blockage. It should also be contraindicated in patients with Crohn’s disease, diabetic ketoacidosis, and pregnant women. AGIs are to be avoided if the individual suffers from bowel obstruction, hepatic cirrhosis, or gastrointestinal ulcers [28].

1.3.2. Amylin mimetics:

The pancreatic hormone known as amylin is a peptide that has 37 amino acids and has a half-life of approximately thirteen minutes. The pancreas releases amylin from its β-cells in conjunction with insulin, and it triggers the satiety response by acting on the brain's hedonic and homoeostatic areas [29]. Everyone who has T1DM or

T2DM is deficient in amylin. Investigations have demonstrated that the amylin analogues, in conjunction with insulin, work together to control blood sugar levels. In light of this, several studies have been carried out to discover amylin analogues that can maintain blood glucose levels through any of the mechanisms that will be detailed here (**Figure 3**).

a) **Slows rapid emptying of the stomach:** Studies have shown that amylin analogues not only lower the amount of food consumed but also slow down the release of several digestive enzymes and bile acids, eventually resulting in a lag in the absorption of nutrients from the stomach.

b) **Suppression of endogenous glucagon production:** Moreover, amylin analogues suppress glucagon secretion, which reduces the liver's glucose production. This result facilitates lowering the amount of extra insulin needed to maintain euglycemia.

c) **Induces satiety by regulation of appetite centre:** Amylin analogue causes an anorectic effect by directly acting on the region postrema and/or nucleus tractus solitarius. This decreases appetite and causes a decrease in food intake [30,31].

Clinical analogues are made to resemble natural amylin since it is described as "glue-like" and is not soluble in solution, making it unsuitable for use as a drug. Pramlintide is the only amylin mimic currently on the market and has been given Food and Drug Administration (FDA) permission for use. It has many physiological functions with native amylin. It might be created as a stable injectable and injected under the skin [32]. The advantages of amylin mimetics in the treatment of T1DM and T2DM are that they reduce weight, so they can be beneficial for people who are overweight or obese. When amylin analogues are

used with insulin, the most common side effects are hypoglycemia, vomiting, nausea, and headaches. Continuous use of this drug makes patients habituated, and the side effects seem to disappear. It is avoided by patients suffering from gastroparesis [22].

1.3.3. Incretin mimetics (GLP–1 agonist and DPP–IV inhibitors):

When nutrients stimulate the gastrointestinal tract cells, they produce peptides known as incretin hormones, which may trigger the pancreas to secrete insulin in a way that is reliant on glucose. When compared to an equivalent intravenous glucose bolus, production of insulin from β cells of the pancreas was more robust after an oral glucose bolus, which first raised the possibility that intestinal peptides were involved in the regulation of after meal insulin release [33]. GLP-1 and also GIP were identified as the gut hormones responsible for this "incretin effect" due to their insulinotropic properties. Most T2DM patients do not respond to GIP in a way that lowers blood sugar. On the other hand, there is insufficient postprandial GLP-1 in the bloodstream despite the insulinotropic response to GLP-1 remaining intact.

GLP-1 engages in the following biological activities (**Figure 3**):

a) Glucose-dependent insulin production to facilitate plasma glucose absorption by tissues

b) Hepatic glucose release is decreased by inhibiting postprandial glucagon.

c) Delaying gastric emptying to prevent glucose from flooding the blood during absorption from the intestines.

d) Reduction of dietary intake (appetite) [34].

A novel family of therapeutic agents known as incretin mimetics has a variety of anti-hyperglycemic activities that simulate specific properties of internal incretin

hormones, such as the acceleration of insulin production in response to glucose. Sadly, Type II transmembrane glycoprotein dipeptidyl peptidase-IV (DPP-IV) quickly deteriorates GLP-1 [half-life ($t_{1/2}$) of < 2 minutes]. Many organs, including the kidney, liver, pancreas, fat cells, and immune cells, express DPP-IV extensively. Consequently, GLP-1 activity is increased with the use of DPP-IV inhibitors [35]. Exenatide was the first GLP-1 agonist used therapeutically; additional GLP-1 agonists in use at the moment include semaglutide, dulaglutide, and liraglutide. The advantages associated with GLP-1 agonists are weight loss and lowering blood pressure. However, many DPP-IV inhibitors are peptides that are derived from alpha-aminoacyl pyrrolidine. The drugs that are currently on the market are sitagliptine, linagliptine, saxagliptine, alogliptine, and vildagliptine. Undesirable effects associated with these medications are joint pain, GI distress, pancreatitis, nausea, and flu-like symptoms [30,36].

1.3.4. Sodium-glucose co-transporter type 2 (SGLT2) inhibitors:

These more recent diabetic medications function by targeting on the renal SGLT2, and which is essential for the reabsorption of glucose in the proximal tubule. As a supplement to another glucose-lowering drug, SGLT2 inhibitors have demonstrated their effectiveness in clinical studies, which were compared to placebo in a study of those undergoing dietary and exercise-based treatment for T2DM. Canagliflozin was the first SGLT2 blocker authorized by the FDA in 2013 to be launched therapeutically, and nowadays, dapagliflozin, empagliflozin, and ipragliflozin are prescribed drugs [37]. SGLT2 blockers work differently than insulin-dependent drugs that lower blood glucose without triggering insulin release by a new way of decreasing renal tubular glucose re-absorption. Other beneficial metabolic benefits of SGLT2 blockers come out as an advantage, as they help in weight loss, reduce

blood pressure, reduce triglycerides, and also reduce diabetics' susceptibility to cardiovascular illness (**Figure 3**). The various unwanted effects of SGLT2 medication are urinary tract infections, hypotension, hypoglycemia, and noticeable sugar in the urine. It is very important to keep in mind when prescribing SGLT2 inhibitors that they are contraindicated in patients with renal impairment and dialysis [30,38].

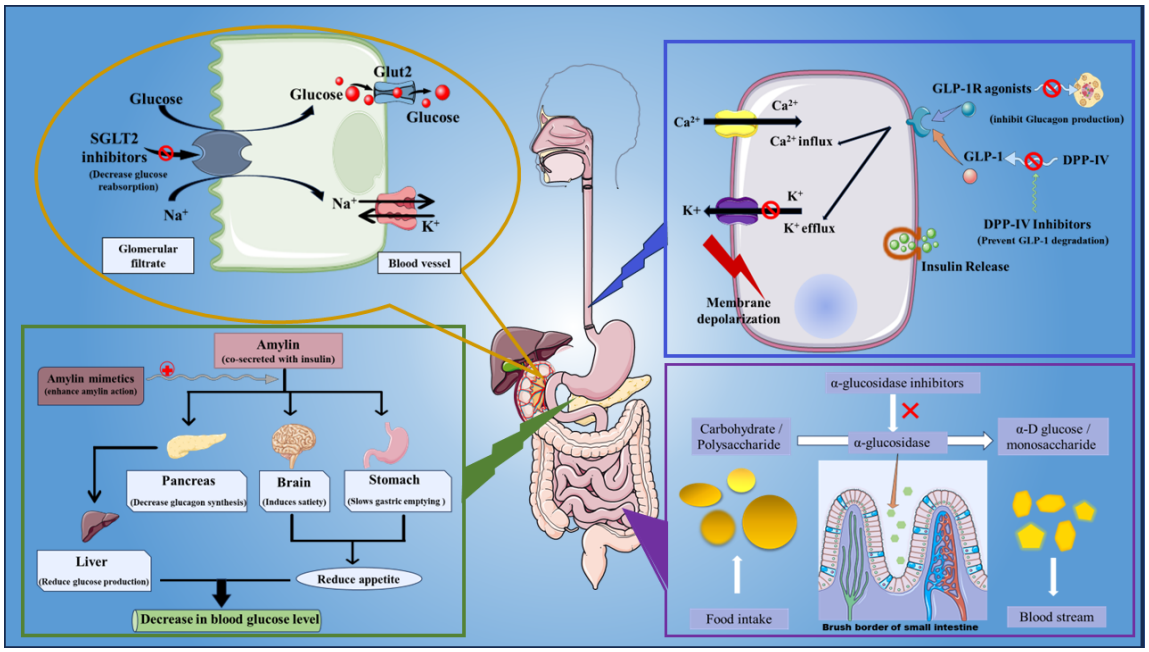

Figure 3: Mechanism of action of newer classes (AGIs, amylin mimetics, incretin mimetics (GLP–1 agonist and DPP-IV inhibitors), and SGLT2 inhibitors) of drugs used in modern therapy for the management of T2DM.

1.4. Treatment approaches for type 2 diabetes mellitus (T2DM):

T2DM is a long-term condition, and there's no permanent cure for it, but there are ways to manage it, such as lifestyle changes, medications, blood sugar monitoring devices, insulin pumps, and surgery. When patients are willing to put in the work, making changes to their diet can be an effective way of controlling their blood sugar, blood pressure, and weight. Not only that, but the benefits of these changes last even longer than the weight-loss results [39]. The improvement in blood sugar is linked to both the

amount of calories they cut out and the amount of weight they lose. Monitoring and controlling the glucose level can be achieved through regular exercise, a low-glycemic diet, ample amount of sleep, stress management, and taking oral anti-hyperglycemic agents. However, some people with T2DM might be tempted to try non-recommended alternative treatments, such as the plethora of natural ingredients in different forms [40].

Making changes to a patient's diet habits and recommended exercise can often be the first step in treating T2DM, while various eminent guidelines are suggested for treating T2DM with medications. There are a lot of treatment options, like monotherapy, dual therapy, and triple therapy, as primary and follow-up treatment options based on the severity and diabetic stage [41]. Alternative or adjuvant medicinal approaches are now introduced to alter blood sugar levels, like amylinomimetic analogues like pramlintide, to co-secrete with insulin to control blood sugar. Additionally, they inhibit frequent food intake, delay gastric emptying, reduce obesity, etc. Next are bile acid sequestrants (Colesevelam), which are primarily lipid-lowering agents but have a significant role in lowering plasma glucose as well as glycosylated haemoglobin levels. In addition to that, dopamine-2 agonist (bromocriptine) is used to control the setting of the drive of the hypothalamus by increasing plasma glucose, fatty acids, and triglycerides in diabetic patients. Other than diabetic diet and exercise, non-medicinal alternative approaches to controlling T2DM are bariatric surgery or metabolic surgery, mainly in obese patients with diabetes, gene therapies, stem cell therapies, pancreatic cell transplantation, artificial pancreas, and the latest innovation, a transdermal insulin patch that releases insulin in a sustained-release form [42]. The conventional and newer treatment algorithms for lowering the glucose in T2DM are discussed below:

1.4.1. Conventional treatment algorithm:

Conventionally, it was believed that one could take charge of his or her T2DM without having to take medication and just make some changes to their lifestyle and opt for natural remedies. Keeping a healthy diet, exercising regularly, losing weight if needed, and quitting smoking will all help to control blood sugar levels. However, these are the conventional and adjuvant therapies associated with T2DM. It is very evident to remember that controlling T2DM without medication takes a prolonged dedication and utmost commitment, which, in reality, most diabetic patients fail to keep; that is why, as per globally appreciated recommendation, concerned physicians start metformin along with lifestyle modifications. This therapy includes anti-hyperglycemic agents primarily based on insulin activities. As per the condition of the patient and the serological test outcome, a considerable glycated haemoglobin (HbA1c) value of ≤ 7.5 is the most commonly used oral anti-hyperglycemic agent, like biguanide derivatives. The primary drug of choice is metformin (both as a form of standard and controlled release) to overcome insulin resistance at the targeted cellular level; along with this or separately, thiazolidinedione (TZD), like pioglitazone, was also recommended as it increases insulin receptor sensitivity. Similarly, when the HbA1c value crosses > 9 with insufficient production of insulin, sulfonylureas (Glimepiride, Glipizide, etc.) would be the drug of choice, with metformin as it increases β-cell insulin secretion. In addition to that, the most conventional remedy for T2DM is regular exercise and a good diet plan, as food impacts heavily on blood sugar levels (**Figure 4**). As diabetes is called a metabolic disorder, to enhance the metabolism, diabetic patients must rely on a low-carbohydrate diet [43].

1.4.2. Newer treatment algorithm:

T2DM is a progressive disease, and sometimes, people will need to take more than one medication to control their blood sugar levels and reach their specific HbA1C goal. Monotherapy, dual therapy, and triple therapy are approaches of therapy suggested by the American Association of Clinical Endocrinologists (AACE)/American College of Endocrinology (ACE) and the American Diabetes Association (ADA) for the management of T2DM. The first line of care for T2DM is advised to involve lifestyle modifications and metformin. The ADA advises first dual treatment if the entry HbA1c level is higher than or equal to 9%, whereas the ACE suggests metformin plus another agent and dietary management for levels over 7.5 per cent. [44]. Current newer treatment options for T2DM include SGLT2 inhibitors, incretin mimetics (GLP-1 receptor agonists and DPP-IV inhibitors), and amylin mimetics. According to the endocrine practice, the glycemic control algorithm is a useful therapy for a person having T2DM and a low risk of any cardiovascular diseases. Amylin mimetics (Pramlintide), incretin mimetics (GLP-1 receptor agonists and DPP-IV inhibitors), Dual GIP and GLP-1 receptor agonists, SGLT2 inhibitors (Anagliflozin, Dapagliflozin, and Empagliflozin), 2nd generation Sulfonylureas, and insulin (Human and analogues) are newer choices of glucose-lowering medications to manage T2DM (**Figure 4**) [45].

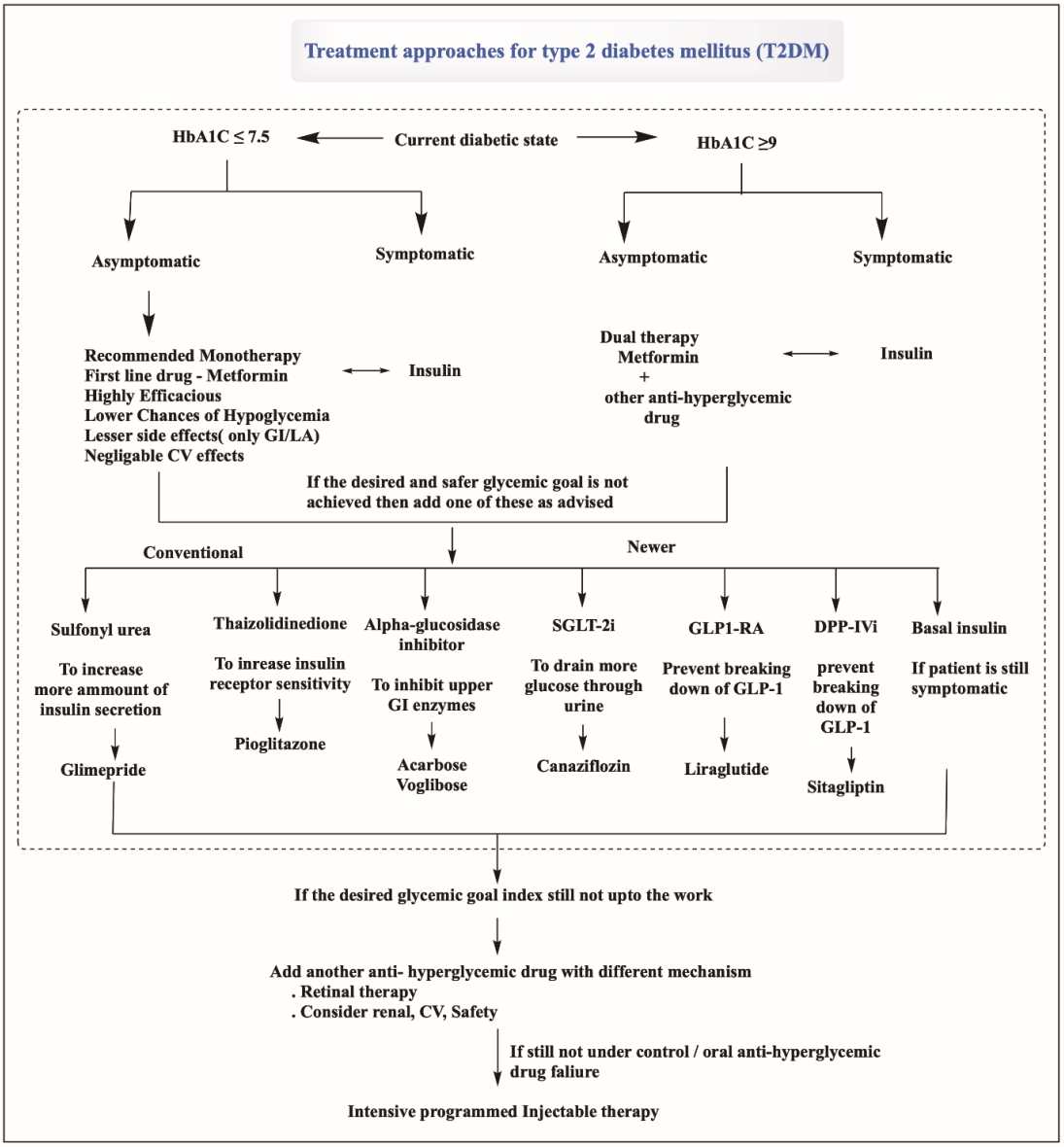

Figure 4: Treatment approaches for the management of T2DM.

1.5. Importance of α-glucosidase inhibition:

The reduction of postprandial hyperglycemia, a main cause of T2DM development, is a major factor for the inhibition of AG. It is a key enzyme in carbohydrate catabolism that hydrolyzes oligosaccharides as well as the terminal glycosidic linkage of alpha- and beta-linked disaccharides. Inhibition of AG will help to slow down the absorption of glucose in the intestines, and effectively reduce the postprandial blood glucose level (**Figure 5**). Inhibition of the AG enzyme has been proven to significantly control

postprandial blood glucose levels in diabetics and to prevent complications like retinopathy and neuropathy [46].

Several molecules have been found to possess AG inhibitory activity, and these molecules may provide a new implication for the management of diabetes. Polyphenolics, in particular, natural products have shown a great potential as AGIs. Isolated plant polyphenols, including those of *Sphallerocarpus gracilis*, are known to show inhibitive effects towards AG as well as general hypoglycemic potential. Furthermore, structural features of the polyphenols are essential for AG inhibitory activity, and specific functional groups are key to their activity. These results highlight the potential of NP-based compounds for the development of AGIs [47,48].

Moreover, synthetic drugs including acarbose, miglitol, and voglibose are clinically used as AGIs. These agents operate through competitive inhibition of the enzyme, resulting in reduced digestion of carbohydrates and glucose absorption, and reduced postprandial hyperglycemia [49]. In clinical trials, patients who take acarbose have shown a lowering of the glycemic index and improved blood glucose control, with average decreases in HbA1c values ranging from about 0.5% to 0.8% when compared to placebo [50,51].

In addition, some thiazole-based, benzimidazole derivatives that have recently appeared in the literature have exhibited interesting inhibitory effects on AG. For instance, recently developed benzothiazole derivatives have been recognized as potent inhibitors, which lead to potential agents for the treatment of diabetes. Technique new double inhibitors of AG and protein tyrosine phosphatase were developed, which indicated the continuing search for better drugs for treatment of diabetes [52,53].

In fact, the role of inhibiting AG cannot be overemphasized in the diabetes therapy. It is one of the pivotal medical interventions to regulate postprandial glucose responses.

By drugs of natural compounds and synthetic inhibitors, more and more effective ways for control of glucose have been found, which brought a new hope for the better treatment of diabetes and its complications.

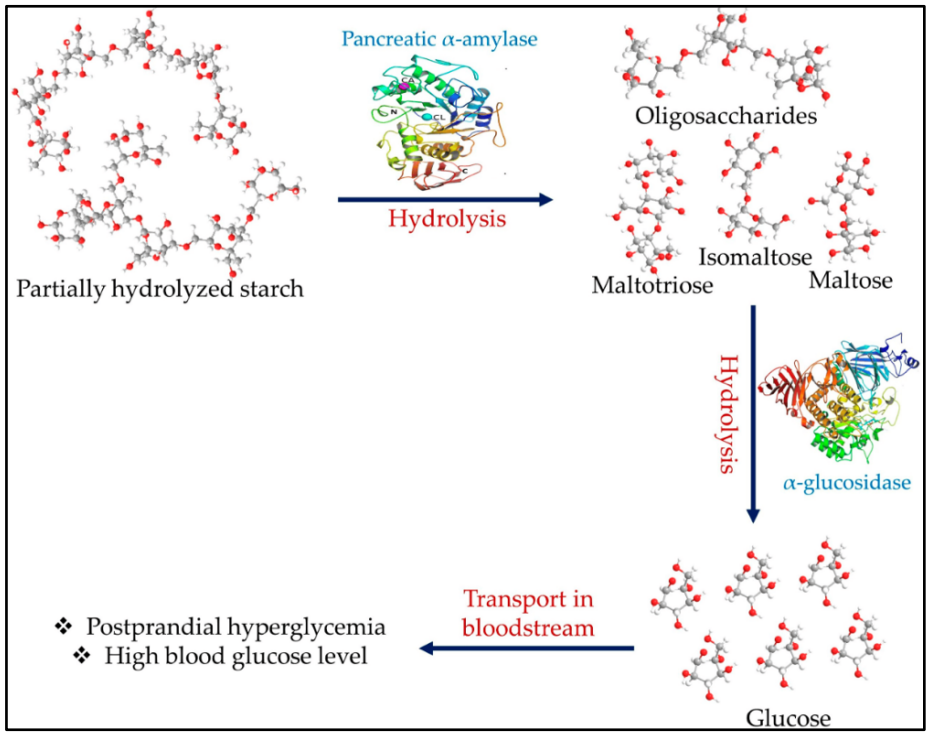

Figure 5: Role of AG in hyperglycemia.

1.6. Overview of 2,4-thiazolidinedione (TZD):

Heterocyclic compounds that include nitrogen and sulphur, particularly those in the thiazole family, have drawn significant attention in synthetic chemistry due to their pharmacological activity as natural compounds and their tremendous potency as agrochemicals and pharmaceuticals [54]. For the purpose of creating novel drugs to treat a variety of pathological/ conditions, such as melanoma, complications from diabetes, cancer, arthritis, and inflammation-related illnesses, the heterocyclic nucleus 2,4-thiazolidinedione (TZD) has been the subject of extensive research. Beside from pharmaceuticals, TZD is used as a brightener in the electroplating industry, a highly sensitive reagent for heavy metals, and for preventing the corrosion of mild steels [55,56]. The well-studied anti-hyperglycemic effect of TZD derivatives is one of them;

this effect has also prompted the creation of therapeutically used "glitazone" drugs, including rosiglitazone, pioglitazone, lobeglitazone, and troglitazone [57]. The historical background and structure of TZD drugs are depicted in **Figure 7** and **Figure 8**.

Thiazolidine-2,4-dione (TZD) is an important heterocyclic nucleus due to its ample reactivity and wide range of applications in medicinal chemistry. TZD is a five-member heterocyclic ring bearing one sulphur, nitrogen, methylene, and carbonyl groups [58]. The molecular formula of TZD is $C_3H_3NO_2S$. The molecular weight, boiling point, melting point, Log P, tPSA, and CLogP are mentioned in **Figure 6**.

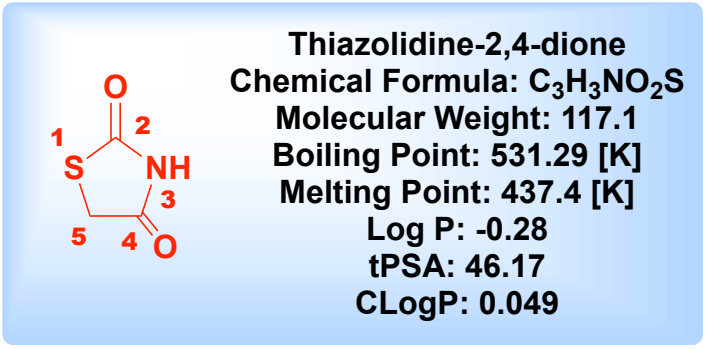

Figure 6: Structure of TZD and its physicochemical properties.

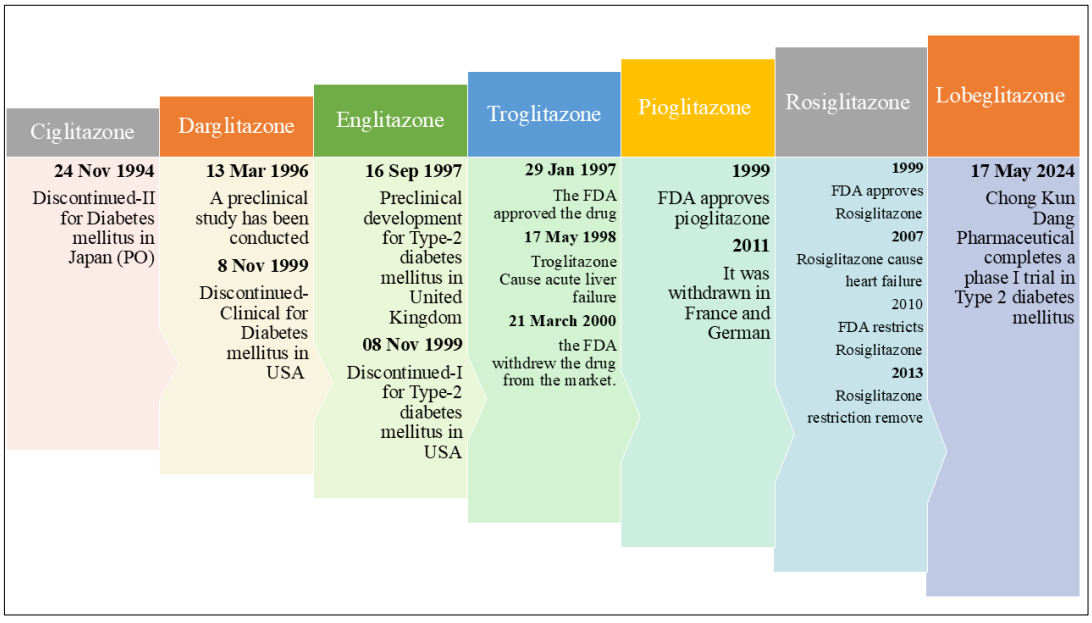

Figure 7: The historical background of thiazolidinediones (TZDs).

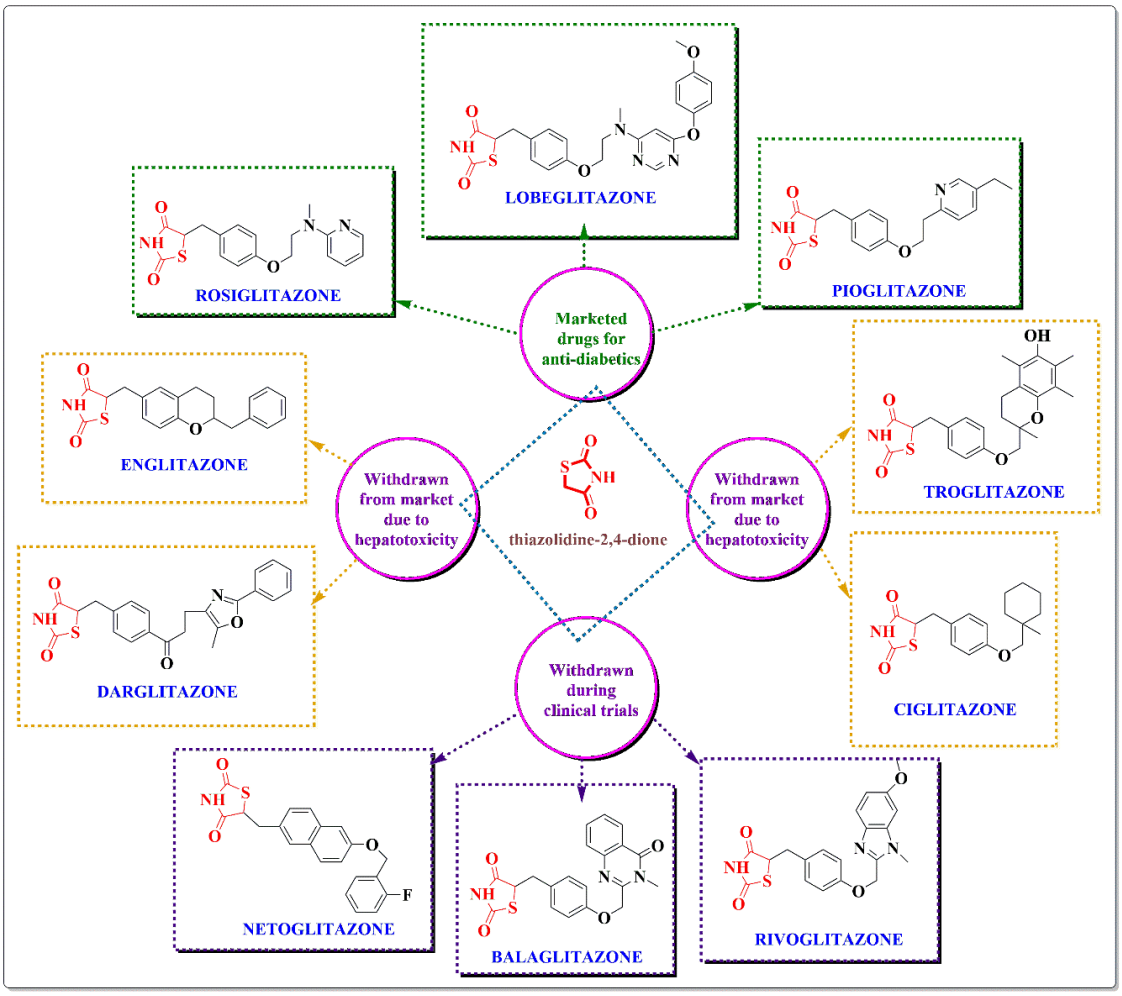

Figure 8: Structure of anti-diabetic medications containing TZD moiety.

The ability of TZDs to be tautomers as a result of the two carbonyl groups and an α-hydrogen further emphasizes the complicated nature of their chemistry (**Figure 9**) [58]. Such tautomeric nature is not solely a chemical curiosity, but would have considerable consequences on the biological effects and possible therapeutic applications of TZD-derived drugs. Further investigation into the role of tautomerism in the structures of TZD that provide medicinal action will provide further insight into the pharmacological nature of these compounds and aid in the rational design of more potent analogues.

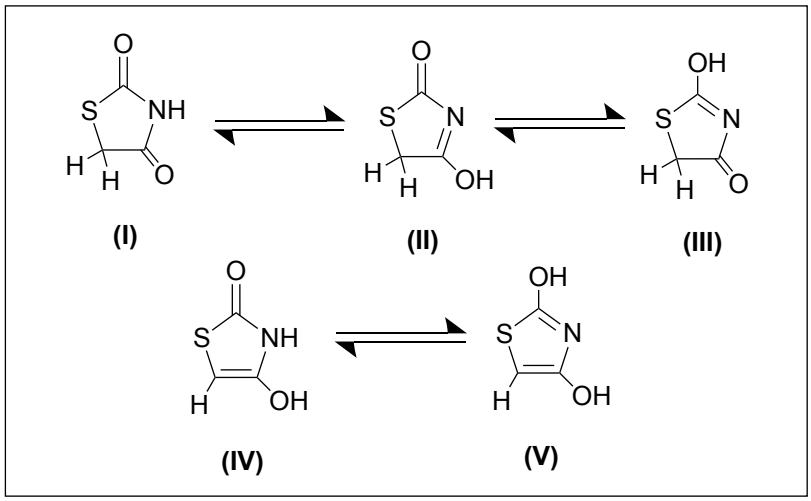

Figure 9: Tautomeric structures of TZD.

1.6.1. Reactivity, synthetic routes and biological effects of TZDs:

The reactivity of TZD hinges critically on its significant capacity to undergo a range of chemical modifications, including enigmatic Knoevenagel condensation and Michael addition, among other chemical reactions that are very important for synthesizing TZD-based analogues with improved pharmacological prospects [59]. The reactivity of the amine (-NH) group in TZD cores is pivotal in various chemical interactions and modifications. The intrinsic reactivity of the -NH group has implications in the synthesis of TZD derivatives and their biological applications. A prime aspect is the ability of the -NH group to participate in hydrogen bonding, which significantly influences the molecular interactions and properties of TZD compounds [59].

The TZD ring, characterized by its -NH linkage, can undergo structural modifications through substitution at this group. Moaty *et al.,* report that structural modifications can be effectuated at the NH groups within the TZD core, such as through Knoevenagel condensation (KC) processes leading to the synthesis of 5-Arylidene-2,4-TZDs [60]. This alteration not only changes the hydrophobicity and

solubility profiles of the TZD compounds but also affects their reactivity towards various biological targets, including enzymes [60].

Furthermore, the presence of electron-rich substituents adjacent to the -NH group enhances its reactivity. In TZD derivatives, the proximity of carbonyl groups can facilitate increased hydrogen bonding capacity, promoting interactions with target proteins, notably with human pancreatic alpha-amylase. The interactions established through the hydrogen bond between the -NH group of TZDs and amino acid residues in the enzyme can modulate enzymatic activity, showcasing how the reactivity of the -NH group is central to the bioactivity of TZDs (**Figure 10**) [61].

The $-CH_2$ unit of the TZD core is crucial for its reactivity and bioactivity. This methylene group is located between the TZD and some functional groups, which affects the interaction between TZDs and biological targets and allows the synthetic modification (**Figure 10**).

The $-CH_2$ function in the TZD scaffold is known to undergo chemical modifications like Michael-type additions and other electrophilic pathways. Recent reports show that TZDs can be chemically modified from reactions at their $-CH_2$ moieties, hence during synthesis of a multitude of TZD derivatives [62,63]. The position of the $-CH_2$ group makes it a nucleophilic site that can participate in various transformation pathways such as electrophilic attacks and rearrangements.

In addition, the chemical effect of the surrounding the $-CH_2$ group has a great effect on its reactivity. It has been pointed out by Kumar et al that changes within the TZD core, for example, different substituents on the phenyl ring at the bridgehead carbon of the TZD moiety, can affect the electronic characteristics of this methylene group and, as such, reaction pathways and efficiencies [63]. The nucleophilicity of $-CH_2$

can be significantly increased by the introduction of an electron-withdrawing or -donating group, making it highly susceptible to attack by electrophiles.

Moreover, investigations on the metabolism of a representative TZD, troglitazone, indicate that the -CH_2 functionality can also serve as a site for metabolic activation, producing reactive intermediates like quinone methides. These metabolites formed on oxidatively opening the TZD ring highlight that the 2-substituent is crucial not only in the synthetic phase, but also in the mitochondria for the bioactivation of the drug [64–66]. Conversion pathways with the -CH_2 group frequently include reactions with hepatic microsomal enzymes, demonstrating such considerations in terms of its reactivity in drug metabolism.

Specifically, with reference to synthetic applications, the -CH_2 moiety in TZDs may either participate in generating new reactive species for further transformation or be exploited to append these onto the TZD scaffold for maintaining or enhancing specific pharmacological activities. For example, the addition of electrophiles or other groups onto the -CH_2 position can substantially modulate biological activity, and this may be a promising area to explore for some potential classes of anti-diabetic agents based on TZD structures [67,68].

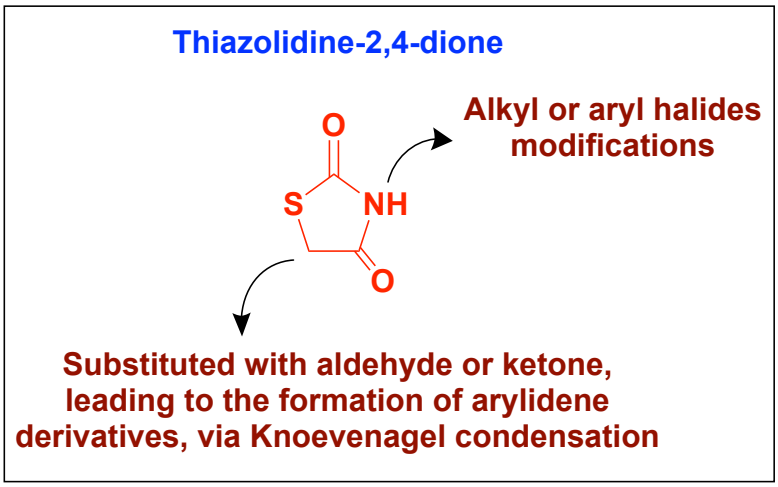

Figure 10: Reactivity of TZD at -CH_2 and -NH.

The initial synthetic procedures for producing the TZD core were documented by Kallenberg in 1923. Kallenberg's approach entails the reaction of carbonyl sulphide with ammonia to produce alkyl thioncarbamate, which is further cyclized under acidic conditions to provide the required TZD (**Scheme 1**). Contemporary techniques entail refluxing α-chloroacetic acid with thiourea, employing water as a solvent for around 12 hours. The proposed reaction mechanism for this process is shown in **Scheme 2**. Similarly, microwave-induced synthesis for the production of TZD is achievable in under 0.5 hours. The procedure entails dissolving chloroacetic acid and thiourea in water, stirring under cryogenic conditions, and subsequently applying microwave initiation. In recent times, TZD was synthesized with the help of mineral acids (HCl/H_2SO_4) in high yield without additional purification (**Scheme 3**). The reaction conducted with HCl as the acid and heated for 7–8 hours yielded the maximum amount of TZD at 94% (**Scheme 4**) [58].

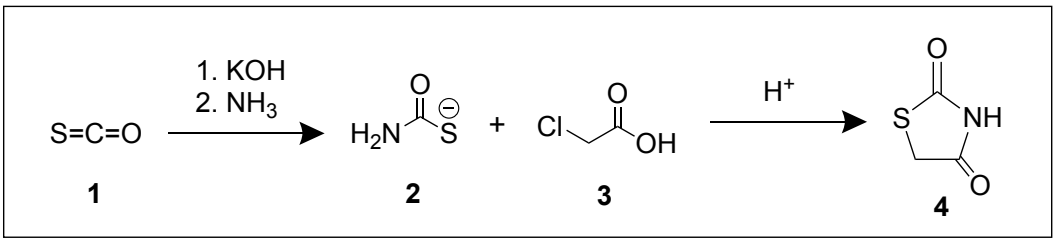

Scheme 1. Initially employed a way to synthesize TZD utilizing carbonyl sulfide.

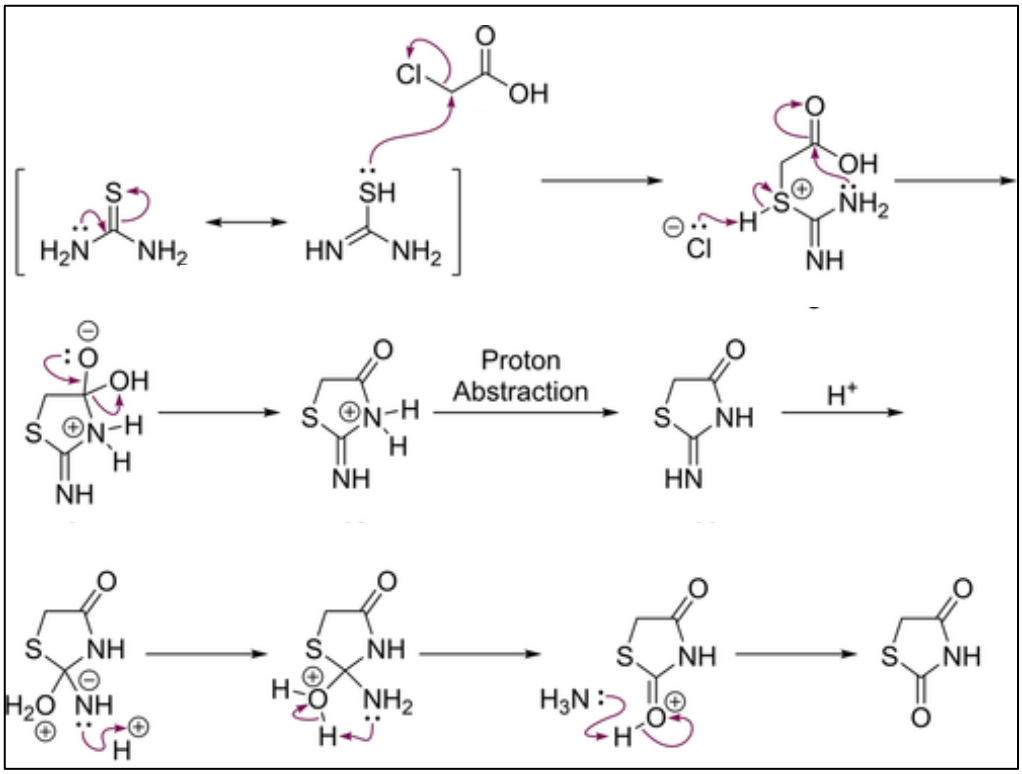

Scheme 2. A mechanistic perspective on the synthetic production of TZD utilizing thiourea and α-chloroacetic acid.

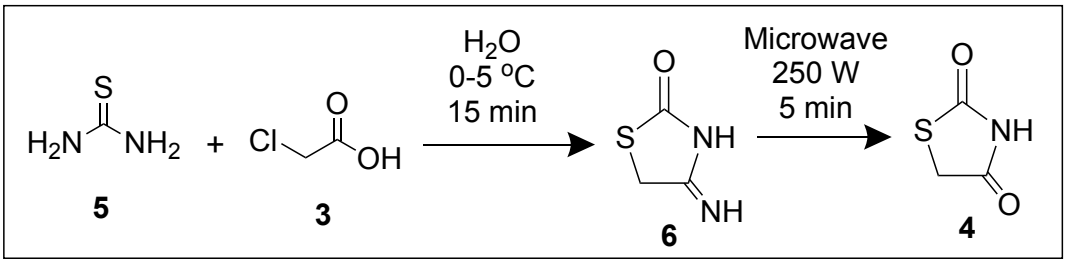

Scheme 3. Synthesis of TZD via microwave irradiation utilizing thiourea and α-chloroacetic acid.

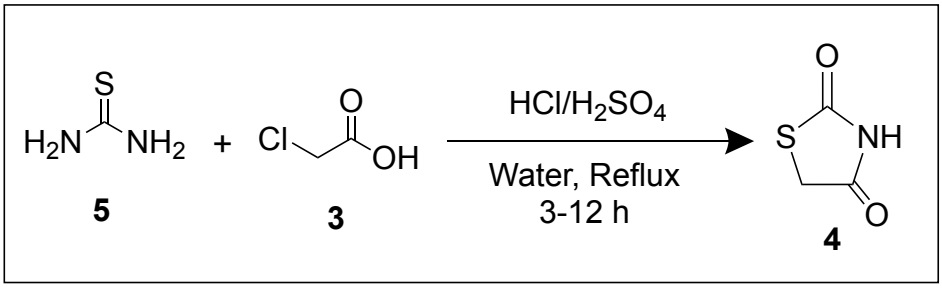

Scheme 4. Synthesis of TZD using mineral acids.

TZD exhibits various biological activities, including anti-diabetic, anticancer, antimicrobial, and anti-inflammatory properties, making it a target for drug development [58,67,68]. Various biological effects of TZDs are attributed to their ability to interfere with major biological pathways and targets. Some analogues were good inhibitors of AG, which are important for the management of T2DM. Furthermore, alterations at the C-5 position of TZD have led to compounds endowed with remarkable anti-diabetic activities, which reinforced their implication in glucose metabolism control and insulin sensitizing activity.

Aside from the pharmacological use, TZDs have been investigated for their antioxidant and anti-inflammatory effects. The presence of different substituents in the TZD scaffold can dramatically shape its biological activity, leading to targeted therapeutic effects. Data accumulated from the literature has highlighted TZD scaffold-containing small molecules as potential multifunctional agents in cellular signalling pathways, supporting the concept of a multitarget approach in drug development. Moreover, novel synthetic methodologies, such as dual-functional and hierarchical synthetic methodologies, are promising to make TZD compounds with favourable properties realistic [54,59].

As a result, TZD is an important structural fragment for organic and medicinal chemistry featuring high reactivity during synthetic transformations and a wide range of biological activities. Studies investigating its mechanisms of action and preparation of new derivatives continue to bring its importance in drug discovery and development to the fore.

1.7. Rationale for Hybrid Molecule Design:

1.7.1. Molecular hybridization in drug discovery:

"Molecular hybridization", a concept that has now gained widespread acceptance in the field of drug discovery, involves the combination of two separate pharmacophores present in two different biologically active molecules toward designing newer entities with better biological activity and suitable physicochemical properties. Essentially, molecular hybridization is the fusion of two or more established pharmacophores into a single hybrid molecule, and may result in new therapeutic agents with the desired advantages of the respective moieties. This approach is especially useful for complicated diseases and conditions that demand multimodal interventions [69].

A major advantage of molecular hybridization is its capacity to develop compounds acting in more than one biological pathway. It has been reported that the hybridization of pharmacophores could neutralize the deleterious side effects of each drug entity or enhance therapeutic efficiency by acting on various biological targets in parallel [70]. The resulting hybrids offer therapeutic potentials as well as reduce drug-drug interactions and pharmacokinetic challenges encountered in traditional drug therapy. The dual-targeting strategy has also been shown to enhance therapeutic efficacy of anti-diabetic agents [71].

Additionally, Siddiki *et al.,* reported that molecular hybridization can produce interesting derivatives like pyrazine-2-carbohydrazide compounds that displayed potent antimicrobial and antitubercular activities [72]. Also, the study of Vinindwa and coworkers on chalcone-quinoline hybrids for potent anti-malarial activities also demonstrated the flexibility of the hybrid strategy and the possibility to design new candidates that are equipotent or more active than their precursors [73]. This shows

the importance of hybrid molecules to access resistance that is observed in different pathogens and cancer cells, encouraging an interest in them in current medicinal chemistry.

The use of computational approaches has greatly improved molecular hybridization in drug design. Using molecular docking and cheminformatics, researchers can improve the efficiency of predicting hybrid compounds' interactions with biological targets. For instance, Aguiar and Camps reviewed the importance of molecular docking as an essential tool for the rapid assessment of the binding affinities of hybrids, to accelerate drug discovery [74]. The combination of hybridization and modern computational approaches allows a rationale design of hybrid molecules and speeds up the hit finding process.

In addition, the case studies of Al-Warhi *et al.,* stress that the hybridization approach is especially useful for the design of anticancer agents were linking pharmacophores could offer improved selectivity and potency towards cancer cell lines [75]. This is also supported by the reported bioactivities of isatin hybrids having good biological activities such as anti-tubercular activity and activity against MDR pathogens [74,76].

In summary, molecular hybridization is a novel approach to drug discovery by integration of pharmacophore, leading to new compounds with better therapeutic applications in terms of greater activity, less side effects and better possibility to combat complex diseases. This strategy not only opens the door to novel chemical entities/metabolites but also fits well with the increasing demand for diversified treatment approaches in the face of the drug resistance, a pressing issue nowadays.

1.7.2. Integration of TZD scaffold with other pharmacophores to enhance anti-diabetic activity:

The TZD scaffolds have been hybridized with other pharmacophores in an endeavour to enhance anti-diabetic potential and outline newer strategies in medicinal chemistry. TZDs (including troglitazone), also known as glitazones, have hypoglycemic effects and act as agonists of PPAR-γ, responsible for inducing insulin sensitivity and subsequently lowering blood glucose levels in T2DM [77–79]. However, for greater potency and expanded therapeutic applications, exploration for methods with incorporation of other medicinal scaffolds is ongoing. Hybridization of the TZD scaffold with various pharmacophores exhibited good potential. For example, a new class of anti-diabetic agents was developed by the synthesis of TZD-based compounds that were fused to different heterocycles such as quinazoline [80]. These combinations, in addition to preserving intrinsic PPAR-γ agonistic activity, lead to the development of new mechanisms of action, which might overcome side effects and resistance to classic TZDs [81,82].

Additionally, generation of TZD derivatives using original synthetic pathways has enabled the incorporation of potent substituents that are able to improve the biological activity. For instance, TZDs in combination with anti-inflammatory or anticancer pharmacophores can give a class of compounds with polypharmacological effect [83,84]. Another recent study brought into evidence the effectiveness of TZDs as dual inhibitors of other pharmacological targets in addition to carbonic anhydrases, shedding light on a novel role of this scaffold beyond diabetes treatment [85,86].

The development of bifunctional compounds based on TZD moieties is especially promising. With TZD in PGL backbones including multi-targeting capability,

researchers have recently reported that this class of compounds showed increasing glucose uptake activity, and some of them also presented with additional anti-inflammation or anticancer activity (compound combined with sulfonylthiourea derivatives) [87,88]. Research into dual-acting TZD hybrids (i.e., activating PPAR-γ and targeting other receptors) has received considerable interest and is a basis for the development of novel anti-diabetic agents [89,90].

TZDs with their distinctive five-membered ring structure present a privileged scaffold to perform numerous modifications, retaining anti-diabetic profile with the least side effects [91]. It is also likely that future directions in this area will emphasize the rational design of new TZD derivative(s) that can combine their targeting against other signalling pathways associated with glucose metabolism and homeostasis. These developments may offer not only better therapeutics for T2DM, but also new models for other metabolic diseases [92,93].

To conclude, the hybridization of TZD templates with other pharmacophores offers a significant scope to develop innovative anti-diabetic drugs with greatly enhanced efficacy and new modes of treatment.

References:

[1] S. Padhi, A.K. Nayak, A. Behera, Type II diabetes mellitus: a review on recent drug based therapeutics, Biomedicine & Pharmacotherapy 131 (2020) 110708. https://doi.org/10.1016/j.biopha.2020.110708.

[2] N. Kerru, A. Singh-Pillay, P. Awolade, P. Singh, Current anti-diabetic agents and their molecular targets: A review, Eur J Med Chem 152 (2018) 436–488. https://doi.org/10.1016/j.ejmech.2018.04.061.

[3] A. Paul, A. Sarkar, T. Banerjee, A. Maji, S. Sarkar, S. Paul, S. Karmakar, N. Ghosh, T.K. Maity, Structural and molecular insights of protein tyrosine phosphatase 1B (PTP1B) and its inhibitors as anti-diabetic agents, J Mol Struct 1293 (2023) 136258. https://doi.org/10.1016/j.molstruc.2023.136258.

[4] S. Wild, G. Roglic, A. Green, R. Sicree, H. King, Global Prevalence of Diabetes: Estimates for the year 2000 and projections for 2030, Diabetes Care 27 (2004) 1047–1053. https://doi.org/10.2337/diacare.27.5.1047.

[5] A. Chaudhury, C. Duvoor, V.S. Reddy Dendi, S. Kraleti, A. Chada, R. Ravilla, A. Marco, N.S. Shekhawat, M.T. Montales, K. Kuriakose, A. Sasapu, A. Beebe, N. Patil, C.K. Musham, G.P. Lohani, W. Mirza, Clinical Review of Anti-diabetic Drugs: Implications for Type 2 Diabetes Mellitus Management, Front Endocrinol (Lausanne) 8 (2017). https://doi.org/10.3389/fendo.2017.00006.

[6] S.Y. Tan, J.L. Mei Wong, Y.J. Sim, S.S. Wong, S.A. Mohamed Elhassan, S.H. Tan, G.P. Ling Lim, N.W. Rong Tay, N.C. Annan, S.K. Bhattamisra, M. Candasamy, Type 1 and 2 diabetes mellitus: A review on current treatment approach and gene therapy as potential intervention, Diabetes and Metabolic Syndrome: Clinical Research and Reviews 13 (2019) 364–372. https://doi.org/10.1016/j.dsx.2018.10.008.

[7] K. Khunti, M.L. Wolden, B.L. Thorsted, M. Andersen, M.J. Davies, Clinical inertia in people with type 2 diabetes: A retrospective cohort study of more than 80,000 people, Diabetes Care 36 (2013) 3411–3417. https://doi.org/10.2337/dc13-0331.

[8] S.E. Inzucchi, R.M. Bergenstal, J.B. Buse, M. Diamant, E. Ferrannini, M. Nauck, A.L. Peters, A. Tsapas, R. Wender, D.R. Matthews, Management of Hyperglycemia in Type 2 Diabetes, 2015: A Patient-Centered Approach: Update to a position statement of the american diabetes association and the european association for the study of diabetes, Diabetes Care 38 (2015) 140–149. https://doi.org/10.2337/dc14-2441.

[9] Y. Handelsman, Z.T. Bloomgarden, G. Grunberger, G. Umpierrez, R.S. Zimmerman, T.S. Bailey, L. Blonde, G.A. Bray, A.J. Cohen, S. Dagogo-Jack, J.A. Davidson, D. Einhorn, O.P. Ganda, A.J. Garber, W.T. Garvey, R.R. Henry, I.B. Hirsch, E.S. Horton, D.L. Hurley, P.S. Jellinger, L. Jovanovič, H.E. Lebovitz, D. LeRoith, P. Levy, J.B. McGill, J.I. Mechanick, J.H. Mestman, E.S. Moghissi, E.A. Orzeck, R. Pessah-Pollack, P.D. Rosenblit, A.I. Vinik, K. Wyne, F. Zangeneh, American Association of Clinical Endocrinologists and American College of Endocrinology – Clinical Practice Guidelines for Developing A Diabetes Mellitus Comprehensive Care Plan – 2015 — Executive Summary, Endocrine Practice 21 (2015) 413–437. https://doi.org/10.4158/EP15672.GL.

[10] H. Li, W. Lu, A. Wang, H. Jiang, J. Lyu, Changing epidemiology of chronic kidney disease as a result of type 2 diabetes mellitus from 1990 to 2017: Estimates from Global Burden of Disease 2017, J Diabetes Investig 12 (2021) 346–356. https://doi.org/10.1111/jdi.13355.

[11] Y. Zeng, Y. Liu, X. Chen, J. Kenny, R. Rong, X. Xia, Global, regional, and national burden of blindness and vision loss attributable to smoking from 1990 to 2021, and forecasts to 2030: findings from the Global Burden of Disease Study 2021, BMC Public Health 25 (2025). https://doi.org/10.1186/s12889-025-21573-2.

[12] W.S. Lee, J. Kim, Diabetic cardiomyopathy: Where we are and where we are going, Korean Journal of Internal Medicine 32 (2017) 404–421. https://doi.org/10.3904/kjim.2016.208.

[13] Y. Zheng, S.H. Ley, F.B. Hu, Global aetiology and epidemiology of type 2 diabetes mellitus and its complications, Nat Rev Endocrinol 14 (2018) 88–98. https://doi.org/10.1038/nrendo.2017.151.

[14] Y. Wu, R. Fu, C. Lei, Y. Deng, W. Lou, L. Wang, Y. Zheng, X. Deng, S. Yang, M. Wang, Z. Zhai, Y. Zhu, D. Xiang, J. Hu, Z. Dai, J. Gao, Estimates of Type 2 Diabetes Mellitus Burden Attributable to Particulate Matter Pollution and Its 30-Year Change Patterns: A Systematic Analysis of Data From the Global Burden of Disease Study 2019, Front Endocrinol (Lausanne) 12 (2021). https://doi.org/10.3389/fendo.2021.689079.

[15] Y. Zhu, C. Zhang, Prevalence of Gestational Diabetes and Risk of Progression to Type 2 Diabetes: a Global Perspective, Curr Diab Rep 16 (2016) 7. https://doi.org/10.1007/s11892-015-0699-x.

[16] E. Dounousi, A. Duni, K. Leivaditis, V. Vaios, T. Eleftheriadis, V. Liakopoulos, Improvements in the Management of Diabetic Nephropathy, The Review of Diabetic Studies 12 (2015) 119–133. https://doi.org/10.1900/RDS.2015.12.119.

[17] C. Bommer, V. Sagalova, E. Heesemann, J. Manne-Goehler, R. Atun, T. Bärnighausen, J. Davies, S. Vollmer, Global Economic Burden of Diabetes in Adults: Projections From 2015 to 2030, Diabetes Care 41 (2018) 963–970. https://doi.org/10.2337/dc17-1962.

[18] P.-C. Mo, H.-Y. Hsu, C.-F. Lin, Y.-S. Cheng, I.-T. Tu, L.-C. Kuo, F.-C. Su, Distinguish different sensorimotor performance of the hand between the individuals with diabetes mellitus and chronic kidney disease through deep learning models, Front Bioeng Biotechnol 12 (2024). https://doi.org/10.3389/fbioe.2024.1351485.

[19] F.K. Alanazi, A. Abdulrahman Almofarh, I. ali Alzahrani, F.A. AlFahid, M.H. alhamdi, M. Gassem Y Alfaifi, F.R. Rabee Alanazi, A. khaledalshehri, H.A. Alharbi, Diabetes Mellitus, International Journal of Engineering Applied Sciences and Technology 8 (2023) 43–52. https://doi.org/10.33564/ijeast.2023.v08i03.006.

[20] D. Asmelash, W. Getnet, B. Biadgo, S. Ambachew, T. Melak, L. Melese, S. Damite, H.W. Baynes, M. Abebe, Undiagnosed diabetes mellitus and associated factors among psychiatric patients receiving antipsychotic drugs at the University of Gondar Hospital, northwest Ethiopia, Ethiop J Health Sci 28 (2018) 3. https://doi.org/10.4314/ejhs.v28i1.2.

[21] N. Shah, M.A. Abdalla, H. Deshmukh, T. Sathyapalan, Therapeutics for type-2 diabetes mellitus: a glance at the recent inclusions and novel agents under development for use in clinical practice, Ther Adv Endocrinol Metab 12 (2021) 204201882110421. https://doi.org/10.1177/20420188211042145.

[22] U. Galicia-Garcia, A. Benito-Vicente, S. Jebari, A. Larrea-Sebal, H. Siddiqi, K.B. Uribe, H. Ostolaza, C. Martín, Pathophysiology of Type 2 Diabetes Mellitus, Int J Mol Sci 21 (2020) 1–34. https://doi.org/10.3390/ijms21176275.

[23] R.A. DeFronzo, R. Eldor, M.A. Bdul-Ghani, Pathophysiologic approach to therapy in patients with newly diagnosed type 2 diabetes, Diabetes Care 36 (2013). https://doi.org/10.2337/dcS13-2011.

[24] A. Singh, K. Singh, A. Sharma, K. Kaur, K. Kaur, R. Chadha, P.M.S. Bedi, Recent developments in synthetic α-glucosidase inhibitors: A comprehensive review with structural and molecular insight, J Mol Struct 1281 (2023) 135115. https://doi.org/10.1016/j.molstruc.2023.135115.

[25] U. Hossain, A.K. Das, S. Ghosh, P.C. Sil, An overview on the role of bioactive α-glucosidase inhibitors in ameliorating diabetic complications, Food and Chemical Toxicology 145 (2020) 111738. https://doi.org/10.1016/j.fct.2020.111738.

[26] A. Mushtaq, U. Azam, S. Mehreen, M.M. Naseer, Synthetic α-glucosidase inhibitors as promising anti-diabetic agents: Recent developments and future challenges, Eur J Med Chem 249 (2023). https://doi.org/10.1016/j.ejmech.2023.115119.

[27] C.M.M. Santos, M. Freitas, E. Fernandes, A comprehensive review on xanthone derivatives as α-glucosidase inhibitors, Eur J Med Chem 157 (2018) 1460–1479. https://doi.org/10.1016/j.ejmech.2018.07.073.

[28] G. Derosa, P. Maffioli, Mini-Special Issue paper Management of diabetic patients with hypoglycemic agents α-Glucosidase inhibitors and their use in clinical practice, Archives of Medical Science 5 (2012). https://doi.org/10.5114/aoms.2012.31621.

[29] M. Camilleri, A. Acosta, Newer pharmacological interventions directed at gut hormones for obesity, Br J Pharmacol (2023) 1–12. https://doi.org/10.1111/bph.16278.

[30] M.O. Mahgoub, I.I. Ali, J.O. Adeghate, K. Tekes, H. Kalász, E.A. Adeghate, An Update on the Molecular and Cellular Basis of Pharmacotherapy in Type 2 Diabetes Mellitus, Int J Mol Sci 24 (2023) 9328. https://doi.org/10.3390/ijms24119328.

[31] E. Adeghate, H. Kalász, Amylin Analogues in the Treatment of Diabetes Mellitus: Medicinal Chemistry and Structural Basis of its Function, Open Med Chem J 5 (2011) 78–81. https://doi.org/10.2174/1874104501105010078.

[32] B.J. Hoogwerf, K.B. Doshi, D. Diab, Pramlintide,the synthetic analogue of amylin: Physiology, pathophysiology, and effects on glycemic control, body weight, and selected biomarkers of vascular risk, Vasc Health Risk Manag 4 (2008). https://doi.org/10.2147/vhrm.s1978.

[33] S. V. Joy, P.T. Rodgers, A.C. Scates, Incretin mimetics as emerging treatments for type 2 diabetes, Annals of Pharmacotherapy 39 (2005). https://doi.org/10.1345/aph.1E245.

[34] D. Hinnen, L.L. Nielsen, A. Waninger, P. Kushner, Incretin mimetics and DPP-IV inhibitors: New paradigms for the treatment of type 2 diabetes, Journal of the American Board of Family Medicine 19 (2006). https://doi.org/10.3122/jabfm.19.6.612.

[35] L.L. Nielsen, Incretin mimetics and DPP-IV inhibitors for the treatment of type 2 diabetes, Drug Discov Today 10 (2005) 703–710. https://doi.org/10.1016/S1359-6446(05)03460-4.

[36] F.K. Knop, Hansen KB, F.K. Knop, Incretin mimetics: a novel therapeutic option for patients with type 2 diabetes – a review, Diabetes Metab Syndr Obes 3 (2010) 155. https://doi.org/10.2147/dmsott.s7004.

[37] A.J. Scheen, Pharmacodynamics, Efficacy and Safety of Sodium–Glucose Co-Transporter Type 2 (SGLT2) Inhibitors for the Treatment of Type 2 Diabetes Mellitus, Drugs 75 (2015) 33–59. https://doi.org/10.1007/s40265-014-0337-y.

[38] D.S. Hsia, O. Grove, W.T. Cefalu, An update on sodium-glucose co-transporter-2 inhibitors for the treatment of diabetes mellitus, Curr Opin Endocrinol Diabetes Obes 24 (2017) 73–79. https://doi.org/10.1097/MED.0000000000000311.

[39] S.I. Taylor, Z.S. Yazdi, A.L. Beitelshees, Pharmacological treatment of hyperglycemia in type 2 diabetes, Journal of Clinical Investigation 131 (2021). https://doi.org/10.1172/JCI142243.

[40] M.J. Davies, V.R. Aroda, B.S. Collins, R.A. Gabbay, J. Green, N.M. Maruthur, S.E. Rosas, S. Del Prato, C. Mathieu, G. Mingrone, P. Rossing, T. Tankova, A. Tsapas, J.B. Buse, Management of Hyperglycemia in Type 2 Diabetes, 2022. A Consensus Report by the American Diabetes Association (ADA) and the European Association for the Study of Diabetes (EASD), Diabetes Care 45 (2022) 2753–2786. https://doi.org/10.2337/dci22-0034.

[41] K. Doyle-Delgado, J.J. Chamberlain, J.H. Shubrook, N. Skolnik, J. Trujillo, Pharmacologic approaches to glycemic treatment of type 2 diabetes: Synopsis of the 2020 American diabetes association's standards of medical care in diabetes clinical guideline, Ann Intern Med 173 (2020). https://doi.org/10.7326/M20-2470.

[42] N. Katsiki, E. Ferrannini, C. Mantzoros, New American Diabetes Association (ADA)/European Association for the Study of Diabetes (EASD) guidelines for the pharmacotherapy of type 2 diabetes: Placing them into a practicing physician's perspective, Metabolism 107 (2020) 813–821. https://doi.org/10.1016/j.metabol.2020.154218.

[43] M.A. Powers, J.K. Bardsley, M. Cypress, M.M. Funnell, D. Harms, A. Hess-Fischl, B. Hooks, D. Isaacs, E.D. Mandel, M.D. Maryniuk, A. Norton, J. Rinker, L.M. Siminerio, S. Uelmen, Diabetes Self-management Education and Support in Adults With Type 2 Diabetes: A Consensus Report of the American Diabetes Association, the Association of Diabetes Care & Education Specialists, the Academy of Nutrition and Dietetics, the American Academy of Family Physicians, the American Academy of PAs, the American Association of Nurse Practitioners, and the American Pharmacists Association, Journal of the American Pharmacists Association 60 (2020). https://doi.org/10.1016/j.japh.2020.04.018.

[44] S.L. Samson, P. Vellanki, L. Blonde, E.A. Christofides, R.J. Galindo, I.B. Hirsch, S.D. Isaacs, K.E. Izuora, C.C. Low Wang, C.L. Twining, G.E. Umpierrez, W.M. Valencia, American Association of Clinical Endocrinology Consensus Statement: Comprehensive Type 2 Diabetes Management Algorithm – 2023 Update, Endocrine Practice 29 (2023). https://doi.org/10.1016/j.eprac.2023.02.001.

[45] N.A. Elsayed, G. Aleppo, V.R. Aroda, R.R. Bannuru, F.M. Brown, D. Bruemmer, B.S. Collins, M.E. Hilliard, D. Isaacs, E.L. Johnson, S. Kahan, K. Khunti, J. Leon, S.K. Lyons, M. Lou Perry, P. Prahalad, R.E. Pratley, J.J. Seley, R.C. Stanton, R.A. Gabbay, 9. Pharmacologic Approaches to Glycemic Treatment: Standards of Care in Diabetes—2023, Diabetes Care 46 (2023). https://doi.org/10.2337/dc23-S009.

[46] E. Nasli-Esfahani, M. Mohammadi-Khanaposhtani, S. Rezaei, Y. Sarrafi, Z. Sharafi, N. Samadi, M.A. Faramarzi, F. Bandarian, H. Hamedifar, B. Larijani, M. Hajimiri, M. Mahdavi, A new series of Schiff base derivatives bearing 1,2,3-triazole: Design, synthesis, molecular docking, and α-glucosidase inhibition, Arch Pharm (Weinheim) 352 (2019). https://doi.org/10.1002/ardp.201900034.

[47] T. Ma, X. Sun, C. Tian, J. Luo, C. Zheng, J. Zhan, Enrichment and Purification of Polyphenol Extract from Sphallerocarpus gracilis Stems and Leaves and in Vitro Evaluation of DNA Damage-Protective Activity and Inhibitory Effects of α-Amylase and α-Glucosidase, Molecules 20 (2015) 21442–21457. https://doi.org/10.3390/molecules201219780.

[48] T. Tian, G.-Y. Chen, H. Zhang, F.-Q. Yang, Personal Glucose Meter for α-Glucosidase Inhibitor Screening Based on the Hydrolysis of Maltose, Molecules 26 (2021) 4638. https://doi.org/10.3390/molecules26154638.

[49] M. Taha, N.H. Ismail, S. Imran, A. Wadood, F. Rahim, M. Ali, A.U. Rehman, Novel quinoline derivatives as potent in vitro α-glucosidase inhibitors: in silico studies and SAR predictions, Medchemcomm 6 (2015) 1826–1836. https://doi.org/10.1039/C5MD00280J.

[50] A. Sukohar, S.U. N, D. Mayasari, A. Suryawinata, Î±-GLUCOSIDASE INHIBITOR AND ANTIOXIDANT ACTIVITY ASSAYS OF GUAVA LEAF, CASHEW LEAF AND THE COMBINATIONS AS ANTI-DIABETIC AGENT, Int J Res Ayurveda Pharm 8 (2017) 86–90. https://doi.org/10.7897/2277-4343.08145.

[51] M.A. Ibrahim, M.J. Bester, A.W.H. Neitz, A.R.M. Gaspar, Structural properties of bioactive peptides with α-glucosidase inhibitory activity, Chem Biol Drug Des 91 (2018) 370–379. https://doi.org/10.1111/cbdd.13105.

[52] J. Liu, J. Li, S. Zhao, Y. Chang, Q. Chen, W. Wu, S. Jiao, H. Xiao, Q. Zhang, J. Zhao, J. Xu, P. Sun, Discovery of N -(phenylsulfonyl)thiazole-2-carboxamides as potent α -glucosidase inhibitors, Drug Dev Res 85 (2024). https://doi.org/10.1002/ddr.22128.

[53] S. Ansariashlaghi, A. Fakhrioliaei, M. Mohammadi-Khanaposhtani, M. Noori, M. Asadi, S. Mojtabavi, M.A. Faramarzi, E.N. Esfahani, H. Rastegar, B. Larijani, H. Azizian, M. Mahdavi, New phenylthiosemicarbazide-phenoxy-1,2,3-triazole- N -phenylacetamides as dual inhibitors against α-glucosidase and PTP-1B for the treatment of type 2 diabetes, Arch Pharm (Weinheim) 357 (2024). https://doi.org/10.1002/ardp.202300517.

[54] H. Kumar, N. Aggarwal, M.G. Marwaha, A. Deep, H. Chopra, M.M. Matin, A. Roy, T. Bin Emran, Y.K. Mohanta, R. Ahmed, T.K. Mohanta, M. Saravanan, R.K. Marwaha, A. Al-Harrasi, Thiazolidin-2,4-Dione Scaffold: An Insight into Recent Advances as Antimicrobial, Antioxidant, and Hypoglycemic Agents, Molecules 27 (2022) 6763. https://doi.org/10.3390/molecules27196763.

[55] N. Chadha, M.S. Bahia, M. Kaur, O. Silakari, Thiazolidine-2,4-dione derivatives: Programmed chemical weapons for key protein targets of various pathological conditions, Bioorg Med Chem 23 (2015) 2953–2974. https://doi.org/10.1016/j.bmc.2015.03.071.

[56] V.S. Jain, D.K. Vora, C.S. Ramaa, Thiazolidine-2,4-diones: Progress towards multifarious applications, Bioorg Med Chem 21 (2013) 1599–1620. https://doi.org/10.1016/j.bmc.2013.01.029.

[57] G. Singh, R. Kumar, D. D.S., M. Chaudhary, C. Kaur, N. Khurrana, Thiazolidinedione as a Promising Medicinal Scaffold for the Treatment of Type 2 Diabetes, Curr Diabetes Rev 20 (2024). https://doi.org/10.2174/0115733998254798231005095627.

[58] N. Long, A. Le Gresley, S.P. Wren, Thiazolidinediones: An In–Depth Study of Their Synthesis and Application to Medicinal Chemistry in the Treatment of Diabetes Mellitus, ChemMedChem 16 (2021) 1717–1736. https://doi.org/10.1002/cmdc.202100177.

[59] A.M. Ibrahim, M.E. Shoman, M.F.A. Mohamed, A.M. Hayallah, G. El-Din A. Abuo-Rahma, Chemistry and Applications of Functionalized 2,4-Thiazolidinediones, European J Org Chem 26 (2023). https://doi.org/10.1002/ejoc.202300184.

[60] M.N. Abd Al Moaty, E.S.H. El Ashry, L.F. Awad, A. Mostafa, M.M. Abu-Serie, M. Teleb, Harnessing ROS-Induced Oxidative Stress for Halting Colorectal Cancer via Thiazolidinedione-Based SOD Inhibitors, ACS Omega 7 (2022) 21267–21279. https://doi.org/10.1021/acsomega.2c02410.

[61] R.N. Devi, M.G. Khrenova, S. Israel, C. Anzline, A.A. Astakhov, V.G. Tsirelson, Testing the ability of rhodanine and 2, 4-thiazolidinedione to interact with the human

pancreatic alpha-amylase: electron-density descriptors complement molecular docking, QM, and QM/MM dynamics calculations, J Mol Model 23 (2017) 252. https://doi.org/10.1007/s00894-017-3418-5.

[62] N. Trotsko, A. Głogowska, B. Kaproń, K. Kozieł, E. Augustynowicz-Kopeć, A. Paneth, The new thiazolidine-2,4-dione-based hybrids with promising antimycobacterial activity: design, synthesis, biological evaluation, and drug interaction analysis, J Enzyme Inhib Med Chem 40 (2025). https://doi.org/10.1080/14756366.2024.2442703.

[63] H. Kumar, N. Aggarwal, M.G. Marwaha, A. Deep, H. Chopra, M.M. Matin, A. Roy, T. Bin Emran, Y.K. Mohanta, R. Ahmed, T.K. Mohanta, M. Saravanan, R.K. Marwaha, A. Al-Harrasi, Thiazolidin-2,4-Dione Scaffold: An Insight into Recent Advances as Antimicrobial, Antioxidant, and Hypoglycemic Agents, Molecules 27 (2022) 6763. https://doi.org/10.3390/molecules27196763.

[64] R. Alvarez-Sánchez, F. Montavon, T. Hartung, A. Pähler, Thiazolidinedione Bioactivation: A Comparison of the Bioactivation Potentials of Troglitazone, Rosiglitazone, and Pioglitazone Using Stable Isotope-Labeled Analogues and Liquid Chromatography Tandem Mass Spectrometry, Chem Res Toxicol 19 (2006) 1106–1116. https://doi.org/10.1021/tx050353h.

[65] K.G. Madsen, G. Grönberg, C. Skonberg, U. Jurva, S.H. Hansen, J. Olsen, Electrochemical Oxidation of Troglitazone: Identification and Characterization of the Major Reactive Metabolite in Liver Microsomes, Chem Res Toxicol 21 (2008) 2035–2041. https://doi.org/10.1021/tx8002214.

[66] J.N. Tettey, J.L. Maggs, W.G. Rapeport, M. Pirmohamed, B.K. Park, Enzyme-Induction Dependent Bioactivation of Troglitazone and Troglitazone Quinone In Vivo, Chem Res Toxicol 14 (2001) 965–974. https://doi.org/10.1021/tx0001981.

[67] Mohd.J. Naim, Md.J. Alam, S. Ahmad, F. Nawaz, N. Shrivastava, M. Sahu, O. Alam, Therapeutic journey of 2,4-thiazolidinediones as a versatile scaffold: An insight into structure activity relationship, Eur J Med Chem 129 (2017) 218–250. https://doi.org/10.1016/j.ejmech.2017.02.031.

[68] N. Long, A. Le Gresley, S.P. Wren, Thiazolidinediones: An In–Depth Study of Their Synthesis and Application to Medicinal Chemistry in the Treatment of Diabetes Mellitus, ChemMedChem 16 (2021) 1717–1736. https://doi.org/10.1002/cmdc.202100177.

[69] P. de Sena Murteira Pinheiro, L.S. Franco, T.L. Montagnoli, C.A.M. Fraga, Molecular hybridization: a powerful tool for multitarget drug discovery, Expert Opin Drug Discov 19 (2024) 451–470. https://doi.org/10.1080/17460441.2024.2322990.

[70] B. Vinindwa, G.A. Dziwornu, W. Masamba, Synthesis and Evaluation of Chalcone-Quinoline Based Molecular Hybrids as Potential Anti-Malarial Agents, Molecules 26 (2021) 4093. https://doi.org/10.3390/molecules26134093.

[71] H. Khamees Thabet, A. Ragab, M. Imran, M.H. Helal, S. Ibrahim Alaqel, A. Alshehri, A. Ash Mohd, M. Rakan Alshammari, M. S. Abusaif, Y. A. Ammar, Discovery of new anti-diabetic potential agents based on paracetamol incorporating sulfa-drugs: Design, synthesis, α-amylase, and α-glucosidase inhibitors with molecular docking simulation, Eur J Med Chem 275 (2024) 116589. https://doi.org/10.1016/j.ejmech.2024.116589.

[72] A.A. Siddiki, S. Parmar, H.K. Chaudhari, S.S. Yadav, R.S. Chauhan, Targeted Hybridization: Pyrazine-2-Carbohydrazide Derivatives as Promising Antitubercular and Antimicrobial Leads, ChemistrySelect 9 (2024). https://doi.org/10.1002/slct.202402487.

[73] B. Vinindwa, G.A. Dziwornu, W. Masamba, Synthesis and Evaluation of Chalcone-Quinoline Based Molecular Hybrids as Potential Anti-Malarial Agents, Molecules 26 (2021) 4093. https://doi.org/10.3390/molecules26134093.

[74] C. Aguiar, I. Camps, Molecular Docking in Drug Discovery: Techniques, Applications, and Advancements, (2024). https://doi.org/10.26434/chemrxiv-2024-gmhtx.

[75] T. Al-Warhi, A.M. El Kerdawy, N. Aljaeed, O.E. Ismael, R.R. Ayyad, W.M. Eldehna, H.A. Abdel-Aziz, G.H. Al-Ansary, Synthesis, Biological Evaluation and In Silico Studies of Certain Oxindole–Indole Conjugates as Anticancer CDK Inhibitors, Molecules 25 (2020) 2031. https://doi.org/10.3390/molecules25092031.

[76] A.A. Siddiki, S. Parmar, H.K. Chaudhari, S.S. Yadav, R.S. Chauhan, Targeted Hybridization: Pyrazine-2-Carbohydrazide Derivatives as Promising Antitubercular and Antimicrobial Leads, ChemistrySelect 9 (2024). https://doi.org/10.1002/slct.202402487.

[77] G. Singh, R. Kumar, D. D.S., M. Chaudhary, C. Kaur, N. Khurrana, Thiazolidinedione as a Promising Medicinal Scaffold for the Treatment of Type 2 Diabetes, Curr Diabetes Rev 20 (2024). https://doi.org/10.2174/0115733998254798231005095627.

[78] S.S. Al Neyadi, A. Adem, N. Amir, I.M. Abdou, Targeting PPAR<i>γ</i> Receptor Using New Phosphazene Derivative Containing Thiazolidinedione: Design, Synthesis, and Glucose Uptake, Open J Med Chem 10 (2020) 35–45. https://doi.org/10.4236/ojmc.2020.102003.

[79] A.M. Ibrahim, M.E. Shoman, M.F.A. Mohamed, A.M. Hayallah, G. El-Din A. Abuo-Rahma, Chemistry and Applications of Functionalized 2,4-Thiazolidinediones, European J Org Chem 26 (2023). https://doi.org/10.1002/ejoc.202300184.

[80] P.S. Auti, G. George, A.T. Paul, Recent advances in the pharmacological diversification of quinazoline/quinazolinone hybrids, RSC Adv 10 (2020) 41353–41392. https://doi.org/10.1039/D0RA06642G.

[81] A. Khamitova, D. Berillo, A. Lozynskyi, Y. Konechnyi, D. Mural, V. Georgiyants, R. Lesyk, Thiadiazole and Thiazole Derivatives as Potential Antimicrobial Agents, Mini-Reviews in Medicinal Chemistry 24 (2024) 531–545. https://doi.org/10.2174/1389557523666230713115947.

[82] W. Ahsan, The Journey of Thiazolidinediones as Modulators of PPARs for the Management of Diabetes: A Current Perspective, Curr Pharm Des 25 (2019) 2540–2554. https://doi.org/10.2174/1381612825666190716094852.

[83] L. Rani, A.S. Grewal, N. Sharma, S. Singh, Recent Updates on Free Fatty Acid Receptor 1 (GPR-40) Agonists for the Treatment of Type 2 Diabetes Mellitus, Mini-Reviews in Medicinal Chemistry 21 (2021) 426–470. https://doi.org/10.2174/1389557520666201023141326.

[84] C.H. Rathod, P.B. Nariya, D. Maliwal, R.R.S. Pissurlenkar, N.P. Kapuriya, A.S. Patel, Design, Synthesis and Anti-diabetic Activity of Biphenylcarbonitrile-Thiazolidinedione Conjugates as Potential α-Amylase Inhibitors, ChemistrySelect 6 (2021) 2464–2469. https://doi.org/10.1002/slct.202004362.

[85] M.A. Abdelgawad, K. El-Adl, S.S.A. El-Hddad, M.M. Elhady, N.M. Saleh, M.M. Khalifa, F. Khedr, M. Alswah, A.A. Nayl, M.M. Ghoneim, N.E.A. Abd El-Sattar, Design, Molecular Docking, Synthesis, Anticancer and Anti-Hyperglycemic Assessments of Thiazolidine-2,4-diones Bearing Sulfonylthiourea Moieties as Potent VEGFR-2 Inhibitors and PPARγ Agonists, Pharmaceuticals 15 (2022) 226. https://doi.org/10.3390/ph15020226.

[86] S.L. Mueller, P.K. Chrysanthopoulos, M.A. Halili, C. Hepburn, T. Nebl, C.T. Supuran, A. Nocentini, T.S. Peat, S.-A. Poulsen, The Glitazone Class of Drugs as Carbonic Anhydrase Inhibitors—A Spin-Off Discovery from Fragment Screening, Molecules 26 (2021) 3010. https://doi.org/10.3390/molecules26103010.

[87] M. Zengin, O. Unsal Tan, S. Sabuncuoglu, R.K. Arafa, A. Balkan, Design and Discovery of New Dual Carbonic Anhydrase IX and VEGFR-2 Inhibitors Based on the Benzenesulfonamide-Bearing 4-Thiazolidinones/2,4-Thiazolidinediones Scaffold, Drug Dev Res 85 (2024). https://doi.org/10.1002/ddr.70030.

[88] A. Citarella, S. Vittorio, C. Dank, L. Ielo, Syntheses, reactivity, and biological applications of coumarins, Front Chem 12 (2024). https://doi.org/10.3389/fchem.2024.1362992.

[89] S. Shaaban, A.Y.M. Alabdali, M.H.A. Mousa, H. Ba-Ghazal, Y.S. Al-Faiyz, I. Elghamry, H.A. Althikrallah, A.O. Al Khatib, M. Alaasar, A.A. Al-Karmalawy, Innovative Multitarget Organoselenium Hybrids With Apoptotic and Anti-Inflammatory Properties Acting as JAK1/STAT3 Suppressors, Drug Dev Res 86 (2025). https://doi.org/10.1002/ddr.70075.

[90] M. Duhan, R. Singh, M. Devi, J. Sindhu, P. Kumar, S. Kumar, R. Kataria, A. Kumar, S. Lal, D. Singh, Thiazolidine-2,4-dione framework containing spiropyrrolidine-oxindole and 1,2,3-triazole scaffold: synthesis, in vitro α-amylase inhibition and in silico studies, New Journal of Chemistry 47 (2023) 5399–5412. https://doi.org/10.1039/D2NJ05059E.

[91] M. Shafiei, H. Toreyhi, L. Firoozpour, T. Akbarzadeh, M. Amini, E. Hosseinzadeh, M. Hashemzadeh, L. Peyton, E. Lotfali, A. Foroumadi, Design, Synthesis, and In Vitro and In Vivo Evaluation of Novel Fluconazole-Based Compounds with Promising Antifungal Activities, ACS Omega 6 (2021) 24981–25001. https://doi.org/10.1021/acsomega.1c04016.

[92] M.S. Sinicropi, J. Ceramella, P. Vanelle, D. Iacopetta, C. Rosano, O. Khoumeri, S. Abdelmohsen, W. Abdelhady, H. El-Kashef, Novel Thiazolidine-2,4-dione-trimethoxybenzene-thiazole Hybrids as Human Topoisomerases Inhibitors, Pharmaceuticals 16 (2023) 946. https://doi.org/10.3390/ph16070946.

[93] B. Nagaraju, M. Rajeswari, N. Vedasree, C.A. Rao, V.R. Srinivasa, T. Prabha, C.V. Rao, S. Maddila, Design, Synthesis, and Molecular Docking Studies of Integrated Benzylidenethiazolidine-2,4-Dione and Thieno[2,3- d]pyrimidine-6-Carboxylate Derivatives as Potent Anti-diabetic agents, ChemistrySelect 8 (2023). https://doi.org/10.1002/slct.202303786.

CHAPTER-II

LITERATURE REVIEW

1. Literature Review:

1.1. Overview of 5-arylidene-2,4-thiazolidinedione (5-A-TZD):

5-Arylidene-2,4-thiazolidinedione (5-A-TZD) is a new class of substituted heterocycles that has been obtained by substitution of an arylidene group at the 5-position of the respective parent 2,4-thiazolidinedione (TZD) moiety (**Figure 1**)[1]. TZD has also been studied for an extended period due to its synthetic diversity, medicinal relevance, and small heterocyclic rings with sulfur and nitrogen atoms. In the area of medicinal chemistry, 5-A-TZD derivatives have received special attention in recent years. Several pharmacological activities such as hypoglycaemic [2], antimicrobial and antiviral [3], analgesic [4], anti-inflammatory [5], antimalarial [6], hypolipidemic [7], antileishmanial [8], and anti-cancer [9] have been recorded for the 5-A-TZD and proved as a versatile precursor molecule [10]. Therefore, the preparation of 5-A-TZDs has become increasingly important. Several synthetic methods have been developed to obtain these derivatives, but Knoevenagel condensation (KC) is one of the most widely used synthetic protocols in medicinal chemistry research. KC of aromatic aldehydes with TZD mainly yield 5-A-TZD [11].

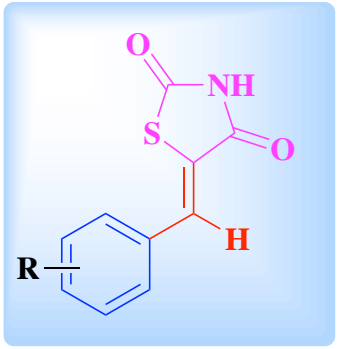

Figure 1: General structure of 5-A-TZD.

KC reaction is a reliable, efficient, versatile, and convenient method for carbon-carbon bond formation, and it is widely used in both industry and academic institutions. The end product is an α,β-unsaturated compound used to build naturally occurring

compounds [12]. KC has been used for the synthesis of several organic molecules like coumarin derivatives [13,14], arylidinemalononitrile derivatives [15], pharmaceutical chemicals [16], antibiotics [17], and chemo-sensors [18]. KC is also valuable for developing clinical drugs and their derivatives, such as pioglitazone and rosiglitazone, epalrestat, sulindac, nifedipine, and atorvastatin [19]. Because of such exceptional features of KC, medicinal chemists have always shown keen interest in using this simple, easy, and effective tool for producing 5-A-TZD. In the literature, several bases, organic catalysts, inorganic catalysts, heterogeneous solid catalysts, ionic liquids (ILs), and bio-catalysts, have been explored under specific reaction conditions to accelerate the KC for synthesizing 5-A-TZD derivatives (**Figure 3**). However, some researchers also developed microwave (MW), ultrasound, and grinding-assisted synthetic protocols to decrease the reaction time and increase the yield of 5-A-TZD derivatives [20–22].

1.2. Knoevenagel condensation and its importance in 5-arylidene-2,4-thiazolidinediones (5-A-TZDs) synthesis:

Knoevenagel condensation (KC) is a transformation reaction in organic chemistry in which an aldehyde or ketone undergoes a reaction with compounds having activated methylene groups under the catalytic activity of organic bases like primary and secondary amines (not tertiary amines), their respective salt of them, and ammonia. The reaction was named after Emil Albert Knoevenagel (a German Chemist), who had investigated and developed this useful reaction (between 1896 and 1898). Another way, we can say that a KC is a nucleophilic attachment of an active methylene compound to a carbonyl group from either ketones or aldehydes, accompanied by a dehydration reaction during which a water molecule is released (therefore, condensation) [23,24]. It is usually done in organic solvents with organic bases like pyridine, piperidine, potassium hydroxide, and sodium hydroxide as mediators. However, since toxic and

unhealthy solvents accompany this reaction, and most of the catalysts used are non-recoverable, their use is limited in the chemical industry. It is a modified aldol condensation in which the reaction of enols with carbonyl compounds affords conjugate enone [11,25].

Generally, KC can be carried out in the presence of a base and catalyst, mainly piperidine. The general mechanism of KC between TZDs and substituted aromatic aldehydes for the synthesis of 5-A-TZDs is shown in (**Figure 2**). The Knoevenagel reaction seems to have two phases: the nucleophilic addition to the carbonyl carbon of an aldehyde, and the formation of an adduct. The second is the 1,2 elimination of a water molecule, which results in forming a carbon-carbon double bond. The lone pair of piperidine N atoms strikes the 5th position (-CH_2-) of the TZD molecule, abstracting one of the H atoms from the structure, forming an intermediate A, and converting the simple piperidine into a piperidinium ion. The nucleophile (intermediate A) then attacked the electrophilic center (C atom) of the aryl aldehyde, resulting in intermediate B. Afterwards, a proton was donated to intermediate B by the piperidinium ion. Then, subsequent dehydration resulted in the final compound 5-A-TZD and the piperidine conjugated acid as a byproduct (**Figure 2**)[26].

Drawanz *et al.,* established a simple, quick, and clean KC reaction method to synthesize 5-A-TZDs using sonochemistry. Different mono- and di-substituted aromatic aldehydes have been reacted with TZDs in the presence of potassium hydroxide (KOH) and ethanol under ultrasonic irradiation (frequency 24 kHz) at room temperature for 10-30 min to form the substituted 5-A-TZDs. Several bases (like triethylamine, sodium acetate, and potassium hydroxide) were used in different equimolar proportions to optimize the reaction. It has been found that in the presence of potassium hydroxide under suitable reaction conditions, the desired products were formed, which were then

analyzed through GC-MS (Gas chromatography Mass spectrometry) and calculated the percentage yields (**Table 1**)[21]. Similarly, Thari *et al.,* explored a one-pot green synthesis of 5-A-TZDs containing isooxazoline derivatives via ultrasound-assisted technique. The compounds were synthesized via KC by the reaction of substituted aldehyde and TZD in the presence of sodium hydroxide as a base in ethanol/water (v/v, 2:1) and stirred at room temperature for 5-6 hrs (**Table 1**)[27]. It has also been noticed that by altering the catalyst and reaction conditions, the mechanism of KC can be optimized even further. In recent advancements, scientists have been using a heterogeneous base and Lewis's acids such as LiOH, $ZnCl_2$, $InCl_3$, $TiCl_4$, and $NbCl_5$ as a catalysts. Given the fact that acids of heavy metals are not suitable in food and pharmaceutical products due to their toxicity [28]. Similarly, for the synthesis of 5-A-TZDs, scientists have also developed a novel MW-assisted KC process. Furthermore, KC was carried out independently with MW-assisted and traditional methods to compare the reaction times for this particular synthesis. As a result, it was revealed that the reaction time in the MW-assisted methodology was significantly reduced compared to the conventional process[29]. Based on the above facts, we can assure that the KC reaction has been one of the most effective methods for synthesizing 5-A-TZDs.

Table 1: Base-catalysed KC for the synthesis of 5-A-TZDs.

Sl. No.	Reactants	Base used	Time	Product	Ref.
1	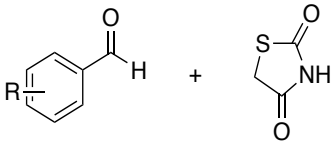 R= EDG/EWG	Potassium hydroxide (KOH) (0.02 mol)	10-30 min	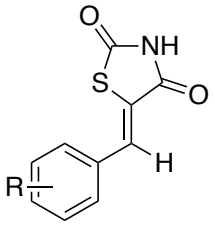 Yield: 25-81%	[21]

2	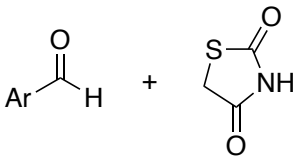 Ar= Substituted Aryl ring with EDG/EWG	Sodium hydroxide (1.1 mmol)	5-6 hrs	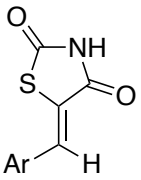 Yield: 55-77%	[27]

*EWG= Electron withdrawing group; EDG= Electron donating group.

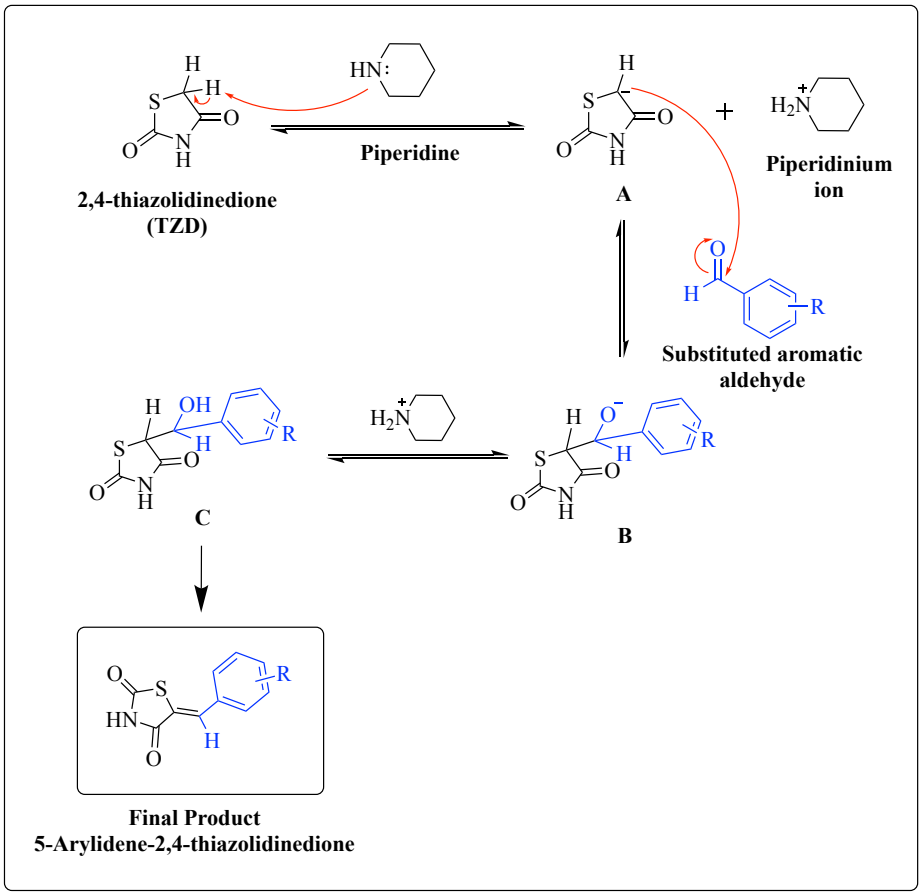

Figure 2: General mechanism of KC between TZD and substituted aromatic aldehydes.

1.3. Recent approaches for the synthesis of 5-A-TZDs via KC:

The synthetic strategy used for synthesizing 5-A-TZDs and their substitution mainly depends on the subtypes of TZDs and substituted aryl aldehydes. One of the most popular and considered procedures for 5-A-TZD synthesis is the KC. By using KC, many medicinal chemists have synthesized numerous potent molecules containing 5-A-TZD as core precursors. KC is a type of aldol condensation reaction in which the

active methylene carbon atoms of any compound react with the carbonyl group of an aldehyde or ketone, followed by the elimination of water in the presence of a base and forms an α,ß-unsaturated compound. The organic base plays a vital role in condensation reactions like KC reactions. Previously, many organic chemists have explored the KC reaction by changing the different reaction conditions (like base catalysts, ionic liquids, and inorganic salts) and optimized the reaction to get better yields in a lesser amount of time. As a result, it has been depicted that the KC reaction produces a better yield in the present base and a precise amount of catalyst. Because of its diverse range of applications in the synthesis of pharmaceutical APIs (active pharmaceutical ingredients), drug intermediates, and agrochemicals (insecticides, pesticides), the KC has garnered considerable attention from industry as well as academia [30–34]. Here, we have discussed the different types of synthetic strategies/methodologies of KC used in the synthesis of 5-A-TZD derivatives, including the use of organic catalysts and ionic liquids (ILs), heterogenous solid catalysts, inorganic catalysts, and bio-catalysts (**Figure 3**).

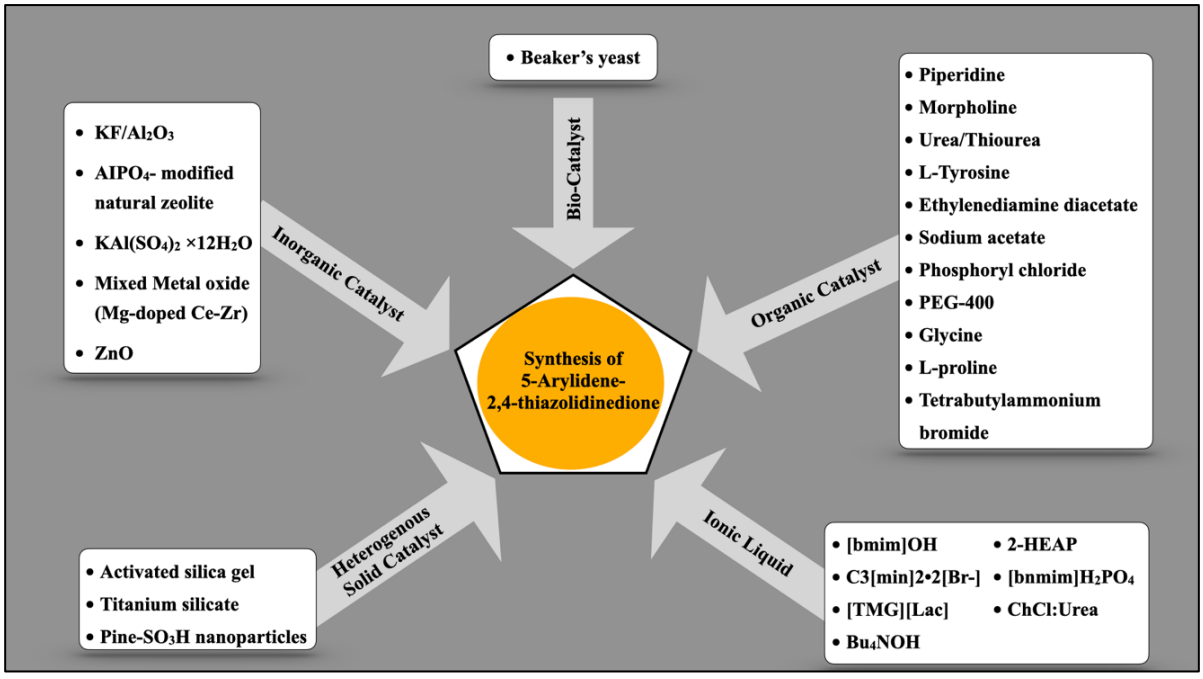

Figure 3: Multiple synthetic approaches of KC for 5-A-TZDs.

1.4. TZD-based hybrids as anti-diabetic agents:

Tien Cong and co-workers designed and synthesized eleven derivatives of TZD, which show dual action against selected strains of both bacteria and fungi along with inhibition of AG activity. The compounds were synthesized through reactions involving aromatic aldehydes, and they showed significant activity as AGIs, as they have IC_{50} values ranging from 7.5 ± 0.5 μM to 290.3 ± 1.9 μM and outperformed the reference drug, voglibose (IC_{50} = 355.8 ± 3.5 μM) regarding activity. Among all synthesized derivatives, the one with a chlorine substituent, **compound 1** (**Figure 4**) (4-chlorobenzylidene moiety), demonstrated the highest activity with an IC_{50} of 7.5 ± 0.5 μM, then **compound 2** (**Figure 4**) (piperonylidene moiety) demonstrated activity with an IC_{50} of 37.3 ± 1.8 μM, thus holding promise to be considered as effective inhibitors. Besides showing the anti-diabetic activity, these compounds were also screened for activity against bacteria and fungi, and their minimum inhibitory concentration (MIC) values lay between 6.25 and 100 μg/mL One of the most relevant findings of the research is the importance of substituents at the fifth position in the thiazolidine molecular structure in modulating biological activities, since compounds lacking this position were shown to be extremely inactive. Furthermore, fifth-position aromatic groups seemed necessary in case of activity, and halogenated compounds proved to be excellent. Docking studies further explained its binding interactions of these compounds with α-glucosidase (AG) enzyme, wherein **compound 1** (-8.1 kcal/mol) and **compound 2** (-9.7 kcal/mol) could establish strong hydrogen bonding and halogen bonding with significant residues and would contribute markedly to the stability of the enzyme-ligand complex [35].

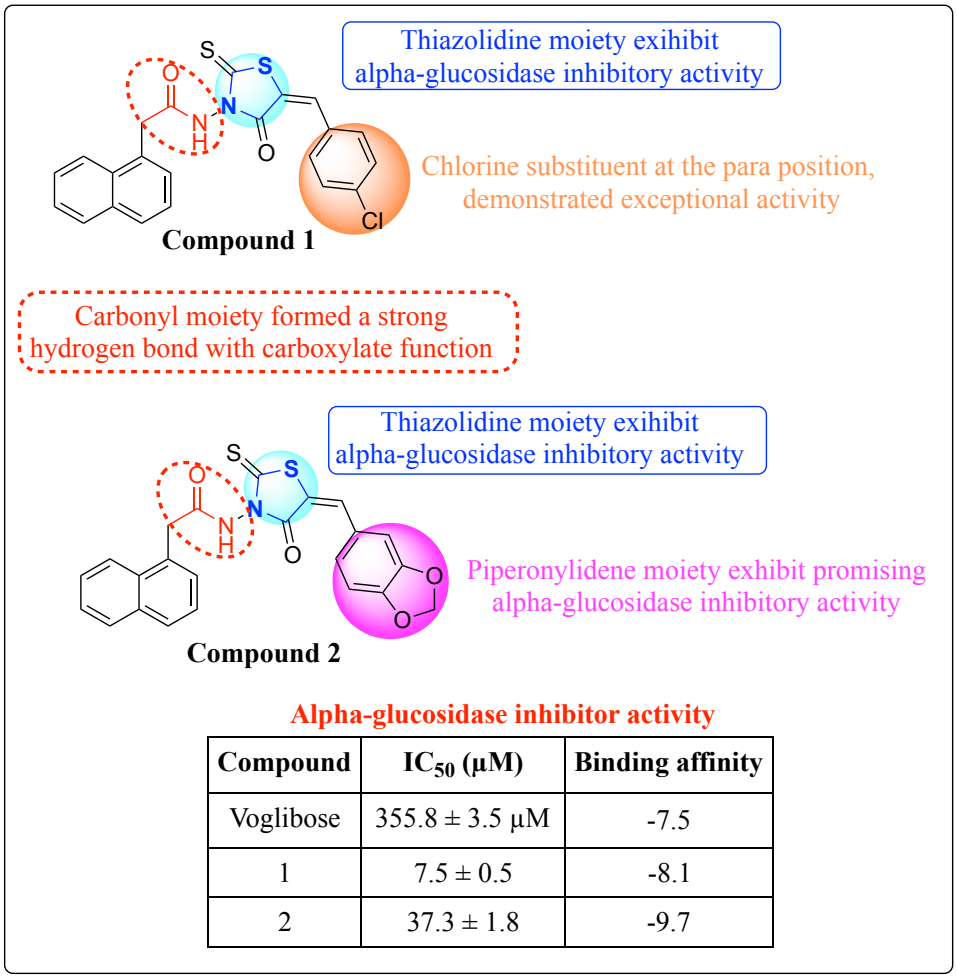

Alpha-glucosidase inhibitor activity

Compound	IC_{50} (µM)	Binding affinity
Voglibose	355.8 ± 3.5 µM	-7.5
1	7.5 ± 0.5	-8.1
2	37.3 ± 1.8	-9.7

Figure 4: SAR and structures of compounds 1 and 2 as potent AGIs.

Liang *et al.,* synthesized and evaluated novel coumarin-TZD hybrids as potential AGIs. The results of the inhibitory activities against AG showed that most of the hybrids (IC_{50}: 5.12 to 24.07 µM) inhibited the enzyme much more strongly as compared to acarbose (IC_{50}: 655.01 µM). Among the synthesized compounds, **compound 3** (**Figure 5**) showed the highest inhibitory activity in terms of non-competitive inhibition. Mechanisms and binding interactions with AG were determined using various approaches, such as fluorescence quenching, CD spectrum, 3D fluorescence and molecular docking simulations. As demonstrated, during binding to the hybrids, conformational changes in the enzyme resulted in inhibition. Furthermore, *in vitro* studies of **compound 3** (**Figure 5**) did not exhibit any notable cytotoxic effect against

HEK 293 cells, indicating that this compound may exhibit a safe profile for this compound. However, oral glucose tolerance test (OGTT) studies (*in vivo*) show that **compound 3** (**Figure 5**) significantly decreases postprandial blood glucose levels in mice, similar to that of acarbose. This affirms that hybridization strategies are important in drug design for potential therapeutic agents [36].

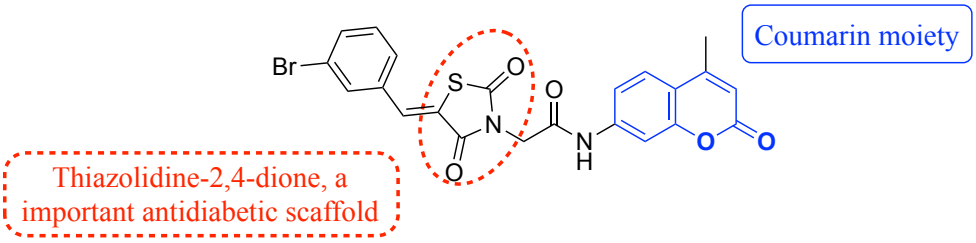

Compound 3

Alpha-glucosidase inhibitor activity

Compound	IC_{50} (µM)	Binding affinity
Acarbose	655.01 ± 52.54	-
3	5.12 ± 0.48	-6.70

Figure 5: SAR and structures of compound 3 as potent AGI.

Sharfuddin and his colleagues synthesized TZD-naphthalene analogues against pancreatic α-amylase (PAA) and intestinal α-glucosidase (IAG) enzymes. *In vitro* inhibition assay showed that several compounds exhibit significant activity, among which **compound 4** (**Figure 6**) is found to be the most potent with IC_{50} values of 4.488 ± 0.10 µM (PAA) and 2.145 ± 0.16 µM (IAG). Antioxidant activity was tested on DPPH assay, in which again **compound 4** showed the highest radical scavenging effect (EC_{50} = 6.36 ± 0.03 µM). In addition, molecular docking studies further show that **compound 4** (**Figure 6**) exhibited high binding affinities (−11.1 kcal/mol and −10.7 kcal/mol, respectively) through hydrogen bonding, pi–pi stacking, and hydrophobic interactions with a few key residues. MM-GBSA showed that **compound 4** (**Figure 6**)

was superior to acarbose in ΔGbind values, thus attesting to such strong and stable interactions. ADMET profiling using SwissADME and OSIRIS tools supported favourable pharmacokinetic properties and low predicted toxicity. All compounds obeyed Lipinski's Rule of Five, which indicated high drug likeness [37].

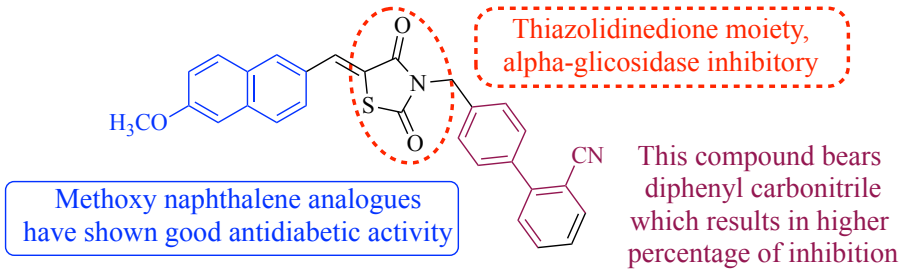

Compound 4

Pancreatic alpha-amylase and intestinal alpha-glucosidase inhibitor activity

Compound	IC_{50} (µM)	Binding affinity (kcal/mol)
Acarbose	8.245 ± 0. 16	-
4	4.488 ± 0.10; 2.145 ± 0.16	-11.1; -10.7

Figure 6: SAR and structures of compound 4 as potent AGI and AAI.

TZDs, a potential drug, are being widely used as a target for treating DM for their inhibition capacity against α-amylase (AA) and AG. Singh *et al.,* have synthesized nineteen derivatives of TZD and examined their inhibitory capacity. The *in vitro* evaluation of AG and AA proved **compound 5** (**Figure 7**) had potent inhibitory activity with IC_{50} of 10.33 ± 0.11 µM and 10.19 ± 0.25 µM, along with good antioxidant property (IC_{50} = 14.93 ± 0.65 µM). Docking scores of -7.5 to -10.7 kcal/mol against AA and a docking score of -7.4 to -10.3 kcal/mol against AG had been found. Through the *in vitro* inhibitory assay, it was seen that the activity of the compounds was greater in the case of AA instead of AG due to lesser micromolar inhibition. In PNAC-1 cells,

these substances also demonstrated significant antioxidant activity and reactive oxygen species inhibition [38].

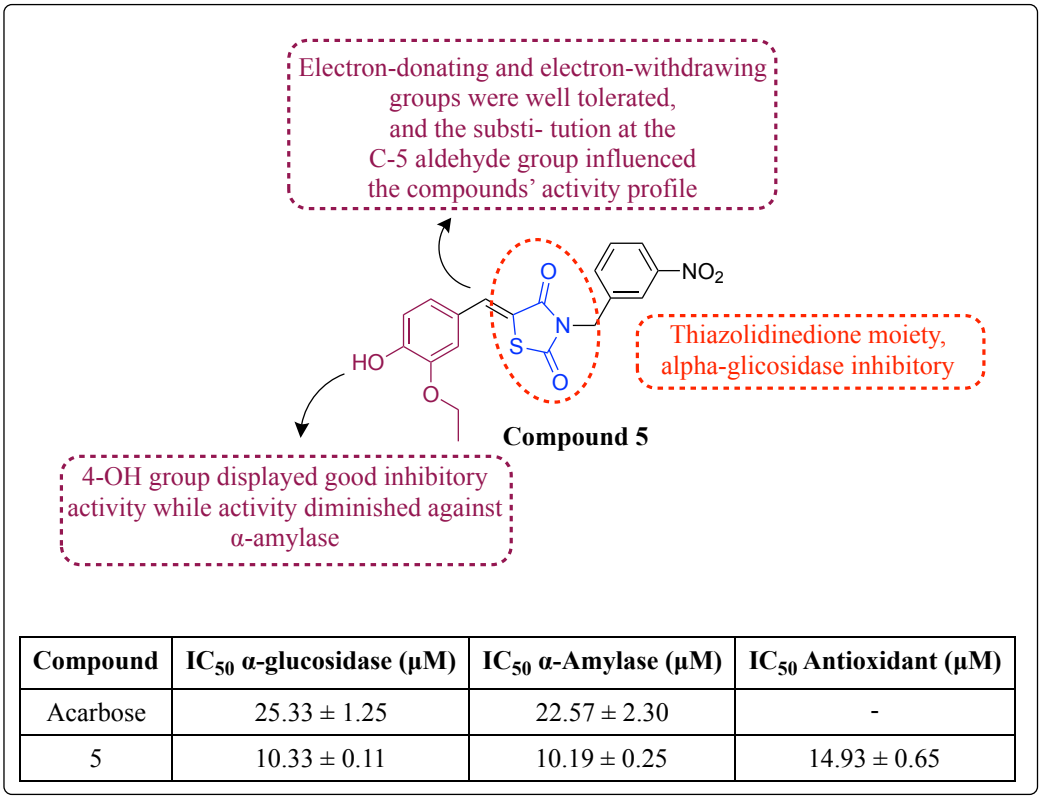

Compound	IC_{50} α-glucosidase (µM)	IC_{50} α-Amylase (µM)	IC_{50} Antioxidant (µM)
Acarbose	25.33 ± 1.25	22.57 ± 2.30	-
5	10.33 ± 0.11	10.19 ± 0.25	14.93 ± 0.65

Figure 7: SAR and structures of compound 5 as potent AGI, AAI, and antioxidant.

Gharge *et al.,* synthesized new 3,5-substituted TZD compounds using a three-step process, including Knoevenagel condensation. The synthesized compounds were thoroughly characterized using techniques like FTIR, HR-MS, ^{1}H NMR, and ^{13}C NMR. They have studied the anti-diabetic potential through both '*In vivo*' studies in Wistar rats and '*In vitro*' assays targeting 'AA', 'AG', and glucose uptake by yeast cells. From all the synthesized compounds, **compound 6** (**Figure 8**) demonstrated the most promising results among the tested compounds. Network pharmacology, molecular docking, and dynamic simulation studies indicated that **compound 6** (**Figure 8**) interacts with key targets like 'AA' and 'AG', modulating relevant signalling pathways ('AMY2A', 'GAA', 'PPARG', 'PIK3CA', 'PRKCB', 'INSR'). '*In vitro*', **compound 6**

(**Figure 8**) showed inhibitory activity against 'AA' (IC_{50} = 86.06 ± 1.1 µM) and 'AG' (IC_{50} = 74.97 ± 1.23 µM), and enhanced glucose uptake (58.23 ± 0.13 %). '*In vivo*', **compound 6** (**Figure 8**) significantly reduced blood glucose levels (114 ± 1.17 mg/dL), comparable to the standard drug pioglitazone. The study concludes that modified TZDs, particularly **compound 6** (**Figure 8**), are promising candidates for new anti-diabetic agents [39].

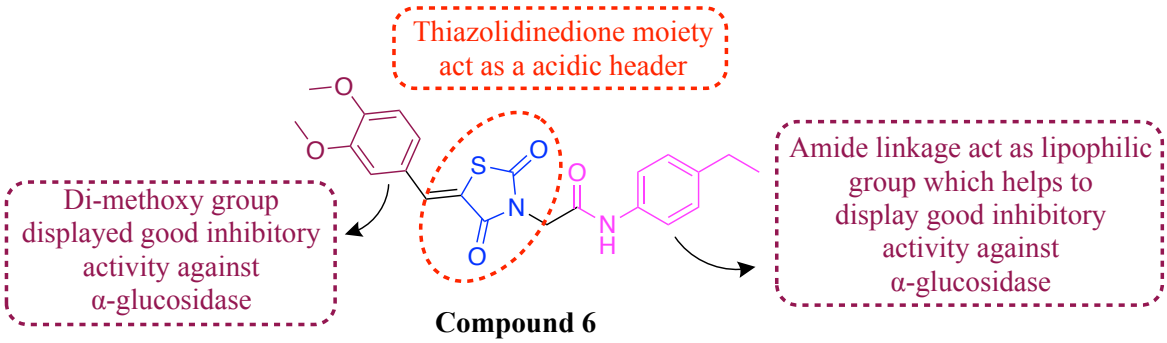

Compound	IC_{50} α-glucosidase (µM)	IC_{50} α-Amylase (µM)
Acarbose	26.89 ± 3.12	26.89 ± 3.12
6	86.06 ± 0.1.1	74.97 ± 1.0

Figure 8: SAR and structures of compound 6 as potent AGI and AAI.

Some novel benzenesulfonamide-TZD hybrids were synthesized by Gamal *et al.,* to target the enzymes AG. The design strategy of **compound 7** as a potent AGI is depicted in **Figure 9**. The results obtained from the biological evaluation indicated that **compound 7** (**Figure 10**) demonstrated the most potent inhibitory activity with IC_{50} values of 0.3456 ± 0.01 µM. Molecular docking studies explained the binding interactions of the active **compound 7** with a binding affinity value of -10.7 kcal/mol. Extended MM-GBSA and molecular dynamic simulations also indicated the potential of **compound 7** (**Figure 10**). Furthermore, an *in vivo* study of OGTT shows that **compound 7** (**Figure 10**) significantly lowers blood glucose levels in diabetic mice

compared to acarbose. Together, these results proved that this compound is efficient in controlling T2DM [40].

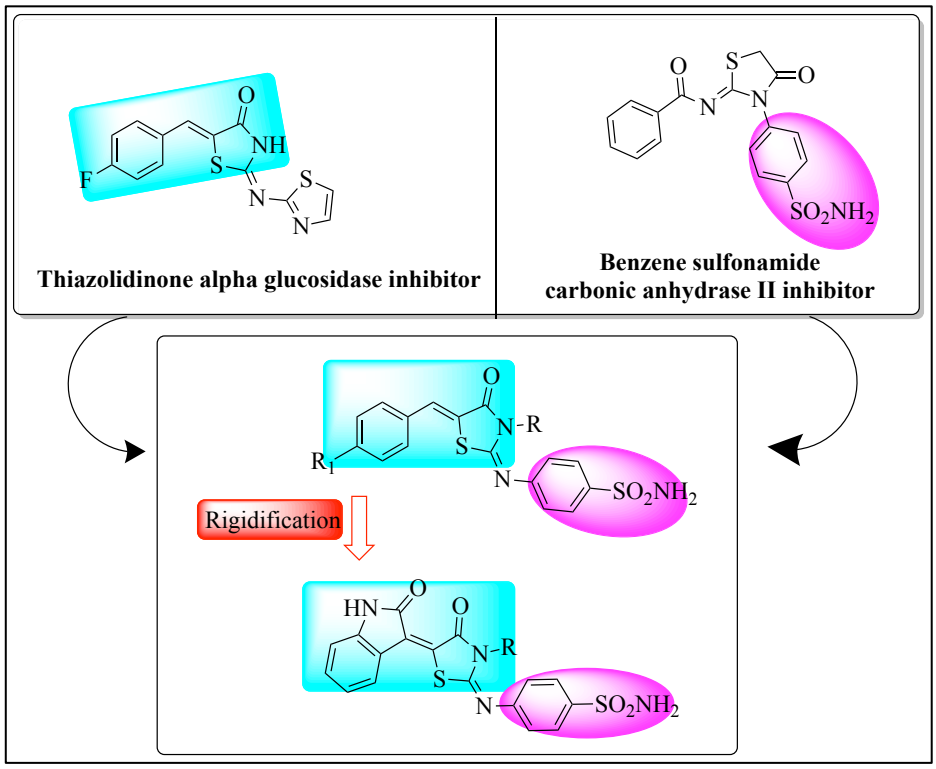

Figure 9: Design strategy of compound 7 as potent AGI.

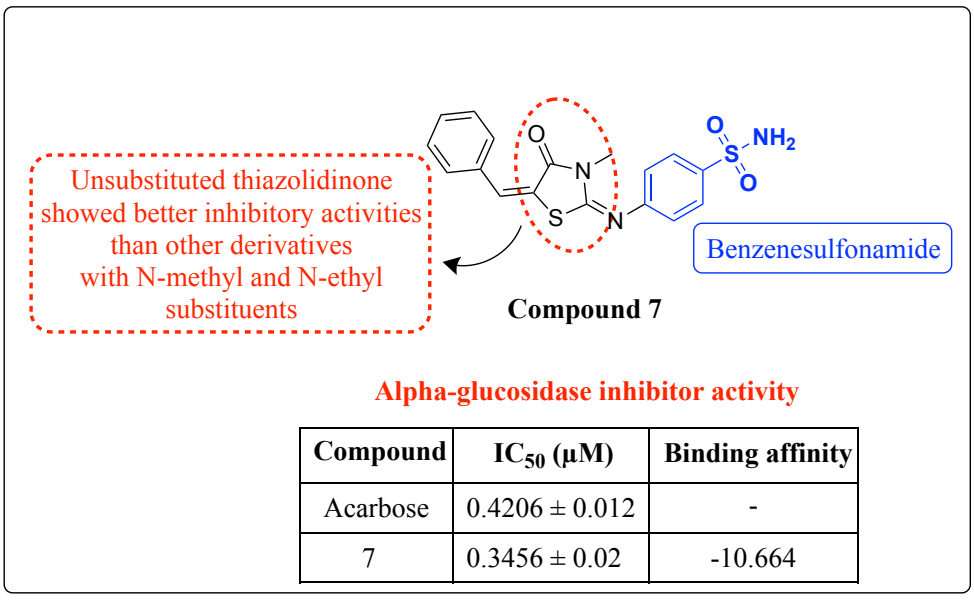

Compound	IC_{50} (µM)	Binding affinity
Acarbose	0.4206 ± 0.012	-
7	0.3456 ± 0.02	-10.664

Figure 10: SAR and structures of compound 7 as potent AGI.

A series of twenty-six indole derivatives containing TZD were synthesized to develop potential AGIs with anti-diabetic activity by Hu *et al.* Hu *et al.,*'s approach to rational

drug design is the combination of indole and TZD moieties employing hybridization chemistry. Not only does this approach exploit the pharmacological advantage of each basic unit, but it may also lead to the discovery of new compounds having a better level of efficacy and different activity profile compared to that of the parent structures (**Figure 11**). The most significant inhibitory capacity had been shown by **compound 8** (**Figure 12**), whose IC_{50} values lie in the range of 2.35 ± 0.11 to 24.36 ± 0.79 µM. The mechanism of inhibition was also measured through 3D fluorescence spectra, molecular docking and CD spectra. *In vivo* anti-diabetic experiments showed that oral administration of **compound 8** (**Figure 12**) suppressed fasting blood glucose levels and improved glucose tolerance and dyslipidemia in diabetic mice [41].

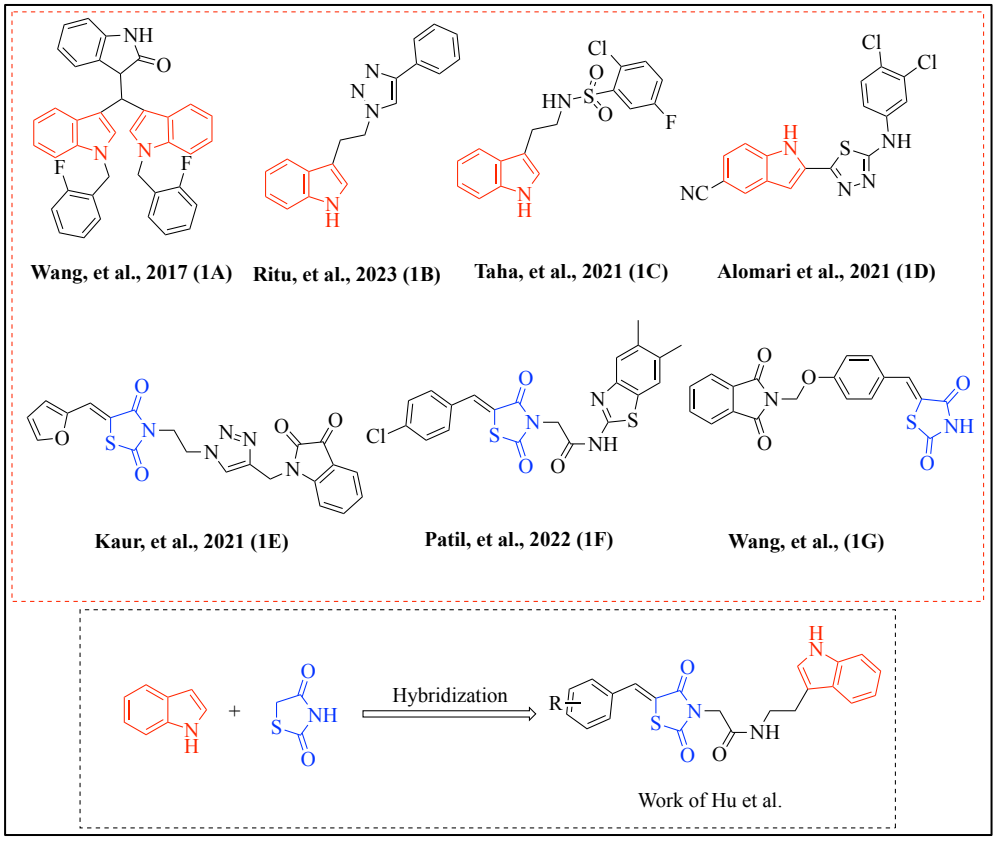

Figure 11: Design strategy of compound 8 as potent AGI.

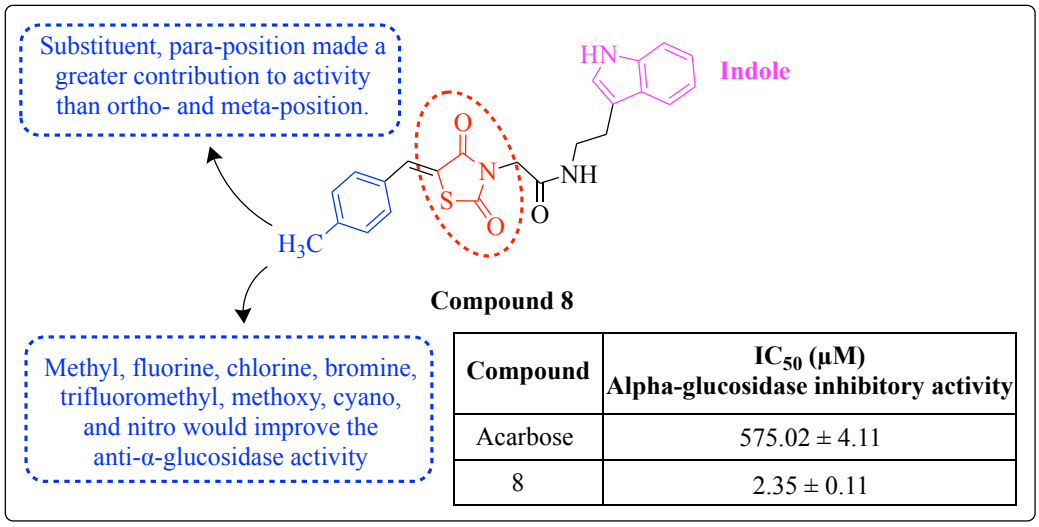

Compound	IC_{50} (μM) Alpha-glucosidase inhibitory activity
Acarbose	575.02 ± 4.11
8	2.35 ± 0.11

Figure 12: SAR and structures of compound 8 as potent AGI.

A series of TZD hybrids was synthesized for the inhibitory action of AG by Mengyue and co-workers. The strategy, a rationale hybridization of the TZD pharmacophore to 1,3,4-thiadiazole tolerating frameworks, led to new compounds which might take advantage of the synergistic or additive effect of the two pharmacophores. This approach not only benefits from previous successes of the field but also it permits additional structural variability at the R-positions for fine-tuning of biological activity and druglike properties toward the newly synthesized hybrids (**Figure 13**). All the compounds showed greater inhibitory action as compared to reference compound acarbose, with the range of IC_{50} values of 0.52 ± 0.06 to 7.76 ± 0.06 μM and **compound 9 (Figure 14)** emerged as the most potent inhibitor, with 1258-fold more power than acarbose. The AG inhibition assay also showed that compounds containing substituents at para-position had greater inhibition capacity than compounds containing substituents at meta- and ortho-position. **Compound 9 (Figure 14)** took a 'U-shaped' conformation in the active pocket of AG enzyme as evaluated from binding reactions of the molecular docking process, and this compound also showed zero cell toxicity against LO2 cells.

The study also included that oral administration of **compound 9 (Figure 14)** lowered the blood glucose levels in mice and increased the glucose tolerance [42].

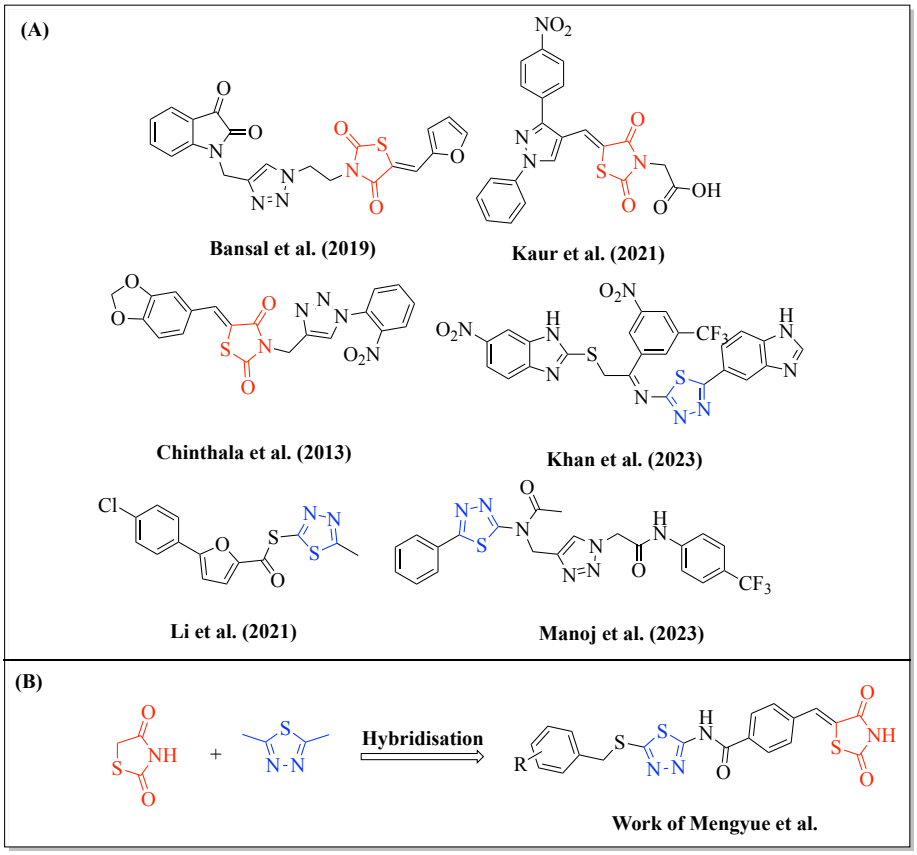

Figure 13: Design strategy of compound 9 as potent AGI.

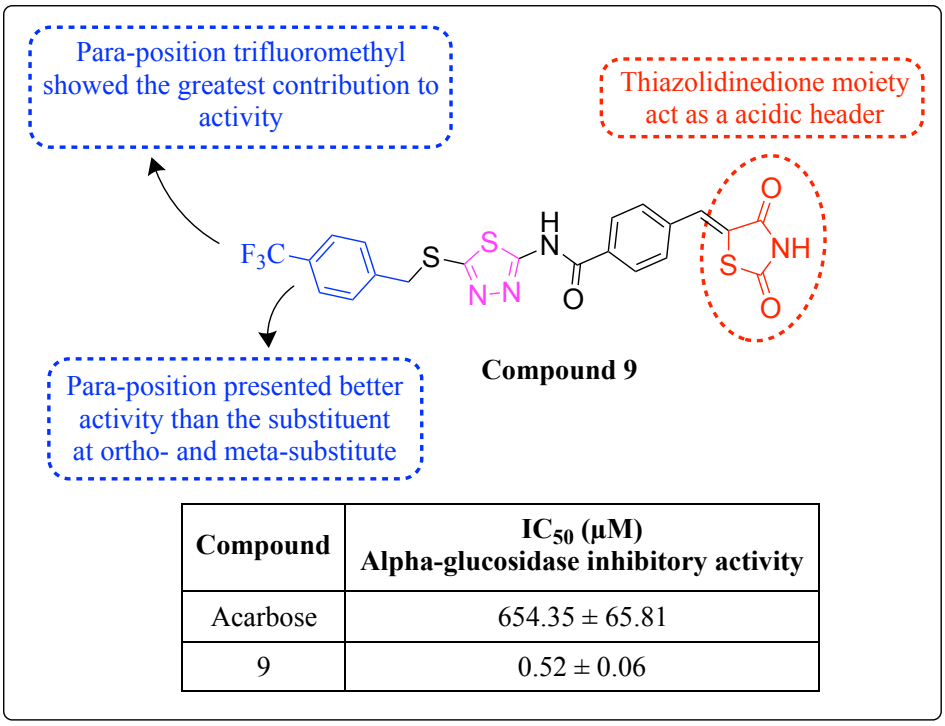

Compound	IC_{50} (µM) Alpha-glucosidase inhibitory activity
Acarbose	654.35 ± 65.81
9	0.52 ± 0.06

Figure 14: SAR and structures of compound 9 as potent AGI.

Singh *et al.,* have synthesized twelve 3,5-disubstituted-TZD hybrids, where they used solution phase chemistry. In their previous research, through antagonism of AG and AA, they evaluated the anti-diabetic potential of 3,5-disubstituted-TZD. The *in vitro* evaluation showed that all the molecules had moderate to potent inhibition activity, but **compound 10** (**Figure 15**) emerged as a significantly promising candidate (5.15 ± 0.0017 µM for AG, 17.10 ± 0.015 µM for AA). **Compound 10** (**Figure 15**) displayed an acceptable fit into the active pocket of both enzymes. From the *in vitro* cytotoxicity assay, it was found that the molecules are without any toxicity. The *in vivo* evaluation of **compound 10** (**Figure 15**) showed remarkable positive changes in Wistar rats, including lower blood glucose, stress, body weight, etc. In terms of ROS inhibitor, **compound 10** (**Figure 15**) was also found potent [43].

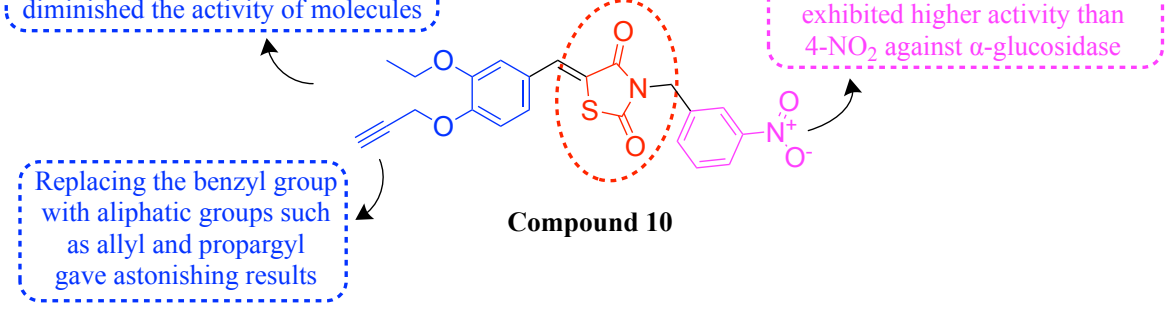

Compound	IC_{50} (µM) Alpha-glucosidase inhibitory activity	IC_{50} (µM) Alpha-amylase inhibitory activity
Acarbose	25.33 ± 1.25	22.57 ± 2.30
10	5.15 ± 0.017	9.2 ± 0.092

Figure 15: SAR and structures of compound 10 as potent AGI and AAI.

Shah *et al.,* in their previous work examined a hybrid of vanillin-TZD as a target inhibitor for AG, AA, PTP-1B, and DPP-4. And in their present research, they developed and synthesized 3-(((1S,3S)-3-((R)-hydroxy(4-(trifluoromethyl) phenyl)

methyl)-4 oxocyclohexyl) methyl) pentane-2,4-dione (S,S, R-D, 4) compound to evaluate its anti-diabetic actions. The study seeks to enhance an initial lead chemical for diabetes therapy by concurrently targeting various pathways. The initial thiazolidine-dione-based therapeutic candidates exhibit a robust binding affinity for DPP-4, PTP-1B, AA, and AG. The amalgamation of central 5-benzylidineTZD, East-side cyclic amines, and West-side hydrophilic hydroxyl groups of gallic acid results in significant *in vitro* inhibitory potencies. From all the synthesized compounds, a few compounds were found to be multipotent compounds. **Compound 11** and **12** (**Figure 16**) with values 0.217 ± 0.016 µM, 0.190 ± 0.019, 0.09 ± 0.011, 0.129 ± 0.012 and 0.185 ± 0.014, 0.241 ± 0.010, 0.036 ± 0.004, 0.042 ± 0.10, respectively, resulted out to be potent multi-target (for AGIs, AAIs, DPP-4, and PTP1B) inhibitors. In the study, the consequences of expanding the West-side of 5-benzylidine core by including amide of gallic acid were also explored [44].

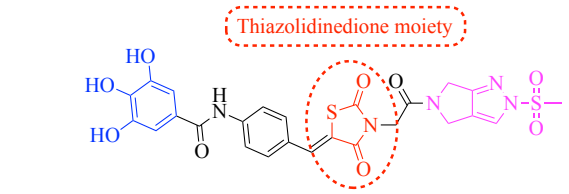

Compound 11

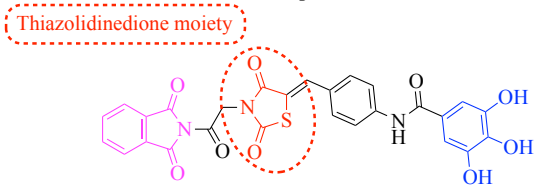

Compound 12

Compound	IC_{50} (µM) Alpha-glucosidase inhibitory activity	IC_{50} (µM) Alpha-amylase inhibitory activity	IC_{50} (µM) DPP-4	IC_{50} (µM) PTP1B
Acarbose	9.78 ± 1.03	10.32 ± 1.03	0.008 ± 1.03	2.49 ± 1.03
11	0.185 ± 0.014	0.241 ± 0.010	0.036 ± 0.004	0.042 ± 0.10
12	0.217 ± 0.016	0.190 ± 0.019	0.09 ± 0.011	0.129 ± 0.012

Figure 16: Structures of compounds 11 and 12 as potent AGIs, AAIs, DPP-4, and PTP1B inhibitors.

Thiazolidine-4-one, which is a heterocyclic compound along with its derivatives, is a pivotal compound in terms of treatment of DM. Fuorenone–thiazolidine-4-one scaffolds were developed by Doddagaddavalli *et al.,* and their structures were confirmed by FTIR, ^{1}H NMR, ^{13}C NMR, and mass spectral data. And its capacity to scavenge DPPH and inhibit AG was assessed. It was revealed that **compound 13** (**Figure 17**), which had hydroxyl functional groups at the para and meta positions, had greater AG inhibition (IC_{50} value of 114.58 ± 1.8 µM), whereas compounds attached with halogen groups showed mild inhibition action. With an IC_{50} value of 81.27 ± 1.3 µM, **compound 13** (**Figure 17**) demonstrated encouraging DPPH scavenging activity. On the other hand, compounds containing substitutions at ortho and para positions have been found to have greater antioxidant properties. Interaction of HAS (Human Serum Albumin) and ct-DNA with derivative **compound 13** (**Figure 17**) demonstrated stronger inhibition capacity, which was found through fluorescence spectroscopy. Compounds obeyed Lipinski's rule of fifth, suggesting that **compound 13** (**Figure 17**) could be a lead compound for the discovery of new anti-diabetic drugs [45].

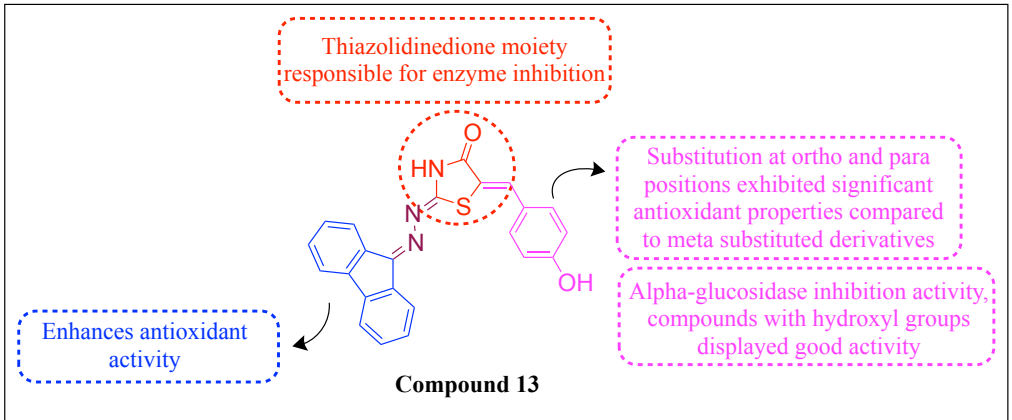

Compound	IC_{50} (µM) Alpha-glucosidase inhibitory activity	IC_{50} (µM) Antioxidant activity
Acarbose / Gallic acid	115.49 ± 2.2	117.92 ± 2.8
13	114.58 ± 1.8	81.27 ± 1.3

Figure 17: SAR and structures of compound 13 as potent AGIs and AAIs.

In recent times, some chromone derivatives have been found they have AG inhibitory activity (**Figure 18**). Zheng *et al.,* synthesized chromone TZD derivatives and examined for their AG inhibitory action and mechanisms. In the evaluation of AG inhibition, it had been found that synthetic derivatives had better AG inhibition where the value of IC_{50} lies in the range from 2.40 ± 0.11 to 5.66 ± 0.15 µM. Among all the compounds, **compound 14** (**Figure 19**) had shown a significant inhibition capacity, which is nearly 267 times that of the positive control acarbose. The molecular docking process demonstrated that **compound 14** (**Figure 19**) can bind to the active pocket of AG. CD spectra and 3D fluorescence spectra of the study also revealed that **compound 14** (**Figure 19**) altered AG's institutional alterations. Furthermore, *in vitro* cytotoxicity revealed that **compound 14** had no definite effect on the viability of L-02 cells [46].

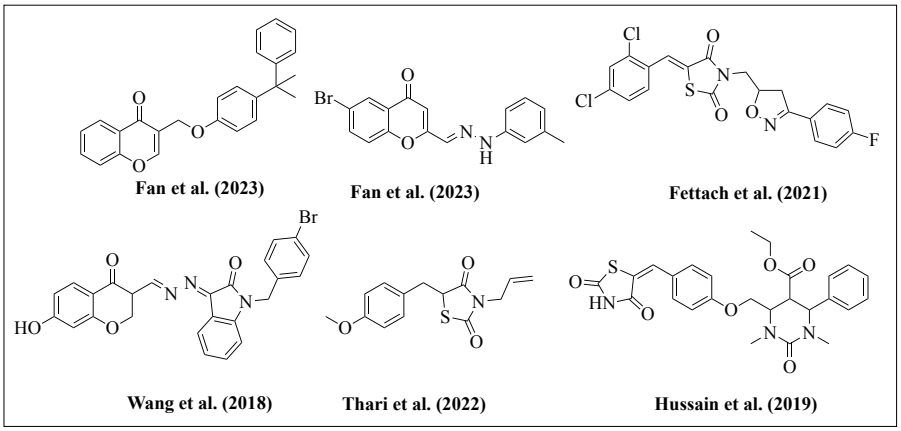

Figure 18: Previously reported compounds as potent AGIs and AAIs.

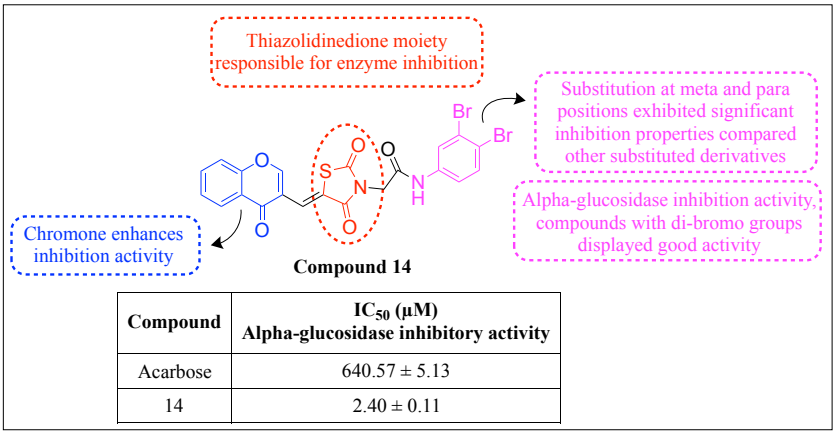

Compound	IC_{50} (µM) Alpha-glucosidase inhibitory activity
Acarbose	640.57 ± 5.13
14	2.40 ± 0.11

Figure 19: SAR and structures of compound 14 as potent AGIs.

Khan *et al.,* synthesized and evaluated thiazole-based TZD derivatives against AG and AA enzymes. By using different spectroscopic techniques, the inhibitory activity of the derivatives was examined, where they showed good to moderate AG and AA inhibition. The IC_{50} values for AG were in the range of 2.40 ± 0.10 to 31.40 ± 0.90 µM, and the IC_{50} value for AA was in the range of 1.80 ± 0.05 to 27.60 ± 0.80 µM. Among those compounds, **compound 15** (**Figure 20**), which bears *meta*-methoxy and *para*-hydroxyl substitutions, showed significant potency against both the enzymes. **Compound 15** (**Figure 20**) (with thiazole and fluorine moieties) emerged as the most potent inhibitor of both AG and AA with IC_{50} values of 2.40 ± 0.10 and 1.80 ± 0.05 µM [47].

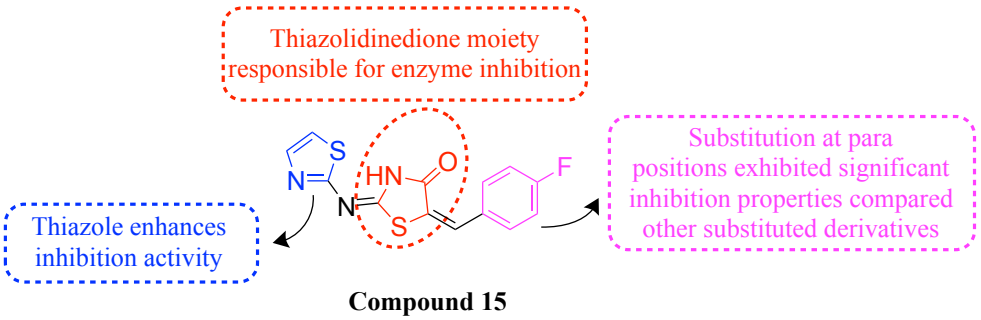

Compound 15

Compound	IC_{50} (µM) Alpha-glucosidase inhibitory activity	IC_{50} (µM) Alpha-amylase inhibitory activity
Acarbose	9.80 ± 0.20	10.30 ± 0.20
15	2.40 ± 0.11	1.80 ± 0.05

Figure 20: SAR and structures of compound 15 as potent AGIs and AAIs.

Khan *et al.,* synthesized a total of twenty TZD-based indole derivatives through different steps and evaluated the derivatives for AG and AA inhibitory activity. The design strategy of **compound 16** as potent AGIs and AAIs is depicted in **Figure 21**. While evaluated, the indole derivatives demonstrated a range of inhibitory potential from IC_{50} = 1.50 ± 0.05 to 29.60 ± 0.40 µM. Among all the derivatives, **compound 16** (**Figure 22**) resulted in better and remarkable inhibition on AA and AG performance,

which is due to its 2-fluoro groups (IC_{50} = 1.50 ± 0.05 µM for AA and 2.40 ± 0.10 µM for AG). While conducting the research, it has been seen that the derivatives with -CL with hydroxyl group or Hydroxyl group resulted as powerful antagonists of the enzymes AG and AA. Fluro-substituted derivative five was discovered to connect uniquely with AA at distances ranging from 4.50 to 6.85 A. Additionally, SAR and interaction of binding were evaluated through molecular docking process [48].

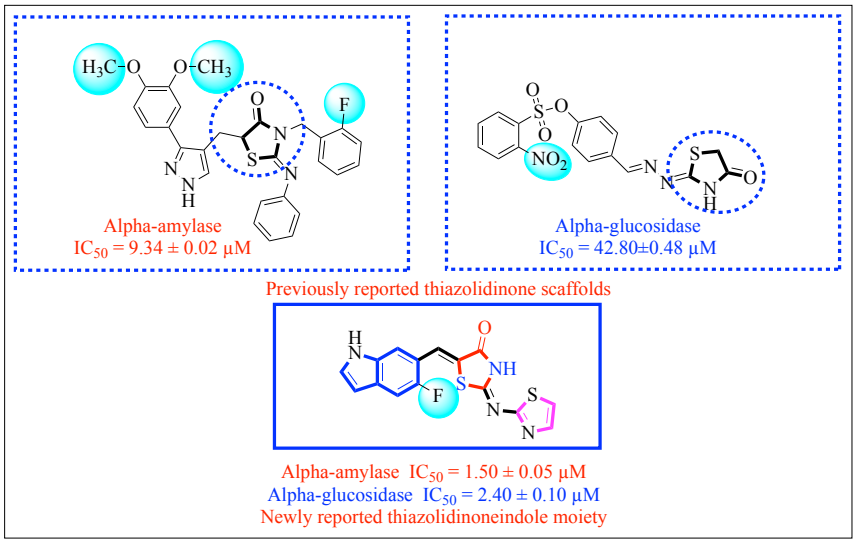

Figure 21: Design strategy of compound 16 as potent AGIs and AAIs.

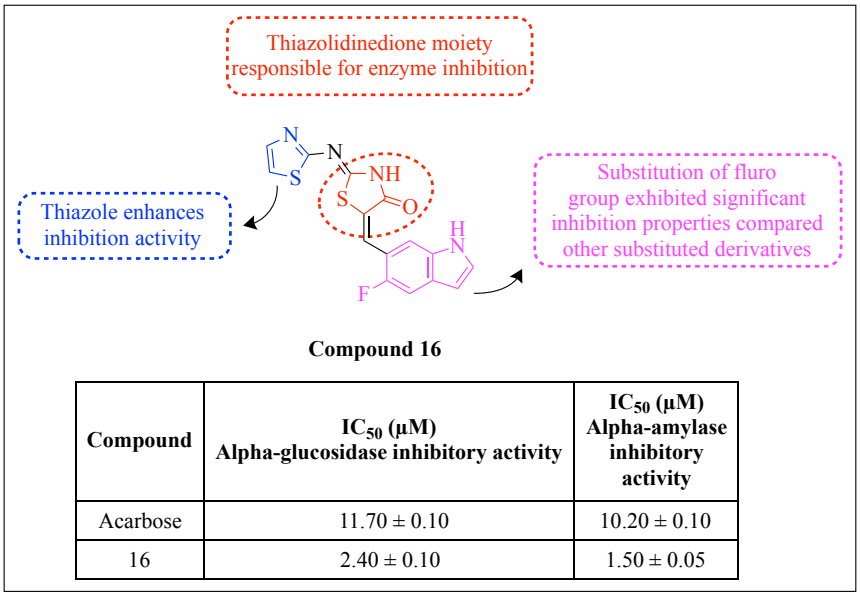

Compound	IC_{50} (µM) Alpha-glucosidase inhibitory activity	IC_{50} (µM) Alpha-amylase inhibitory activity
Acarbose	11.70 ± 0.10	10.20 ± 0.10
16	2.40 ± 0.10	1.50 ± 0.05

Figure 22: SAR and structures of compound 16 as potent AGIs and AAIs.

Khan *et al.,* designed and synthesized TZD-based benzothiazole through several stepwise reactions, and after that, their biological significance against AG and AA was

also evaluated. The design strategy of **compound 17** as potent AGIs and AAIs is depicted in **Figure 23**. Almost all the derivatives, **compound 17** (**Figure 24**), showed significant action against those enzymes, where IC_{50} against AA was 2.10 ± 0.70 µM and against AG it was 3.20 ±0.05 µM. **Compound 17** (**Figure 24**)showed remarkable results due to the phenyl ring linked with it, where other derivatives also proved to contain better folds than other compounds. Other than **compound 17** (**Figure 24**), there is a decreased activity due to the chlorine group. **Compound 17,** comprising exceptional activities against both AA and AG, revealed diverse interactions at various stages, which further indicates the site of activity in the molecule and both enzymes [49].

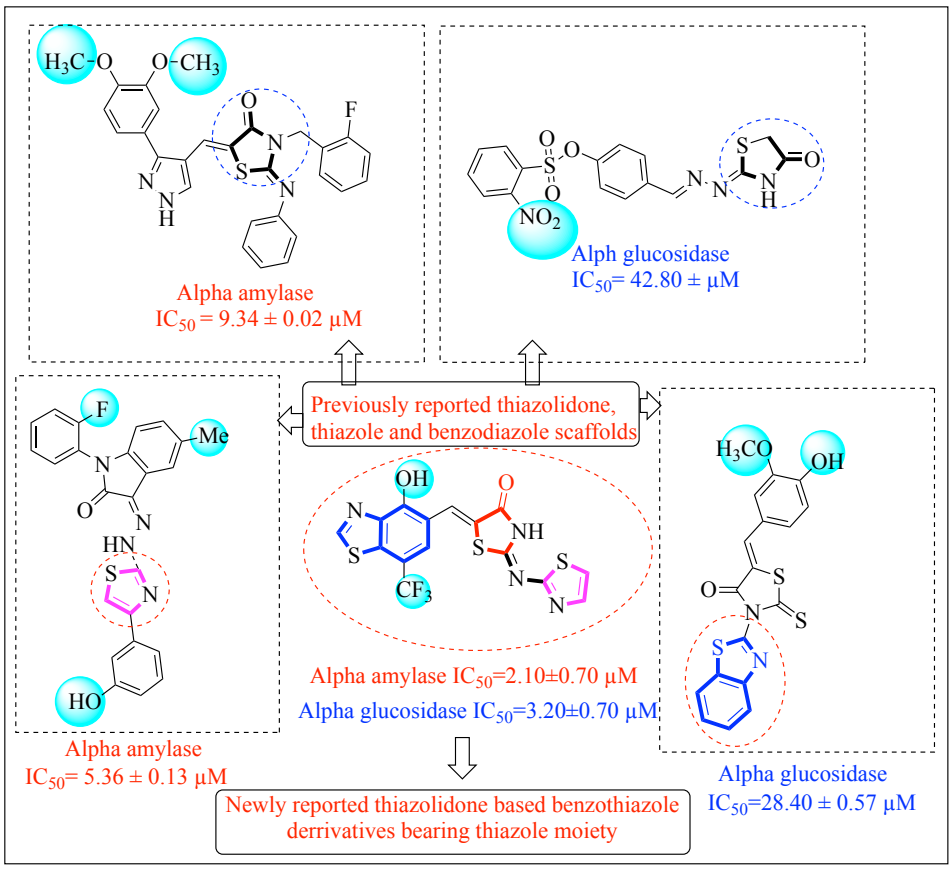

Figure 23: Design strategy of compound 17 as potent AGIs and AAIs.

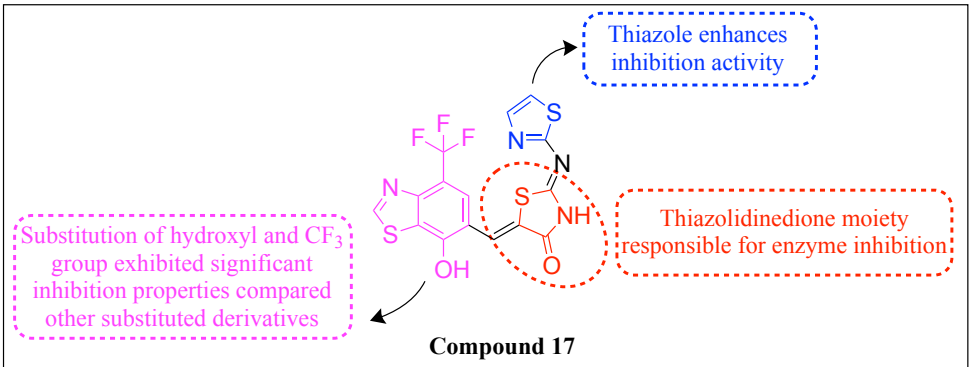

Compound	IC_{50} (µM) Alpha-glucosidase inhibitory activity	IC_{50} (µM) Alpha-amylase inhibitory activity
Acarbose	10.70 ± 0.10	9.10 ± 0.10
17	3.20 ± 0.70	2.10 ± 0.70

Figure 24: SAR and structures of compound 17 as potent AGI and AAI.

A series of N-substituted 5-benzylidene-2,4-TZD derivatives as potential AGIs were synthesized by Vijay and his researchers. Design strategy of compounds 18, 19, and 20 as potent AGIs is shown in **Figure 25**. The compounds were further screened *in silico* using SwissADME and OSIRIS tools to predict drug-likeness, solubility, lipophilicity, polar surface area (PSA), and bioavailability. All candidates exhibited properties consistent with oral drug absorption and low toxicity. *In vitro* AG inhibition assay results indicated that several derivatives exhibited IC_{50} values < 65 µM, outperformed acarbose (IC_{50} = 67.06 µM). The most potent inhibitor was thus **compound 18** (IC_{50} = 29.91 µM; **Figure 26**), followed by **compound 19** (36.52 µM; **Figure 26**) and **compound 20** (39.19 µM; **Figure 26**). Structural elucidation indicated that chloro substitution on the phenyl and benzothiazole rings and methyl substitution are responsible for this potency. Docking scores ranged from −7.9 to −9.3 kcal/mol, indicating strong binding affinities. Key interactions were observed with crucial residues such as Asp232, Asn237, Ala234, and Asp568, which are essential for enzyme inhibition. For instance, **compound 18** formed hydrogen bonds with Asp232, Ser497,

and Ser505 and adopted a U-shaped conformation at the active site, which supports their research [50].

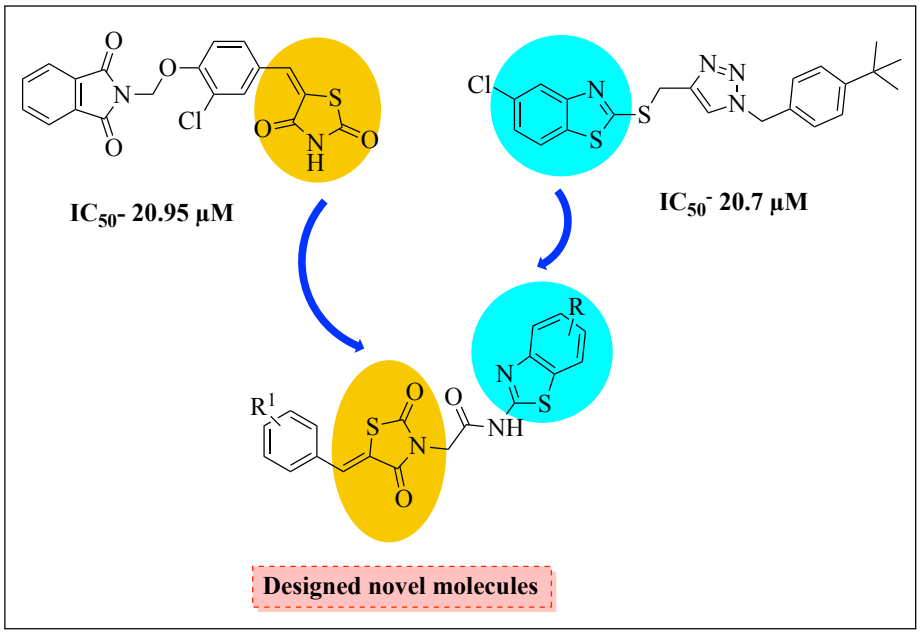

Figure 25: Design strategy of compounds 18, 19, and 20 as potent AGIs.

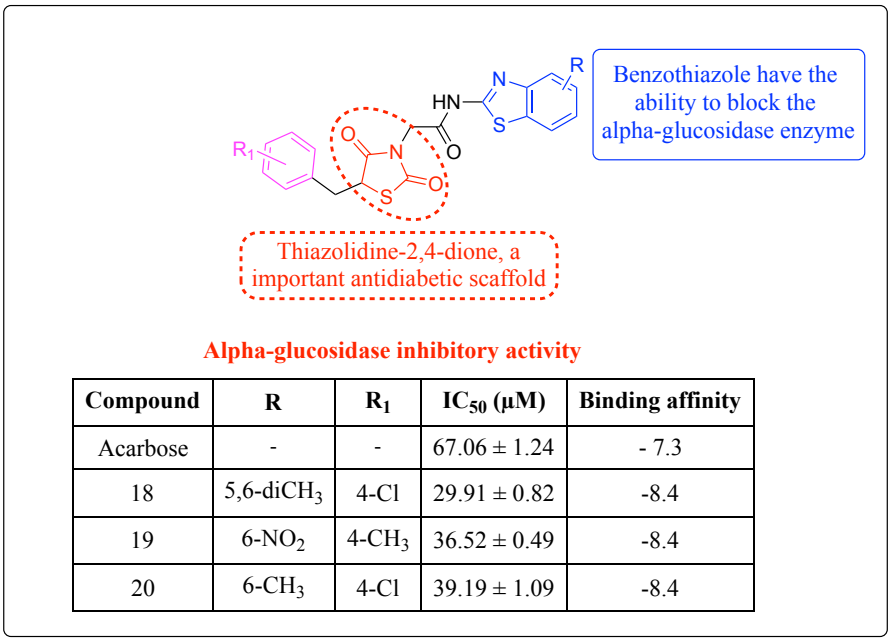

Alpha-glucosidase inhibitory activity

Compound	R	R_1	IC_{50} (µM)	Binding affinity
Acarbose	-	-	67.06 ± 1.24	- 7.3
18	5,6-diCH_3	4-Cl	29.91 ± 0.82	-8.4
19	6-NO_2	4-CH_3	36.52 ± 0.49	-8.4
20	6-CH_3	4-Cl	39.19 ± 1.09	-8.4

Figure 26: SAR and structures of compounds 18, 19, and 20 as potent AGIs.

Ullah *et al.,* synthesized and evaluated sixteen benzohydrazide-based imines and sixteen thiazolidine-4-one analogues against AG and AA as dual inhibitors. The

inhibition of AG was significant *in vitro* for the imine series, with **compound 21** exhibiting an IC_{50} of 5.60 ± 0.30 µM, followed by **compound 22** (IC_{50} = 7.30 ± 0.10 µM; **Figure 27**). The efficacy of these inhibitors was enhanced by the substitution of hydroxyl groups on the aryl rings, facilitating hydrogen bonding with the enzyme's active site. Similarly, AA inhibition was evaluated against the thiazolidine-4-one series with **compound 23** being the most active (IC_{50} = 0.40 ± 0.05 µM; **Figure 27**). The SAR suggested that activities were enhanced by such electron-donating groups as –O and $–OCH_3$ in concert through hydrogen bonding and polar interactions, while activity was diminished by bulky electron-withdrawing substituents. In molecular docking findings, **compound 23** showed the most favourable binding profile with a docking score of -14.23 kcal/mol while forming multiple hydrogen bonds and π–π interactions with the key active site residues: Trp59, Asp197, Asp300 and Arg195. The kinetic analysis of AG confirmed competitive inhibition and the applicability of Michaelis-Menten kinetics to all tested drugs. The enzyme kinetics and docking data lend support to a mechanistic basis for their inhibition, and therefore, **compound 23** exhibited the most potent activity [51].

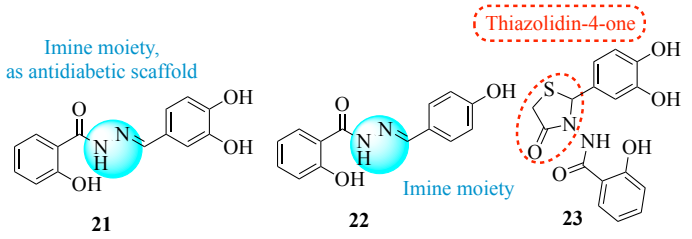

Alpha-glucosidase and alpha-amylase inhibitory activity

Compound	IC_{50} (µM)	Binding affinity (kcal/mol)
Acarbose alpha-glucosidase	38.45 ± 0.80	-11.7209
21 (alpha-glucosidase)	5.60 ± 0.30	-
22 (alpha-glucosidase)	7.30 ± 0.10	-10.6412
Acarbose alpha-amylase	0.91 ± 0.20	-
23 (alpha-amylase)	0.40 ± 0.05	-14.23

Figure 27: SAR and structures of compounds 21, 22, and 23 as potent AGIs and AAIs.

A series of novel TZD derivatives were synthesized via microwave-assisted Knoevenagel by Saad and co-workers. The synthesized compounds were evaluated for their inhibitory activity against AG and AA enzymes. The IC_{50} values of most of the compounds ranged between 43.85 and 380.10 µM for AG and 18.19 to 208.10 µM for AA. Nonetheless, **compound 24** (**Figure 28**) revealed itself as the most effective dual inhibitor, demonstrating IC_{50} values of 43.85 ± 1.06 µM (AG) and 18.19 ± 0.11 µM (AA). The bioactivity of the parent compounds was improved significantly by N-allylation, suggesting that the allyl moiety takes part in the enzyme binding. Docking analysis pinpoints residues involved in hydrogen bond formation and hydrophobic interactions. Moreover, extensive *in silico* studies showed the dual target capability of this compound towards T2DM [52].

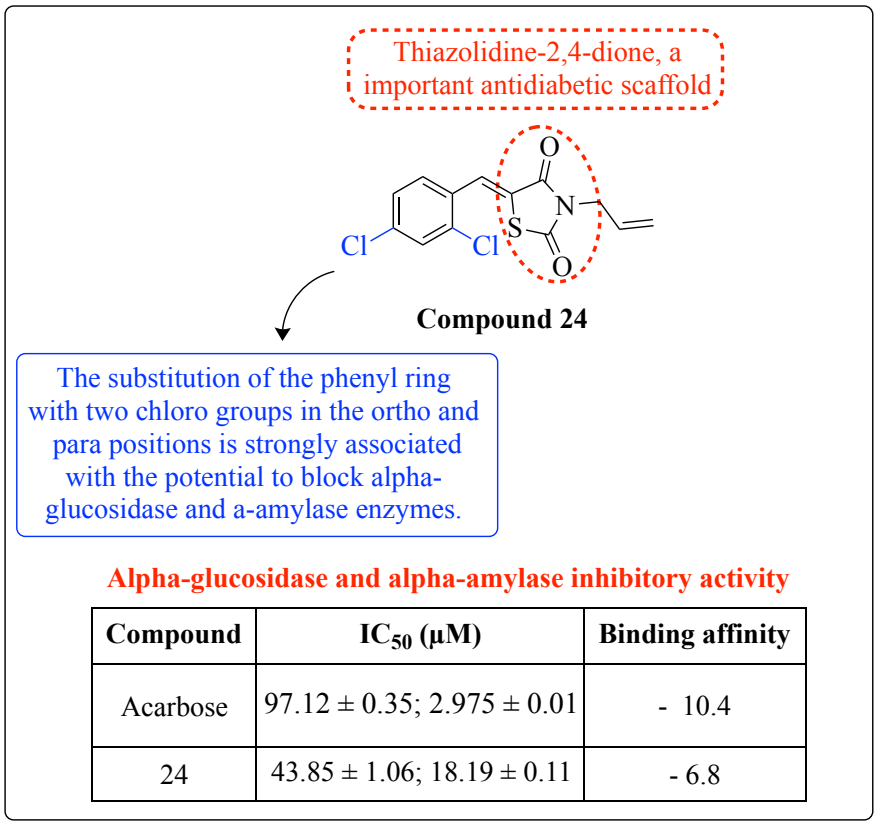

Alpha-glucosidase and alpha-amylase inhibitory activity

Compound	IC_{50} (µM)	Binding affinity
Acarbose	97.12 ± 0.35; 2.975 ± 0.01	- 10.4
24	43.85 ± 1.06; 18.19 ± 0.11	- 6.8

Figure 28: SAR and structures of compound 24 as potent AGI.

Novel diarylthiazolidin-4-one derivatives were synthesized and screened for their *in vitro* activity against AG by Ebrahim Saeedian and colleagues. All of the synthesized compounds were found to inhibit AG enzyme activity with an IC_{50} value in the range of 90-704 µM, better than the standard drug acarbose (IC_{50} = 750 µM). The most potent compound that was studied further was **compound 25** (90 µM; **Figure 29**). Enzyme kinetics study revealed that **compound 25** (**Figure 29**) acts as a competitive inhibitor with a Ki value of 87 µM. Molecular docking studies corroborated the experimental data, showing that the lead **compound 25** interacts strongly with the enzyme active site, involving key residues such as THR310, ARG315, TYR158, ASP307, etc., by hydrogen bonding, π-π stacking, π-anion, and hydrophobic interactions. This indicates it as a potential inhibitor [53].

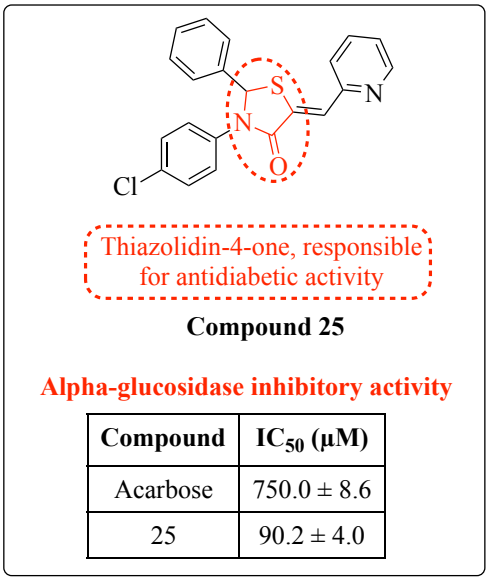

Compound	IC_{50} (µM)
Acarbose	750.0 ± 8.6
25	90.2 ± 4.0

Figure 29: SAR and structures of compound 25 as potent AGI.

Thari *et al.,* designed and developed two TZD derivatives and evaluated them for AGIs and AAIs. The heterocyclic compound TZD contains oxygen, nitrogen and sulphur as heteroatoms. Molecular geometry, along with thermodynamic properties of this compound, was examined through DFT studies. It was observed that **compound 26**

(**Figure 30**) contains an amine substitution which was responsible for its greater AA and AG inhibition. Negative binding energy was observed by joining the place of docked **compound 26** (**Figure 30**) and binding site of amino acids of AG and AA, which clearly pointed out the thermodynamic advantages caused by enzymatic inhibition. Due to their low binding energy and strong affinity for the active sites of enzymes, **compound 26** (**Figure 30**) has been described as an efficient inhibitor of these enzymes. These results confirm the premise that the structural characteristics of the synthesized TZD derivatives have a pronounced effect on their inhibitory activities [54].

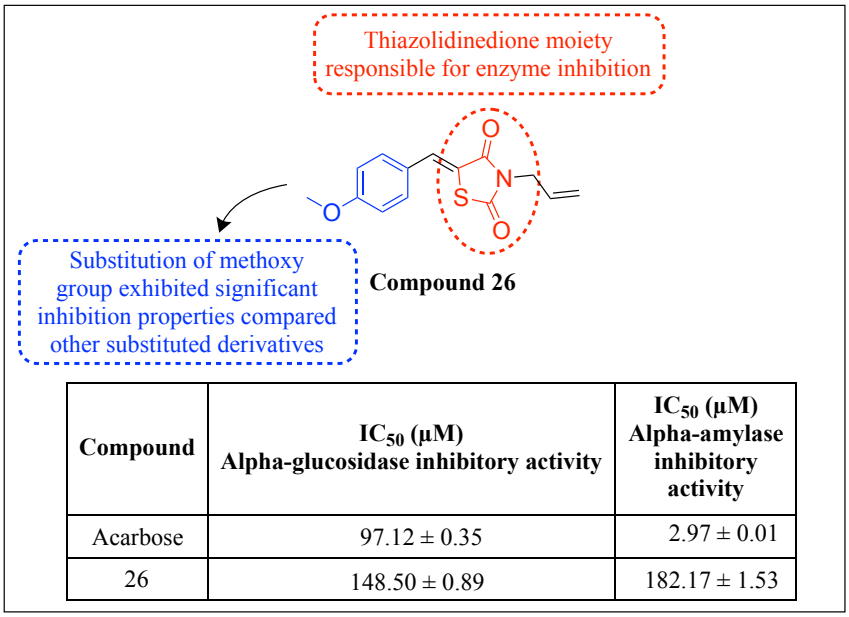

Compound	IC_{50} (µM) Alpha-glucosidase inhibitory activity	IC_{50} (µM) Alpha-amylase inhibitory activity
Acarbose	97.12 ± 0.35	2.97 ± 0.01
26	148.50 ± 0.89	182.17 ± 1.53

Figure 30: SAR and structures of compound 26 as potent AGI and AAI.

Gummidi *et al.,* developed a protocol to synthesize hybrids of 1,3,4-thiadiazole-thiazolidine-4-one. *In vitro* assay of AA and AG showed significant inhibitory potency of hybrid **compound 27** (**Figure 31**) against those enzymes, where the IC_{50} value was below 500 µM. The strongest inhibitory activity for AA was shown by **compound 27** (**Figure 31**) with an IC_{50} value of 2.59 µM. Using free radical scavenging ability of hybrids, HNO_3 scavenging assays, and ferric reducing antioxidant power, the

antioxidant potential of those hybrids was measured, and 4c hybrid was found to have fair antioxidant activity. Hybrid **compound 27** (**Figure 31**) emerged as the most potent AG inhibitor, whose orientation at the active site of the enzyme was almost similar to acarbose. Furthermore, the molecular docking method proved the significance of para-thiomethyl unit for stronger inhibition.

The introduction of a bromine or iodine atom at the para-position of the phenyl ring by replacing the hydrogen resulted in lowering both AG and AA inhibitory activity. However, with the para-SCH_3 substituted derivative (**Compound 27**), the inhibition of both enzymes is the most potent among the compounds tested. This remarkable activity could be seen from its IC_{50} values, **compound 27** (2.59 µM for both AG and AA) is more potent than the standard drug acarbose (3.87 µM for AG, 35.62 µM for AA), which establishes that the nature and position of the substituents on the phenyl ring plays a significant role in the modulation of biological activity [55].

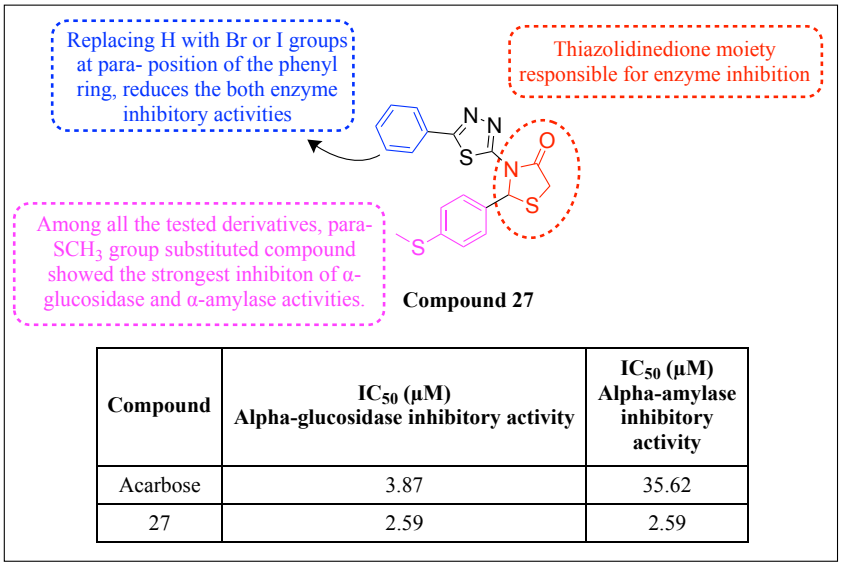

Compound	IC_{50} (µM) Alpha-glucosidase inhibitory activity	IC_{50} (µM) Alpha-amylase inhibitory activity
Acarbose	3.87	35.62
27	2.59	2.59

Figure 31: SAR and structures of compound 27 as potent AGI and AAI.

A library of novel triazole-linked TZD-isatin hybrids was designed and synthesized as potential AGIs by Ramandeep and colleagues. The molecular design rationale was a complementary action of three bioactive pharmacophores-TZD, isatin, and 1,2,3-

triazole-in conjunction with click chemistry to increase enzyme inhibition, potency, and safety. From among all the synthesized hybrids, the most potent compound was **compound 28** with an IC_{50} value of 24.73 ± 0.93 µM (**Figure 32**), and the EC_{50} value of antioxidant activity was 15.90 ± 0.28. Enzyme kinetic studies showed that **compound 28** (**Figure 32**) inhibited AG in a competitive manner as directed by the Lineweaver–Burk plots. In *in vivo* studies, **compound 28** (**Figure 32**) showed a significant decrease in postprandial blood glucose levels at both 10 mg/kg and 20 mg/kg, thus confirming its effect in a physiological context. The results of the in-silico studies, including MM-GBSA, molecular docking and dynamic simulations, showed that **compound 28** (**Figure 32**) established stable complexes through multiple interactions like hydrogen bonds, π–π stacking, and hydrophobic contacts with crucial residues in the active site. *In silico* ADME profiling also supported favourable drug-likeness and pharmacokinetic properties of **compound 28** (**Figure 32**) [56].

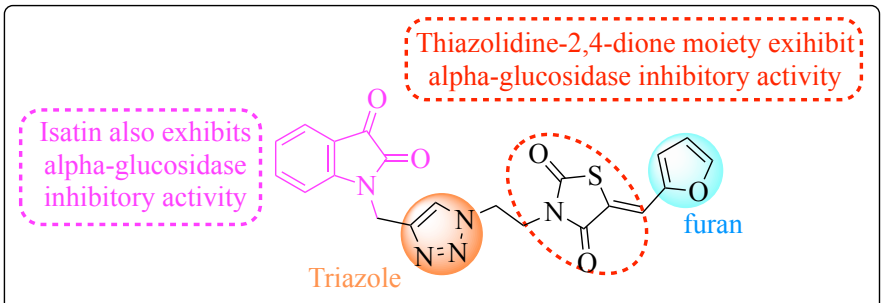

Compound 28

Alpha-glucosidase inhibitory activity

Compound	IC_{50} (µM)	Binding affinity
Acarbose	478.07 ± 1.53	-
28	24.73 ± 0.93	-7.0

Figure 32: SAR and structures of compound 28 as potent AGI.

A novel set of substituted benzimidazole derivatives bearing N-methyl and N-benzyl groups was designed, synthesized, and biologically evaluated by Gagandeep and colleagues for possible identification of multifunctional types of therapeutic agents

targeting T2DM. The rational design of these molecules was undertaken by the hybridization of three important pharmacophores, namely benzimidazole, TZD, and acyclic analogues such as DMM and DEM, which could work as extra electron-withdrawing units and hydrogen bond acceptors. The outcomes of the *in vitro* biological activity showed that several compounds demonstrated excellent inhibitory potency with IC_{50} values ranging from 4.10-9.12 µM, out of which **compound 29** (**Figure 33**) turned out to be the best active (IC_{50} = 4.10 µM). The compound's antioxidant activity was evaluated using the DPPH radical scavenging assay, and among the compounds tested, **compound 29** (**Figure 33**) exhibited excellent antioxidant activity (EC_{50} of 0.176 ± 0.002 µM). Given that **compound 29** docking results revealed good binding affinities and strong interactions through hydrogen bonds and hydrophobic contacts, the further synthesized compounds were docked onto the active sites of the PPARγ protein and may act as dual-acting agents with AG inhibitory effects and PPARγ agonistic properties, which could have the benefits of insulin sensitization [57].

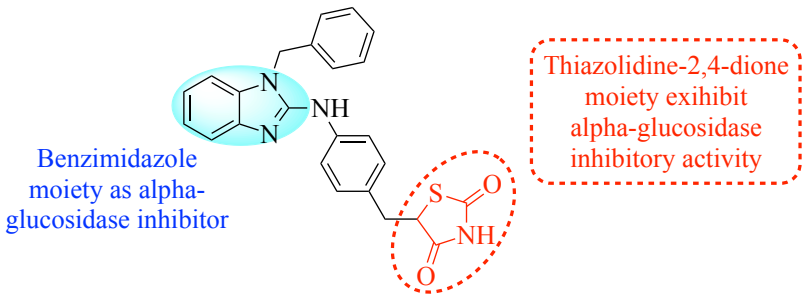

Compound 29

Alpha-glucosidase inhibitory activity

Compound	IC_{50} (µM)	Binding affinity
Acarbose	478.07 ± 1.53	-160.51
29	4.10 ± 0.01	-216.80

Figure 33: SAR and structures of compound 29 as potent AGI.

A drug with dual action of both anti-inflammatory (AI) and anti-diabetic has certain market limitations. Khaled *et al.,* synthesized two new series comprising a pyrazole ring with vicinal diaryl a ring, which acts as a selective COX-2 moiety and anti-diabetic moiety TZD; methylene was used to bind the two moieties. Using an enzyme immunoassay, the *in vitro* COX-1/COX-2 isozyme inhibition tests assessed the target thiazolidine-pyrazole derivatives' capacity to inhibit human recombinant COX-2 and ovine COX-1. Derivatives were evaluated *in vivo* for anti-inflammatory activity in the carrageenan-induced rat paw oedema assay. It has been found that **compound 30** (**Figure 34**) has the highest potential against COX-2. The **compound 30** (**Figure 34**) has a comparatively higher selectivity index than drug celecoxib, and it also showed remarkable AI activities. Also, **compound 30** (**Figure 34**) resulted in tter inhibitor activity against AA and AG [58].

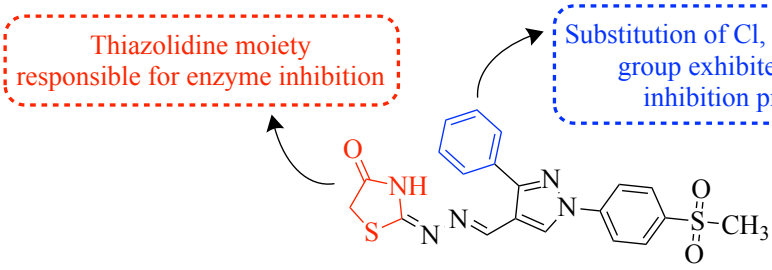

Compound 30

Compound	IC_{50} (µM) Alpha-glucosidase inhibitory activity
Acarbose	49.5 ± 1.73
30	19.32 ± 1.02

Figure 34: SAR and structures of compound 30 as potent AGI.

Postprandial hyperglycemic condition in diabetes patients is caused by dietary carbohydrate hydrolysis by AG and AA enzymes. This condition can be addressed by blocking these enzymes. Thiazolidin-4-one and pyrazolyl pharmacophore (THZP)-based molecular hybrids have been synthesized by Kumar *et al.,* as novel anti-diabetic

agents. Their biological potential in inhibiting AG and AA has been investigated, and these compounds revealed intriguing nonlinear optical characteristics (NLO). The compounds' structures were validated by spectroscopic investigations, and compounds displayed encouraging NLO. Compared to common acarbose compound, **compounds 31** and **32** (**Figure 35**) revealed significant inhibition of AA and AG, where the IC_{50} values were 54.46 µM and 4.84 µM, respectively. Furthermore, in the docking study, it was seen that **compound 31** (**Figure 35**) has 6 hydrogen bonds, 2 electrostatic, 7 hydrophobic and 2 other interactions entangled in the enzyme's active pocket [59].

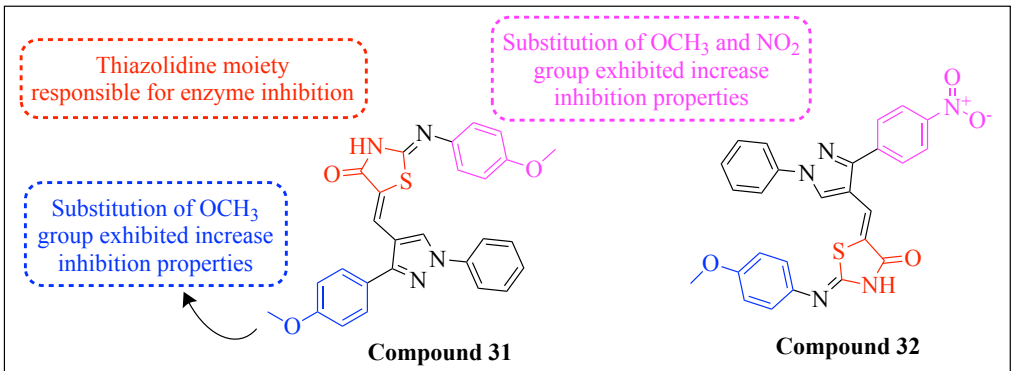

Compound	IC_{50} (µM) Alpha-glucosidase inhibitory activity
Acarbose	10.53 ± 1.38
31	54.46 ± 1.23
32	4.48 ± 1.38

Figure 35: SAR and structures of compounds 31 and 32 as potent AGIs.

A new series of fused TZD-azole moieties like benzimidazole, indazole, pyrazole, imidazole, and azaindole hybrids have been developed by Senthil Kumar and co-workers against AA and AG inhibition. All the compounds synthesized were assessed for their inhibition against the enzymes AA and AG. Among the tested compounds, the highest inhibition was exhibited by compounds between 35 to 40% at 250 µg/mL, comparable to standard drug acarbose. These results were supported further by glucose

diffusion study, during which it was observed that these lead compounds significantly reduced glucose movement through bio-membranes over a time of 3 h. The SAR study exhibited that the enhanced activity of **compound 33** (**Figure 36**) will be due to fluorinated aryl amine substituents at the 7th position of the azaindole moiety, increasing between lipophilicity (6.49, 5.63, 6.45) and molar refractivity (125, 117, 123) which is associated almost proportionally with better binding efficiency and selectivity [60].

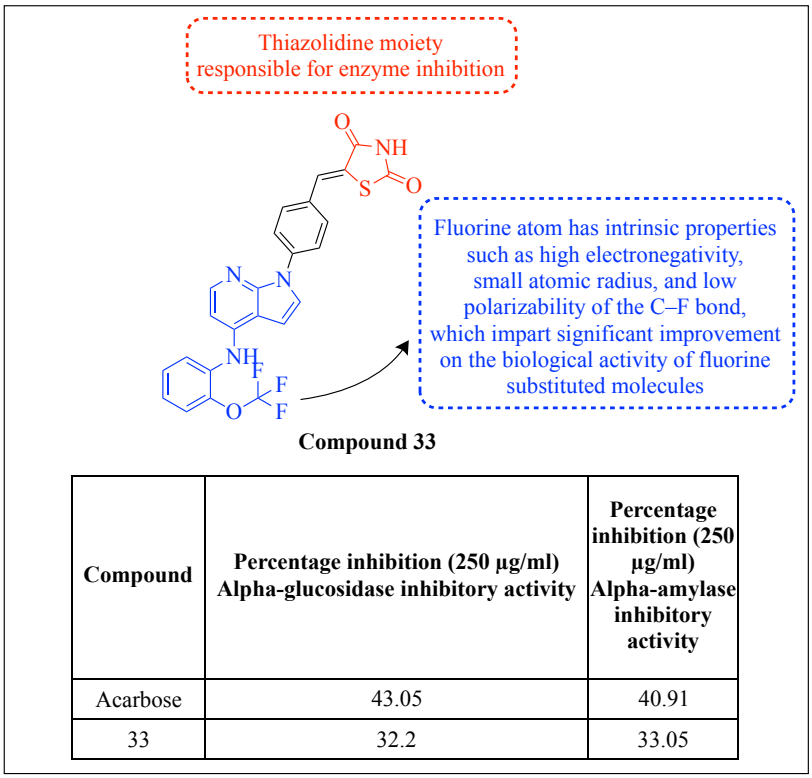

Compound 33

Compound	Percentage inhibition (250 µg/ml) Alpha-glucosidase inhibitory activity	Percentage inhibition (250 µg/ml) Alpha-amylase inhibitory activity
Acarbose	43.05	40.91
33	32.2	33.05

Figure 36: SAR and structures of compound 33 as potent AGI and AAI.

Hussain *et al.,* developed and evaluated AG inhibition of TZD derivatives along with pyrrolidine-2,5-dione. The synthesized compounds were tested against yeast AG, where almost all pyrrolidine-2,5-dione derivatives showed low to moderate inhibitory action. SAR studies of **compound 34** (**Figure 37**) show that the thiazolidine ring of a/all of the compounds is essential for their AG inhibition, because it contributes directly to enzyme inhibition. Furthermore, para-substitutions on the phenyl ring (the

hydrogen by methyl (CH_3) or chlorine (Cl)) significantly decrease the inhibitory activity of the compound toward the enzyme. Biologically, **compound 34** (**Figure 37**) displays a higher inhibitory activity of AG (IC_{50} = 0.98 ± 0.008 µM) than the market drug acarbose (IC_{50} = 10.6 ± 0.10 µM), indicating that **compound 34** (**Figure 37**) could be a promising inhibitor. The study of antioxidant potential showed that only a few compounds exhibit moderate anti-oxidant activity. The *in vivo* anti-diabetic study of selected compounds was able to lower blood glucose levels in comparison with drug glibenclamide. Interactions of active compounds with important residues like Asp214, Glu276 and Phe157 resulted in high potency of the compounds, which were evaluated by bioassay and binding mode method [61].

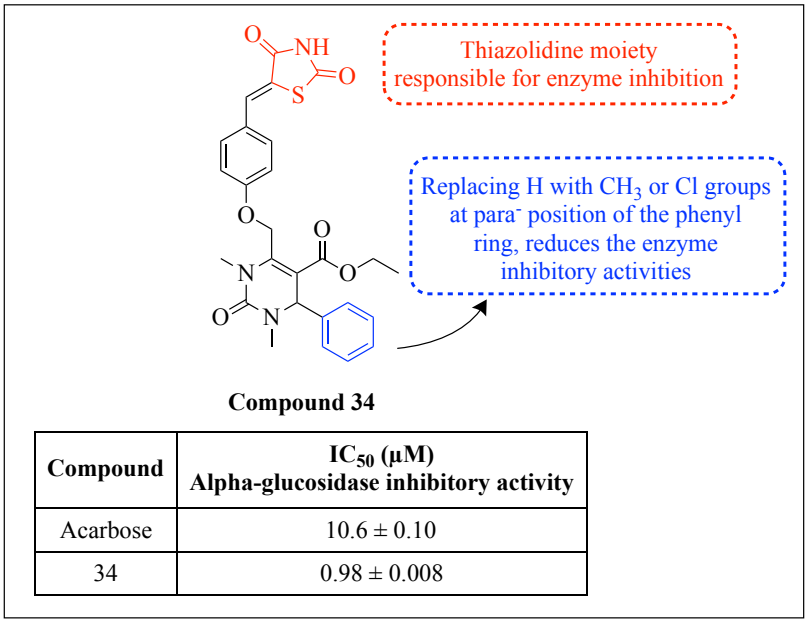

Compound	IC_{50} (µM) Alpha-glucosidase inhibitory activity
Acarbose	10.6 ± 0.10
34	0.98 ± 0.008

Figure 37: SAR and structures of compound 34 as potent AGI.

Guang-cheng *et al.,* synthesized the newer derivatives of TZD and evaluated their AG inhibitory action. Among all these compounds, **compound 35** (**Figure 38**) showed significant inhibitory capacity AG in the *in vitro* assay, where the IC_{50} values of compounds were 5.44 ± 0.13 µM, respectively. SAR studies of **compound 35** (**Figure 38**) show that the thiazolidine ring of a/all of the compounds is essential for their AG

inhibition, because it contributes directly to enzyme inhibition. Furthermore, ortho-substitutions on the phenyl ring by chlorine significantly decrease the inhibitory activity of the compound toward the enzyme. The molecular docking process showed that **compound 35** (**Figure 38**) resulted in a 'L-shape' conformation in the pocket of AG. **Compound 35** (**Figure 38**) also showed almost similar docking activity with a slight difference due to the oxygen atom of **compound 35** (**Figure 38**), which created one extra hydrogen bond [62].

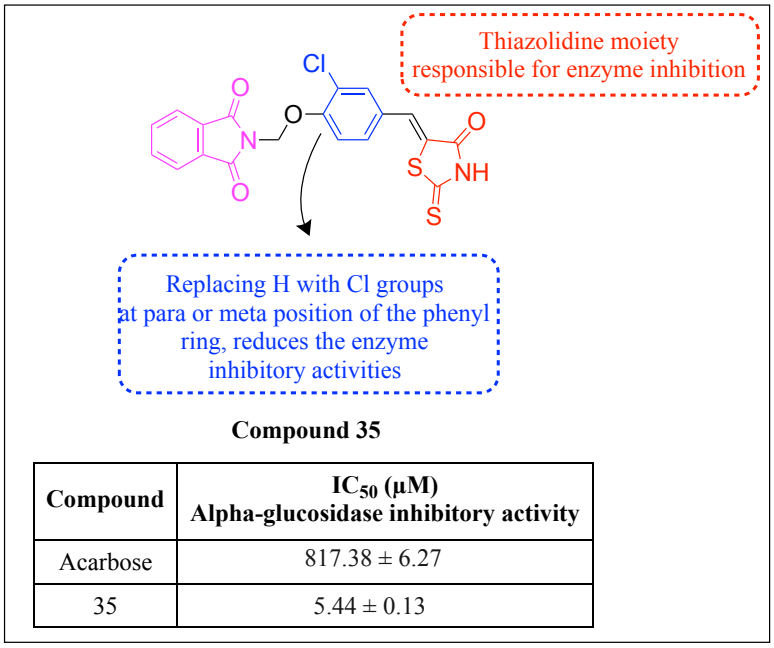

Compound 35

Compound	IC_{50} (µM) Alpha-glucosidase inhibitory activity
Acarbose	817.38 ± 6.27
35	5.44 ± 0.13

Figure 38: SAR and structures of compound 35 as potent AGI.

1.5. Cuminaldehyde:

Cuminaldehyde (CUM; CAS Registry Number: 122-03-2 and PubChem CID: 326; **Figure 39**) is a terpenoid class of compounds isolated from essential oil components and is found in cumin (*C. cyminum*) seeds and other plants [63]. Traditionally, fruits and seeds of *C. cyminum* were used for the treatment of cough, inflammation, ulcers, and boils. The essential oil components have been extracted using various extraction techniques, and hydrodistillation is one of the beneficial techniques with 30-35% yields of essential oil components. Cumin essential oil (CEO) was also explored in

nutraceuticals and perfumes and as a flavour in culinary dishes due to its aromatic nature [64–66]. There are several bioactive secondary metabolites discovered in *C. cyminum* seeds, which have been shown to have antibacterial, anti-inflammatory, antioxidant, anti-cancer, and anti-diabetic effects [67]. The composition of essential oil components has been studied using GC-MS, and the analytical result indicates that CUM is a prominent chemical in essential oil components. As a result, scientists believe CUM has potential benefits as an antioxidant, antibacterial, and anti-diabetic agent.

Recent research studies revealed that CUM has also been demonstrated to have phytotoxic action, preventing the growth of a variety of plant species and promoting the generation of reactive oxygen species (ROS) and programmed cell death in the roots of onions [68]. It has also been demonstrated that CUM forms a stable combination with bovine serum albumin (BSA) through hydrogen bonding and hydrophobic forces [69]. Furthermore, against Pseudomonas aeruginosa, CUM has shown antibiofilm efficacy by preventing ROS buildup, which prevents biofilm development [70]. **Figure 40** illustrates the various pharmacological effects that CUM provides, together with their mechanisms of action.

Structurally, CUM is a member of the benzaldehyde class, where the isopropyl group is attached at position 4. The structure, chemical formula, molecular weight, melting point, logP, and tPSA of CUM are depicted in **Figure 39**. CUM can be structurally confirmed with the help of ^{1}H NMR, Fourier-transform infrared (FT-IR) spectroscopy, and mass spectrometry. In ^{1}H NMR, CUM showed specific chemical shift in ppm value as follows: at 1.2 ppm (assigned to -CH_3 group, doublet), 3.1 ppm (assigned to -CH group, multiplate), 7.4 ppm (assigned to -CH of aromatic ring, doublet), 7.8 ppm (assigned to -CH of aromatic ring, doublet), and 10.0 ppm (assigned to -H of aldehyde group, singlet). In FT-IR spectroscopy, CUM exhibited characteristic vibrational peaks

at 2930, 2871, and 2824 cm^{-1}, while the C–H stretching vibration in the aromatic ring was at 2662 cm^{-1}, the CO– stretching vibration was at 1698 cm^{-1}, the C–H bending vibration in the aromatic ring plane was at 1211−1015 cm^{-1}, and the C–H bending vibration out of the aromatic ring was at 826 cm^{-1}. Similarly, in mass spectrometry, CUM showed a base peak at an m/z value of 133 and a molecular ion peak at an m/z value of 148 [71].

Numerous extraction methodologies (like plant selection, techniques, and solvents have been developed by researchers to extract essential oils and purify CUM from them. Recently, high-speed counter-current chromatography (HSCCC) was used to purify CUM from essential oils. Similarly, different HPLC methods have been developed for the analysis of CUM from essential oils. For both academic and commercial research institutes, CUM is a crucial topic of study due to its possible biological usefulness. Nevertheless, there are published review studies that provide a thorough presentation of CUM, which consists of an overview of CUM's isolation and purification processes, HPLC methods for the analysis, and therapeutic applications with their molecular mechanism of action. Therefore, CUM is a therapeutic agent that may be utilized therapeutically to address a variety of ailments.

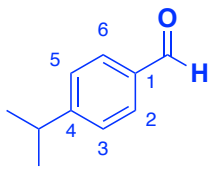

Cuminaldehyde (CUM)

Chemical Formula:	$C_{10}H_{12}O$
Molecular Weight:	148.21
Melting Point:	267.9 [K]
LogP:	3.02
tPSA:	17.07

Figure 39: Structure, chemical formula, molecular weight, melting point, logP, and tPSA of CUM (Chemical formula, molecular weight, melting point, logP, and tPSA were calculated from ChemBioDraw Ultra 12.0.).

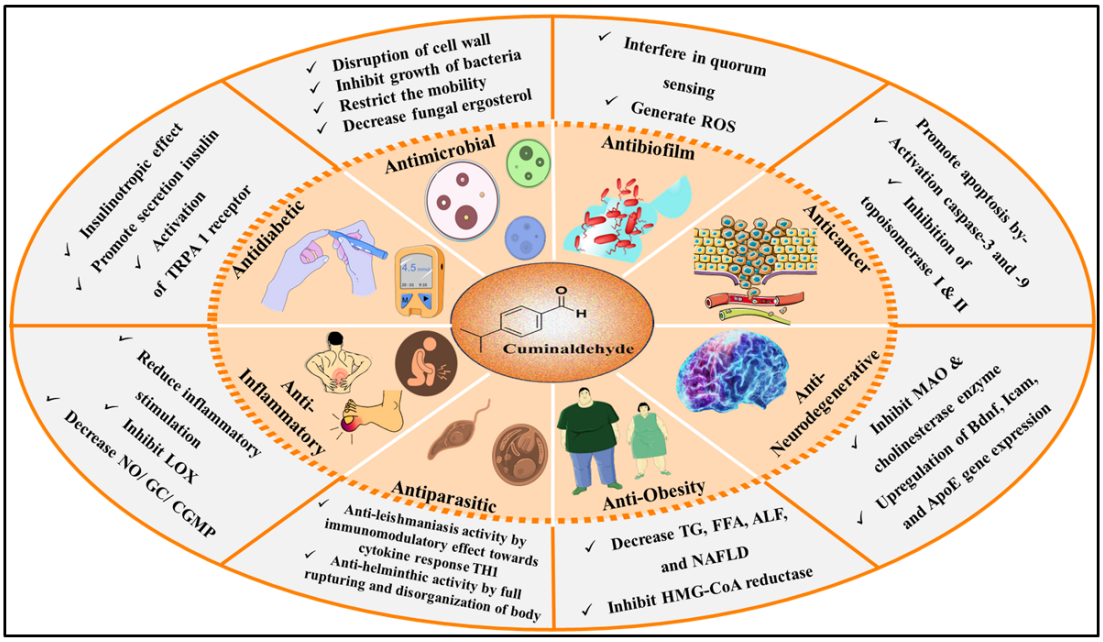

Figure 40: Therapeutic potential of CUM with its schematic mode of action.

1.6. Biological activity potentials of Cuminaldehyde analogues:

CUM analogues have also been explored by researchers in the last few years to identify the best possible analogue for diverse biological activities. Hydrazone, oxadiazole, pyrazoline, isoxazoline, thiosemicarbazone, hydrazide with thiophene, and Schiff bases are a few of the heterocyclic cores that have been mostly explored for the development of synthetic CUM analogues. Presented below is an extensive overview of the possible biological effects of CUM analogues.

Meenatchi *et al.,* synthesized cuminaldehyde-3-hydroxy-2-napthoichydrazone (**Compound 36**) (**Figure 41**), a new essential oil component derivative, using the ultrasonication method. The CUM derivatives have been evaluated for antibacterial activity using the agar-well diffusion method, which showed a significant growth inhibition zone against *B. subtilis* (21 ± 0.2 mm) and *E. coli* (18 ± 0.3 mm). These bactericidal effects may be attributed to the disruption of the cell wall and cytoplasmic membranes, as well as the release of pathogen cytoplasm. In addition, it has been

determined that the biological activity of an essential oil component, CUM was retained even if its derivative was synthesized by condensation with polycyclic aryl hydrazide. This novel CUM derivative has also shown remarkable promise as an antioxidant with nonlinear optical activity [72]. By modifying the natural scaffold CUM, a series of oxadiazoles were designed, synthesized by Hamdy *et al.,* and evaluated for antifungal activity. At sub-micromolar MIC_{50} concentrations, the novel series inhibited *Candida albicans* and *Candida auris*, with **compound 37** (**Figure 41**) being the most potent analogue that did not exhibit toxicity on normal mammalian cells. Additionally, they carried out molecular dynamics simulations of the *C. auris* CYP51 enzyme using molecular docking and homology modelling, demonstrating the stability and effectiveness of **compound 37**. Furthermore, a 70% decrease in the fungal ergosterol content was shown by **compound 37**, and the ADME prediction suggested that **compound 37** meets the requirements for drug resemblance as a potential antifungal medication (**Figure 41**) [73]. Zhang *et al.,* planned and created two sets of new CUM derivatives, which include pyrazoline and isoxazoline components. They assessed their antifungal activity against six plant-pathogenic fungal strains. **Compounds 38** and **39** (**Figure 41**) with potent antifungal properties should undergo further assessment *in vivo* and in field conditions, as reported. Remarkably, **compound 38**, which has a fluorine atom, exhibited exceptional antifungal properties, surpassing those of commercially available fungicides. The CUM derivatives in this research showed notable antifungal activity against the fungi that were examined. Compared to CUM alone, around half of the reported compounds showed more potent inhibitory effects. Specifically, **compound 38** outperformed CUM by 3.5 times in activities against *Ph. Piricola* (7.25 vs. 25.50 μg·mL−1), while **compound 39** outperformed CUM by around five times in potential against *S. sclerotiorum* (12.75 vs. 63.62 μg·mL−1) [74].

Francesca and his fellow researchers have effectively synthesized semi-carbazone, a compound derived from CUM thiosemicarbazone (**compound 40; Figure 41**), in which the sulphur atom has been replaced with an oxygen atom. This modification aimed to investigate the role of sulphur and oxygen in forming hydrogen bonds of varying strength, as well as their redox potentials. Typically, sulphur has weaker hydrogen bonds compared to oxygen because of its lower electronegativity. Additionally, sulphur is more prone to oxidation by creating disulfide bridges. Thiosemicarbazones may function as reducers due to their ability to undergo thione-thiol tautomerism in their thiolic form. As a result, they can also operate as producers of reactive oxygen species or scavengers of radicals. The selection of the ortho-Htcum and meta-Htcum isopropyl derivatives of Htcum is determined by the similarity in hydrophobicity to CUM while exhibiting distinct geometries. This study seeks to determine if the position of the isopropyl group serves as a general hydrophobic segment that enables the molecule to enter the cell or whether its placement is part of a more specialized molecule recognition process [75].

Regarding the biochemical characterization of hydrazide with thiophene moiety produced from CUM, no research has been done until Rajavel *et al.,* reported a synthesis of **compound 41;** [(*E*)-*N*-(4-isopropyl benzylidene) thiophene-2-carbohydrazide] (**Figure 41**). CUM and 2-thiophenecarboxylic acid hydrazide were condensed to create **compound 41.** The findings indicate that **compound 41** exhibits lower activity against the tested microorganisms in comparison to the standards. In addition, **compound 41** has modest efficacy against two bacterial strains (*P. aeruginosa* and *E. coli*) and two fungal strains (*Mucor sp.* and *Rhizopus sp.*), as seen by the MIC values. The **compound 41** also exhibited a mild antioxidant property. The compound's notable activity may be attributed to the existence of the thiophene ring

[76]. Witold and his colleagues researched the stereoisomers of CUM derivatives. They showed trans-lactones with a (4S,5R,6S)-framework more activity than other compounds. The trans-lactone and cis-lactone enantiomers with a 1,3-benzodioxole substituent (**compound 42; Figure 41)** showed a moderate variation (IC_{50} = 34.75 and 14.48 vs. 38.93 and 20.28 for the Jurkat and GL-1 cancer lines, respectively). The observed relationship in the case of cis-isomers was dependent on an aryl substituent and tested cancer line [77]. Degola *et al.,* researched the function of a series of modified thiosemicarbazones CUM derivatives. They carried out antifungal and antimycotoxin activity. Two compounds exhibited distinct toxicological characteristics against *Aspergillus* and *Fusarium*, two genera of mycotoxigenic fungi that affect cereal. This provides an illustration of the differences between the impacts of **compound 43** (**Figure 41**) thiosemicarbazones on the growth of *A. flavus* mycelium. These initial findings demonstrated that the CUM and trans-cinnamaldehyde moieties are critical to the potential. **Compound 43's** IC_{50} was 49 μM, and it caused significant cytotoxicity with a dose-response relationship. Thiosemicarbazones are a significant class of chemicals containing sulphur and nitrogen. They have drawn considerable interest due to their physical and chemical features, which include cancer prevention and antimicrobial activities in human pharmacotherapy [78]. Bisceglie *et al.,* synthesized and characterized a trans-cinnamaldehyde thiosemicarbazone (**compound 44; Figure 41**), CUM thiosemicarbazone (**compound 45; Figure 41**), and their copper and nickel complexes for antileukemic activity. All the compounds were evaluated *in vitro* in the U937 cell line, which exhibited negligible cytotoxicity on healthy human fibroblasts. Despite their molecular similarity, these compounds exhibit a variety of behaviours. In U935 cells, **compound 44** does not show any inhibition activity, whereas both of its metal complexes inhibit proliferation with an IC_{50} at μM concentrations. In addition to

inhibiting proliferation, the other ligand, **compound 45**, and its metal complexes induce apoptosis. The G2/M checkpoint halt is emphasized in the cell cycle analysis, which implies a potential direct action on topoisomerase IIa or DNA. The DNA is not the primary target of any of these compounds, as evidenced by CD and UV spectroscopy experiments. However, both copper complexes are effective inhibitors of topoisomerase IIa. Both cinnamonaldehyde metal complexes substantially induce caspase-8 activity, while all of these compounds activate caspase-9 and caspase-3. The compounds accumulate in the cytoplasm, and the cells are unable to expel copper and nickel ions, as evidenced by tests on PgP and intracellular metal concentrations (determined by the mean of atomic absorption spectrometry) [79]. Arish *et al.,* developed a Schiff base (L) by the condensation of CUM and L-histidine as antimicrobial agents. This Schiff-base ligand is synthesized and characterized by elemental analysis, molar conductance, mass, IR, electronic spectra, magnetic moment, electron spin resonance (ESR), CV, TG/DTA, granular XRD, and SEM. The complexes of Co(II), Ni(II), Cu(II), and Zn(II) are also involved. The Schiff base is a tridentate monobasic donor, as IR data indicates. It coordinates through carboxylate oxygen, imidazole nitrogen, and azomethine nitrogen. The crystalline nature of the Co(II), Cu(II), and Zn(II) complexes is demonstrated by XRD and SEM. In contrast, the Ni(II) complex is amorphous, and the particles are in the nanocrystalline phase. The disc diffusion method was employed to evaluate the *in vitro* biological activities of the synthesized compounds against the bacterial species. The biological investigation suggests complexes demonstrate more significant activity than their ligand counterparts. In the presence and absence of H_2O_2, the nuclease activity of the ligand and its complexes is evaluated on CT DNA using gel electrophoresis. Experiments on

CT-DNA cleavage and antimicrobial activity indicate that the complex (**Compound 46; Figure 41**) exhibits more significant activity than the ligand [80].

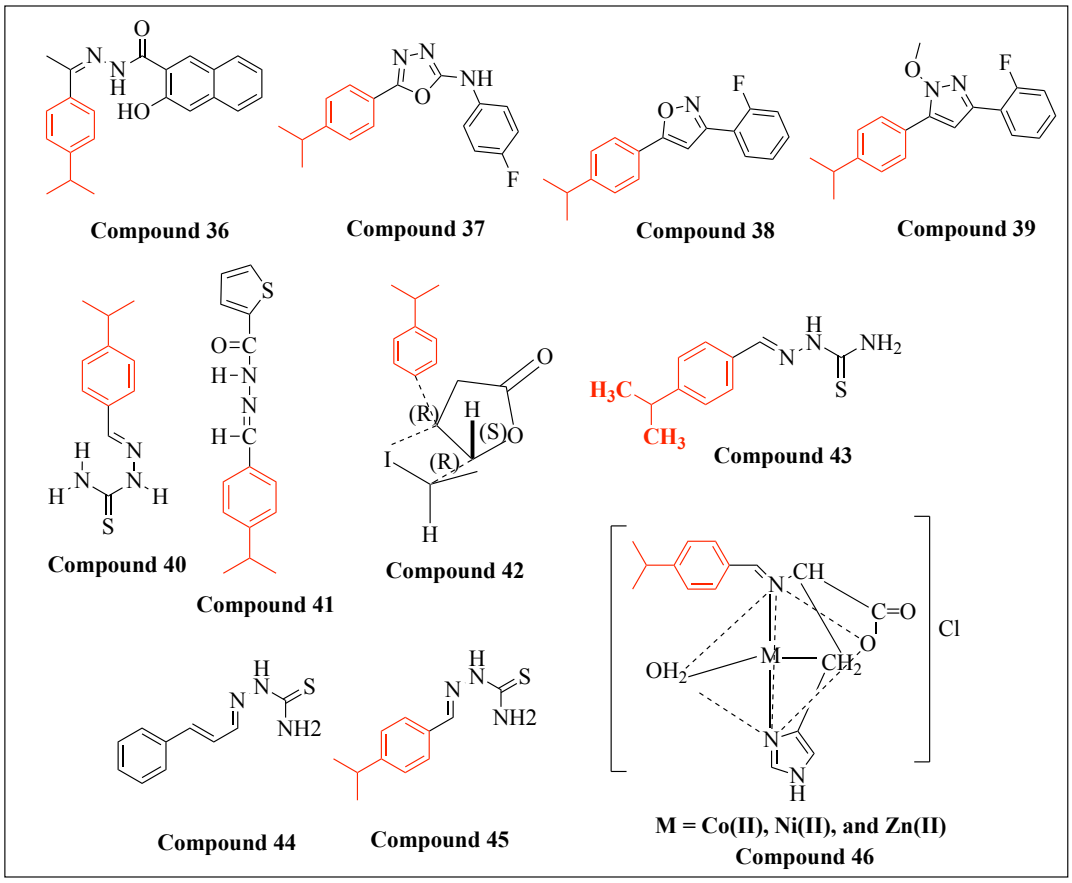

Figure 41: Structure of potential CUM analogues.

1.7. Comparative studies between Cuminaldehyde and its analogues:

In the last decade, CUM has been extensively studied for numerous biological activities with appropriate pharmacological mechanisms, and we have highlighted those in the above section. Similarly, we have also emphasized different synthetic analogues of CUM as reported in various research articles [73–82]. When we examined the biological activities and efficacy of CUM and analogues, we found that both showed comparable biological activities and efficacy in various pharmacological models of diseases. However, we lack any data on *in vivo* or *in vitro* experimental support to compare the safety and toxicity profiles. Lastly, we can say that extensive future

research on the preclinical and clinical study of CUM, including the synthesis, biological study and toxicological study of its synthetic analogues, is necessary to develop CUM-based medicine.

References:

[1] G. Bansal, P.V. Thanikachalam, R.K. Maurya, P. Chawla, S. Ramamurthy, An overview on medicinal perspective of thiazolidine-2,4-dione: A remarkable scaffold in the treatment of type 2 diabetes, J Adv Res 23 (2020) 163–205. https://doi.org/10.1016/j.jare.2020.01.008.

[2] N. Long, A. Le Gresley, S. Wren, Thiazolidinediones: An in depth study of their synthesis and application to medicinal chemistry in the treatment of Diabetes Mellitus, ChemMedChem n/a (2021). https://doi.org/10.1002/cmdc.202100177.

[3] R.S. Bahare, S. Ganguly, K. Choowongkomon, S. Seetaha, Synthesis, HIV-1 RT inhibitory, antibacterial, antifungal and binding mode studies of some novel N-substituted 5-benzylidine-2,4-thiazolidinediones, DARU, Journal of Pharmaceutical Sciences 23 (2015) 6. https://doi.org/10.1186/s40199-014-0086-1.

[4] A.M. Ali, G.E. Saber, N.M. Mahfouz, M.A. El-Gendy, A.A. Radwan, M.A.E. Hamid, Synthesis and three-dimensional qualitative structure selectivity relationship of 3,5-disubstituted-2,4-thiazolidinedione derivatives as COX2 inhibitors, Arch Pharm Res 30 (2007) 1186–1204. https://doi.org/10.1007/BF02980259.

[5] C.D. Barros, A.A. Amato, T.B. de Oliveira, K.B.R. Iannini, A.L. da Silva, T.G. da Silva, E.S. Leite, M.Z. Hernandes, M. do C.A. de Lima, S.L. Galdino, F. de A.R. Neves, I. da R. Pitta, Synthesis and anti-inflammatory activity of new arylidene-thiazolidine-2,4-diones as PPARγ ligands, Bioorg Med Chem 18 (2010) 3805–3811. https://doi.org/10.1016/j.bmc.2010.04.045.

[6] R.K. Sharma, Y. Younis, G. Mugumbate, M. Njoroge, J. Gut, P.J. Rosenthal, K. Chibale, Synthesis and structure-activity-relationship studies of thiazolidinediones as antiplasmodial inhibitors of the Plasmodium falciparum cysteine protease falcipain-2, Eur J Med Chem 90 (2015) 507–518. https://doi.org/10.1016/j.ejmech.2014.11.061.

[7] S. Mehendale-Munj, R. Ghosh, C.S. Ramaa, Synthesis and evaluation of the hypoglycemic and hypolipidemic activity of novel 5-benzylidene-2,4-thiazolidinedione analogs in a type-2 diabetes model, Medicinal Chemistry Research 20 (2011) 642–647. https://doi.org/10.1007/s00044-010-9359-5.

[8] F.S.M. Neri, D.B.C. Júnior, T.Q. Froes, P.B.G. da Silva, M.S. do Egito, P.O.L. Moreira, F. de Pilla Varotti, M.S. Castilho, R.G. Teixeira-Neto, J.F.C. de Albuquerque, F.H.A. Leite, Antileishmanial activity evaluation of thiazolidine-2,4-dione against Leishmania infantum and Leishmania braziliensis, Parasitol Res 119 (2020) 2263–2274. https://doi.org/10.1007/s00436-020-06706-3.

[9] N.S. Sethi, D.N. Prasad, R.K. Singh, Synthesis, Anti-cancer, and Antibacterial Studies of Benzylidene Bearing 5-substituted and 3,5-disubstituted-2,4-Thiazolidinedione Derivatives, Med Chem (Los Angeles) 17 (2020) 369–379. https://doi.org/10.2174/1573406416666200512073640.

[10] M.J. Naim, M.J. Alam, S. Ahmad, F. Nawaz, N. Shrivastava, M. Sahu, O. Alam, Therapeutic journey of 2,4-thiazolidinediones as a versatile scaffold: An insight into structure activity relationship, Eur J Med Chem 129 (2017) 218–250. https://doi.org/10.1016/j.ejmech.2017.02.031.

[11] R. Khare, J. Pandey, S. Smriti, R. Ruchi, The Importance and Applications of Knoevenagel Reaction (Brief Review), Oriental Journal of Chemistry 35 (2019) 423–429. https://doi.org/10.13005/ojc/350154.

[12] M.M. Heravi, F. Janati, V. Zadsirjan, Applications of Knoevenagel condensation reaction in the total synthesis of natural products, Monatsh Chem 151 (2020) 439–482. https://doi.org/10.1007/s00706-020-02586-6.

[13] A. Shaabani, R. Ghadari, A. Rahmati, A.H. Rezayan, Coumarin synthesis via knoevenagel condensation reaction in 1,1,3,3-N,N,N',N'- tetramethylguanidinium trifluoroacetate ionic liquid, Journal of the Iranian Chemical Society 6 (2009) 710–714. https://doi.org/10.1007/BF03246160.

[14] P. Verdía, F. Santamarta, E. Tojo, Knoevenagel reaction in [MMIm][MSO4]: Synthesis of coumarins, Molecules 16 (2011) 4379–4388. https://doi.org/10.3390/molecules16064379.

[15] K. Laskar, P. Bhattacharjee, M. Gohain, D. Deka, U. Bora, Application of bio-based green heterogeneous catalyst for the synthesis of arylidinemalononitriles, Sustain Chem Pharm 14 (2019) 100181. https://doi.org/10.1016/j.scp.2019.100181.

[16] P. Leelavathi, S.R. Kumar, Niobium (V) chloride catalyzed Knoevenagel condensation: An efficient protocol for the preparation of electrophilic alkenes, J Mol Catal A Chem 240 (2005) 99–102. https://doi.org/10.1016/j.molcata.2005.06.026.

[17] J. Boukouvalas, C. Thibault, Step-Economical Synthesis of the Marine Ascidian Antibiotics Cadiolide A, B, and D, Journal of Organic Chemistry 80 (2015) 681–684. https://doi.org/10.1021/jo502503w.

[18] Y. Chen, W. Shi, Y. Hui, X. Sun, L. Xu, L. Feng, Z. Xie, A new highly selective fluorescent turn-on chemosensor for cyanide anion, Talanta 137 (2015) 38–42. https://doi.org/10.1016/j.talanta.2015.01.018.

[19] Lednicer, Daniel, Strategies for Organic Drug Synthesis and Design, 2nd Edition, John Wiley & Sons, n.d.

[20] A. Khazaei, H. Veisi, M. Safaei, H. Ahmadian, Green synthesis of 5 arylidene-2,4-thiazolidinedione, 5-benzylidene rhodanine and dihydrothiophene derivatives catalyzed by hydrated ionic liquid tetrabutylammonium hydroxide in aqueous medium, Journal of Sulfur Chemistry 35 (2014) 270–278. https://doi.org/10.1080/17415993.2013.860142.

[21] B.B. Drawanz, C.S. Ribeiro, H.G. Masteloto, P.D. Neuenfeldt, C.M.P. Pereira, G.M. Siqueira, W. Cunico, Sonochemistry: A good, fast and clean method to promote the synthesis of 5-arylidene-2,4-thiazolidinediones, Ultrason Sonochem 21 (2014) 1615–1617. https://doi.org/10.1016/j.ultsonch.2014.04.013.

[22] N.H. Metwally, N.M. Rateb, H.F. Zohdi, A simple and green procedure for the synthesis of 5-arylidene-4-thiazolidinones by grinding, Green Chem Lett Rev 4 (2011) 225–228. https://doi.org/10.1080/17518253.2010.544330.

[23] G. Jones, The Knoevenagel Condensation, Organic Reactions (2011) 204–599. https://doi.org/10.1002/0471264180.or015.02.

[24] J. van Schijndel, L.A. Canalle, D. Molendijk, J. Meuldijk, The green knoevenagel condensation: Solvent-free condensation of benzaldehydes, Green Chem Lett Rev 10 (2017) 404–411. https://doi.org/10.1080/17518253.2017.1391881.

[25] J.J. Li, Knoevenagel condensation, in: J.J. Li (Ed.), Name Reactions, Springer International Publishing, Cham, 2014: pp. 344–346. https://doi.org/10.1007/978-3-319-03979-4_147.

[26] B.R.P. Kumar, M.D. Karvekar, L. Adhikary, M.J. Nanjan, B. Suresh, Microwave induced synthesis of the thiazolidine-2,4-dione motif and the efficient solvent free-solid phase parallel syntheses of 5-benzylidene- thiazolidine-2,4-dione and 5-benzylidene-2-thioxo-thiazolidine-4-one compounds, J Heterocycl Chem 43 (2006) 897–903. https://doi.org/10.1002/jhet.5570430413.

[27] F.Z. Thari, H. Tachallait, N.E. El Alaoui, A. Talha, S. Arshad, E. Álvarez, K. Karrouchi, K. Bougrin, Ultrasound-assisted one-pot green synthesis of new N-substituted-5-arylidene-thiazolidine-2,4-dione-isoxazoline derivatives using

NaCl/Oxone/Na3PO4 in aqueous media, Ultrason Sonochem 68 (2020) 105222. https://doi.org/10.1016/j.ultsonch.2020.105222.

[28] A.V. Narsaiah, K. Nagaiah, An Efficient Knoevenagel Condensation Catalyzed by LaCl 3 .7H2O in Heterogeneous Medium #, Synth Commun 33 (2003) 3825–3832. https://doi.org/10.1081/SCC-120025194.

[29] A.R. Bhat, M.H. Najar, R.S. Dongre, M.S. Akhter, Microwave assisted synthesis of Knoevenagel Derivatives using water as green solvent, Current Research in Green and Sustainable Chemistry 3 (2020) 100008. https://doi.org/10.1016/j.crgsc.2020.06.001.

[30] H. V. Chavan, B.P. Bandgar, Aqueous extract of Acacia concinna pods: An efficient surfactant type catalyst for synthesis of 3-carboxycoumarins and cinnamic acids via knoevenagel condensation, ACS Sustain Chem Eng 1 (2013) 929–936. https://doi.org/10.1021/sc4000237.

[31] G. Kwak, M. Fujiki, Colored and luminous aliphatic polyester via one-pot intra- and intermolecular Knoevenagel reactions, Macromolecules 37 (2004) 2021–2025. https://doi.org/10.1021/ma035679g.

[32] J. Nokami, K. Kataoka, K. Shiraishi, M. Osafune, I. Hussain, S.I. Sumida, Convenient formation of 4-hydroxyalk-2-en-1-one functionality via a Knoevenagel-type carbon chain elongation reaction of aldehyde with 1-arylsulfinylalkan-2-one, Journal of Organic Chemistry 66 (2001) 1228–1232. https://doi.org/10.1021/jo001323g.

[33] P. De, G. Koumba Yoya, P. Constant, F. Bedos-Belval, H. Duran, N. Saffon, M. Daffé, M. Baltas, Design, synthesis, and biological evaluation of new cinnamic derivatives as antituberculosis agents, J Med Chem 54 (2011) 1449–1461. https://doi.org/10.1021/jm101510d.

[34] H. Cho, M. Ueda, M. Tamaoka, M. Hamaguchi, K. Aisaka, Y. Kiso, T. Inoue, R. Ogino, T. Tatsuoka, T. Ishihara, T. Noguchi, I. Morita, S. itsu Murota, Novel Caffeic Acid Derivatives: Extremely Potent Inhibitors of 12-Lipoxygenase, J Med Chem 34 (1991) 1503–1505. https://doi.org/10.1021/jm00108a039.

[35] T.C. Nguyen, T.D. Le, T.K.D. Hoang, C.T. Pham, J.A. Alhaji, T.C. Nguyen, N.A. Truong, C.P. Dinh, L. Van Meervelt, Synthesis, evaluation of α-glucosidase inhibitory and antimicrobial activities of novel N-(5-arylidene-4-oxo-2-thioxothiazolidin-3-yl)-2-(naphthalen-1-yl)acetamide derivatives, J Mol Struct 1326 (2025) 141068. https://doi.org/10.1016/j.molstruc.2024.141068.

[36] B. Liang, J. Li, S. Wu, X. Kou, T. Liu, X. Xu, Novel coumarin-thiazolidine-2,4-dione hybrids as potential α-glucosidase inhibitors: Synthesis and bioactivity evaluation, J Mol Struct 1322 (2025) 140481. https://doi.org/10.1016/j.molstruc.2024.140481.

[37] S. Mohd, V. Sharma, V. Harish, R. Kumar, G. Pilli, Exploring Thiazolidinedione-Naphthalene Analogues as Potential Anti-diabetic Agents: Design, Synthesis, Molecular Docking and In-vitro Evaluation, Cell Biochem Biophys 83 (2024) 2213–2226. https://doi.org/10.1007/s12013-024-01632-y.

[38] G. Singh, R. Singh, V. Monga, S. Mehan, 3,5-Disubstituted-thiazolidine-2,4-dione hybrids as anti-diabetic agents: Design, synthesis, in-vitro and In vivo evaluation, Eur J Med Chem 266 (2024) 116139. https://doi.org/10.1016/j.ejmech.2024.116139.

[39] S. Gharge, S.G. Alegaon, S. Jadhav, S.D. Ranade, R.S. Kavalapure, Design, synthesis, characterization and anti-diabetic evaluation of 3,5-substituted thiazolidinediones: Evidenced by network pharmacology, Molecular docking, dynamic simulation, in vitro and in vivo assessment, European Journal of Medicinal Chemistry Reports 12 (2024) 100213. https://doi.org/10.1016/j.ejmcr.2024.100213.

[40] M.A. Gamal, S.H. Fahim, S. Giovannuzzi, M.A. Fouad, A. Bonardi, P. Gratteri, C.T. Supuran, G.S. Hassan, Probing benzenesulfonamide–thiazolidinone hybrids as multitarget directed ligands for efficient control of type 2 diabetes mellitus through targeting the enzymes: α-glucosidase and carbonic anhydrase II, Eur J Med Chem 271 (2024) 116434. https://doi.org/10.1016/j.ejmech.2024.116434.

[41] C. Hu, B. Liang, J. Sun, J. Li, Z. Xiong, S.-H. Wang, X. Xuetao, Synthesis and biological evaluation of indole derivatives containing thiazolidine-2,4-dione as α-glucosidase inhibitors with anti-diabetic activity, Eur J Med Chem 264 (2024) 115957. https://doi.org/10.1016/j.ejmech.2023.115957.

[42] M. Li, J. Sun, B. Liang, X. Min, J. Hu, R. Wu, X. Xu, Thiazolidine-2,4-dione derivatives as potential α-glucosidase inhibitors: Synthesis, inhibitory activity, binding interaction and hypoglycemic activity, Bioorg Chem 144 (2024) 107177. https://doi.org/10.1016/j.bioorg.2024.107177.

[43] G. Singh, R. Singh, V. Monga, S. Mehan, Thiazolidine-2,4-dione hybrids as dual alpha-amylase and alpha-glucosidase inhibitors: design, synthesis, in vitro and in vivo anti-diabetic evaluation, RSC Med Chem 15 (2024) 2826–2854. https://doi.org/10.1039/D4MD00199K.

[44] M. Shah, M.S. Jan, A. Sadiq, S. Khan, U. Rashid, SAR and lead optimization of (Z)-5-(4-hydroxy-3-methoxybenzylidene)-3-(2-morpholinoacetyl)thiazolidine-2,4-dione as a potential multi-target anti-diabetic agent, Eur J Med Chem 258 (2023) 115591. https://doi.org/10.1016/j.ejmech.2023.115591.

[45] M.A. Doddagaddavalli, V.K.A. Kalalbandi, T.R.R. Naik, S.D. Joshi, J. Seetharamappa, Fluorenone–thiazolidine-4-one scaffolds as anti-diabetic and antioxidant agents: design, synthesis, X-ray crystal structures, and binding and computational studies, New Journal of Chemistry 47 (2023) 13581–13599. https://doi.org/10.1039/D3NJ01922E.

[46] Y. Zheng, M. Li, S. Wu, L. Li, Z. Xiong, X. Xu, K. Zhang, Y. Wen, Synthesis and biological evaluation of chromone-thiazolidine-2,4-dione derivatives as potential α-glucosidase inhibitors, Arabian Journal of Chemistry 16 (2023) 105279. https://doi.org/10.1016/j.arabjc.2023.105279.

[47] S. Khan, H. Ullah, F. Rahim, M. Taha, R. Hussain, M.S. Khan, H. Ali, M.U. Khan, S.A.A. Shah, K.M. Khan, New thiazole-based thiazolidinone derivatives: Synthesis, in vitro α-amylase, α-glucosidase activities and silico molecular docking study, Chemical Data Collections 42 (2022) 100967. https://doi.org/10.1016/j.cdc.2022.100967.

[48] S. Khan, S. Iqbal, F. Rahim, M. Shah, R. Hussain, H. Alrbyawi, W. Rehman, A.A. Dera, L. Rasheed, H.H. Somaily, R.A. Pashameah, E. Alzahrani, A.-E. Farouk, New Biologically Hybrid Pharmacophore Thiazolidinone-Based Indole Derivatives: Synthesis, In Vitro Alpha-Amylase and Alpha-Glucosidase Along with Molecular Docking Investigations, Molecules 27 (2022) 6564. https://doi.org/10.3390/molecules27196564.

[49] S. Khan, S. Iqbal, M. Khan, W. Rehman, M. Shah, R. Hussain, L. Rasheed, Y. Khan, A.A. Dera, R.A. Pashameah, E. Alzahrani, A.-E. Farouk, Design, Synthesis, In Silico Testing, and In Vitro Evaluation of Thiazolidinone-Based Benzothiazole Derivatives as Inhibitors of α-Amylase and α-Glucosidase, Pharmaceuticals 15 (2022) 1164. https://doi.org/10.3390/ph15101164.

[50] V.M. Patil, K.N. Tilekar, N.M. Upadhyay, C.S. Ramaa, Synthesis, In-Vitro Evaluation and Molecular Docking Study of N-Substituted Thiazolidinediones as α-Glucosidase Inhibitors, ChemistrySelect 7 (2022). https://doi.org/10.1002/slct.202103848.

[51] H. Ullah, I. Uddin, F. Rahim, F. Khan, Sobia, M. Taha, M.U. Khan, S. Hayat, M. Ullah, Z. Gul, S. Ullah, H. Zada, J. Hussain, In vitro α-glucosidase and α-amylase inhibitory potential and molecular docking studies of benzohydrazide based imines and thiazolidine-4-one derivatives, J Mol Struct 1251 (2022) 132058. https://doi.org/10.1016/j.molstruc.2021.132058.

[52] S. Fettach, F.Z. Thari, Z. Hafidi, H. Tachallait, K. Karrouchi, M. El achouri, Y. Cherrah, H. Sefrioui, K. Bougrin, M.E.A. Faouzi, Synthesis, α-glucosidase and α-amylase inhibitory activities, acute toxicity and molecular docking studies of thiazolidine-2,4-diones derivatives, J Biomol Struct Dyn 40 (2022) 8340–8351. https://doi.org/10.1080/07391102.2021.1911854.

[53] E.S. Moghadam, M.H. Tehrani, R. Abdel-Jalil, M.A. Faramarzi, M. Amini, Design, Synthesis and Bioactivity Investigation of Novel 2,3-Diarylthiazolidine-4-Ones as Potent α-Glucosidase Inhibitors, Polycycl Aromat Compd 42 (2022) 5748–5766. https://doi.org/10.1080/10406638.2021.1962369.

[54] F.Z. Thari, S. Fettach, E.H. Anouar, H. Tachallait, H. Albalwi, Y. Ramli, J.T. Mague, K. Karrouchi, M.E.A. Faouzi, K. Bougrin, Synthesis, crystal structures, α-glucosidase and α-amylase inhibition, DFT and molecular docking investigations of two thiazolidine-2,4-dione derivatives, J Mol Struct 1261 (2022) 132960. https://doi.org/10.1016/j.molstruc.2022.132960.

[55] L. Gummidi, N. Kerru, O. Ebenezer, P. Awolade, O. Sanni, Md.S. Islam, P. Singh, Multicomponent reaction for the synthesis of new 1,3,4-thiadiazole-thiazolidine-4-one molecular hybrids as promising anti-diabetic agents through α-glucosidase and α-amylase inhibition, Bioorg Chem 115 (2021) 105210. https://doi.org/10.1016/j.bioorg.2021.105210.

[56] R. Kaur, R. Kumar, N. Dogra, A. Kumar, A.K. Yadav, M. Kumar, Synthesis and Studies of Thiazolidinedione–Isatin Hybrids As α-Glucosidase Inhibitors for Management of Diabetes, Future Med Chem 13 (2021) 457–485. https://doi.org/10.4155/fmc-2020-0022.

[57] G. Singh, A. Singh, V. Singh, R.K. Verma, J. Tomar, R. Mall, Synthesis, molecular docking, α-glucosidase inhibition, and antioxidant activity studies of novel benzimidazole derivatives, Medicinal Chemistry Research 29 (2020) 1846–1866. https://doi.org/10.1007/s00044-020-02605-5.

[58] K.R.A. Abdellatif, W.A.A. Fadaly, G.M. Kamel, Y.A.M.M. Elshaier, M.A. El-Magd, Design, synthesis, modeling studies and biological evaluation of thiazolidine derivatives containing pyrazole core as potential anti-diabetic PPAR-γ agonists and anti-inflammatory COX-2 selective inhibitors, Bioorg Chem 82 (2019) 86–99. https://doi.org/10.1016/j.bioorg.2018.09.034.

[59] P. Kumar, M. Duhan, J. Sindhu, K. Kadyan, S. Saini, N. Panihar, Thiazolidine-4-one clubbed pyrazoles hybrids: Potent α-amylase and α-glucosidase inhibitors with NLO properties, J Heterocycl Chem 57 (2020) 1573–1587. https://doi.org/10.1002/jhet.3882.

[60] N. Senthilkumar, V. Vijayakumar, S. Sarveswari, G.A. Gayathri, M. Gayathri, Synthesis of New Thiazolidine-2,-4-dione-azole Derivatives and Evaluation of Their α-Amylase and α-Glucosidase Inhibitory Activity, Iranian Journal of Science and Technology, Transactions A: Science 43 (2019) 735–745. https://doi.org/10.1007/s40995-018-0593-x.

[61] F. Hussain, Z. Khan, M.S. Jan, S. Ahmad, A. Ahmad, U. Rashid, F. Ullah, M. Ayaz, A. Sadiq, Synthesis, in-vitro α-glucosidase inhibition, antioxidant, in-vivo anti-diabetic and molecular docking studies of pyrrolidine-2,5-dione and thiazolidine-2,4-

dione derivatives, Bioorg Chem 91 (2019) 103128. https://doi.org/10.1016/j.bioorg.2019.103128.

[62] G. Wang, Y. Peng, Z. Xie, J. Wang, M. Chen, Synthesis, α-glucosidase inhibition and molecular docking studies of novel thiazolidine-2,4-dione or rhodanine derivatives, Medchemcomm 8 (2017) 1477–1484. https://doi.org/10.1039/C7MD00173H.

[63] N. Singh, S.S. Yadav, S. Kumar, B. Narashiman, A review on traditional uses, phytochemistry, pharmacology, and clinical research of dietary spice Cuminum cyminum L., Phytotherapy Research 35 (2021) 5007–5030. https://doi.org/10.1002/ptr.7133.

[64] H. V. Gangadharappa, K. Mruthunjaya, R.P. Singh, Cuminum cyminum -A popular spice: An updated review, Pharmacognosy Journal 9 (2017) 292–301. https://doi.org/10.5530/pj.2017.3.51.

[65] H.B. Sowbhagya, Chemistry, Technology, and Nutraceutical Functions of Cumin (cuminum cyminum L): An Overview, Crit Rev Food Sci Nutr 53 (2013) 1–10. https://doi.org/10.1080/10408398.2010.500223.

[66] H.B. Sowbhagya, P. Srinivas, K.T. Purnima, N. Krishnamurthy, Enzyme-assisted extraction of volatiles from cumin (Cuminum cyminum L.) seeds, Food Chem 127 (2011) 1856–1861. https://doi.org/10.1016/j.foodchem.2011.02.001.

[67] S. Ramya, T. Loganathan, M. Chandran, R. Priyanka, K. Kavipriya, G.L. Grace Lydial Pushpalatha, D. Aruna, GC. Abraham, R. Jayakumararaj, ADME-Tox profile of Cuminaldehyde (4-Isopropylbenzaldehyde) from Cuminum cyminum seeds for potential biomedical applications, Journal of Drug Delivery and Therapeutics 12 (2022) 127–141. https://doi.org/10.22270/jddt.v12i2-s.5286.

[68] Y. Sunohara, K. Nakano, S. Matsuyama, T. Oka, H. Matsumoto, Cuminaldehyde, a cumin seed volatile component, induces growth inhibition, overproduction of reactive oxygen species and cell cycle arrest in onion roots, Sci Hortic 289 (2021) 110493. https://doi.org/10.1016/j.scienta.2021.110493.

[69] M.S. Ali, M.T. Rehman, H.A. Al-Lohedan, M.F. Alajmi, Study of the Binding of Cuminaldehyde with Bovine Serum Albumin by Spectroscopic and Molecular Modeling Methods, Journal of Spectroscopy 2023 (2023) 1–11. https://doi.org/10.1155/2023/4191046.

[70] S. Chatterjee, P. Paul, P. Chakraborty, S. Das, R.K. Sarker, S. Sarkar, A. Das, P. Tribedi, Cuminaldehyde exhibits potential antibiofilm activity against Pseudomonas aeruginosa involving reactive oxygen species (ROS) accumulation: a way forward towards sustainable biofilm management, 3 Biotech 11 (2021). https://doi.org/10.1007/s13205-021-03013-1.

[71] Q. Chen, X. Hu, J. Li, P. Liu, Y. Yang, Y. Ni, Preparative isolation and purification of cuminaldehyde and p-menta-1,4-dien-7-al from the essential oil of Cuminum cyminum L. by high-speed counter-current chromatography, Anal Chim Acta 689 (2011) 149–154. https://doi.org/10.1016/j.aca.2011.01.038.

[72] V. Meenatchi, S.M. Zo, S.Y. Won, J.W. Nam, L. Cheng, S.S. Han, Cuminaldehyde-3-hydroxy-2-napthoichydrazone: Synthesis, effect of solvents, nonlinear optical activity, antioxidant activity, antimicrobial activity, and DFT analysis, Spectrochim Acta A Mol Biomol Spectrosc 302 (2023). https://doi.org/10.1016/j.saa.2023.123071.

[73] R. Hamdy, A.M. Hamoda, M. Al-Khalifa, V. Menon, R. El-Awady, S.S.M. Soliman, Efficient selective targeting of Candida CYP51 by oxadiazole derivatives designed from plant cuminaldehyde, RSC Med Chem 13 (2022) 1322–1340. https://doi.org/10.1039/d2md00196a.

[74] T. Zhang, M. Dong, J. Zhao, X. Zhang, X. Mei, Synthesis and antifungal activity of novel pyrazolines and isoxazolines derived from cuminaldehyde, J Pestic Sci 44 (2019) 181–185. https://doi.org/10.1584/jpestics.D19-028.

[75] F. Degola, F. Bisceglie, M. Pioli, S. Palmano, L. Elviri, G. Pelosi, T. Lodi, F.M. Restivo, Structural modification of cuminaldehyde thiosemicarbazone increases inhibition specificity toward aflatoxin biosynthesis and sclerotia development in Aspergillus flavus, Appl Microbiol Biotechnol 101 (2017). https://doi.org/10.1007/s00253-017-8426-y.

[76] A. Rajavel, T. Jeyakumar, M.L. Sundararajan, T. Srinivasan, D. Velmurugan, Synthesis, crystal structure, characterization, and microbial evaluation of (E)-N-(4-isopropylbenzylidene)thiophene-2-carbohydrazide, Molecular Crystals and Liquid Crystals 631 (2016). https://doi.org/10.1080/15421406.2016.1170285.

[77] W. Gładkowski, A. Skrobiszewski, M. Mazur, A. Gliszczyńska, M. Czarnecka, A. Pawlak, B. Obmińska-Mrukowicz, G. Maciejewska, A. Białońska, Chiral δ-iodo-γ-lactones derived from cuminaldehyde, 2,5-dimethylbenzaldehyde and piperonal: Chemoenzymatic synthesis and antiproliferative activity, Tetrahedron Asymmetry 27 (2016). https://doi.org/10.1016/j.tetasy.2016.02.003.

[78] F. Degola, C. Morcia, F. Bisceglie, F. Mussi, G. Tumino, R. Ghizzoni, G. Pelosi, V. Terzi, A. Buschini, F.M. Restivo, T. Lodi, In vitro evaluation of the activity of thiosemicarbazone derivatives against mycotoxigenic fungi affecting cereals, Int J Food Microbiol 200 (2015). https://doi.org/10.1016/j.ijfoodmicro.2015.02.009.

[79] F. Bisceglie, S. Pinelli, R. Alinovi, M. Goldoni, A. Mutti, A. Camerini, L. Piola, P. Tarasconi, G. Pelosi, Cinnamaldehyde and cuminaldehyde thiosemicarbazones and their copper(II) and nickel(II) complexes: A study to understand their biological activity, J Inorg Biochem 140 (2014). https://doi.org/10.1016/j.jinorgbio.2014.07.014.

[80] D. Arish, M.S. Nair, Synthesis, characterization, antimicrobial, and nuclease activity studies of some metal Schiff-base complexes, J Coord Chem 63 (2010). https://doi.org/10.1080/00958972.2010.483729.

[81] P.K. Kaushik, V.K. Varshney, P. Kumar, P. Bhatia, S. V. Shukla, Microwave-assisted synthesis, characterization, and antimicrobial activity of some odorant Schiff bases derived from naturally occurring carbonyl compounds and anthranilic acid, Synth Commun 46 (2016). https://doi.org/10.1080/00397911.2016.1245749.

[82] H. A. Saad, S. H. Abdel-Hafez, Synthesis and Biological Activity of Some Nucleoside Analogs of 3-Cyanopyridin-2- one, Curr Org Synth 9 (2012). https://doi.org/10.2174/157017912801270540.

CHAPTER-III

Synthesis, single crystal XRD, *in vitro* evaluation, molecular docking and ADMET studies of cuminaldehyde-thiazolidine-2,4-dione hybrids as potential α-glucosidase inhibitors

1. Introduction:

Diabetes mellitus (DM) is a chronic, progressive condition characterized by hyperglycemia and long-term microvascular and macrovascular consequences. It impacts millions globally and is projected to affect 700 million by 2045 [1–3]. Patients with type 2 diabetes (T2D) utilize hypoglycemic agents to manage postprandial hyperglycemia. DM results in significant health complications, including cardiovascular illnesses, hypertension, obesity, renal disorders, and visual impairment [4–9]. α-glucosidase inhibitors serve as a treatment to manage DM by obstructing the digestion of dietary carbohydrates, which generate monosaccharide units that subsequently enter the circulation. α-glucosidase inhibitors, including acarbose, voglibose, and miglitol, serve as first-line oral hypoglycemic medicines under moderate circumstances and as adjunct therapy in acute scenarios [10]. Although contemporary α-glucosidase inhibitors are beneficial, their adverse effects, including stomach discomfort, gas, and diarrhoea, might pose challenges [11]. Therefore, novel α-glucosidase inhibitors are significant since they assist researchers and pharmaceutical companies in identifying safer and more efficacious treatments. This has the potential to enhance the quality of life for individuals living with DM by leading to more effective treatment alternatives.

Among various bioactive heterocyclic nuclei, thiazolidinedione (TZD) plays a crucial role in providing molecules that are potent anti-diabetic agents [12,13]. Glitazones, or TZDs, are recognized for their PPAR-gamma agonistic properties, which enhance insulin production and modulate glucose metabolism. Troglitazone, rosiglitazone, and pioglitazone received approval from the US FDA in 1997, 1999, and 2007, respectively, for the treatment of T2D. However, troglitazone and rosiglitazone have been pulled from the market due to hepatotoxicity and myocardial infarction [14]. Pioglitazone is

only available globally [1,15]. TZD derivatives have a wide spectrum of pharmacological activities such as anti-cancer [16–18], antimicrobial [19,20], anti-tubercular [21], antioxidant [22,23], anti-inflammatory [24,25], anti-obesity [26,27] agents.

Molecular hybridization is an attractive approach in drug design that aids in the discovery of pharmacological agents for diverse diseases, promoting the development novel therapeutic agents with enhanced efficacy and diminished adverse effects [28]. About 20% of approved drugs have used this approach in recent years. Recently, many studies employed this strategy to synthesize synthetic α-glucosidase inhibitors and elucidated their mechanism of α-glucosidase inhibition [29–33].

TZD-heterocyclic hybrids have a favored pharmacophore in medicinal chemistry, prompting research to investigate their pharmacological significance [34,35]. Moreover, in recent times, various TZD derivatives and their hybrids have been investigated as possible α-glucosidase inhibitors for the management of T2D, as presented in **Figure 1** [1,2,36–38]. In 2004, Li *et al.* developed TZD-thiadiazole derivatives as effective α-glucosidase inhibitors (**1A**; **Figure 1**) [36]. Hu *et al.* developed indole-TZD hybrids as effective α-glucosidase inhibitors (**1B**; **Figure 1**) [37]. Similarly, Singh *et al.* discovered 3,5-Disubstituted-TZD hybrids as anti-diabetic agents by targeting α-glucosidase (**1C and 1D**; **Figure 1**) [1,2]. On the other hand, Daud *et al.* developed ibuprofen and mefenamic acid Schiff base analogues as α-glucosidase inhibitors (**1E**; **Figure 1**) [38]. In 2005, Lee *et al.* also revealed that cuminaldehyde has α-glucosidase inhibitory action with an IC_{50} value of 0.50 mg/ml (**1F**; **Figure 1**) [39].

These prior results indicate that TZD and cuminaldehyde may serve as viable pharmacophoric fragments for the identification and development of newer α-glucosidase inhibitors. Encouraged by the earlier research and our ongoing endeavours

to discover TZD-derived possible α-glucosidase inhibitors, we planned to synthesize cuminaldehyde-TZD hybrids (**6a-6h**, **6i-6l**, and **6m**) as potential anti-diabetic agents through the inhibition of α-glucosidase (**Figure 1**). All synthesized substances were evaluated for their α-glucosidase inhibitory activities *in vitro*. Additionally, the interaction mechanism between α-glucosidase and the best molecule was investigated by enzyme kinetic fluorescence quenching circular dichroism spectroscopy. Further, the best molecule was subjected to *in silico* molecular docking and ADMET predictions. The cell viability assay of the best molecule was also carried out against the human embryonic kidney (HEK-293) cell line.

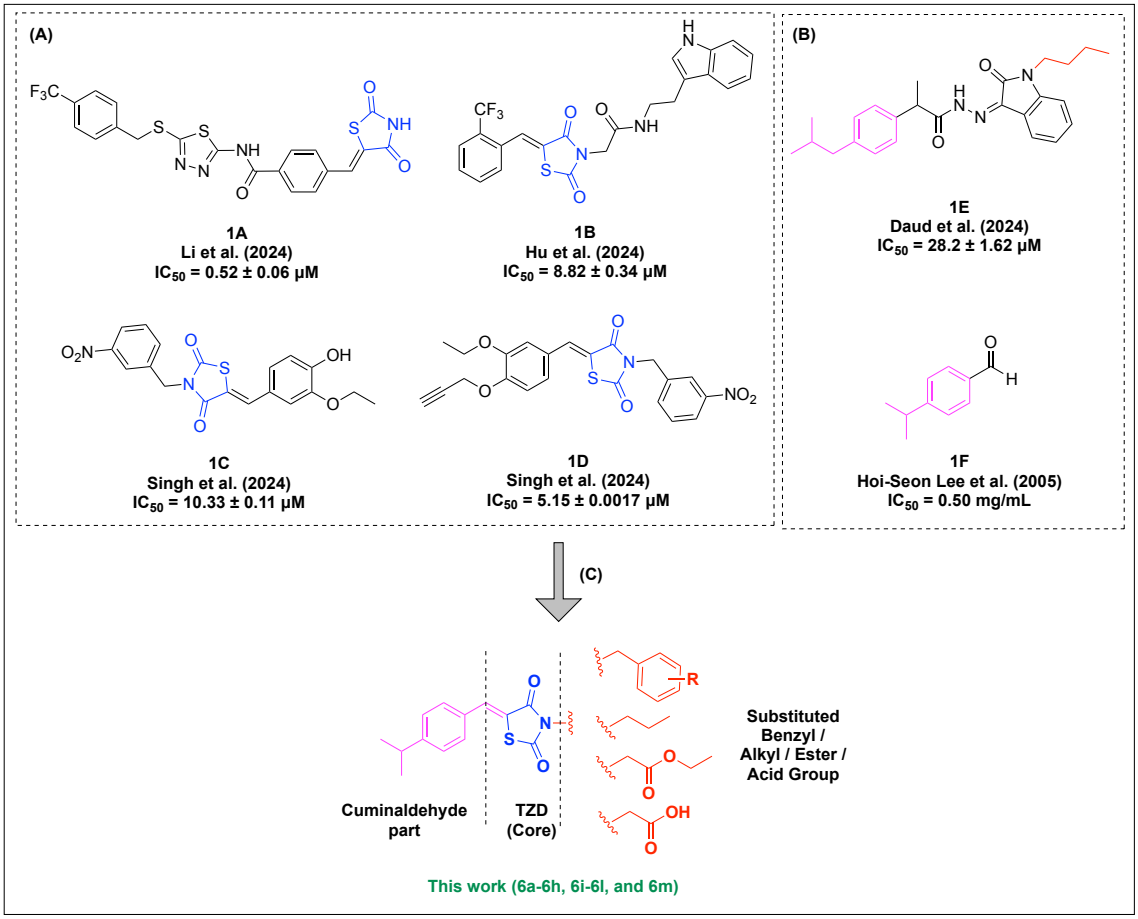

Figure 1: (A) Structure of α-glucosidase inhibitors containing TZD [1,2,36]; (B) Structure of α-glucosidase inhibitors (ibuprofen Schiff base and cuminaldehyde) [38,39]; (C) Designing of cuminaldehyde-TZD hybrids for potential α-glucosidase inhibitors.

2. Experimental section:

2.1. Chemistry:

All required chemicals and solvents of the highest grades for this research work were purchased from commercial suppliers. Thin layer chromatography (TLC) was performed on 0.20 mm Silica Gel 60 F254 plates, and an ultraviolet light chamber (short and long wavelength) was used to monitor the synthesis process. The melting point of the synthesized compounds was determined using the VEEGO melting point apparatus. Nuclear magnetic resonance (NMR) spectra at 400/300 MHz (^{1}H NMR) and 101/75 MHz (^{13}C NMR) were recorded on a Bruker Avance NMR Spectrophotometer (Germany), respectively, using $CDCl_3$ and DMSO-d_6 as solvent. The chemical shifts were reported in parts per million (ppm) concerning the internal standard tetramethylsilane (TMS) (δ = 0.00 ppm), and coupling constant values were reported in Hertz (Hz). The following are the descriptions of the peak splitting: dd (doublet of doublets), t (triplet), q (quartet), m (multiplet), and s (singlet). Mass spectra (*m/z*) were recorded using an ESI (ETM, positive/negative ion mode) mass spectrometry instrument (API 2000 ABSCIEX). X-ray crystal structure determination was performed using a single-crystal X-ray diffractometer (Bruker SMART, Germany).

2.1.1. Synthesis of thiazolidine-2,4-dione (TZD; Compound 3):

In a 150 mL round-bottomed flask, 28.35 g chloroacetic acid (compound **1**; 0.3 mol) and 22.83 g thiourea (compound **2;** 0.3 mol) were dissolved in 35 mL of water. The mixture was stirred for 1 h to form a white precipitate, accompanied by considerable cooling. To the contents of the flask, 18 mL of concentrated hydrochloric acid was then added slowly from a dropping funnel, and the flask was then connected with a reflux condenser, and gentle

heat was applied to produce a complete solution, after which the reaction mixture was stirred and refluxed for 8–10 h at 100–110 °C. The progress of the reaction was monitored by using TLC using n-hexane/ethyl acetate 3:2 as an eluent. On cooling, the contents of the flask solidified to a cluster of white needles; the TZD (compound **3**) was filtered and washed with double distilled water to remove traces of hydrochloric acid and dried. Finally, the TZD (compound **3**) was purified by recrystallization from ethyl alcohol [2,40].

2.1.2. (Z)-5-(4-isopropylbenzylidene)thiazolidine-2,4-dione (Compound 5):

To get the Knoevenagel condensation (KC) product, 0.550 g TZD (Compound **3**; 0.004 mol) and 0.7 g of cuminaldehyde (compound **4**; 0.004 mol) were taken in 50 mL of RBF and added 10 mL of acetic acid with stirring for 5 mins. Then, 0.423 g urea (0.007 mol) was added and stirred for 15 mins. After 15 mins, the reaction mixture was set up for reflux condition at 100 ^{o}C for 10-12 h, and the reaction was monitored by performing TLC. After completion of the reaction, the reaction mixture was poured into crushed ice in a beaker. The precipitated solid was filtered under vacuum, dried at RT, and recrystallized from EtOH/Methanol to obtain pure product **5** [40].

(Z)-5-(4-isopropylbenzylidene)thiazolidine-2,4-dione (Compound 5):

^{1}H NMR (300 MHz, $CDCl_3$) δ 9.482 (s, 1H), 7.866 (s, 1H), 7.459 – 7.424 (m, 2H), 7.355 – 7.327 (m, 2H), 2.96 (p, *J* = 6.9 Hz, 1H), 1.27 (d, *J* = 6.9 Hz, 6H). **^{13}C NMR** (101 MHz, $CDCl_3$) δ 167.6, 167.0, 152.4, 134.7, 130.6, 130.5, 127.5, 121.1, 34.2, 23.7. **FT-IR** (ATR) υmax/cm^{-1}: 3739.49 (-NH

str.), 2385.53, 2312.26 (C-H str.), 1694.79, 1516.27 (CH_3-CH_3 str.). **MS (ESI)** *m/z:* $[M-H]^+$ calcd. for $C_{13}H_{12}NO_2S^+$: 244.8; found 245.8

2.1.3. General procedure for synthesis of (Z)-3-substituted-5-(4-isopropylbenzylidene)thiazolidine-2,4-dione (Compound 6a-6l):

First, anhydrous K_2CO_3 (2 equiv) in a 100 mL flat bottom flask was taken and heated for 2-3 mins to remove the excess moisture. Then, the (Z)-5-(4-isopropylbenzylidene)thiazolidine-2,4-dione (Compound **5**; 0.002 mol) was dissolved in 15 ml of dimethylformamide (DMF) in a 100 mL flat bottom flask and stirred for 15-20 mints in an RT condition. Then, the substituted benzyl chlorides (1.2 equiv)/ alkyl halides (1.2 equiv) were added dropwise and stirred (400-600 rpm) on a magnetic stirrer at RT for 10-12 h. After completion of the reaction, TLC was performed to monitor the reaction. After that, the reaction mixture was diluted with ethyl acetate and extracted from water using a separating funnel. Finally, the ethyl acetate phase was concentrated under a vacuum to give substituted target compounds (Compound **6a-6l**). The physicochemical properties of synthesized compounds (Compound **5** and **6a-6m**) are presented in **Table 1**.

Table 1: Physiochemical properties of synthesized compounds (Compound **5** and **6a-6m**).

Compound	Molecular formula	Molecular mass (g/mol)	Appearance	% yield	Melting point (°C)	R_f (H-EA: 4:1)
5	$C_{13}H_{13}NO_2S$	247.1	Creamy brown solid	88.32%	160-162 °C	0.72
6a	$C_{20}H_{19}NO_2S$	337.1	White solid	79.12%	138-140 °C	0.63
6b	$C_{21}H_{21}NO_2S$	351.1	Creamy white crystal	76.82%	130-132 °C	0.54
6c	$C_{20}H_{18}ClNO_2S$	371.1	Creamy white crystal	77.22%	158-160 °C	0.64
6d	$C_{20}H_{17}Cl_2NO_2S$	405.0	Shining white crystals	75.81%	142-144 °C	0.68

6e	$C_{20}H_{18}FNO_2S$	355.1	White crystal	72.35%	125-127 °C	0.65
6f	$C_{20}H_{18}ClNO_2S$	371.1	Shining white crystals	74.71%	118-120 °C	0.60
6g	$C_{20}H_{17}Cl_2NO_2S$	405.0	Creamy white crystal	72.68%		0.67
6h	$C_{20}H_{18}BrNO_2S$	416.3	White flakes	77.42%	158-160 °C	0.58
6i	$C_{17}H_{21}NO_2S$	303.1	White crystal	75.34%	104-106 °C	0.64
6j	$C_{18}H_{23}NO_2S$	317.1	White flakes	72.41%	109-111 °C	0.56
6k	$C_{17}H_{21}NO_2S$	303.1	White flakes	82.12%	80-82 °C	0.64
6l	$C_{17}H_{19}NO_4S$	333.1	White flakes	75.20%	104-110 °C	0.46
6m	$C_{15}H_{15}NO_4S$	305.1	Pale yellow solid	86.22%	-	0.2

H-EA: Hexane: Ethyl acetate

(Z)-3-benzyl-5-(4-isopropylbenzylidene)thiazolidine-2,4-dione

*(Compound **6a):***

^{1}H NMR (400 MHz, $CDCl_3$) δ 7.89 (s, 1H), 7.45 (d, *J* = 1.8 Hz, 1H), 7.44 (s, 1H), 7.43 (s, 1H), 7.42 (s, 1H), 7.36 (d, *J* = 1.9 Hz, 1H), 7.34 (s, 1H), 7.32 (s, 1H), 7.29 (d, *J* = 7.8 Hz, 1H), 4.90 (s, 2H), 2.95 (p, *J* = 6.9 Hz, 1H), 1.27 (d, *J* = 6.9 Hz, 6H). **^{13}C NMR** (101 MHz, $CDCl_3$) δ 168.0, 166.3, 152.1, 135.2, 134.2, 130.8, 130.5, 128.9, 128.8, 128.3, 127.4, 120.2, 45.2, 34.2, 23.7. **FT-IR** (ATR) υmax/cm^{-1}: 3850.88, 3739.03, 3600.03 (Benzyl C-H str.), 2810.88 (CH_2 str.), 2312.29 (C-H str.), 1643.35 (C=O str.), 1513.07, 1378.21 (CH_3-CH_3 str.), 1169.35 (Benzyl C-H str.), 833.83 (Benzyl C-H str.). **MS (ESI)** *m/z:* $[M-H]^+$ calcd. for $C_{20}H_{18}NO_2S^+$: 334.7; found 335.7

(Z)-5-(4-isopropylbenzylidene)-3-(4-methylbenzyl)thiazolidine-2,4-dione (Compound 6b):

^{1}H NMR (400 MHz, $CDCl_3$) δ 7.88 (s, 1H), 7.44 (s, 1H), 7.42 (s, 1H), 7.35 (s, 1H), 7.33 (s, 1H), 7.31 (s, 1H), 7.15 (s, 1H), 7.13 (s, 1H), 4.86 (s, 2H), 2.95 (p, *J* = 7.0 Hz, 1H), 2.32 (s, 3H), 1.27 (d, *J* = 6.9 Hz, 6H). **^{13}C NMR** (101 MHz, $CDCl_3$) δ 168.0, 166.3, 152.1, 138.1, 134.1, 132.3, 130.9, 130.5, 129.4, 128.9, 127.4, 120.3, 45.0, 34.2, 23.7, 21.2. **FT-IR** (ATR) υmax/cm^{-1}: 3862.36, 3735.88 (Benzyl C-H str.), 3390.32 (CH_2 str.), 2311.48 (C-H str.), 1660.63 (C=O str.), 1516.37, 1375.09 (CH_3-CH_3 str.), 1160.64 (Benzyl C-H str.), 829.02 (Benzyl C-H str.). **MS (ESI)** *m/z:* $[M+H]^+$ calcd. for $C_{21}H_{22}NO_2S^+$: 352.1; found 352.2

(Z)-3-(4-chlorobenzyl)-5-(4-isopropylbenzylidene)thiazolidine-2,4-dione (Compound 6c):

^{1}H NMR (400 MHz, $CDCl_3$) δ 7.89 (s, 1H), 7.43 (d, *J* = 7.9 Hz, 2H), 7.38 (d, *J* = 8.0 Hz, 2H), 7.31 (t, *J* = 9.3 Hz, 4H), 4.86 (s, 2H), 2.95 (p, *J* = 7.0 Hz, 1H), 1.27 (s, 3H), 1.26 (s, 3H). **^{13}C NMR** (101 MHz, $CDCl_3$) δ 168.0, 166.2, 152.3, 134.5, 134.3, 133.7, 130.7, 130.5, 130.4, 128.9, 127.4, 120.0, 44.5, 34.2, 23.7. **FT-IR** (ATR) υmax/cm-1: 3863.32, 3736.45 (Benzyl C-H str.), 3613.06 (CH2 str.), 2384.68, 2311.68 (C-H str.), 1667.07 (C=O str.), 1517.55, 1376.96 (CH3-CH3 str.), 1153.29 (Benzyl C-H str.), 698.46 (Benzyl C-H str.). **MS (ESI)** *m/z:* $[M-H]^+$ calcd. for $C_{20}H_{17}ClNO_2S^+$: 370.1; found 370.2

(Z)-3-(2,4-dichlorobenzyl)-5-(4-isopropylbenzylidene)thiazolidine-2,4-dione (*Compound* ***6d):***

^{1}H NMR (400 MHz, $CDCl_3$) δ 7.92 (d, *J* = 1.9 Hz, 1H), 7.48 – 7.43 (m, 2H), 7.41 (d, *J* = 2.7 Hz, 1H), 7.37 – 7.33 (m, 2H), 7.21 (d, *J* = 8.3 Hz, 1H), 7.16 (d, *J* = 1.9 Hz, 1H), 5.00 (d, *J* = 2.0 Hz, 2H), 3.00 – 2.92 (m, 1H), 1.29 – 1.28 (m, 3H), 1.26 (d, *J* = 2.1 Hz, 3H). **^{13}C NMR** (101 MHz, $CDCl_3$) δ 167.7, 166.1, 152.4, 134.8, 134.4, 130.7, 130.6, 129.8, 129.7, 127.5, 127.3, 119.6, 42.4, 34.2, 23.7. **FT-IR** (ATR) υmax/cm^{-1}: 3850.82, 3736.94 (Benzyl C-H str.), 3598.64 (CH_2 str.), 2385.05, 2311.75 (C-H str.), 1696.13 (C=O str.), 1516.40, 1378.58 (CH_3-CH_3 str.), 704.09 (Benzyl C-H str.). **MS (ESI)** *m/z:* $[M+H]^+$ calcd. for $C_{20}H_{18}Cl_2NO_2S^+$: 406.0; found 406.2

(Z)-3-(4-fluorobenzyl)-5-(4-isopropylbenzylidene)thiazolidine-2,4-dione (*Compound* ***6e):***

^{1}H NMR (400 MHz, $CDCl_3$) δ 7.89 (s, 1H), 7.45 (d, *J* = 5.8 Hz, 2H), 7.42 (d, *J* = 1.7 Hz, 2H), 7.33 (d, *J* = 7.3 Hz, 2H), 7.05 – 6.98 (m, 2H), 4.86 (s, 2H), 2.95 (p, *J* = 6.8 Hz, 1H), 1.27 (s, 3H), 1.26 (d, *J* = 1.6 Hz, 3H). **^{13}C NMR** (101 MHz, $CDCl_3$) δ 168.0, 166.3, 152.2, 134.4, 131.1, 131.1, 131.0, 130.9, 130.8, 130.5, 127.4, 115.8, 44.5, 34.2, 23.7, 23.7. **FT-IR** (ATR) υmax/cm^{-1}: 3859.39, 3736.35 (Benzyl C-H str.), 3609.23 (CH_2 str.), 2387.81, 2309.36 (C-H str.), 1689.27 (C=O str.), 1513.01, 1378.06 (CH_3-CH_3 str.), 1158.86 (Benzyl C-H str.), 704.74 (Benzyl C-H str.). **MS (ESI)** *m/z:* $[M+H]^+$ calcd. for $C_{20}H_{19}FNO_2S^+$: 356.1; found 356.2

(Z)-3-(3-chlorobenzyl)-5-(4-isopropylbenzylidene)thiazolidine-2,4-dione (Compound 6f):

^{1}H NMR (400 MHz, $CDCl_3$) δ 7.90 (s, 1H), 7.45 (s, 1H), 7.43 (s, 2H), 7.33 (d, *J* = 8.1 Hz, 3H), 7.28 (s, 2H), 4.86 (s, 2H), 2.95 (p, *J* = 6.9 Hz, 1H), 1.28 (s, 3H), 1.26 (s, 3H). **^{13}C NMR** (101 MHz, $CDCl_3$) δ 167.9, 166.2, 152.3, 137.0, 134.6, 134.6, 130.5, 130.0, 129.0, 128.5, 127.5, 127.1, 119.9, 44.6, 34.2, 23.7. **FT-IR** (ATR) υmax/cm^{-1}: 3851.20, 3736.95 (Benzyl C-H str.), 3598.85 (CH_2 str.), 2311.78 (C-H str.), 1697.32 (C=O str.), 1516.57, 1378.48 (CH_3-CH_3 str.), 1168.88 (Benzyl C-H str.), 705.13 (Benzyl C-H str.). **MS (ESI)** *m/z:* $[M+H]^+$ calcd. for $C_{20}H_{19}ClNO_2S^+$: 372.1; found 372.3

(Z)-3-(3,4-dichlorobenzyl)-5-(4-isopropylbenzylidene)thiazolidine-2,4-dione (Compound 6g):

^{1}H NMR (400 MHz, $CDCl_3$) δ 7.90 (s, 1H), 7.54 (d, *J* = 2.0 Hz, 1H), 7.45 – 7.41 (m, 2H), 7.39 (s, 1H), 7.33 (d, *J* = 8.1 Hz, 2H), 7.29 (dd, *J* = 8.3, 2.1 Hz, 1H), 4.83 (s, 2H), 2.97-2.93 (m, 1H), 1.27 (d, *J* = 6.9 Hz, 6H). **^{13}C NMR** (101 MHz, CDCl3) δ 167.9, 166.1, 152.4, 135.2, 134.8, 130.9, 130.7, 130.7, 130.6, 128.4, 127.5, 119.8, 44.00, 34.2, 23.7. **FT-IR** (ATR) υmax/cm^{-1}: 3862.83, 3737.20 (Benzyl C-H str.), 3612.95 (CH_2 str.), 2310.98 (C-H str.), 1661.96 (C=O str.), 1593.28, 1372.37 (CH_3-CH_3 str.), 1140.18 (Benzyl C-H str.), 812.84 (Benzyl C-H str.). **MS (ESI)** *m/z:* $[M+H]^+$ calcd. for $C_{20}H_{18}Cl_2NO_2S^+$: 405.1; found 406.1

(Z)-3-(4-bromobenzyl)-5-(4-isopropylbenzylidene)thiazolidine-2,4-dione (Compound 6h):

^{1}H NMR (400 MHz, $CDCl_3$) δ 7.89 (s, 1H), 7.46 (d, *J* = 8.2 Hz, 2H), 7.43 (d, *J* = 7.8 Hz, 2H), 7.32 (dd, *J* = 8.3, 3.2 Hz, 3H), 4.84 (s, 2H), 3.00 – 2.88

(m, 1H), 1.27 (d, *J* = 7.0 Hz, 6H). **^{13}C NMR** (101 MHz, $CDCl_3$) δ 167.9, 166.2, 152.3, 134.9, 134.5, 134.2, 131.9, 130.7, 130.5, 127.4, 122.4, 120.0, 44.6, 34.2, 23.7. **FT-IR** (ATR) υmax/cm^{-1}: 3864.50, 3736.83 (Benzyl C-H str.), 3613.69 (CH_2 str.), 2385.16, 2311.72 (C-H str.), 1674.27 (C=O str.), 1516.47, 1378.20 (CH_3-CH_3 str.), 1161.49 (Benzyl C-H str.), 697.62 (Benzyl C-H str.). **MS (ESI)** *m/z:* $[M-H]^+$ calcd. for $C_{20}H_{17}BrNO_2S^+$: 415.3; found 415.1

(Z)-3-isobutyl-5-(4-isopropylbenzylidene)thiazolidine-2,4-dione

(*Compound* ***6i):***

^{1}H NMR (400 MHz, $CDCl_3$) δ 7.87 (s, 1H), 7.45 (d, *J* = 7.9 Hz, 2H), 7.33 (d, *J* = 7.9 Hz, 2H), 3.58 (dd, *J* = 7.5, 1.3 Hz, 2H), 2.95 (p, *J* = 7.0 Hz, 1H), 2.18 – 2.10 (m, 1H), 1.27 (dd, *J* = 7.0, 1.3 Hz, 6H), 0.94 (dd, *J* = 6.7, 1.2 Hz, 6H). **^{13}C NMR** (101 MHz, $CDCl_3$) δ 168.3, 166.8, 152.0, 133.8, 130.9, 130.5, 127.4, 120.3, 49.0, 34.2, 27.2, 23.7, 20.0. **FT-IR** (ATR) υmax/cm^{-1}: 3864.47, 3736.81 (Benzyl C-H str.), 3391.67 (CH_2 str.), 2311.75 (C-H str.), 1696.46 (C=O str.), 1516.36, 1376.79 (CH_3-CH_3 str.), 1166.91 (CH-CH_3-CH_3 C-H str.), 830.57 (C-H str.). **MS (ESI)** *m/z:* $[M+H]^+$ calcd. for $C_{17}H_{22}NO_2S^+$: 304.1; found 304.1

(Z)-3-isopentyl-5-(4-isopropylbenzylidene)thiazolidine-2,4-dione

(*Compound* ***6j):***

^{1}H NMR (400 MHz, $CDCl_3$) δ 7.87 (d, *J* = 2.0 Hz, 1H), 7.45 (dd, *J* = 8.3, 2.1 Hz, 2H), 7.33 (dd, *J* = 8.3, 2.1 Hz, 2H), 3.80 – 3.73 (m, 2H), 2.94 (dt, *J* = 13.1, 6.4 Hz, 1H), 1.62 (s, 1H), 1.59 – 1.51 (m, 2H), 1.27 (dd, *J* = 7.0, 2.0 Hz, 6H), 0.96 (dd, *J* = 6.4, 2.0 Hz, 6H). **^{13}C NMR** (101 MHz, $CDCl_3$) δ 168.1, 166.5, 152.0, 133.7, 130.9, 130.5, 127.4, 120.4, 40.6, 36.5, 34.2, 26.0,

23.7, 22.4. **FT-IR** (ATR) υmax/cm^{-1}: 3864.23, 3736.39 (Benzyl C-H str.), 3598.58 (CH_2 str.), 2311.45 (C-H str.), 1696.27 (C=O str.), 1516.65, 1377.66 (CH_3-CH_3 str.), 1167.76 (CH-CH_3-CH_3 C-H str.), 831.40 (C-H str.). **MS (ESI)** *m/z:* $[M+H]^+$ calcd. for $C_{18}H_{24}NO_2S^+$: 317.1; found 318.0

(Z)-3-butyl-5-(4-isopropylbenzylidene)thiazolidine-2,4-dione (*Compound **6k):***

^{1}H NMR (400 MHz, $CDCl_3$) δ 7.81 (s, 1H), 7.40 – 7.36 (m, 2H), 7.27 (d, *J* = 7.1 Hz, 2H), 3.69 (t, *J* = 7.3 Hz, 2H), 2.89 (p, *J* = 6.7 Hz, 1H), 1.64 – 1.57 (m, 2H), 1.30 (h, *J* = 7.7 Hz, 2H), 1.23 – 1.18 (m, 6H), 0.89 (t, *J* = 7.3 Hz, 3H). **^{13}C NMR** (101 MHz, $CDCl_3$) δ 168.2, 166.6, 152.0, 133.8, 130.9, 130.5, 127.4, 120.4, 41.8, 34.2, 29.8, 29.8, 23.7, 20.0, 13.6. **FT-IR** (ATR) υmax/cm^{-1}: 3850.85, 3736.24 (Benzyl C-H str.), 3391.53 (CH_2 str.), 2311.70 (C-H str.), 1641.03 (C=O str.), 1375.72 (CH_3-CH_3 str.), 1259.77, 1166.60 (CH_2-CH_2-CH_2-CH_3 C-H str.), 830.04 (C-H str.). **MS (ESI)** *m/z:* $[M-H]^+$ calcd. for $C_{17}H_{20}NO_2S^+$: 302.1; found 302.2

Ethyl (Z)-2-(5-(4-isopropylbenzylidene)-2,4-dioxothiazolidin-3-yl)acetate (*Compound **6l):***

^{1}H NMR (400 MHz, CDCl3) δ 7.92 (s, 1H), 7.49 – 7.42 (m, 2H), 7.38 – 7.31 (m, 2H), 4.47 (s, 2H), 4.24 (q, J = 7.1 Hz, 2H), 3.02 – 2.89 (m, 1H), 1.30 (d, J = 7.1 Hz, 3H), 1.28 – 1.26 (m, 6H) **^{13}C NMR** (101 MHz, $CDCl_3$) δ 167.7, 166.3, 165.8, 152.4, 134.9, 130.7, 130.6, 127.5, 119.8, 62.2, 42.1, 34.2, 23.7, 14.1. **FT-IR (ATR)** υmax/cm^{-1}: 3864.47, 3735.87 (Benzyl C-H str.), 3597.55 (CH_2 str.), 2311.67 (C-H str.), 1681.10 (C=O str.), 1516.61 (CH-$(CH_3)_2$ C-H str.), 1377.58 (Ester CH_2 C-H str.), 1203.70 (Aromatic C-H str.),

829.54 (CH_2-CH_3 C-H str.). **MS (ESI)** *m/z:* $[M+H]^+$ calcd. for $C_{17}H_{20}NO_4S^+$: 334.1; found 334.3

2.1.4. General procedure for synthesis of (Z)-2-(5-(4-isopropylbenzylidene)-2,4-dioxothiazolidin-3-yl)acetic acid (Compound 6m):

0.5 g of compound **6l** (0.5 mmol) was taken in a 150 ml round-bottomed flask. To the same flask, 3 mL of concentrated hydrochloric acid and 6 mL of glacial acetic acid were added in a 1:2 ratio and kept for reflux at 100 ºC for 2 to 3 hours. The reaction mixture was then cooled to room temperature and poured into ice-cold water. After a few minutes, the pale-yellow color precipitate was recovered by filtering under a vacuum, washing it with water for several times, and drying it at room temperature to get the target compound **6m** [41].

(Z)-2-(5-(4-isopropylbenzylidene)-2,4-dioxothiazolidin-3-yl)acetic acid (Compound 6m):

^{1}H NMR (300 MHz, $CDCl_3$) δ 7.93 (s, 1H), 7.48 – 7.43 (m, 2H), 7.34 (d, *J* = 8.3 Hz, 2H), 6.24 (s, 1H), 4.54 (s, 2H), 2.96 (p, *J* = 6.9 Hz, 1H), 1.27 (d, *J* = 6.9 Hz, 6H). **^{13}C NMR** (101 MHz, $CDCl_3$) δ 171.0, 167.6, 165.7, 152.5, 135.2, 133.9, 130.6, 127.5, 119.5, 41.7, 34.2, 23.7. **FT-IR (ATR)** υmax/cm^{-1}: 3735.25 (Benzyl C-H str.), 3597.68 (CH_2 str.), 3391.81, 2982.52 (OH bond in carboxylic acid O-H str.), 2893.69 (CH_2 C-H str.), 2386.09, 2311.36 (C-H str.), 1851.57 (Ester C=O str), 1743.13, 1695.87 (TZD C=O str.), 1516.60 (Dimethyl attached with aromatic ring C-H str.), 1378.30, 1166.64 (CH_2 C-H str.), 830.78 (O-H bond), 703.61 (O-H str.). **MS (ESI)** *m/z:* $[M-H]^+$ calcd. for $C_{15}H_{14}NO_4S^+$: 305.1; found 304.0

2.2. In vitro assay of α-glucosidase inhibitory activity:

The α-glucosidase inhibition assay was conducted in 96-well plates with minor modifications to the prior methodology, which was denoted by Meiyan Fan *et al.* [42]. The α-glucosidase enzyme derived from *Saccharomyces cerevisiae* (>100U/mg), p-nitrophenyl-α-d-glucopyranoside (pNPG) and acarbose were purchased from Sisco Research Laboratories Pvt. Ltd. In this assay, pNPG served as the substrate, whereas acarbose provided as the positive control. In 96-well plates, 20 µL of various concentrations of test samples and acarbose, dissolved in methanol, and 10 µL of α-glucosidase (0.5 U/mL) soluble in 0.1 mM phosphate buffer (pH 6.8) were allowed to incubate at 37 °C for 15 minutes. Subsequent to pre-incubation, 20 µL of PNPG substrate, which was soluble in the previously mentioned phosphate buffer (pH 6.8), was introduced into each well and again incubated at 37 °C for 25 minutes. The alteration in absorbance was measured at 405 nm using a SpectraMax M5 multi-mode microplate reader (Molecular Devices, California, USA). The percentage of inhibition for examined substances, control, and positive control was represented as % inhibition and calculated by using the following formula-

$$\% \text{ Inhibition} = \frac{\mathbf{Abs(control) - Abs(sample)}}{\mathbf{Abs(control)}} \times 100$$

The IC_{50} values of the examined substances or positive control were determined using the linear regression curve utilizing the Logit technique.

2.3. Inhibition kinetics:

A kinetic investigation of the chosen substance compound **6i** against α-glucosidase was conducted following established literature procedures with slight modifications to determine the type of inhibition of the enzyme and the inhibition constant [42]. A substrate of p-NPG with concentrations of 0.10, 0.15, 0.20, and 0.30 µM was incorporated into a mixture containing a fixed concentration of α-glucosidase (0.5

U/mL) and varying amounts of **compound 6i** with varying concentrations of 0, 4.882, 9.756, 19.531, 39.062, 78.125 and 156.25 µg/ml. The absorbance at 405 nm was detected 15 times over a duration of 30 seconds using SpectraMax M5 multi-mode microplate reader (Molecular Devices, California, USA). The inhibition type was ascertained using the Lineweaver-Burk plot, and the Michaelis-Menten constant (Km) was calculated from the plot depicting the reciprocal of varying pNGP concentrations (1/[S]) against the reciprocal of enzyme activity (1/V) across different inhibitor concentrations.

2.4. Fluorescence quenching:

The slightly modified approach from a prior article was employed to assess the fluorescence quenching of α-glucosidase in either the absence or presence of **compound 6i** [42]. 3.5 U/mL α-glucosidase which was dissolved in phosphate buffer at pH 6.8, was combined with different concentrations of inhibitors (0, 4.882, 9.765, 19.531, 39.062, 78.125 and 156.250 µg/ml) for 10 minutes at 25 °C. The fluorescence intensities of α-glucosidase were measured using an emission wavelength ranging from 300 to 450 nm using an excitation wavelength of 280 nm by SpectraMax M5 multi-mode microplate reader (Molecular Devices, California, USA). The **compound 6i** exhibited fluorescence at an excitation wavelength of 280 nm and subtracted the initial fluorescence value. Additionally, the fluorescence spectrum of phosphate buffer was evaluated under identical conditions and subtracted as the background.

2.5. Circular dichroism spectra:

The circular dichroism (CD) spectra of α-glucosidase solution (0.5 U/mL) were analyzed with and without incremental concentrations of **compound 6i** at 0, 15, 30 and 60 µg/ml within the wavelength range of 190–260 nm. The bandwidth of 1 nm

was measured using a CD spectrometer (J-1500 CD spectrometer, JASCO) at ambient temperature under consistent nitrogen conditions. The solvent background of the phosphate buffer signal was subtracted to rectify the CD spectra. The CDNN software was utilized to assess the impact of **compound 6i** by calculating the alteration of α- helix, random coils, β-sheets, and β-turn content of α-glucosidase [43].

2.6. Molecular docking:

2.6.1. Protein preparation:

The crystal structures (3D) were acquired with the integration of Protein Data Bank (https://www.rcsb.org) of AG (PDB ID: 5NN8) with the resolution 2.45 Å. Inhibitors, unnecessary water molecules and all heteroatoms were filtered with DiscoveryStudio Visualizer (v21.1.020298), and the macromolecule preparation protocol was carried out using AutoDockTools 1.5.7. Gasteiger charges were introduced post-merging the non-polar hydrogens, and docking evaluations were performed on the prepared complex structures [44,45].

2.6.2. Ligand preparation:

The .mol2 files containing the 3D structures of **6i** and **6h** molecules were minimized using the mmff94 method. Additionally, hydrogen atoms were incorporated into the ligand molecules. Finally, to determine the most stable conformation of ligands, molecular docking research was performed using AutoDockTools 1.5.7 [46].

2.6.3. Docking:

The ligand-protein interactions were studied using molecular docking. AutoDockTools 1.5.7 performed the docking analysis using a grid-based

methodology with x, y, and z coordinates of -14.597930, -33.591140, and 95.075744, respectively. Every protein-ligand complex binding energy (Kcal/mol) was calculated using the docking results [47]. The docking score quantitatively indicates the binding affinity of the ligands, with lower values suggesting better interaction. The ligands interact with the receptor through many bonding interactions [48]. According to Agu *et al.* such interactions may contribute to an understanding of the mechanism of action of the compounds and their probable therapeutic efficacies. Using Discovery Studio Visualizer, the interaction features of the protein-ligand complex were examined [45,49].

2.7. In vitro cytotoxicity:

The cell viability assay was performed to assess the cytotoxic effects of compound **6i** on HEK293 cells, according to Gupta *et al.* with slight modifications [50]. In brief, cells were cultured in DMEM at 37 ^{o}C. After reaching confluence, 6000 cells were seeded into each well of 96 well plates and incubated for 24 h. Following 24 h of incubation, the cells were treated with concentrations ranging from 3.9 to 250 µM of compound **6i** for 24 h. After 24 h, 5 mg/mL MTT was added to the wells, followed by incubation for 3 h. After 3 h, formazan crystals were solubilized in DMSO. The resulting absorbance was recorded using SpectraMax-M5 (Molecular Devices, USA) at 570 nm [51]. The percentage cell viability was determined according to:

$$Cell\ viability\ (\%) = \left(\frac{ODsample}{ODcontrol}\right) x\ 100$$

2.8. ADME, drug-likeness and toxicity assessment:

The physicochemical and pharmacokinetic characteristics of the chosen candidates were assessed using the SwissADME online tool (http://www.swissadme.ch), created by the Swiss Institute of Bioinformatics (SIB) in Lausanne, Switzerland, for evaluating their ADME predictions and drug-likeness attributes [52]. Additionally, the toxicity profiles of the following picked endpoints of chosen potent analogues were investigated using the online Deep-PK webserver: Ames (Mutagenicity), Maximum Tolerated Dose, Carcinogenesis, Liver Injury, hERG Blockers, Fathead Minnow, Skin Sensitization, and Acute and Chronic Rat toxicity [53].

3. Result and discussion:

3.1. Chemistry:

In this research work, 14 new heterocyclic compounds bearing cuminaldehyde-TZD hybrids (**Table 1**) were synthesized, starting with chloroacetic acid and thiourea. The TZD, intermediate compound **5**, and proposed compounds (**6a-6l** and **6m**) were synthesized using a synthetic procedure involving three steps and 1 step. The synthetic schemes are outlined in **Scheme 1** and **Scheme 1A**. All the compounds (compound **5**, **6a-6m**) were characterized by NMR, FT-IR, and ESI mass (**Spectral figures**). Similarly, the molecular geometry and tabular data of compound **6i** crystal was analyzed and presented in **spectral figures.**

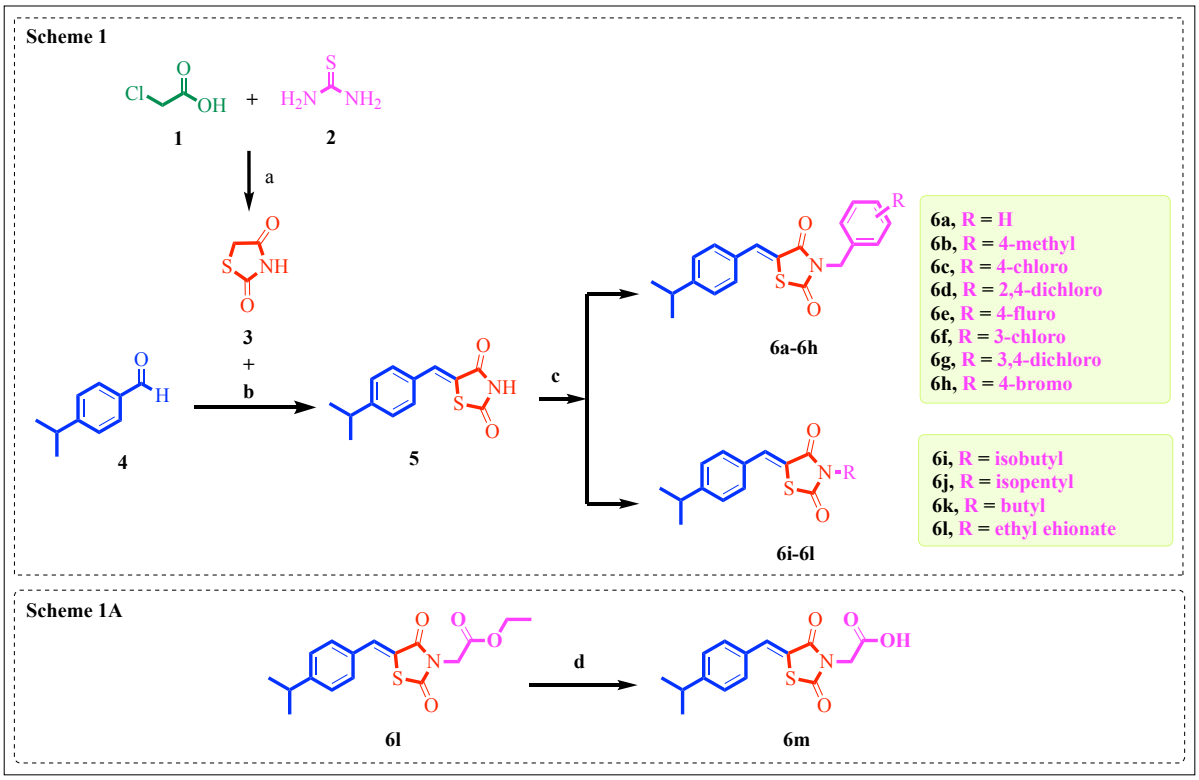

Scheme 1: Synthesis of target compounds **6a-h**, **6i-6l,** and **6m**. **Reagents and conditions:** a) Concentrated hydrochloric acid, water, 100-110 ^{0}C, reflux, 8–10 hrs; b) Urea (1.5 equiv), Glacial acetic acid, 100 ^{0}C, Reflux, 8–10 hrs; c) Substituted benzyl chlorides/ Alkyl halides, K_2CO_3, DMF, rt; 18-24 hrs. **Scheme 1A:** Synthesis of target compound **6m** from **6l**. **Reagents and conditions:** d) Conc. HCl:AcOH (1:2), reflux 2 h.

3.2. X-ray crystallographic analysis with ORTEP diagram of compounds 6i:

To verify the suggested structure, we carried out an X-ray crystallographic investigation on compound **6i** (**Scheme 1**). The structures of other compounds were determined by analogy and verified by spectral data (^{1}H, ^{13}C, and MS-ESI data analysis). The crystallization was accomplished in compounds **6i** using Methanol solvents via a gradual evaporation method. **Spectral figure** (**S43** and **Table S1**) provides additional information on these crystals. We were interested in offering the product stereochemistry, for which we have already supplied the data examined using X-ray crystallography (**Scheme 1**).

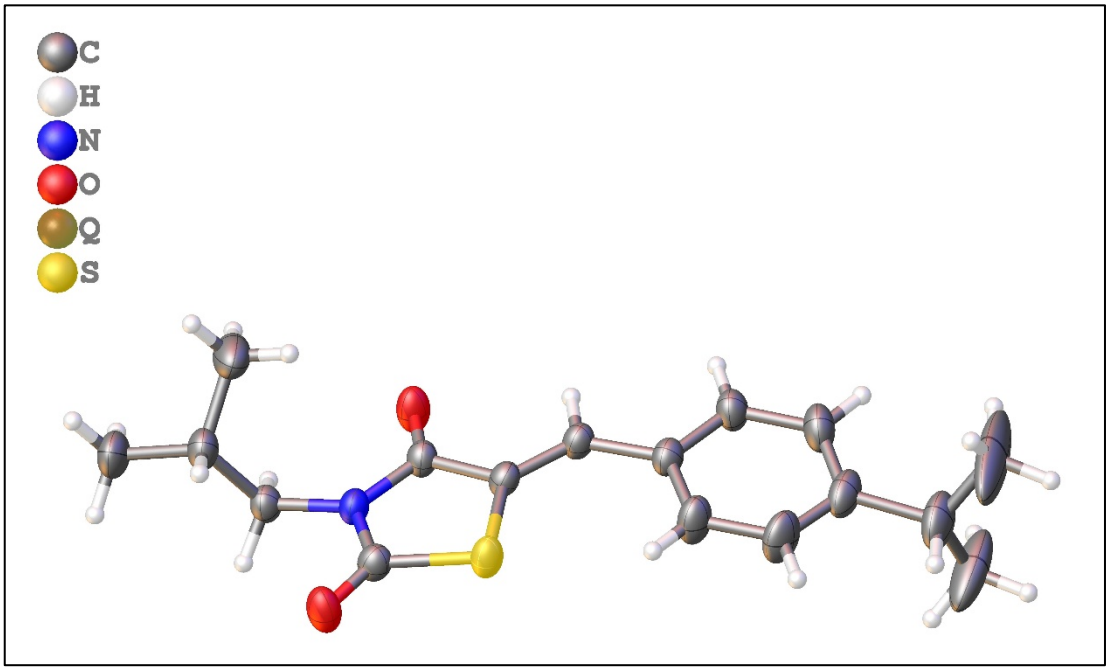

Figure 2: ORTEP diagram of compound **6i** (**CCDC-** 2402983) (**Scheme 1**).

3.3. In vitro assay of α-glucosidase inhibitory activity:

All synthetic molecules, compounds **5** and **6a-6m,** were evaluated for their *in vitro* antagonistic effect of α-glucosidase activity by using acarbose as a standard through a modified established method, which was previously discussed (**Table 2**). Several distinct synthetic compounds exhibited α-glucosidase inhibitory activity, with IC_{50} values ranging from 31.29 ± 0.94 µM to greater than 600 µM. Compounds

named compound **6i**, compound **6h**, compound **6b** and compound **5** exhibited better α-glucosidase inhibitory action, compared with others, with IC_{50} values ranging from 31.29 ± 0.94 µM to 196.75 ± 1.02 µM. Among them, **compound 6i** exhibited the most promising antagonistic activity with an IC_{50} value of 31.29 ± 0.94 µM in comparison to Acarbose (IC_{50} = 61.24 ± 1.81 µM).

However, it is worth mentioning that the series has a cuminaldehyde part and a TZD core ring as one of the moieties. It has also previously been reported that this heterocyclic ring structure has a potential antagonistic activity towards the α-glucosidase enzyme in the management of hyperglycemic conditions [36].

Table 2: The *in vitro* α-glucosidase inhibitory activity screening and IC_{50} values data of synthesized compounds (**6a-6h**, **6i-6l**, and **6m**).

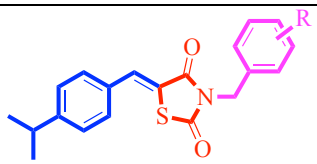

6a-6h

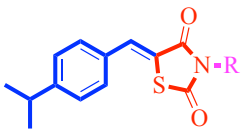

6i-6m

Sl. no.	Compound	R	IC_{50} (µM)
1	5	-	196.75 ± 1.02
2	6a	-H	>600
3	6b	4-methyl	75.71 ± 0.82
4	6c	4-chloro	>600
5	6d	2,4-dichloro	>600
6	6e	4-fluro	>600
7	6f	3-chloro	>600
8	6g	3,4-dichloro	>600
9	6h	4-bromo	68.86 ± 1.25
10	6i	-isobutyl	31.29 ± 0.94
11	6j	-isopentyl	116.36 ± 2.14
12	6k	-butyl	>600

13	6l	-ethyl ehionate	>600
14	6m	-acetic acid	>600
15	Acarbose	-	61.24 ± 1.81

3.4. Structure-activity relationships (SARs):

To study the activity of different N-benzyl, alkyl, and acid substitutions at cuminaldehyde-TZD intermediate (**compound 5**) on α-glucosidase inhibitory activity, the structure-activity relationship (SAR) was analyzed. From all the benzyl substitution at cuminaldehyde-TZD intermediate (**compound 5; Figure 3**), the 4-bromo group resulted in an increase in the α-glucosidase inhibitory activity as **compound 6h** (68.8636 µM). Similarly, the substitution of the alkyl chain towards cuminaldehyde-TZD intermediate (**compound 5; Figure 3**) also enhances the α-glucosidase inhibitory activity as **compound 6i** (31.29 ± 0.94 µM). The attachment of the acetic acid group at the cuminaldehyde-TZD intermediate (**compound 5; Figure 3**) resulted in a decrease in the α-glucosidase inhibitory activity. The findings on SARs informed the enhancement of inhibitory action in subsequent structural modifications.

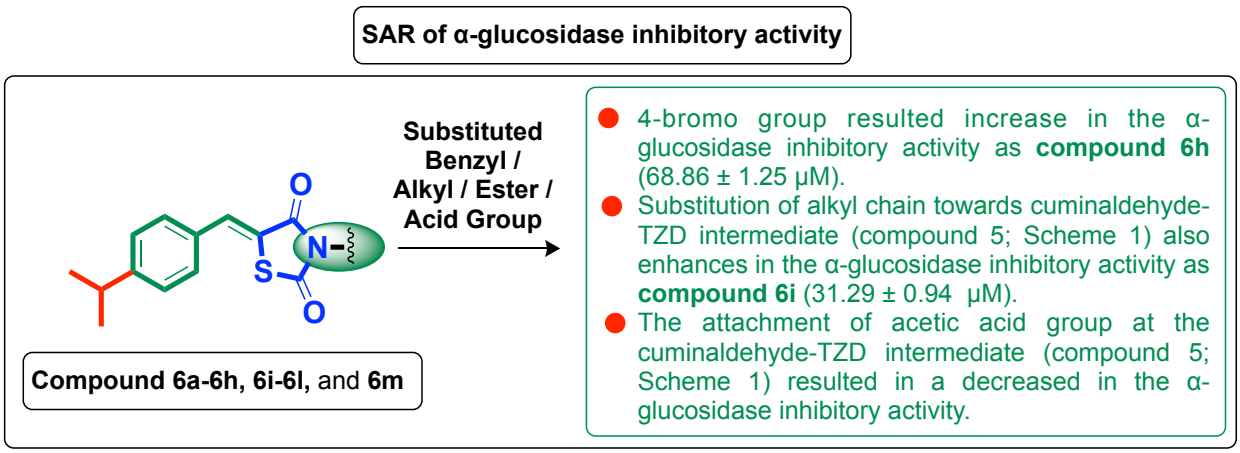

Figure 3: SAR of compound series for α-glucosidase inhibitory activity.

3.5. Enzyme kinetic study:

To investigate the inhibitory mechanism of **compound 6i** on α-glucosidase, the results of an inhibition kinetics study were evaluated using the Lineweaver-Burk method (**Figure 4)**. The plots of 1/V versus 1/[S] exhibited a series of straight lines with varying slopes that didn't intersect the X-axis or Y-axis but converged in the second quadrant. The results indicated that Km values increased while Vmax was unaffected with higher concentrations of **compound 6i,** which implies competitive inhibition mechanisms against α-glucosidase by **compound 6i**. So, it can be explained that compound 6i has a tendency to bind the active site of the enzyme and inhibit the formation of the enzyme-substrate (ES) complex by competing with the substrate (S) [54]. The plot of Km with the concentration of **compound 6i** was mentioned in (**Figure 5**).

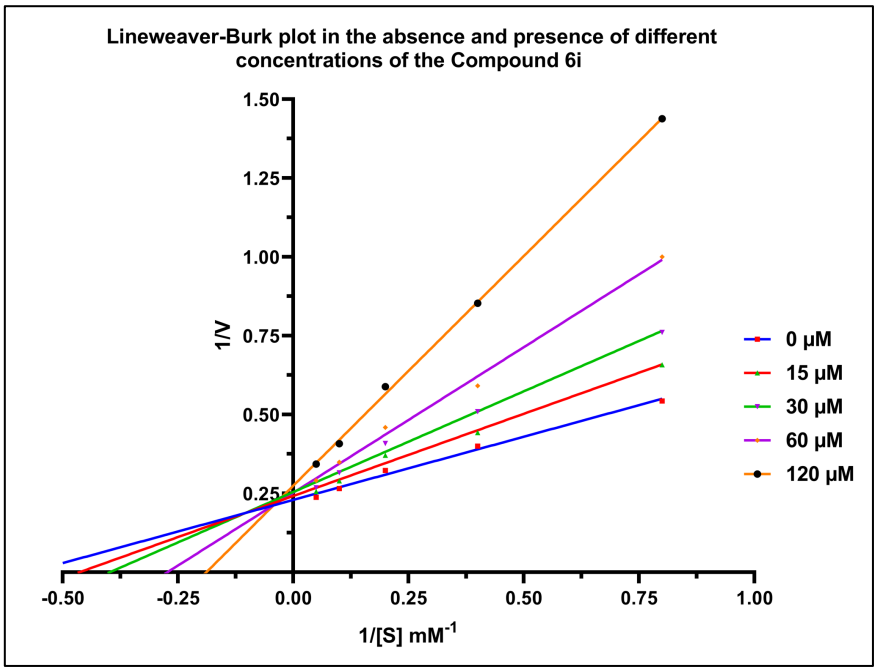

Figure 4: Kinetics of α-glucosidase inhibition by compound **6i** and the Lineweaver-Burk plot in the absence and presence of different concentrations of compound **6i**.

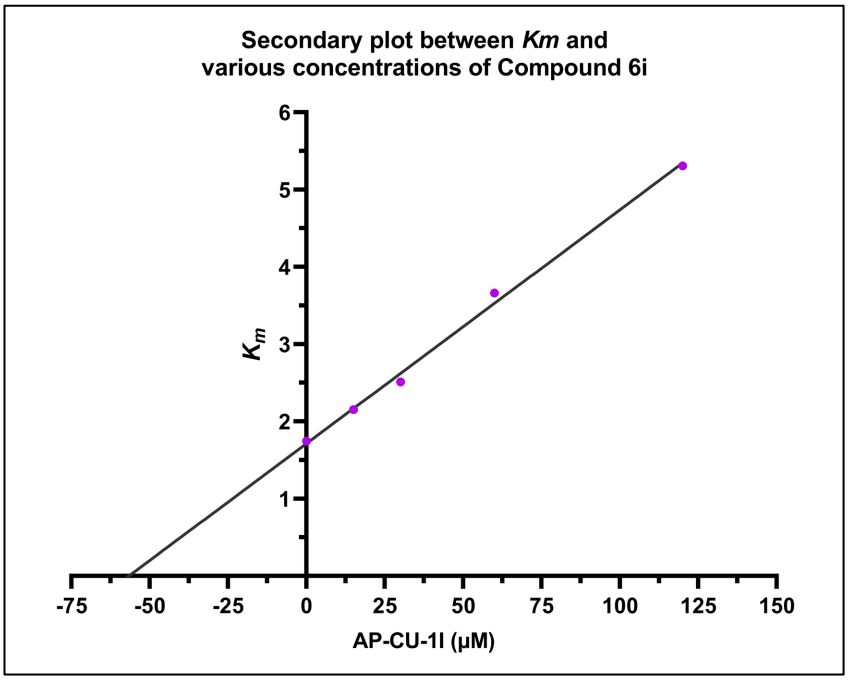

Figure 5: The secondary plot between *Km* and various concentrations of compound **6i**.

3.6. Fluorescence quenching:

To extend this finding, fluorescence quenching studies were conducted to investigate the interactions between compound **6i** and α-glucosidase (**Figure 6** and **Figure 7**). The fluorescence quenching technique is frequently employed in the interaction analysis of macromolecules and ligand compounds [55]. The application of **compound 6i**, ranging from 0 to 156.25 µg/ml, resulted in a variable reduction of fluorescence intensity across different cases, indicating that compound **6i** may have interacted with α-glucosidase, subsequently quenching its intrinsic fluorescence. The fluorescence value of the system diminished as the concentration of the compound increased, and the maximum emission wavelength exhibited a minor blue shift. The fluorescence quenching data were evaluated using the Stern-Volmer equation.

$$\frac{F0}{F} = 1 + Ksv[Q] = 1 + Kq\,\tau 0[Q]$$

In the aforementioned equation, F0 and F denote the fluorescence intensity of α-glucosidase in the absence and presence of the quencher compound **6i**, respectively. Ksv and Kq represent the fluorescence quenching constant and the bimolecular quenching constant, respectively. τ0 denotes the mean lifespan of biomolecules absent a quencher (10^{-8} s), while [Q] indicates the concentration of quencher at compound **6i**. The Stern-Volmer plot (**Figure 8**) exhibits a robust linear correlation, suggesting that the enzyme's quenching effect is due to a solitary quenching mechanism. The values of Ksv and Kq were ascertained to be 1.44×10^4 L/mol and 1.44×10^{12} L·mol^{-1}·S^{-1}, respectively.

Considering that the Kq value substantially surpasses the maximum dynamic rate constant for bimolecular interactions (2×10^{10} L·mol^{-1}·S^{-1}), it can be concluded that the quenching mechanism of compound **6i** on the intrinsic fluorescence of α-glucosidase is static quenching due to complex formation.

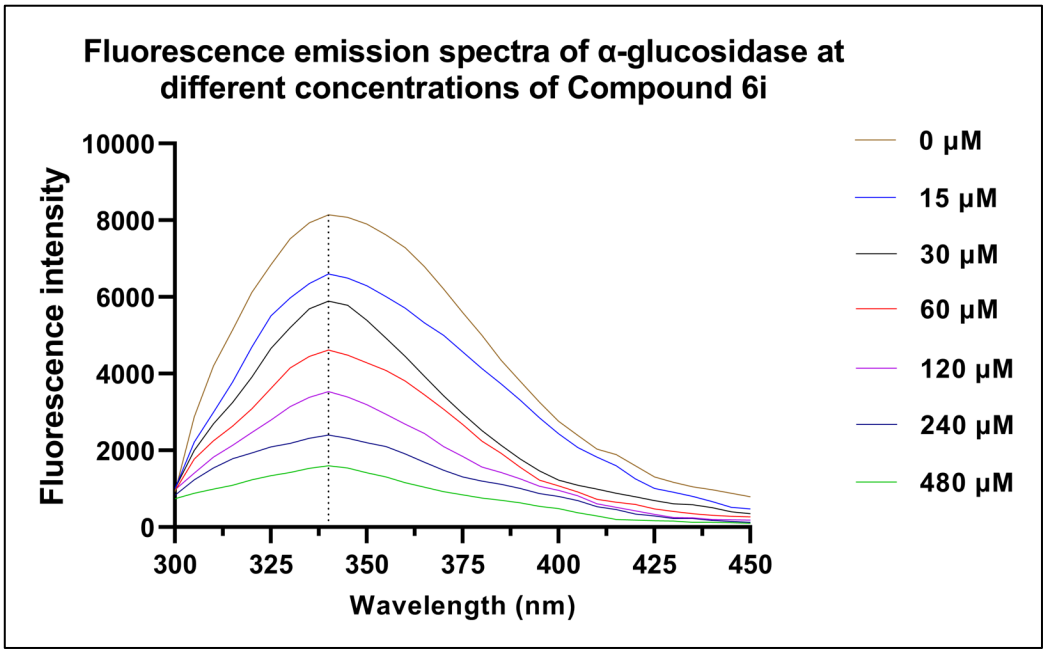

Figure 6: Fluorescence emission spectra at different concentrations of compound **6i**.

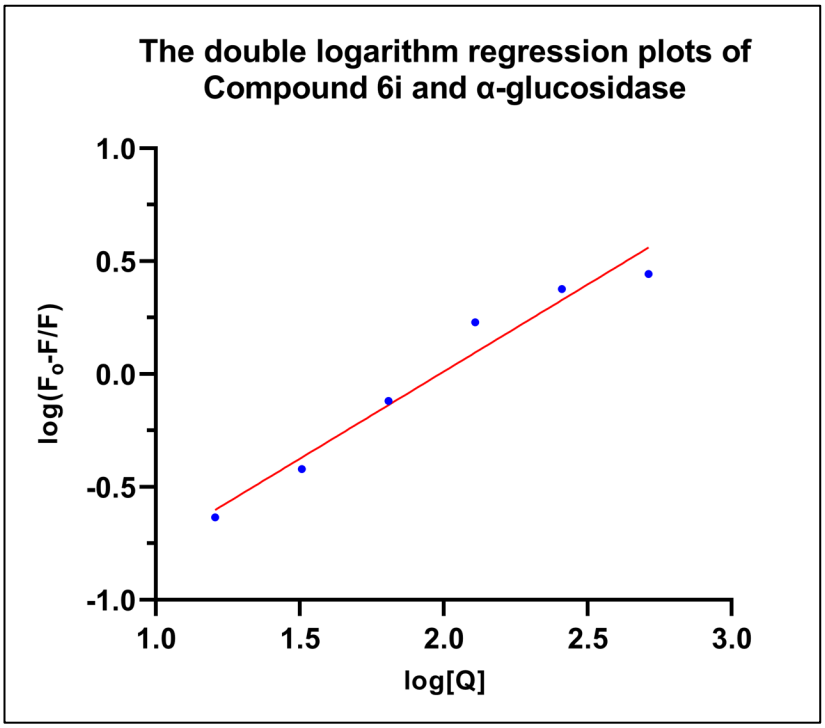

Figure 7: Double logarithm regression plots of compound **6i** and α-glucosidase.

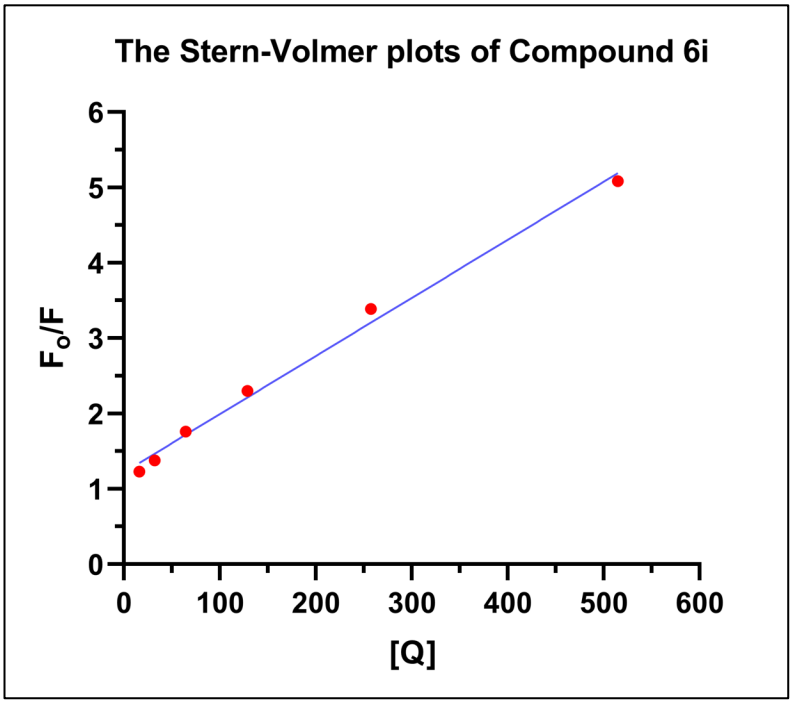

Figure 8: Stern-Volmer plots of compound **6i**.

3.7. Circular dichroism spectra:

Circular dichroism (CD) was employed to study alterations in the secondary structure of proteins. Two negative bands at around 210 and 220 nm were detected

in the far-UV CD spectra of α-glucosidase (**Figure 9**), with alterations in the size and shape of the peaks, indicative of the α-helix structure of α-glucosidase. The computed results indicate that treatment with compound **6i** (molar ratios: 2:1) resulted in an increase in α-helix content (from 34.4% to 62.9%), alongside decreases in β-sheet (from 13.8% to 7.48%), β-turn (from 12.3% to 9.2%), and random coil (from 41.0% to 21.1%) (**Table 3**). The results indicated that the structure of α-glucosidase became more flexible and unstable; **compound 6i** induced alterations in the secondary structure of α-glucosidase, modifying its hydrophobicity, thereby obstructing active site formation or impeding substrate binding, which subsequently impacts the enzymatic activity.

Table 3: Secondary structural analysis of compound **6i** with α-glucosidase from CD.

μM	α-helix (%)	β-sheet (%)	β-turn (%)	Random coil (%)
0	34.4	13.8	12.3	41.0
10	42.1	12.5	11.2	39.3
15	45.5	7.78	10.8	34.5
30	48.4	6.36	10.4	25.2
60	62.9	7.48	9.2	21.1

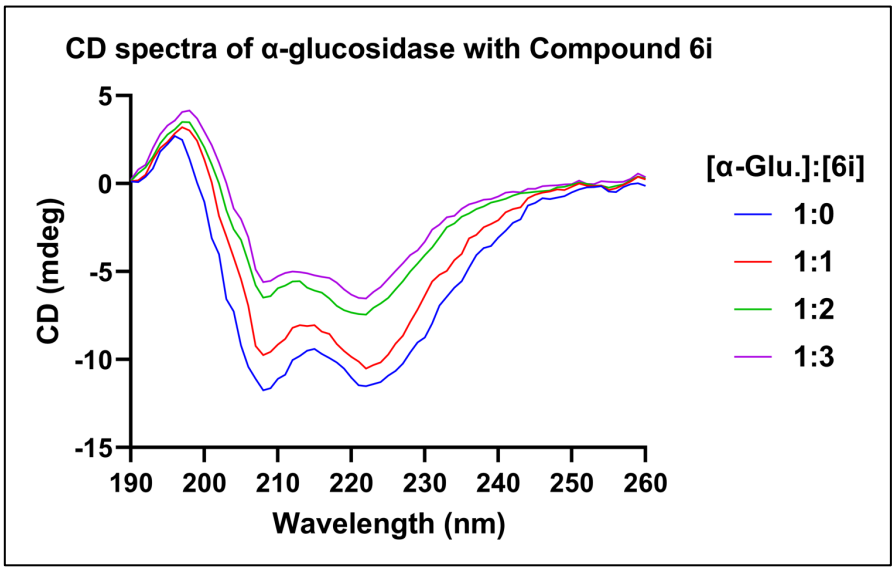

Figure 9: CD spectra of α-glucosidase with compound **6i**.

3.8. Molecular docking:

3.8.1. Molecular docking analysis:

To investigate the binding pattern, screening, and identify the structural feature responsible for the activity and selectivity of the ligands towards the studied targets, compound **6i** and **6h** were docked using the Lamarckian genetic algorithm (LGA) method on AG (PDB ID: 5NN8) Various analyses were conducted based on the docking results, which are detailed below:

3.8.1.1. Docking score and binding interaction analysis of Compound 6i and 6h:

The enzyme AG in the small intestine catalyzes the hydrolysis of long-chain dietary carbohydrates, yielding monosaccharide units that enter the circulation, resulting in hyperglycemia [56]. Thus, the inhibition of α-glucosidase has become a significant therapeutic target capable of lowering blood sugar levels by diminishing carbohydrate digestion. The AG inhibitors primarily target hyperglycemia without directly influencing insulin secretion [10]. The synthesized compounds were docked into the active sites of AG (PDB ID: 5NN8), as given in **Table 4**. It was observed that both the compounds were docked in the active areas of the corresponding macromolecules (**Figure 10**). The molecular docking studies on the AG (PDB ID: 5NN8) revealed that the binding energies of compound **6i** and **6h** were -6.54 and -6.19, respectively. Thus, compound **6i** is the most potent compound among all three test compounds. Considering the better binding scores of compounds **6i** and **6h** against the AG protein, it is worth exploring the inhibitory pathways of these compounds in the management of diabetes mellitus by inhibiting

AG [2]. **Figure 11** illustrates the 2D and 3D interactions that occur between compound **6i** (**Figure 11;** A and B) and compound **6h** (**Figure 11;** C and D) and the active site of the AG.

The activity of compound **6i** against AG could be due to the formation of several interactions with active side residues. The TZD ring in compound **6i** formed one pi-pi and two pi-alkyl interactions with the amino acid residues PHE649, LEU678 and LEU650, as shown in **Figure 11;** A and B. In contrast, the =O group at the 2 position forms two vital conventional hydrogen bonds with LEU677 and LEU678, respectively. Other than that, the phenyl group core forms two pi-pi T-shaped bonds along with one pi-anionic interaction with PHE649, ASP616, and TRP481. The terminal methyl group in the isopropyl chain were found to possess a couple of pi-alkyl interactions with TRP481 and MET519. Furthermore, the 2-methylpropyl group in the TZD end also possessed significant hydrophobic interactions with TRP618, LEU678 and LEU650.

In the case of compound **6h**, the terminal methyl groups in the isopropyl chain possessed several hydrophobic interactions with TRP376, TRP481, LEU405, ILE441, HIS674 and TRP516 residues. The phenyl group core forms one pi-pi T-shaped bond along with one pi-anionic and pi-sulfur interaction with TRP481, ASP616 and MET519. Furthermore, the TZD ring in compound **6h** formed one pi-anionic interaction with the amino acid residue ASP282 (Figure 2C and 2D). Apart from several hydrophobic interactions, the –Br in the bromophenyl group of compound **6h** was found to interact with ALA555 through a carbon-

hydrogen bond ((**Figure 11;** C). In addition, the 3D structures of the interaction between compound **6i** and **6h**, as well as the active site of AG, demonstrate that the TZD components of the compounds engage in both polar and non-polar interactions with the amino acid residues. The higher binding scores of the compound **6i** and **6h** can be attributed to the presence of several non-polar and polar contacts facilitated by the heterocyclic rings (**Figure 11;** A and C). The image illustrates the 2D and 3D interactions between compound **6h** and the active region of the AG protein.

Table 4: Molecular docking scores of the most potent compound **6i** and **6h**.

Compound	Docking Score against AG (PDB: 5NN8)	Conventional -H Bond	Hydrophobic interactions	Active site pocket residues
6i	-6.54	LEU677, LEU678	TRP618, LEU650 (2), TRP481 (2), MET519, PHE649 (2), ASP616, LEU678 (2)	TRP618, LEU650, TRP481, MET519, PHE649, ASP616, LEU678, ARG600, TRP613, ASP518, TRP376, SER676, SER679, GLY651
6h	-6.19	-	ASP616, MET519, TRP376, TRP481 (2), LEU405, ILE441 (2), HIS674, TRP516, ASP282, ALA555	ASP616, MET519, TRP376, TRP481, LEU405, ILE441, HIS674, TRP516, ASP282, ALA555, PHE649, ASP404, ARG600, ASP518, PHE525, ASN524

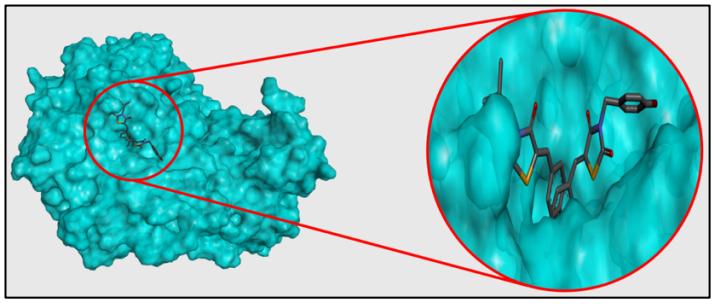

Figure 10: 3D representation of all the Aligned TZD derivatives at the active site of AG (PDB: 5NN8).

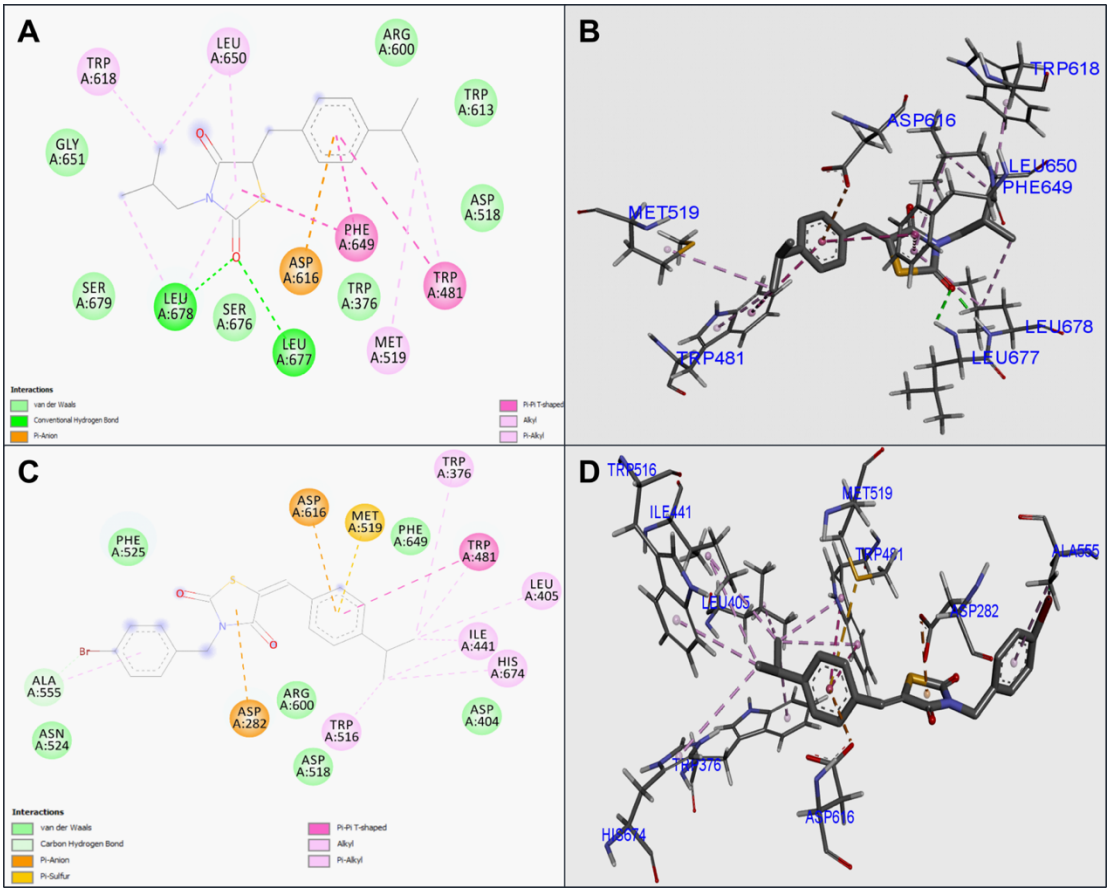

Figure 11: 2D and 3D docking representation of AG–TZD derivatives **6i** (A and B) and **6h** (C and D).

3.9. In vitro cytotoxicity:

The cell viability assay by MTT assay is a vital approach for determining the therapeutic and adverse effects of chemicals on live cells, hence assuring their safety for therapeutic use [57]. HEK293 cells are regarded as an established human cell line model, characteristic of human cells, and are regularly used to assess the cytotoxicity of compounds [58]. The assay involved the exposure of various increasing concentrations of compound **6i** (3.9–250 µM). The experiment indicated that compound **6i** exhibited cytotoxicity at an IC_{50} of 543.3 µM (**Figure 12**). Furthermore, the *in vitro* cytotoxicity assay against HEK293 cells revealed that compound **6i** is nontoxic in lower doses. The viability decreases in a dose-dependent manner. This assay showed that even at 250 µM, the viability of HEK293 cells was 78.22267 ± 4.121515 % and at 3.9 µM, it increased up to 103.0176 ±

1.948184 % when compared with the control. In a nutshell, this study concludes that compound **6i** is nontoxic against normal cells and thus can be used as a potent candidate in therapeutic studies.

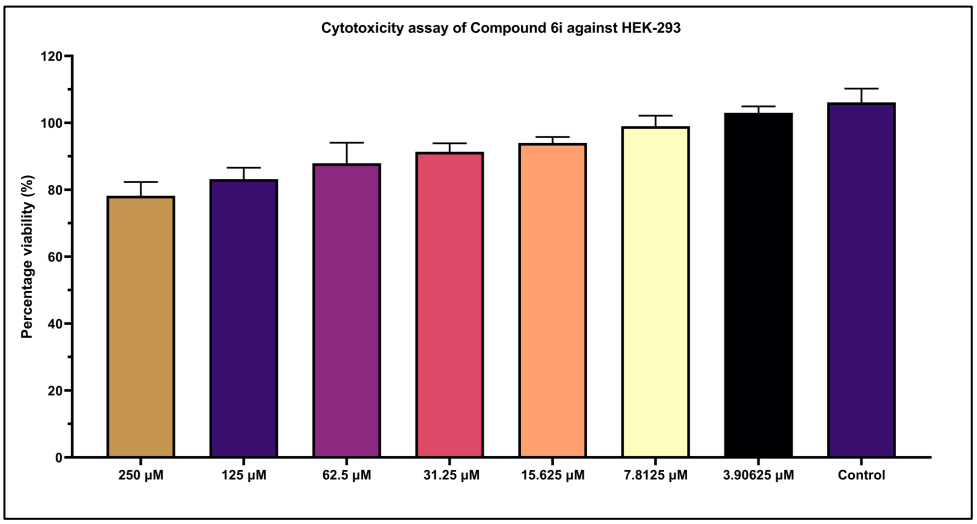

Figure 12: Cell viability assay of compound **6i** against HEK293.

3.10. ADME, drug-likeness and toxicity assessment:

In drug discovery and development, the absorption, distribution, metabolism, excretion, and toxicity (ADMET) profiles of compounds have a significant role. Pharmacokinetic (pK) and pharmacodynamic (pD) profiles of any compounds provide confidence for the development of the drugs to indicate various diseases. Orally, bioavailable compounds are more inclined to exhibit drug-like properties and fulfil the Lipinski and Veber principles. Molecules, due to their drug-like properties, may equal or surpass the efficacy of currently available pharmaceuticals [52].

ADME prognosis indicates that **compounds 6h** and **6i** do not break any of the rules of drug-likeness. Both compounds adhere to the criteria set by Lipinski, Veber, and Ghose, achieving a bioavailability score of 0.55, indicative of satisfactory drug resemblance. In contrast, **compound 6h**

seemed to violate Lipinski's rule with one infraction (MLOGP>4.15). **Compounds 6h** and **6i** possess four rotatable bonds and two hydrogen bond acceptors and lack hydrogen bond donors. Their TPSA values are 62.68 Å², which is below the acceptable limit of 140 Å², indicating favourable oral bioavailability and suggesting excellent gastrointestinal absorption. The radar plot (**Figure 13**) illustrates that **compound 6i** is situated inside the pink area, affirming its strong drug similarity and superior bioavailability profile, while **compound 6h** exhibits permissible bioavailability (**Table 5**).

In addition, pharmacokinetics was checked using the Boiled-Egg model, wherein **compounds 6h** and **6i** were situated in the yellow zone (**Figure 13**), indicating their enhanced gastrointestinal absorption and a significant likelihood of penetrating the blood-brain barrier (BBB). Additionally, it showed that both compounds had negative log Kp values, which indicates reduced skin permeation, and that they might block CYP2C19 and CYP2C9 but not CYP2D6 (**Table 6**).

The computational toxicity evaluation executed through the Deep-PK web server reveals that compounds **6h** and **6i** are non-AMES, lack carcinogenic qualities, exhibit reasonable toxicity towards the liver and skin, and are also safely biodegradable. Compound **6h** and **6i** have higher maximum tolerated doses of 0.86 and 0.82 logs (mg/kg/day), respectively, with the standard threshold for low being below or equivalent to 0.477 logs (mg/kg/day), while high doses are defined as over 0.477 logs (mg/kg/day). Furthermore, the compounds **6h** and **6i** exhibit LD_{50} values of 2.23 mM and 2.11 mM, accordingly indicating low or satisfactory acute toxicity, as LD_{50} values less

than 0.5 mM (Log LD_{50} < 0.3) are regarded as having high acute toxicity (**Table 7**).

The aforementioned *in silico* ADME metrics and toxicology predictions of the most potent analogues may facilitate the advancement of potential novel drugs with improved oral bioavailability, which gives them the property of acceptable lead-like potential for future development of safe and efficient drugs.

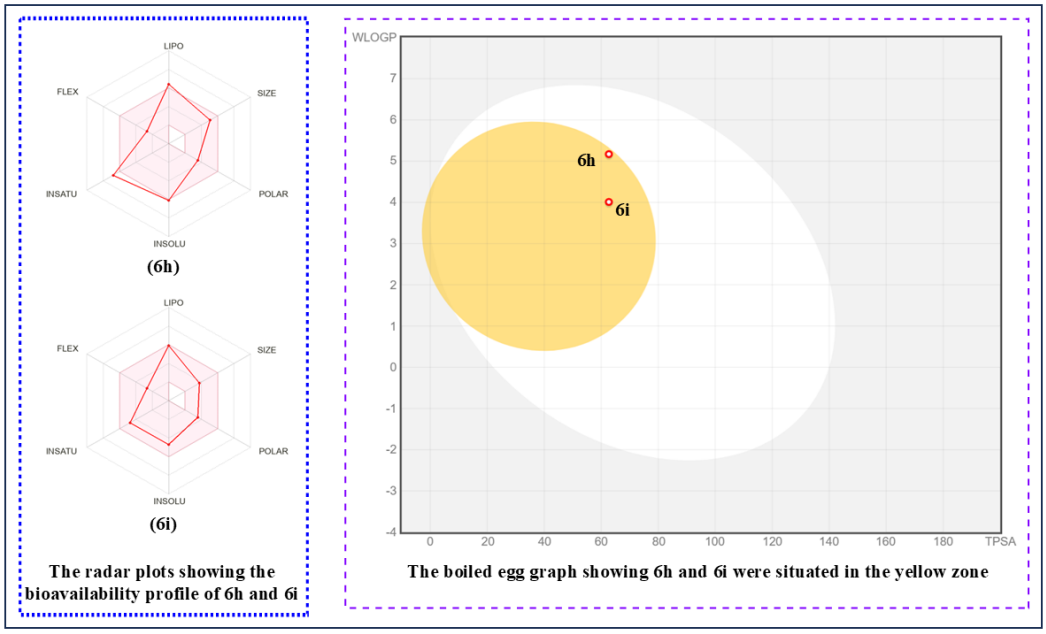

Figure 13: Radar plot and Boiled-Egg model of compound **6i** and **6h.**

Table 5: ADME prognosis using SwissADME, Physiochemical and Drug-likeness properties. ((MW=Molecular Weight, TPSA=total polar surface area, Consensus Log P =average of all predicted Log Po/w).

Compound Name	MW (g/mol)	Rotatable bonds	H-bond acceptors	H-bond donors	TPSA	Consensus Log P	Lipinski violations	Ghose violations	Veber violations	Egan violations	Muegge violations	Bioavailability Score	Synthetic Accessibility
6i	303.42	4	2	0	62.68	3.92	0	0	0	0	0	0.55	3.51
6h	416.33	4	2	0	62.68	4.85	1	0	0	0	1	0.55	3.53

Table 6: Pharmacokinetics prediction of synthesized compounds (**6i** and **6h**) from the SwissADME server.

Compound Name	GI absorption	BBB permeant	Pgp substrate	CYP1A2 inhibitor	CYP2C19 inhibitor	CYP2C9 inhibitor	CYP2D6 inhibitor	CYP3A4 inhibitor	log Kp (cm/s)
6i	High	Yes	No	Yes	Yes	Yes	No	No	-4.71
6h	High	Yes	No	No	Yes	Yes	No	Yes	-4.8

Table 7: Toxicology predictions. Information was retrieved via the Deep-PK database.

Compound Name	AMES Mutagenesis	Maximum Tolerated Dose	Biodegradation	Carcinogenesis	Liver Injury I	Liver Injury II	hERG Blockers	NR-PPAR-gamma	T. Pyriformis	Rat (Acute)	Rat (Chronic)	Fathead Minnow	Skin Sensitisation
6i	Safe	0.82	Safe	Safe	Safe	Toxic	Safe	Safe	3.9	2.11	1.88	4.5	Toxic
6h	Safe	0.86	Safe	Safe	Toxic	Toxic	Toxic	Safe	2.27	2.23	1.8	4.97	Toxic

4. Spectral data:

I. ^{1}H and ^{13}C NMR data (Compound **5** and **6a-6m**):

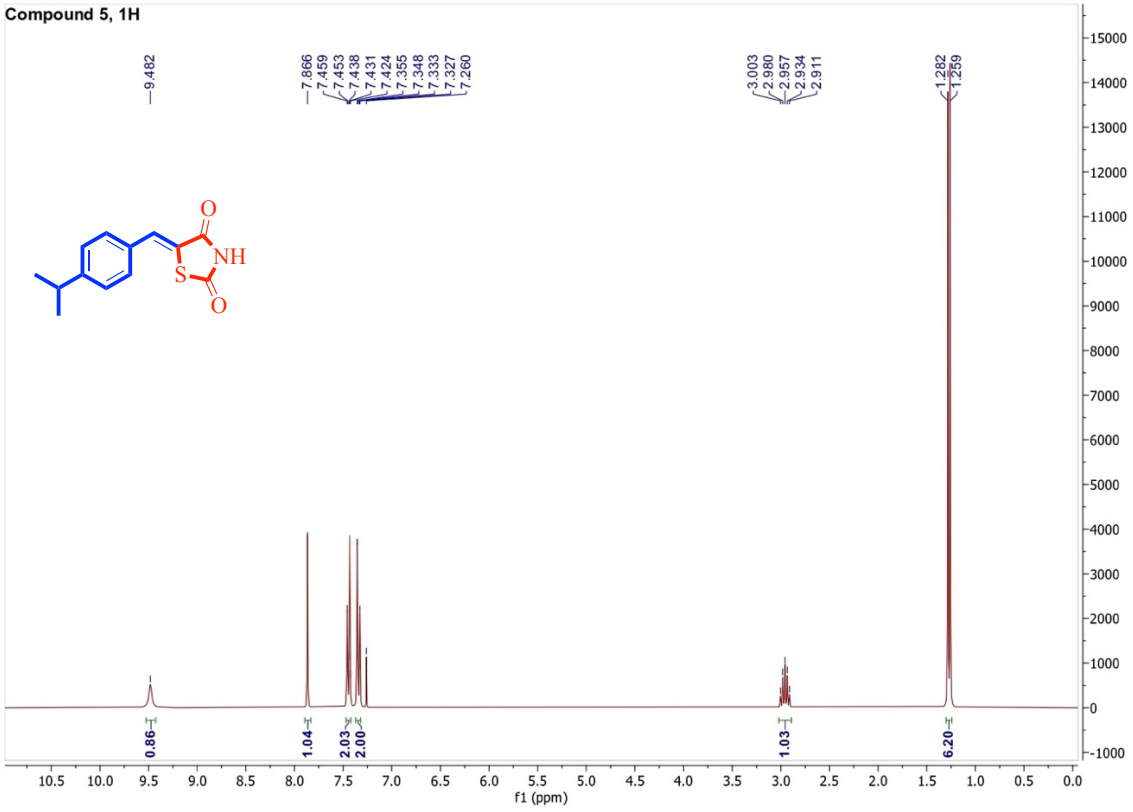

S.F1′: ^{1}H NMR of compound **5**

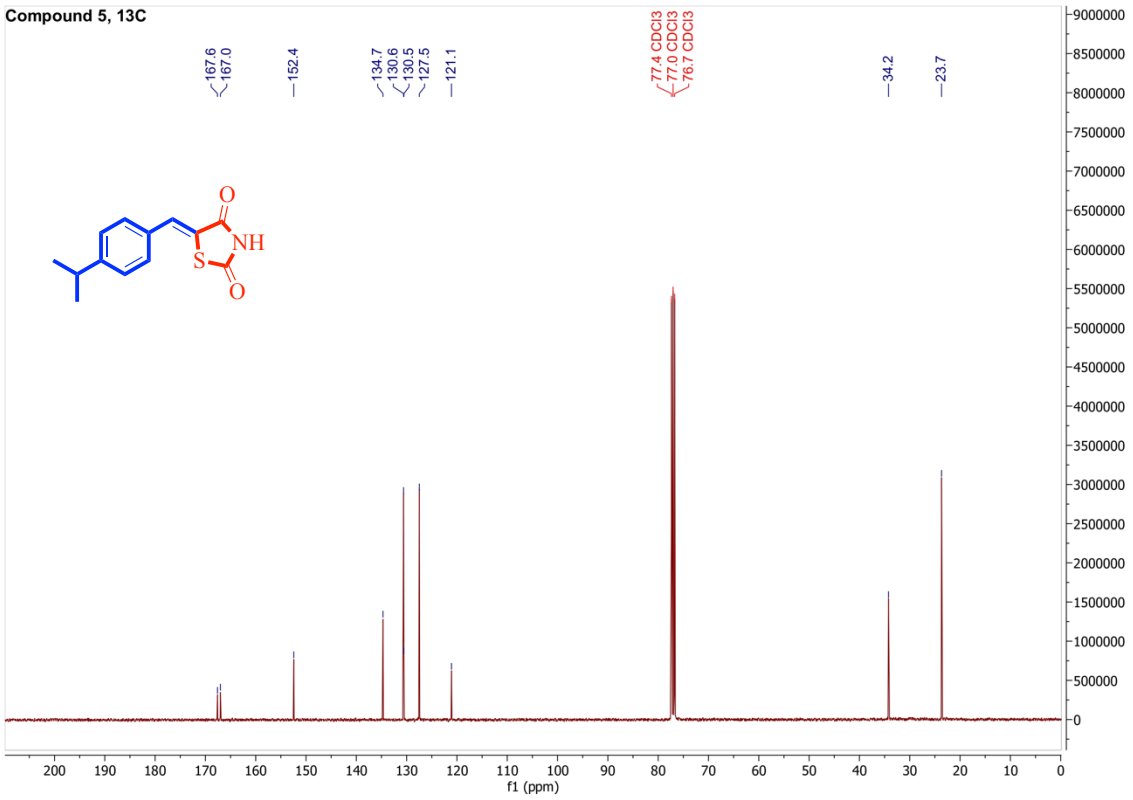

S.F1″: ^{13}C NMR of compound **5**

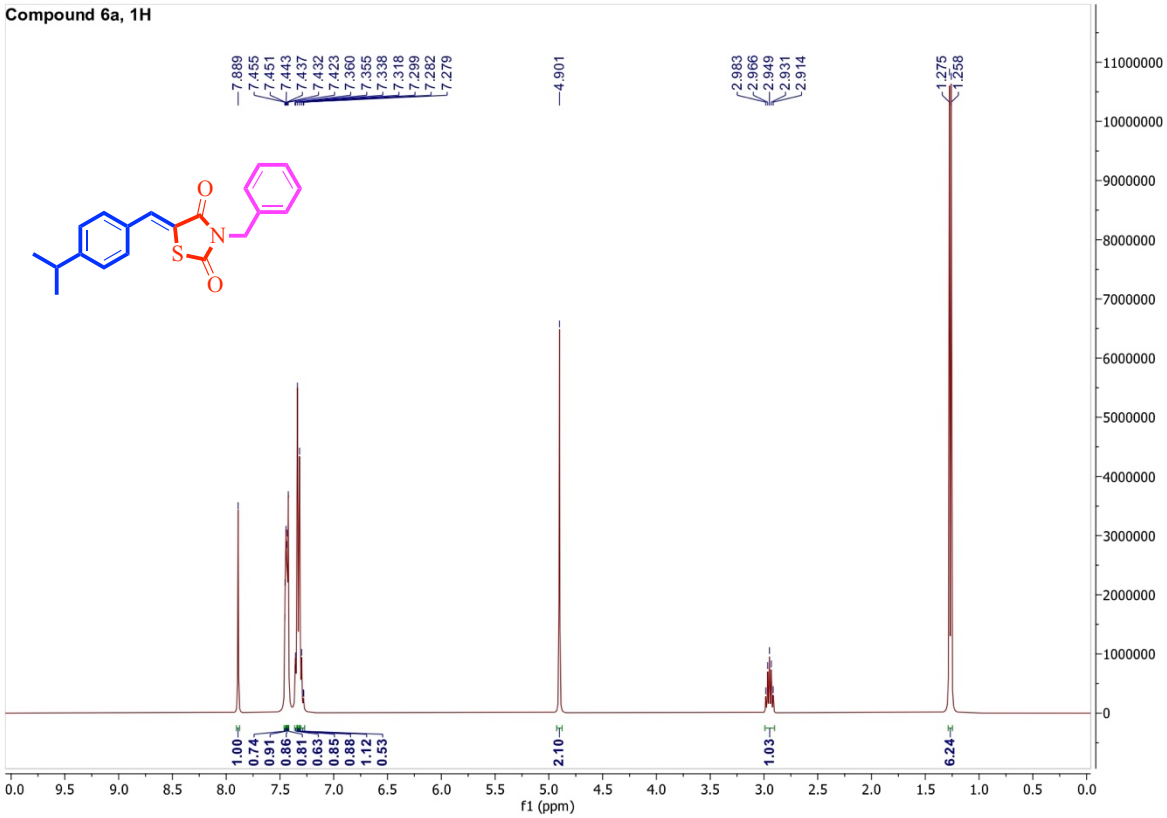

S.F2′: ^{1}H NMR of compound **6a**

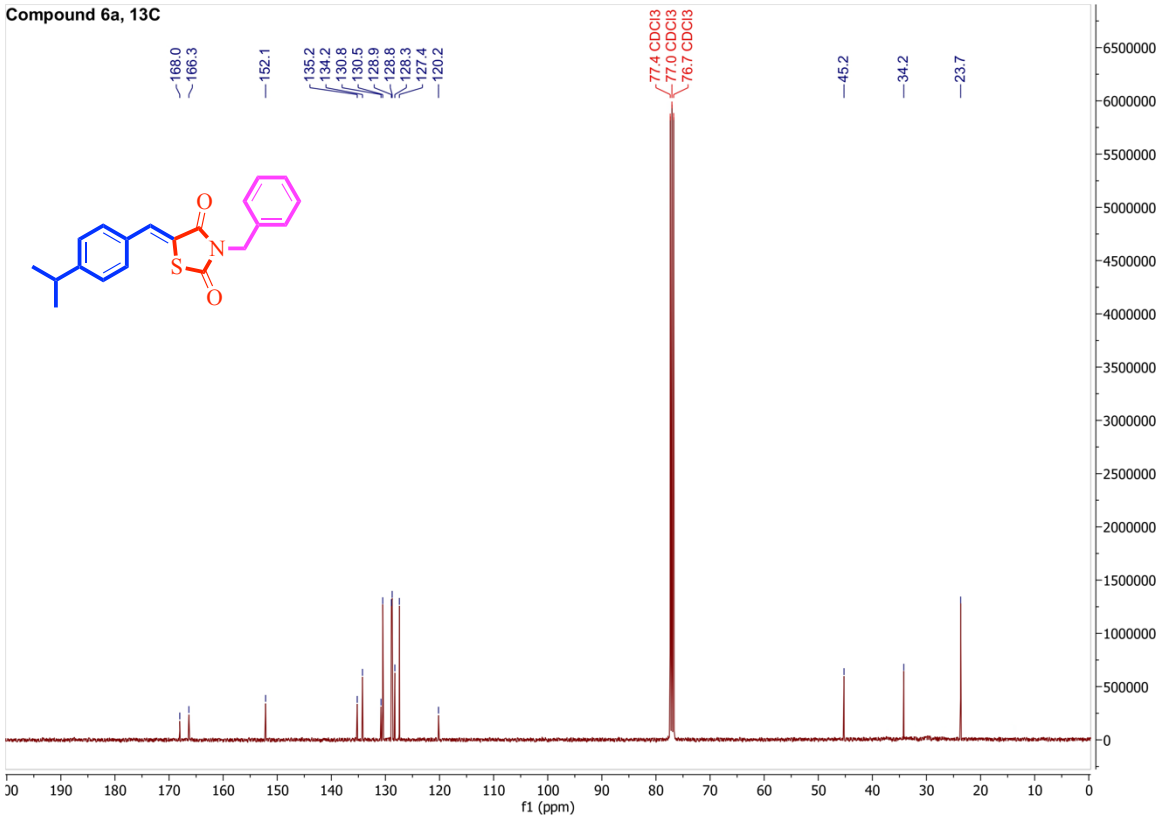

S.F2″: ^{13}C NMR of compound **6a**

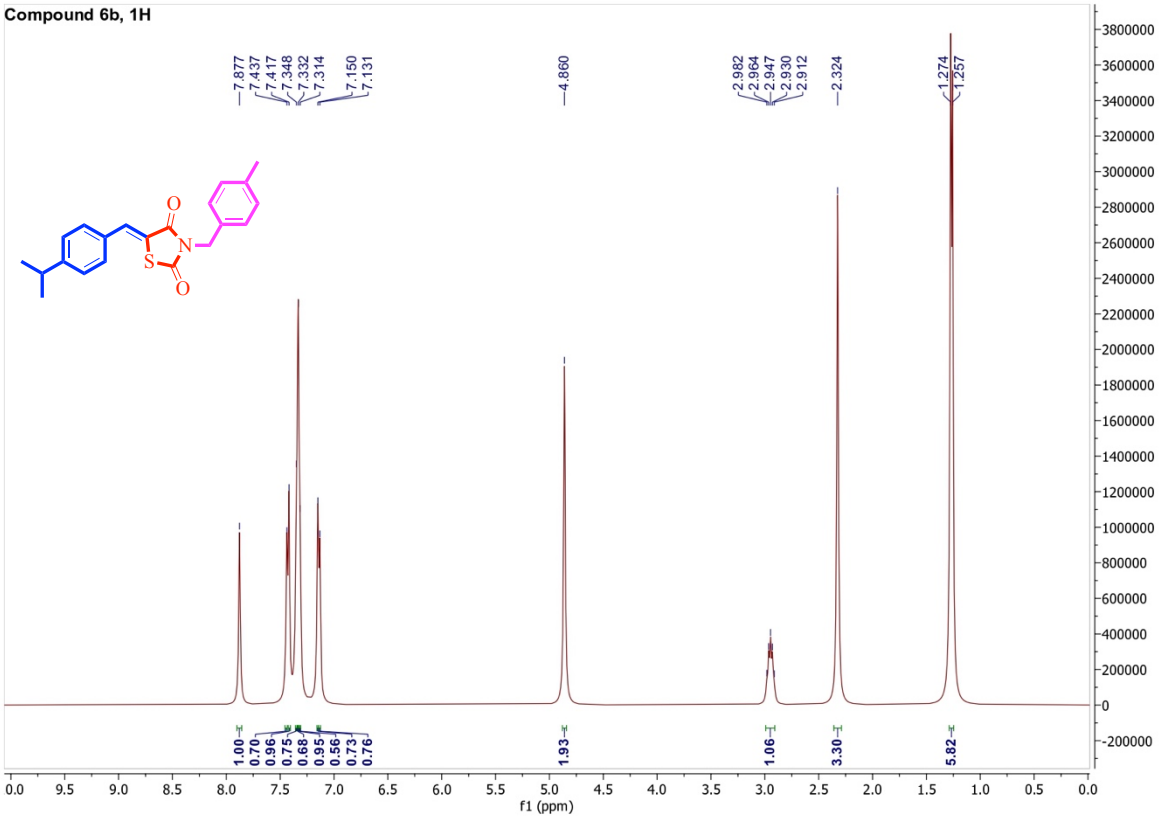

S.F3′: ^{1}H NMR of compound **6b**

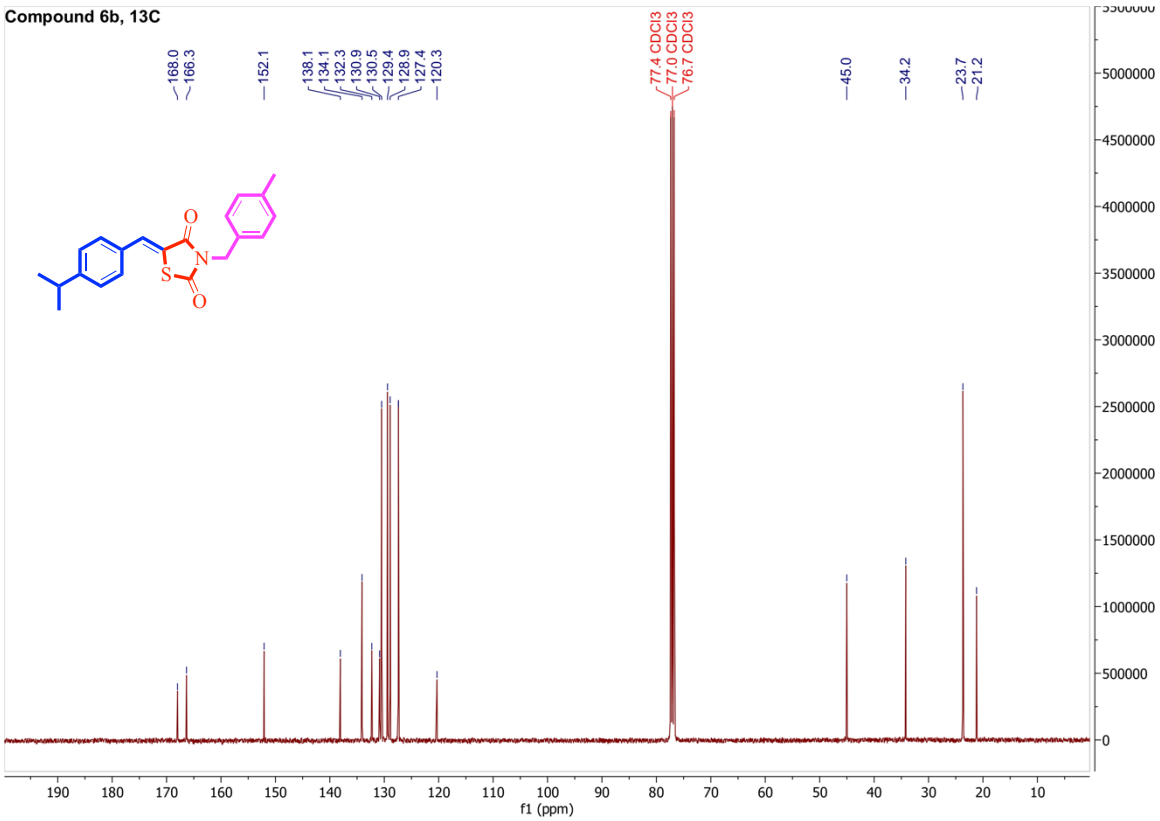

S.F3″: ^{13}C NMR of compound **6b**

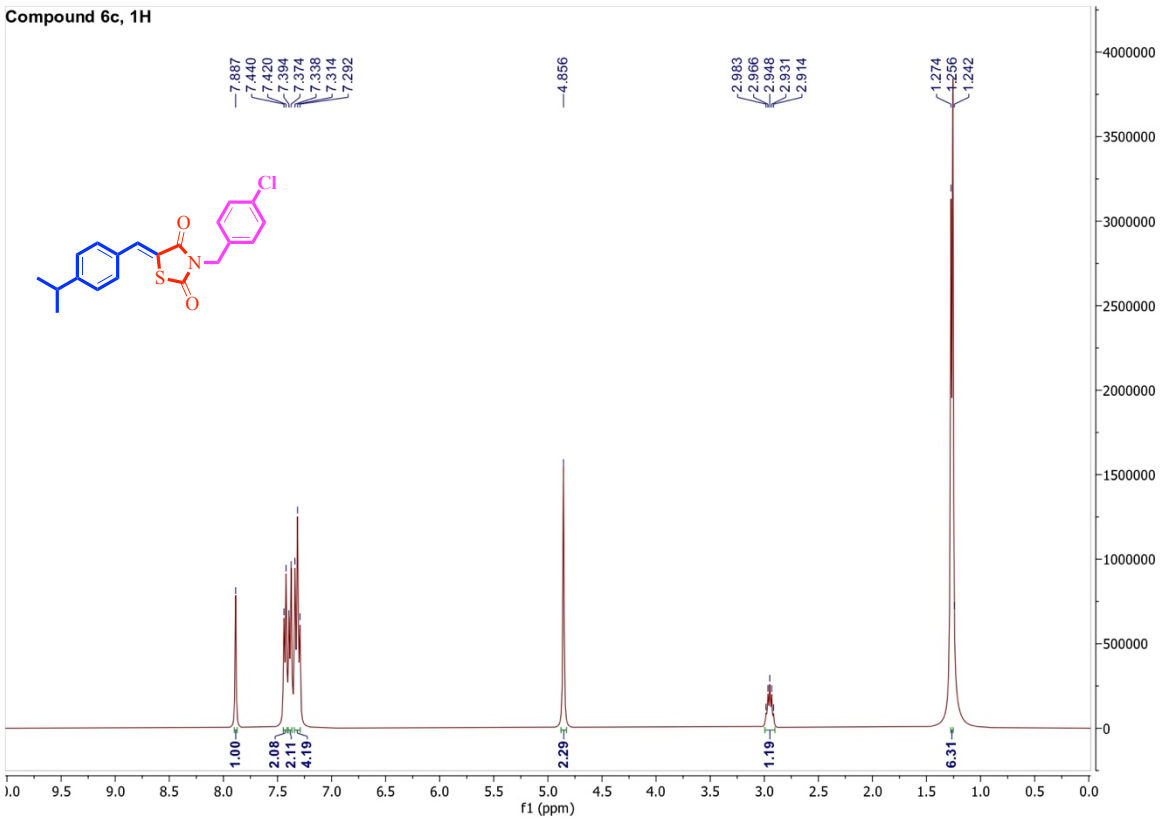

S.F4′: ^{1}H NMR of compound **6c**

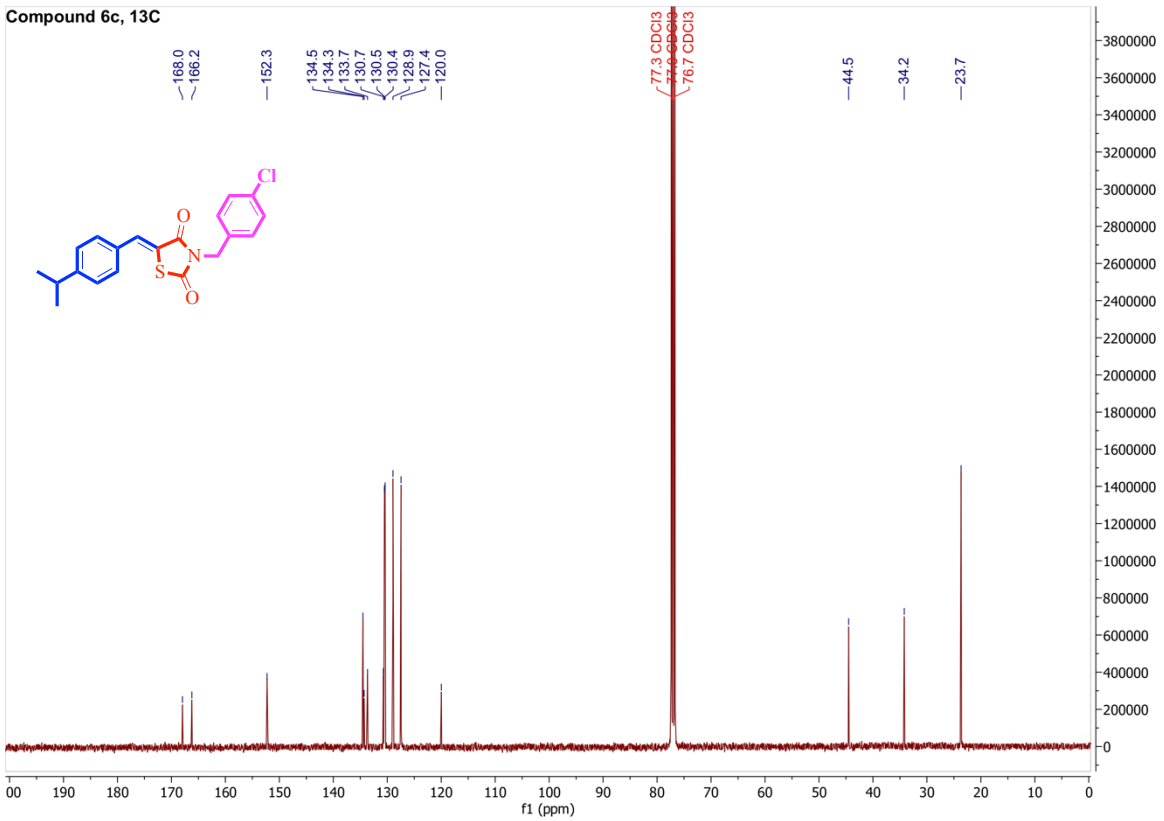

S.F4″: ^{13}C NMR of compound **6c**

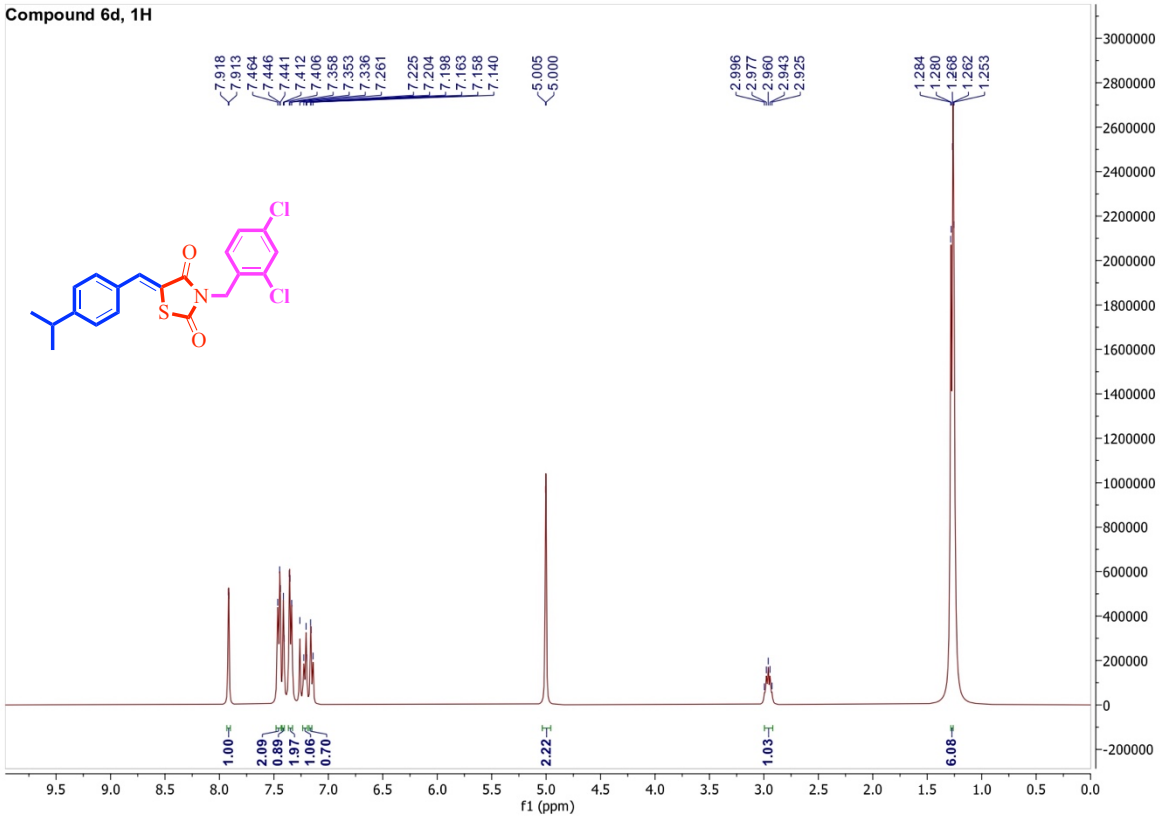

S.F5′: ^{1}H NMR of compound **6d**

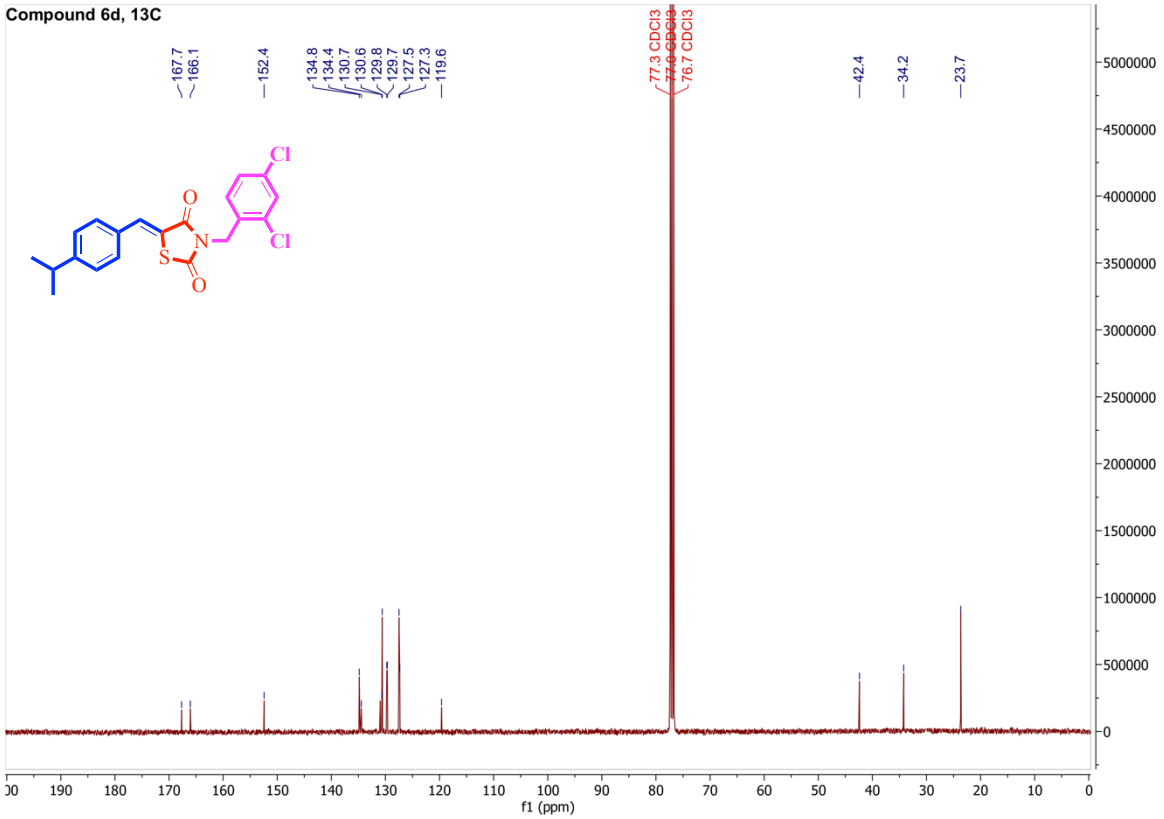

S.F5″: ^{13}C NMR of compound **6d**

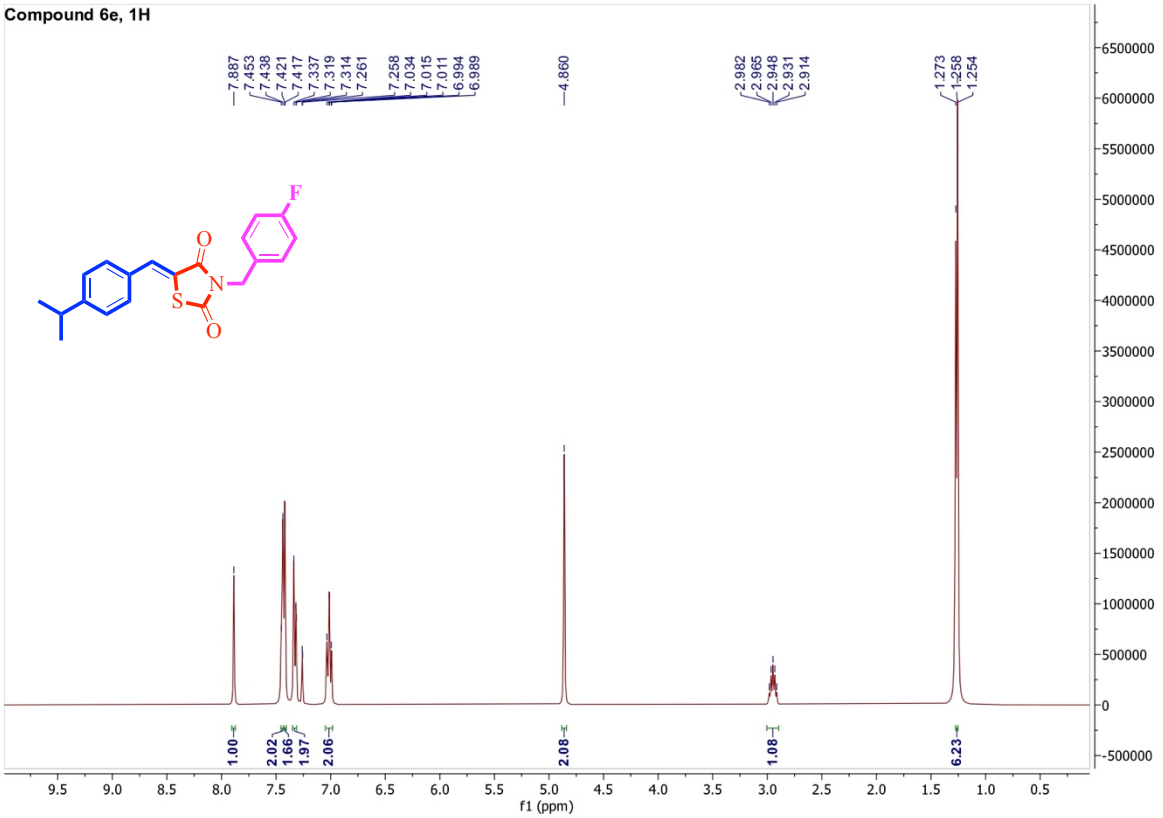

S.F6′: ^{1}H NMR of compound **6e**

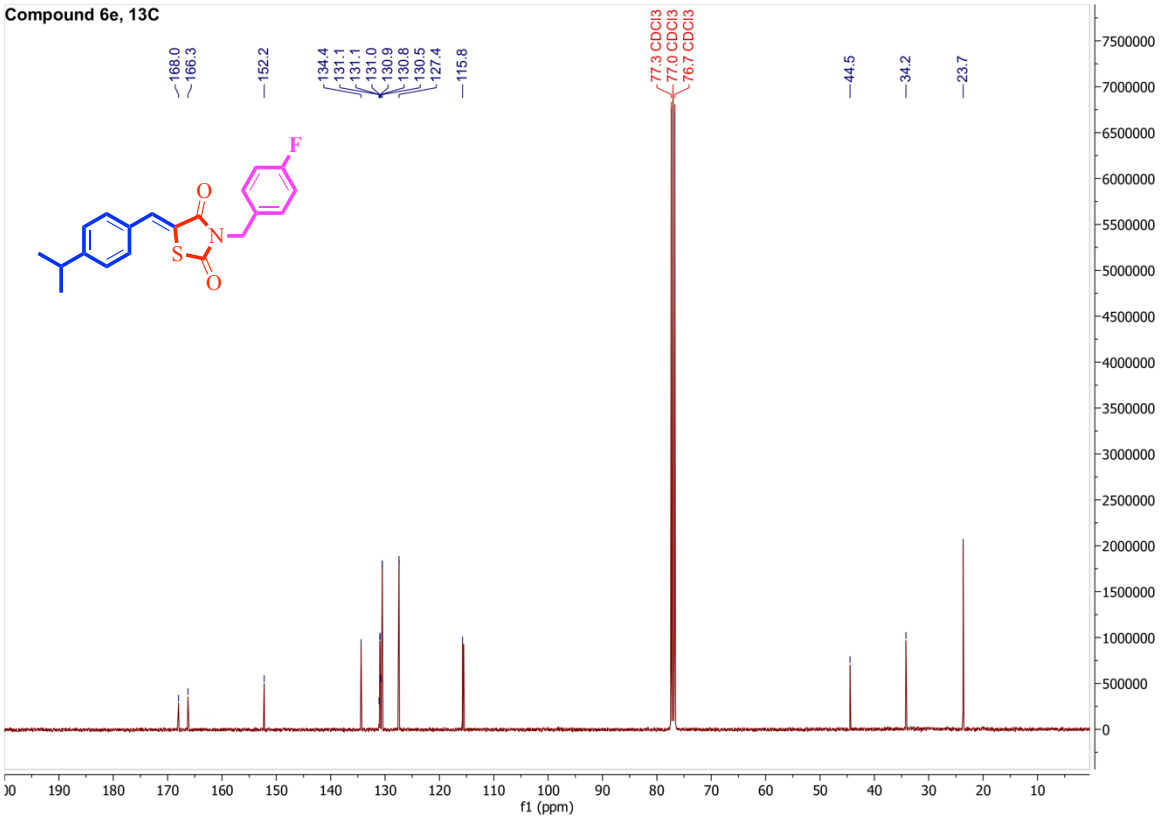

S.F6″: ^{13}C NMR of compound **6e**

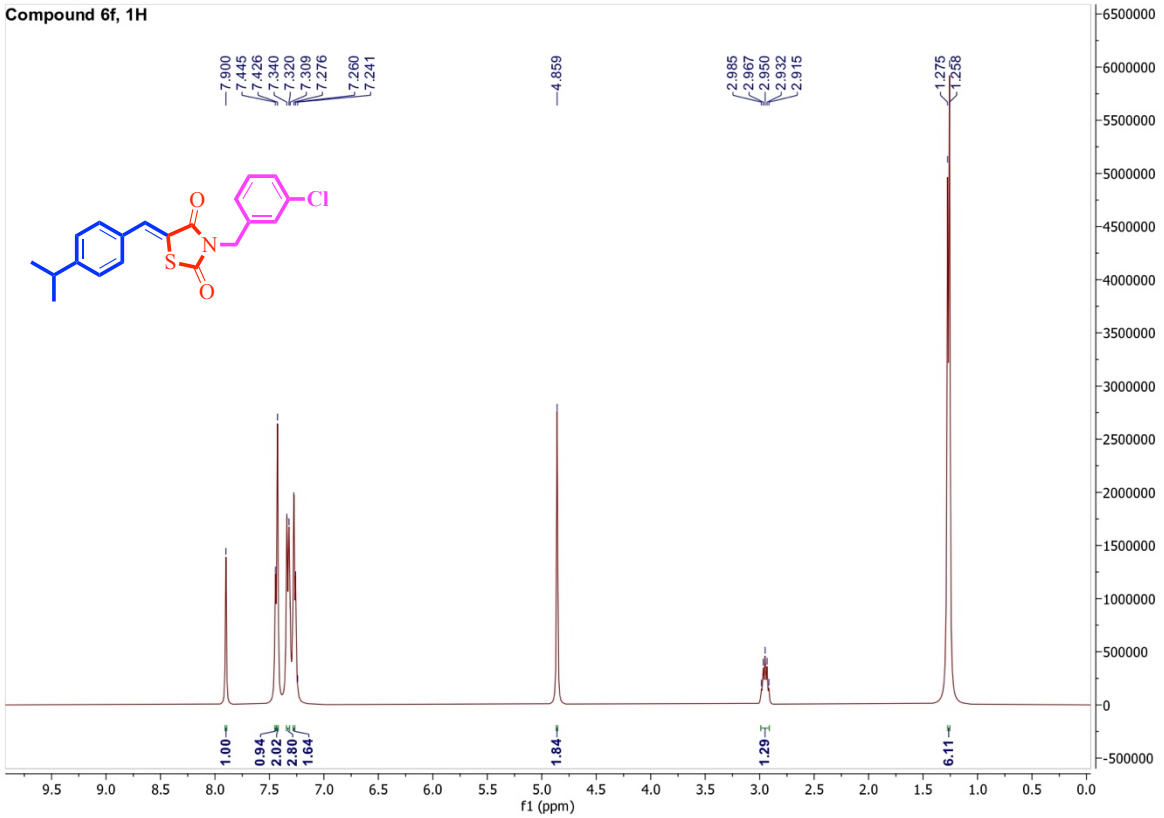

S.F7′: ^{1}H NMR of compound **6f**

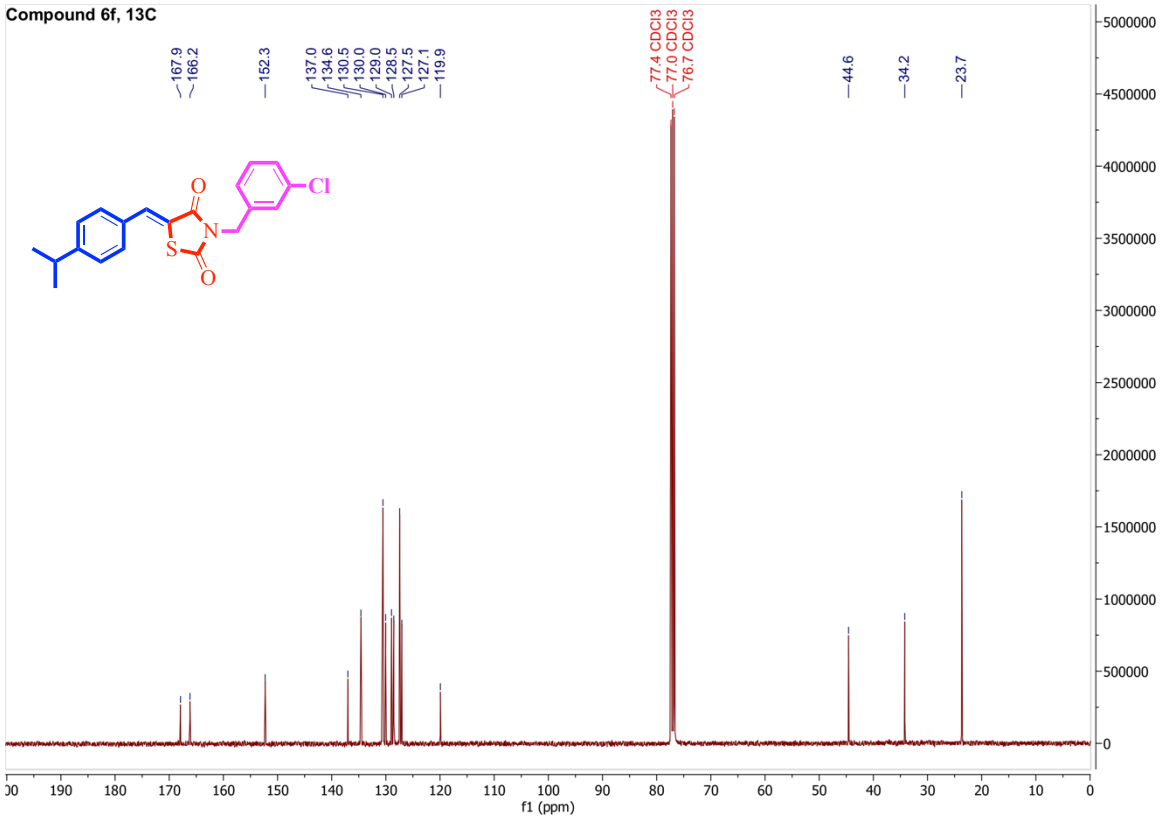

S.F7″: ^{13}C NMR of compound **6f**

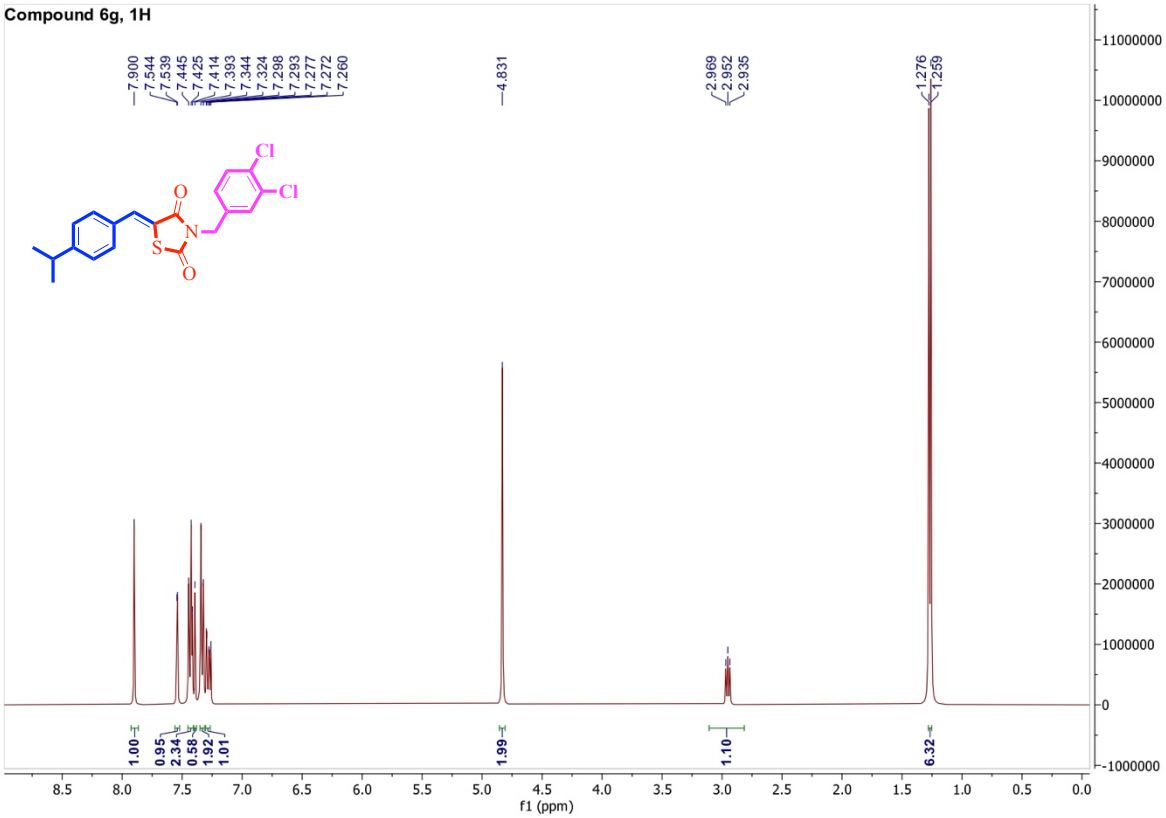

S.F8′: ^{1}H NMR of compound **6g**

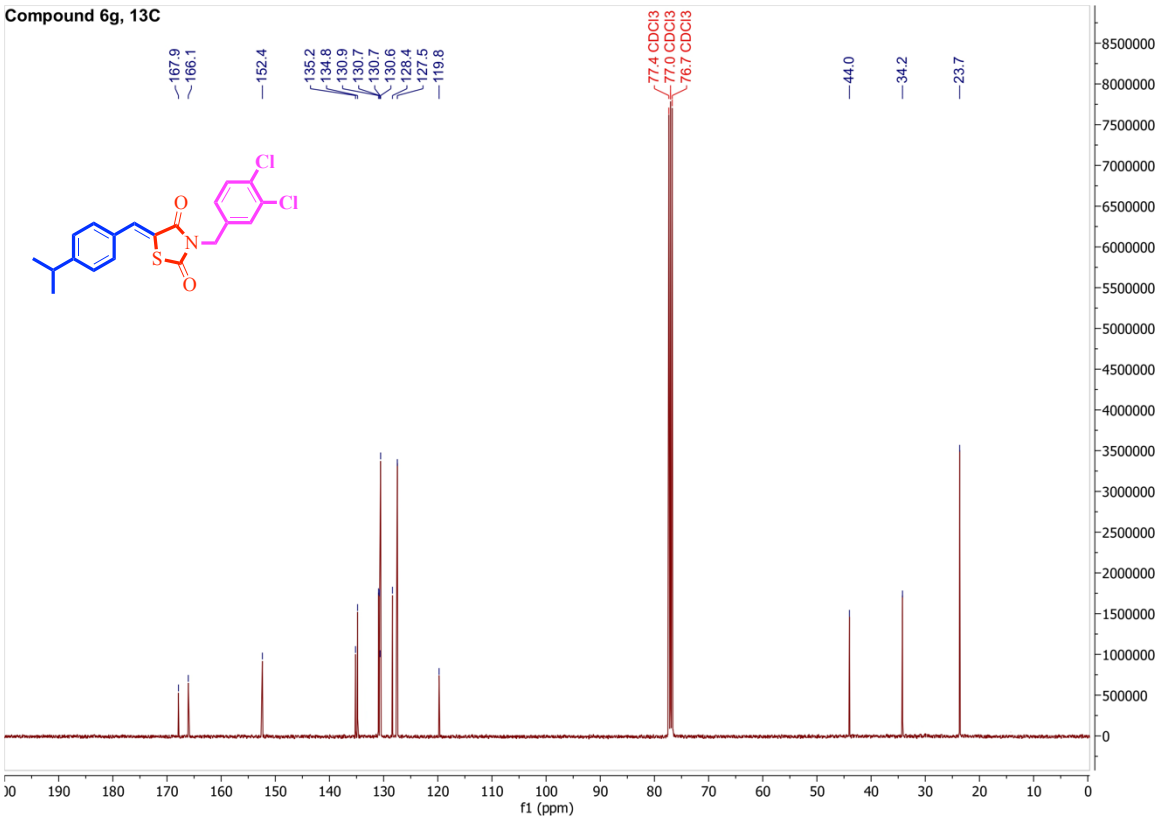

S.F8″: ^{13}C NMR of compound **6g**

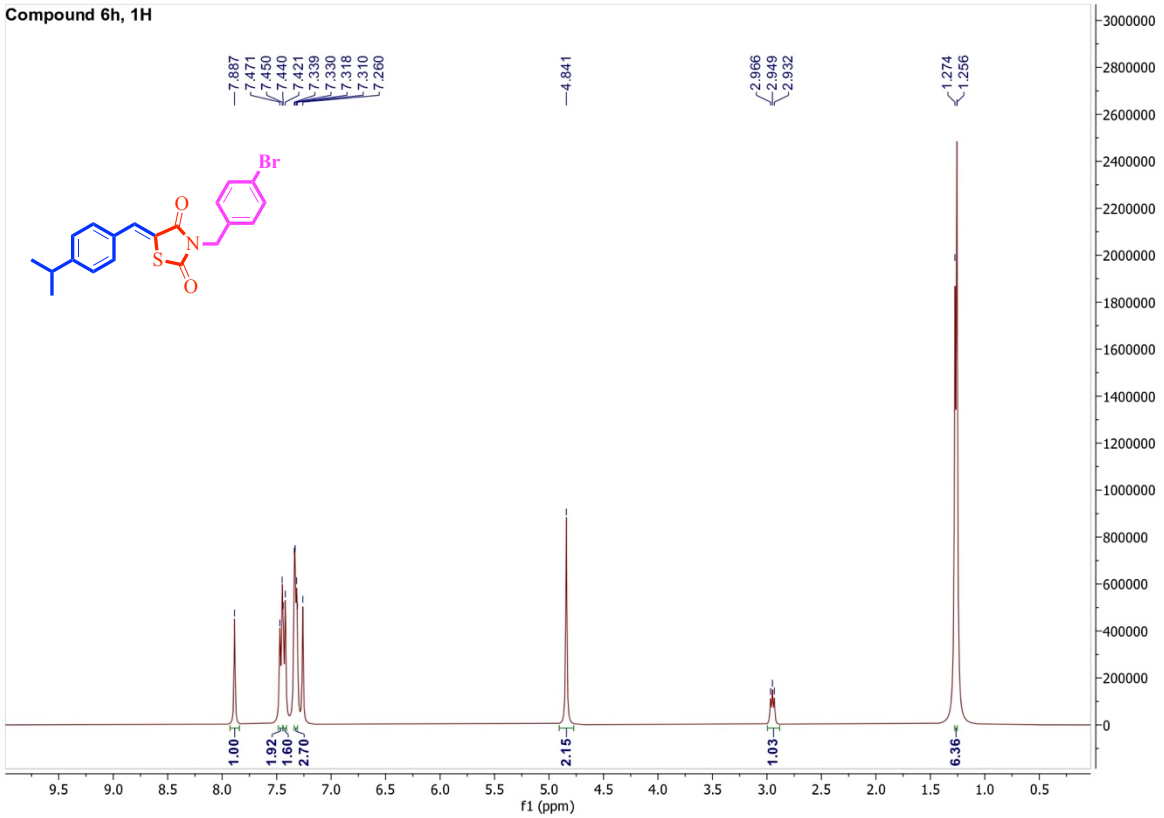

S.F9′: ^{1}H NMR of compound **6h**

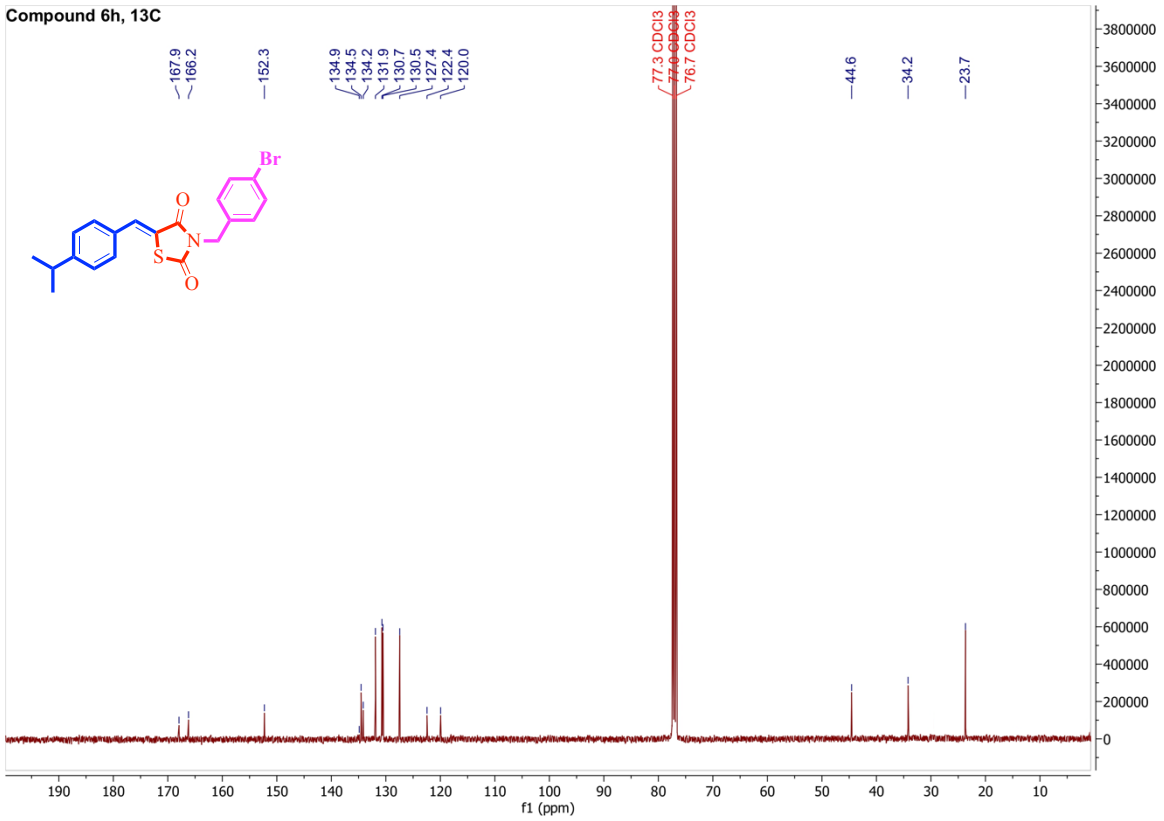

S.F9″: ^{13}C NMR of compound **6h**

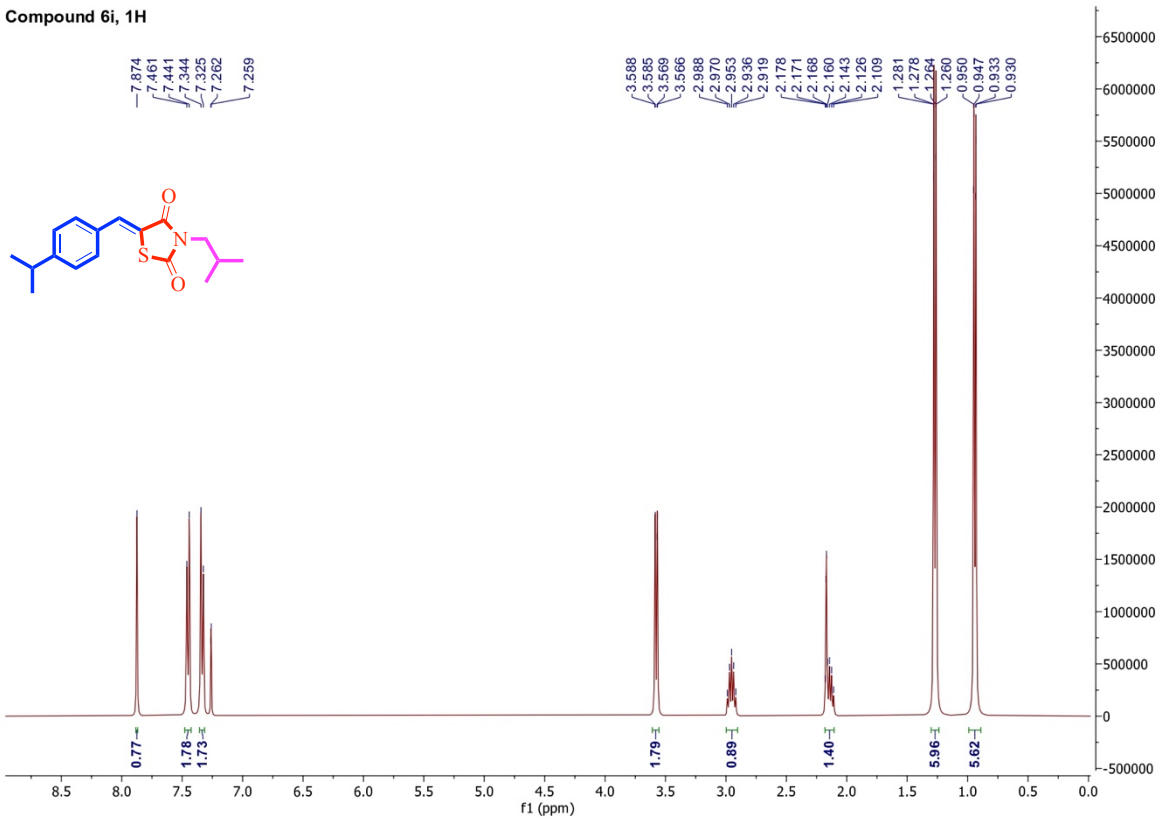

S.F10′: ^{1}H NMR of compound **6i**

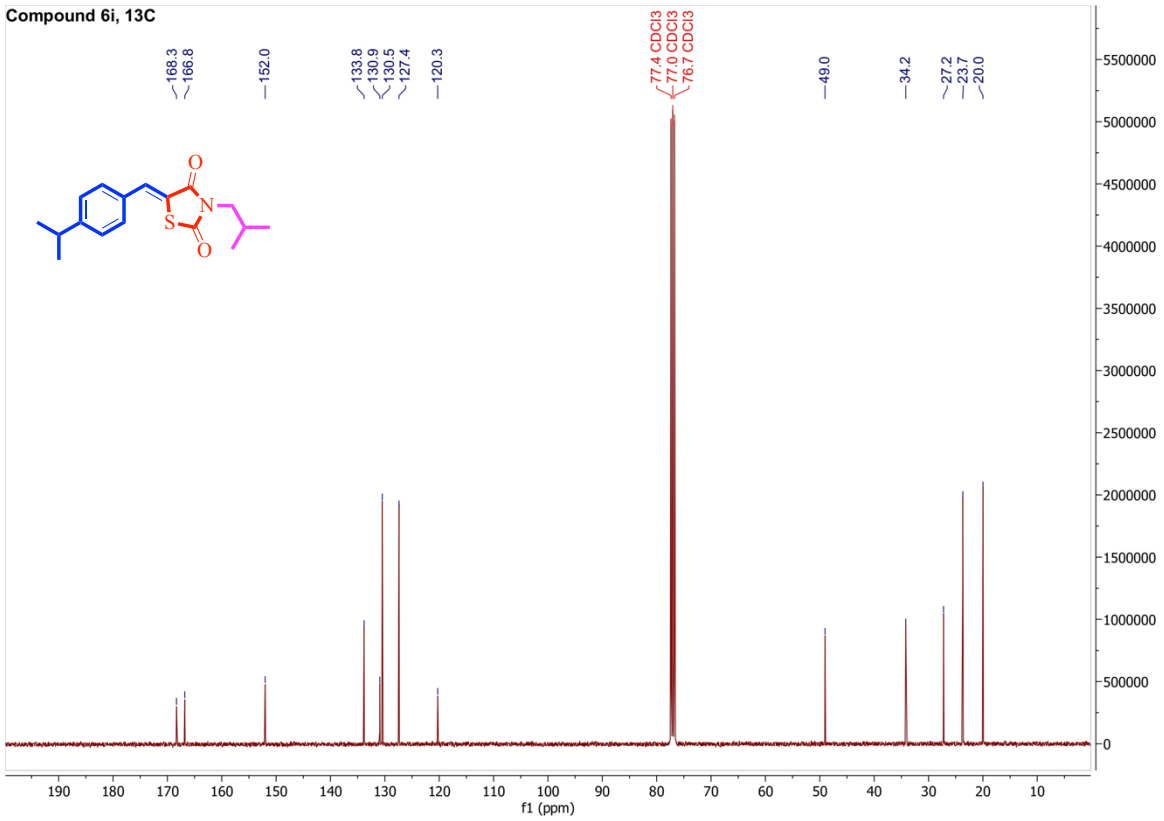

S.F10″: ^{13}C NMR of compound **6i**

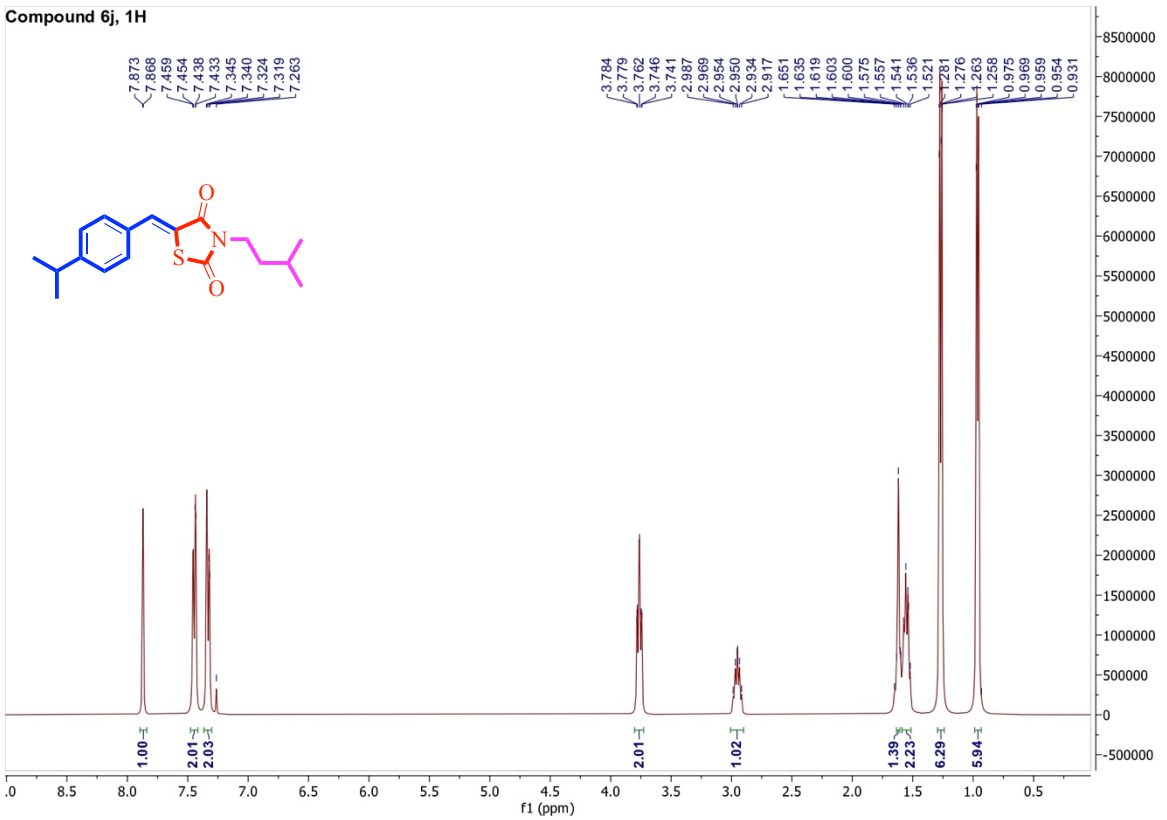

S.F11′: ^{1}H NMR of compound **6j**

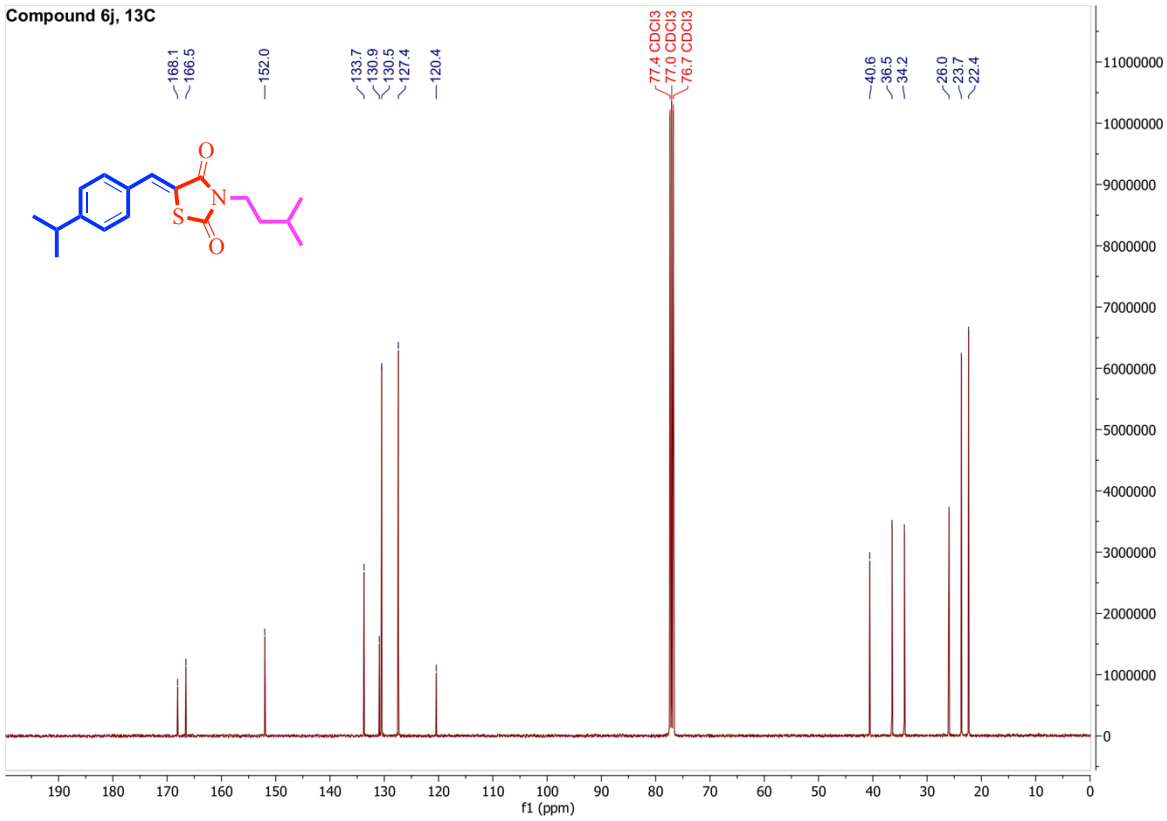

S.F11″: ^{13}C NMR of compound **6j**

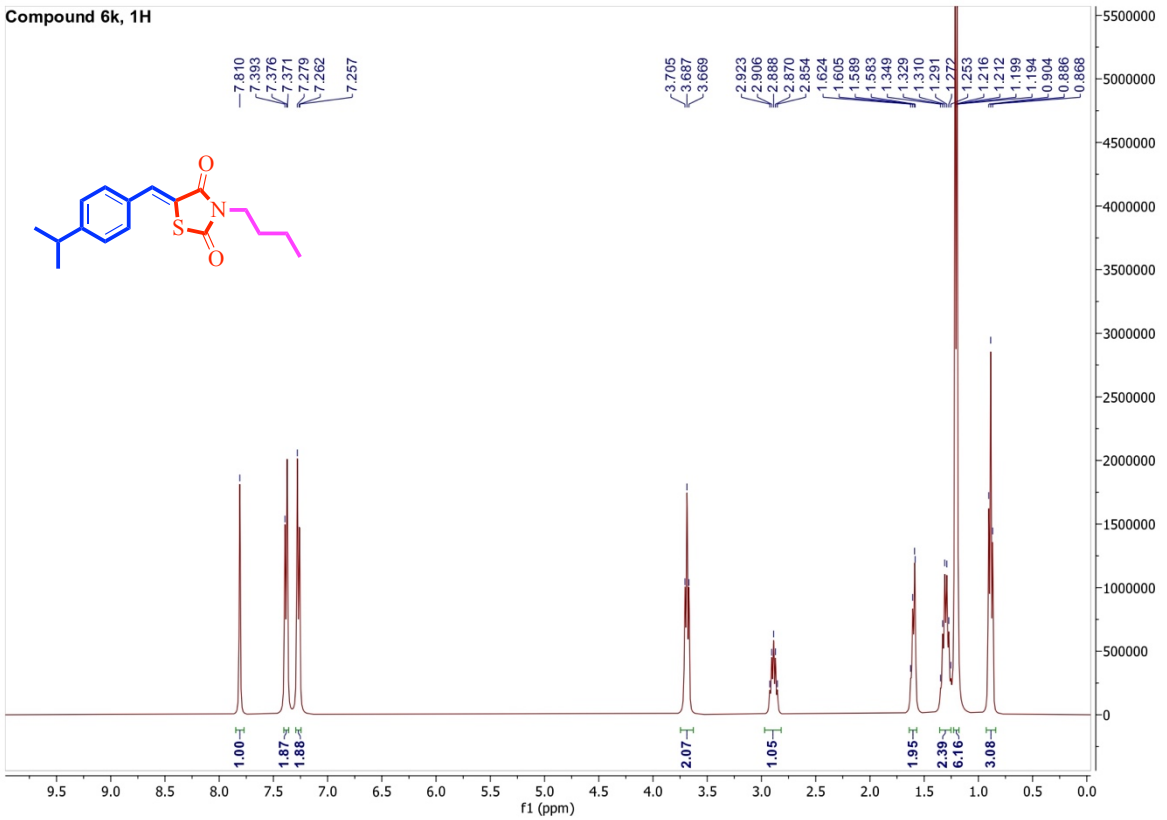

S.F12′: ^{1}H NMR of compound **6k**

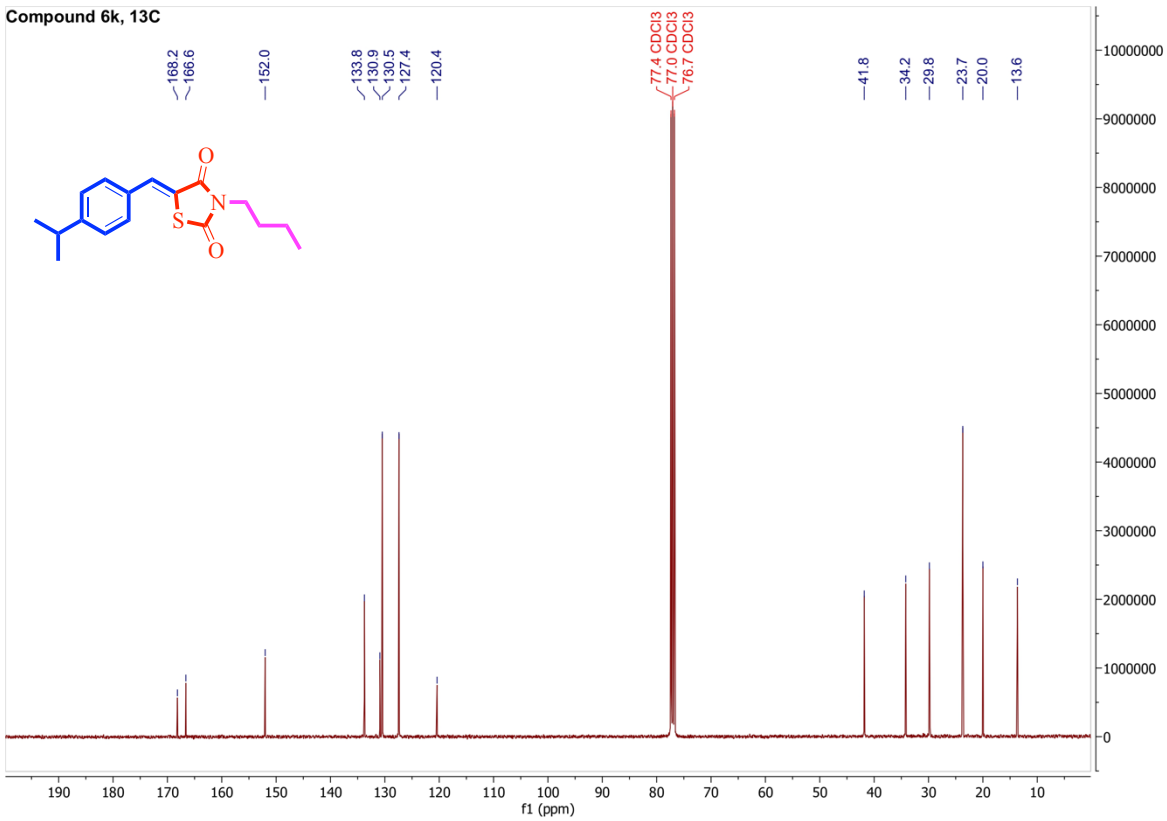

S.F12″: ^{13}C NMR of compound **6k**

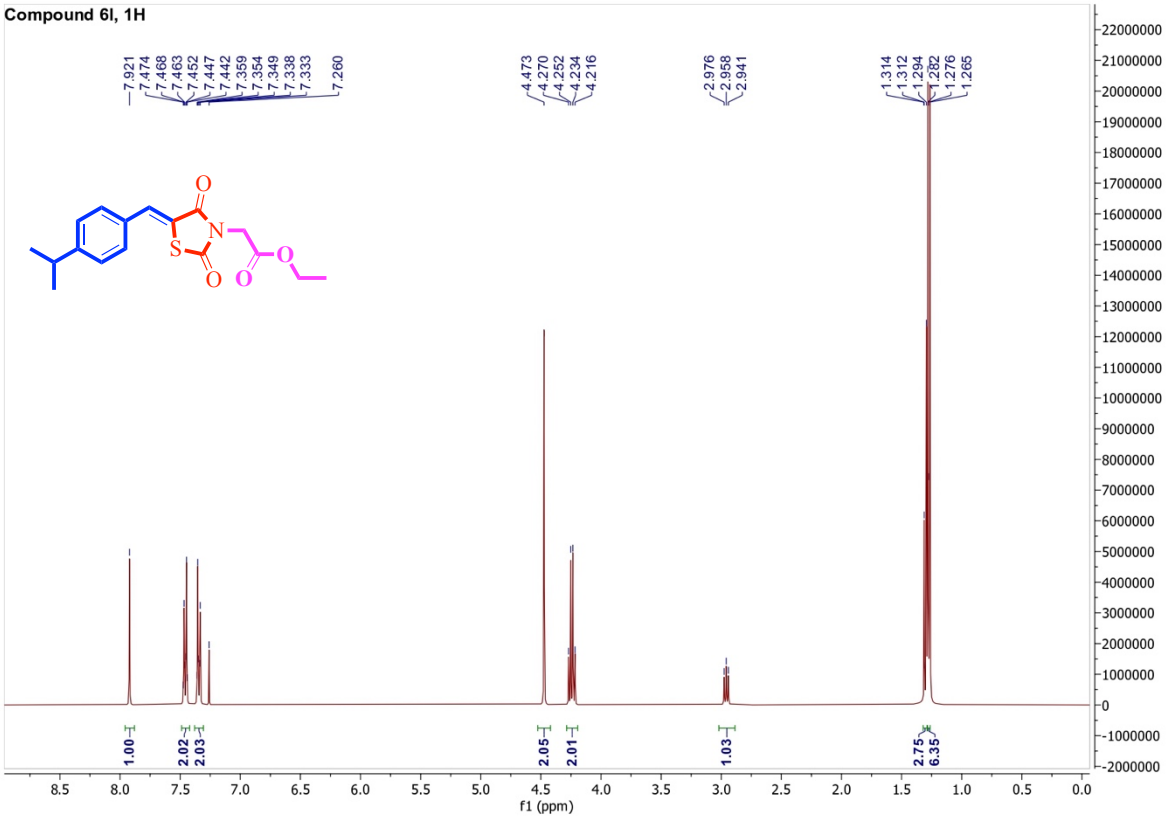

S.F13′: ^{1}H NMR of compound **6l**

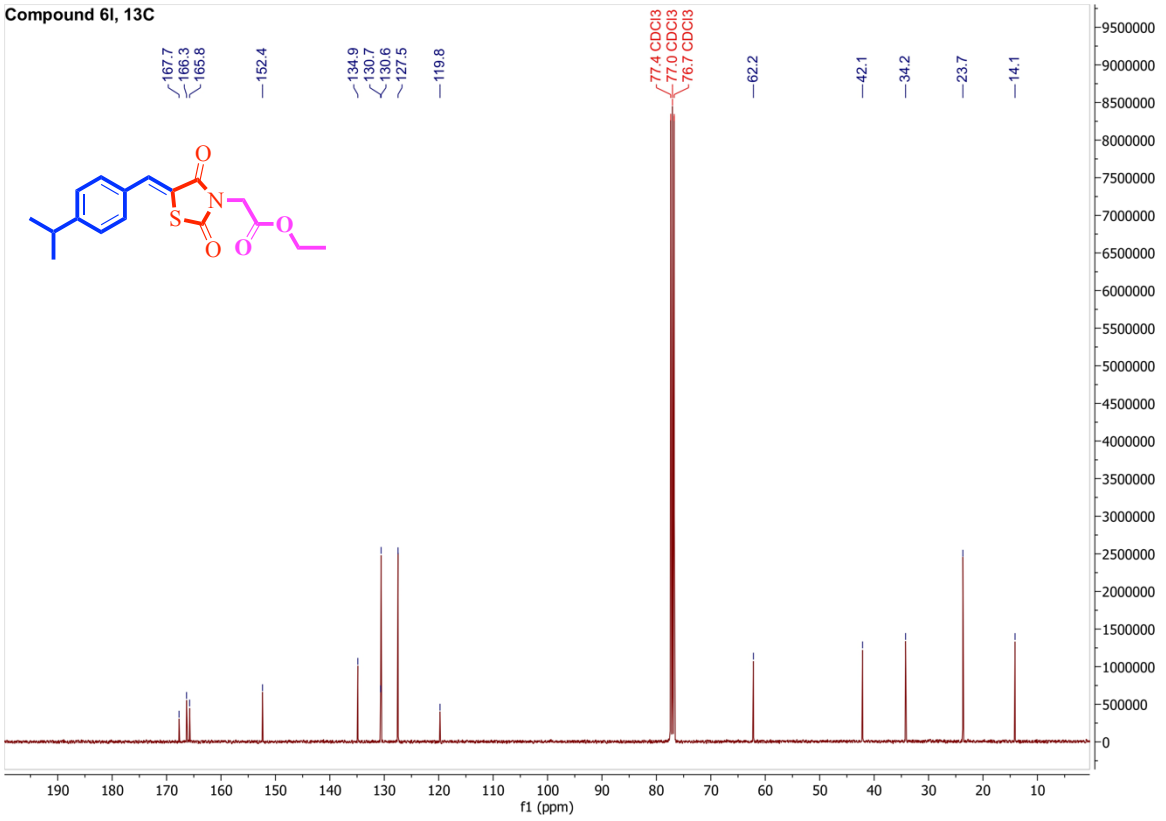

S.F13″: ^{13}C NMR of compound **6l**

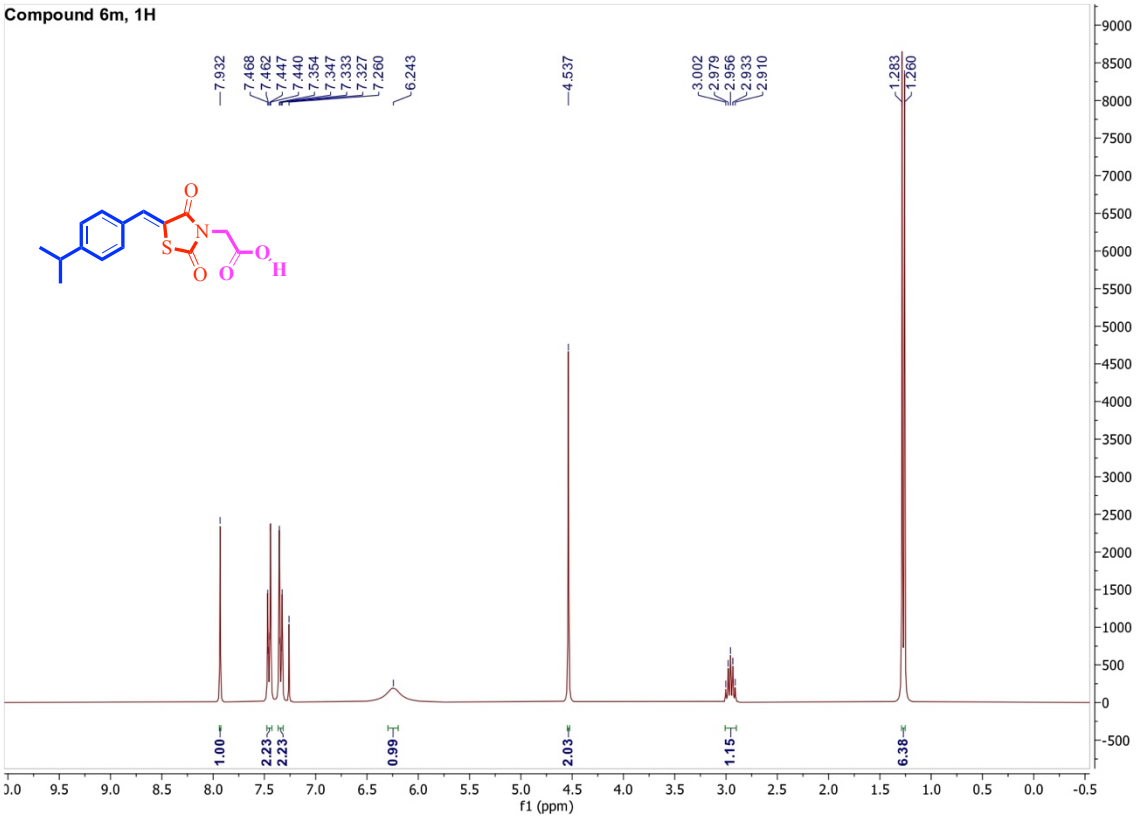

S.F14′: ^{1}H NMR of compound **6m**

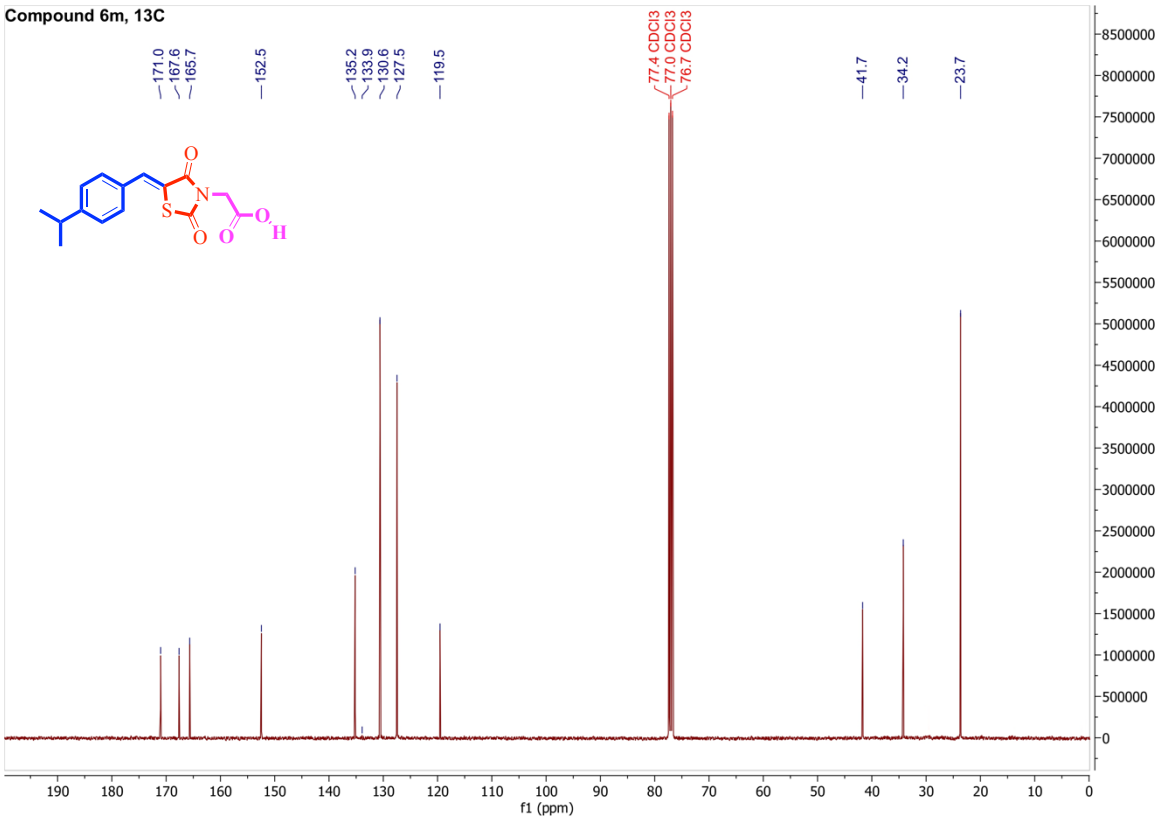

S.F14″: ^{13}C NMR of compound **6m**

II. FT-IR data (Compound **5** and **6a-6m):**

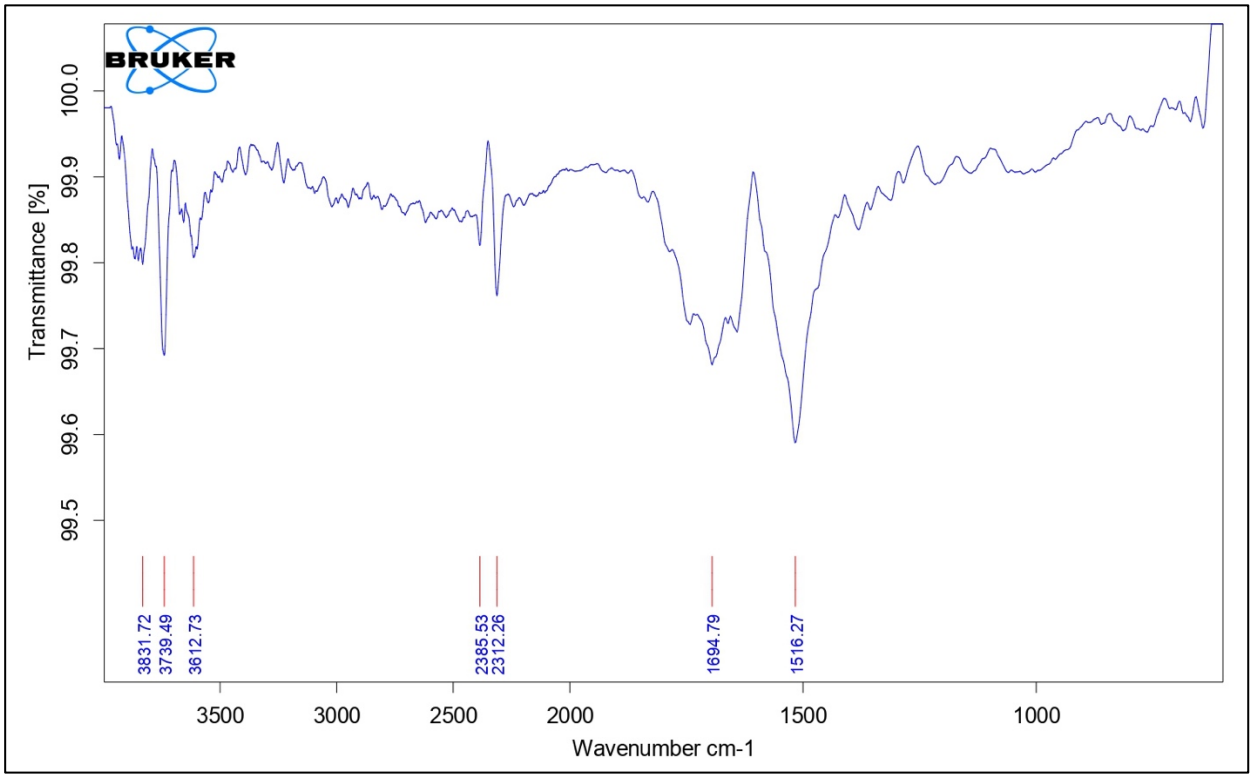

S.F15: FT-IR of compound **5**

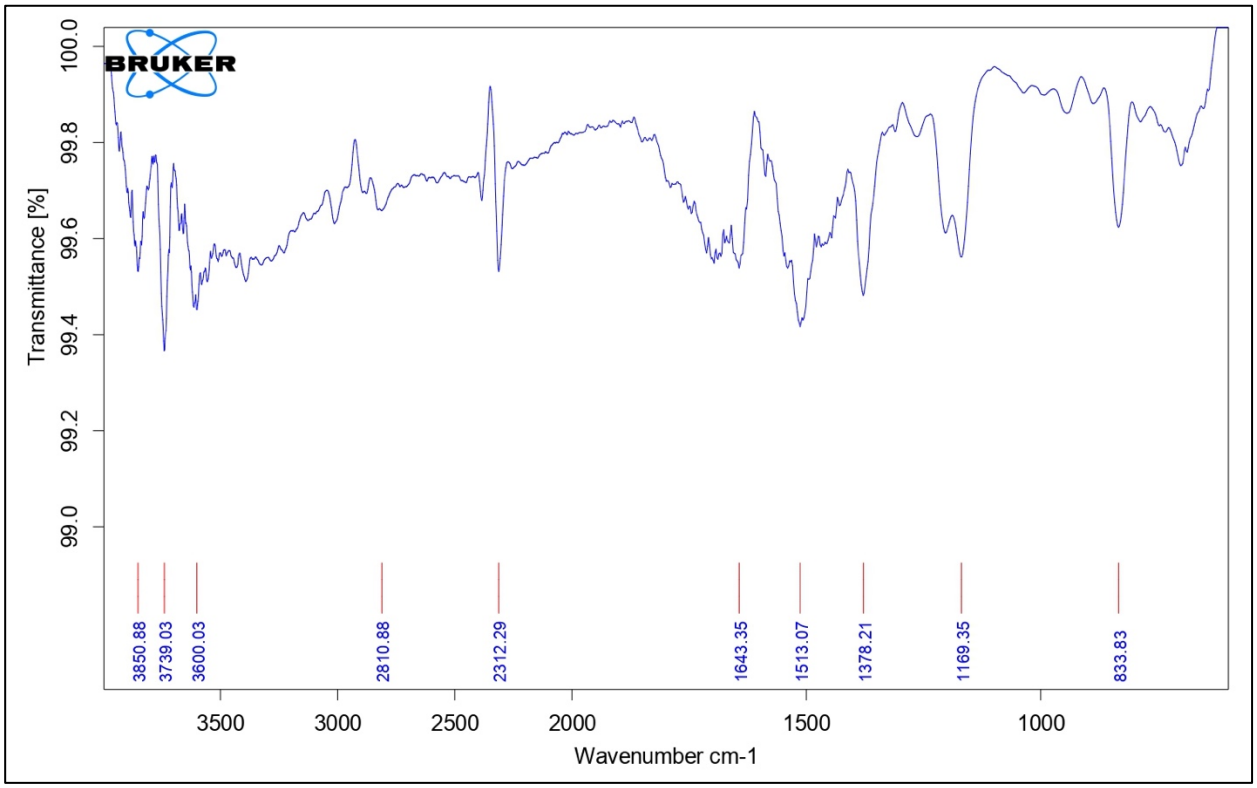

S.F16: FT-IR of compound **6a**

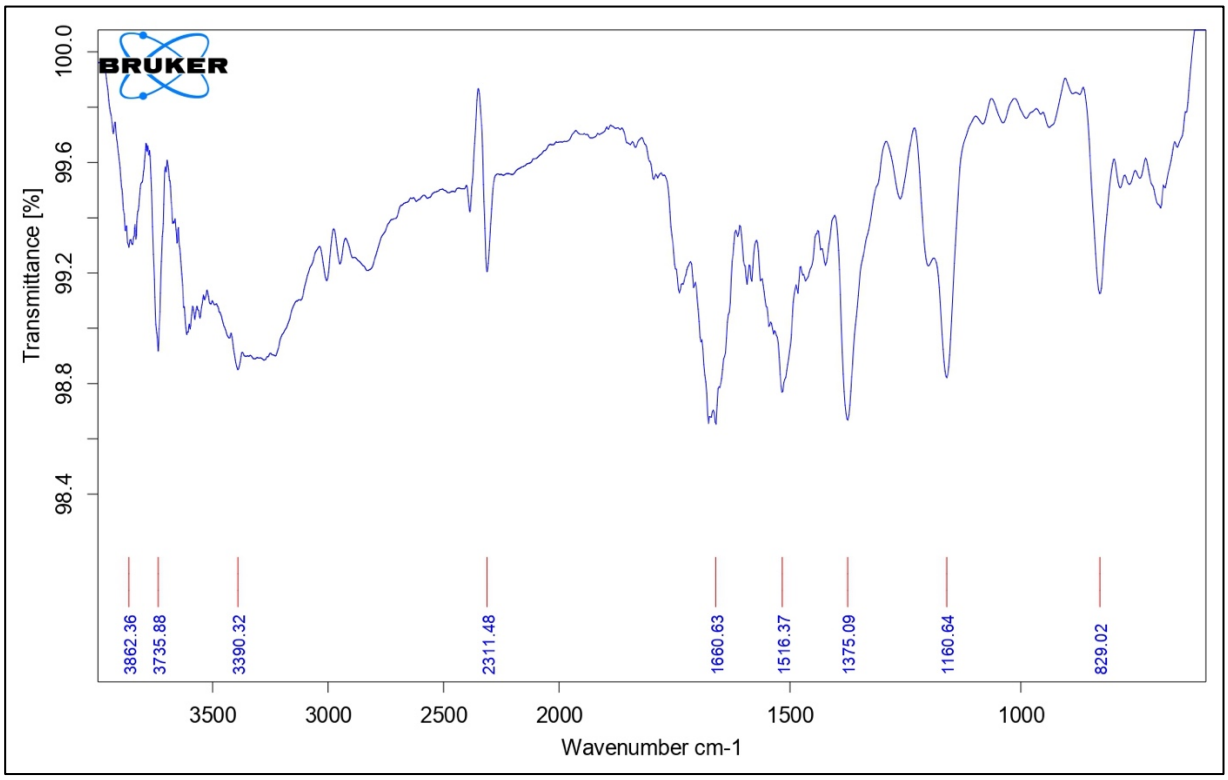

S.F17: FT-IR of compound **6b**

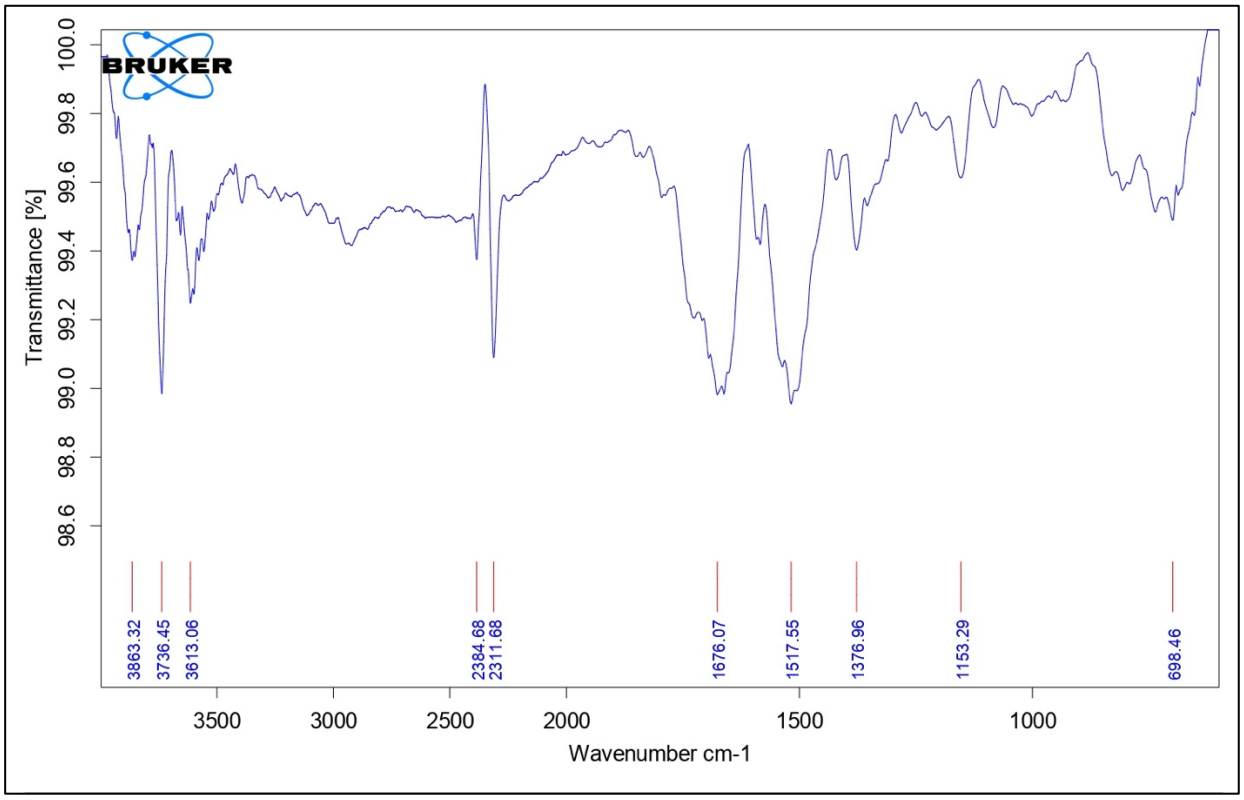

S.F18: FT-IR of compound **6c**

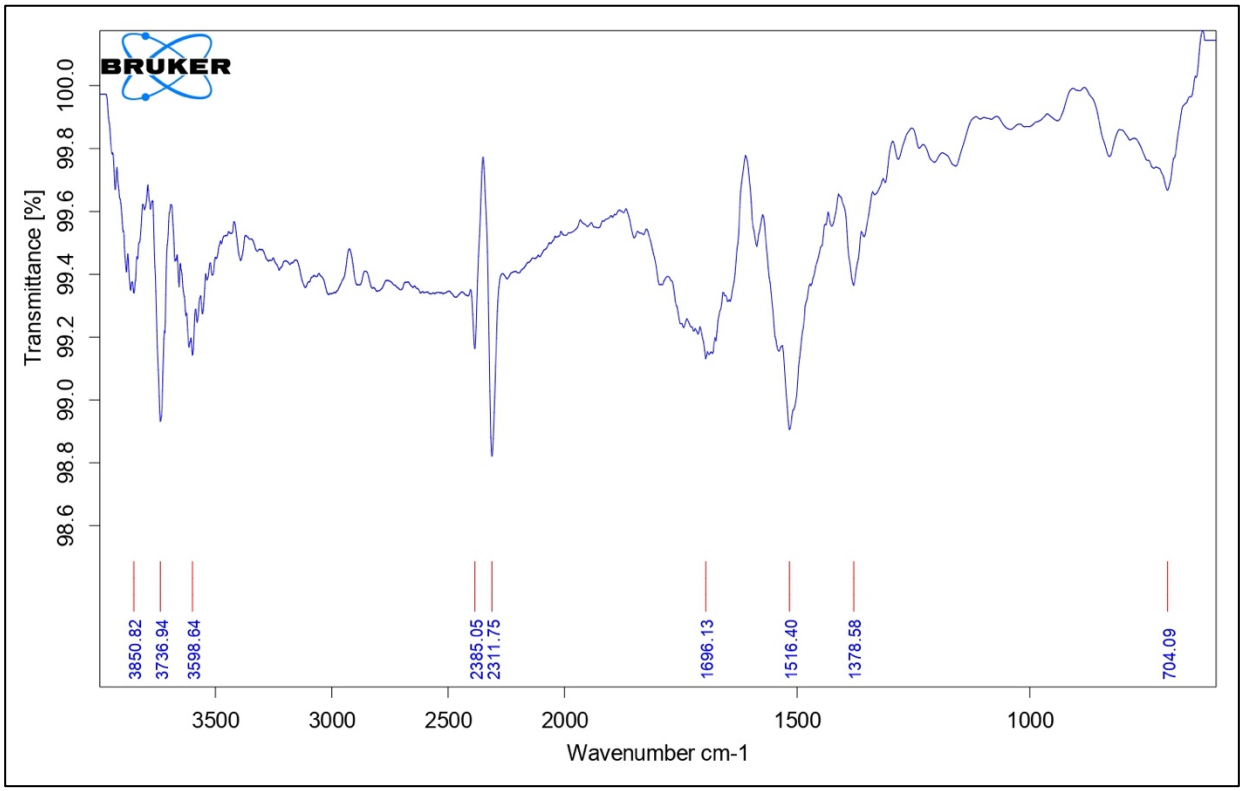

S.F19: FT-IR of compound **6d**

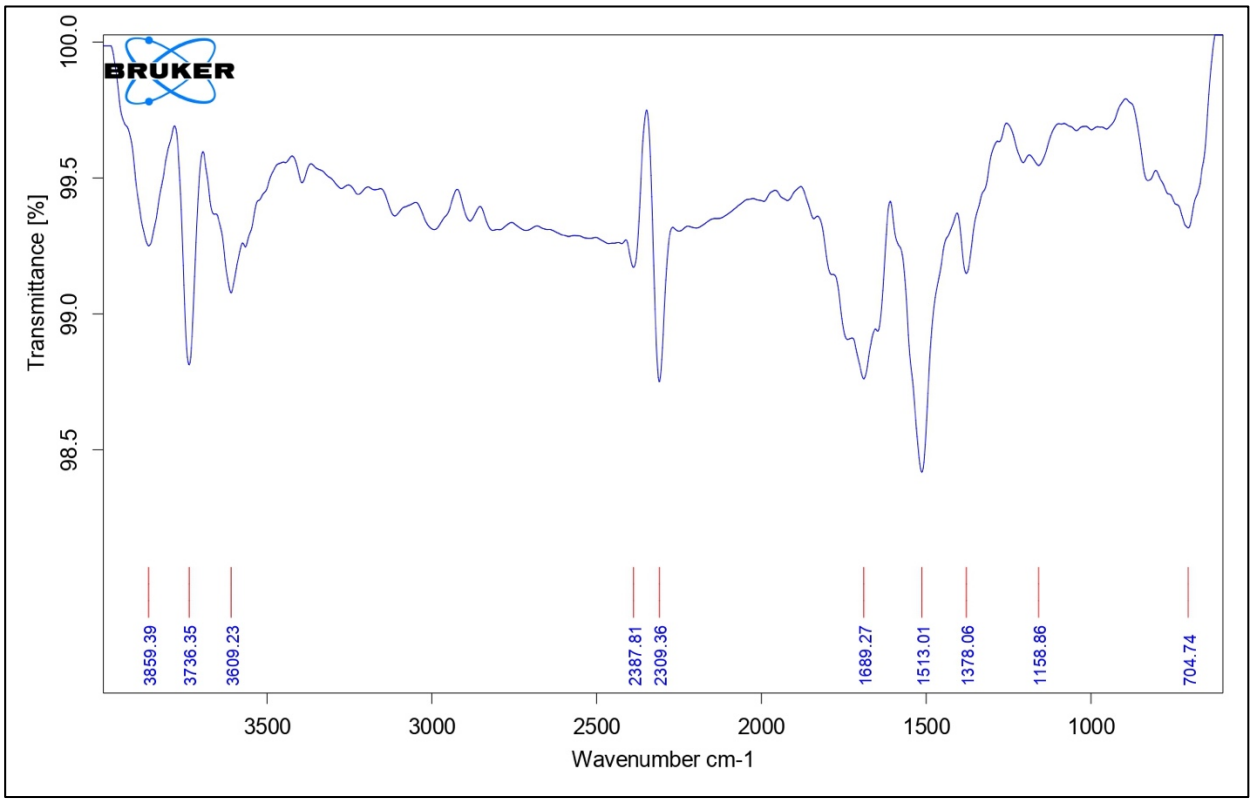

S.F20: FT-IR of compound **6e**

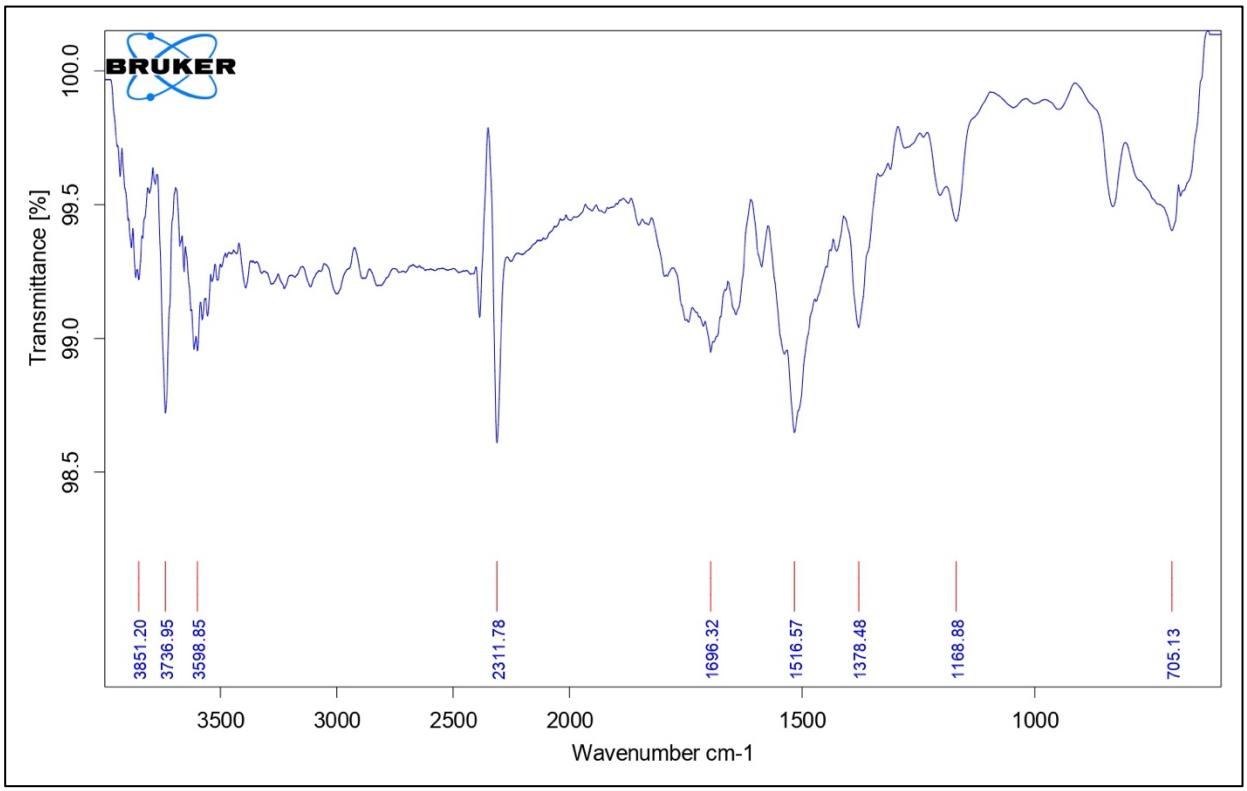

S.F21: FT-IR of compound **6f**

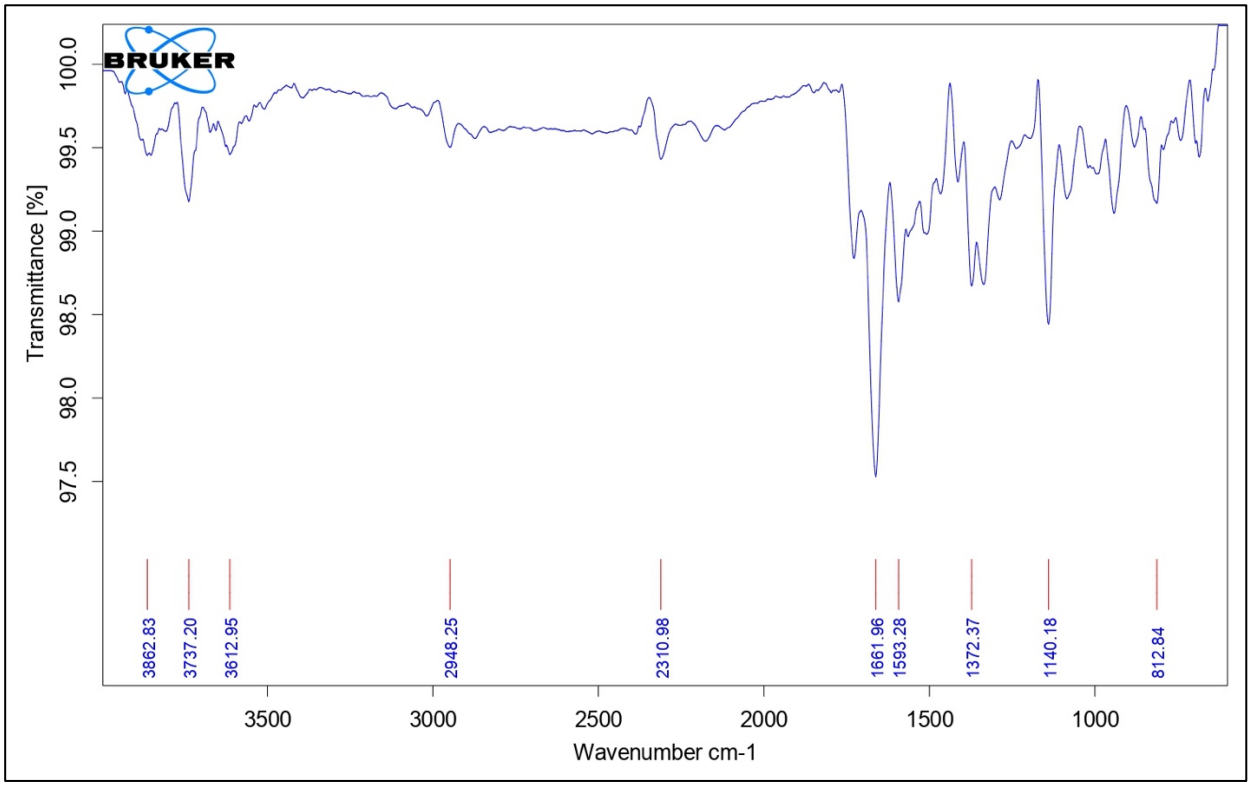

S.F22: FT-IR of compound **6g**

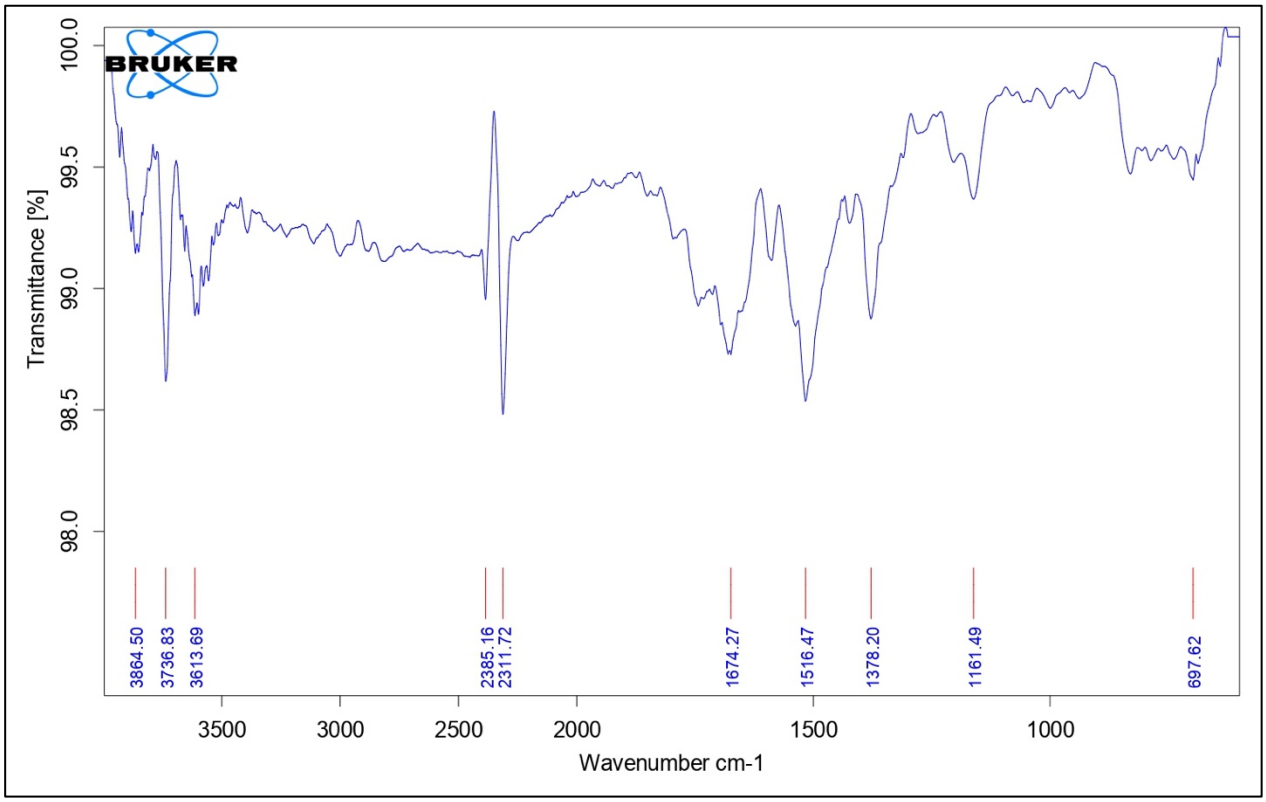

S.F23: FT-IR of compound **6h**

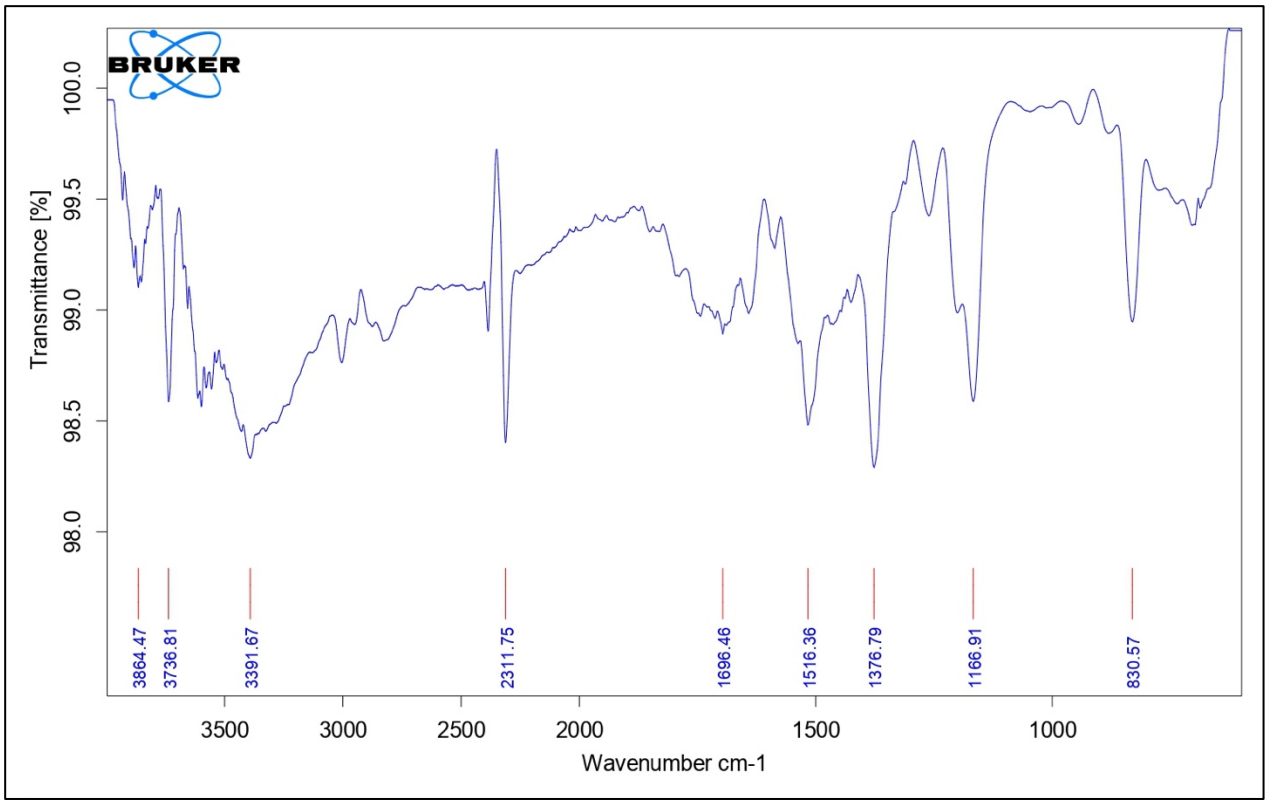

S.F24: FT-IR of compound **6i**

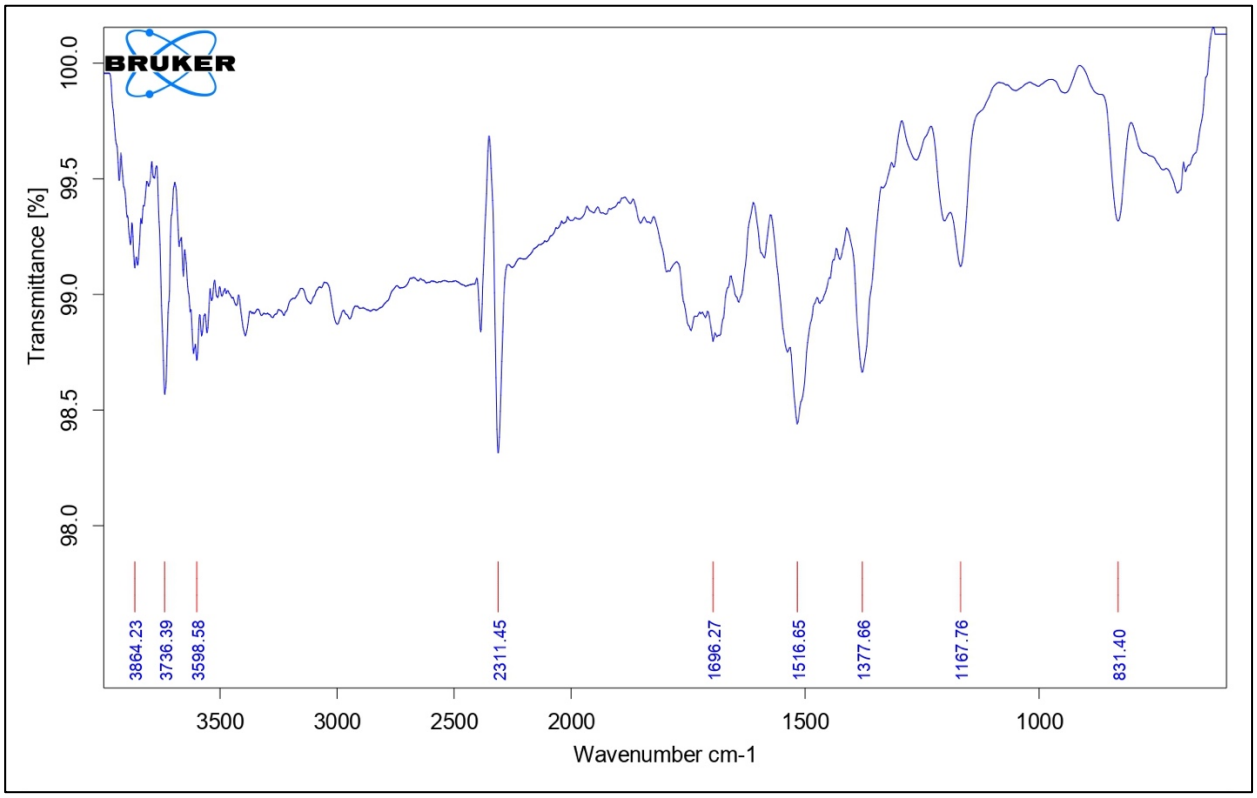

S.F25: FT-IR of compound **6j**

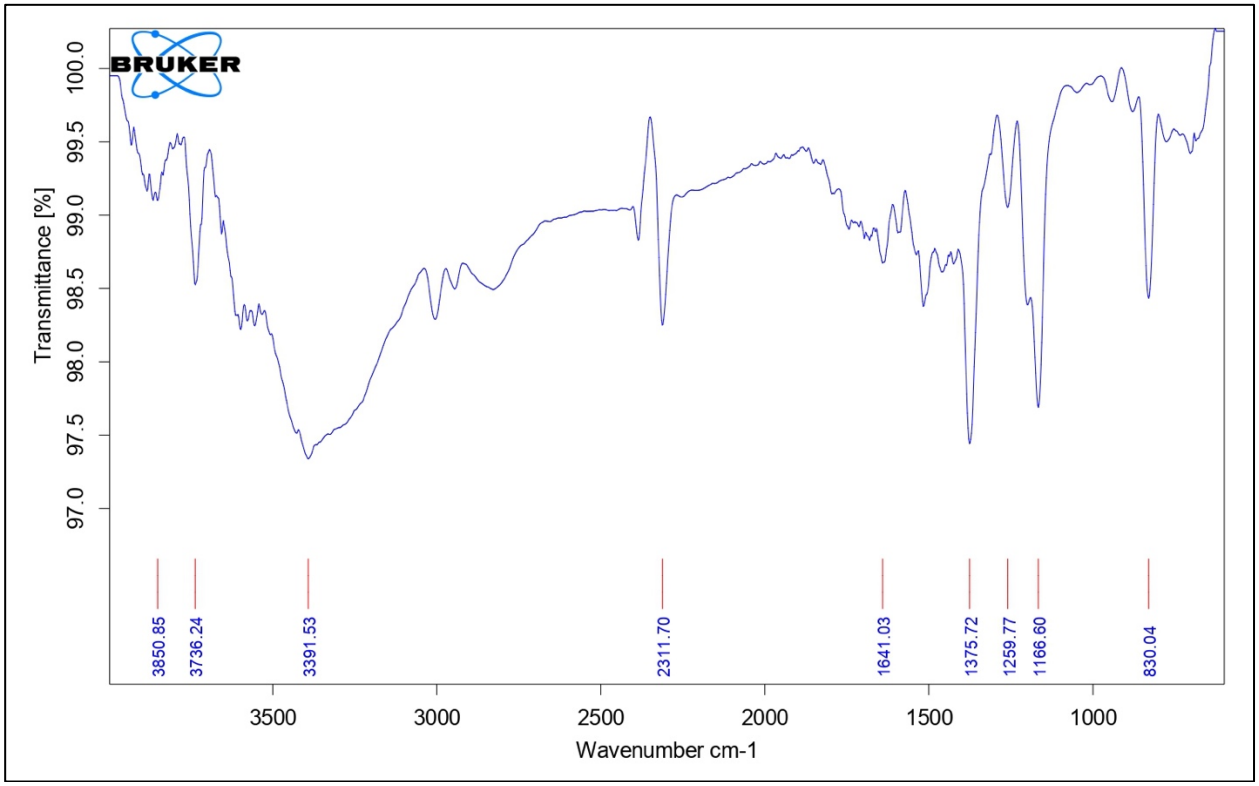

S.F26: FT-IR of compound **6k**

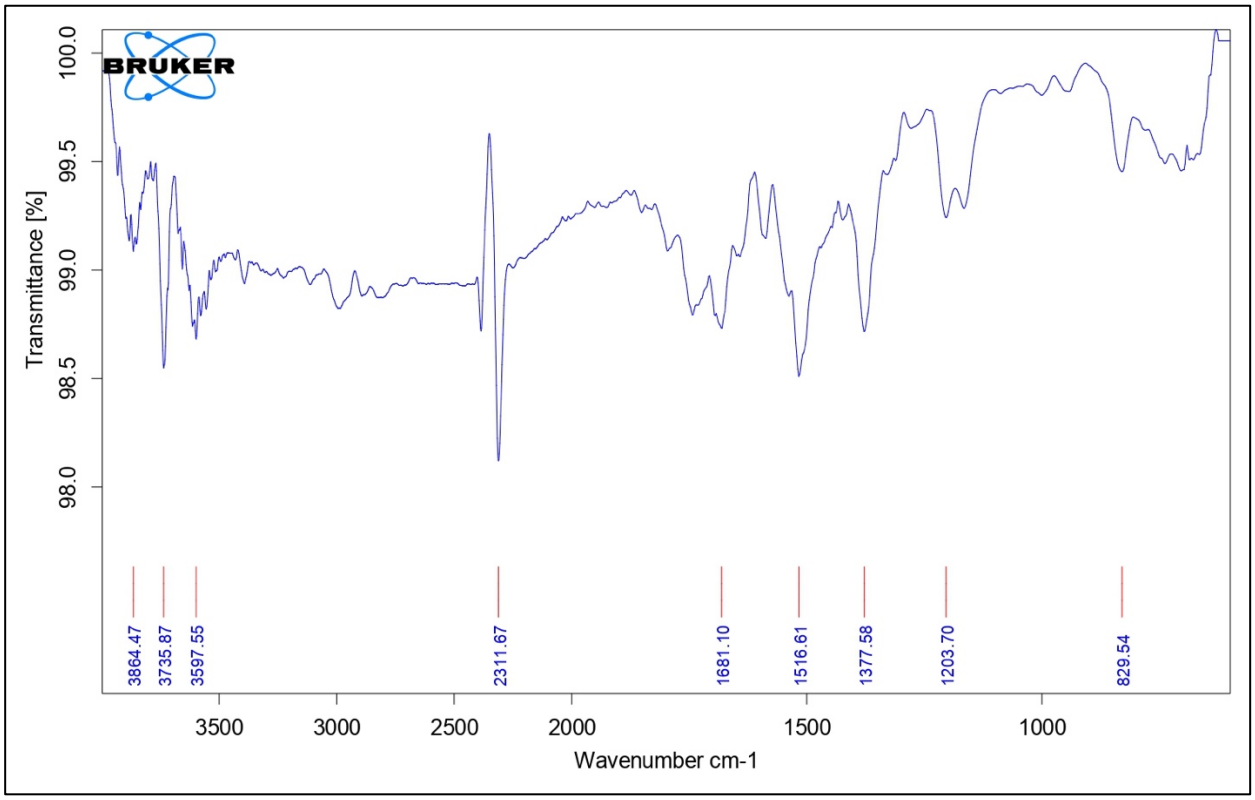

S.F27: FT-IR of compound **6l**

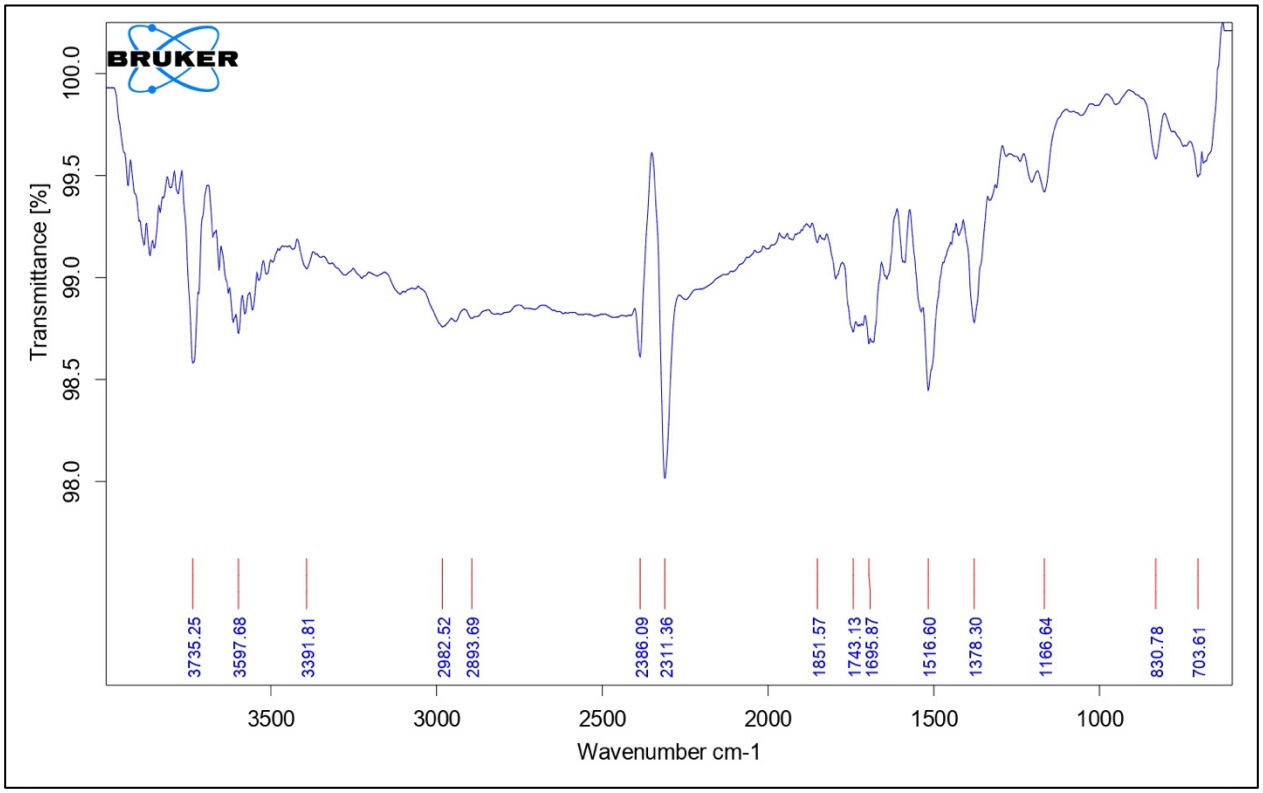

S.F28: FT-IR of compound **6m**

III. ESI mass data (Compound **5** and **6a-6m**):

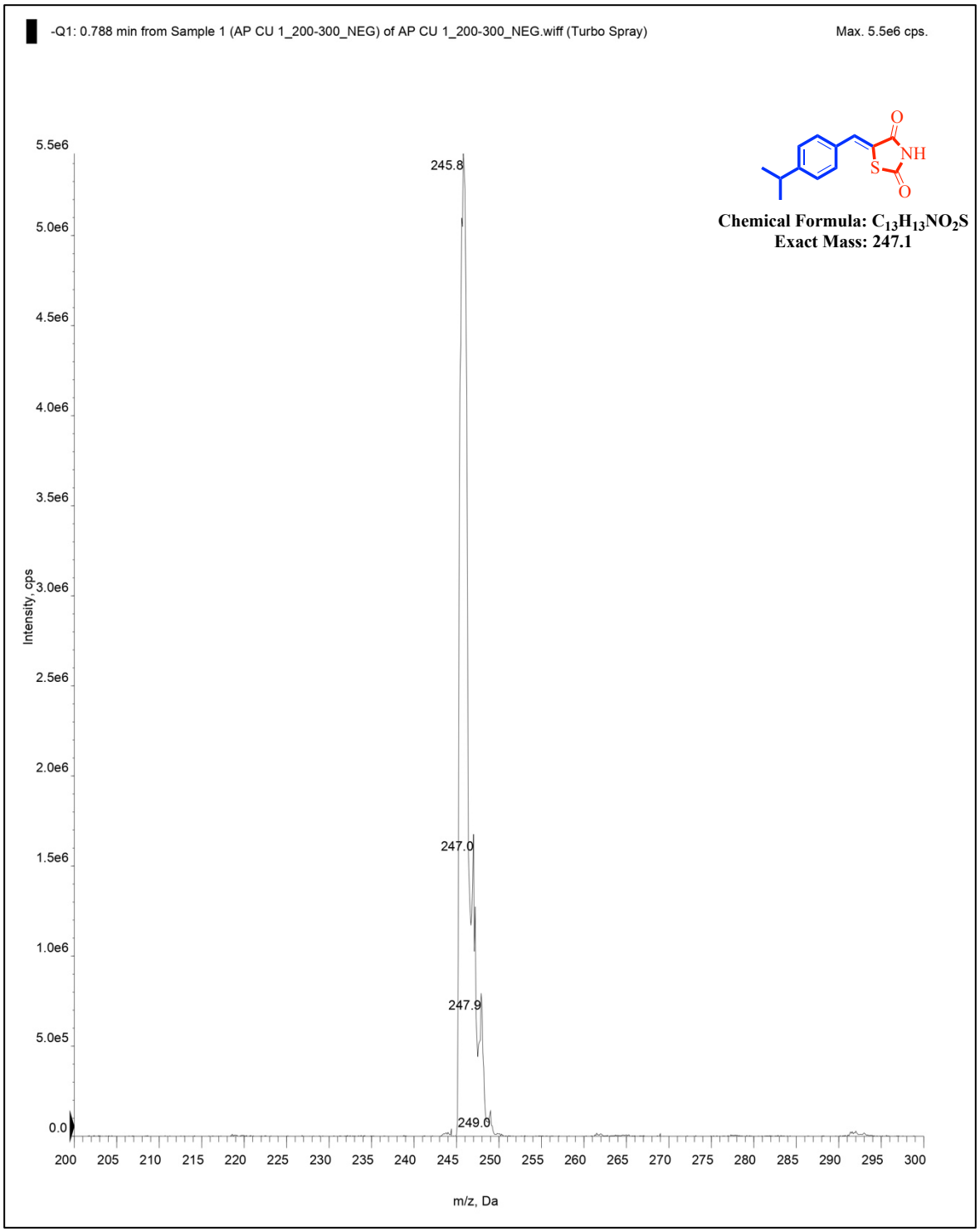

S.F29: MS (ESI, m/z) of Compound **5**

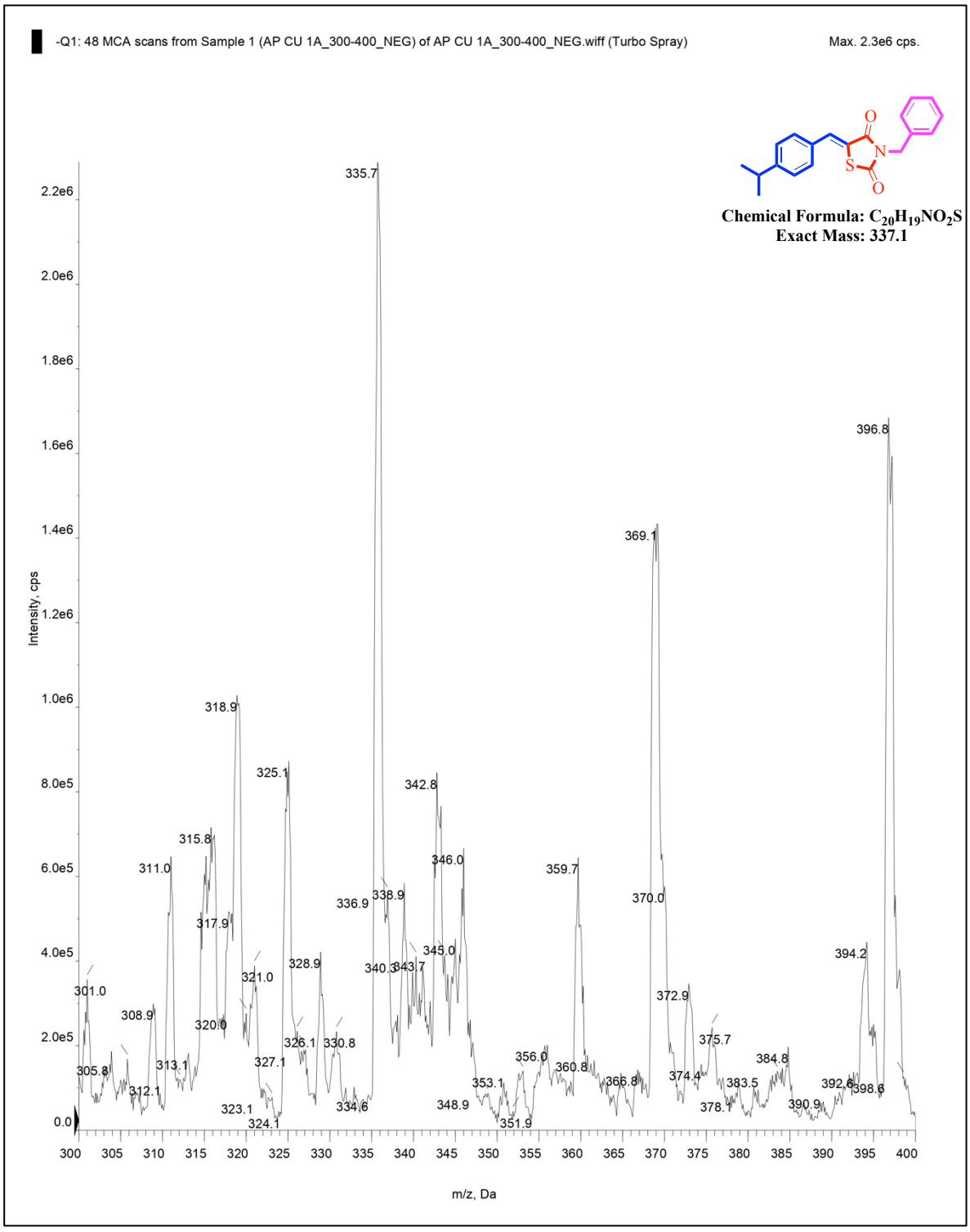

S.F30: MS (ESI, m/z) of Compound **6a**

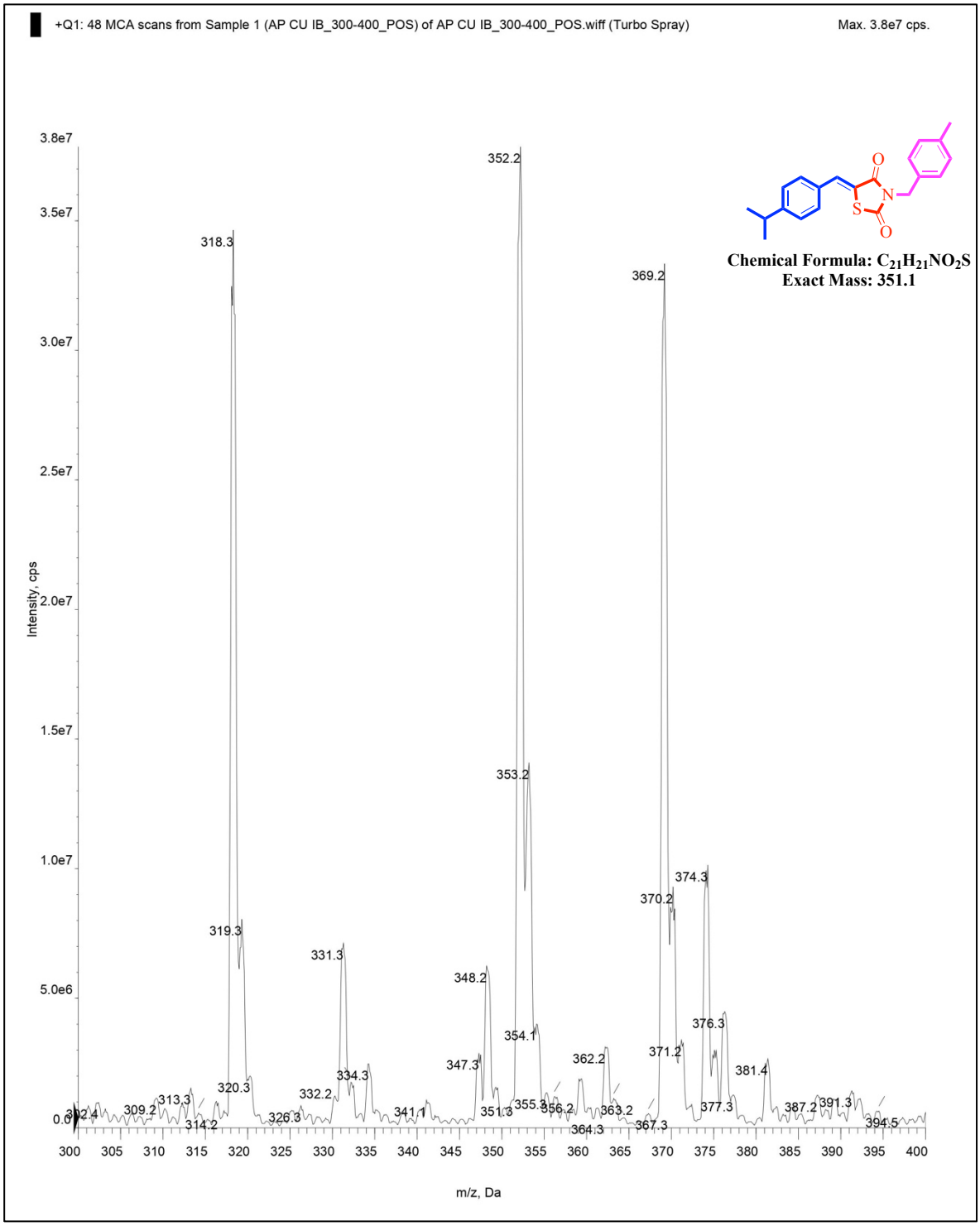

S.F31: MS (ESI, m/z) of Compound **6b**

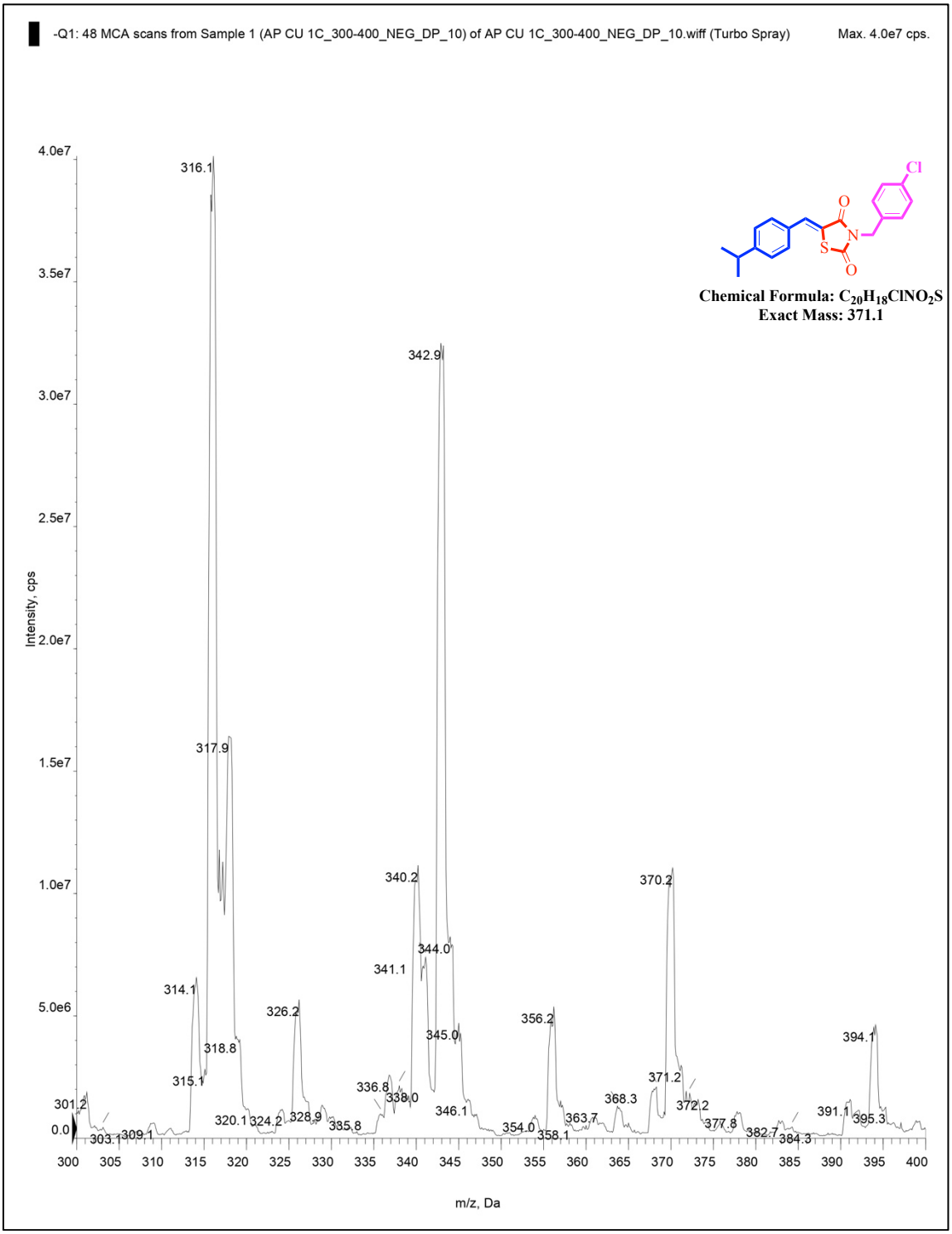

S.F32: MS (ESI, m/z) of Compound **6c**

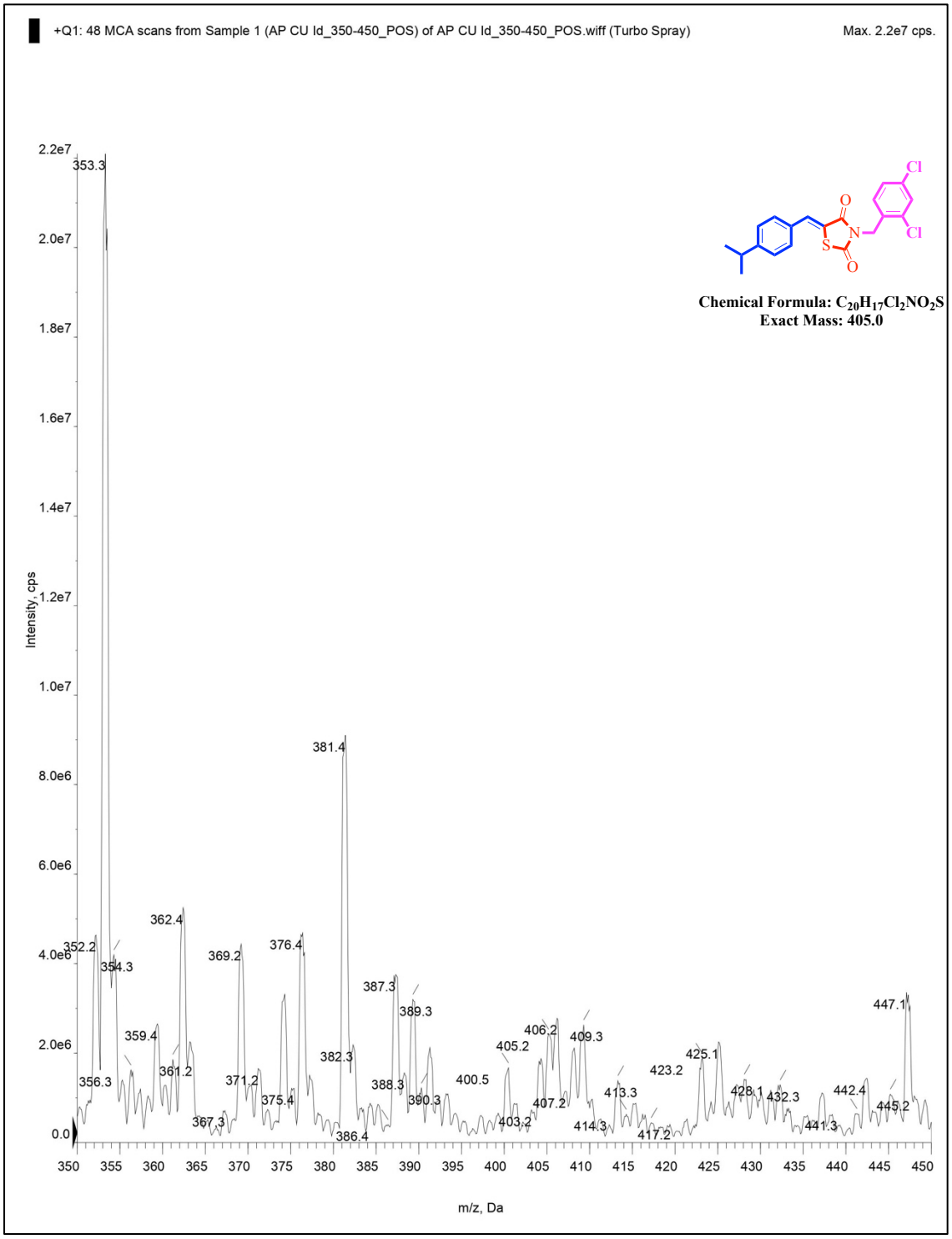

S.F33: MS (ESI, m/z) of Compound **6d**

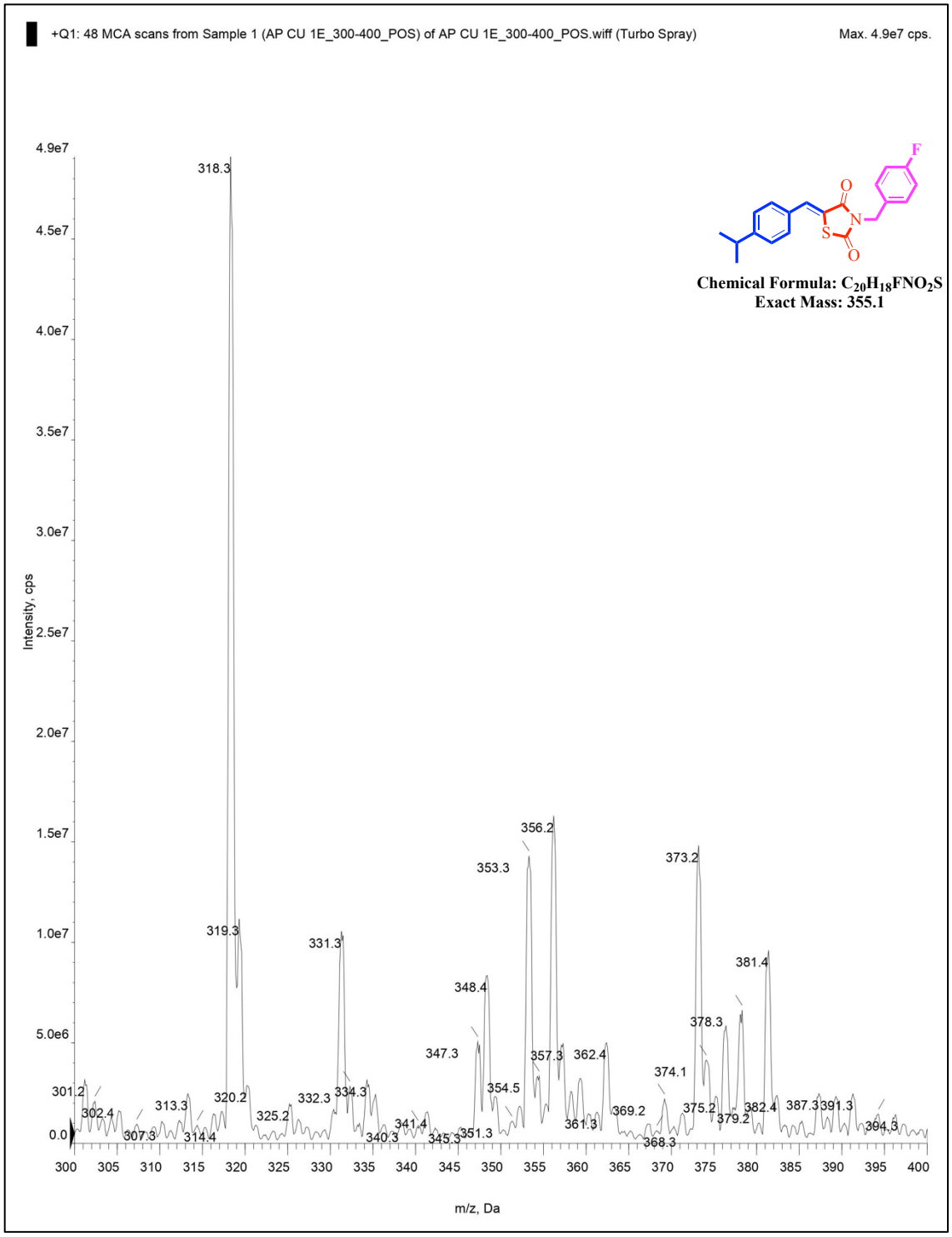

S.F34: MS (ESI, m/z) of Compound **6e**

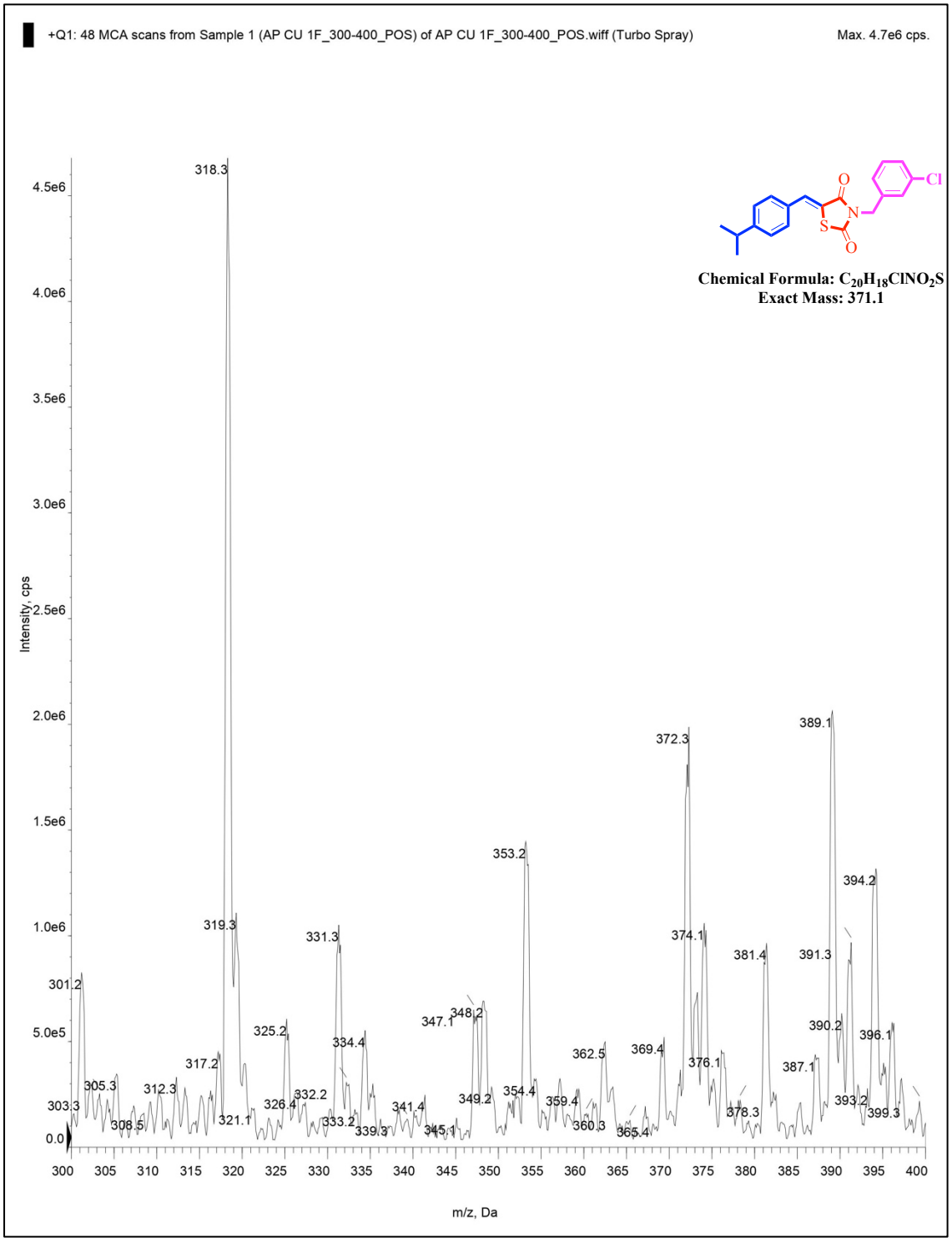

S.F35: MS (ESI, m/z) of Compound **6f**

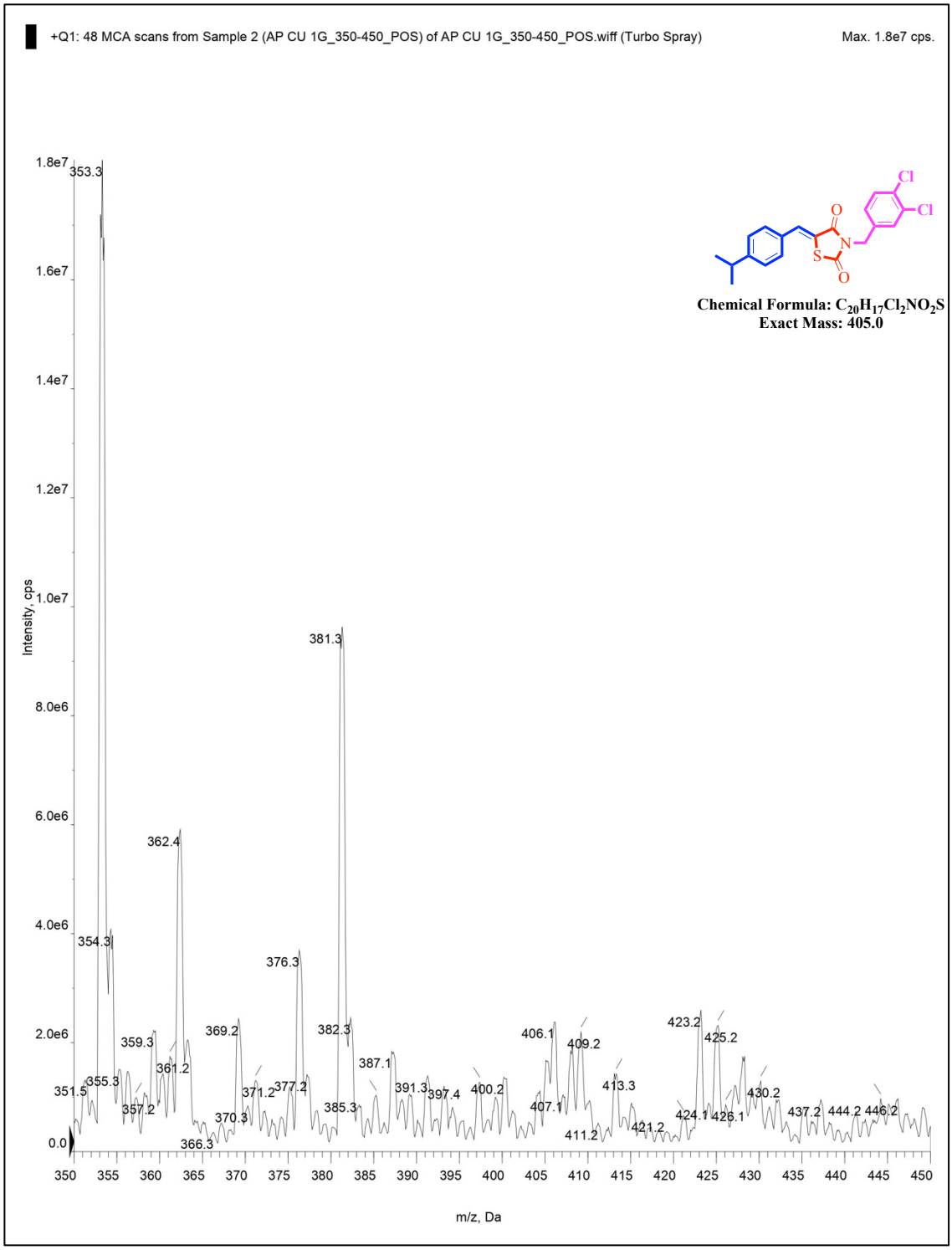

S.F36: MS (ESI, m/z) of Compound **6g**

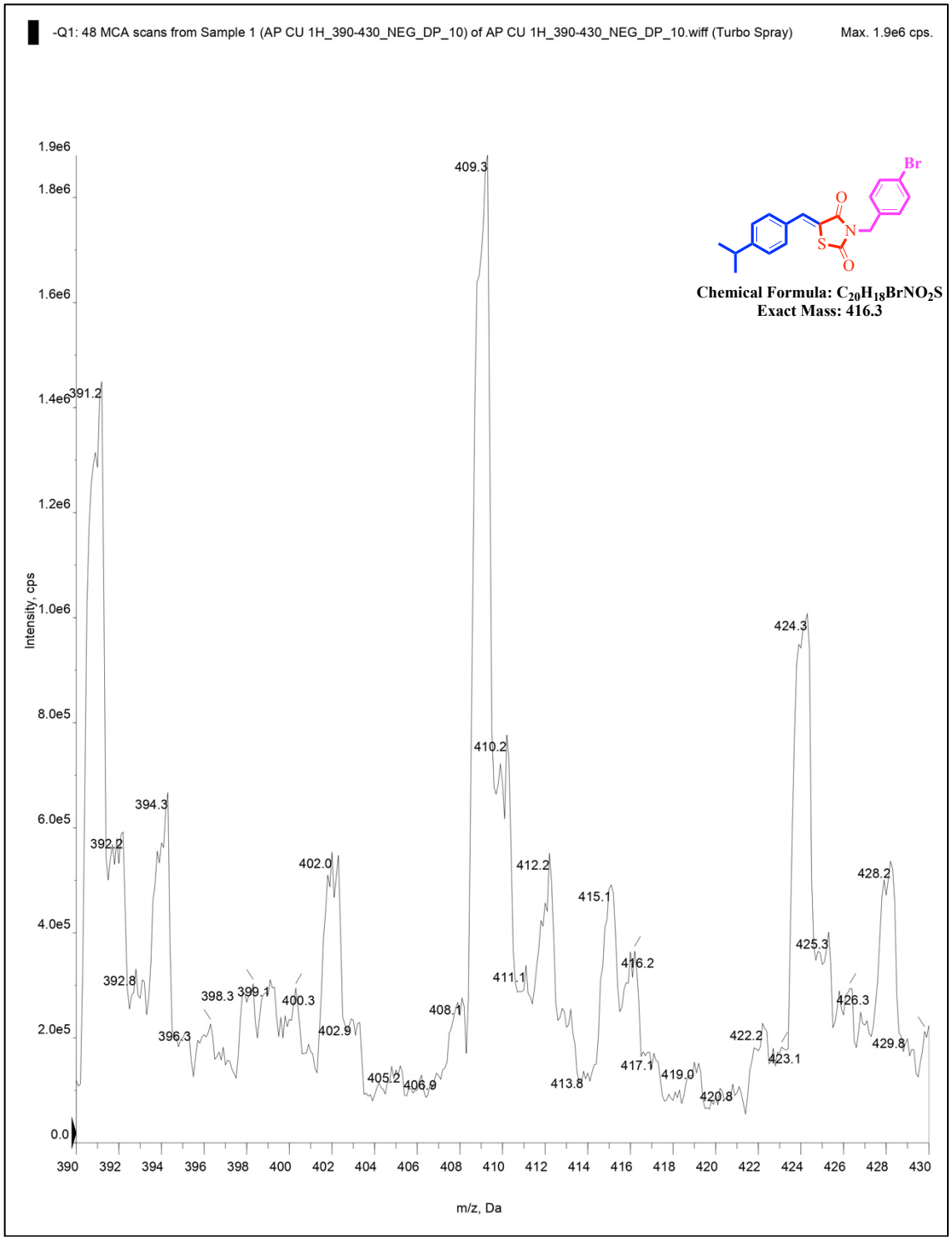

S.F37: MS (ESI, m/z) of Compound **6h**

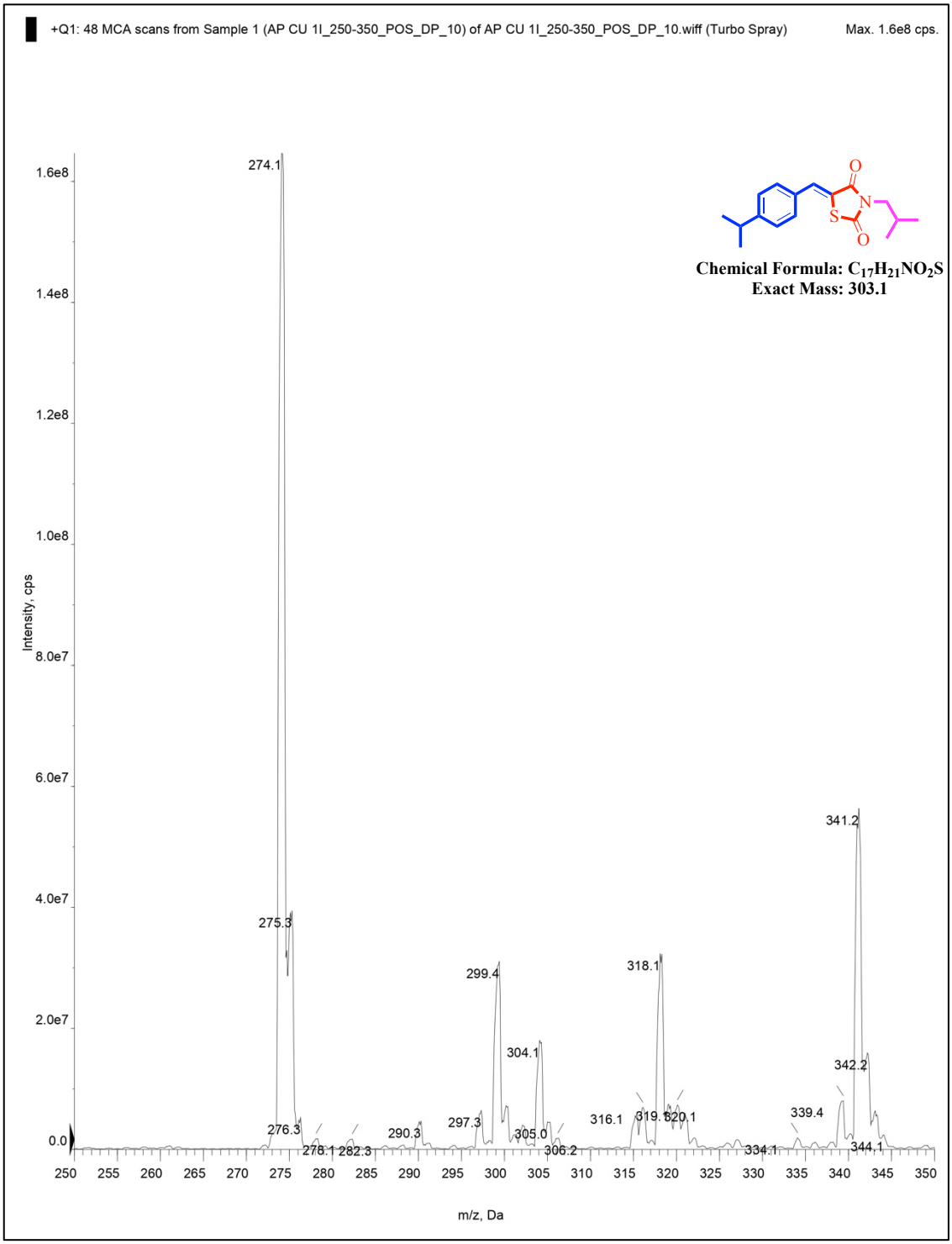

S.F38: MS (ESI, m/z) of Compound **6i**

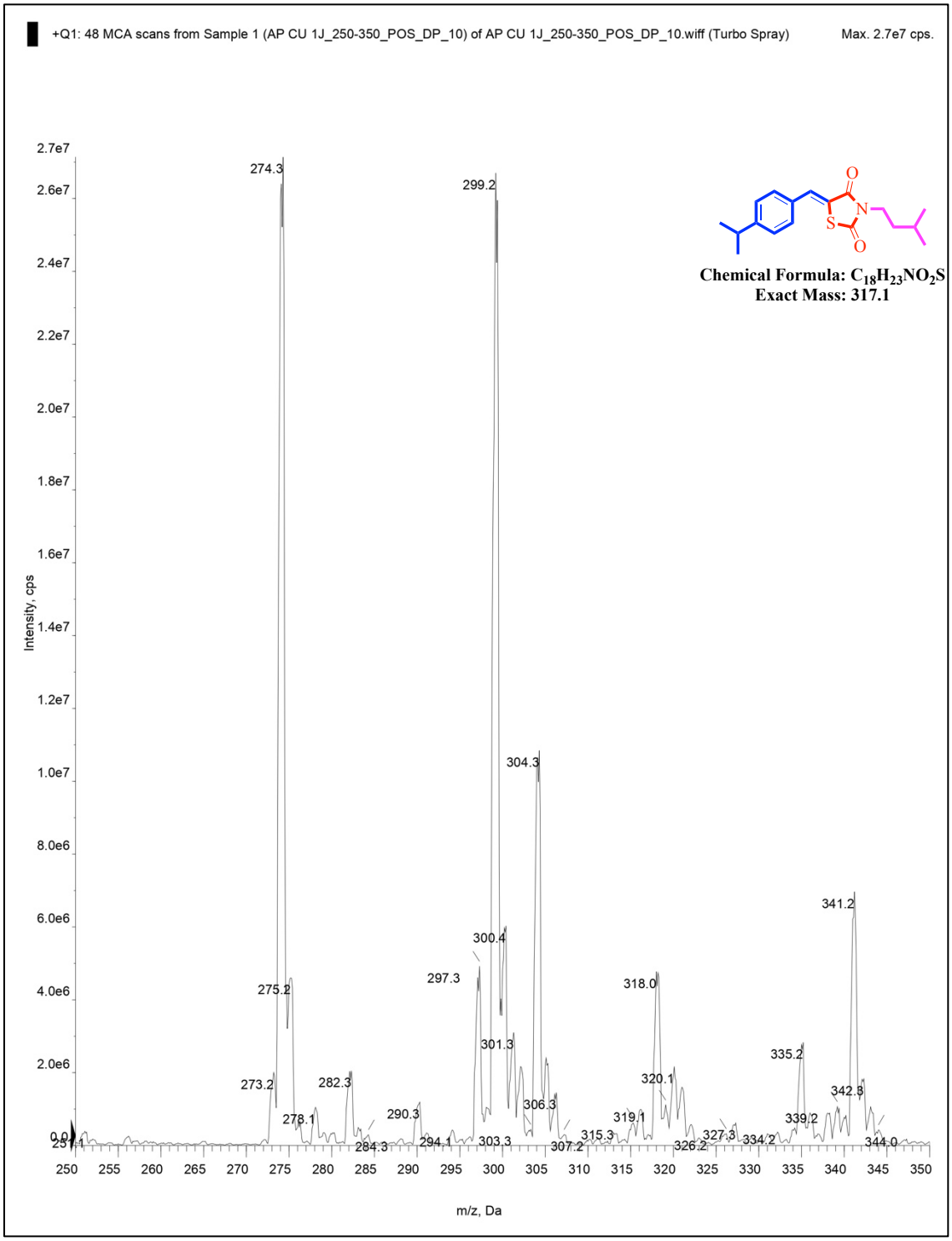

S.F39: MS (ESI, m/z) of Compound **6j**

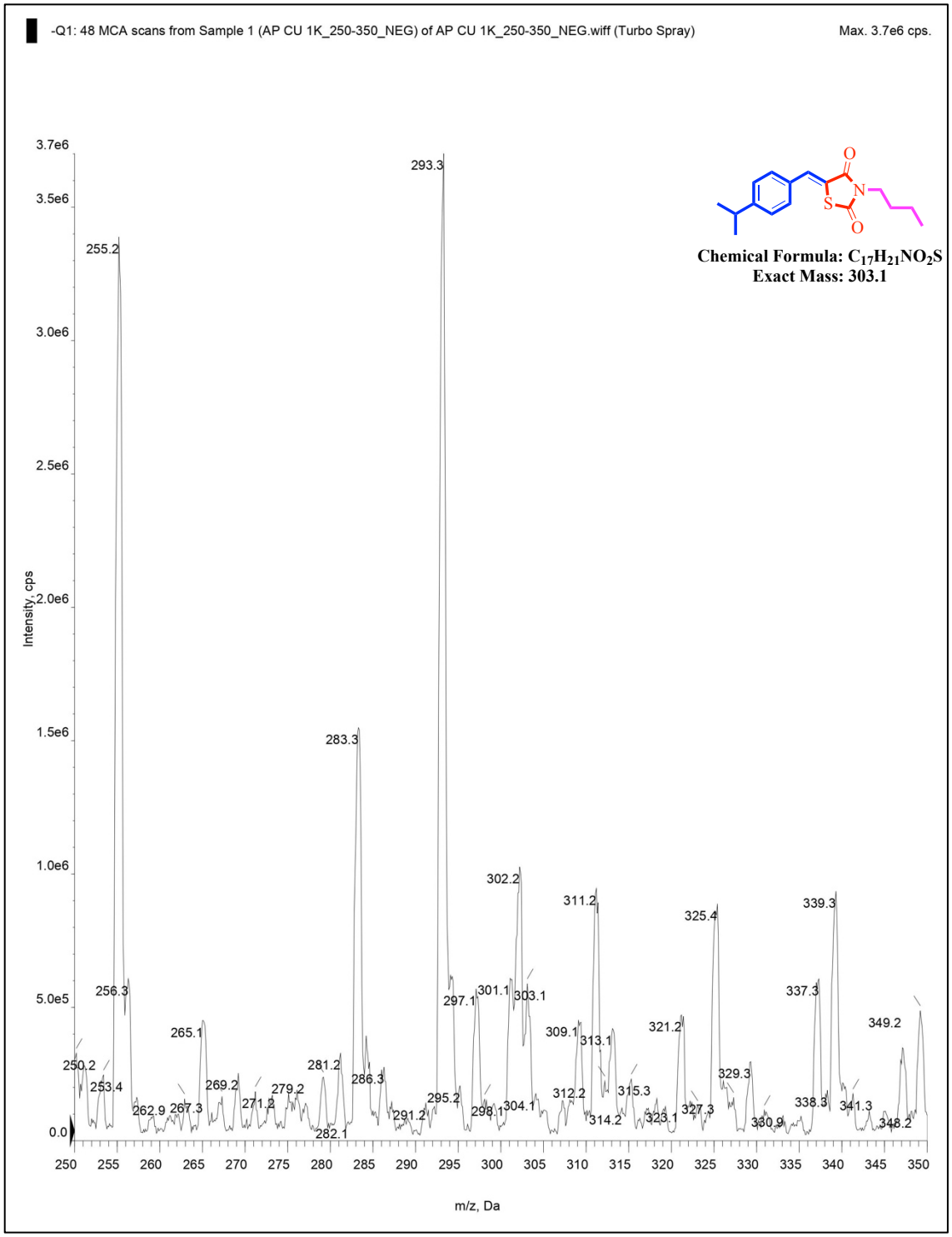

S.F40: MS (ESI, m/z) of Compound **6k**

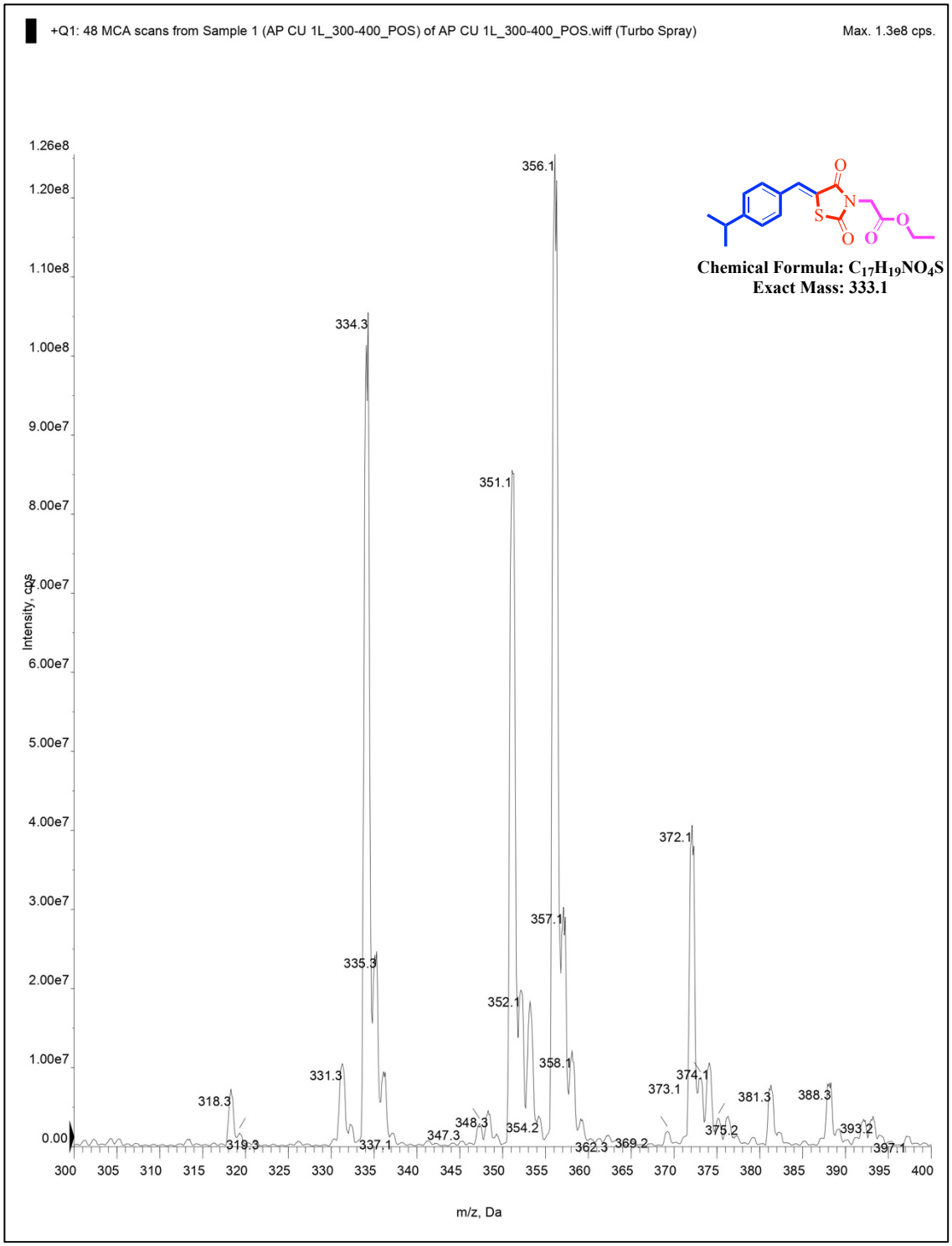

S.F41: MS (ESI, m/z) of Compound **6l**

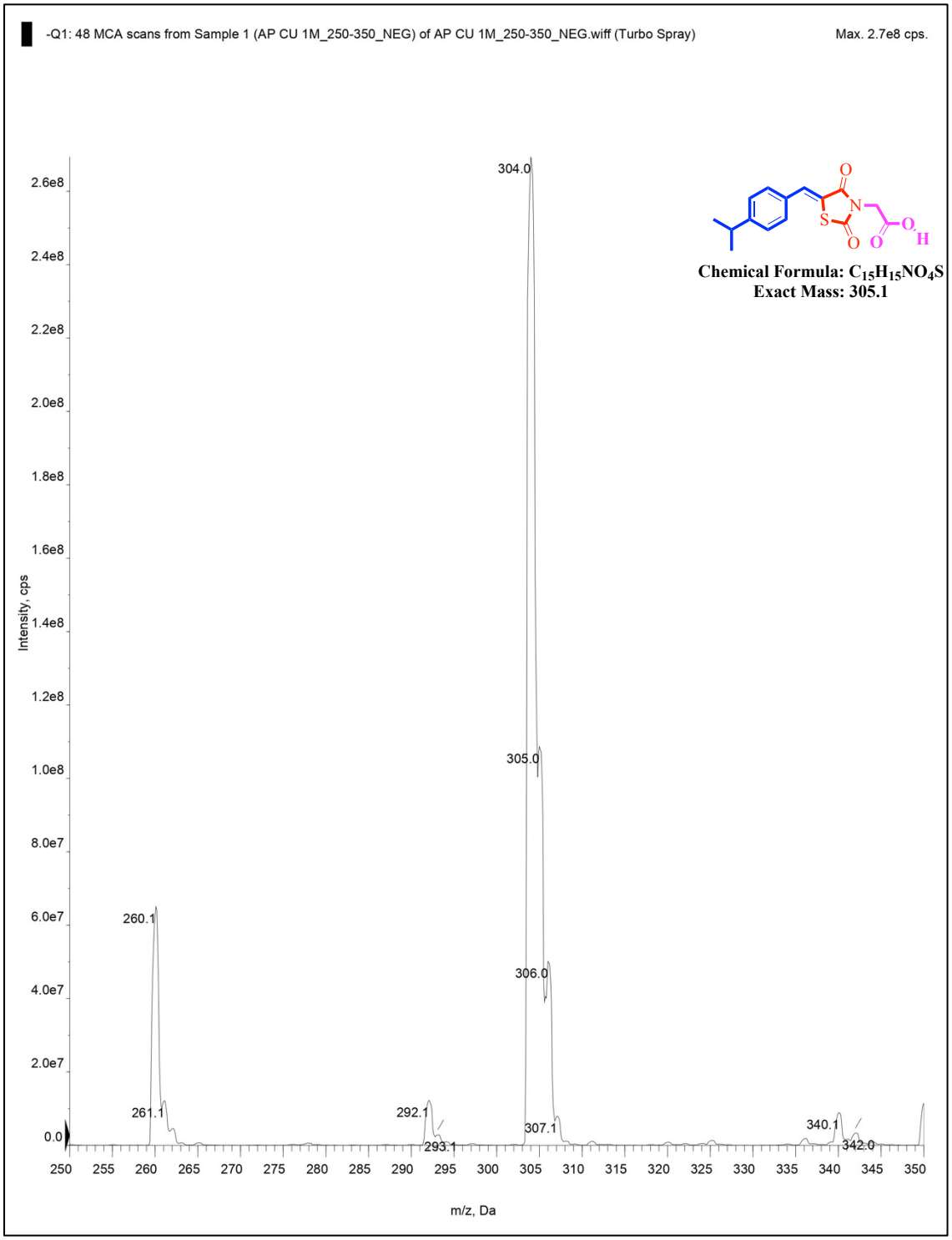

S.F42: MS (ESI, m/z) of Compound **6m**

IV. X-Ray Crystallographic data:

a) Molecular geometries of compound 6i

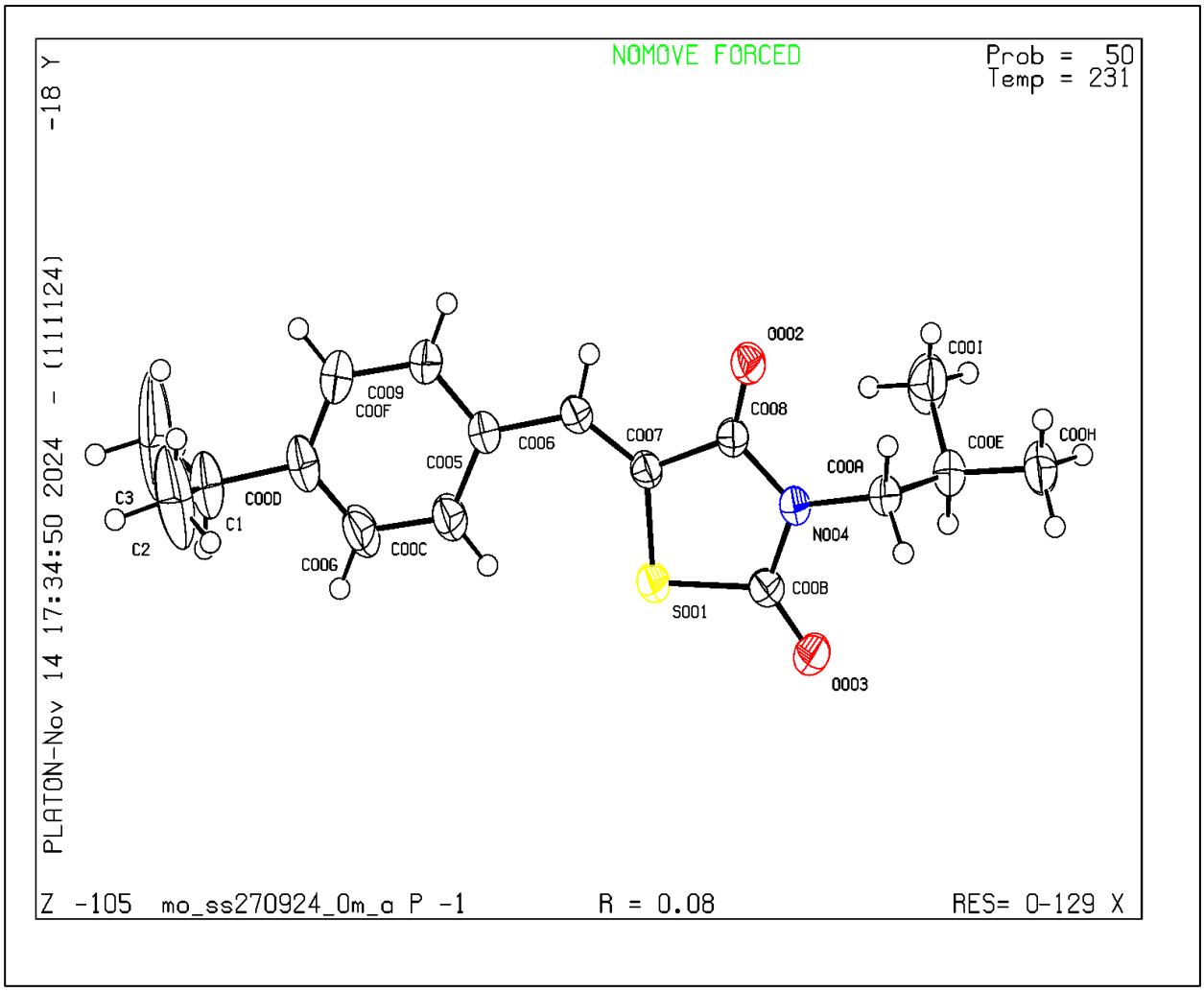

S.F43: Molecular geometries of compound **6i** in crystal.

b) Tabular data of crystal:

Table S1: Crystallographic table:

Complexes	6i
CCDC	2402983
formula	$C_{17}H_{21}NO_2S$
fw	303.41
crystal system	triclinic
space group	P -1
a (Å)	5.5659(9)

b (Å)	10.8650(19)
c(Å)	14.029(3)
α (°)	74.617(6)
β (°)	84.389(6)
γ (°)	79.193(6)
V (Å^3)	802.5(2)
Z	2
T (K)	231
Dx, g cm-3	1.256
μ (mm^{-1})	0.206
R1[a][I>2*σ*(I)]/GOF [b]	0.0792/ 1.038
*w*R2[c] (I>2*σ* (I))	0.2448
Observation criterion: [a]R1 = Σ||F_o|-|F_c||/Σ|F_o|. [b]GOF = {Σ[w(F_o^2-F_c^2)^2]/(n-p)}$^{1/2}$, [c]*w*R2 = [Σ[*w*(F_o^2-F_c^2)^2]/Σ[*w*(F_o^2)^2]]$^{1/2}$ where *w* = 1/[σ^2(F_o^2) + (aP)^2+bP], P = (F_o^2+2F_c^2)/3.	

References:

[1] G. Singh, R. Singh, V. Monga, S. Mehan, Thiazolidine-2,4-dione hybrids as dual alpha-amylase and alpha-glucosidase inhibitors: design, synthesis, in vitro and in vivo anti-diabetic evaluation, RSC Med. Chem. 15 (2024) 2826–2854. https://doi.org/10.1039/D4MD00199K.

[2] G. Singh, R. Singh, V. Monga, S. Mehan, 3,5-Disubstituted-thiazolidine-2,4-dione hybrids as antidiabetic agents: Design, synthesis, in-vitro and In vivo evaluation, Eur J Med Chem 266 (2024). https://doi.org/10.1016/j.ejmech.2024.116139.

[3] A. Paul, S. Nahar, P. Nahata, A. Sarkar, A. Maji, A. Samanta, S. Karmakar, T.K. Maity, Synthetic GPR40/FFAR1 agonists: An exhaustive survey on the most recent chemical classes and their structure-activity relationships, Eur J Med Chem 264 (2024) 115990. https://doi.org/10.1016/j.ejmech.2023.115990.

[4] A. Zeng, R. Yang, S. Yu, W. Zhao, A novel hypoglycemic agent: Polysaccharides from laver (: Porphyra spp.), Food Funct 11 (2020). https://doi.org/10.1039/d0fo01195a.

[5] A.K. Saini, A. Kumar H.S., S.S. Sharma, Preventive and curative effect of edaravone on nerve functions and oxidative stress in experimental diabetic neuropathy, Eur J Pharmacol 568 (2007). https://doi.org/10.1016/j.ejphar.2007.04.016.

[6] C.M. Hu, W.J. Wang, Y.N. Ye, Y. Kang, J. Lin, P.P. Wu, D.L. Li, L.P. Bai, X.T. Xu, B.Q. Li, K. Zhang, Novel cinnamic acid magnolol derivatives as potent α-glucosidase and α-amylase inhibitors: Synthesis, in vitro and in silico studies, Bioorg Chem 116 (2021). https://doi.org/10.1016/j.bioorg.2021.105291.

[7] Y.Y. Yang, L.X. Shi, J.H. Li, L.Y. Yao, D.X. Xiang, Piperazine ferulate ameliorates the development of diabetic nephropathy by regulating endothelial nitric oxide synthase, Mol Med Rep 19 (2019). https://doi.org/10.3892/mmr.2019.9875.

[8] L. Liu, Y. Zhou, X. Zhao, X. Yang, X. Wan, Z. An, H. Zhang, J. Tian, C. Ge, X. Song, Bone Marrow Mesenchymal Stem Cell-Derived Exosomes Alleviate Diabetic Kidney Disease in Rats by Inhibiting Apoptosis and Inflammation, Frontiers in Bioscience - Landmark 28 (2023). https://doi.org/10.31083/j.fbl2809203.

[9] D. Xiong, W. Hu, X. Han, Y. Cai, Rhein Inhibited Ferroptosis and EMT to Attenuate Diabetic Nephropathy by Regulating the Rac1/NOX1/β-Catenin Axis, Frontiers in Bioscience - Landmark 58 (2023). https://doi.org/10.31083/j.fbl2805100.

[10] A. Mushtaq, U. Azam, S. Mehreen, M.M. Naseer, Synthetic α-glucosidase inhibitors as promising anti-diabetic agents: Recent developments and future challenges, Eur J Med Chem 249 (2023). https://doi.org/10.1016/j.ejmech.2023.115119.

[11] M. Fan, X. Zhong, Y. Huang, Z. Peng, G. Wang, Synthesis, biological evaluation and molecular docking studies of chromone derivatives as potential α-glucosidase inhibitors, J Mol Struct 1274 (2023). https://doi.org/10.1016/j.molstruc.2022.134575.

[12] A. Sharma, N. Kumar, H.K. Gulati, R. Rana, Jyoti, A. Khanna, Muskan, J.V. Singh, P.M.S. Bedi, Antidiabetic potential of thiazolidinedione derivatives with efficient design, molecular docking, structural activity relationship, and biological activity: an update review (2021–2023), Mol Divers (2024). https://doi.org/10.1007/s11030-023-10793-6.

[13] K. Kajal, G. Singh, T. Pradhan, D. Bhurta, V. Monga, The medicinal perspective of 2,4-thiazolidinediones based ligands as antimicrobial, antitumor and antidiabetic agents: A review, Arch Pharm (Weinheim) 355 (2022). https://doi.org/10.1002/ardp.202100517.

[14] A. Paul, A. Sarkar, T. Banerjee, A. Maji, S. Sarkar, S. Paul, S. Karmakar, N. Ghosh, T.K. Maity, Structural and molecular insights of protein tyrosine phosphatase 1B (PTP1B) and its inhibitors as anti-diabetic agents, J Mol Struct 1293 (2023) 136258. https://doi.org/10.1016/j.molstruc.2023.136258.

[15] M. Saw, V.W. Wong, I. Van Ho, G. Liew, New anti-hyperglycaemic agents for type 2 diabetes and their effects on diabetic retinopathy, Eye (Basingstoke) 33 (2019). https://doi.org/10.1038/s41433-019-0494-z.

[16] K. Tilekar, O. Shelke, N. Upadhyay, A. Lavecchia, C.S. Ramaa, Current status and future prospects of molecular hybrids with thiazolidinedione (TZD) scaffold in anticancer drug discovery, J Mol Struct 1250 (2022). https://doi.org/10.1016/j.molstruc.2021.131767.

[17] A. Paneth, B. Kaproń, T. Plech, R. Paduch, N. Trotsko, P. Paneth, Combined In Silico and In Vitro Analyses to Assess the Anticancer Potential of Thiazolidinedione–Thiosemicarbazone Hybrid Molecules, Int J Mol Sci 24 (2023). https://doi.org/10.3390/ijms242417521.

[18] N. Savin, A. Erofeev, R. Timoshenko, A. Vaneev, A. Garanina, S. Salikhov, N. Grammatikova, I. Levshin, Y. Korchev, P. Gorelkin, Investigation of the Antifungal and Anticancer Effects of the Novel Synthesized Thiazolidinedione by Ion-Conductance Microscopy, Cells 12 (2023). https://doi.org/10.3390/cells12121666.

[19] P. Moorthy, S.P. Ekambaram, S.S. Perumal, Synthesis, characterization and antimicrobial evaluation of imidazolyl thiazolidinedione derivatives, Arabian Journal of Chemistry 12 (2019). https://doi.org/10.1016/j.arabjc.2014.08.010.

[20] S.G. Alegaon, V. U, K.R. Alagawadi, D. Kumar, R.S. Kavalapure, S.D. Ranade, S. Priya A, S.S. Jalalpure, Synthesis, molecular docking and ADME studies of thiazole-thiazolidinedione hybrids as antimicrobial agents, J Biomol Struct Dyn 40 (2022). https://doi.org/10.1080/07391102.2021.1880479.

[21] M.S. Raghu, C.B. Pradeep Kumar, K. Yogesh Kumar, M.K. Prashanth, F. Alharethy, B.H. Jeon, Synthesis, biological evaluation and molecular docking study of pyrimidine linked thiazolidinedione derivatives as potential antimicrobial and antitubercular agents, Bioorg Med Chem Lett 103 (2024). https://doi.org/10.1016/j.bmcl.2024.129707.

[22] Archna, P.A. Chawla, G. Teli, S. Pathania, S. Singh, V. Srivastava, Exploration of Antioxidant, Anti-inflammatory and Anticancer Potential of Substituted 4-Thiazolidinone Derivatives: Synthesis, Biological Evaluation and Docking Studies, Polycycl Aromat Compd 43 (2023). https://doi.org/10.1080/10406638.2021.2019796.

[23] N. Swathi, T.D.A. Kumar, Insights into Thiazolidinedione Analogues: Unveiling Antioxidant Activity through Descriptor-Based Quantitative Structure-Activity Relationship Investigations, Asian Journal of Applied Chemistry Research 15 (2024). https://doi.org/10.9734/ajacr/2024/v15i1277.

[24] M.H. Shaikh, D.D. Subhedar, S. V. Akolkar, A.A. Nagargoje, A. Asrondkar, V.M. Khedkar, B.B. Shingate, New 1,2,3-Triazole-Tethered Thiazolidinedione Derivatives: Synthesis, Bioevaluation and Molecular Docking Study, Polycycl Aromat Compd 43 (2023). https://doi.org/10.1080/10406638.2022.2069132.

[25] A. Paul, A. Maji, A. Sarkar, S. Saha, P. Janah, T.K. Maity, Recent Approaches in the Synthesis of 5-Arylidene-2,4-thiazolidinedione Derivatives Using Knoevenagel Condensation, Mini Rev Org Chem 20 (2023). https://doi.org/10.2174/1570193X19666220331155705.

[26] G. George, P.S. Auti, P. Sengupta, N. Yadav, A.T. Paul, Synthesis, molecular modelling and pharmacological evaluation of novel indole-thiazolidinedione based hybrid analogues as potential pancreatic lipase inhibitors, J Biomol Struct Dyn (2023). https://doi.org/10.1080/07391102.2023.2293255.

[27] P. Dhiman, N. Yadav, P.S. Auti, S. Jaswal, G. Singh, S. Mehan, B. Ghosh, A.T. Paul, V. Monga, Discovery of thiazolidinedione-based pancreatic lipase inhibitors as anti-obesity agents: synthesis, in silico studies and pharmacological investigations, J Biomol Struct Dyn (2024). https://doi.org/10.1080/07391102.2024.2310799.

[28] P. de Sena Murteira Pinheiro, L.S. Franco, T.L. Montagnoli, C.A.M. Fraga, Molecular hybridization: a powerful tool for multitarget drug discovery, Expert Opin Drug Discov 19 (2024) 451–470. https://doi.org/10.1080/17460441.2024.2322990.

[29] B. Liang, J. Li, S. Wu, X. Kou, T. Liu, X. Xu, Novel coumarin-thiazolidine-2,4-dione hybrids as potential α-glucosidase inhibitors: Synthesis and bioactivity evaluation, J Mol Struct 1322 (2025) 140481. https://doi.org/10.1016/j.molstruc.2024.140481.

[30] M. Feng, B. Liang, J. Sun, X. Min, S.-H. Wang, Y. Lu, X. Xu, Synthesis, anti-α-glucosidase activity, inhibition interaction, and anti-diabetic activity of novel cryptolepine derivatives, J Mol Struct 1310 (2024) 138311. https://doi.org/10.1016/j.molstruc.2024.138311.

[31] X. Min, S. Guo, Y. Lu, X. Xu, Investigation on the inhibition mechanism and binding behavior of cryptolepine to α-glucosidase and its hypoglycemic activity by multi-spectroscopic method, J Lumin 269 (2024) 120437. https://doi.org/10.1016/j.jlumin.2024.120437.

[32] B. Liang, D. Xiao, S.-H. Wang, X. Xu, Novel thiosemicarbazide-based β-carboline derivatives as α-glucosidase inhibitors: Synthesis and biological evaluation, Eur J Med Chem 275 (2024) 116595. https://doi.org/10.1016/j.ejmech.2024.116595.

[33] X.-Z. Wu, W.-J. Zhu, L. Lu, C.-M. Hu, Y.-Y. Zheng, X. Zhang, J. Lin, J.-Y. Wu, Z. Xiong, K. Zhang, X.-T. Xu, Synthesis and anti-α-glucosidase activity evaluation of betulinic acid derivatives, Arabian Journal of Chemistry 16 (2023) 104659. https://doi.org/10.1016/j.arabjc.2023.104659.

[34] P. Seboletswe, N. Cele, P. Singh, Thiazolidinone-Heterocycle Frameworks: A Concise Review of Their Pharmacological Significance, ChemMedChem 18 (2023). https://doi.org/10.1002/cmdc.202200618.

[35] A. Singh, K. Singh, A. Sharma, K. Kaur, K. Kaur, R. Chadha, P.M.S. Bedi, Recent developments in synthetic α-glucosidase inhibitors: A comprehensive review with structural and molecular insight, J Mol Struct 1281 (2023) 135115. https://doi.org/10.1016/j.molstruc.2023.135115.

[36] M. Li, J. Sun, B. Liang, X. Min, J. Hu, R. Wu, X. Xu, Thiazolidine-2,4-dione derivatives as potential α-glucosidase inhibitors: Synthesis, inhibitory activity, binding interaction and hypoglycemic activity, Bioorg Chem 144 (2024). https://doi.org/10.1016/j.bioorg.2024.107177.

[37] C. Hu, B. Liang, J. Sun, J. Li, Z. Xiong, S.H. Wang, X. Xuetao, Synthesis and biological evaluation of indole derivatives containing thiazolidine-2,4-dione as α-glucosidase inhibitors with antidiabetic activity, Eur J Med Chem 264 (2024). https://doi.org/10.1016/j.ejmech.2023.115957.

[38] S. Daud, O. Abid, M. Saadullah, M. Fakhar-e-Alam, S. Carradori, A. Sardar, B. Niaz, M. Atif, S. Zara, M. Rashad, Isatin-based ibuprofen and mefenamic acid Schiff base derivatives as dual inhibitors against urease and α–glucosidase: In vitro, in silico and cytotoxicity studies, Journal of Saudi Chemical Society 28 (2024) 101905. https://doi.org/https://doi.org/10.1016/j.jscs.2024.101905.

[39] H.S. Lee, Cuminaldehyde: Aldose reductase and α-glucosidase inhibitor derived from Cuminum cyminum L. seeds, J Agric Food Chem 53 (2005) 2446–2450. https://doi.org/10.1021/jf048451g.

[40] A. Paul, A. Maji, A. Sarkar, S. Saha, P. Janah, T.K. Maity, Recent Approaches in the Synthesis of 5-Arylidene-2,4-thiazolidinedione Derivatives Using Knoevenagel Condensation, Mini Rev Org Chem 20 (2023) 5–34. https://doi.org/10.2174/1570193X19666220331155705.

[41] R.M. Christoff, T.P. Soares da Costa, S. Bayat, J.K. Holien, M.A. Perugini, B.M. Abbott, Synthesis and structure-activity relationship studies of 2,4-thiazolidinediones and analogous heterocycles as inhibitors of dihydrodipicolinate synthase, Bioorg Med Chem 52 (2021). https://doi.org/10.1016/j.bmc.2021.116518.

[42] M. Fan, X. Zhong, Y. Huang, Z. Peng, G. Wang, Synthesis, biological evaluation and molecular docking studies of chromone derivatives as potential α-glucosidase

inhibitors, J Mol Struct 1274 (2023). https://doi.org/10.1016/j.molstruc.2022.134575.

[43] P.S. Gaikwad, L. Panicker, M. Mohole, S. Sawant, R. Mukhopadhyaya, B.B. Nath, Differential sensitivity of Chironomus and human hemoglobin to gamma radiation, Biochem Biophys Res Commun 476 (2016). https://doi.org/10.1016/j.bbrc.2016.05.129.

[44] A. Aispuro-Pérez, J. López-Ávalos, F. García-Páez, J. Montes-Avila, L.A. Picos-Corrales, A. Ochoa-Terán, P. Bastidas, S. Montaño, L. Calderón-Zamora, U. Osuna-Martínez, J.I. Sarmiento-Sánchez, Synthesis and molecular docking studies of imines as α-glucosidase and α-amylase inhibitors, Bioorg Chem 94 (2020). https://doi.org/10.1016/j.bioorg.2019.103491.

[45] S. Singha, B. Das Gupta, A. Sarkar, S. Jana, P.K. Bharadwaj, N. Sharma, P.K. Haldar, P.K. Mukherjee, A. Kar, Chemo-profiling and exploring therapeutic potential of Momordica dioica Roxb. ex Willd. for managing metabolic related disorders: In-vitro studies, and docking based approach, J Ethnopharmacol 331 (2024) 118351. https://doi.org/https://doi.org/10.1016/j.jep.2024.118351.

[46] S. Ghannay, M. Snoussi, S. Messaoudi, A. Kadri, K. Aouadi, Novel enantiopure isoxazolidine and C-alkyl imine oxide derivatives as potential hypoglycemic agents: Design, synthesis, dual inhibitors of α-amylase and α-glucosidase, ADMET and molecular docking study, Bioorg Chem 104 (2020). https://doi.org/10.1016/j.bioorg.2020.104270.

[47] L. Durmaz, H. Kiziltas, H. Karagecili, S. Alwasel, İ. Gulcin, Potential antioxidant, anticholinergic, antidiabetic and antiglaucoma activities and molecular docking of spiraeoside as a secondary metabolite of onion (Allium cepa), Saudi Pharmaceutical Journal 31 (2023). https://doi.org/10.1016/j.jsps.2023.101760.

[48] M.M. Hasan, Z. Khan, M.S. Chowdhury, M.A. Khan, M.A. Moni, M.H. Rahman, In silico molecular docking and ADME/T analysis of Quercetin compound with its evaluation of broad-spectrum therapeutic potential against particular diseases, Inform Med Unlocked 29 (2022). https://doi.org/10.1016/j.imu.2022.100894.

[49] P.C. Agu, C.A. Afiukwa, O.U. Orji, E.M. Ezeh, I.H. Ofoke, C.O. Ogbu, E.I. Ugwuja, P.M. Aja, Molecular docking as a tool for the discovery of molecular targets of nutraceuticals in diseases management, Sci Rep 13 (2023). https://doi.org/10.1038/s41598-023-40160-2.

[50] S. Gupta, G.S. Baweja, S. Singh, M. Irani, R. Singh, V. Asati, Integrated fragment-based drug design and virtual screening techniques for exploring the antidiabetic potential of thiazolidine-2,4-diones: Design, synthesis and in vivo studies, Eur J Med Chem 261 (2023). https://doi.org/10.1016/j.ejmech.2023.115826.

[51] A. Majie, R. Saha, A. Sarkar, R. Bhowmik, S. Karmakar, V. Sharma, K. Deokar, A. ul Haque, S.S. Tripathy, B. Sarkar, A novel chitosan–PEG hydrogel embedded with in situ silver nanoparticles of Clerodendrum glandulosum Lindl. extract: evaluation of its in vivo diabetic wound healing properties using an image-guided machine

learning model, Biomater. Sci. 12 (2024) 4242–4261. https://doi.org/10.1039/D4BM00349G.

[52] A. Daina, O. Michielin, V. Zoete, SwissADME: A free web tool to evaluate pharmacokinetics, drug-likeness and medicinal chemistry friendliness of small molecules, Sci Rep 7 (2017). https://doi.org/10.1038/srep42717.

[53] Y. Myung, A.G.C. de Sá, D.B. Ascher, Deep-PK: deep learning for small molecule pharmacokinetic and toxicity prediction, Nucleic Acids Res (2024) gkae254. https://doi.org/10.1093/nar/gkae254.

[54] T.P. Kenakin, Chapter 6 - Enzymes as Drug Targets, in: Pharmacology in Drug Discovery and Development, 2017.

[55] O. Duman, S. Tunç, B. Kancı Bozoğlan, Characterization of the binding of metoprolol tartrate and guaifenesin drugs to human serum albumin and human hemoglobin proteins by fluorescence and circular dichroism spectroscopy, J Fluoresc 23 (2013). https://doi.org/10.1007/s10895-013-1177-y.

[56] U. Ghani, Re-exploring promising α-glucosidase inhibitors for potential development into oral anti-diabetic drugs: Finding needle in the haystack, Eur J Med Chem 103 (2015). https://doi.org/10.1016/j.ejmech.2015.08.043.

[57] R. Islam, A. Deb, A.J. Ghosh, D. Dutta, A. Ray, A. Dutta, S. Ghosh, S. Sarkar, M. Bahadur, A. Kumar, T. Saha, Toxicological profiling of methanolic seed extract of Abutilon indicum (L.) Sweet: in-vitro and in-vivo analysis, J Ethnopharmacol 335 (2024) 118655. https://doi.org/https://doi.org/10.1016/j.jep.2024.118655.

[58] E.J. Jeyaraj, Y.Y. Lim, W.S. Choo, Antioxidant, cytotoxic, and antibacterial activities of Clitoria ternatea flower extracts and anthocyanin-rich fraction, Sci Rep 12 (2022). https://doi.org/10.1038/s41598-022-19146-z.

CHAPTER-IV

Synthesis, crystal structure, and *in vitro* evaluation of newer 2,4-thiazolidinedione hybrids as α-glucosidase inhibitors

1. Introduction:

Diabetes mellitus (DM) is a worldwide health concern marked by increased blood glucose levels, resulting in serious complications such as cardiovascular disease, cerebrovascular accident, renal failure, and neuropathy. Prevalent varieties encompass type 1, type 2, and gestational diabetes. It affects millions worldwide and is anticipated to influence 700 million by 2045 [1–4]. Individuals with type 2 diabetes (T2D) employ hypoglycemic medications to regulate postprandial hyperglycemia. Alongside TZD medicines, a notable treatment strategy for diabetes management includes the utilization of synthetic α-glucosidase inhibitors (AGIs). AGIs represent an alternative treatment strategy for diabetes management, regulating postprandial glucose levels and providing advantages such as improved glycemic control. AGIs must be administered with meals and may induce gastrointestinal adverse effects. AGIs function as a therapeutic intervention for DM by inhibiting the breakdown of dietary carbohydrates, hence preventing the release of monosaccharides into the bloodstream. AGIs, such as Acarbose, voglibose, and miglitol, function as first-line oral hypoglycemic agents in moderate conditions and as adjunctive therapy in acute situations [5]. While modern AGIs are advantageous, their side effects, such as abdominal pain, flatulence, and diarrhoea, may provide difficulties [6]. Consequently, novel AGIs are crucial as they aid researchers and pharmaceutical businesses in discovering safer and more effective therapies. This could improve the quality of life for patients with DM by providing more effective treatment options.

Thiazolidinedione (TZD) is a bioactive heterocyclic nucleus that is known for its potent anti-diabetic properties [7,8]. TZDs, including troglitazone, rosiglitazone, and pioglitazone, have been approved by the US FDA for treating T2D. However, these drugs have faced market withdrawal due to hepatotoxicity and myocardial infarction

[9]. TZD-heterocyclic hybrids represent a prominent pharmacophore in pharmaceutical chemistry, leading to investigations into their medicinal importance [10,11]. Recent studies have explored various TZD derivatives and their hybrids as potential AGIs for T2D management, as illustrated in **Figure 1.** In 2025, Liang *et al.* developed novel coumarin-TZD hybrids for effective AGIs (**1A**; **Figure 1**) [12]. Nguyen *et al.* discovered naphthalene-based TZD hybrid inhibitors for dual activities against AG enzyme and some strains of bacteria and fungi (**1B**; **Figure 1**) [13]. In 2024, Gharge *et al.* developed new compounds with 3,5-substituted TZD as effective AGIs (**1C; Figure 1**) [14]. Similarly, Singh *et al.* discovered 3,5-Disubstituted-TZD hybrids as anti-diabetic agents by targeting AG (**1D and 1E**; **Figure 1**) [2,3]. In our previous work, we have developed cuminaldehyde-TZD hybrids as potential AGIs (**1F**; **Figure 1**)[1].

Similarly, veratraldehyde (VD), a compound with the chemical structure 3,4-dimethoxybenzaldehyde (**1G**; **Figure 1**), is a compound derived from vanillin. It has been identified and extracted from a variety of sources, including peppermint, ginger, bourbon vanilla, and certain fruits like raspberry [15]. It also exhibits a range of biological and pharmacological properties, such as antioxidant, antimicrobial activities [16], and antihypertensive effects [17]. It is primarily recognized for its role as a precursor in various industrial applications, including the production of flavouring agents, odorants, and pharmaceuticals [18]. The compound's biological activities and pharmacokinetics have been explored in several studies, revealing its potential in different therapeutic areas [19]. Moreover, VD is widely utilized in the pharmaceutical industry as an essential intermediate in the synthetic generation of organic compounds [20,21].

Natural substances possess a wide range of medicinal properties and are essential for the advancement of therapeutic agents [22]. In the past few years, many medicinal

chemists have synthesized diverse derivatives from natural product frameworks to create AGIs by using a molecular hybridization strategy [23]. Molecular hybridization represents a valuable strategy in the development of drugs, facilitating the identification of medicinal agents for multiple illnesses and fostering the creation of new therapeutics with improved efficacy and reduced negative consequences [24]. Approximately 20% of recently approved drugs have utilized this method of development. Several studies have utilized this approach to synthesize synthetic AGIs and establish the structure and function of AG inhibition [25–29].

The previous findings suggest that TZD and VD could function as effective pharmacophoric fragments for the discovery and advancement of novel AGIs. Establishing on prior research and our continuous efforts to identify TZD-derived potential AGIs, our laboratory aimed to synthesize VD-TZD hybrids (**6a-6h**, **6i-6l**, and **6m**) as prospective anti-diabetic agents via AG inhibition (**Figure 1**). A simple and efficient method was applied for synthesizing VD-TZD hybrids with various substitutions at the intermediate (compound **5)** in high yields. Every compound that was synthesized was assessed for its *in vitro* inhibitory effects on AG. Furthermore, the best molecule's interaction mechanism with AG was examined using enzyme kinetic fluorescence quenching and circular dichroism (CD) spectroscopy. Additionally, ADMET predictions and *in silico* molecular docking were applied to the best compound. The best compound was further tested against the human embryonic kidney (HEK-293) cell line to determine its cell viability.

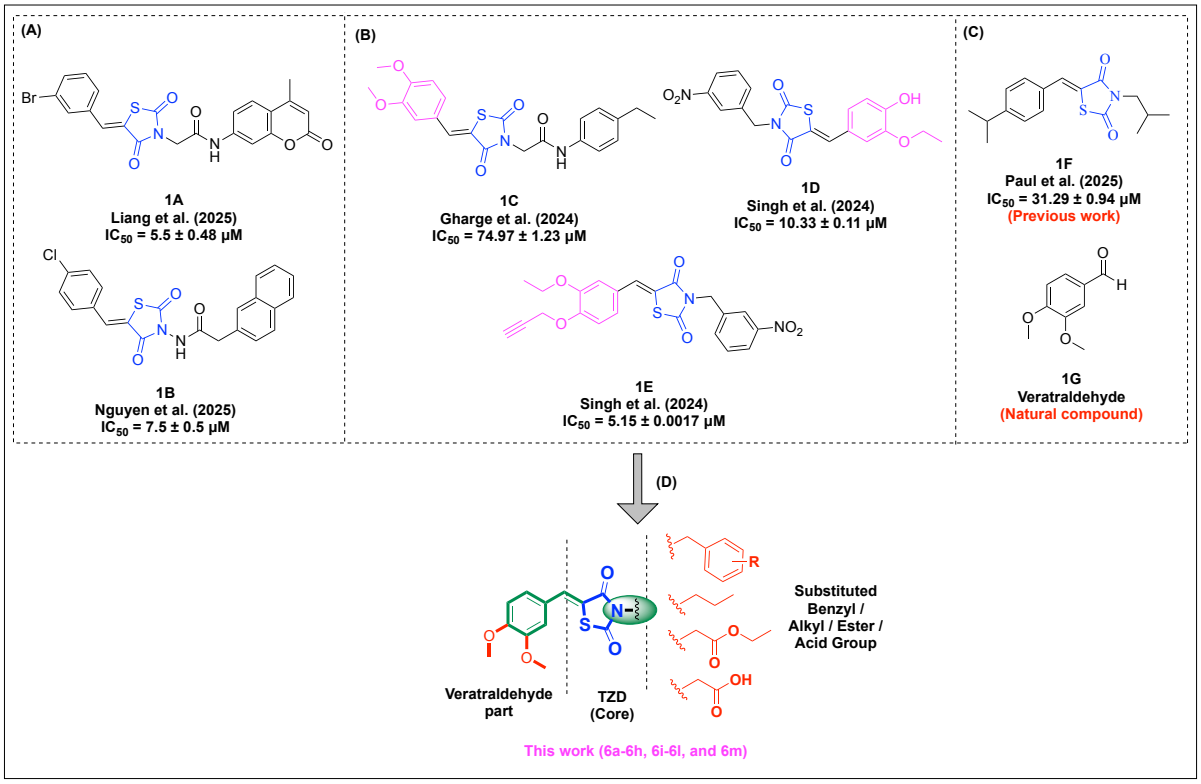

Figure 1: (A) The structure of TZD-containing AGIs [1–3,12–14]; (B) Structure of some AGIs having veratraldehyde (VD) part [2,3,14]; (C) Structure of cuminaldehyde-TZD hybrids as an AG inhibitor [1] and structure of VD; (D) The process of designing hybrids of VD and TZD for the purpose of developing potential AGIs.

2. Experimental section:

2.1. Chemistry:

All essential chemical compounds and solvents of the highest quality for the present study were acquired from commercial operations vendor partners. Thin layer chromatography (TLC) was conducted using 0.20 mm Silica Gel 60 F254 plates, with an ultraviolet light chamber employed to observe the synthesis process under both short and long wavelengths. The synthesized compounds' melting points were evaluated using VEEGO melting point apparatus. Nuclear magnetic resonance (NMR) spectra were obtained at 400/300 MHz for ^{1}H NMR and 101/75 MHz for ^{13}C NMR using a Bruker Avance NMR Spectrophotometer (Germany), with $CDCl_3$ and DMSO-d_6 serving as solvents. Chemical shifts were expressed in parts per million (ppm) relative to the internal standard tetramethylsilane (TMS) (δ = 0.00 ppm) while coupling constant values were indicated in Hertz (Hz). The descriptions of peak splitting include: dd (doublet of doublets), t (triplet), q (quartet), m (multiplet), and s (singlet). Mass spectra (m/z) were obtained using an ESI (ETM, positive/negative ion mode) mass spectrometry instrument (API 2000 ABSCIEX). The analysis of the X-ray crystal structure was conducted utilizing a single-crystal X-ray diffractometer (Bruker SMART, Germany).

2.1.1. Synthesis of thiazolidine-2,4-dione (TZD; Compound 3):

The TZD (compound **3**) was synthesized according to our previously described procedure [1]. In this method, chloroacetic acid (compound **1**; 0.3 mol) and thiourea (compound **2**; 0.3 mol) were used as starting material. The TZD (compound **3**) was ultimately refined through recrystallization from ethyl alcohol [1,30].

2.1.2. (Z)-5-(3,4-dimethoxybenzylidene)thiazolidine-2,4-dione (Compound 5):

To obtain the Knoevenagel condensation (KC) product, 0.550 g of TZD (Compound **3**; 0.004 mol) and 0.664 g of VD (Compound **4**; 0.004 mol) were placed in a 50 mL round-bottom flask, to which 10 mL of acetic acid was added while stirring for 5 minutes. Subsequently, 0.423 g of urea (0.007 mol) was incorporated and stirred for 15 minutes. Following 15 minutes, the reaction mixture was subjected to reflux conditions at 100 °C for 10 to 12 hours, with progress monitored via thin-layer chromatography (TLC). Upon completion of the reaction, the reaction mixture was transferred into a beaker containing crushed ice. The solid was filtered under vacuum, dried at room temperature, and recrystallized from ethanol/methanol to yield pure product 5 (Compound **5**) [1,30].

(Z)-5-(3,4-dimethoxybenzylidene)thiazolidine-2,4-dione (Compound 5):

^{1}H NMR (300 MHz, DMSO-d_6) δ 12.50 (s, 1H), 7.73 (s, 1H), 7.19 – 7.16 (m, 1H), 7.15 (d, *J* = 2.0 Hz, 1H), 7.12 (s, 1H), 3.81 (d, *J* = 5.5 Hz, 6H).**^{13}C NMR** (75 MHz, DMSO-d_6) δ 168.44, 167.84, 151.27, 149.40, 132.69, 126.14, 124.19, 120.87, 113.71, 112.53, 56.14, 55.99. **FT-IR** (ATR) υmax/cm^{-1}: 3113.31 (aromatic =C–H str.), 2981.24, 2775.32 (C–H str., –OCH_3), 11768.48, 1726.45 (C=O str., TZD), 1681.17 (C=C str., aromatic + exocyclic alkene), 1586.51, 1506.87, 1451.10 (C–H bending, aromatic), 1327.23, 1261.69 (C–O str., –OCH_3), 1146.11 (C–N str., TZD ring), 1016.03 (C–H bending), 959.06–686.64 (C–H, aromatic substitution pattern). **MS (ESI)** *m/z:* $[M-H]^+$ calcd. for $C_{12}H_{10}NO_4S^+$: 264.0; found 263.7

2.1.3. General procedure for synthesis of (Z)-3-substituted-5-(3,4-dimethoxybenzylidene)thiazolidine-2,4-dione (Compound 6a-6l):

First, to eliminate extra moisture, anhydrous K_2CO_3 (2 equiv) was placed in a 100 mL flask with a flat bottom and heated for two to three minutes. Subsequently, (Z)-5-(3,4-dimethoxybenzylidene)thiazolidine-2,4-dione (Compound **5**; 0.002 mol) was solubilized in 15 mL of dimethylformamide (DMF) within a 100 mL flat-bottom flask and agitated for 15-20 minutes at room temperature. After that, the substituted benzyl chlorides (1.2 equiv) and alkyl halides (1.2 equiv) were added dropwise and agitated (400–600 rpm) for 10–12 hours at room temperature using a magnetic stirrer. Upon completion of the reaction, thin-layer chromatography (TLC) was conducted to assess the reaction progress. The reaction mixture was subsequently diluted with ethyl acetate and removed from water utilizing a separating funnel. In order to obtain substituted target compounds (Compound **6a-6l**), the ethyl acetate phase was lastly concentrated under vacuum. **Table 1** illustrates the physicochemical characteristics of the synthesized compounds (Compound **5** and **6a-6m**).

Table 1: Physiochemical properties of synthesized compounds (Compound **5** and **6a-6m**).

Compound	Molecular formula	Molecular mass (g/mol)	Appearance	% yield	Melting point (°C)	R_f (H-EA: 4:1)
5	$C_{12}H_{11}NO_4S$	265.3	Light yellow solid	87.42%	201-203 °C	0.35
6a	$C_{19}H_{17}NO_4S$	355.4	Light brown solid	82.02%	132-134 °C	0.40
6b	$C_{20}H_{19}NO_4S$	369.4	Yellow crystal	74.20%	146-148 °C	0.38
6c	$C_{19}H_{16}ClNO_4S$	389.9	Light yellow solid	81.12%	147-149 °C	0.52
6d	$C_{19}H_{15}Cl_2NO_4S$	424.3	Light brown solid	78.18%	163-165 °C	0.48

6e	$C_{19}H_{16}FNO_4S$	373.4	Yellow solid	79.53%	144-146 °C	0.46
6f	$C_{19}H_{16}ClNO_4S$	389.9	Light pink solid	74.43%	148-150 °C	0.47
6g	$C_{19}H_{15}Cl_2NO_4S$	423.0	White solid	80.12%	160-162 °C	0.41
6h	$C_{19}H_{16}BrNO_4S$	433.0	Yellow crystal	79.87%	136-138 °C	0.44
6i	$C_{16}H_{19}NO_4S$	321.1	Light yellow solid	77.82%	180-182 °C	0.42
6j	$C_{17}H_{21}NO_4S$	335.1	Yellow crystal	76.21%	178-180 °C	0.65
6k	$C_{16}H_{19}NO_4S$	321.1	Yellow crystal	84.76%	167-169 °C	0.55
6l	$C_{16}H_{17}NO_6S$	351.1	Light brown crystal	76.80%	113-115 °C	0.62
6m	$C_{14}H_{13}NO_6S$	323.0	Light yellow solid	88.90%	106-108 °C	0.30

H-EA: Hexane: Ethyl acetate

(Z)-3-benzyl-5-(3,4-dimethoxybenzylidene)thiazolidine-2,4-dione

*(Compound **6a):***

^{1}H NMR (300 MHz, $CDCl_3$) δ 7.84 (s, 1H), 7.46 – 7.40 (m, 2H), 7.36 – 7.28 (m, 3H), 7.11 (dd, *J* = 8.4, 2.1 Hz, 1H), 6.99 (d, *J* = 2.0 Hz, 1H), 6.94 (d, *J* = 8.4 Hz, 1H), 4.89 (s, 2H), 3.92 (d, *J* = 3.8 Hz, 6H). **^{13}C NMR** (75 MHz, $CDCl_3$) δ 167.85, 166.26, 151.27, 149.36, 135.27, 134.18, 128.85, 128.74, 128.23, 126.16, 124.75, 118.70, 112.38, 111.41, 77.50, 76.65, 56.08, 55.97, 45.22. **FT-IR** (ATR) υmax/cm^{-1}: 3343.78, 2925.99, 2372.79, 2310.26 (C–H str., aliphatic/aromatic and –OCH_3), 1722.96, 1667.27 (C=O str., TZD ring), 1590.29, 1507.04 (C=C str., aromatic + exocyclic alkene), 1451.34, 1418.72, 1369.43, 1342.43, (C–H bending, aromatic rings), 1270.49, 1283.33 (C–O str., –OCH_3 groups), 1143.18, 1089.75 (C–N str., TZD ring), 1019.73, 1019.73 (C–H bending, out-of-plane, substituted aromatic), 957.70-688.27

(Aromatic C–H oop bending). **MS (ESI)** *m/z:* $[M-H]^+$ calcd. for $C_{19}H_{16}NO_4S^+$: 354.1; found 352.9

(Z)-5-(3,4-dimethoxybenzylidene)-3-(4-methylbenzyl)thiazolidine-2,4-dione (*Compound* ***6b):***

^{1}H NMR (300 MHz, $CDCl_3$) δ 7.83 (s, 1H), 7.36 – 7.30 (m, 2H), 7.17 – 7.08 (m, 3H), 7.00 – 6.90 (m, 2H), 4.86 (s, 2H), 3.92 (d, *J* = 3.8 Hz, 6H), 2.32 (s, 3H). **^{13}C NMR** (75 MHz, $CDCl_3$) δ 167.85, 166.28, 151.23, 149.35, 138.04, 134.05, 132.33, 129.39, 128.87, 126.20, 124.72, 118.81, 112.36, 111.40, 56.07, 55.96, 45.01, 21.18. **FT-IR** (ATR) υmax/cm^{-1}: 2898.33, 2824.13, 2386.78, 2310.31 (C–H str., aliphatic and aromatic, including –CH_3 and –OCH_3), 1729.57 (C=O str., TZD ring), 1672.98 (C=C str., aromatic + alkene), 1579.20, 1501.84 (C–H bending, aromatic), 1421.14, 1315.06 (C–H bending, –CH_3 of p-tolyl group), 1267.20 (C–O str., –OCH_3 groups), 1165.28, 1120.53 (C–N str., TZD ring), 1010.31 (C–H oop bending, aromatic), 933.84-667.84 (Aromatic C–H oop bending, substituted rings). **MS (ESI)** *m/z:* $[M-H]^+$ calcd. for $C_{20}H_{18}NO_4S^+$: 368.1; found 367.0

(Z)-3-(4-chlorobenzyl)-5-(3,4-dimethoxybenzylidene)thiazolidine-2,4-dione (*Compound* ***6c):***

^{1}H NMR (300 MHz, $CDCl_3$) δ 7.84 (s, 1H), 7.41 – 7.34 (m, 2H), 7.33 – 7.27 (m, 2H), 7.12 (dd, *J* = 8.4, 2.1 Hz, 1H), 7.01 – 6.91 (m, 2H), 4.85 (s, 2H), 3.93 (d, *J* = 4.3 Hz, 6H). **^{13}C NMR** (75 MHz, $CDCl_3$) δ 167.82, 166.15, 151.36, 149.39, 134.48, 134.25, 133.70, 130.36, 128.93, 126.06, 124.81, 118.45, 112.39, 111.42, 56.08, 55.97, 44.48. **FT-IR** (ATR) υmax/cm^{-1}: 3056.92, 2942.31, 2832.45, 2311.10 (C–H str., aliphatic and aromatic, including –OCH_3), 1729.28 (C=O str., TZD ring), 1676.66 (C=C str.,

aromatic + alkene), 1587.54, 1506.14, 1455.67, 1424.77, 1374.58, 1324.61 (C–H bending, aromatic), 12672.87 (C–O str., –OCH_3 groups), 1139.33 (C–N str., TZD ring), 1095.17 (C–Cl str., aryl chloride), 1019.99 (C–H oop bending, substituted aromatic rings), 950.51–676.09 (Aromatic C–H oop bending, characteristic of para-substituted benzene rings). **MS (ESI)** *m/z:* $[M-H]^+$ calcd. for $C_{19}H_{15}ClNO_4S^+$: 388.9; found 388.7

(Z)-3-(2,4-dichlorobenzyl)-5-(3,4-dimethoxybenzylidene)thiazolidine-2,4-dione (*Compound* ***6d):***

^{1}H NMR (300 MHz, $CDCl_3$) δ 7.87 (s, 1H), 7.40 (d, *J* = 2.0 Hz, 1H), 7.21 (dd, *J* = 8.4, 2.1 Hz, 1H), 7.17 – 7.11 (m, 2H), 7.03 – 6.93 (m, 2H), 4.99 (s, 2H), 3.94 (d, *J* = 3.9 Hz, 6H). **^{13}C NMR** (75 MHz, $CDCl_3$) δ 167.53, 165.99, 151.47, 149.42, 134.79, 134.41, 133.94, 131.00, 129.67, 129.64, 127.33, 126.00, 124.92, 118.07, 112.44, 111.45, 56.10, 55.99, 42.38. **FT-IR** (ATR) υmax/cm^{-1}: 3077.08, 2925.67, 2386.80, 2310.06 (C–H str., aliphatic and aromatic including –OCH_3), 1730.66 (C=O str., TZD ring), 1673.62, 1580.76 (C=C str., aromatic + exocyclic alkene), 1580.76, 1508.76, 1455.22, 1418.38, 1362.83, 1334.56 (C–H bending, aromatic), 1256.22 (C–O str., –OCH_3 groups), 1141.92 (C–N str., TZD ring), 1086.61 (C–Cl str., aryl chlorides), 1014.82, 914.63 (C–H bending, out-of-plane), 829.23–658.80 (C–H oop bending, disubstituted benzene ring). **MS (ESI)** *m/z:* $[M-H]^+$ calcd. for $C_{19}H_{14}Cl_2NO_4S^+$: 423.3; found 422.9

(Z)-5-(3,4-dimethoxybenzylidene)-3-(4-fluorobenzyl)thiazolidine-2,4-dione (*Compound* ***6e):***

^{1}H NMR (300 MHz, $CDCl_3$) δ 7.84 (s, 1H), 7.47 – 7.40 (m, 2H), 7.12 (dd, *J* = 8.4, 2.1 Hz, 1H), 7.05 – 6.99 (m, 2H), 6.99 – 6.92 (m, 2H), 4.86 (s, 2H),

3.93 (d, *J* = 4.3 Hz, 6H). **^{13}C NMR** (75 MHz, $CDCl_3$) δ 167.85, 166.19, 164.27, 161.00, 151.34, 149.38, 134.37, 130.94, 130.83, 126.09, 124.79, 118.55, 115.78, 115.49, 112.38, 111.42, 56.08, 55.97, 44.45. **FT-IR** (ATR) υmax/cm^{-1}: 3067.01, 2943.98, 2835.14, 2386.81, 2310.22 (C–H str., aliphatic and aromatic, including –OCH_3), 1728.91 (C=O str., TZD ring), 1674.73 (C=C str., aromatic + alkene), 1587.70, 1505.47, 1427.21, 1370.99, 1322.46 (C–H bending, aromatic), 1272.25, 1213.09 (C–O str., –OCH_3 groups), 1134.58 (C–N str., TZD ring), 1089.61 (C–F str., aryl fluoride), 1012.57 (C–H oop bending, substituted aromatic rings), 947.21–668.89 (Aromatic C–H oop bending, characteristic of para-substituted benzene rings). **MS (ESI)** *m/z:* $[M+H]^+$ calcd. for $C_{19}H_{17}FNO_4S^+$: 374.1; found 374.0

(Z)-3-(3-chlorobenzyl)-5-(3,4-dimethoxybenzylidene)thiazolidine-2,4-dione (*Compound* ***6f):***

^{1}H NMR (300 MHz, $CDCl_3$) δ 7.84 (s, 1H), 7.42 – 7.39 (m, 1H), 7.32 – 7.26 (m, 2H), 7.26 – 7.23 (m, 1H), 7.14 – 7.09 (m, 1H), 6.98 (d, *J* = 2.1 Hz, 1H), 6.93 (d, *J* = 8.4 Hz, 1H), 4.84 (s, 2H), 3.92 (d, *J* = 4.1 Hz, 6H). **^{13}C NMR** (75 MHz, $CDCl_3$) δ 167.77, 166.09, 151.37, 149.39, 137.06, 134.58, 134.56, 130.03, 128.90, 128.50, 127.01, 126.06, 124.82, 118.40, 112.40, 111.43, 56.08, 55.97, 44.55. **FT-IR** (ATR) υmax/cm^{-1}: 3257.14, 3067.01–2081.13 (C–H str., aliphatic and aromatic, including –OCH_3), 1734.83 (C=O str., TZD ring), 1666.91 (C=C str., aromatic + alkene), 1595.63–1343.72 (C–H bending, aromatic), 1267.97 (C–O str., –OCH_3 groups), 1148.94 (C–N str., TZD ring), 1089.46 (C–Cl str., aryl chloride), 1019.65 (C–H oop bending, substituted aromatic rings), 823.89–675.34 (Aromatic C–H oop bending,

characteristic of meta-substituted benzene rings). **MS (ESI)** *m/z:* $[M+H]^+$ calcd. for $C_{19}H_{17}ClNO_4S^+$: 390; found 389.8

(Z)-3-(3,4-dichlorobenzyl)-5-(3,4-dimethoxybenzylidene)thiazolidine-2,4-dione (*Compound* ***6g):***

^{1}H NMR (300 MHz, $CDCl_3$) δ 7.85 (s, 1H), 7.53 (d, *J* = 2.0 Hz, 1H), 7.40 (d, *J* = 8.2 Hz, 1H), 7.29 (d, *J* = 2.1 Hz, 1H), 7.12 (dd, *J* = 8.4, 2.1 Hz, 1H), 6.99 (d, *J* = 2.1 Hz, 1H), 6.95 (d, *J* = 8.4 Hz, 1H), 4.82 (s, 2H), 3.93 (d, *J* = 4.5 Hz, 6H). **^{13}C NMR** (75 MHz, $CDCl_3$) δ 167.76, 166.01, 151.45, 149.40, 135.24, 134.78, 132.82, 132.60, 130.90, 130.73, 128.34, 125.99, 124.87, 118.21, 112.42, 111.44, 56.09, 55.98, 43.98. **FT-IR** (ATR) υmax/cm^{-1}: 3084.10, 2925.24, 2310.49 (C–H str., aliphatic and aromatic, including –OCH_3), 1724.97 (C=O str., TZD ring), 1667.26 (C=C str., aromatic + alkene), 1592.08–1337.76 (C–H bending, aromatic), 1260.54 (C–O str., –OCH_3 groups), 1143.59 (C–N str., TZD ring), 1086.37 (C–Cl str., aryl chlorides), 1016.75, 938.72 (C–H oop bending, substituted aromatic rings), 865.72–678.50 (Aromatic C–H oop bending, characteristic of disubstituted benzene rings). **MS (ESI)** *m/z:* $[M+H]^+$ calcd. for $C_{19}H_{16}Cl_2NO_4S^+$: 424.0; found 424.8

(Z)-3-(4-bromobenzyl)-5-(3,4-dimethoxybenzylidene)thiazolidine-2,4-dione (*Compound* ***6h):***

^{1}H NMR (300 MHz, $CDCl_3$) δ 7.84 (s, 1H), 7.49 – 7.41 (m, 2H), 7.36 – 7.28 (m, 2H), 7.12 (dd, *J* = 8.5, 2.1 Hz, 1H), 6.98 (d, *J* = 2.1 Hz, 1H), 6.94 (d, *J* = 8.4 Hz, 1H), 4.84 (s, 2H), 3.93 (d, *J* = 4.4 Hz, 6H). **^{13}C NMR** (75 MHz, $CDCl_3$) δ 167.80, 166.13, 151.38, 149.40, 134.49, 134.20, 131.89, 130.67, 126.07, 124.81, 122.42, 118.44, 112.41, 111.44, 56.08, 55.98, 44.54. **FT-IR**

(ATR) υmax/cm^{-1}: 3282.08, 3177.52, 3005.97, 2943.11, 2874.48, 2824.08, 2447.24, 2325.55 (C–H str., aliphatic and aromatic, including –OCH_3), 1725.65 (C=O str., TZD ring), 1670.93 (C=C str., aromatic + alkene), 1576.94, 1500.51, 1420.73, 1370.52, 1321.92 (C–H bending, aromatic), 1265.25 (C–O str., –OCH_3 groups), 1134.30 (C–N str., TZD ring), 1089.61 (C–Br str., aryl bromide), 1096.79, 1009.52 (C–H oop bending, substituted aromatic rings), 907.36–663.74 (Aromatic C–H oop bending, characteristic of para-substituted benzene rings). **MS (ESI)** *m/z:* $[M+H]^+$ calcd. for $C_{19}H_{17}BrNO_4S^+$: 435.3; found 435.7

(Z)-5-(3,4-dimethoxybenzylidene)-3-isobutylthiazolidine-2,4-dione (Compound 6i):

^{1}H NMR (300 MHz, $CDCl_3$) δ 7.83 (s, 1H), 7.13 (dd, *J* = 8.4, 2.1 Hz, 1H), 7.01 (d, *J* = 2.1 Hz, 1H), 6.95 (d, *J* = 8.4 Hz, 1H), 3.93 (d, *J* = 2.7 Hz, 6H), 3.57 (d, *J* = 7.5 Hz, 2H), 2.19 – 2.09 (m, 1H), 0.93 (d, *J* = 6.7 Hz, 6H). **^{13}C NMR** (75 MHz, $CDCl_3$) δ 167.86, 166.42, 150.87, 149.06, 133.45, 125.97, 124.36, 118.49, 112.10, 111.11, 76.94, 55.76, 55.66, 48.72, 26.93, 19.66. **FT-IR** (ATR) υmax/cm^{-1}: 2983.41, 2890.91, 2497.12, 2325.93 (C–H str., aliphatic –CH_3, –CH_2–, isobutyl and –OCH_3 groups), 1733.19 (C=O str., TZD ring), 1684.59, 1580.15 (C=C str., aromatic + exocyclic alkene), 1510.15, 1450.09 (C–H bending, aromatic), 1385.70, 1367.00, 1312.86 (C–H bending, –$CH(CH_3)_2$ of isobutyl), 1260.23, 1202.34 (C–O str., methoxy groups), 1141.94 (C–N str., TZD ring), 1096.43, 1012.40 (C–H oop bending, substituted aromatic), 950.10–663.79 (Aromatic C–H oop bending, 1,2,3-trisubstituted ring pattern). **MS (ESI)** *m/z:* $[M-H]^+$ calcd. for $C_{16}H_{18}NO_4S^+$: 320.1; found 320.7

(Z)-5-(3,4-dimethoxybenzylidene)-3-isopentylthiazolidine-2,4-dione

*(Compound **6j**):*

^{1}H NMR (300 MHz, $CDCl_3$) δ 7.82 (s, 1H), 7.13 (dd, *J* = 8.5, 2.1 Hz, 1H), 7.00 (d, *J* = 2.1 Hz, 1H), 6.95 (d, *J* = 8.4 Hz, 1H), 3.93 (d, *J* = 2.7 Hz, 6H), 3.81 – 3.71 (m, 2H), 1.60 (d, *J* = 6.0 Hz, 1H), 1.55 (ddd, *J* = 8.4, 4.6, 1.3 Hz, 2H), 0.96 (d, *J* = 6.3 Hz, 6H). **^{13}C NMR** (75 MHz, $CDCl_3$) δ 167.92, 166.47, 151.18, 149.36, 133.67, 126.27, 124.67, 118.95, 112.39, 111.41, 56.06, 55.96, 40.56, 36.47, 25.96, 22.35. **FT-IR** (ATR) υmax/cm^{-1}: 3007.66, 2311.22 (C–H str., aliphatic –CH_3, –CH_2–, isobutyl and –OCH_3 groups), 1727.67, 1667.07 (C=O str., TZD ring), 1600.35 (C=C str., aromatic + exocyclic alkene), 1373.75 (C–H bending of isopentyl), 1202.50 (C–O str., methoxy groups), 1110.19 (C–N str., TZD ring), 1016.38 (C–H oop bending, substituted aromatic), 831.15, 658.13 (Aromatic C–H oop bending, 1,2,3-trisubstituted ring pattern). **MS (ESI)** *m/z:* $[M+H]^+$ calcd. for $C_{17}H_{22}NO_4S^+$: 336.4; found 337.8

(Z)-3-butyl-5-(3,4-dimethoxybenzylidene)thiazolidine-2,4-dione

*(Compound **6k**):*

^{1}H NMR (300 MHz, $CDCl_3$) δ 7.82 (s, 1H), 7.13 (dd, *J* = 8.5, 2.1 Hz, 1H), 7.00 (d, *J* = 2.1 Hz, 1H), 6.95 (d, *J* = 8.4 Hz, 1H), 3.93 (d, *J* = 2.7 Hz, 6H), 3.79 – 3.71 (m, 2H), 1.70 – 1.54 (m, 3H), 1.42 – 1.29 (m, 2H), 0.94 (t, *J* = 7.3 Hz, 3H). **^{13}C NMR** (75 MHz, $CDCl_3$) δ 167.98, 166.52, 151.18, 149.36, 133.70, 126.26, 124.66, 118.92, 112.40, 111.41, 56.06, 55.96, 41.80, 29.84, 19.98, 13.62. **FT-IR** (ATR) υmax/cm^{-1}: 2942.58, 2318.45 (C–H str., aliphatic –CH_3, –CH_2– and –OCH_3), 1741.85 (C=O str., TZD ring), 1602.41 (C=C str., aromatic and alkene), 1433.66 (C–H bending, aromatic), 1368.90

(C–H bending, aliphatic chain), 1257.22 (C–O str., –OCH_3 groups), 1107.81 (C–N str., TZD ring), 1091.66 (C–H bending, out-of-plane), 660.86 (Aromatic C–H oop bending, 1,2,3-trisubstituted ring). **MS (ESI)** *m/z:* $[M+H]^+$ calcd. for $C_{16}H_{20}NO_4S^+$: 322.4; found 323.0

Ethyl (Z)-2-(5-(3,4-dimethoxybenzylidene)-2,4-dioxothiazolidin-3-yl)acetate (*Compound* ***6l):***

^{1}H NMR (300 MHz, $CDCl_3$) δ 7.87 (s, 1H), 7.14 (dd, *J* = 8.5, 2.1 Hz, 1H), 7.01 (d, *J* = 2.1 Hz, 1H), 6.96 (d, *J* = 8.4 Hz, 1H), 4.47 (s, 2H), 4.24 (q, *J* = 7.1 Hz, 2H), 3.93 (d, *J* = 3.3 Hz, 6H), 1.29 (t, *J* = 7.1 Hz, 3H). **^{13}C NMR** (75 MHz, $CDCl_3$) δ 167.23, 166.01, 165.37, 151.12, 149.10, 134.46, 125.71, 124.54, 117.94, 112.15, 111.14, 76.94, 61.81, 55.78, 55.67, 41.80, 13.79. **FT-IR** (ATR) υmax/cm^{-1}: 3374.00, 2937.78 (C–H str., aliphatic –CH_3, –CH_2– and –OCH_3), 1729.13 (C=O str., ester group), 16662.46 (C=O str., TZD ring), 1662.46 (C=C str., aromatic and exocyclic alkene), 1596.81 (C–H bending, aromatic), 1443.90, 1370.03 (C–H bending, –CH_2– and –CH_3 groups), 1257.11 (C–O str., methoxy groups and ester), 1162.14 (C–N str., TZD ring), 1015.06 (C–O–C str., ethyl ester and methoxy), 941.87 (C–H bending, out-of-plane), 827.28 (Aromatic C–H oop bending, 1,2,3-trisubstituted ring). **MS (ESI)** *m/z:* $[M+H]^+$ calcd. for $C_{16}H_{18}NO_6S^+$: 352.4; found 352.9

2.1.4. General procedure for synthesis of (Z)-2-(5-(3,4-dimethoxybenzylidene)-2,4-dioxothiazolidin-3-yl)acetic acid (Compound 6m):

The compound **6m** was synthesized as per our previous published method [1]. A round-bottomed flask with a volume of 150 ml was used to collect 0.5 grams of compound **6l**, which is equivalent to 0.5 millimoles. In the same

flask, 3 mL of concentrated hydrochloric acid and 6 mL of glacial acetic acid were combined in a 1:2 ratio and subjected to reflux at 100 ºC for 2 to 3 hours. The reaction mixture was subsequently cooled to ambient temperature and transferred into ice-cold water. After a few minutes, the light-yellow solid precipitate was obtained by vacuum filtration, washed multiple times with water, and dried at room temperature to provide the target compound **6m**.

(Z)-2-(5-(3,4-dimethoxybenzylidene)-2,4-dioxothiazolidin-3-yl)acetic acid (*Compound* ***6m):***

^{1}H NMR (400 MHz, $CDCl_3$) δ 7.88 (s, 1H), 7.14 (s, 1H), 7.02 (s, 1H), 6.96 (d, *J* = 8.4 Hz, 1H), 4.50 (s, 2H), 3.94 (d, *J* = 4.6 Hz, 6H). **^{13}C NMR** (101 MHz, $CDCl_3$) δ 168.41, 151.40, 149.39, 142.24, 134.78, 124.84, 118.32, 112.44, 111.44, 77.23, 56.09, 55.98, 29.71. **FT-IR** (ATR) υmax/cm^{-1}: 3391.50 (O–H str.), 2943.35, 2800.98 (C–H str., aliphatic and –OCH_3), 1693.72 (C=O str., carboxylic acid), 1758.99 (C=O str., cyclic imide/dione from TZD), 1516.05 (C=C str., aromatic and alkene), 1381.74 (C–H bending, aliphatic –CH_2), 1144.39 (C–N str., TZD ring). **MS (ESI)** *m/z:* [M-H]$^+$ calcd. for $C_{14}H_{12}NO_6S^+$: 322.3; found 322.7

2.2. In vitro assay of α-glucosidase inhibitory activity:

The AG inhibition experiment was performed in 96-well plates according to our previous protocol [1]. The AG enzyme sourced from *Saccharomyces cerevisiae*, p-nitrophenyl-α-d-glucopyranoside (pNPG), and Acarbose were obtained from SRL. In this experiment, pNPG functioned as the substrate, while Acarbose acted as the positive control. In well plates, 20 µL of diverse quantities of test samples and Acarbose, solubilized in methanol, together with 10 µL of AG (0.5 U/mL) in 0.1

mM phosphate buffer (pH 6.8), were incubated at 37 °C for 15 minutes. 20 µL of pNPG substrate, soluble in the aforementioned PBS, was added to each well and kept at 37 °C for 25 minutes. The absorbance was quantified at 405 nm. The percentage of inhibition for the analyzed drugs, control, and positive control was expressed as % inhibition using the following formula-

$$\% \text{ Inhibition} = \frac{\mathbf{Abs(control)} - \mathbf{Abs(sample)}}{\mathbf{Abs(control)}} \times 100$$

The IC_{50} of the analyzed compounds or positive control were ascertained by Logit method for linear regression analysis.

2.3. Inhibition kinetics:

A kinetic study of compound **6f** against AG was performed according to our previous technique to ascertain the type of enzyme inhibition and the inhibition constant [1]. pNPG at concentrations of 0.10, 0.15, 0.20, and 0.30 µM was integrated with a constant amount of AG (0.5 U/mL) and different concentration of compound **6f** at values of 0, 15, 30, 60 and 120 µM. The absorbance with 405 nm was measured 15 times over 30 seconds. The antagonistic effect was determined using the Lineweaver-Burk plot, and the Michaelis-Menten constant (Km) was derived from the plot illustrating the reciprocal of variable pNGP concentrations (1/[S]) against the reciprocal of enzyme activity (1/V) at varied doses.

2.4. Fluorescence quenching:

The method from our previous work was utilized to evaluate the fluorescence quenching of AG in compound **6f** [1]. 3.5 U/mL AG, solubilized in PBS at pH 6.8, was mixed with various amounts of inhibitors (0, 0, 10, 20, 40, 80 and 160 µM) for 10 minutes at 25 °C. The fluorescence intensities of AG were quantified with an emission wavelength of 300 to 450 nm and an excitation wavelength of 280 nm. The compound **6f** demonstrated fluorescence at an excitation wavelength of 280

nm and subtracted the baseline fluorescence value. The fluorescence spectra of the PBS were assessed under the same conditions.

2.5. Circular dichroism spectra:

The CD spectra of AG solution (0.5 U/mL) were examined with and without varying doses of compound compound **6f** at 0, 10, 20, 40, and 80 µM across the wavelength range of 190–260 nm. The 1 nm bandwidth was quantified utilizing a CD spectrometer (Chirascan qCD, Applied Photophysics) at RT under stable nitrogen circumstances. The solvent background of the PBS signal was eliminated to correct the CD spectra. The CDNN program was employed to evaluate the effect of compound **6f** by quantifying the changes in α-helix, random coils, β-sheets, and β-turn content of AG [1].

2.6. Molecular docking:

2.6.1. Protein preparation:

The three-dimensional crystal structure of AG (PDB ID: 5NN8) with a resolution of 2.45 Å was retrieved from the Protein Data Bank (https://www.rcsb.org). Using Discovery Studio Visualizer (v21.1.020298), all co-crystallized ligands, non-essential water molecules, and other heteroatoms were removed. The macromolecule was subsequently prepared for docking using AutoDockTools version 1.5.7. This involved merging non-polar hydrogens and applying Gasteiger charges. The prepared structure was then used for further docking simulations [31].

2.6.2. Ligand preparation:

The 3D conformer of compound **6f**, in .mol2 format, was energy-minimized using MMFF94 force field. Hydrogen atoms were also added to the ligand

structure. To identify the most favourable binding conformation, molecular docking was carried out through AutoDockTools 1.5.7 [32].

2.6.3. Docking:

The ligand-protein interactions were investigated using molecular docking. AutoDockTools 1.5.7 carried out the docking study utilizing a grid-based methodology using x, y, and z coordinates of -14.597930, -33.591140, and 95.075744, respectively. The binding energy (Kcal/mol) of each protein-ligand complex was determined using the docking results. The docking score quantitatively reflects the binding affinity of the ligands, with lower values indicating superior interaction. The ligands engage with the receptor via several bonding interactions. However, Agu *et al.* suggest that these interactions may enhance the comprehension of the compounds' mechanisms of action and their potential therapeutic efficacies. The interaction characteristics of the protein-ligand complex were analyzed using Discovery Studio Visualiser [33].

2.7. In vitro cytotoxicity:

The cell viability assay was conducted to evaluate the cytotoxic effects of compound **6f** on HEK-293 cells, following our established technique [1]. Cells were grown in DMEM at 37 °C. Upon achieving confluence, 6000 cells were inoculated into each well of 96-well plates and incubated for 24 hours. After 24 hours of incubation, the cells were exposed to doses of compound 6f varying from 3.9 to 250 µM for an additional 24 hours. After 24 hours, 5 mg/mL MTT was introduced to the wells, followed by a 3 hour incubation period. After three hours, formazan crystals were dissolved in DMSO. The absorbance was measured at 570 nm. The percentage cell viability was determined according to:

$$Cell\ viability\ (\%) = \left(\frac{ODsample}{ODcontrol}\right) x\ 100$$

2.8. ADME, drug-likeness and toxicity assessment:

The SwissADME online tool (http://www.swissadme.ch), designed by the Swiss Institute of Bioinformatics (SIB) in Lausanne, Switzerland, was used to evaluate the physicochemical and pharmacokinetic properties of the selected candidates to determine their ADME predictions and drug-like features. Likewise, the online Deep-PK webserver was used to examine the toxicity characteristics of the specified endpoints of selected potent molecules: Skin Sensitization, Carcinogenesis, Liver Injury, hERG Blockers, Fathead Minnow, Maximum Tolerated Dose, Ames (Mutagenicity), and Acute and Chronic Rat Toxicology [34][35].

3. Result and discussion:

3.1. Chemistry:

The present study developed 14 new heterocyclic compounds employing VD based TZD hybrids (**Table 1**), beginning with thiourea and chloroacetic acid. A synthetic process consisting of three steps, one step of which was used for developing the TZD, intermediate compound **5**, and suggested compounds (**6a-6l** and **6m**). **Scheme 1** and **Scheme 1A** describe the synthesis schemes. NMR, FT-IR, and MS-ESI were used to characterize all of the compounds (compound **5**, **6a-6m**) (**Spectral figure**). Additionally, the molecular geometry and table data of compound **6b** crystal were studied and shown in **spectral figure**.

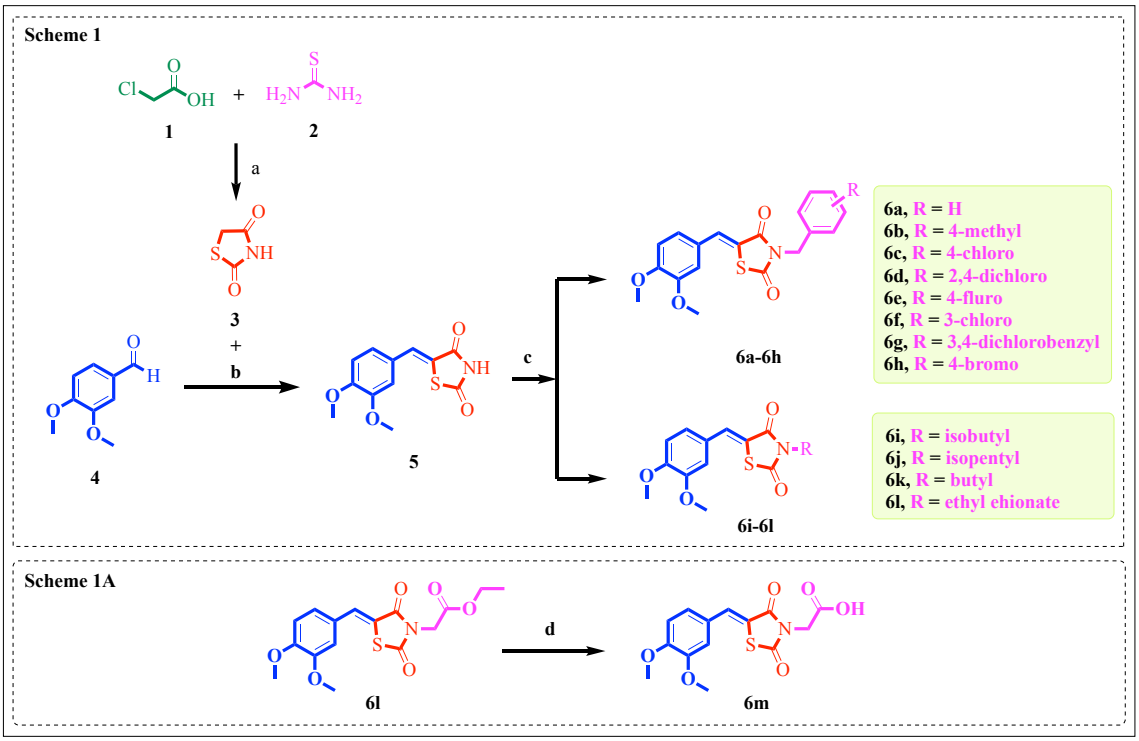

Scheme 1: Synthesis of target compounds **6a-h**, **6i-6l,** and **6m**. **Reagents and conditions:** a) Concentrated hydrochloric acid, water, 100-110 ^{0}C, reflux, 8–10 hrs; b) Urea (1.5 equiv), Glacial acetic acid, 100 ^{0}C, Reflux, 8–10 hrs; c) Substituted benzyl chlorides/ Alkyl halides, K_2CO_3, DMF, rt; 18-24 hrs. **Scheme 1A:** Synthesis of target compound **6m** from **6l**. **Reagents and conditions:** d) Conc. HCl: AcOH (1:2), reflux 2 h [1].

3.2. X-ray crystallographic analysis with ORTEP diagram of compounds 6b:

We conducted an X-ray crystallographic investigation on compound **6b** (**Scheme 1**). to verify the proposed structure. The structures of additional compounds were established through analogy and corroborated by spectral data, including ^{1}H, ^{13}C, and MS-ESI analysis. The crystallization of compound **6b** was achieved using methanol solvents through a gradual evaporation method. The **spectral figure** (**S43** and **Table S1**) contains further details regarding these crystals. We aimed to provide the product stereochemistry, for which we have already supplied the data analyzed through X-ray crystallography (**Scheme 1**).

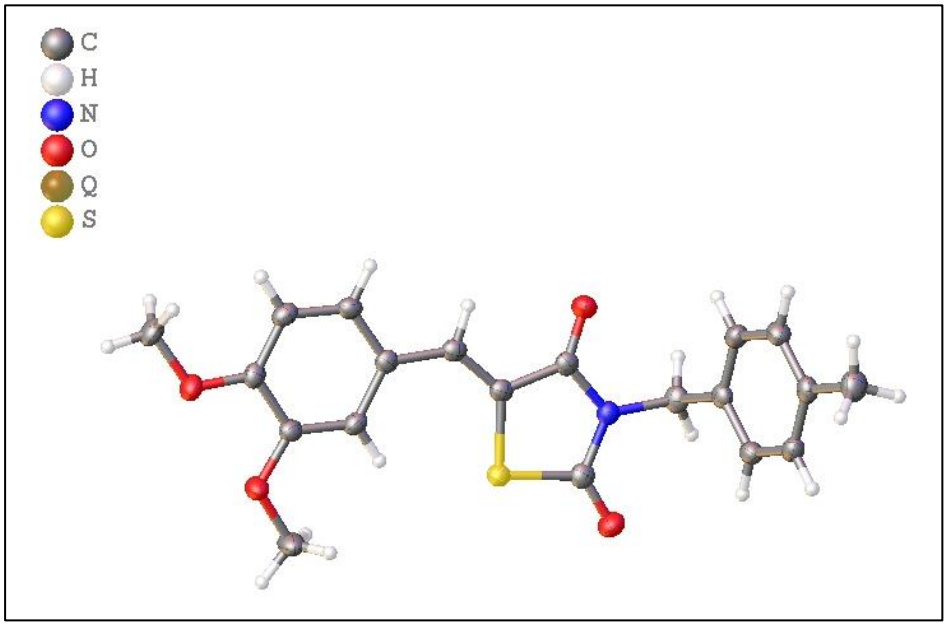

Figure 2: ORTEP diagram of compound **6b** (**CCDC-** 2445001) (**Scheme 1**).

3.3. In vitro assay of α-glucosidase inhibitory activity:

All synthetic compounds (compound **5** to compounds **6a-6m**) were assessed for their *in vitro* antagonistic effect on AG activity, utilizing Acarbose as a reference, employing an established method which was previously described (**Table 2**). Multiple different synthesized compounds demonstrated AGI action, with IC_{50} values spanning from 18.16 ± 0.41 µM to over 500 µM. The compounds compound **6f**, **6g**, **6d**, **6h**, and **6e** showed superior AGI activity compared to others, with IC_{50}

values between 18.16 ± 0.41 µM and 66.09 ± 1.95 µM. Among the compounds, compound **6f** demonstrated the most promising antagonistic activity, with an IC_{50} value of 18.16 ± 0.41 µM, in contrast to Acarbose, which had an IC_{50} of 55.04 ± 1.51 µM. However, it is noteworthy that the VD-TZD series has a TZD ring as one of its moieties. This heterocyclic ring structure has been previously reported to exhibit possible antagonistic activity against the AG enzyme in the control of hyperglycemia [36].

Table 2: The *in vitro* AGI activity screening and IC_{50} values data of synthesized compounds (**6a-6h**, **6i-6l**, and **6m**).

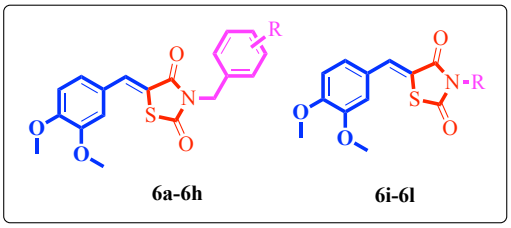

Sl. no.	Compound	R	IC_{50} (µM)
1	5	-	>500
2	6a	-H	>500
3	6b	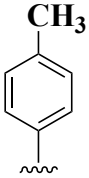	66.77 ± 0.58
4	6c	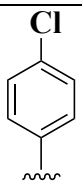	97.62 ± 1.24
5	6d	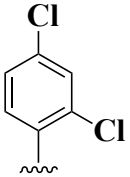	21.60 ± 0.97

6	6e	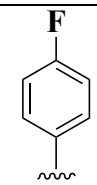	66.09 ± 1.95
7	6f	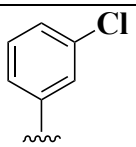	18.16 ± 0.41
8	6g	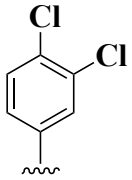	19.59 ± 0.78
9	6h	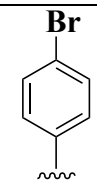	42.15 ± 1.25
10	6i	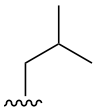	>500
11	6j	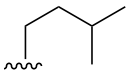	>500
12	6k	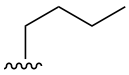	104.29 ± 0.58
13	6l	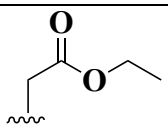	116.96 ± 1.10
14	6m	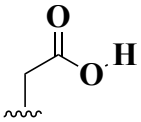	>500
15	Acarbose	-	55.04 ± 1.51

3.4. Structure-activity relationships (SARs):

The activity of various N-benzyl, alkyl, and acid substitutions at the VD-TZD intermediate (compound **5**) on AGI activity was examined by a structure-activity relationship (SAR) analysis. The introduction of a 3-chloro group in the benzyl

substitution of the VD-TZD intermediate (compound **5; Figure 3**) enhanced the AGI activity, achieving compound **6f** with an IC_{50} of 18.16 ± 0.41 µM. The replacement of the 3,4-dichloro group similarly improves the AGI activity, as demonstrated by compound **6g** (IC_{50} = 19.59 ± 0.78 µM). The incorporation of the alkyl, ester, and acetic acid moieties into the VD-TZD intermediate (compound **5; Figure 3**) led to a reduction in AGI activity. The results regarding SARs guided the improvement of inhibitory efficacy in later structural alterations.

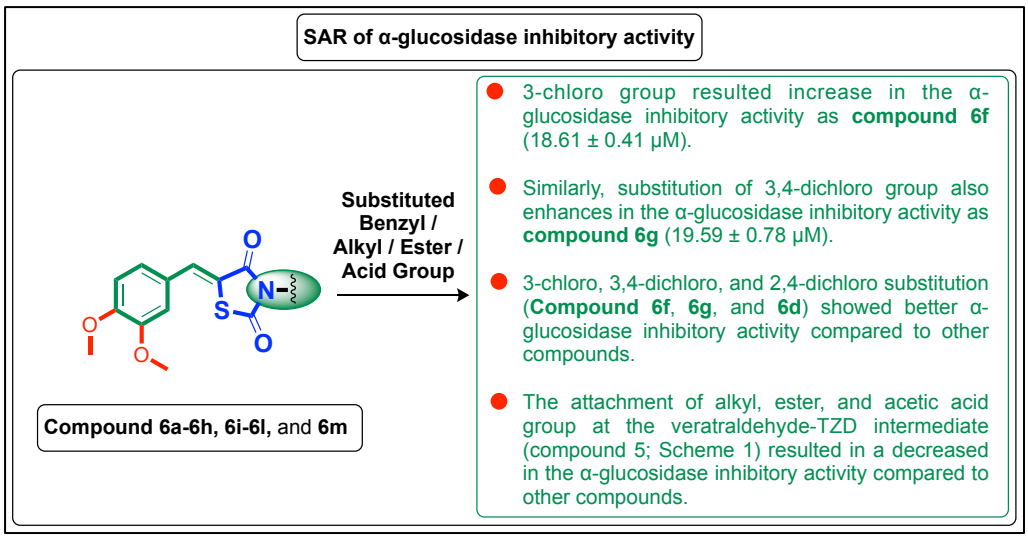

Figure 3: SAR of VD-TZD series for AGI activity.

3.5. Enzyme kinetic study:

The antagonistic effect of **6f** on AG was examined using inhibition kinetics research analyzed via the Lineweaver-Burk method (**Figure 4**). The graphs of 1/V against 1/[S] displayed a succession of linear relationships with differing gradient that converged in the second quadrant. The results demonstrated that Km values rose while Vmax remained unchanged with elevated level of compound **6f**, suggesting competitive inhibition mechanisms of AG by **6f**. Compound **6f** exhibits a propensity to occupy the reactive site of the enzyme, hence inhibiting the enzyme-substrate (ES) complex by competitive interaction with the substrate (S) [37] referenced in (**Figure 5**).

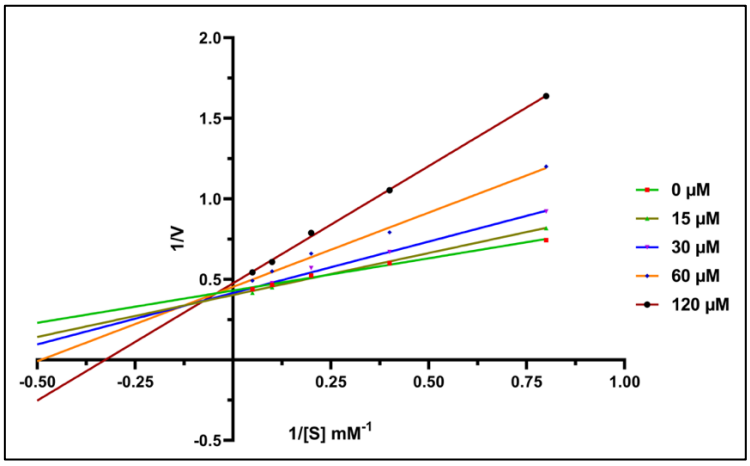

Figure 4: Kinetics of AG inhibition by compound **6f** and the Lineweaver-Burk plot in the absence and presence of different concentrations of compound **6f**.

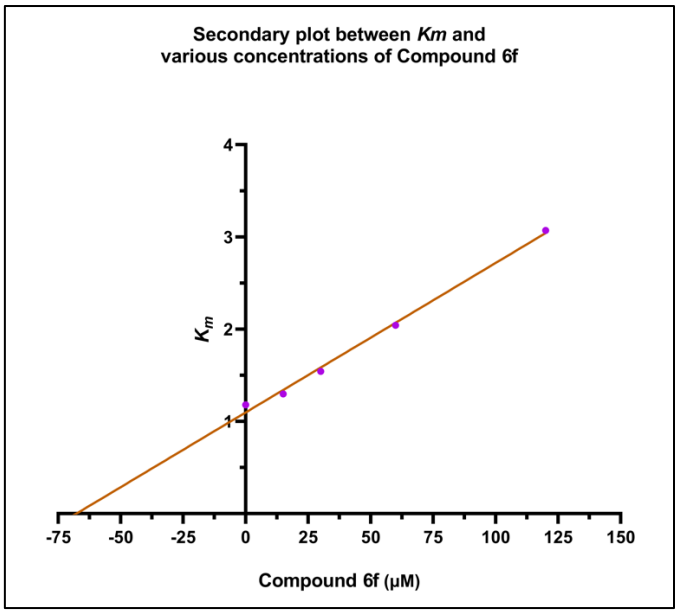

Figure 5: The secondary plot between *Km* and various concentrations of compound **6f**.

3.6. Fluorescence quenching:

Fluorescence quenching tests were performed to explore the effect of compound compound **6f** with enzyme, hence extending this finding. The fluorescence quenching method is generally utilized for the investigation of interactions between macromolecules and ligand chemicals. The administration of **6f**, at concentrations between 0 and 160 µM, led to a variable decrease in fluorescence intensity across various instances, suggesting that compound **6f** may have interacted with AG, hence quenching its intrinsic fluorescence (**Figure 6** and **Figure 7**). The

fluorescence value of the system was lower with increasing compound concentration, and the maximum emission wavelength displayed a little blue shift. The fluorescence quenching data were analyzed using the Stern-Volmer equation [38].

$$\frac{F0}{F} = 1 + Ksv[Q] = 1 + Kq\,\tau 0[Q]$$

In the specified equation, F0 and F represent the fluorescence activity of AG without and with **6f**, respectively. τ0 represents the average lifespan of biomolecules in the absence of a quencher (10^{-8} s), whereas [Q] signifies the concentration of quencher in compound **6f**. The Stern-Volmer graph demonstrates a strong linear connection, indicating that the enzyme's quenching action results from a singular quenching process. The values of Ksv (fluorescence quenching constant) and Kq (bimolecular quenching constant) were discovered to be 1.4 $\times 10^4$ L/mol and 1.44 $\times 10^{12}$ L·mol-1·S-1, respectively (**Figure 8**). It can be inferred that the quenching technique of compound **6f** on the intrinsic fluorescence of AG is static quenching resulting from complex formation.

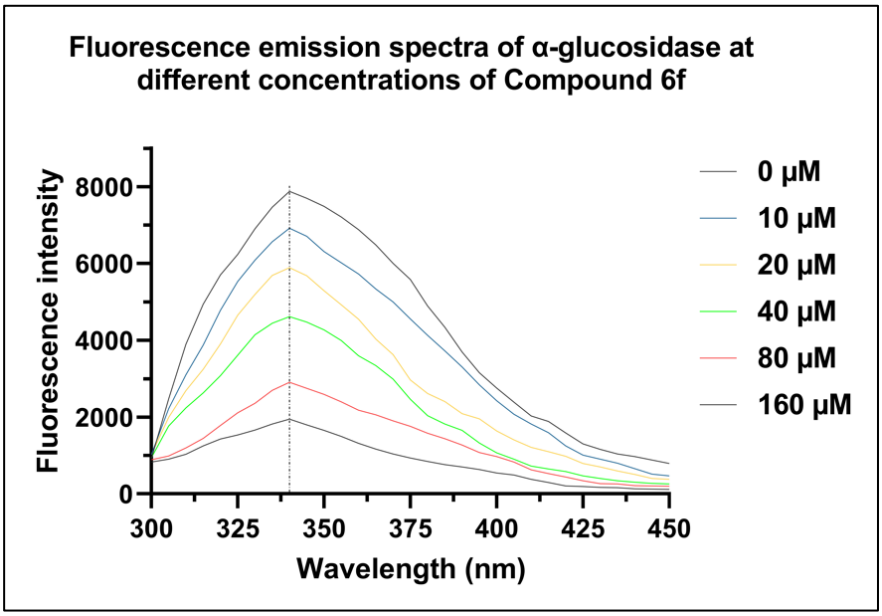

Figure 6: Fluorescence emission spectra at different concentrations of compound **6f**.

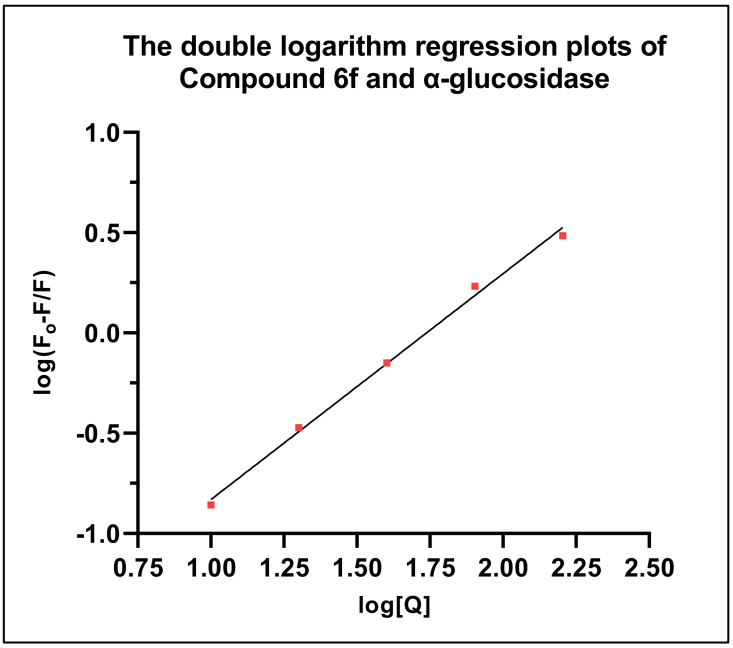

Figure 7: Double logarithm regression plots of compound **6f** and AG.

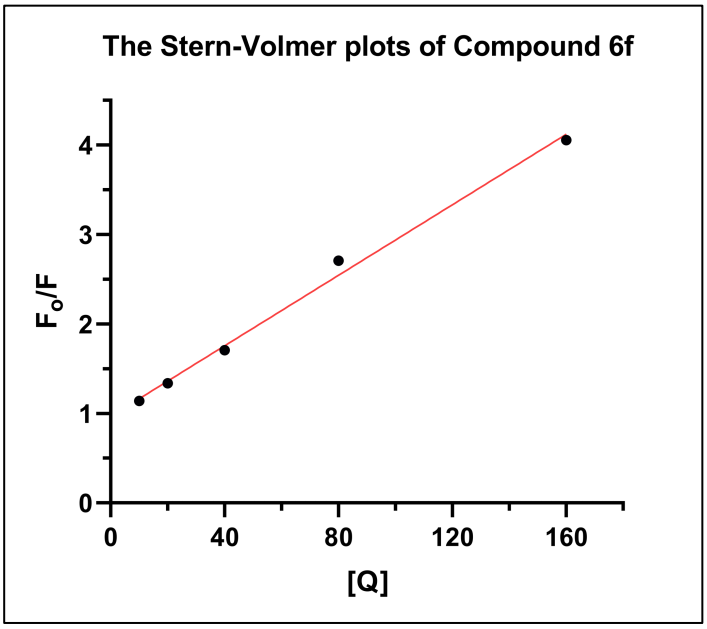

Figure 8: Stern-Volmer plots of compound **6f**.

3.7. Circular dichroism spectra:

CD was utilized to examine changes in the secondary structure of proteins. Two negative bands at approximately 210 and 220 nm were observed in the far-UV CD spectra of AG (**Figure 9**), with variations in peak size and shape, indicative of the α-helix conformation of AG. The calculated outcomes demonstrate that dissolved with compound **6f** (molar ratios: 2:1) led to an augmentation in α-helix content

(from 35.6% to 60.4%), concomitantly with reductions in β-sheet (from 14.6% to 7.02%), β-turn (from 12.8% to 8.8%), and random coil (from 44.2% to 26.4%). The outcome demonstrated that the structure of AG exhibited increased flexibility and instability; compound **6f** caused changes in the secondary structure of AG, altering its hydrophobicity, which hindered active site formation or obstructed substrate binding, consequently affecting enzymatic activity.

Table 3: Secondary structural analysis of compound **6f** with AG from CD.

µM	α-helix (%)	β-sheet (%)	β-turn (%)	Random coil (%)
0	35.6	14.6	12.8	44.2
10	38.3	13.1	10.9	40.1
15	41.4	12.3	10.2	36.3
30	47.8	7.68	10.2	28.8
60	60.4	7.02	8.8	26.4

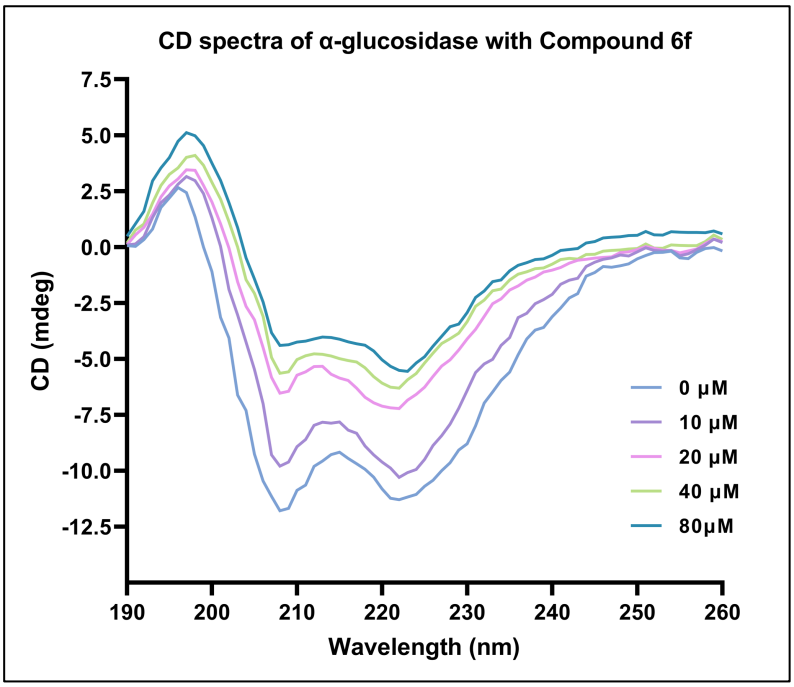

Figure 9: CD spectra of AG with compound **6f**.

3.8. Molecular docking:

AG primarily active in the small intestine, catalyzes the hydrolysis of complex carbohydrates into monosaccharides, which are subsequently absorbed into the

bloodstream, contributing to elevated blood glucose levels [39]. As a result, AG has become a key target for managing hyperglycemia by delaying carbohydrate breakdown. Notably, AG inhibitors modulate blood glucose levels without directly stimulating insulin secretion [5]. Docking analysis of compound **6f** with AG (PDB ID: 5NN8) obtained a binding energy of −7.50 kcal/mol, indicating favorable interaction of 6f with the macromolecule. Due to this significant binding affinity, compound 6f needs to be further investigated for its inhibitory mechanism and potential role in DM management through AG inhibition. (**Table 4)**.

The two- and three-dimensional interaction profiles of compound **6f** within the AG active site are shown in **Figure 10**. The strong binding potential of **6f** can be attributed to multiple interactions with key active site residues. Specifically, the TZD ring forms one π–π stacking interaction and three π–alkyl contacts with TRP376, LEU677, and LEU678 (**Figure 11)**. Additionally, the carbonyl (=O) group forms two conventional hydrogen bonds with LEU677 and LEU678. The two phenyl rings in the compound contribute to one π–π T-shaped interaction and one π–alkyl contact with LEU678 and TRP376. The 3D interaction model further highlights the involvement of both polar and non-polar interactions facilitated by the TZD moiety of compound **6f** with surrounding amino acid residues.

Table 4: Molecular docking scores of compound **6f**.

Compound	Docking Score against AG (PDB: 5NN8)	Conventional -H Bond	Hydrophobic interactions	Active site pocket residues
6f	-7.50	LEU A:678 LEU A:677 ARG A:411(2)	TRP A:376 LEU A:678(2)	LEU A:678 LEU A:677 ARG A:411 TRP A:376 LEU A:678 LEU A:650 GLY A:651 ASNA:652, SER A:679,

				SER A:676, TRP A:481

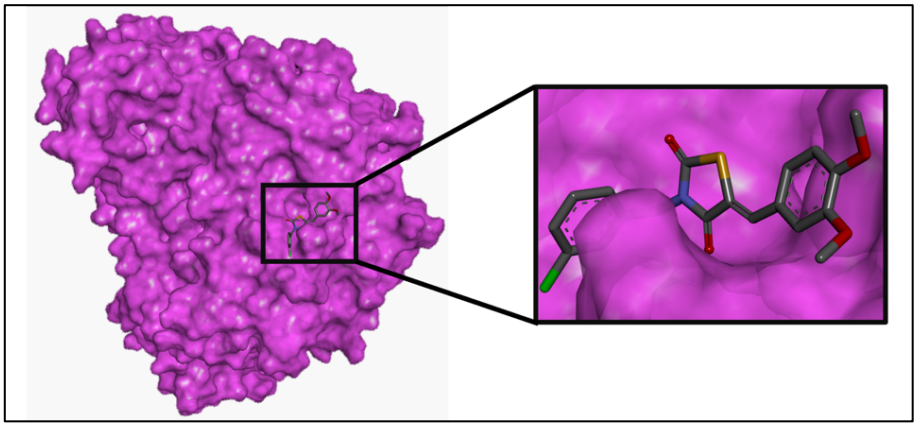

Figure 10: 3D representation of all the Aligned TZD derivatives at the active site of AG (PDB: 5NN8).

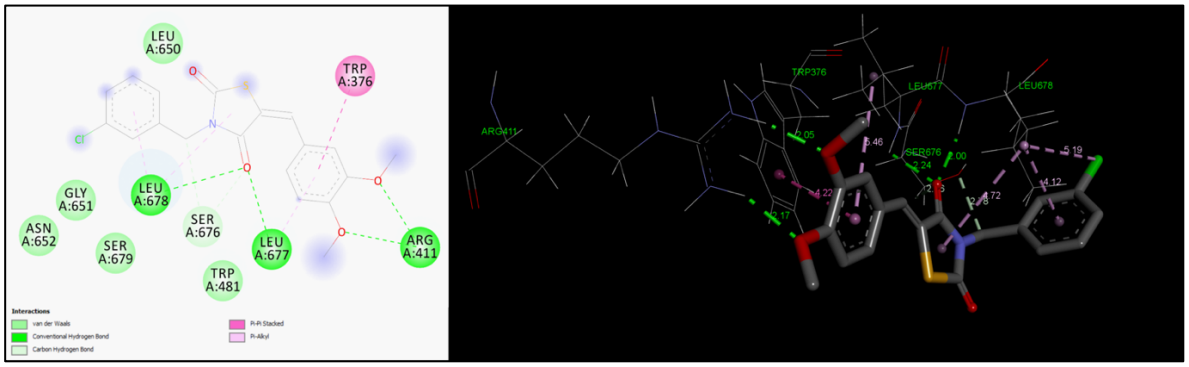

Figure 11: 2D and 3D docking representation of VD–TZD derivatives **6f**.

3.9. In vitro cytotoxicity:

The MTT assay is a widely utilized technique for evaluating the effects of chemical compounds on cell viability, playing a critical role in determining both therapeutic potential and cytotoxic risk, thereby supporting their suitability for clinical applications. HEK-293 cells, a well-established human cell line, serve as a representative model for evaluating the cytotoxic effects of various agents [40]. In this study, HEK-293 cells were treated with increasing concentrations of compound **6f**, ranging from 3.9 to 250 µM (**Figure 12**). The results revealed that compound **6f** exhibited cytotoxic activity with an IC_{50} value of 449.64 µM.

The *in vitro* cytotoxicity assay indicated that compound 6f exhibited no toxicity at lower concentrations. A dose-dependent decline in cell viability was observed. Specifically, treatment with 250 µM of compound **6f** resulted in 72.82 ± 5.12% cell viability, whereas treatment with 3.9 µM showed a viability of 98.76 ± 0.95%, relative to the untreated control. These findings suggest that compound 6f is relatively safe for normal cells at lower concentrations, supporting its potential for further investigation in therapeutic applications.

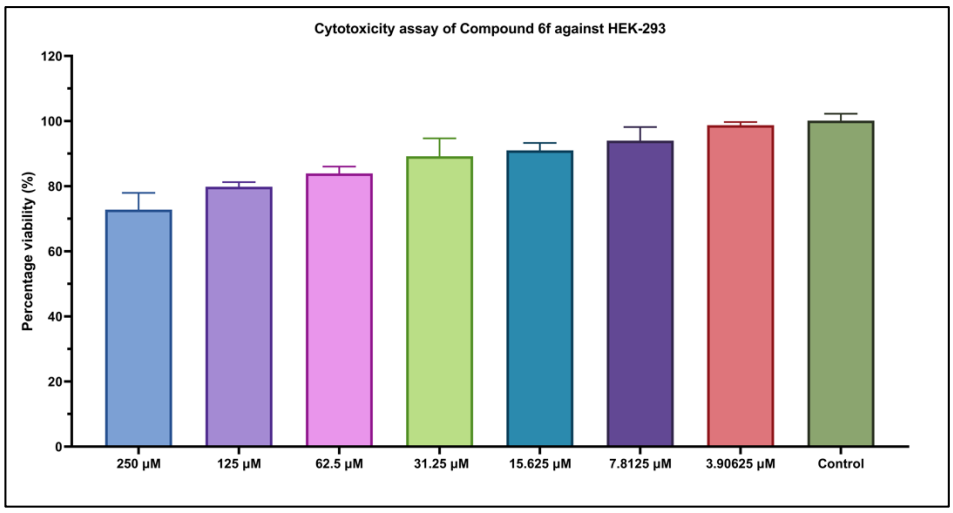

Figure 12: Cell viability assay of compound **6f** against HEK293.

3.10. ADME, drug-likeness and toxicity assessment:

An essential part of developing new drugs is studying their ADMET (absorption, distribution, metabolism, excretion, and toxicity) profiles. Any compound's pharmacokinetic (pK) and pharmacodynamic (pD) profiles give promise for the creation of medications that can detect a range of illnesses. The Lipinski and Veber criteria are more likely to be met by substances that are bioavailable orally and have drug-like characteristics. Because molecules resemble drugs, they may be just as effective as or perhaps more so than medications that are currently on the market [34].

Compounds **6f** and **6g** do not violate any of the drug-likeness requirements, according to the ADME prediction. The two compounds reach a bioavailability score of 0.55, which indicates acceptable drug similarity, meeting the standards established by Lipinski, Veber, and Ghose. On the other hand, compound **6g** appeared to have one breach of Muegge's rule (MLOGP>4.15). Neither compound **6f** nor **6g** has a hydrogen bond donor; instead, they have five rotatable bonds as well as four hydrogen bond acceptors. Their TPSA values of 81.14 Å² are lower than the permitted limit of 140 Å², meaning they have good oral bioavailability and may be absorbed very well by the gastrointestinal tract. Compounds **6f** and **6g** are seen inside the pink region of the radar map (**Figure 13**), confirming their intended pharmacological similarity and allowable bioavailability (**Table 5**).

Further, the Boiled-Egg concept was used to investigate pharmacokinetics. Compounds **6f** and **6g** were located outside the yellow zone (**Figure 13**), suggesting that they had improved gastrointestinal absorption and had little to no probability of crossing the blood-brain barrier (BBB). Also, studies revealed that the two drugs may inhibit CYP1A2, CYP2C19, CYP3A4, and CYP2C9 but not CYP2D6 and that their negative log Kp values suggest decreased skin penetration (**Table 6**).

The computational toxicological evaluation conducted via the Deep-PK web server indicates that compounds **6f** and **6g** are non-AMES, devoid of carcinogenic properties, demonstrate moderate toxicity against the liver and skin, and are compostable without risk. The conventional criterion for low doses is less than or equal to 0.477 logs (mg/kg/day), whereas elevated doses are defined as more than 0.477 logs (mg/kg/day). Compounds **6f** and **6g**

possess higher maximum tolerated amounts of 1.35 and 1.32 logs (mg/kg/day), accordingly. Moreover, although LD_{50} values below 0.5 mM (Log LD_{50} < 0.3) are considered to have significant acute toxicity, Compounds **6f** and **6g** show LD_{50} values of 2.13 mM and 2.31 mM, in that order, indicating low or tolerable acute toxicity (**Table 7**).

The toxicology forecasts of the highest-activity analogues and the previously discussed *in silico* ADME metrics could contribute to advancing novel drugs with enhanced oral bioavailability, thereby providing them with the ability to be accepted as lead-like candidates for the development of safe and effective medications in the future.

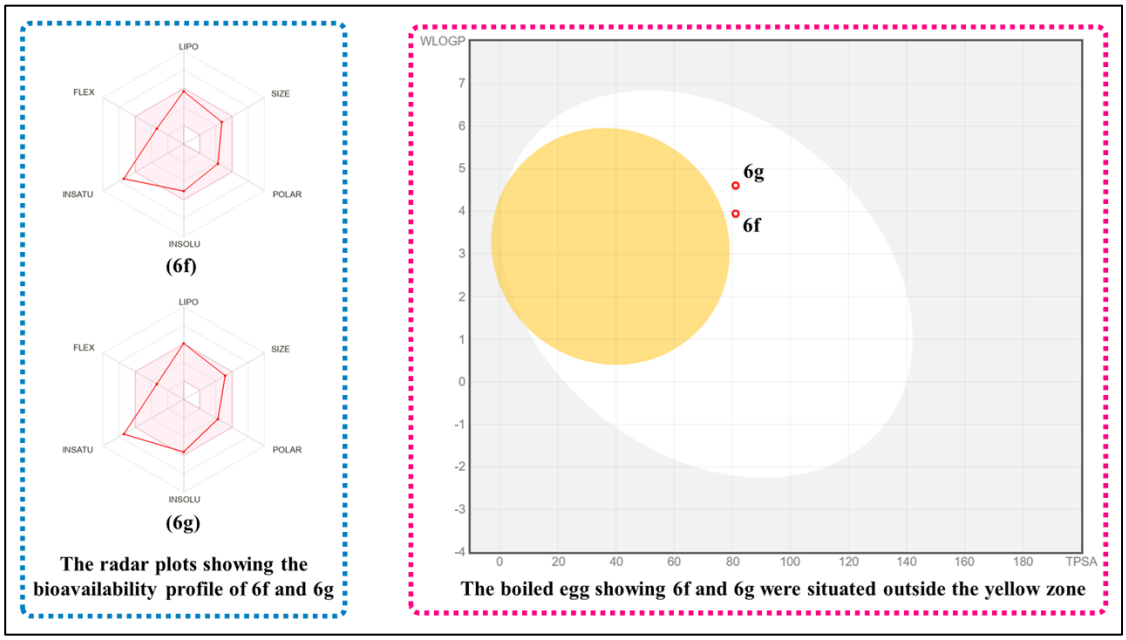

Figure 13: Radar plot and Boiled-Egg model of compounds **6f** and **6g.**

Table 5: ADME prognosis using SwissADME, Physiochemical and Drug-likeness properties. ((MW=Molecular Weight, TPSA=total polar surface area, Consensus Log P =average of all predicted Log Po/w).

Compound Name	MW (g/mol)	Rotatable bonds	H-bond acceptors	H-bond donors	TPSA	Consensus Log P	Lipinski violations	Ghose violations	Veber violations	Egan violations	Muegge violations	Bioavailability Score	Synthetic Accessibility
6f	389.85	5	4	0	81.14	3.78	0	0	0	0	0	0.55	3.46
6g	424.3	5	4	0	81.14	4.29	0	0	0	0	1	0.55	3.48

Table 6: Pharmacokinetics prediction of synthesized compounds (**6f** and **6g**) from the SwissADME server.

Compound Name	GI absorption	BBB permeant	Pgp substrate	CYP1A2 inhibitor	CYP2C19 inhibitor	CYP2C9 inhibitor	CYP2D6 inhibitor	CYP3A4 inhibitor	log Kp (cm/s)
6f	High	No	No	Yes	Yes	Yes	No	Yes	-5.53
6g	High	No	No	Yes	Yes	Yes	No	Yes	-5.29

Table 7: Toxicology predictions. Information was retrieved via the Deep-PK database.

Compound Name	AMES Mutagenesis	Maximum Tolerated Dose	Biodegradation	Carcinogenesis	Liver Injury I	Liver Injury II	hERG Blockers	NR-PPAR-gamma	T. Pyriformis	Rat (Acute)	Rat (Chronic)	Fathead Minnow	Skin Sensitisation
6f	Safe	1.35	Safe	Safe	Toxic	Toxic	Safe	Safe	-0.59	2.13	1.84	5.02	Toxic
6g	Safe	1.32	Safe	Safe	Safe	Toxic	Toxic	Safe	-2.45	2.31	1.78	5.21	Toxic

4. Spectral data:

I. ^{1}H and ^{13}C NMR data (Compound **5** and **6a-6m**):

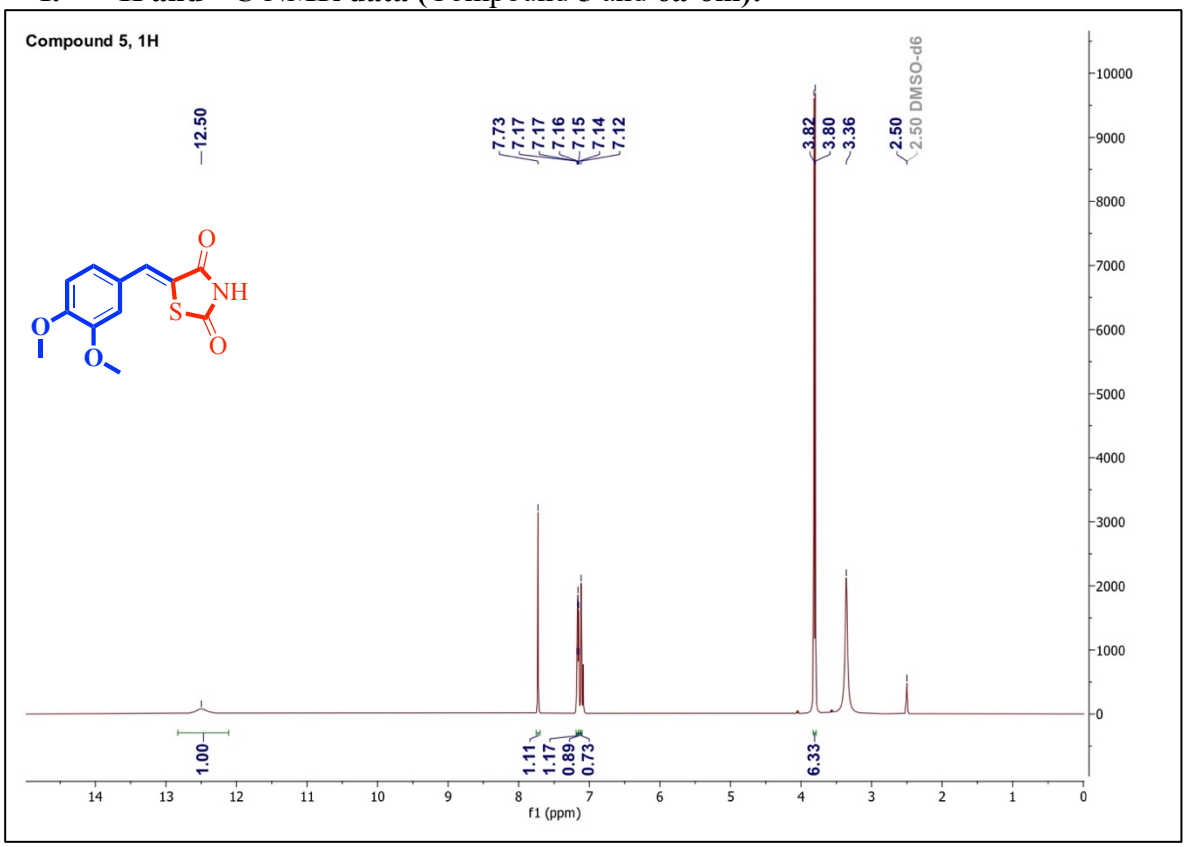

S.F1′: ^{1}H NMR of compound **5**

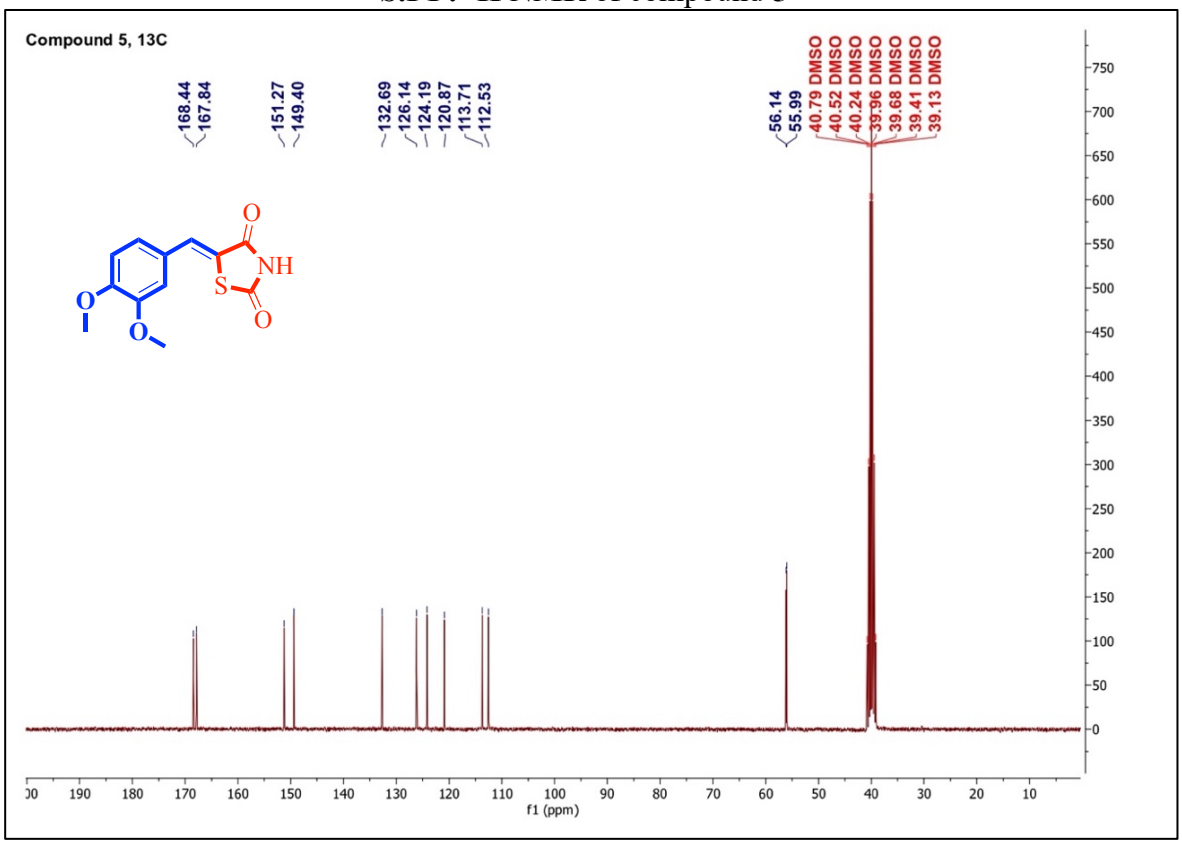

S.F1″: ^{13}C NMR of compound **5**

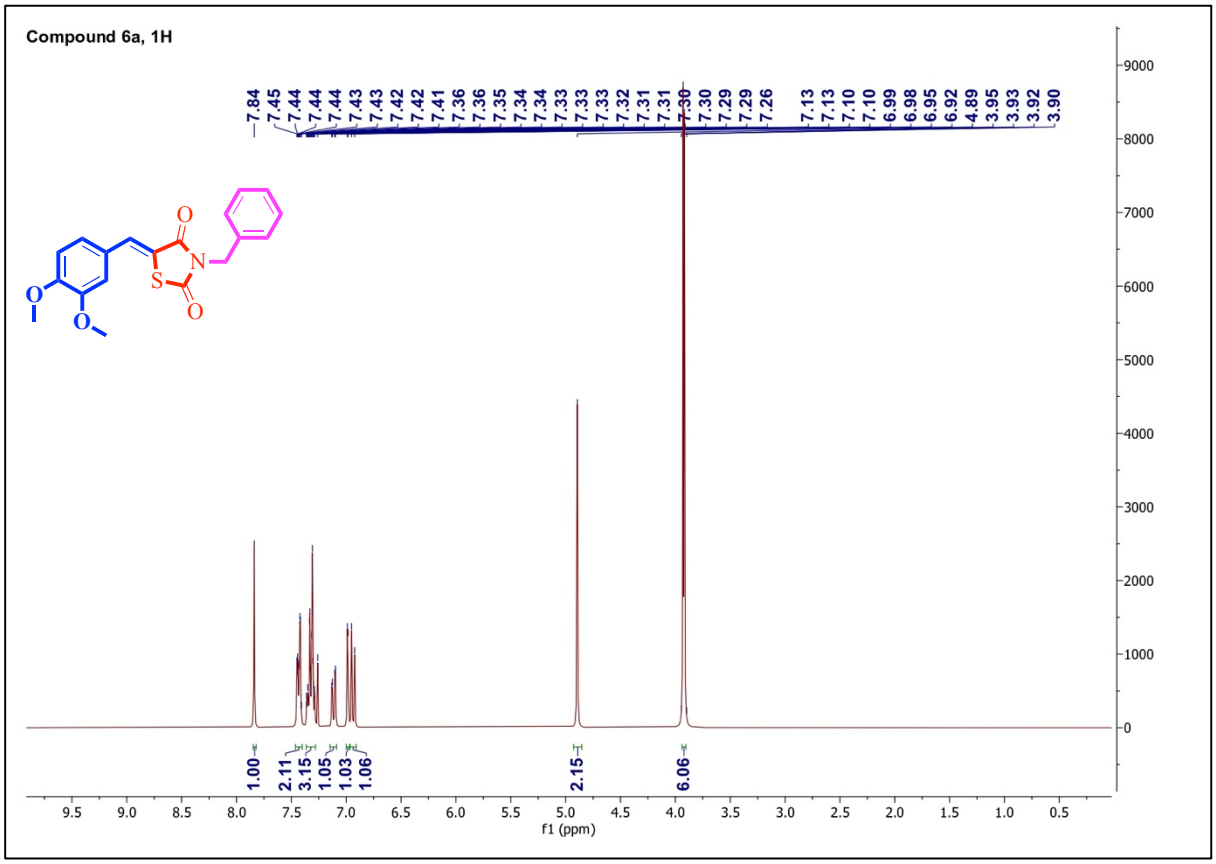

S.F2′: ^{1}H NMR of compound **6a**

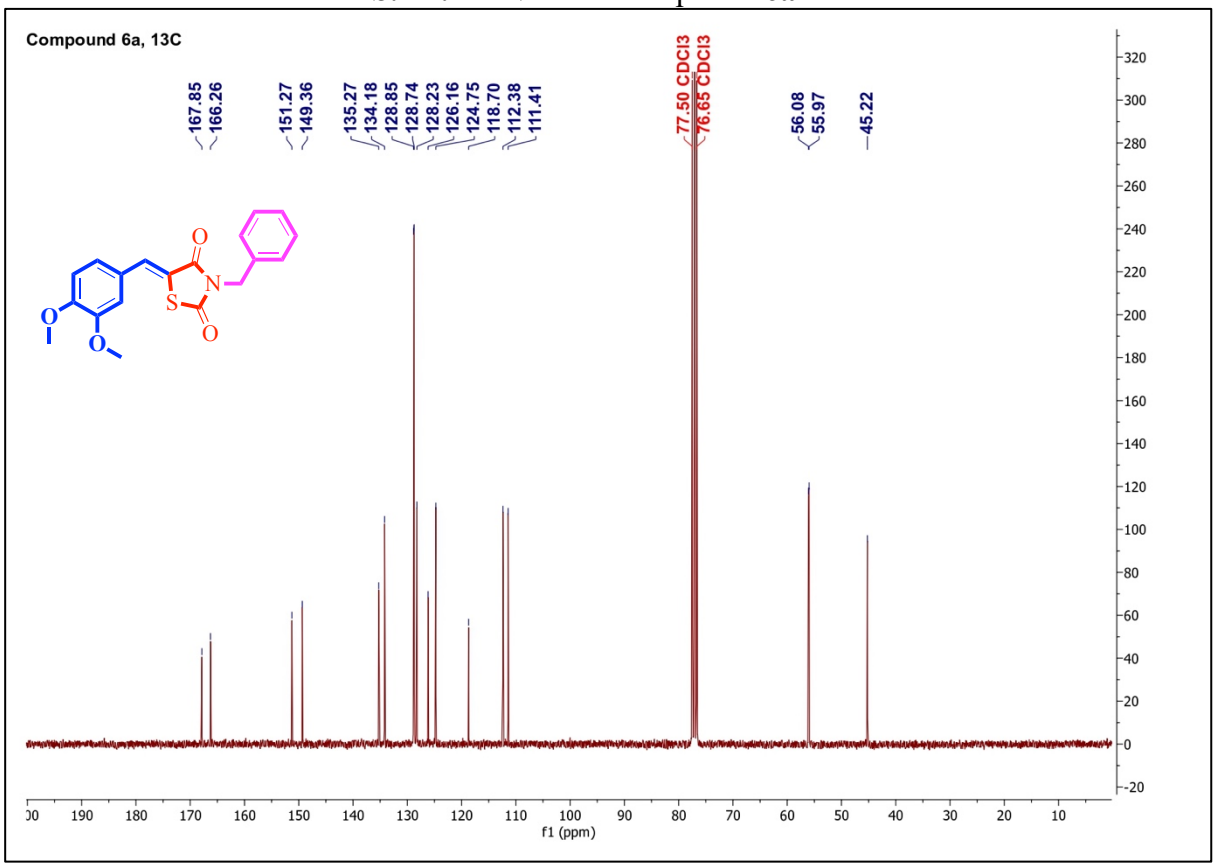

S.F2″: ^{13}C NMR of compound **6a**

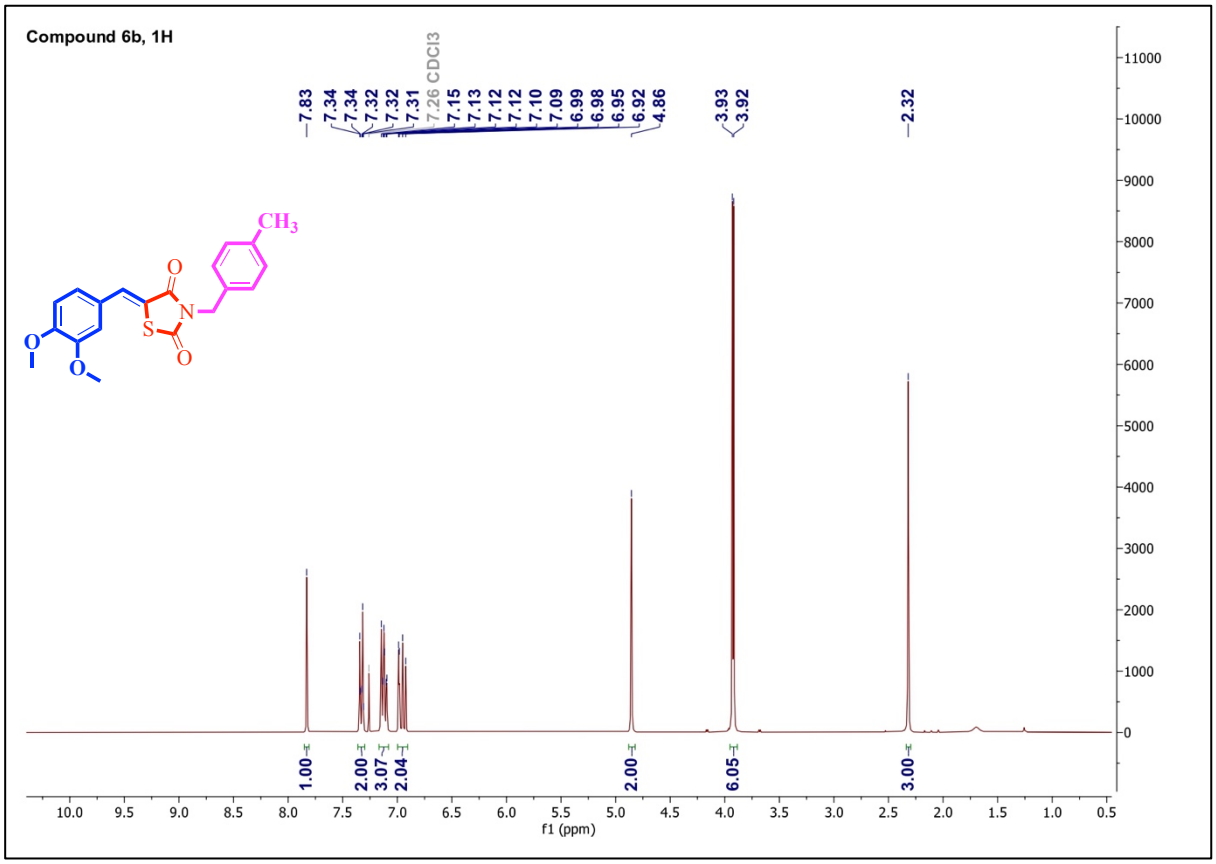

S.F3′: ^{1}H NMR of compound **6b**

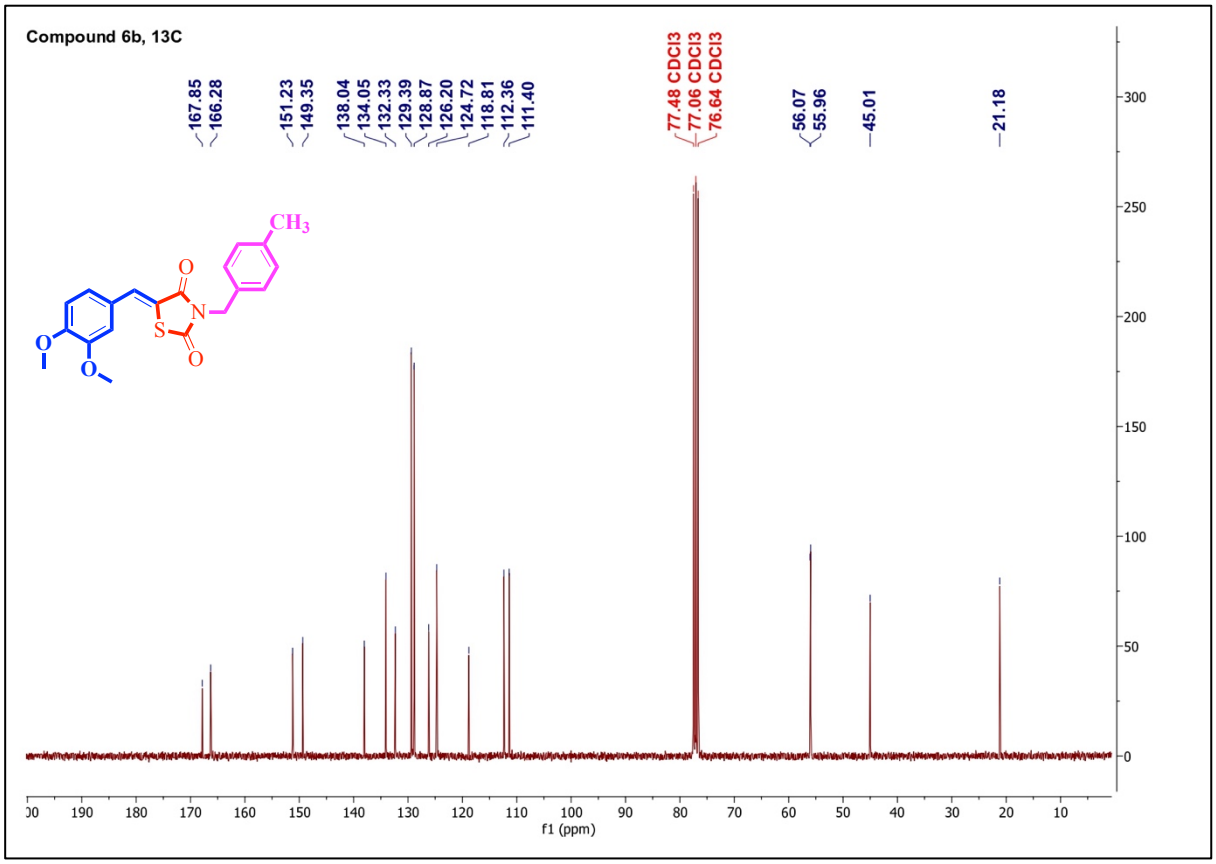

S.F3″: ^{13}C NMR of compound **6b**

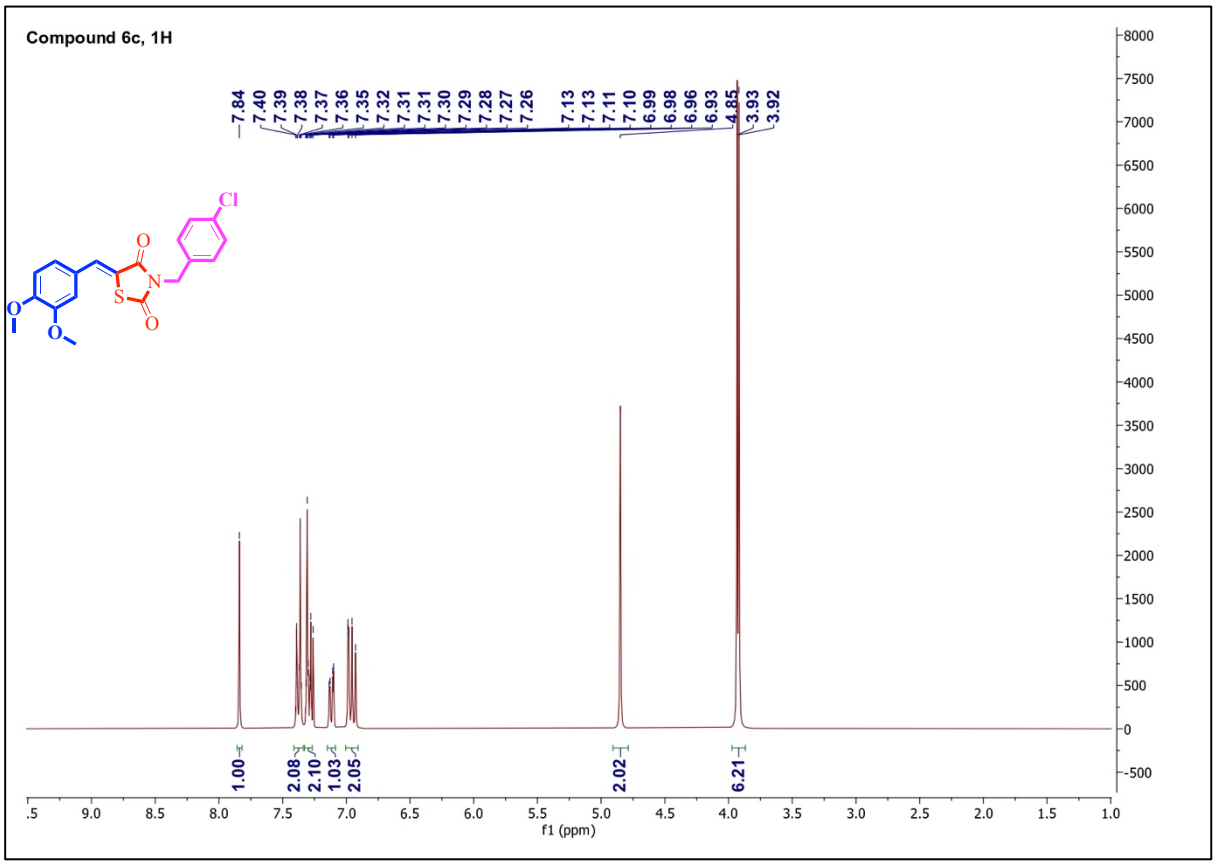

S.F4′: ^{1}H NMR of compound **6c**

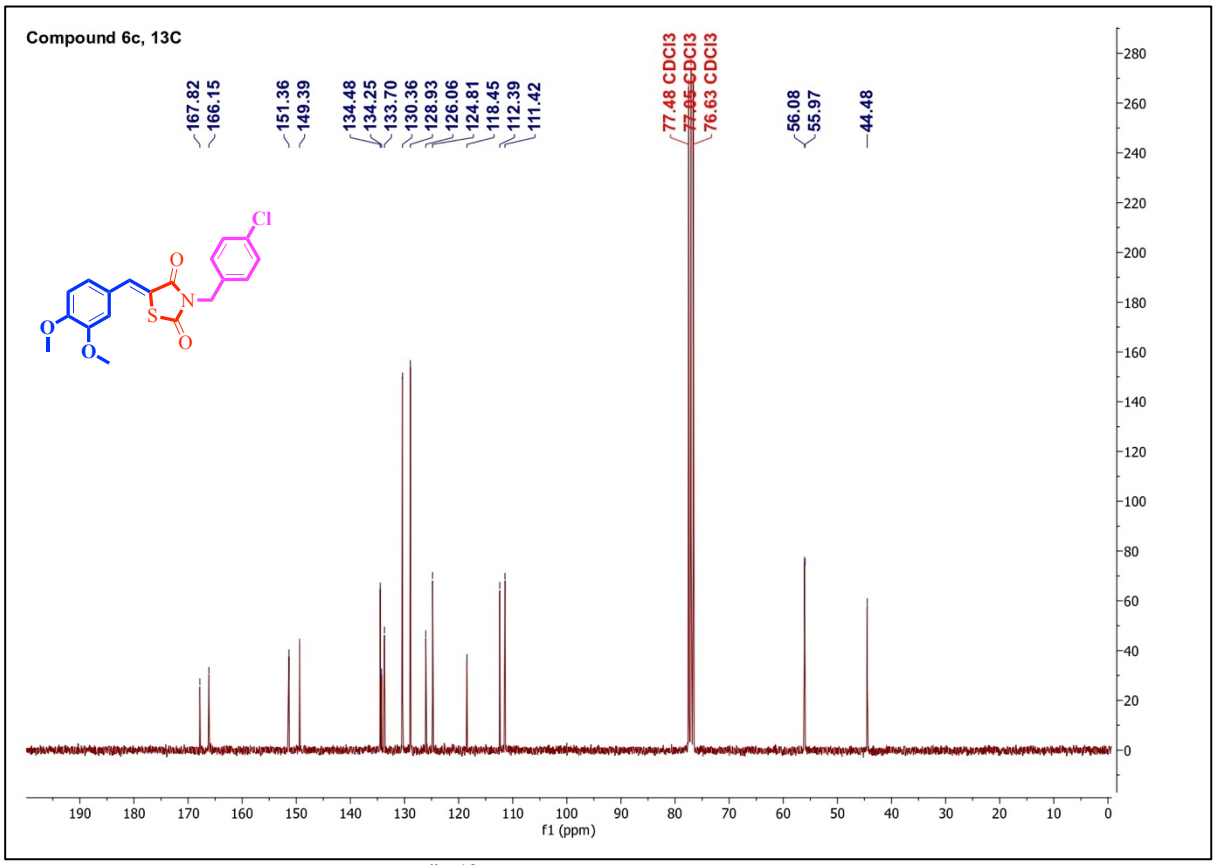

S.F4″: ^{13}C NMR of compound **6c**

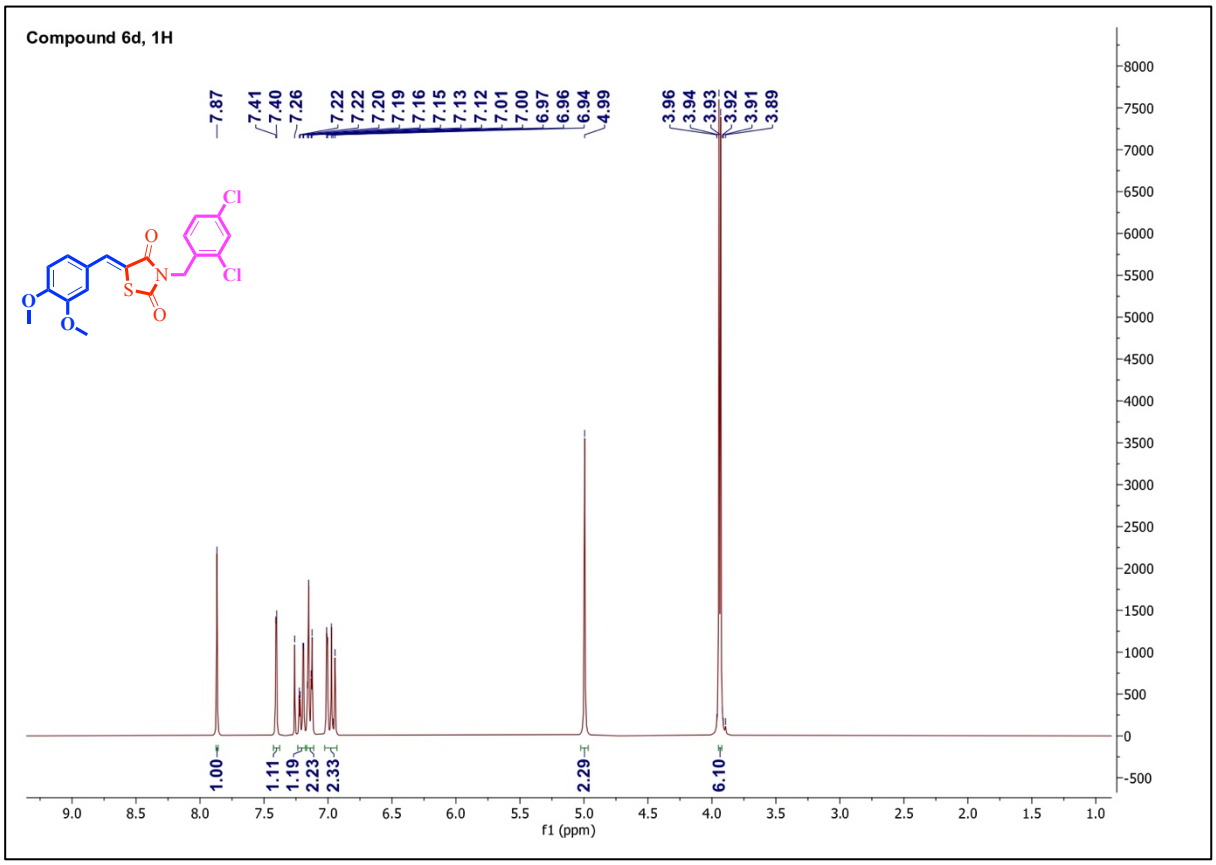

S.F5′: ^{1}H NMR of compound **6d**

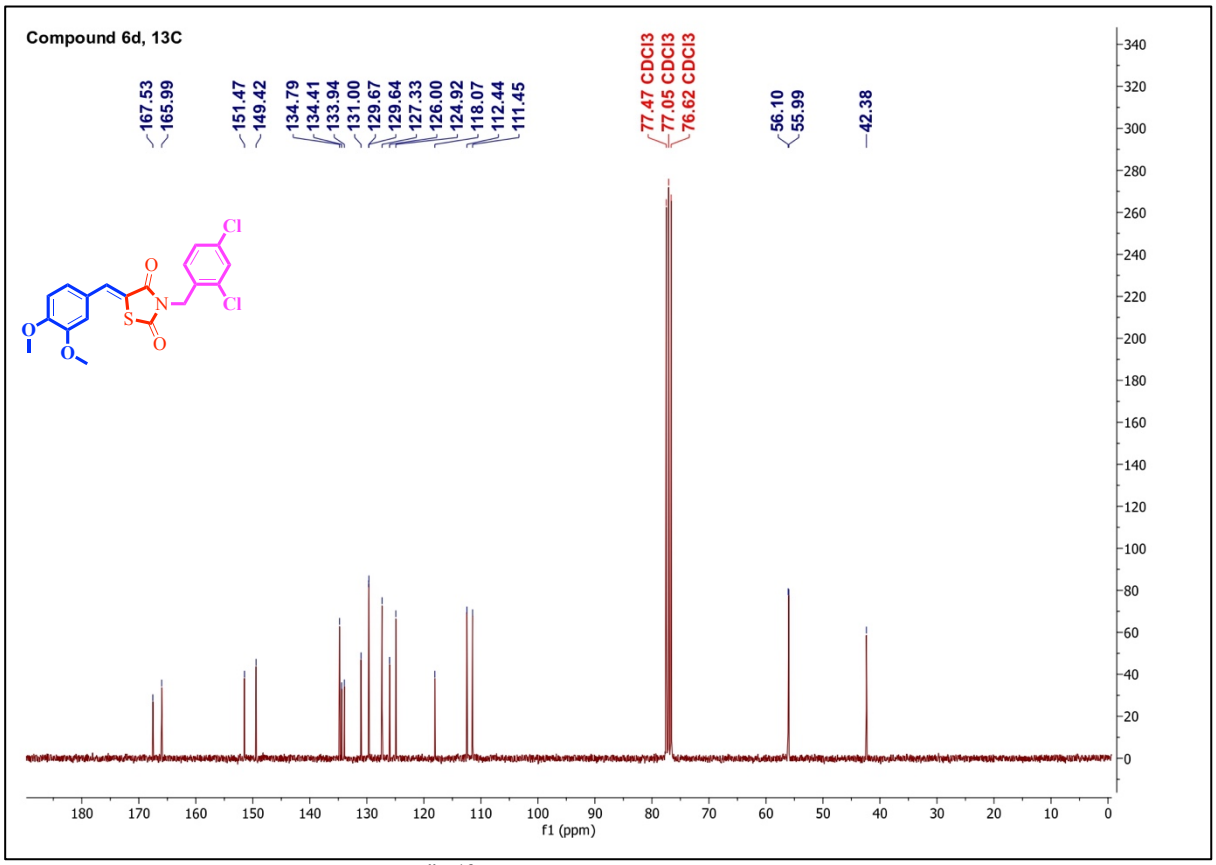

S.F5″: ^{13}C NMR of compound **6d**

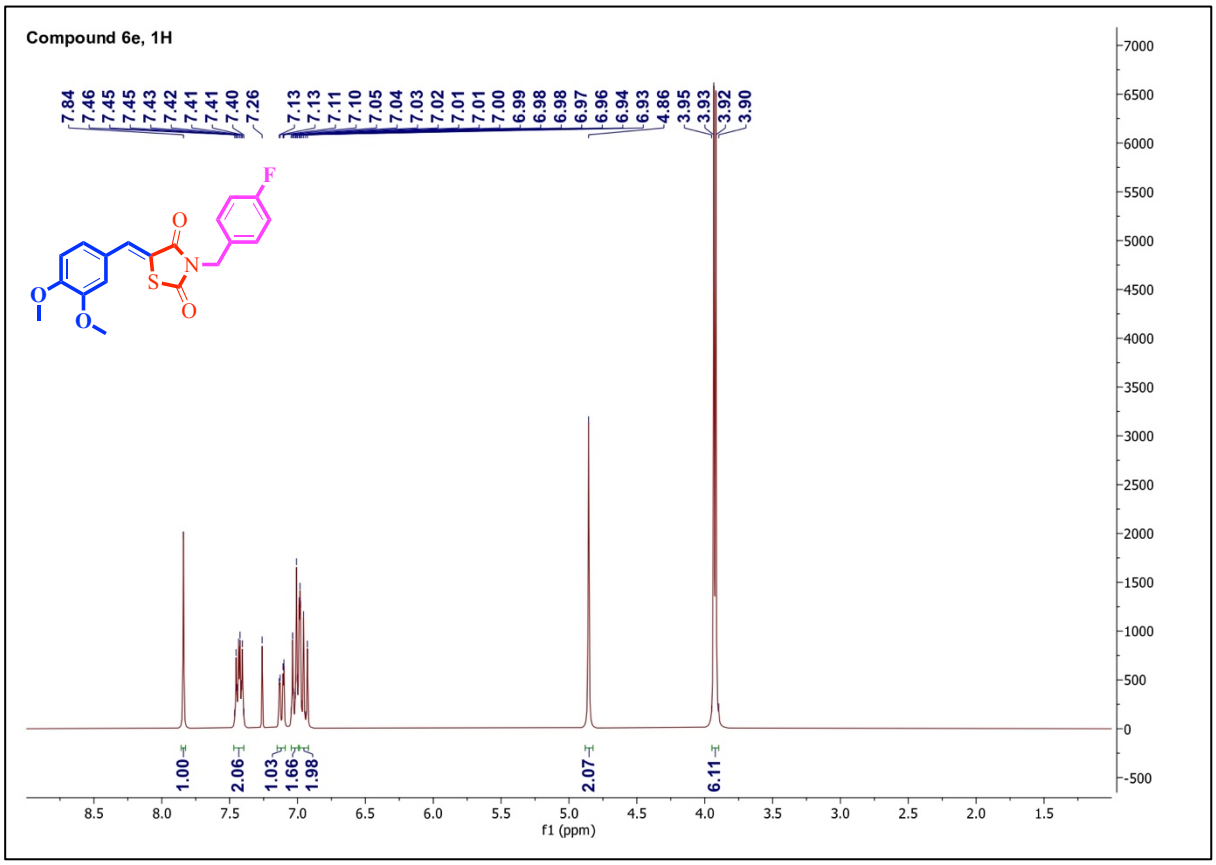

S.F6′: ^{1}H NMR of compound **6e**

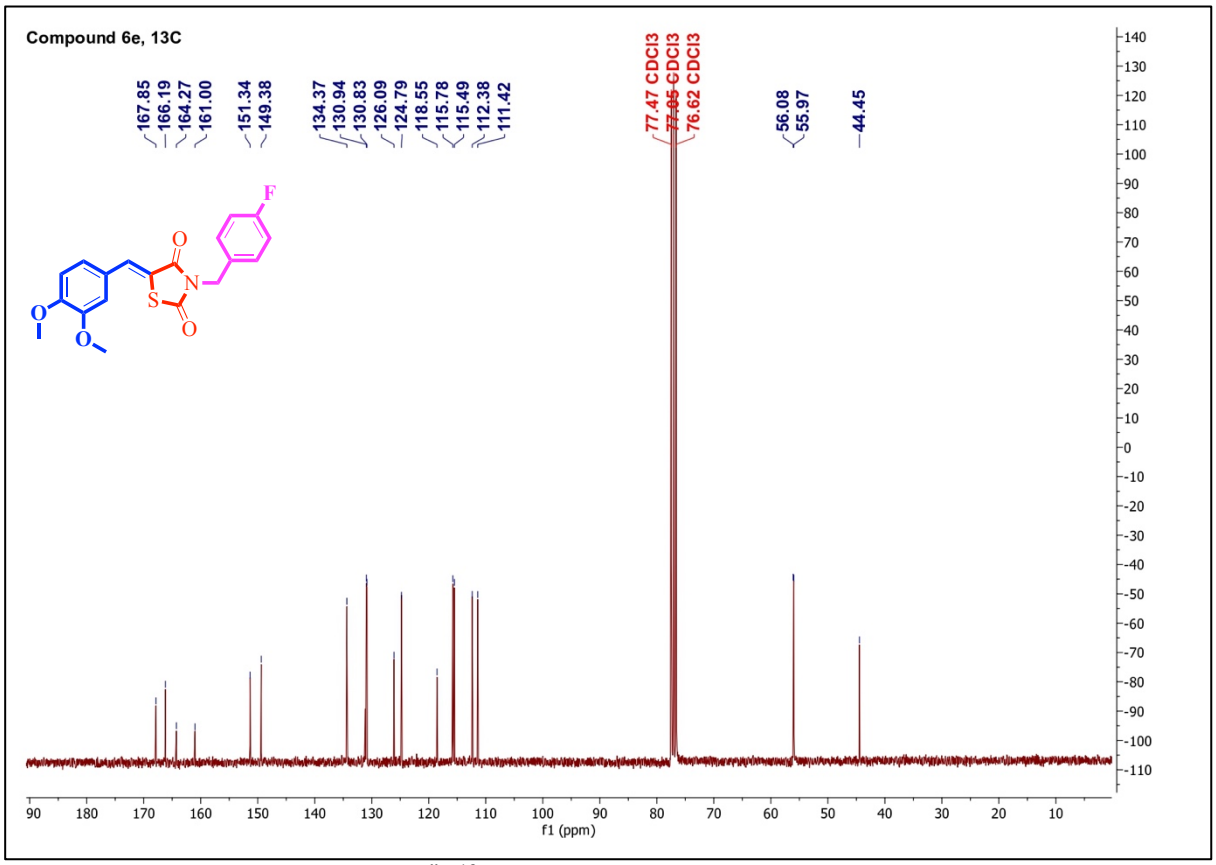

S.F6″: ^{13}C NMR of compound **6e**

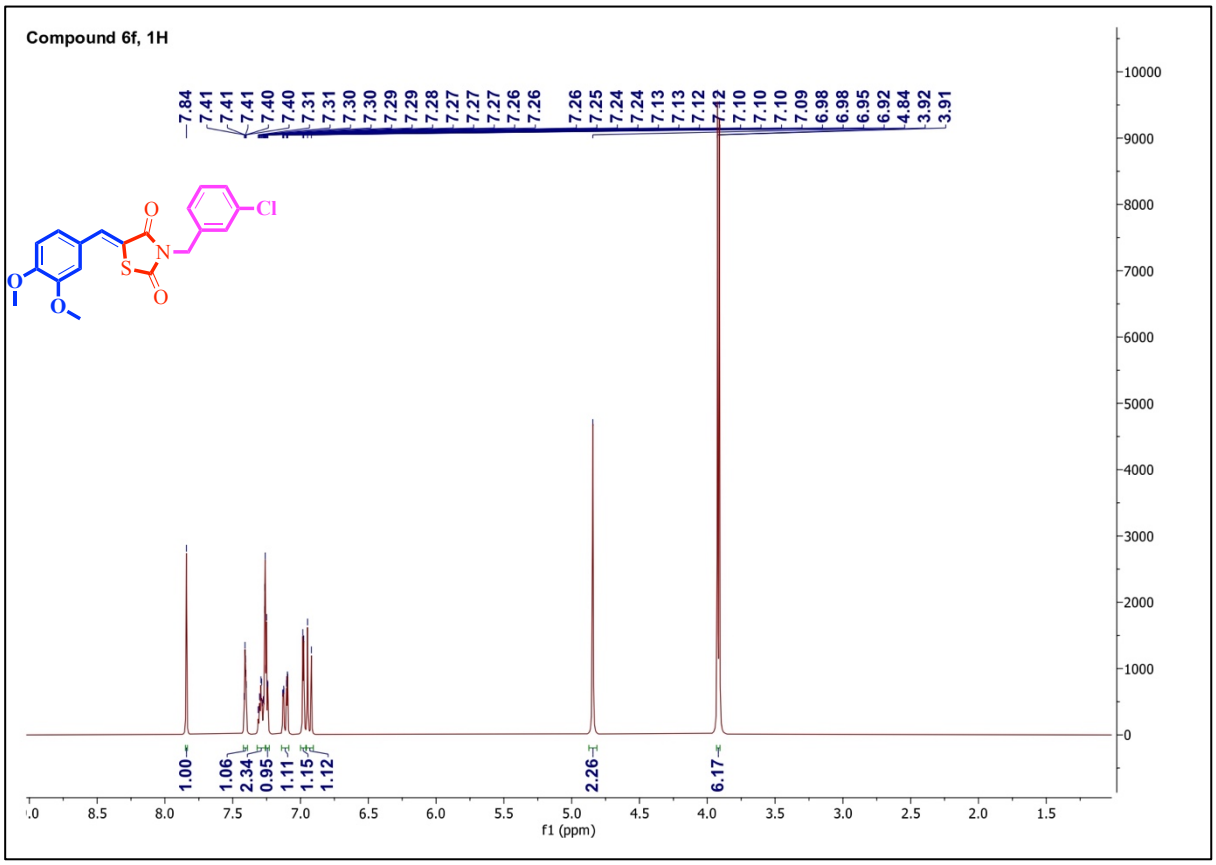

S.F7′: ^{1}H NMR of compound **6f**

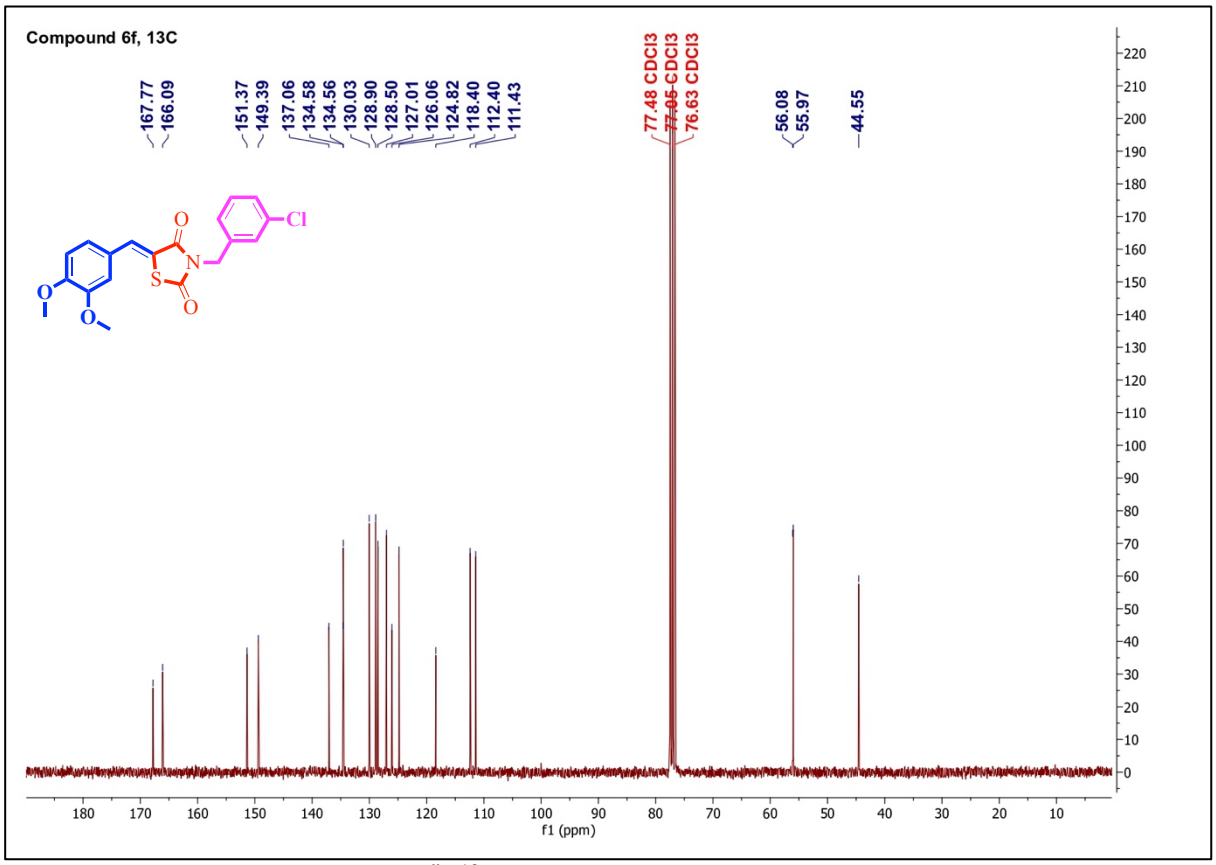

S.F7″: ^{13}C NMR of compound **6f**

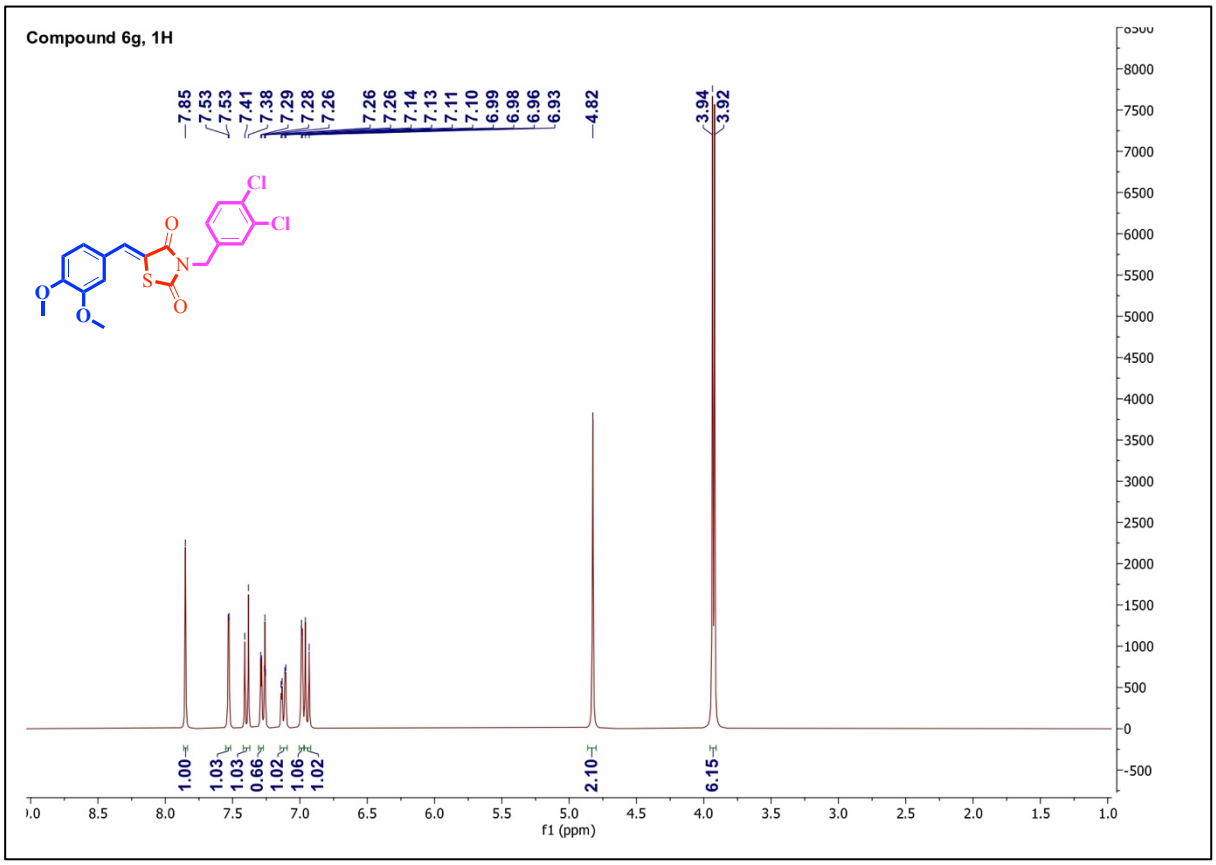

S.F8′: ^{1}H NMR of compound **6g**

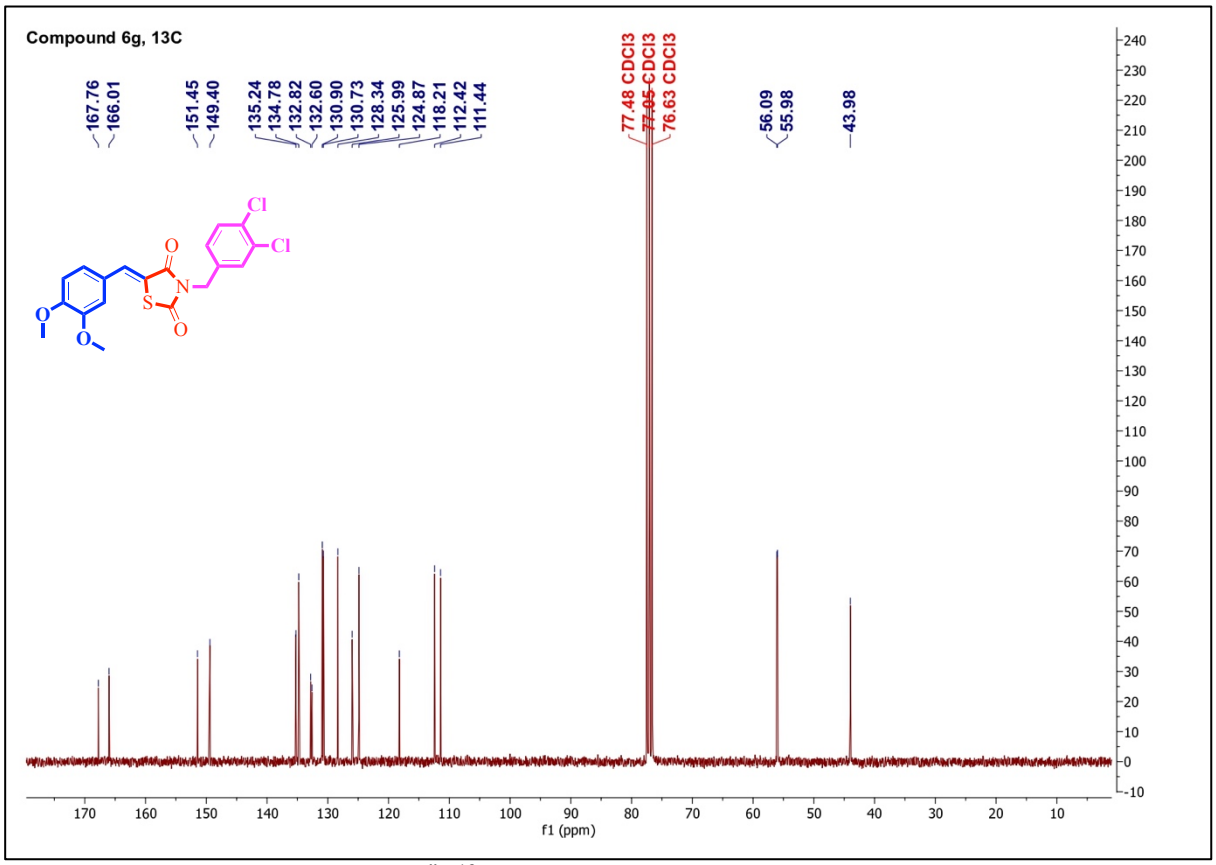

S.F8″: ^{13}C NMR of compound **6g**

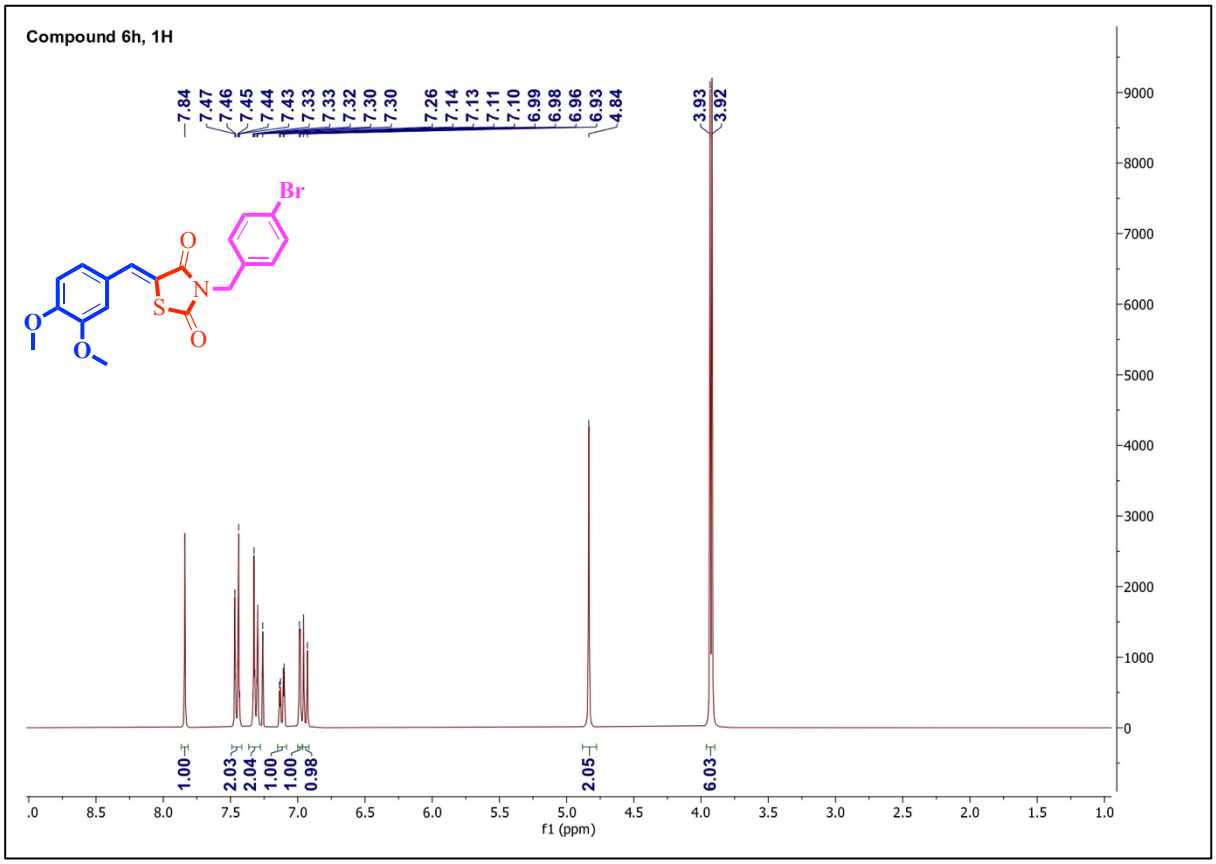

S.F9′: ^{1}H NMR of compound **6h**

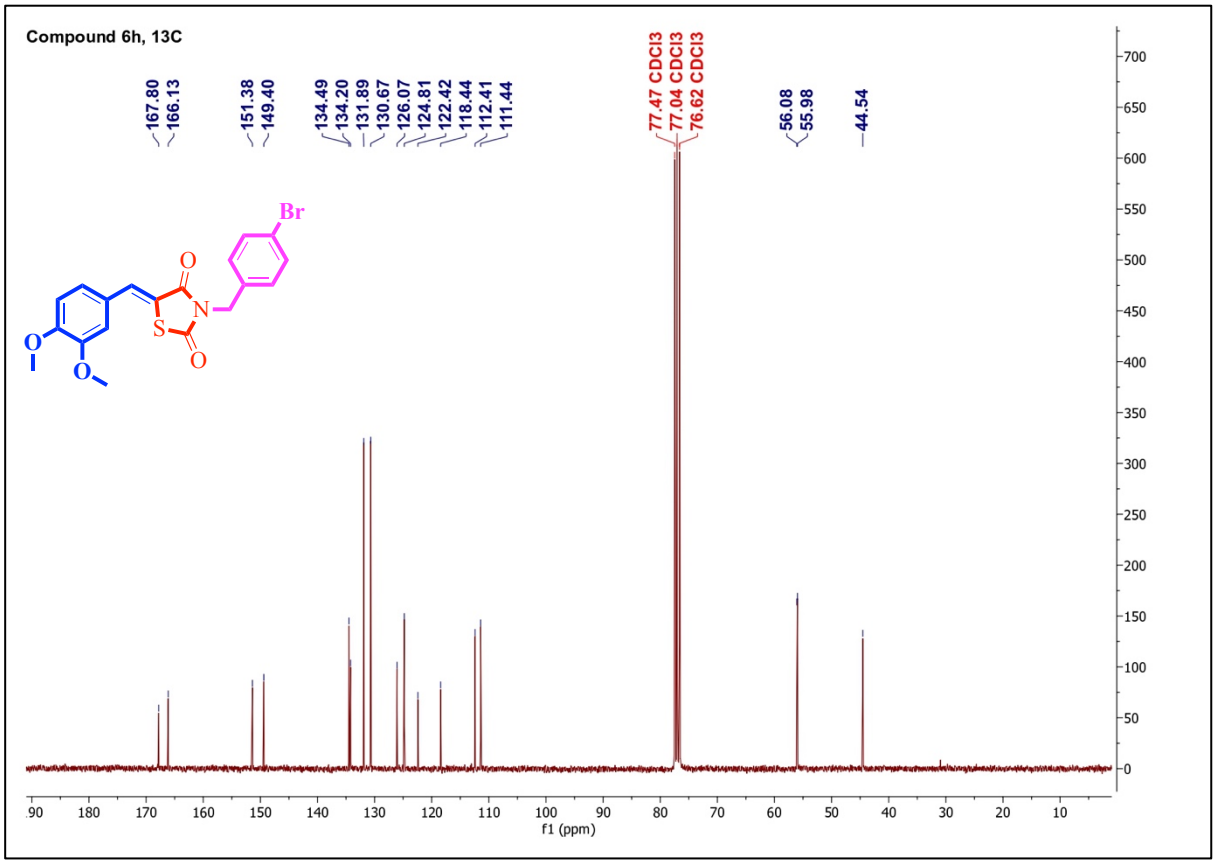

S.F9″: ^{13}C NMR of compound **6h**

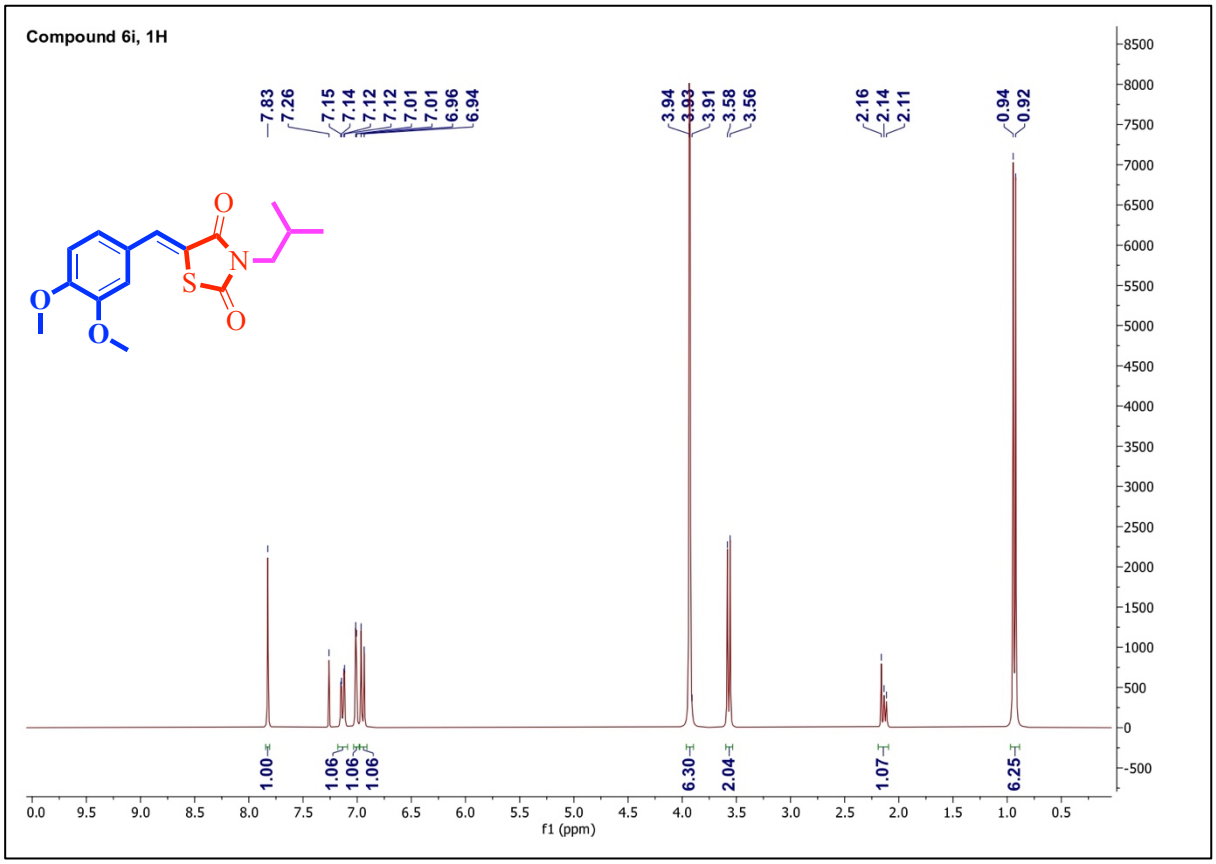

S.F10′: ^{1}H NMR of compound **6i**

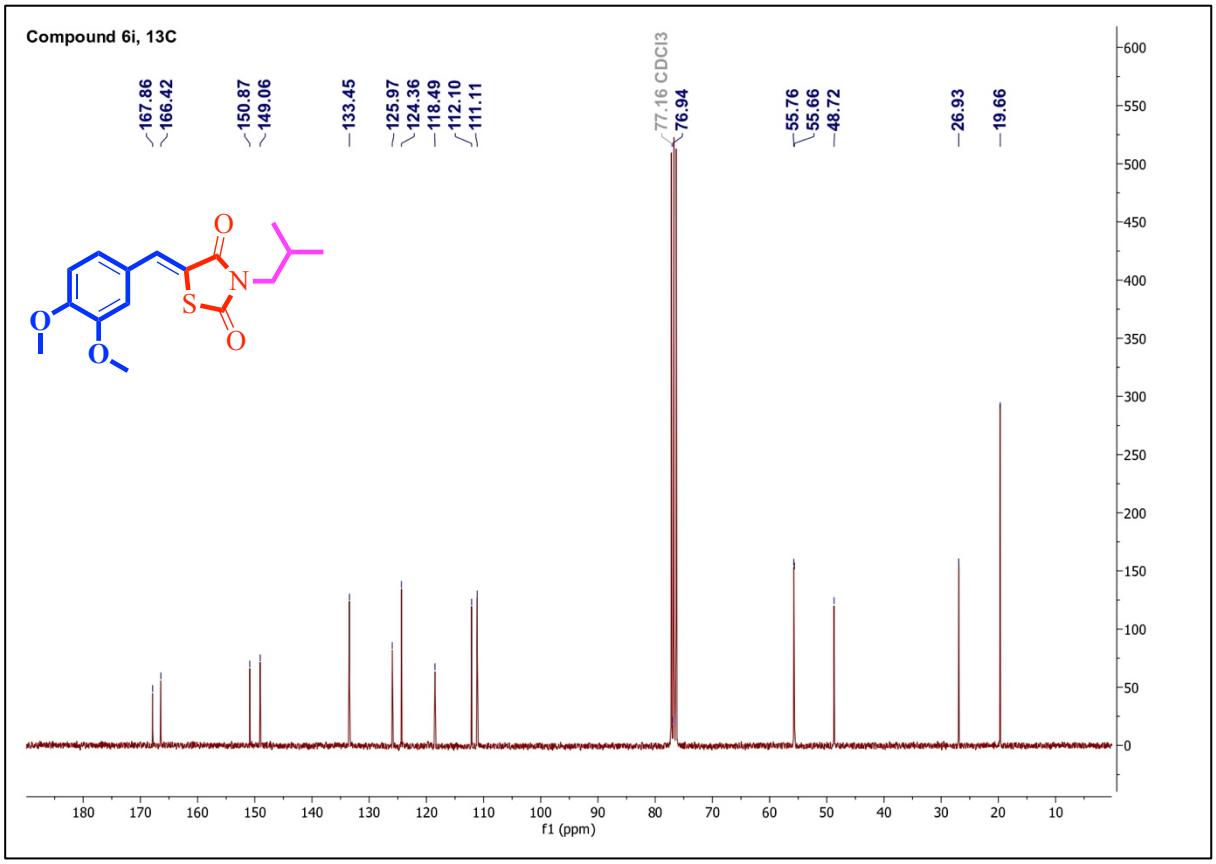

S.F10″: ^{13}C NMR of compound **6i**

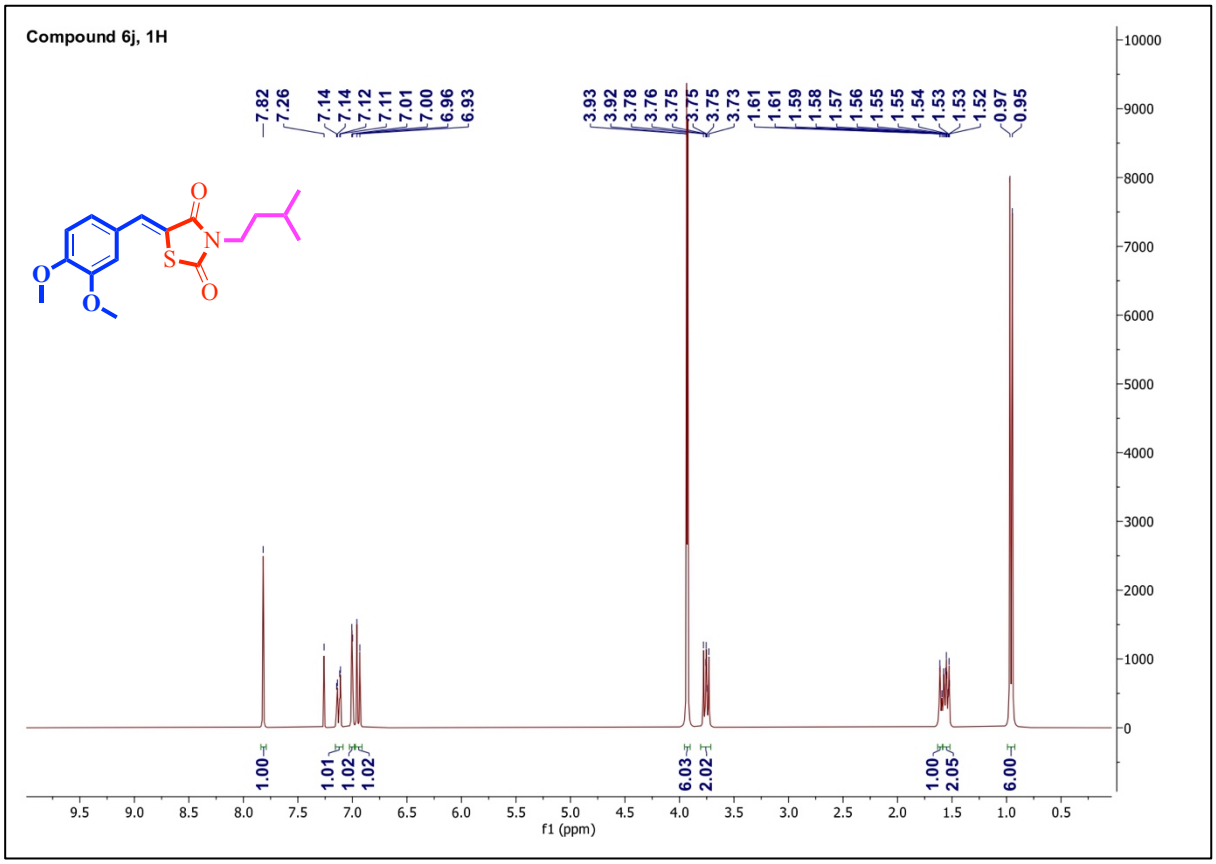

S.F11′: ^{1}H NMR of compound **6j**

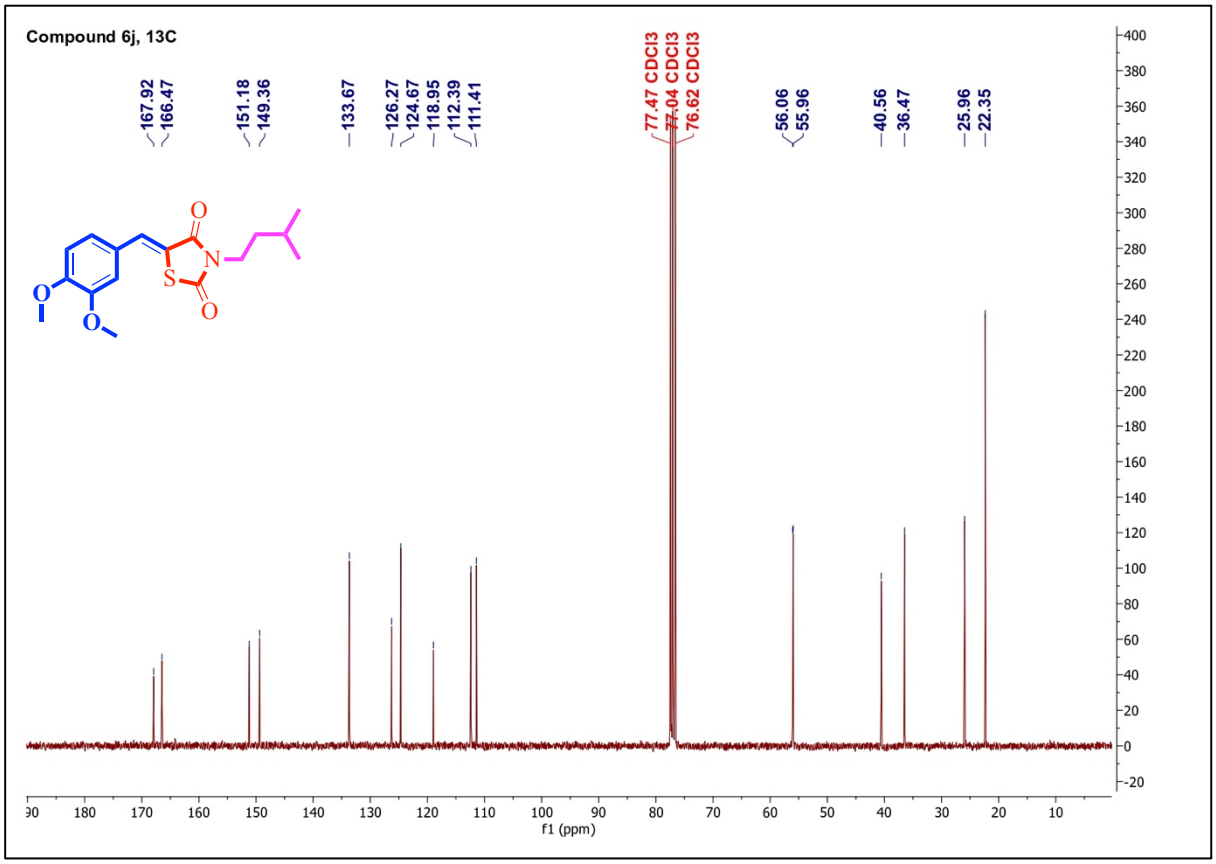

S.F11″: ^{13}C NMR of compound **6j**

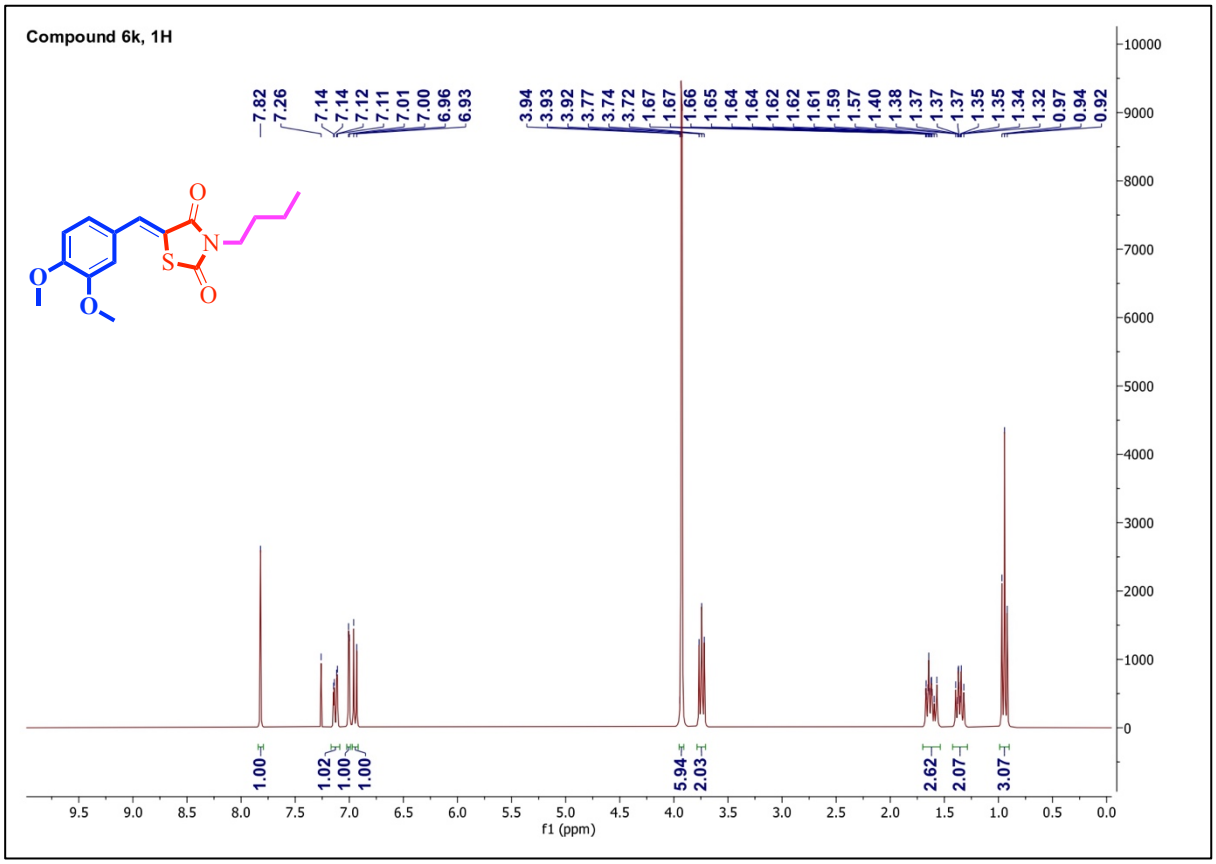

S.F12′: ^{1}H NMR of compound **6k**

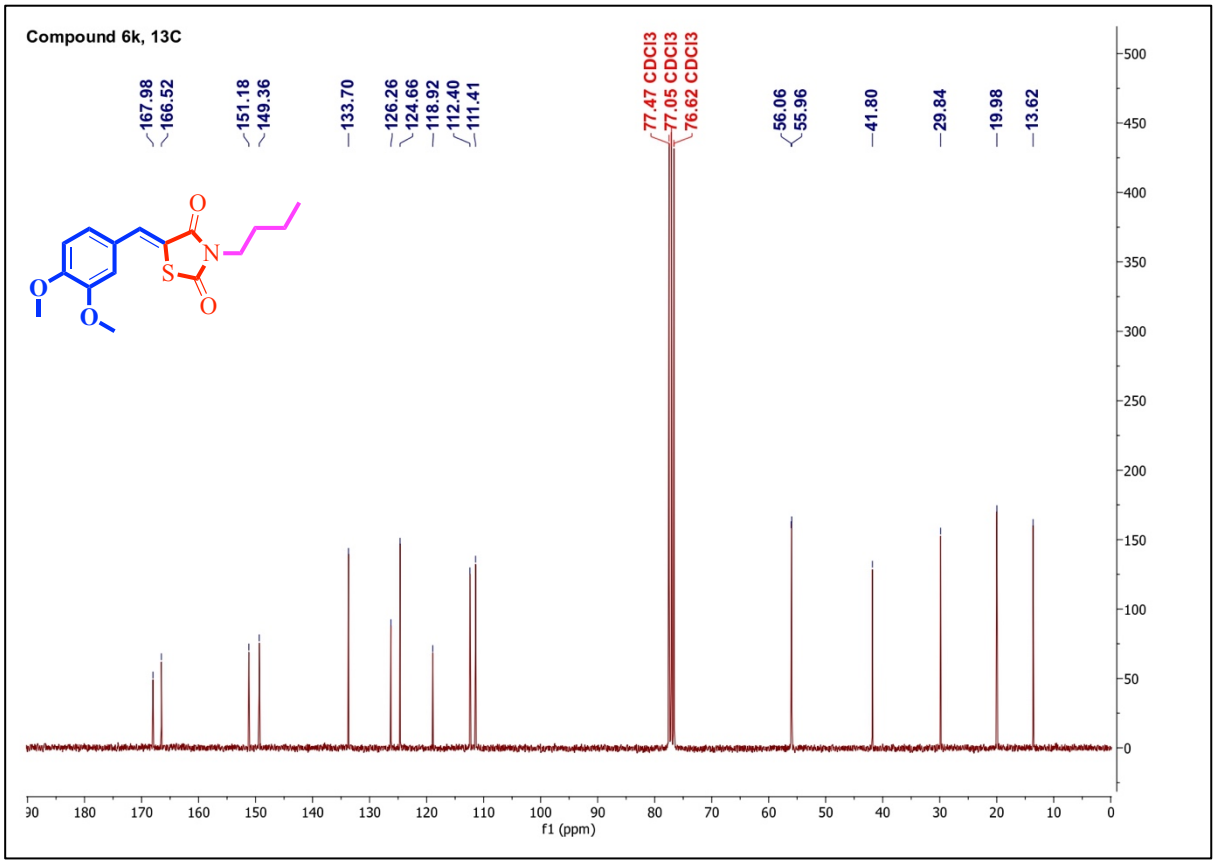

S.F12″: ^{13}C NMR of compound **6k**

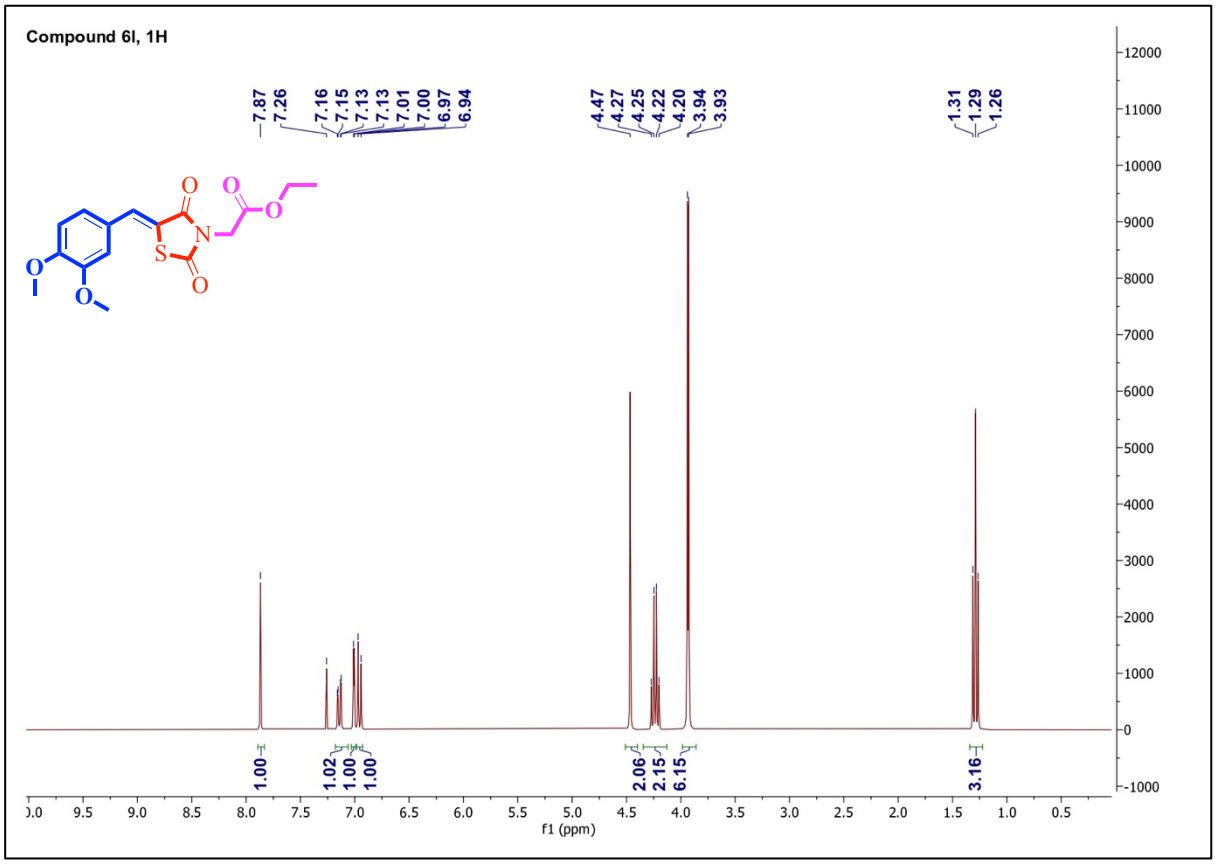

S.F13′: ^{1}H NMR of compound **6l**

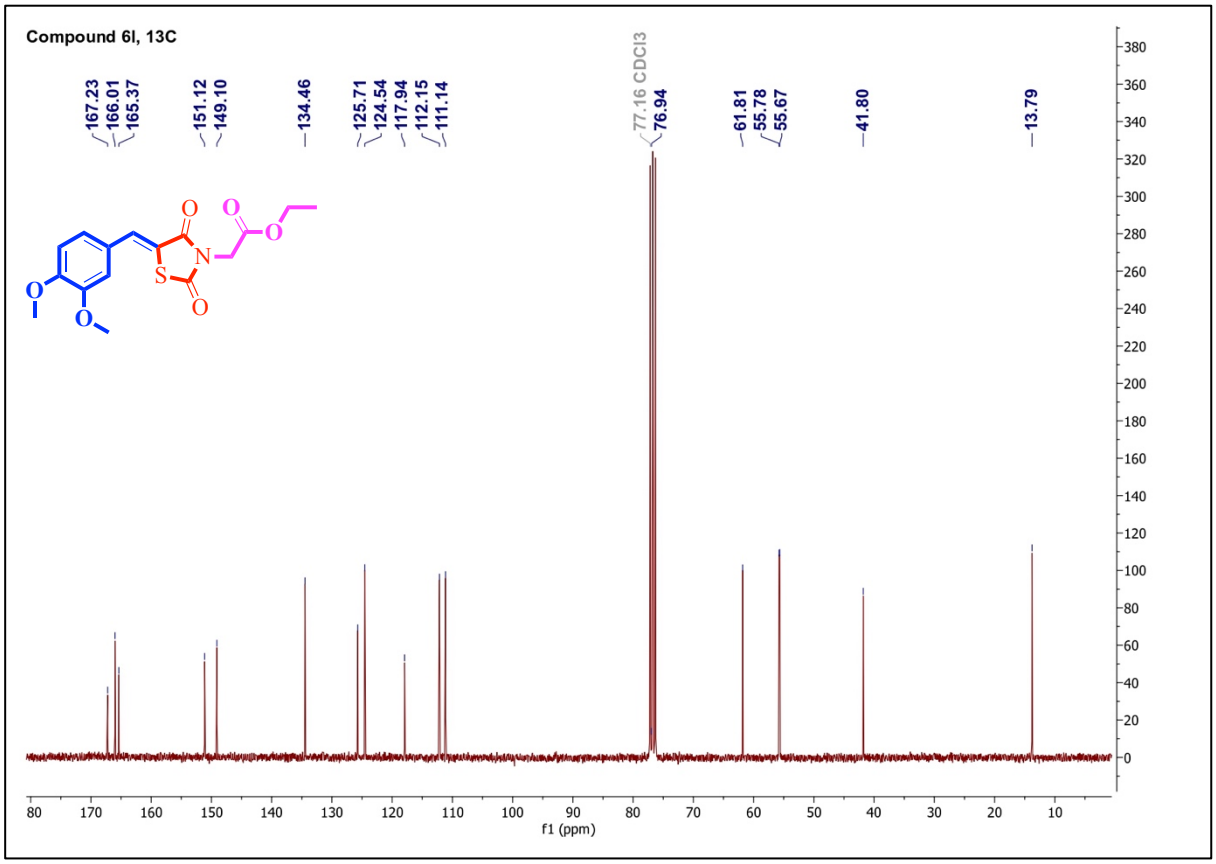

S.F13″: ^{13}C NMR of compound **6l**

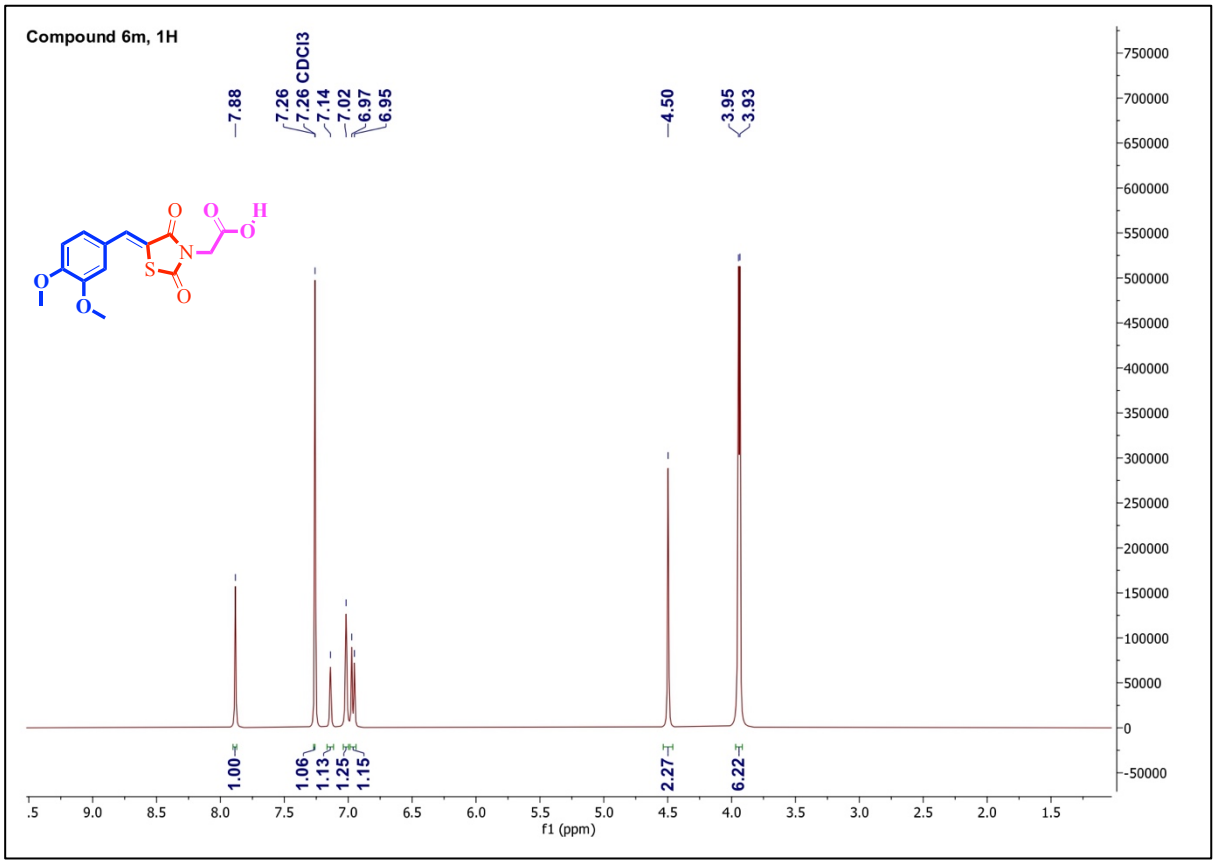

S.F14′: ^{1}H NMR of compound **6m**

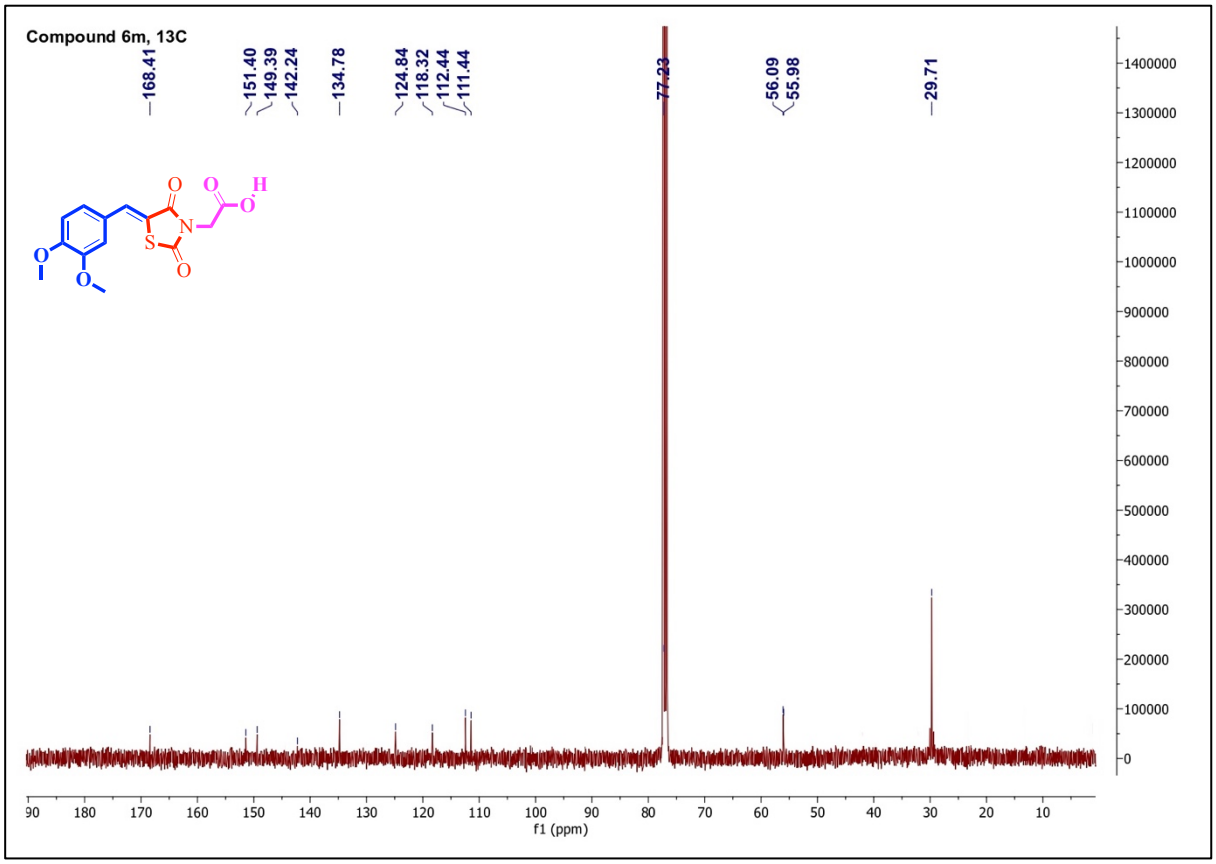

S.F14″: ^{13}C NMR of compound **6m**

II. FT-IR data (Compound **5** and **6a-6m):**

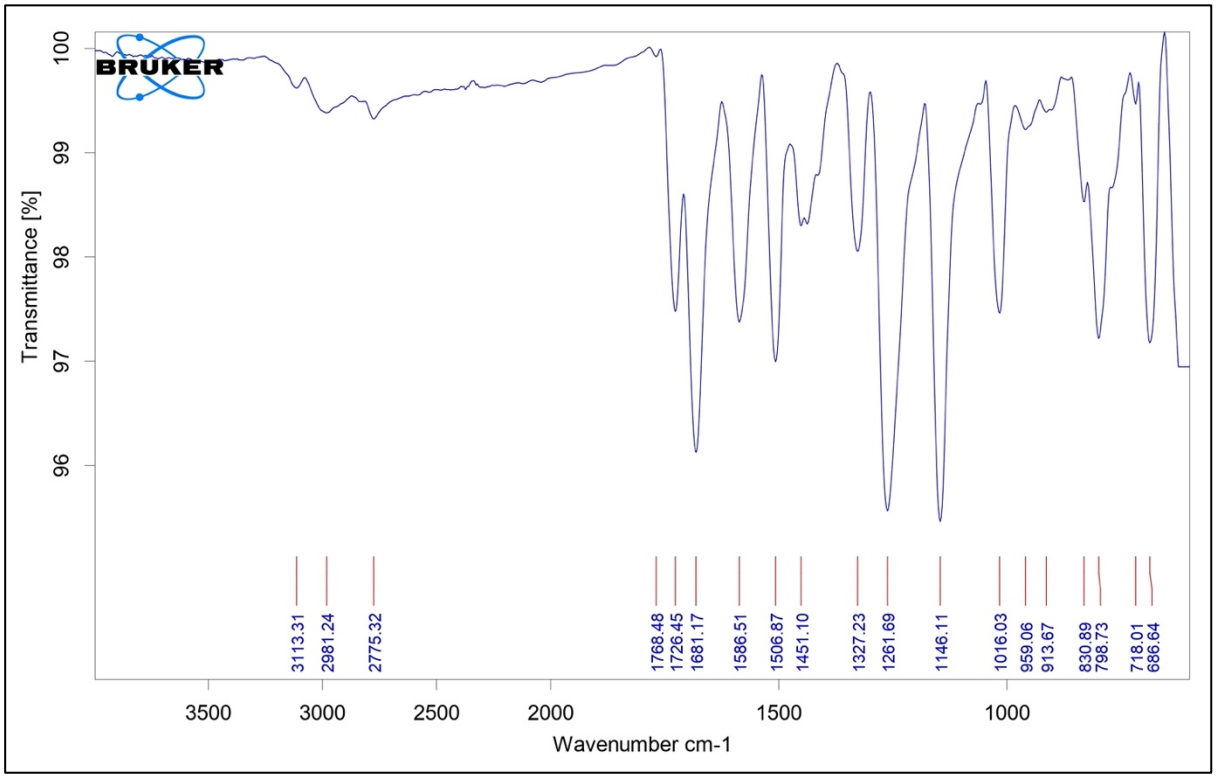

S.F15: FT-IR of compound **5**

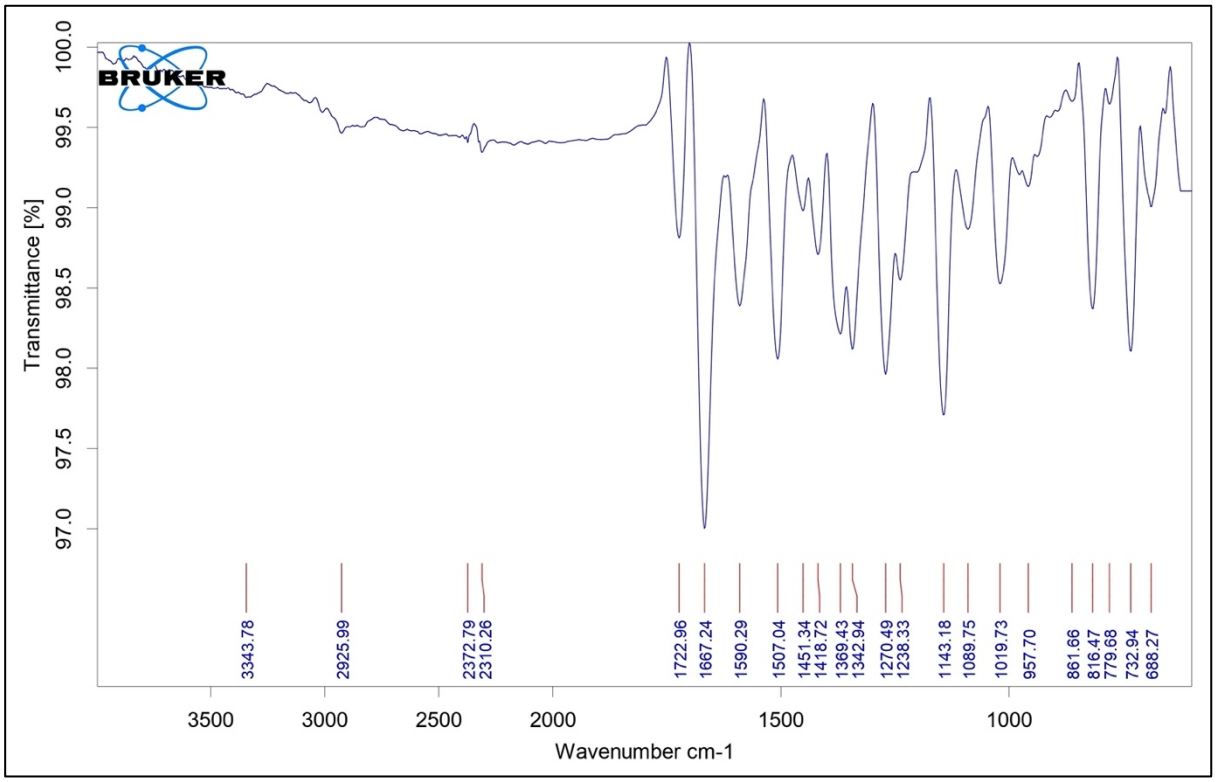

S.F16: FT-IR of compound **6a**

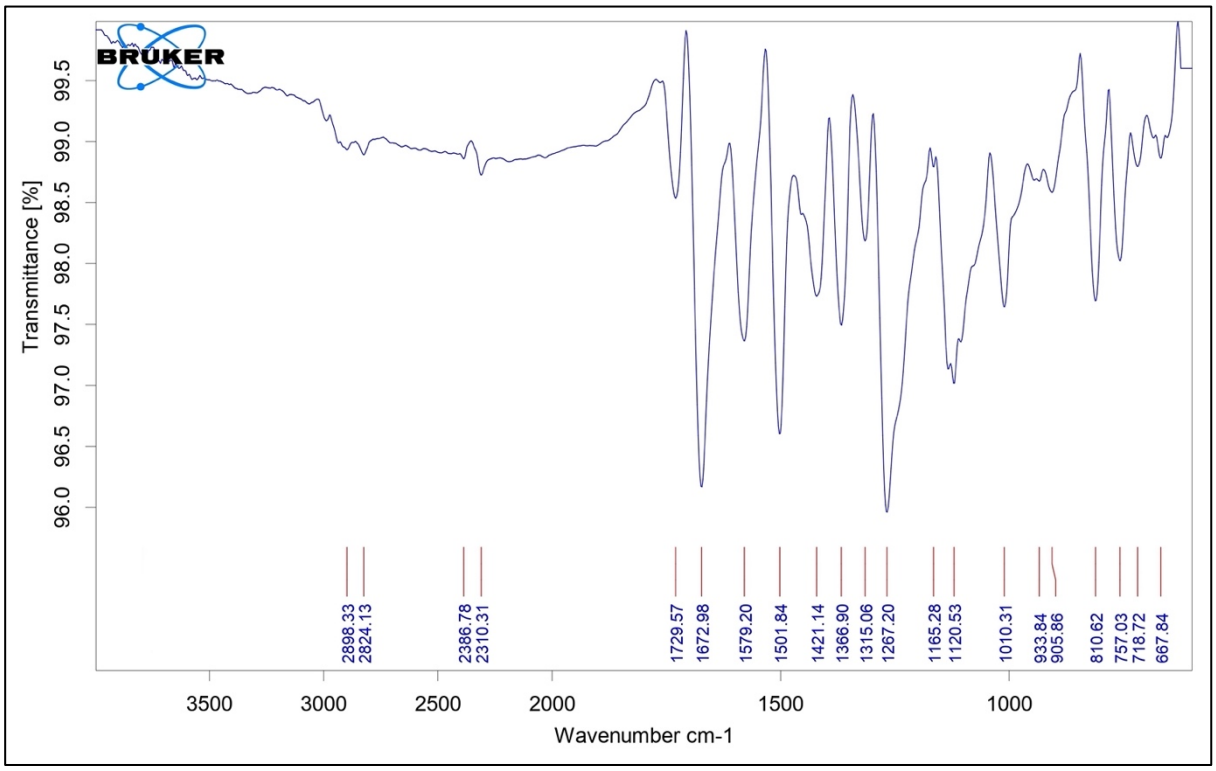

S.F17: FT-IR of compound **6b**

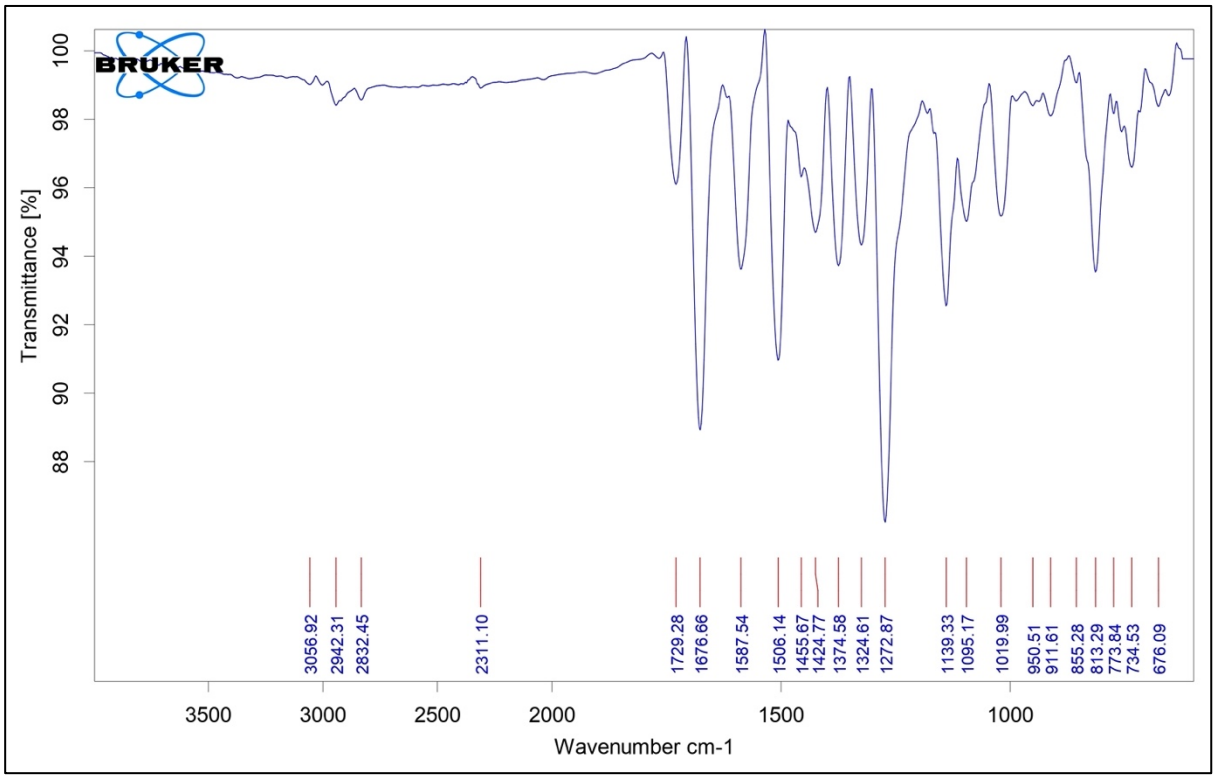

S.F18: FT-IR of compound **6c**

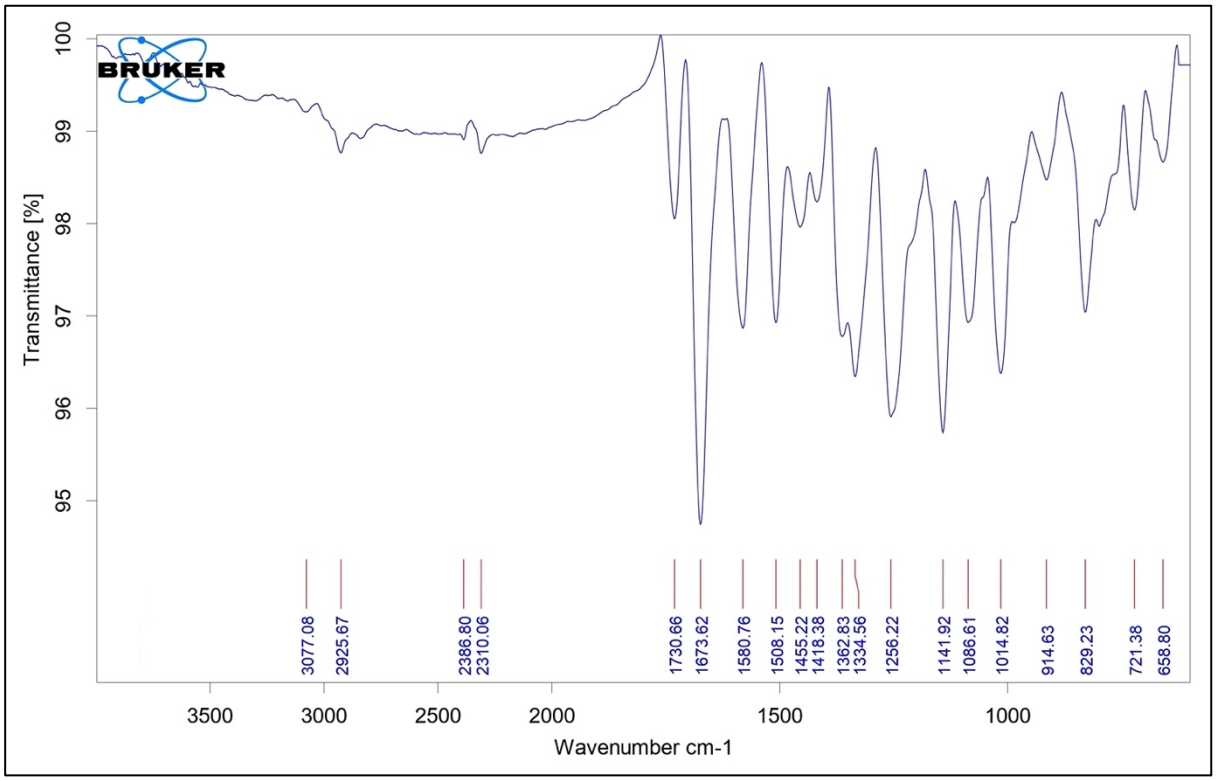

S.F19: FT-IR of compound **6d**

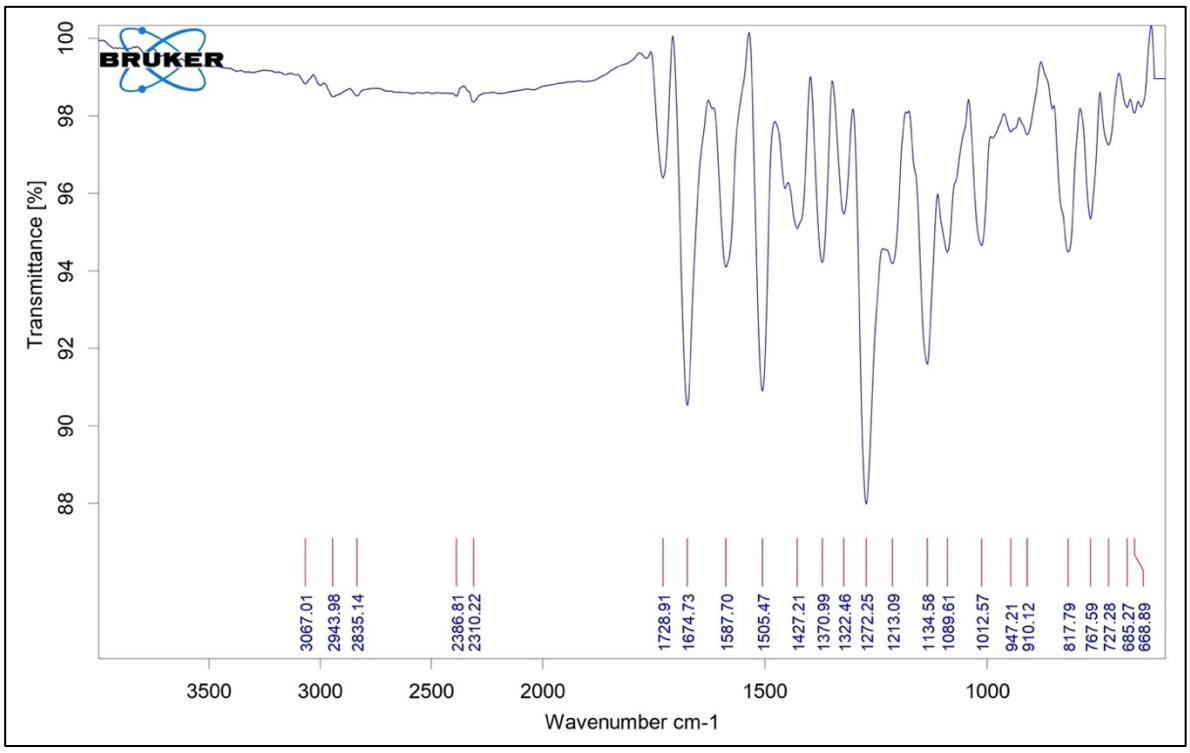

S.F20: FT-IR of compound **6e**

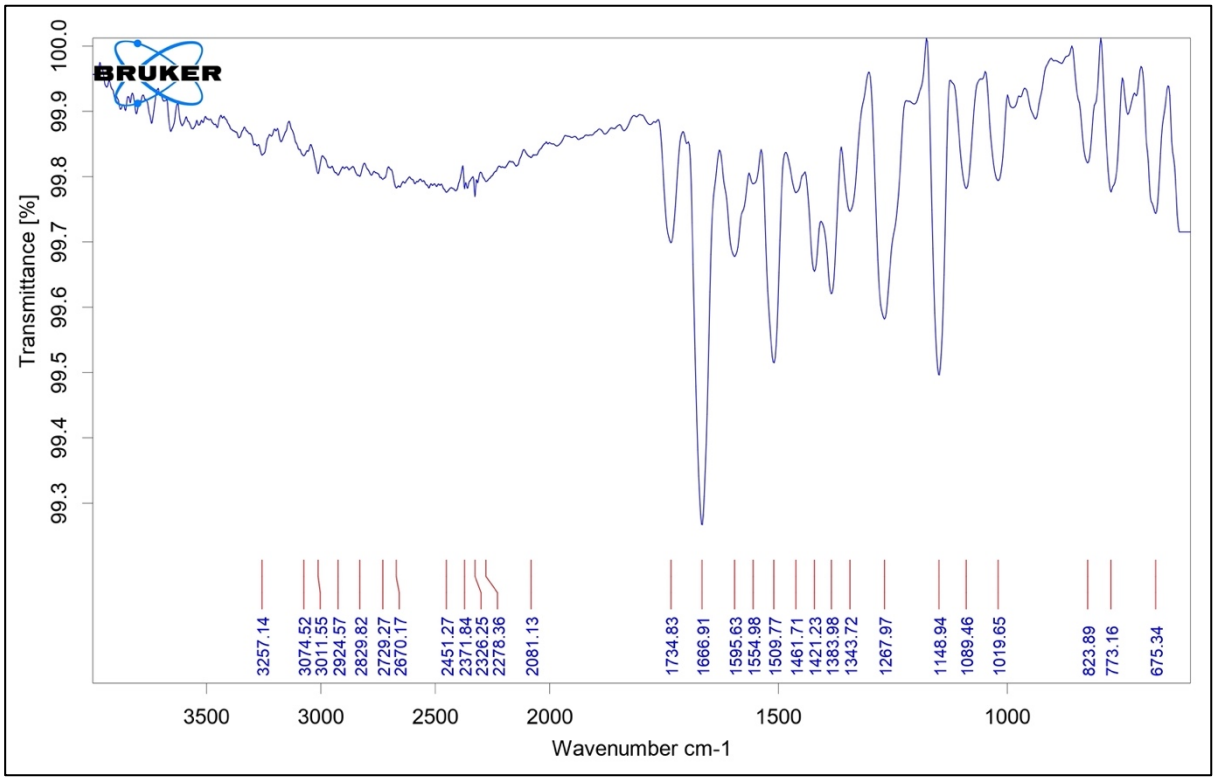

S.F21: FT-IR of compound **6f**

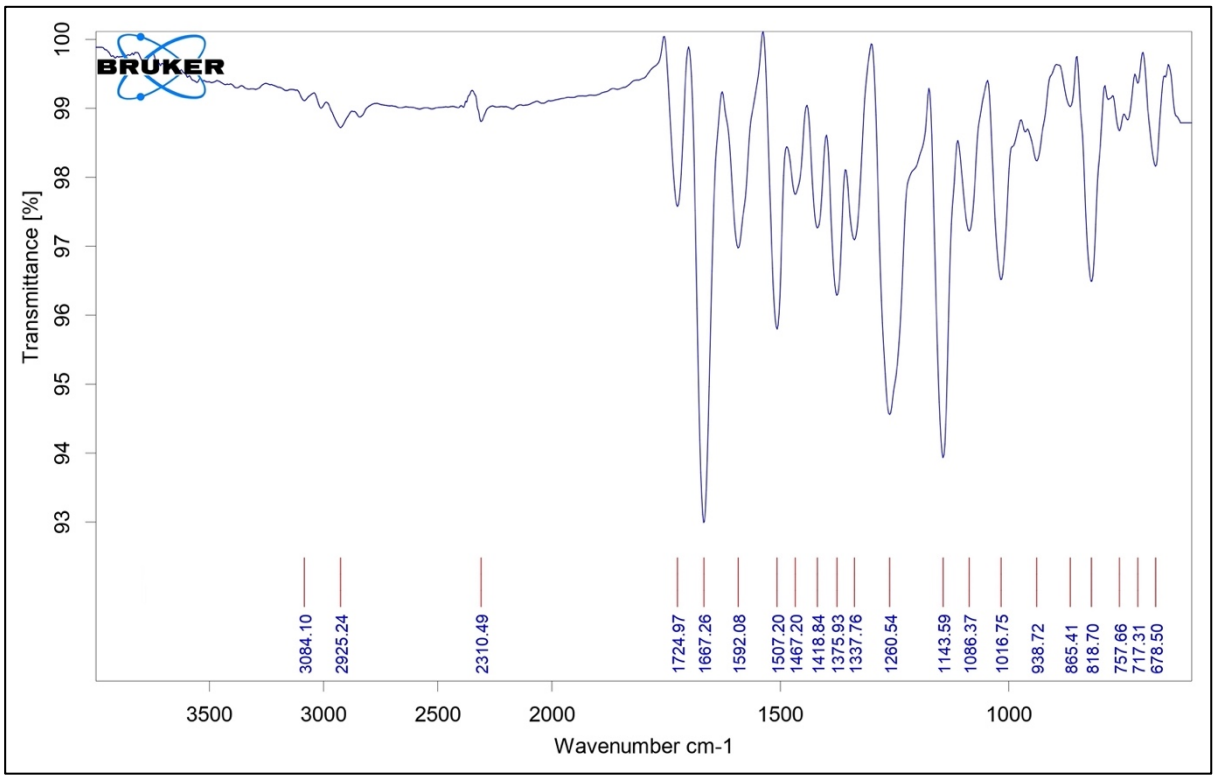

S.F22: FT-IR of compound **6g**

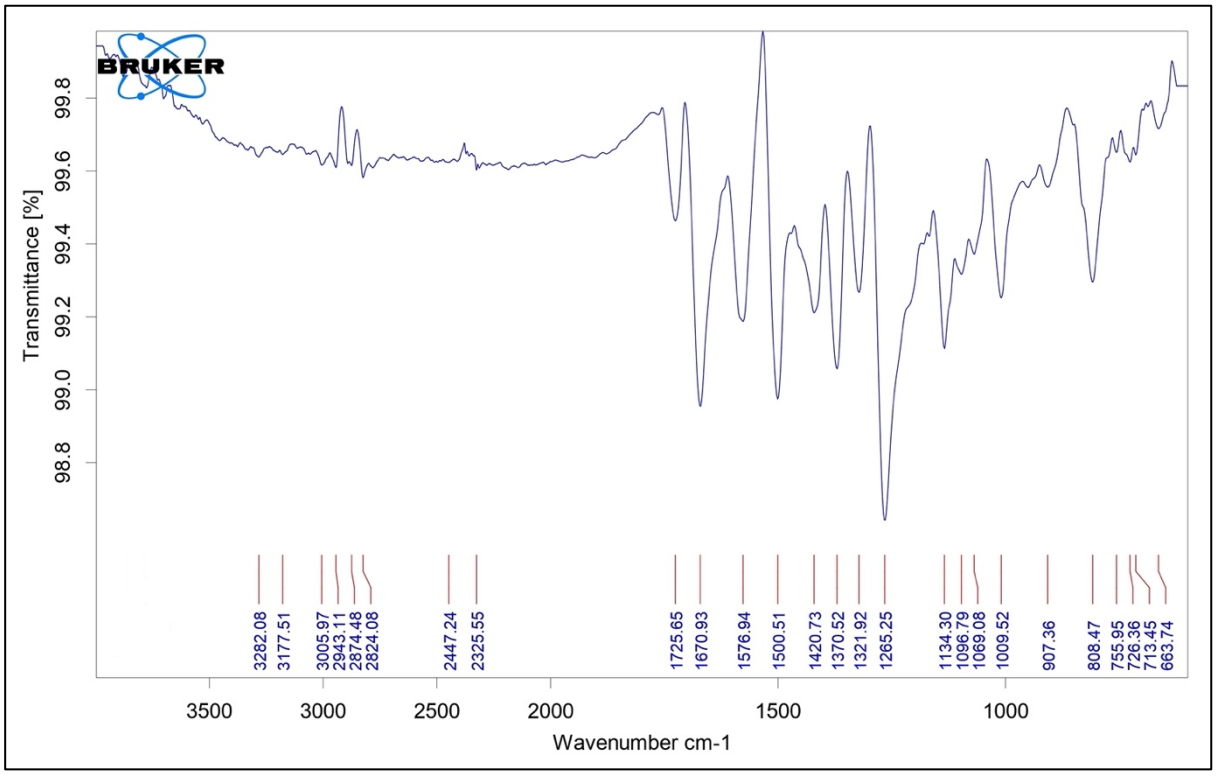

S.F23: FT-IR of compound **6h**

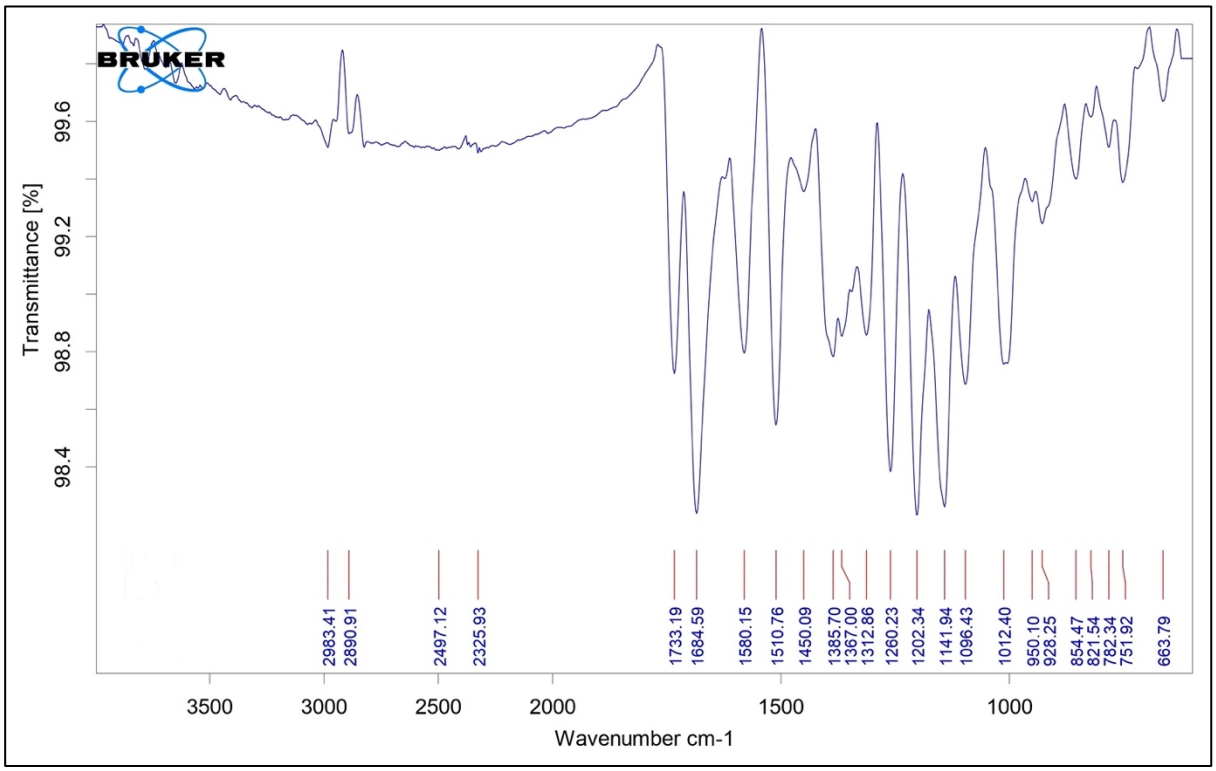

S.F24: FT-IR of compound **6i**

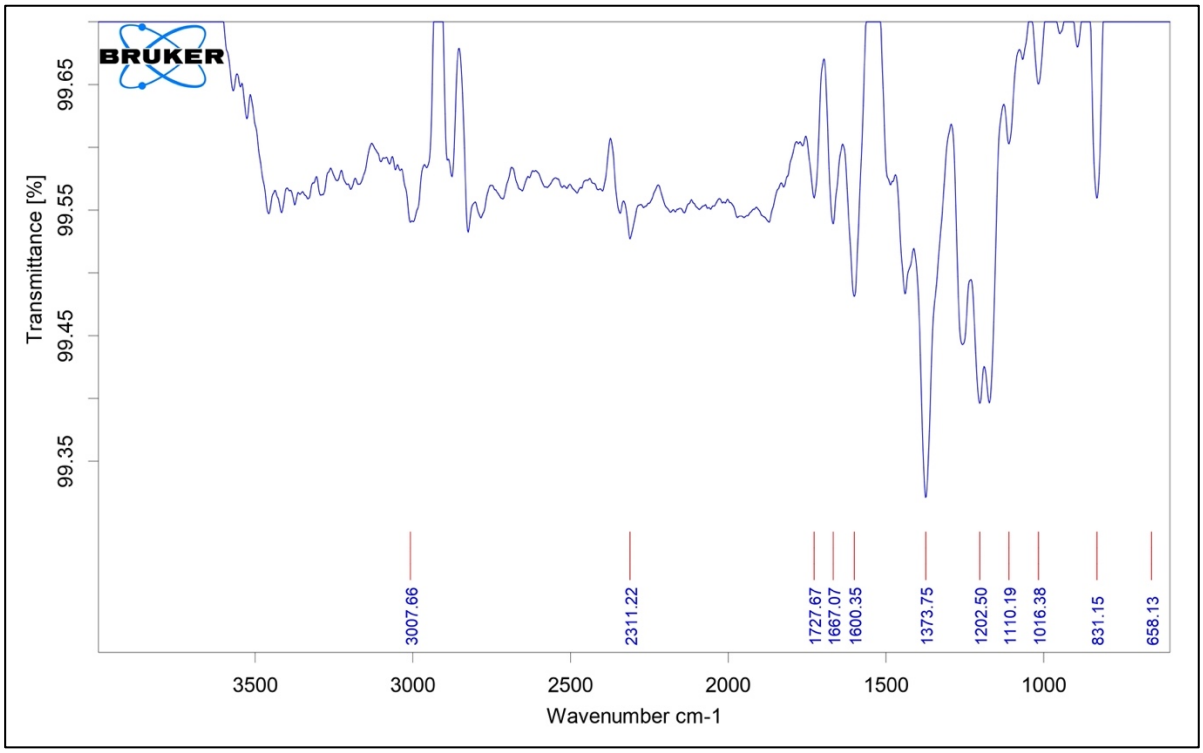

S.F25: FT-IR of compound **6j**

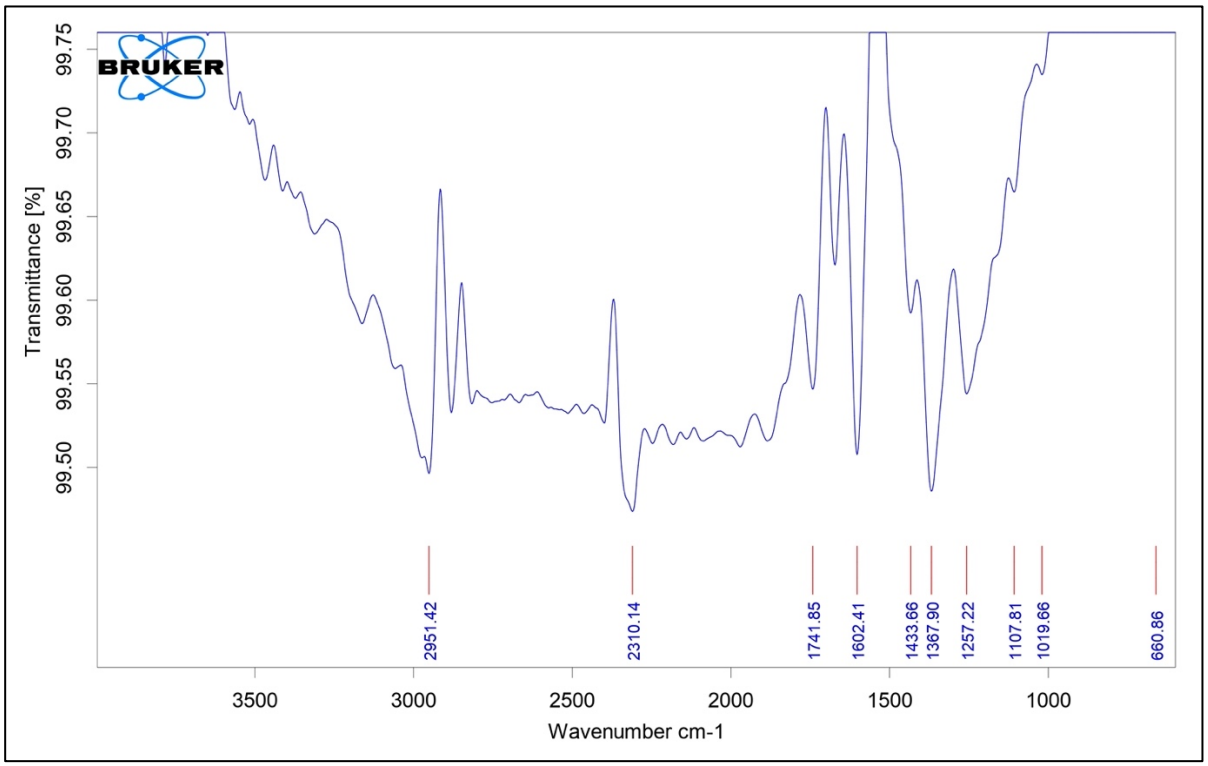

S.F26: FT-IR of compound **6k**

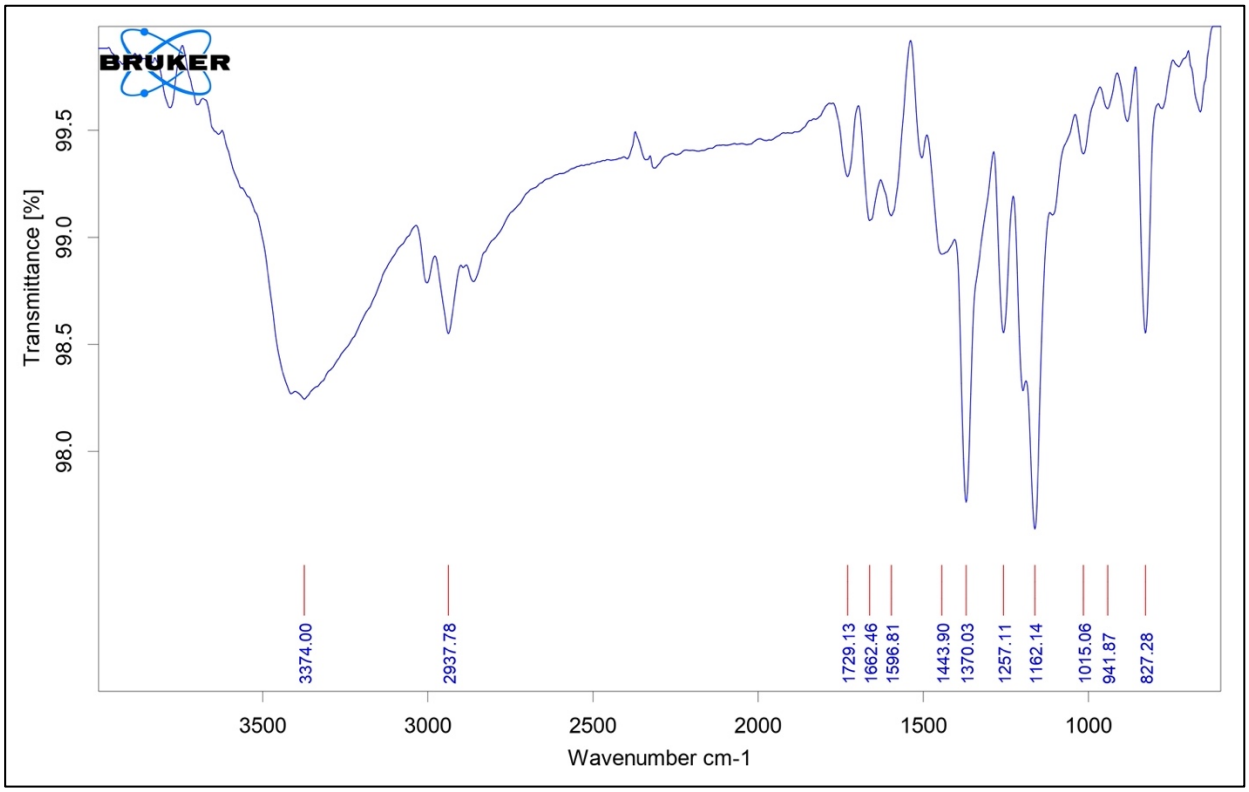

S.F27: FT-IR of compound **6l**

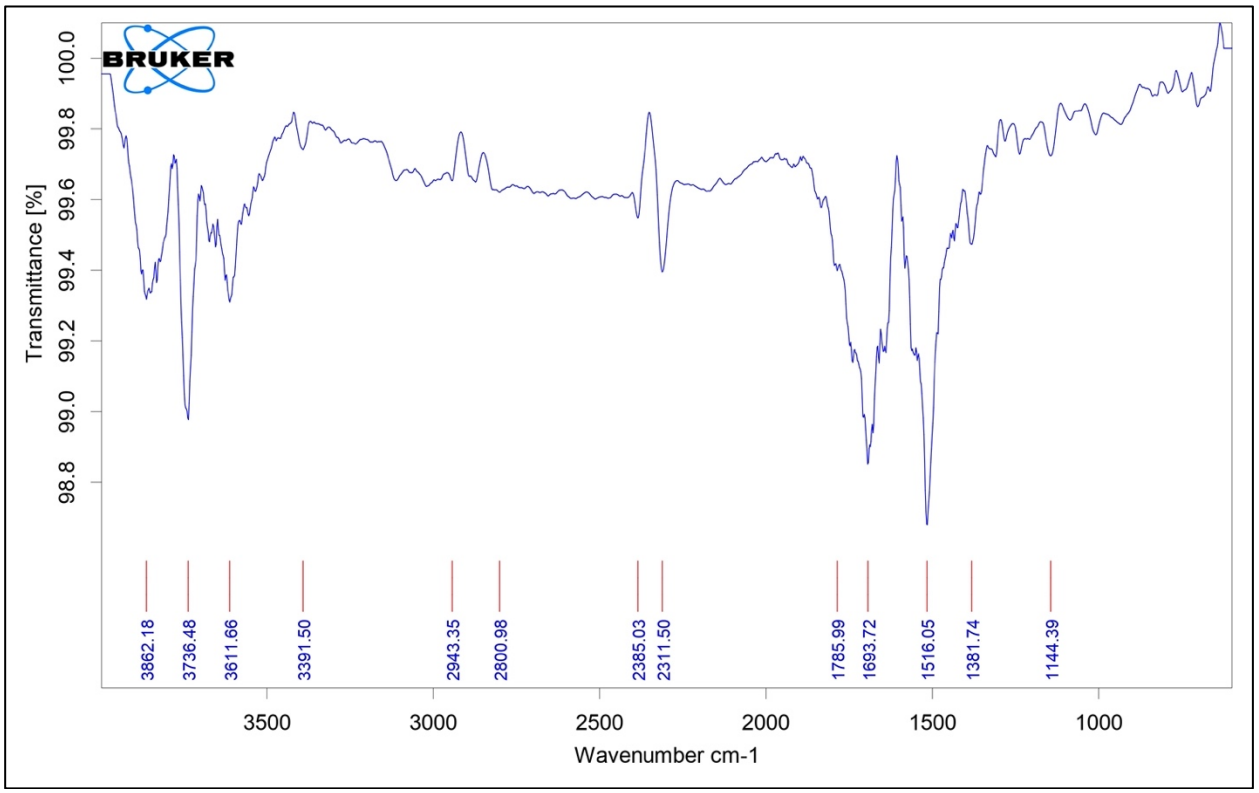

S.F28: FT-IR of compound **6m**

III. ESI mass data (Compound **5** and **6a-6m**):

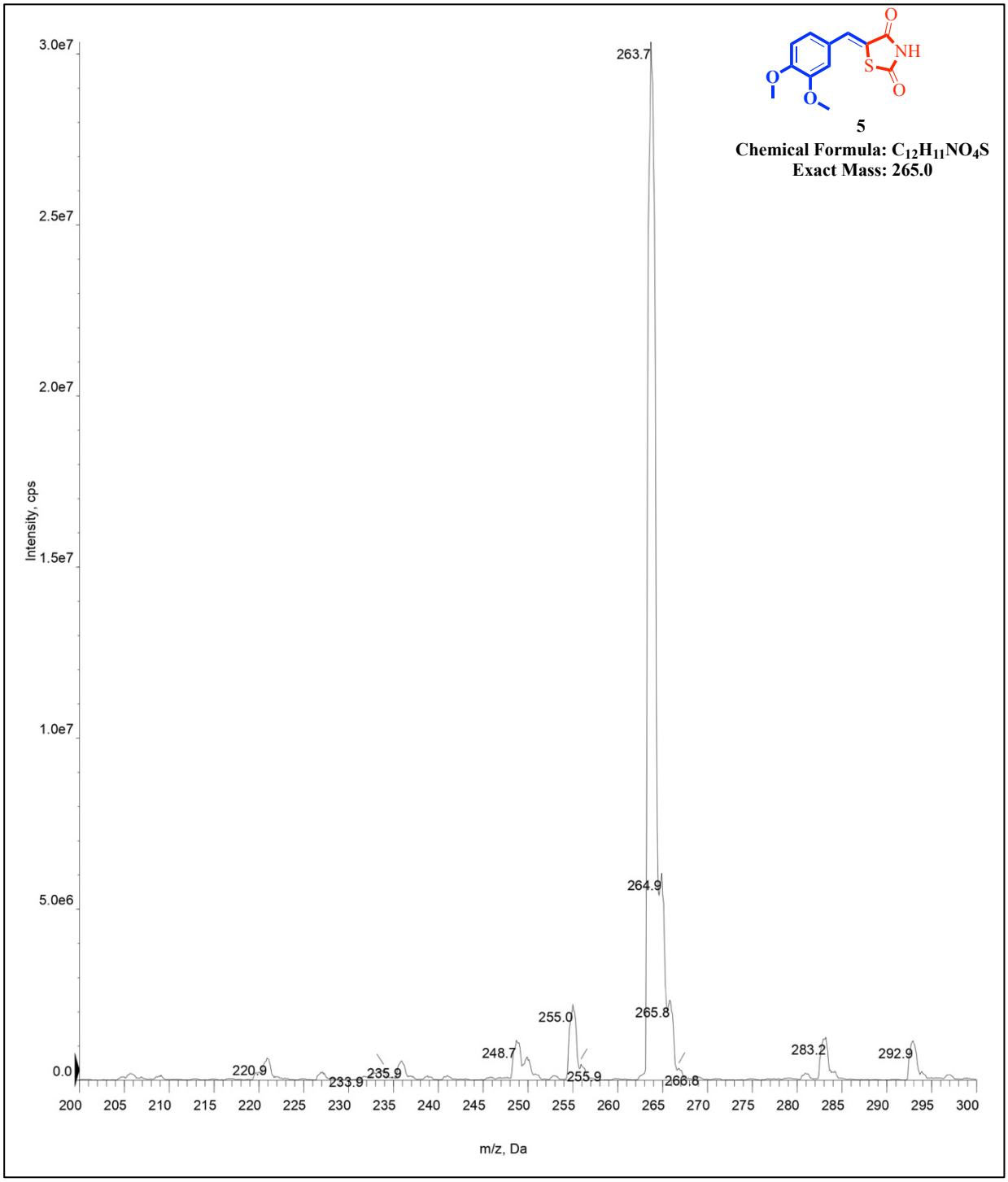

S.F29: MS (ESI, m/z) of Compound **5**

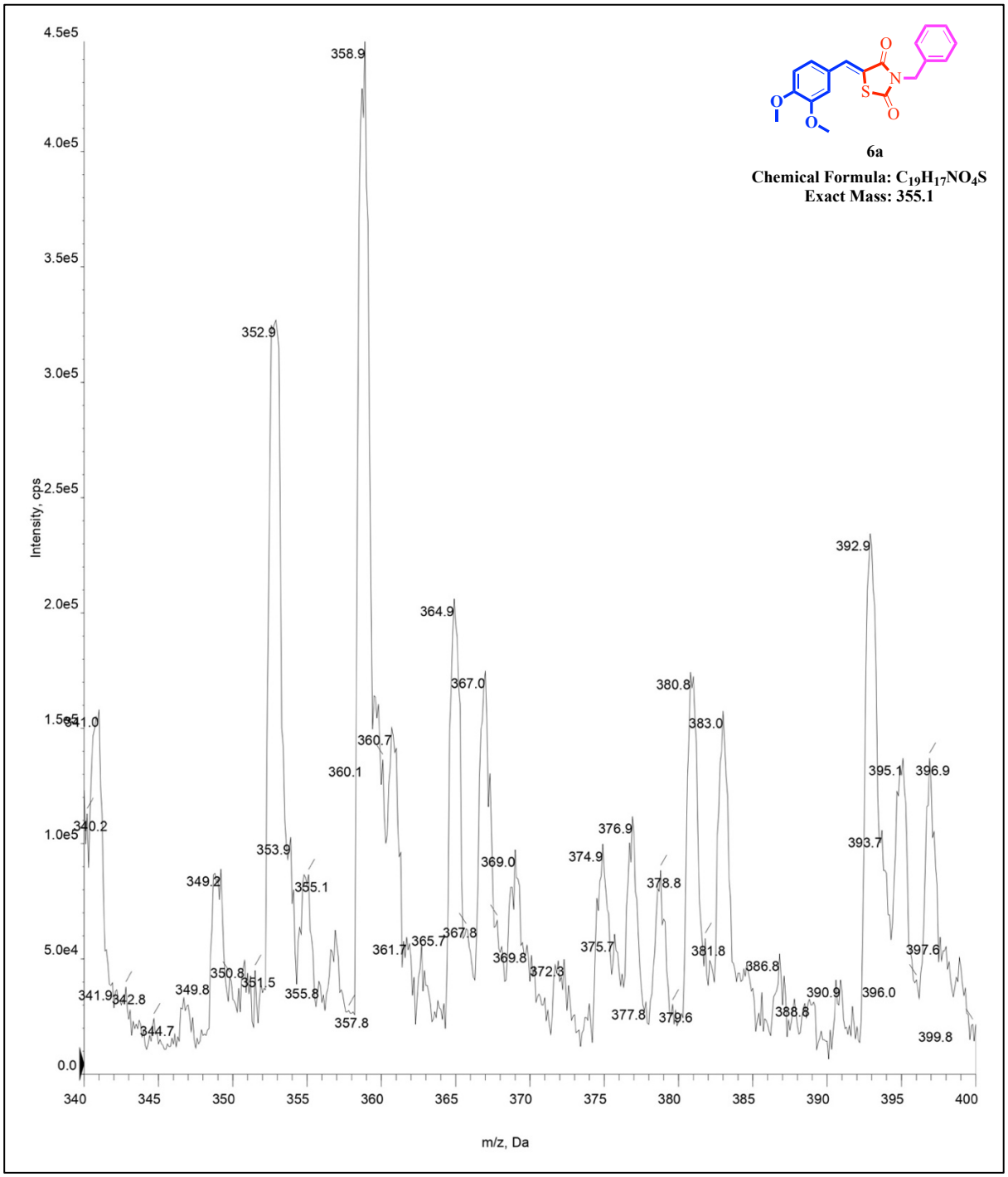

S.F30: MS (ESI, m/z) of Compound **6a**

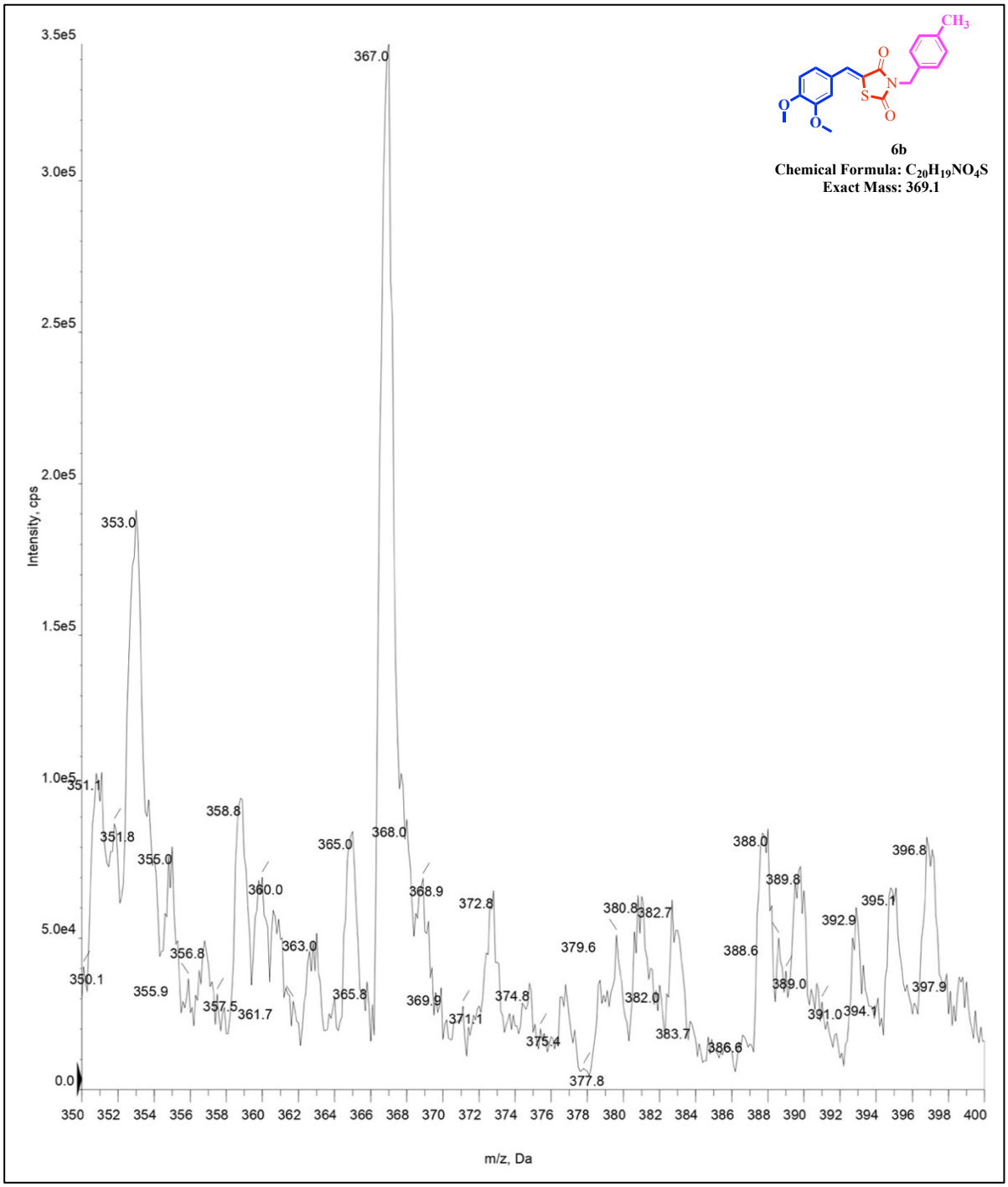

S.F31: MS (ESI, m/z) of Compound **6b**

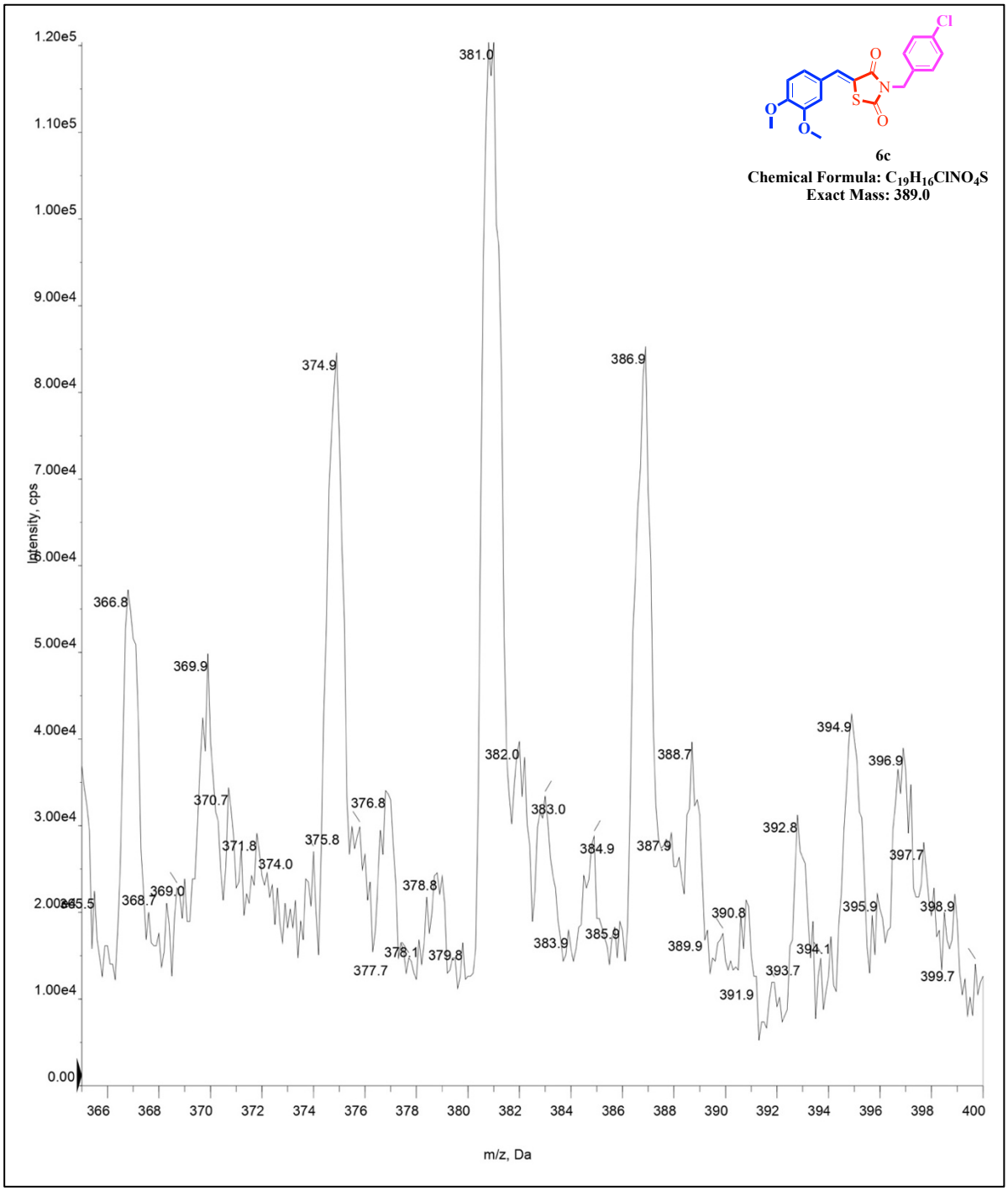

S.F32: MS (ESI, m/z) of Compound **6c**

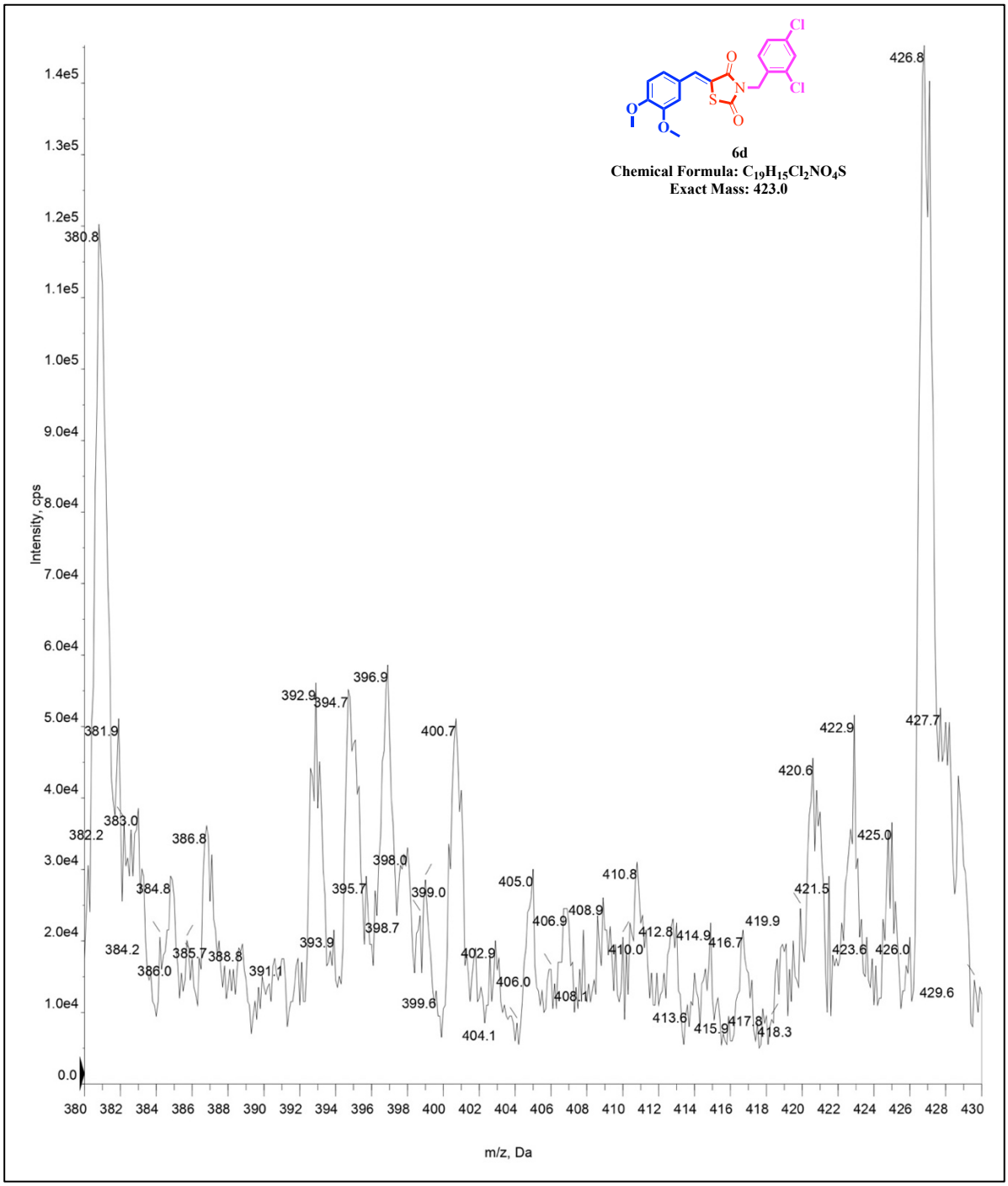

S.F33: MS (ESI, m/z) of Compound **6d**

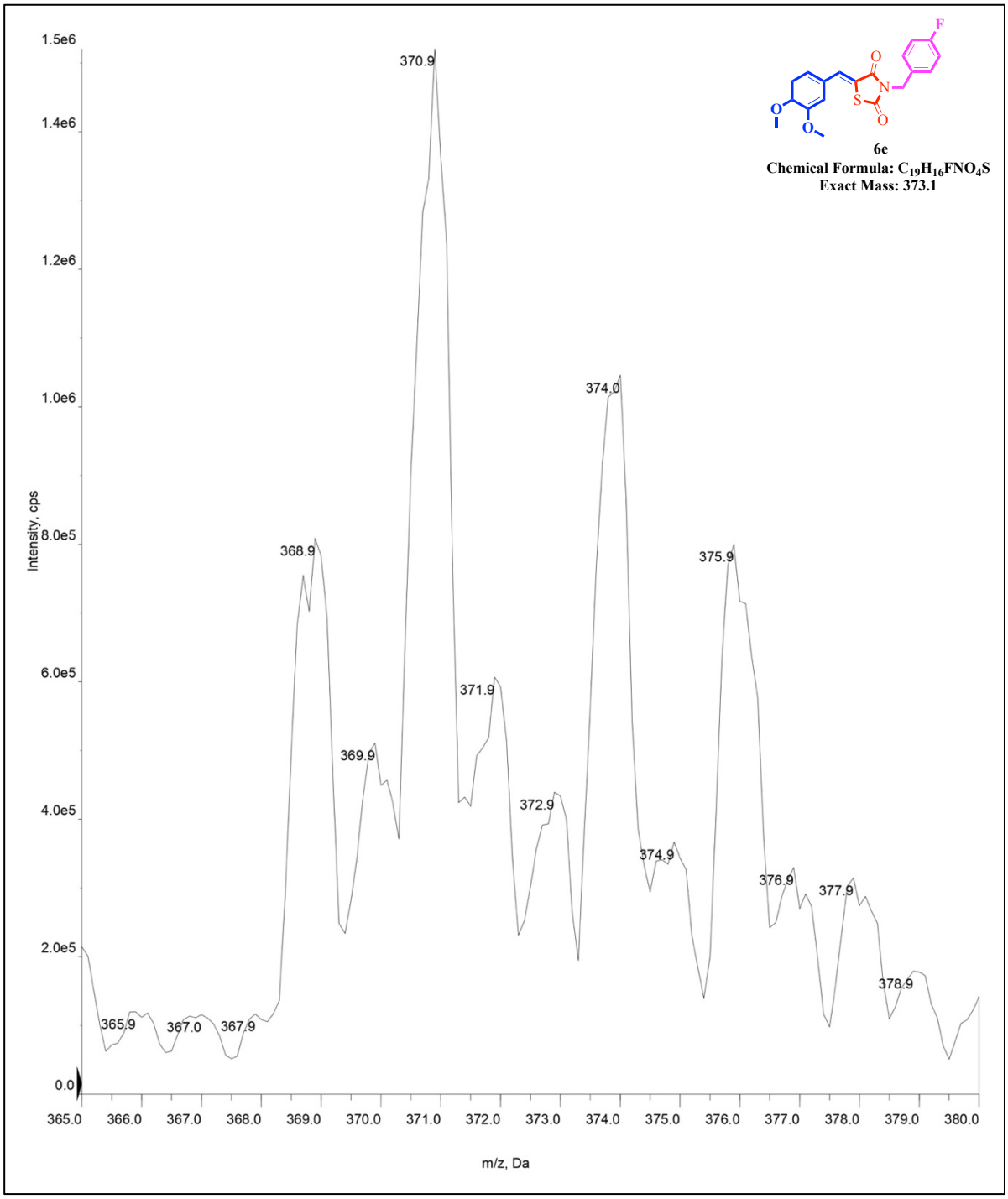

S.F34: MS (ESI, m/z) of Compound **6e**

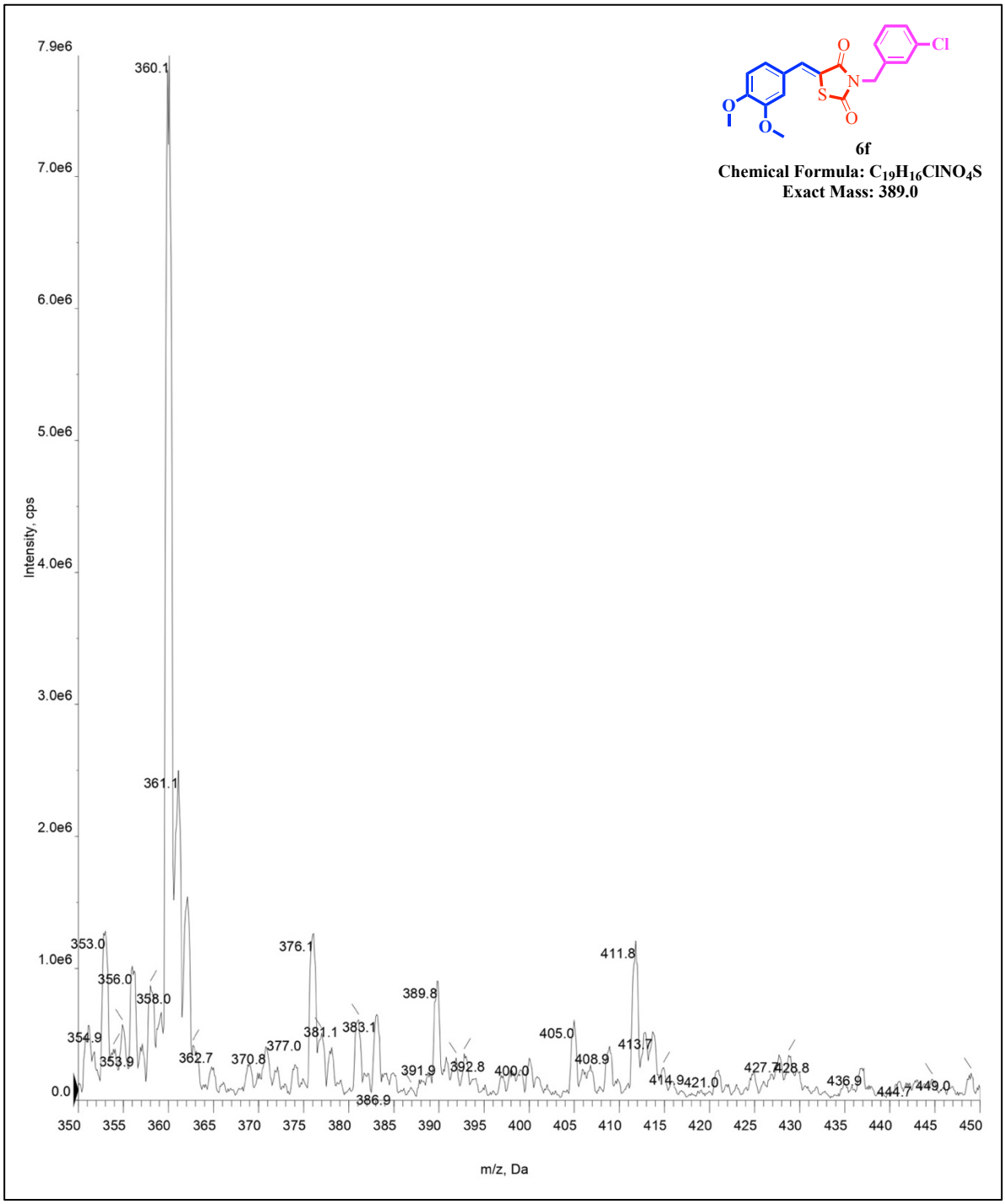

S.F35: MS (ESI, m/z) of Compound **6f**

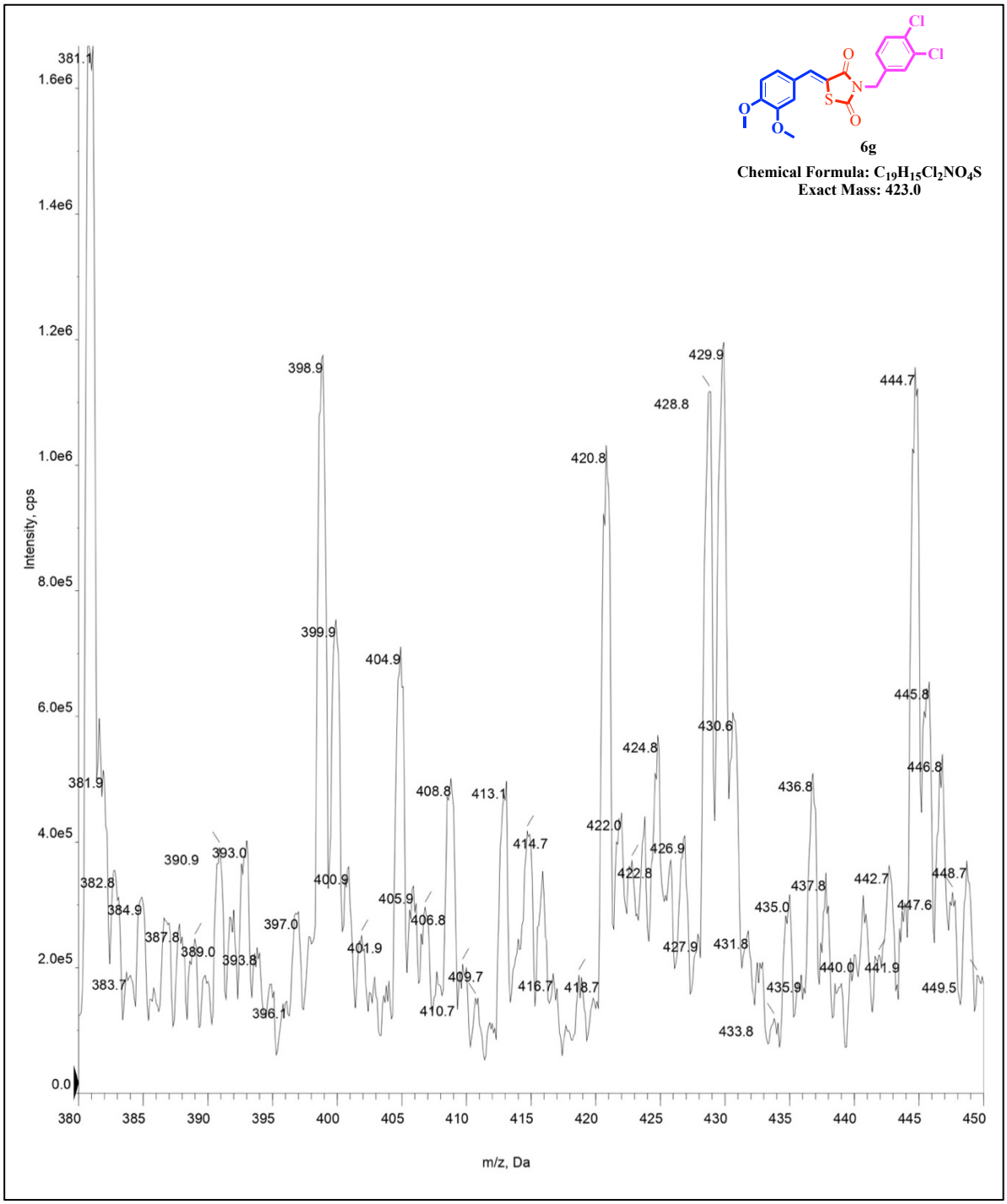

S.F36: MS (ESI, m/z) of Compound **6g**

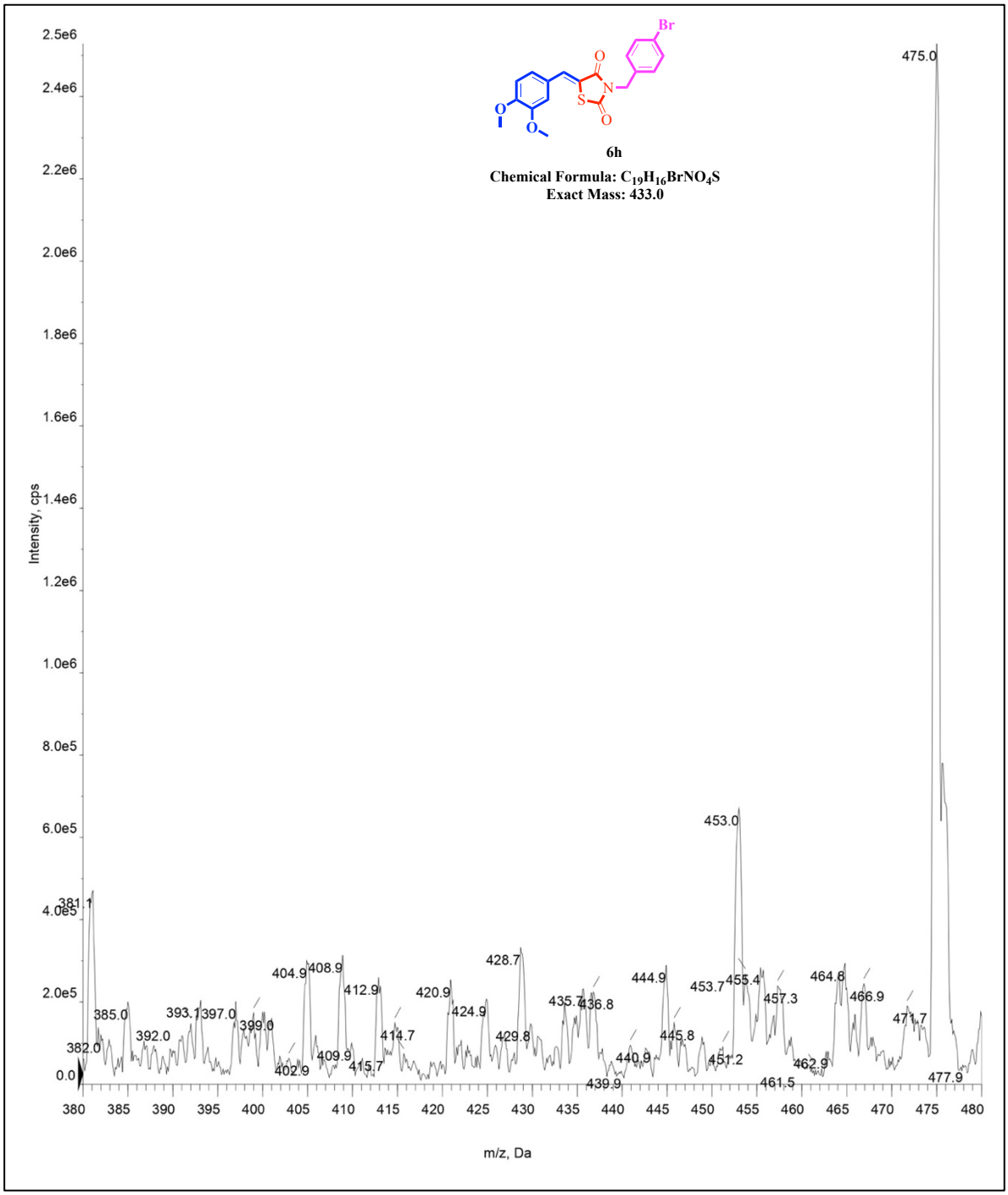

S.F37: MS (ESI, m/z) of Compound **6h**

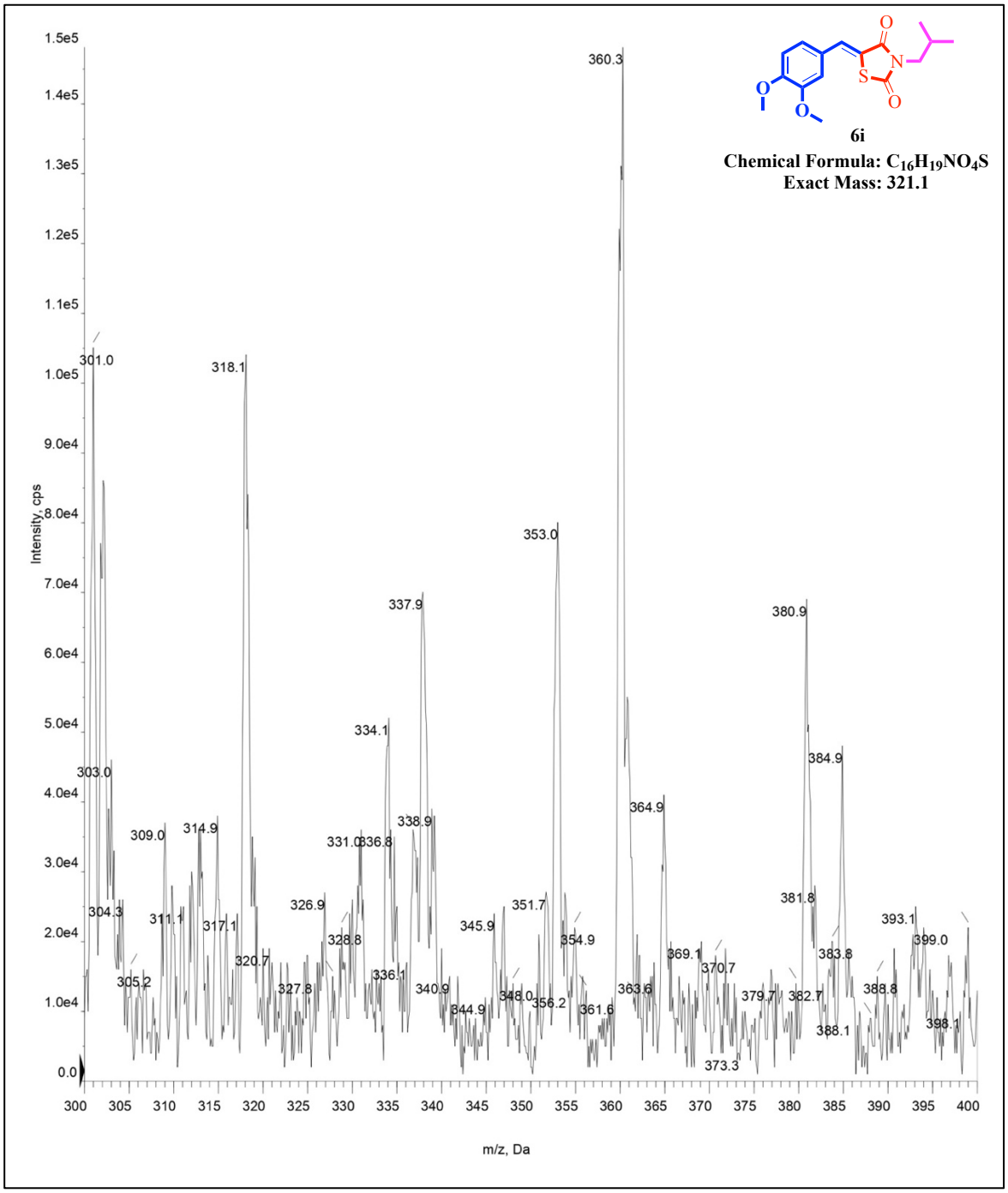

S.F38: MS (ESI, m/z) of Compound **6i**

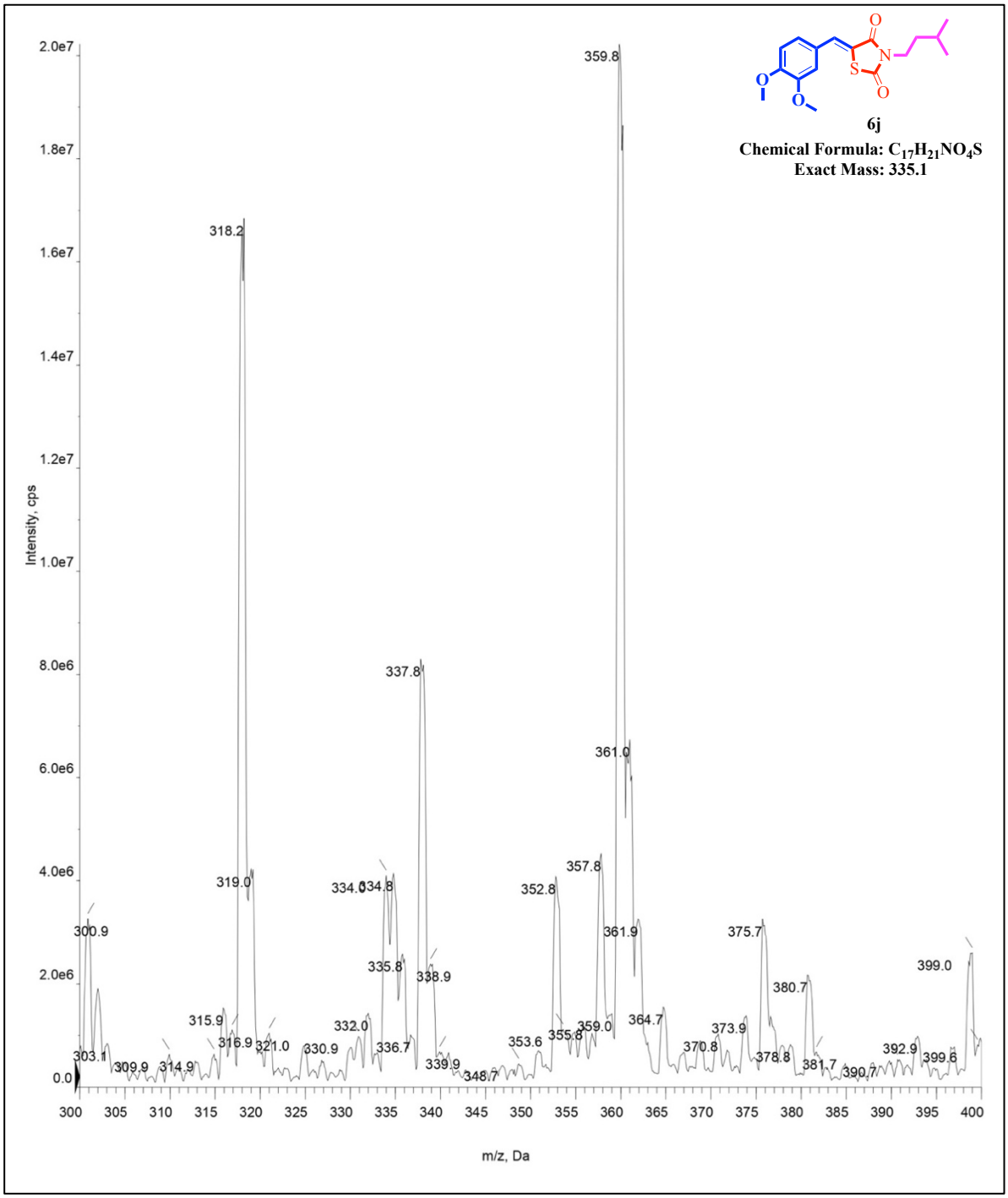

S.F39: MS (ESI, m/z) of Compound **6j**

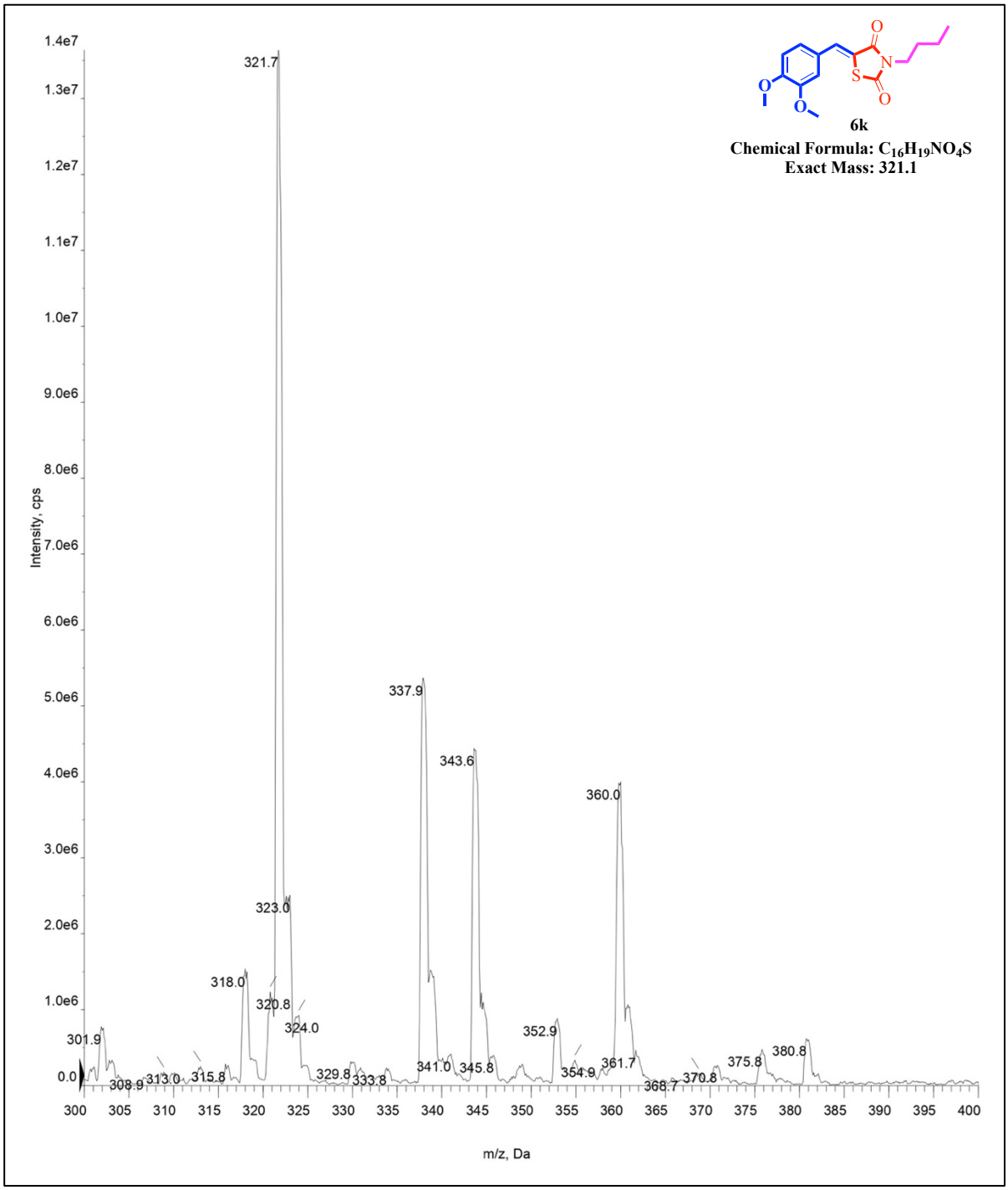

S.F40: MS (ESI, m/z) of Compound **6k**

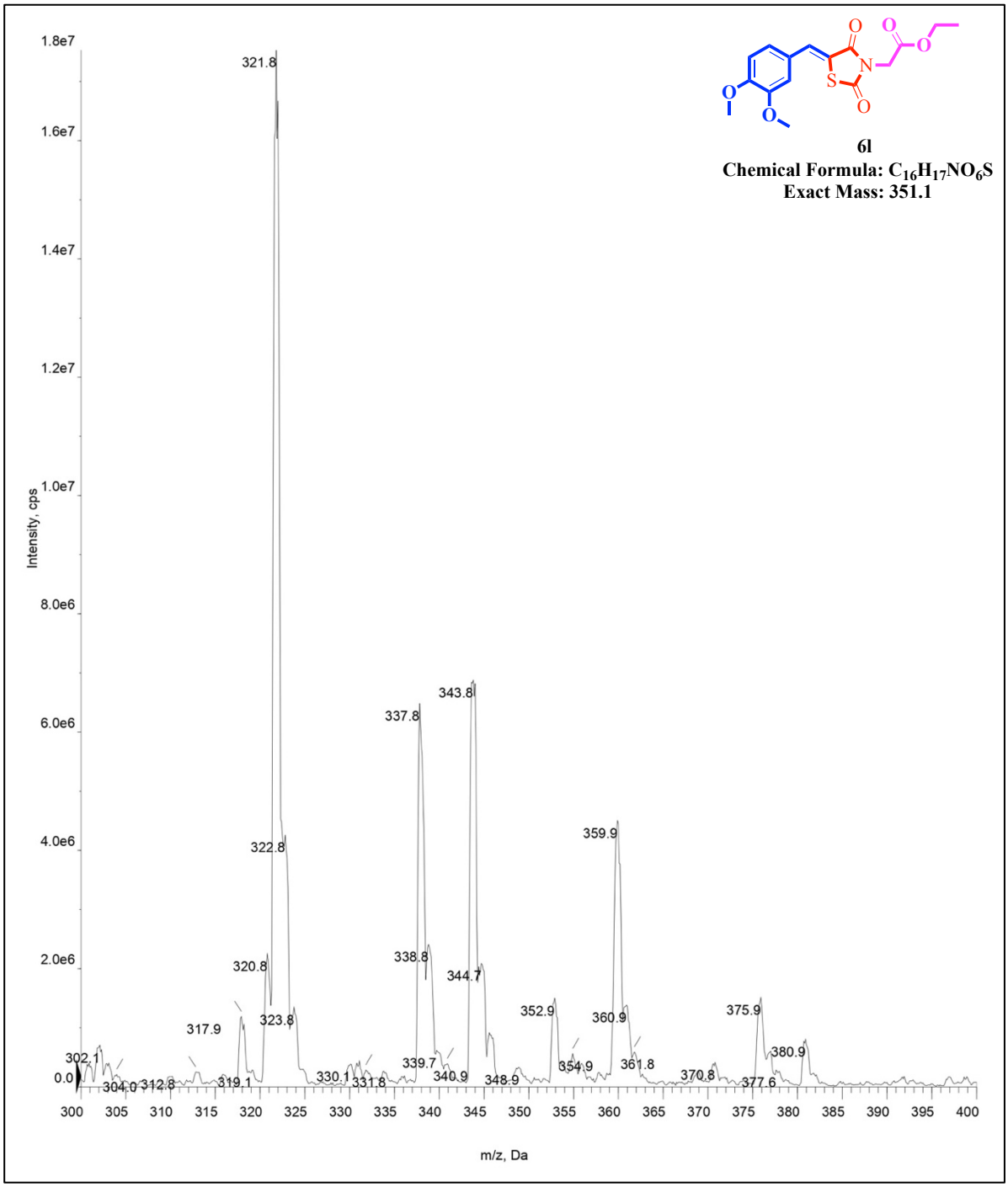

S.F41: MS (ESI, m/z) of Compound **6l**

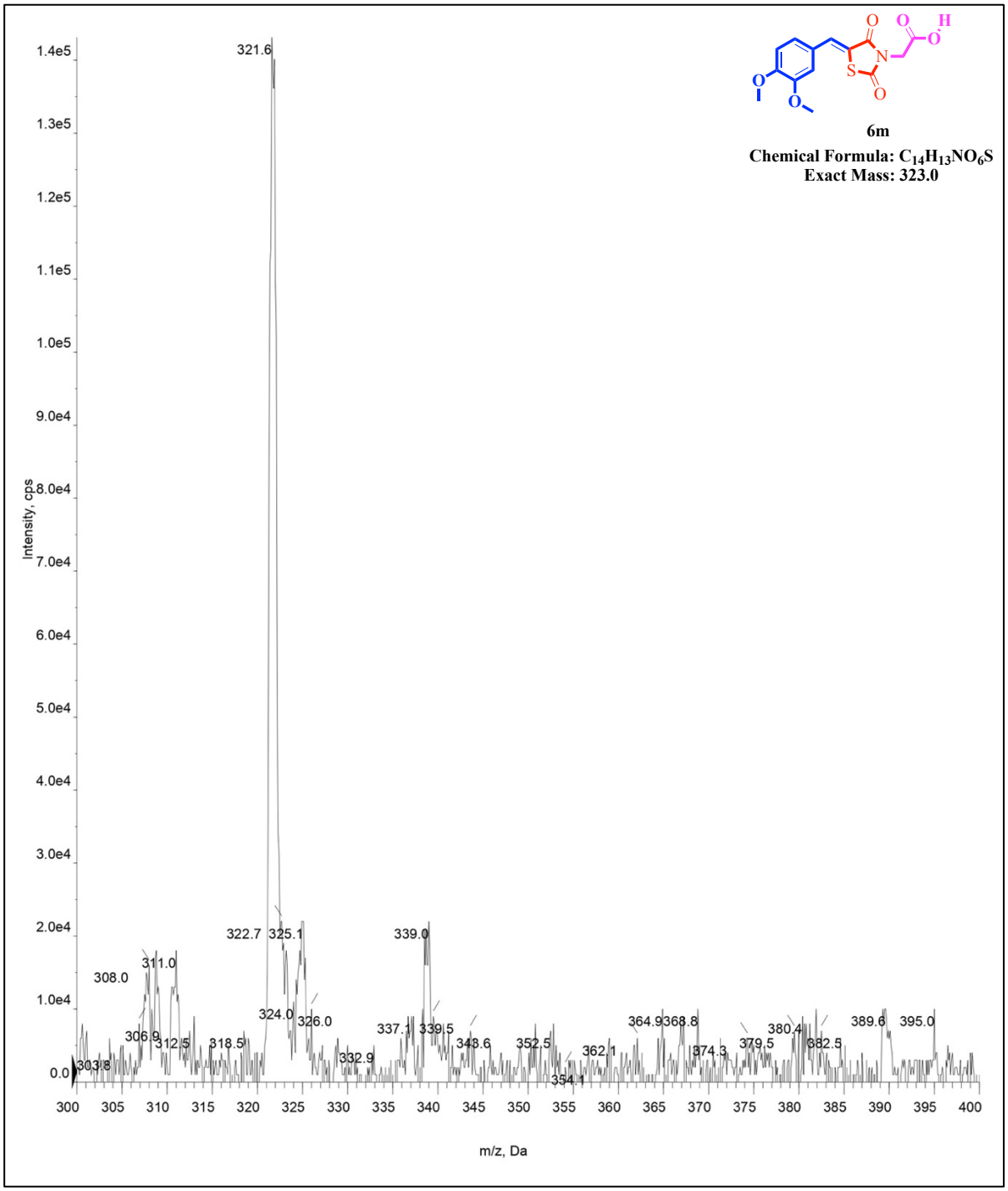

S.F42: MS (ESI, m/z) of Compound **6m**

IV. X-Ray Crystallographic data:

a) Molecular geometries of compound 6b

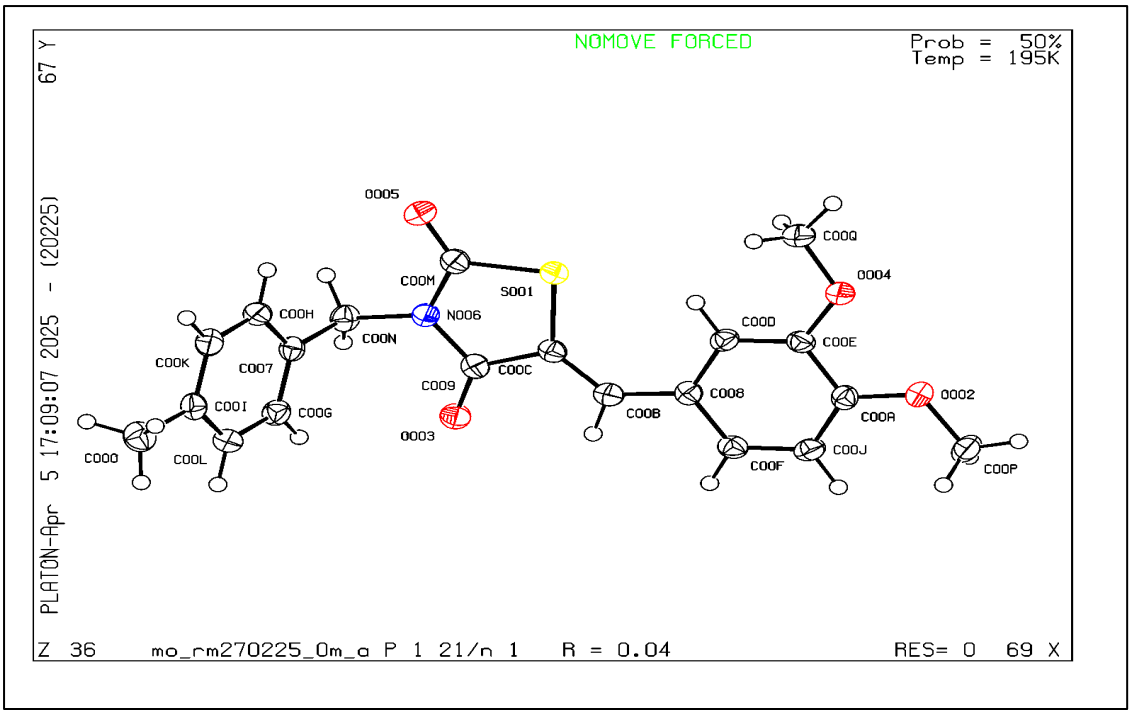

S.F43: Molecular geometries of compound **6b** in crystal.

b) Tabular data of crystal:

Table S1: Crystallographic table:

Complexes	Compound 6b
CCDC	2445001
formula	C20 H19 N O4 S
fw	369.42
crystal system	block
space group	P21/n
a (Å)	4.2415(2)
b (Å)	24.1911(11)
c(Å)	16.9988(7)
α (°)	90
β (°)	95.848(2)
γ (°)	90
V (Å^3)	1735.11(13)

Z	4
T (K)	195
Dx, g cm-3	1.414
μ (mm^{-1})	0.213
R1[a][I>2σ(I)]/GOF [b]	0.0404/ 1.123
*w*R2[c] (I>2σ (I))	0.1088
observation criterion: [a]R1 = $\Sigma\|\|F_o\|-\|F_c\|\|/\Sigma\|F_o\|$. [b]GOF = $\{\Sigma[w(F_o^2-F_c^2)^2]/(n-p)\}^{1/2}$, [c]*w*R2 = $[\Sigma[w(F_o^2-F_c^2)^2]/\Sigma[w(F_o^2)^2]]^{1/2}$ where $w = 1/[\sigma^2(F_o^2) + (aP)^2+bP]$, $P = (F_o^2+2F_c^2)/3$.	

References:

[1] A. Paul, S.S. Mishra, A. Sarkar, R. Bhowmik, A. De, A. Maji, U. Shee, A. Samanta, S. Karmakar, T.K. Maity, Synthesis, single crystal XRD, in vitro evaluation, molecular docking and ADMET studies of cuminaldehyde-thiazolidine-2,4-dione hybrids as potential α-glucosidase inhibitors, J Mol Struct 1331 (2025) 141510. https://doi.org/10.1016/j.molstruc.2025.141510.

[2] G. Singh, R. Singh, V. Monga, S. Mehan, Thiazolidine-2,4-dione hybrids as dual alpha-amylase and alpha-glucosidase inhibitors: design, synthesis, in vitro and in vivo anti-diabetic evaluation, RSC Med. Chem. 15 (2024) 2826–2854. https://doi.org/10.1039/D4MD00199K.

[3] G. Singh, R. Singh, V. Monga, S. Mehan, 3,5-Disubstituted-thiazolidine-2,4-dione hybrids as antidiabetic agents: Design, synthesis, in-vitro and In vivo evaluation, Eur J Med Chem 266 (2024). https://doi.org/10.1016/j.ejmech.2024.116139.

[4] A. Paul, S. Nahar, P. Nahata, A. Sarkar, A. Maji, A. Samanta, S. Karmakar, T.K. Maity, Synthetic GPR40/FFAR1 agonists: An exhaustive survey on the most recent chemical classes and their structure-activity relationships, Eur J Med Chem 264 (2024) 115990. https://doi.org/10.1016/j.ejmech.2023.115990.

[5] A. Mushtaq, U. Azam, S. Mehreen, M.M. Naseer, Synthetic α-glucosidase inhibitors as promising anti-diabetic agents: Recent developments and future challenges, Eur J Med Chem 249 (2023). https://doi.org/10.1016/j.ejmech.2023.115119.

[6] M. Fan, X. Zhong, Y. Huang, Z. Peng, G. Wang, Synthesis, biological evaluation and molecular docking studies of chromone derivatives as potential α-glucosidase inhibitors, J Mol Struct 1274 (2023). https://doi.org/10.1016/j.molstruc.2022.134575.

[7] A. Sharma, N. Kumar, H.K. Gulati, R. Rana, Jyoti, A. Khanna, Muskan, J.V. Singh, P.M.S. Bedi, Antidiabetic potential of thiazolidinedione derivatives with efficient design, molecular docking, structural activity relationship, and biological activity: an update review (2021–2023), Mol Divers (2024). https://doi.org/10.1007/s11030-023-10793-6.

[8] K. Kajal, G. Singh, T. Pradhan, D. Bhurta, V. Monga, The medicinal perspective of 2,4-thiazolidinediones based ligands as antimicrobial, antitumor and antidiabetic agents: A review, Arch Pharm (Weinheim) 355 (2022). https://doi.org/10.1002/ardp.202100517.

[9] A. Paul, A. Sarkar, T. Banerjee, A. Maji, S. Sarkar, S. Paul, S. Karmakar, N. Ghosh, T.K. Maity, Structural and molecular insights of protein tyrosine phosphatase 1B (PTP1B) and its inhibitors as anti-diabetic agents, J Mol Struct 1293 (2023) 136258. https://doi.org/10.1016/j.molstruc.2023.136258.

[10] P. Seboletswe, N. Cele, P. Singh, Thiazolidinone-Heterocycle Frameworks: A Concise Review of Their Pharmacological Significance, ChemMedChem 18 (2023). https://doi.org/10.1002/cmdc.202200618.

[11] A. Singh, K. Singh, A. Sharma, K. Kaur, K. Kaur, R. Chadha, P.M.S. Bedi, Recent developments in synthetic α-glucosidase inhibitors: A comprehensive review with structural and molecular insight, J Mol Struct 1281 (2023) 135115. https://doi.org/10.1016/j.molstruc.2023.135115.

[12] B. Liang, J. Li, S. Wu, X. Kou, T. Liu, X. Xu, Novel coumarin-thiazolidine-2,4-dione hybrids as potential α-glucosidase inhibitors: Synthesis and bioactivity evaluation, J Mol Struct 1322 (2025) 140481. https://doi.org/10.1016/j.molstruc.2024.140481.

[13] T.C. Nguyen, T.D. Le, T.K.D. Hoang, C.T. Pham, J.A. Alhaji, T.C. Nguyen, N.A. Truong, C.P. Dinh, L. Van Meervelt, Synthesis, evaluation of α-glucosidase inhibitory and antimicrobial activities of novel N-(5-arylidene-4-oxo-2-thioxothiazolidin-3-yl)-2-(naphthalen-1-yl)acetamide derivatives, J Mol Struct 1326 (2025) 141068. https://doi.org/10.1016/j.molstruc.2024.141068.

[14] S. Gharge, S.G. Alegaon, S. Jadhav, S.D. Ranade, R.S. Kavalapure, Design, synthesis, characterization and antidiabetic evaluation of 3,5-substituted thiazolidinediones: Evidenced by network pharmacology, Molecular docking, dynamic simulation, in vitro and in vivo assessment, European Journal of Medicinal Chemistry Reports 12 (2024) 100213. https://doi.org/10.1016/j.ejmcr.2024.100213.

[15] A. Olatunde, A. Mohammed, M.A. Ibrahim, N. Tajuddeen, M.N. Shuaibu, Vanillin: A food additive with multiple biological activities, European Journal of Medicinal Chemistry Reports 5 (2022) 100055. https://doi.org/10.1016/j.ejmcr.2022.100055.

[16] M. Naz, Z. Akhter, A. Zaka, B. Mirza, V. McKee, E. Ullah, M. Bolte, Structural characterization, biological evaluation and DNA interaction of some potential drugs based on bifunctional aldehyde functionality, European Journal of Chemistry 8 (2017) 195–202. https://doi.org/10.5155/eurjchem.8.3.195-202.1576.

[17] Y. Cong, Y. Wu, S. Shen, X. Liu, J. Guo, A Structure-Activity Relationship between the Veratrum Alkaloids on the Antihypertension and DNA Damage Activity in Mice, Chem Biodivers 17 (2020). https://doi.org/10.1002/cbdv.201900473.

[18] S. Venkataraman, J.K. Athilakshmi, D.S. Rajendran, P. Bharathi, V.V. Kumar, A comprehensive review of eclectic approaches to the biological synthesis of vanillin and their application towards the food sector, Food Sci Biotechnol 33 (2024) 1019–1036. https://doi.org/10.1007/s10068-023-01484-x.

[19] H.W. Huh, H.-Y. Song, Y.-G. Na, M. Kim, M. Han, T.M.A. Pham, H. Lee, J. Suh, S.-J. Lee, H.-K. Lee, C.-W. Cho, Bioanalytical Method Development and Validation of Veratraldehyde and Its Metabolite Veratric Acid in Rat Plasma: An Application for a Pharmacokinetic Study, Molecules 25 (2020) 2800. https://doi.org/10.3390/molecules25122800.

[20] Synthesis, anticancer activity, and docking study of N-acetyl pyrazolines from veratraldehyde, J Appl Pharm Sci 9 (2019) 14–20. https://doi.org/10.7324/JAPS.2019.90303.

[21] A.A.T. Suma, T.D. Wahyuningsih, D. Pranowo, Synthesis and Antibacterial Activities of N-Phenylpyrazolines from Veratraldehyde, Materials Science Forum 901 (2017) 124–132. https://doi.org/10.4028/www.scientific.net/MSF.901.124.

[22] L. Han, H. Wang, J. Cao, Y. Li, X. Jin, C. He, M. Wang, Inhibition mechanism of α-glucosidase inhibitors screened from Tartary buckwheat and synergistic effect with acarbose, Food Chem 420 (2023) 136102. https://doi.org/10.1016/j.foodchem.2023.136102.

[23] M. Dhameja, P. Gupta, Synthetic heterocyclic candidates as promising α-glucosidase inhibitors: An overview, Eur J Med Chem 176 (2019) 343–377. https://doi.org/10.1016/j.ejmech.2019.04.025.

[24] P. de Sena Murteira Pinheiro, L.S. Franco, T.L. Montagnoli, C.A.M. Fraga, Molecular hybridization: a powerful tool for multitarget drug discovery, Expert Opin Drug Discov 19 (2024) 451–470. https://doi.org/10.1080/17460441.2024.2322990.

[25] B. Liang, J. Li, S. Wu, X. Kou, T. Liu, X. Xu, Novel coumarin-thiazolidine-2,4-dione hybrids as potential α-glucosidase inhibitors: Synthesis and bioactivity evaluation, J Mol Struct 1322 (2025) 140481. https://doi.org/10.1016/j.molstruc.2024.140481.

[26] M. Feng, B. Liang, J. Sun, X. Min, S.-H. Wang, Y. Lu, X. Xu, Synthesis, anti-α-glucosidase activity, inhibition interaction, and anti-diabetic activity of novel cryptolepine derivatives, J Mol Struct 1310 (2024) 138311. https://doi.org/10.1016/j.molstruc.2024.138311.

[27] X. Min, S. Guo, Y. Lu, X. Xu, Investigation on the inhibition mechanism and binding behavior of cryptolepine to α-glucosidase and its hypoglycemic activity by multi-spectroscopic method, J Lumin 269 (2024) 120437. https://doi.org/10.1016/j.jlumin.2024.120437.

[28] B. Liang, D. Xiao, S.-H. Wang, X. Xu, Novel thiosemicarbazide-based β-carboline derivatives as α-glucosidase inhibitors: Synthesis and biological evaluation, Eur J Med Chem 275 (2024) 116595. https://doi.org/10.1016/j.ejmech.2024.116595.

[29] X.-Z. Wu, W.-J. Zhu, L. Lu, C.-M. Hu, Y.-Y. Zheng, X. Zhang, J. Lin, J.-Y. Wu, Z. Xiong, K. Zhang, X.-T. Xu, Synthesis and anti-α-glucosidase activity evaluation of betulinic acid derivatives, Arabian Journal of Chemistry 16 (2023) 104659. https://doi.org/10.1016/j.arabjc.2023.104659.

[30] A. Paul, A. Maji, A. Sarkar, S. Saha, P. Janah, T.K. Maity, Recent Approaches in the Synthesis of 5-Arylidene-2,4-thiazolidinedione Derivatives Using Knoevenagel Condensation, Mini Rev Org Chem 20 (2023) 5–34. https://doi.org/10.2174/1570193X19666220331155705.

[31] A. Aispuro-Pérez, J. López-Ávalos, F. García-Páez, J. Montes-Avila, L.A. Picos-Corrales, A. Ochoa-Terán, P. Bastidas, S. Montaño, L. Calderón-Zamora, U. Osuna-Martínez, J.I. Sarmiento-Sánchez, Synthesis and molecular docking studies of imines as α-glucosidase and α-amylase inhibitors, Bioorg Chem 94 (2020) 103491. https://doi.org/10.1016/j.bioorg.2019.103491.

[32] S. Ghannay, M. Snoussi, S. Messaoudi, A. Kadri, K. Aouadi, Novel enantiopure isoxazolidine and C-alkyl imine oxide derivatives as potential hypoglycemic agents: Design, synthesis, dual inhibitors of α-amylase and α-glucosidase, ADMET and molecular docking study, Bioorg Chem 104 (2020) 104270. https://doi.org/10.1016/j.bioorg.2020.104270.

[33] P.C. Agu, C.A. Afiukwa, O.U. Orji, E.M. Ezeh, I.H. Ofoke, C.O. Ogbu, E.I. Ugwuja, P.M. Aja, Molecular docking as a tool for the discovery of molecular targets of nutraceuticals in diseases management, Sci Rep 13 (2023) 13398. https://doi.org/10.1038/s41598-023-40160-2.

[34] A. Daina, O. Michielin, V. Zoete, SwissADME: A free web tool to evaluate pharmacokinetics, drug-likeness and medicinal chemistry friendliness of small molecules, Sci Rep 7 (2017). https://doi.org/10.1038/srep42717.

[35] Y. Myung, A.G.C. de Sá, D.B. Ascher, Deep-PK: deep learning for small molecule pharmacokinetic and toxicity prediction, Nucleic Acids Res (2024) gkae254. https://doi.org/10.1093/nar/gkae254.

[36] M. Li, J. Sun, B. Liang, X. Min, J. Hu, R. Wu, X. Xu, Thiazolidine-2,4-dione derivatives as potential α-glucosidase inhibitors: Synthesis, inhibitory activity, binding interaction and hypoglycemic activity, Bioorg Chem 144 (2024). https://doi.org/10.1016/j.bioorg.2024.107177.

[37] T.P. Kenakin, Chapter 6 - Enzymes as Drug Targets, in: Pharmacology in Drug Discovery and Development, 2017.

[38] O. Duman, S. Tunç, B. Kancı Bozoğlan, Characterization of the binding of metoprolol tartrate and guaifenesin drugs to human serum albumin and human hemoglobin proteins by fluorescence and circular dichroism spectroscopy, J Fluoresc 23 (2013). https://doi.org/10.1007/s10895-013-1177-y.

[39] U. Ghani, Re-exploring promising α-glucosidase inhibitors for potential development into oral anti-diabetic drugs: Finding needle in the haystack, Eur J Med Chem 103 (2015). https://doi.org/10.1016/j.ejmech.2015.08.043.

[40] X. Jiang, C. Lu, M. Tang, Z. Yang, W. Jia, Y. Ma, P. Jia, D. Pei, H. Wang, Nanotoxicity of Silver Nanoparticles on HEK293T Cells: A Combined Study Using Biomechanical and Biological Techniques, ACS Omega 3 (2018) 6770–6778. https://doi.org/10.1021/acsomega.8b00608.

CHAPTER-V

CONCLUSION AND FUTURE PERSPECTIVE

Conclusion and future perspective:

In summary, a series of cuminaldehyde-TZD hybrids were designed, synthesized and evaluated their α-glucosidase inhibitory activity by using *in vitro* study (**Figure 1**). Among all synthesized compounds, **compound 6i** and **compound 6h** with isobutyl and 4-bromobenzyl moiety on the N-position of the TZD ring exhibited the most potent α-glucosidase inhibitory activity, with IC_{50} values of 31.29 ± 0.94 and 68.86 ± 1.25 μM. The enzyme kinetic analysis demonstrated that **compound 6i** functions as a mixed-competitive inhibitor of α-glucosidase. The fluorescence quenching experiment demonstrated that **compound 6i** had a strong affinity for α-glucosidase, with the contact occurring via a static mechanism. The CD spectral data indicated that the relationship between **compound 6i** and α-glucosidase promoted conformational and microenvironmental alterations in α-glucosidase, as evidenced by the analysis of its α-helix, β-turn and random coil content, hence impacting the overall protein structure, characteristics, and catalytic activity. The molecular docking experiments of **compound 6i** and **compound 6h** indicated that compounds have a better binding affinity for α-glucosidase (PDB: 5NN8). The carbonyl group of **compound 6i** interacted with hydrogen bonding with the amino acid residues of LEU677 and LEU678. Similarly, the *in silico* absorption, distribution, metabolism, excretion, and toxicity (ADMET) profile of **compound 6i** and **compound 6h** suggests their satisfactory oral drug-likeness without toxic effects. The cell viability showed that **compound 6i** exhibited low cytotoxic activity against HEK-293 cells. While the current work focuses on preliminary investigations, future studies will aim to explore the hypoglycemic activity of the potent compound in diabetic animal models. These studies will provide deeper insights into its therapeutic potential for managing diabetes.

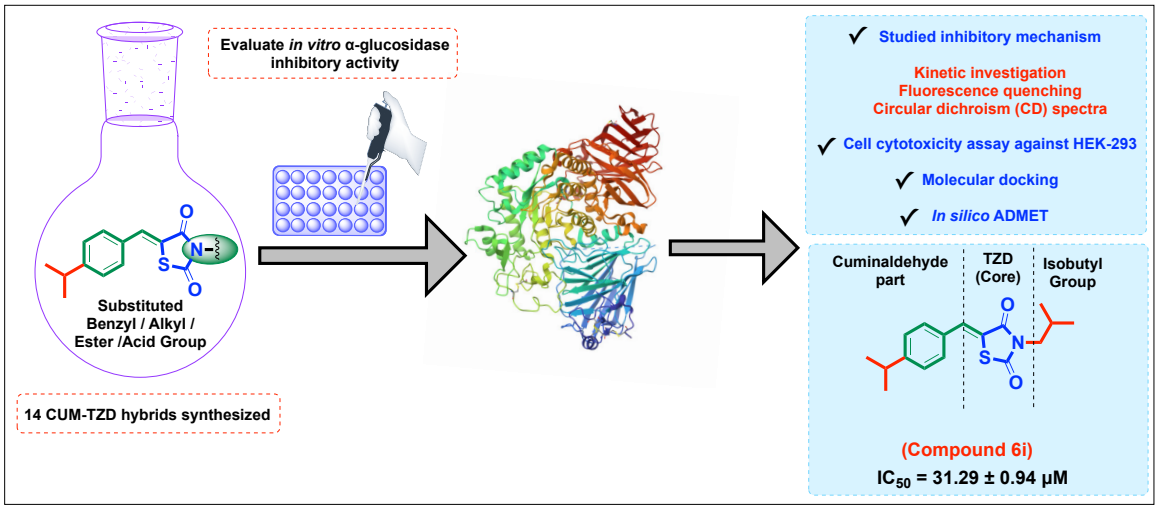

Figure 1: Graphical representation of synthesis, single crystal XRD, *in vitro* evaluation, molecular docking and ADMET studies of cuminaldehyde-TZD hybrids as potential α-glucosidase inhibitors.

Similarly, a number of veratraldehyde-TZD (VD-TZD) hybrids were designed and synthesized, and their AGI activity was assessed through *in vitro* experimentation (**Figure 2**). Compound **6f** and compound **6g**, which contain a 3-chloro and 3,4-dichloro moiety on the N-position of the TZD ring, were found to have the most effective AGI action among all the compounds that were developed. Their IC_{50} values were 18.16 ± 0.41 and 19.59 ± 0.78 µM, respectively. According to the enzyme kinetic analysis, compound **6f** inhibits AG competitively. The fluorescence quenching experiment showed that compound **6f** had a strong affinity for AG and that a static mechanism was responsible for the contact. The CD spectral data showed that the interaction between compound **6f** and AG influenced the protein's overall structure, properties, and catalytic activity by promoting conformational and microenvironmental changes in AG, as demonstrated by the analysis of its α-helix, β-turn, and random coil content. The molecular docking studies of compound **6f** shown that the compounds have superior binding affinity for AG (PDB: 5NN8). The amino acid residues of LEU677, LEU678, and ARG411 were in contact with the carbonyl group of

compound **6f** by hydrogen bonding. Cell viability assays indicated that compound **6f** had minimal cytotoxicity against HEK-293 cells at a concentration of 3.9 µM. The *in silico* ADMET profiles of compounds **6f** and **6g** indicate their acceptable oral drug-likeness and absence of harmful effects, meeting the drug-likeness criteria. Consequently, these compounds may represent promising candidates for the development of novel anti-diabetic agents. This study concentrates on initial findings, while subsequent research will seek to examine the hypoglycemic effects of the active compound in diabetic animal models. These investigations will yield profound insights into its therapeutic efficacy for diabetes management.

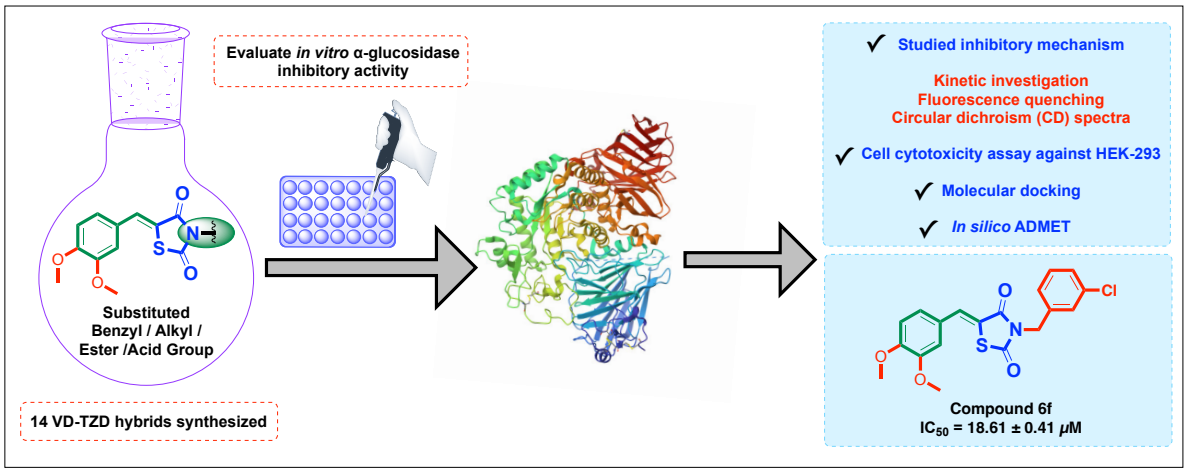

Figure 2: Graphical representation of synthesis, crystal structure, and *in vitro* evaluation of newer 2,4-thiazolidinedione hybrids as α-glucosidase inhibitors.

APPENDICES

PUBLICATIONS & CERTIFICATES

Journal of Molecular Structure 1331 (2025) 141510

Contents lists available at ScienceDirect

Journal of Molecular Structure

journal homepage: www.elsevier.com/locate/molstr

Synthesis, single crystal XRD, *in vitro* evaluation, molecular docking and ADMET studies of cuminaldehyde-thiazolidine-2,4-dione hybrids as potential α-glucosidase inhibitors

Abhik Paul [a,b], Sai Satyaprakash Mishra [a,1], Arnab Sarkar [a,1], Rudranil Bhowmik [a], Akash De [a], Avik Maji [a], Uday Shee [c], Ajeya Samanta [a], Sanmoy Karmakar [a], Tapan Kumar Maity [a,*]

[a] Department of Pharmaceutical Technology, Jadavpur University, West Bengal, Kolkata 700032, India
[b] Department of Pharmaceutical Technology, NSHM Knowledge Campus, Kolkata- Group of Institutions, 124, 60, BL Saha Road, Kolkata 700053, India
[c] Department of Chemistry, Jadavpur University, Kolkata 700032, West Bengal, India

ARTICLE INFO

Keywords:
Thiazolidinedione (TZD)
Cuminaldehyde
α-glucosidase inhibitors
Type 2 diabetes
Circular dichroism spectra
Molecular docking
ADMET

ABSTRACT

In order to find effective α-glucosidase inhibitors, a series of cuminaldehyde-TZD hybrids were designed, synthesized and evaluated for their α-glucosidase inhibitory activity by using *in vitro* study. The synthesized molecules (**6a-6h, 6i-6l**, and **6m**) were characterized by ^{1}H NMR, ^{13}C NMR, mass spectrometry, FT-IR, and x-ray crystallographic analysis. Compared to positive control acarbose ($IC_{50} = 61.24 \pm 1.81$ μM), few compounds (**6b, 6i, 6j,** and **6h**) showed good α-glucosidase inhibitory activity with IC_{50} values of $31.29 \pm 0.94 \sim 196.75 \pm 1.02$ μM. From all the synthetic compounds, compound **6i** demonstrated promising α-glucosidase inhibitory activity with an IC_{50} value of 31.29 ± 0.94 μM. Similarly, enzyme kinetic study demonstrated that compound **6i** involves both competitive and uncompetitive inhibition mechanisms with a steady-state inhibition constant (*Ki*) value of 16.87 μM. Circular dichroism spectra further substantiated that the binding of compound **6i** altered the secondary structure of α-glucosidase. The molecular docking experiments of compound **6i** and compound **6h** indicated that compounds have a better binding affinity for α-glucosidase (PDB ID: 5NN8), as seen from docking scores -6.54 and -6.19 kcal/mol. The carbonyl group of compound **6i** interacted with hydrogen bonding with the amino acid residues of LEU677 and LEU678. Similarly, the *in-silico* absorption, distribution, metabolism, excretion, and toxicity (ADMET) profile of compound **6i** and compound **6h** suggests their satisfactory oral drug-likeness without toxic effects. Cell cytotoxicity assay showed compound **6i** had low cytotoxic activity against HEK-293 cell lines. Therefore, it can be concluded that both compound **6i** and compound **6h** serve as potent lead compounds for the advancement of α-glucosidase inhibitors in the treatment of T2DM.

1. Introduction

Diabetes mellitus (DM) is a chronic, progressive condition characterized by hyperglycemia and long-term microvascular and macrovascular consequences. It impacts millions globally and is projected to affect 700 million by 2045 [1–3]. Patients with type 2 diabetes (T2D) utilize hypoglycemic agents to manage postprandial hyperglycemia. DM results in significant health complications, including cardiovascular illnesses, hypertension, obesity, renal disorders, and visual impairment [4–9]. α-glucosidase inhibitors serve as a treatment to manage DM by obstructing the digestion of dietary carbohydrates, which generate monosaccharide units that subsequently enter the circulation.

* Corresponding author at: Department of Pharmaceutical Technology, Synthetic and Natural Product Research Laboratory, Jadavpur University, Kolkata 700 032, West Bengal, India.
E-mail addresses: abhik.jupharm@gmail.com, abhikp.pharma.rs@jadavpuruniversity.in (A. Paul), saisatyaprakash.19@gmail.com (S.S. Mishra), sarkar.arnab54@yahoo.com (A. Sarkar), rudranilz@yahoo.in (R. Bhowmik), akashonway100@gmail.com (A. De), avikmaji12@gmail.com, avikmaji.pharma.rs@jadavpuruniversity.in (A. Maji), udayshee410@gmail.com (U. Shee), ajeyas.pharma.rs@jadavpuruniversity.in (A. Samanta), sanmoy.karmakar@jadavpuruniversity.in (S. Karmakar), tapan.maity@jadavpuruniversity.in (T.K. Maity).
[1] Contributed equally.

https://doi.org/10.1016/j.molstruc.2025.141510
Received 25 November 2024; Received in revised form 16 January 2025; Accepted 20 January 2025
Available online 21 January 2025

Phytochem Rev
https://doi.org/10.1007/s11101-025-10069-x

REVIEW ARTICLE

Exploring the therapeutic potentials of cuminaldehyde: a comprehensive review of biological activities, mechanisms, and novel delivery systems

Abhik Paul · Sai Satyaprakash Mishra · Avik Maji · Ajeya Samanta · Sourin Nahar · Tapan Kumar Maity

Received: 7 February 2024 / Accepted: 2 January 2025

Abstract Cuminaldehyde (CUM) is a bioactive compound majorly present in the seeds of *Cuminum cyminum*. The plant *C. cyminum* is the hub of numerous bioactive compounds that have various pharmacological significance, and CUM is one of them. Various extraction and purification methodologies have been developed to isolate CUM from plant origins and study its effectiveness in treating a range of disorders. The present study comprises recent pharmacological properties of CUM that have been reported to exert various pharmacological properties, such as anti-microbial, anti-neurodegenerative, anti-inflammatory, anti-cancer, anti-diabetic, anti-obesity, and anti-parasitic. Additionally, CUM improved the effects of other anti-microbial drugs, including vancomycin, tobramycin, and ciprofloxacin. Similarly, we have outlined many targeted delivery systems that have been used to deliver CUM to the disease-specific target system, such as microemulsions, inclusion complexes, mesoporous silica nanoparticles, and smart hydrogel. The absorption, distribution, metabolism, excretion, and toxicity (ADMET) profiles of CUM have also been predicted using SwissADME and Deep-PK. Moreover, this review provides a complete overview of CUM's isolation and purification processes, its synthetic analogues, biological activities with mechanisms of action, novel delivery systems, and pK-pD profile with *in silico* ADMET parameters. All of this will be beneficial for researchers assessing CUM's pre-clinical and clinical outcomes in the near future.

A. Paul · S. S. Mishra · A. Maji · A. Samanta · T. K. Maity (✉)
Synthetic and Natural Product Research Laboratory, Department of Pharmaceutical Technology, Jadavpur University, Kolkata, West Bengal 700032, India
e-mail: tapan.maity@jadavpuruniversity.in; jutkmaity@yahoo.com

A. Paul
e-mail: abhik.jupharm@gmail.com; abhikp.pharma.rs@jadavpuruniversity.in

S. S. Mishra
e-mail: saisatyaprakash.19@gmail.com

A. Maji
e-mail: avikmaji12@gmail.com; avikmaji.pharma.rs@jadavpuruniversity.in

A. Samanta
e-mail: ajeyas.pharma.rs@jadavpuruniversity.in

A. Paul
Department of Pharmaceutical Technology, NSHM Knowledge Campus, Kolkata-Group of Institutions, 124, 60, BL Saha Road, Kolkata 700053, India

S. Nahar
Department of Pharmaceutical Chemistry, School of Pharmacy, Techno India University, Kolkata, West Bengal 700091, India
e-mail: sourinnahar1913@gmail.com

Published online: 22 January 2025

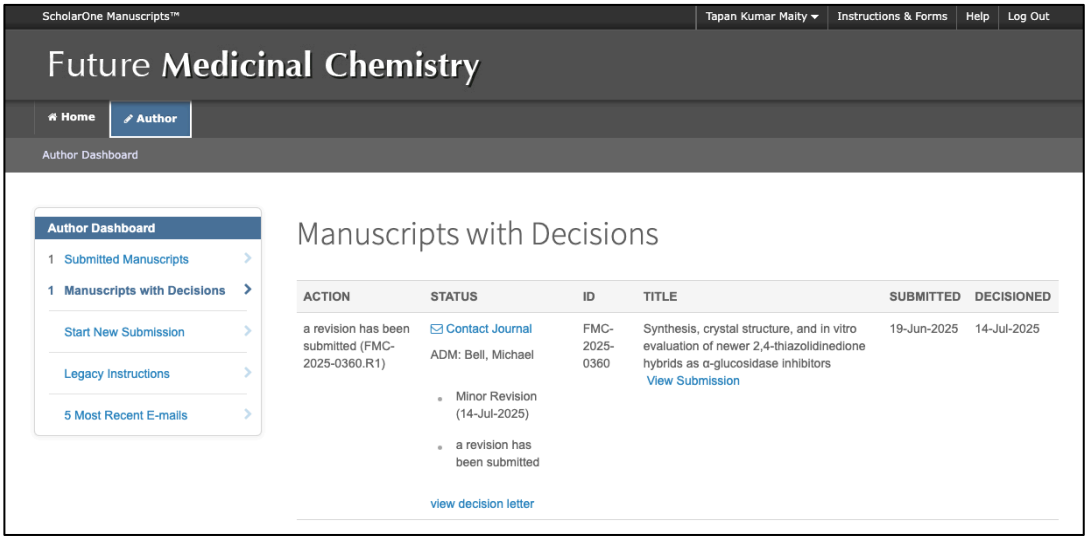
ScholarOne Manuscripts™
Tapan Kumar Maity
Instructions & Forms
Help
Log Out
Future Medicinal Chemistry
Home
Author
Author Dashboard
Author Dashboard
1 Submitted Manuscripts
1 Manuscripts with Decisions
Start New Submission
Legacy Instructions
5 Most Recent E-mails
Manuscripts with Decisions
ACTION
STATUS
ID
TITLE
SUBMITTED
DECISIONED
a revision has been submitted (FMC-2025-0360.R1)
Contact Journal
ADM: Bell, Michael
Minor Revision (14-Jul-2025)
a revision has been submitted
view decision letter
FMC-2025-0360
Synthesis, crystal structure, and in vitro evaluation of newer 2,4-thiazolidinedione hybrids as α-glucosidase inhibitors
View Submission
19-Jun-2025
14-Jul-2025

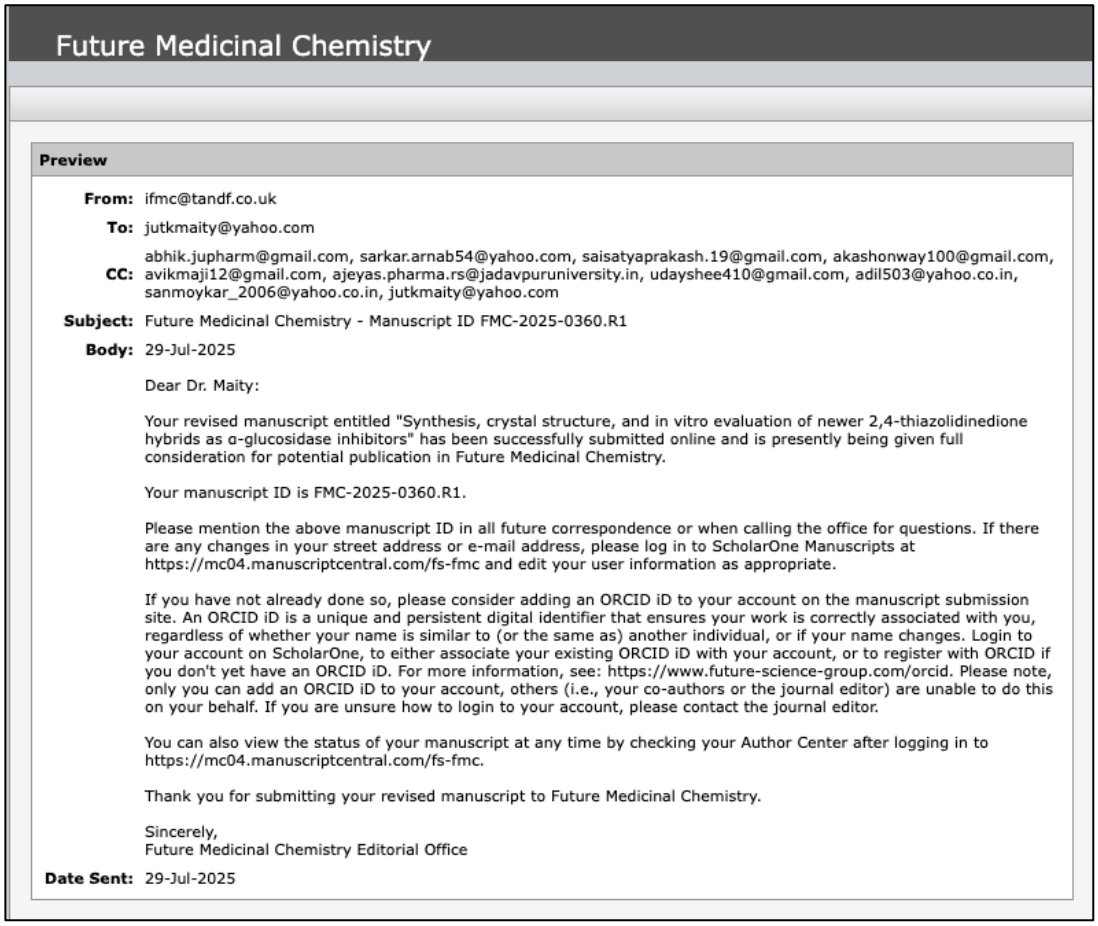
Future Medicinal Chemistry
Preview
From: ifmc@tandf.co.uk
To: jutkmaity@yahoo.com
CC: abhik.jupharm@gmail.com, sarkar.arnab54@yahoo.com, saisatyaprakash.19@gmail.com, akashonway100@gmail.com, avikmaji12@gmail.com, ajeyas.pharma.rs@jadavpuruniversity.in, udayshee410@gmail.com, adil503@yahoo.co.in, sanmoykar_2006@yahoo.co.in, jutkmaity@yahoo.com
Subject: Future Medicinal Chemistry - Manuscript ID FMC-2025-0360.R1
Body: 29-Jul-2025
Dear Dr. Maity:
Your revised manuscript entitled "Synthesis, crystal structure, and in vitro evaluation of newer 2,4-thiazolidinedione hybrids as α-glucosidase inhibitors" has been successfully submitted online and is presently being given full consideration for potential publication in Future Medicinal Chemistry.
Your manuscript ID is FMC-2025-0360.R1.
Please mention the above manuscript ID in all future correspondence or when calling the office for questions. If there are any changes in your street address or e-mail address, please log in to ScholarOne Manuscripts at https://mc04.manuscriptcentral.com/fs-fmc and edit your user information as appropriate.
If you have not already done so, please consider adding an ORCID iD to your account on the manuscript submission site. An ORCID iD is a unique and persistent digital identifier that ensures your work is correctly associated with you, regardless of whether your name is similar to (or the same as) another individual, or if your name changes. Login to your account on ScholarOne, to either associate your existing ORCID iD with your account, or to register with ORCID if you don't yet have an ORCID iD. For more information, see: https://www.future-science-group.com/orcid. Please note, only you can add an ORCID iD to your account, others (i.e., your co-authors or the journal editor) are unable to do this on your behalf. If you are unsure how to login to your account, please contact the journal editor.
You can also view the status of your manuscript at any time by checking your Author Center after logging in to https://mc04.manuscriptcentral.com/fs-fmc.
Thank you for submitting your revised manuscript to Future Medicinal Chemistry.
Sincerely,
Future Medicinal Chemistry Editorial Office
Date Sent: 29-Jul-2025

European Journal of Medicinal Chemistry 264 (2024) 115990

Contents lists available at ScienceDirect

European Journal of Medicinal Chemistry

journal homepage: www.elsevier.com/locate/ejmech

Review article

Synthetic GPR40/FFAR1 agonists: An exhaustive survey on the most recent chemical classes and their structure-activity relationships

Abhik Paul [a], Sourin Nahar [a,1], Pankaj Nahata [a,1], Arnab Sarkar [a,b], Avik Maji [a], Ajeya Samanta [a], Sanmoy Karmakar [a,b], Tapan Kumar Maity [a,*]

[a] Department of Pharmaceutical Technology, Jadavpur University, West Bengal, Kolkata, 700 032, India
[b] Bioequivalence Study Centre, Department of Pharmaceutical Technology, Jadavpur University, Kolkata, 700032, India

ARTICLE INFO

Keywords:
GPR40 agonists
Free fatty acid receptor 1
Type 2 diabetes mellitus
Structure-activity relationships
Chemico-biological interactions

ABSTRACT

Free fatty acid receptor 1 (FFAR1 or GPR40) is a potential target for treating type 2 diabetes mellitus (T2DM) and related disorders that have been extensively researched for many years. GPR40/FFAR1 is a promising anti-diabetic target because it can activate insulin, promoting glucose metabolism. It controls T2DM by regulating glucose levels in the body through two separate mechanisms: glucose-stimulated insulin secretion and incretin production. In the last few years, various synthetic GPR40/FFAR1 agonists have been discovered that fall under several chemical classes, viz. phenylpropionic acid, phenoxyacetic acid, and dihydrobenzofuran acetic acid. However, only a few synthetic agonists have entered clinical trials due to various shortcomings like poor efficacy, low lipophilicity and toxicity issues. As a result, pharmaceutical firms and research institutions are interested in developing synthetic GPR40/FFAR1 agonists with superior effectiveness, lipophilicity, and safety profiles. This review encompasses the most recent research on synthetic GPR40/FFAR1 agonists, including their chemical classes, design strategies and structure-activity relationships. Additionally, we have emphasised the structural characteristics of the most potent GPR40/FFAR1 agonists from each chemical class of synthetic derivatives and analysed their chemico-biological interactions. This work will hopefully pave the way for developing more potent and selective synthetic GPR40/FFAR1 agonists for treating T2DM and related disorders.

1. Introduction

Free fatty acid receptor 1 (FFAR1), also known as GPR40, is a member of the family of G protein-coupled receptors (GPCRs) that are highly expressed in pancreatic β-cells and activated by long-chain fatty acids (LCFAs) [1–3]. LCFAs are a type of fat molecule that is commonly found in foods like meat, dairy, and vegetable oils. LCFAs mainly activate two receptors, known as GPR40/FFAR1 and GPR120/FFAR4. The GPR40 receptor signals towards increased insulin release from glucose-stimulated β-cells when free fatty acids (FFAs) are present. The GPR40/FFAR1 receptor controls insulin release in response to glucose and FFAs [4,5]. GPR40 also plays a role in regulating the release of incretins in response to FFAs. The study suggests that there is a conserved role for Ipf1/Pdx1 and GPR40 in the secretion of hormones that regulate glucose and overall energy homeostasis [6]. Similarly, GPR40/FFAR1 regulates glucose homeostasis via two distinct mechanisms, namely glucose-stimulated insulin secretion and incretin production [7–11]. Due to this fact, GPR40 agonists have the potential to be utilised for the management of type 2 diabetes mellitus (T2DM) and related disorders, including insulin resistance, obesity, cardiovascular disease, and dyslipidemia [12]. Similarly, recent research shows us that the GPR40 agonist can be explored and developed for therapeutic reasons in diseases other than diabetes, such as neurological disorders, infections, cancer, inflammation, and allergies.

T2DM is one of the most serious problems among the world's most common metabolic conditions, and cardiovascular diseases, nephropathy, neuropathy, and retinopathy are expected consequences [13–15]. According to the International Diabetes Federation (IDF), there are currently 537 million diabetics worldwide, with 783 million diabetics

* Corresponding author. Department of Pharmaceutical Technology, Synthetic and Natural Product Research Laboratory, Jadavpur University, Kolkata, 700 032, West Bengal, India.
E-mail addresses: abhik.jupharm@gmail.com, abhikp.pharma.rs@jadavpuruniversity.in (A. Paul), sourinnahar1913@gmail.com (S. Nahar), pankajnahata1996@gmail.com (P. Nahata), sarkar.arnab54@yahoo.com (A. Sarkar), avikmaji.pharma.rs@jadavpuruniversity.in (A. Maji), ajeyas.pharma.rs@jadavpuruniversity.in (A. Samanta), sanmoy.karmakar@jadavpuruniversity.in (S. Karmakar), tapan.maity@jadavpuruniversity.in, jutkmaity@yahoo.com (T.K. Maity).
[1] Authors have equal contributions.

https://doi.org/10.1016/j.ejmech.2023.115990
Received 24 September 2023; Received in revised form 18 November 2023; Accepted 20 November 2023
Available online 25 November 2023

Journal of Molecular Structure 1293 (2023) 136258

Contents lists available at ScienceDirect

Journal of Molecular Structure

journal homepage: www.elsevier.com/locate/molstr

Structural and molecular insights of protein tyrosine phosphatase 1B (PTP1B) and its inhibitors as anti-diabetic agents

Abhik Paul [a], Arnab Sarkar [a,b], Tanmoy Banerjee [a], Avik Maji [a], Shrabanti Sarkar [a], Sourav Paul [c], Sanmoy Karmakar [a,b], Nilanjan Ghosh [a], Tapan Kumar Maity [a,*]

[a] Department of Pharmaceutical Technology, Jadavpur University, West Bengal, Kolkata 700 032, India
[b] Bioequivalence Study Centre, Department of Pharmaceutical Technology, Jadavpur University, Kolkata, India
[c] Department of Biotechnology, National Institute of Technology, Durgapur 713 209, India

ARTICLE INFO

Keywords:
Type 2 diabetes mellitus (T2DM)
Structural features
PTP1B
Natural inhibitors
Synthetic inhibitors
Protein-inhibitor interactions

ABSTRACT

Diabetes mellitus (DM), especially type 2 diabetes mellitus (T2DM), is the most disruptive metabolic disorder globally affecting human health. To effectively manage this medical condition, the quest for a new medication to treat T2DM continues. The emergence of medication resistance to the insulin and leptin receptors leads to significant concerns. The compounds which can tackle this resistance issue may be helpful in the therapeutic management of T2DM. Protein tyrosine phosphatase 1B (PTP1B) is a promising therapeutic target for treating T2DM. Diverse natural bioactive and synthetic molecules have offered great opportunities for developing lead molecules with significant inhibitory action in *in vitro* and *in vivo* against PTP1B. Numerous PTP1B inhibitors have recently been found from natural sources or synthesized by organic synthesis and shown effectiveness for treating T2DM. This review comprehensively updates the latest research findings in developing potent natural and synthetic PTP1B inhibitors over the past six years, including structural features of PTP1B, classification of inhibitors, biological effects, and protein-inhibitors interaction modalities. These studies will be highly helpful for the medicinal chemists working in this field to design and develop novel selective PTP1B inhibitors as anti-diabetic agents in the future.

Abbreviations

Akt	Tyrosine kinase b
C2C12	Immortalized mouse myoblast cell line
DM	Diabetes mellitus
ER	Endoplasmic reticulum
ERK	Extracellular signal regulated kinase
EtOAc	Ethyl acetate
HO-1	Heme oxygenase-1
hr	Hour
IC_{50}	Half maximal inhibitory concentration
IR	Insulin receptor
IRK	Insulin receptor kinase
IRS-1	Insulin receptor substrate-1
JAK2	Janus kinase 2
K_i	Inhibition constant
LAR	Leukocyte common antigen-related
LepR	Leptin receptor
mL	Mililiter
Nrf2	Nuclear factor erythroid-2-related factor 2
ObR	Astrocyte leptin receptor
°C	Degree celsius
PAMPA	Parallel artificial membrane permeability assay
PI3K	Phosphatidylinositol-3-kinase
PKC	Protein kinase C
pNPP	p-nitrophenyl phosphate
PTMs	Posttranslational modifications
PTP	Protein tyrosine phosphatase
PTP1B	Protein tyrosine phosphatase 1B
RH	Rohitukine
SAR	Structure-activity relationship
Ser	Serine
SH3	Src homology 3
SHP-2	Src homology-2 domain-containing protein tyrosine

* Corresponding author at: Department of Pharmaceutical Technology, Synthetic and Natural Product Research Laboratory, Jadavpur University, Kolkata 700 032, West Bengal, India.
E-mail address: jutkmaity@yahoo.com (T.K. Maity).

https://doi.org/10.1016/j.molstruc.2023.136258
Received 17 May 2023; Received in revised form 19 July 2023; Accepted 20 July 2023
Available online 20 July 2023

Send Orders for Reprints to reprints@benthamscience.net

Mini-Reviews in Organic Chemistry, 2023, *20*, 5-34

MINI-REVIEW ARTICLE

Recent Approaches in the Synthesis of 5-Arylidene-2,4-thiazolidinedione Derivatives Using Knoevenagel Condensation

Abhik Paul[1], Avik Maji[1], Arnab Sarkar[1], Sanjukta Saha[1], Pritha Janah[1] and Tapan Kumar Maity[1,*]

[1]*Department of Pharmaceutical Technology, Jadavpur University, West Bengal, Kolkata-700032, India*

ARTICLE HISTORY

Received: August 12, 2021
Revised: December 08, 2021
Accepted: January 26, 2022

DOI:
10.2174/1570193X19666220331155705

Abstract: 5-Arylidene-2,4-thiazolidinedione (5-A-TZD) is an emerging precursor molecule in medicinal chemistry for discovering multifunctional therapeutic agents. For synthesizing this precursor molecule, Knoevenagel Condensation (KC) is one of the most excellent tools in modern organic chemistry. The 5-A-TZD framework has a variety of therapeutic functions such as antidiabetic, anticancer, antimicrobial, and anti-inflammatory. As a result, several approaches and methods of KC have been established for the synthesis of this multifunctional precursor. However, the use of highly corrosive catalysts, prolonged reaction times, by-products formation, and poor product yields are the main drawbacks in 5-A-TZDs synthesis *via* KC. Therefore, several authors have been successfully established fast, effective, and environmentally sustainable protocols of KC using organic catalysts, inorganic catalysts, heterogeneous solid catalysts, ionic liquids (ILs), and bio-catalysts to synthesize 5-A-TZD derivatives with high conversion yield and selectivity. In this review, we have summarized the recent approaches for synthesizing 5-A-TZDs *via* KC and their therapeutic application as a precursor molecule in medicinal chemistry.

Keywords: 5-Arylidene-2,4-thiazolidinediones (5-A-TZDs), Knoevenagel condensation (KC), Synthetic methods, Organic catalysts, Ionic liquids (ILs), Heterogeneous solid catalysts, Inorganic catalysts, Bio-catalysts.

1. INTRODUCTION

5-Arylidene-2,4-thiazolidinedione (5-A-TZD) is a new class of substituted heterocycle that has been obtained by substitution of an arylidene group at 5-position of the respective parent 2,4-thiazolidinedione (TZD) moiety (Fig. **1**) [1]. TZD has also been studied for an extended period due to its synthetic diversity, medicinal relevance, and small heterocyclic rings with sulfur and nitrogen atoms. In the area of medicinal chemistry, 5-A-TZD derivatives have received special attention in recent years. Several pharmacological activities such as hypoglycaemic [2], antimicrobial and antiviral [3], analgesic [4], anti-inflammatory [5], antimalarial [6], hypolipidemic [7], antileishmanial [8], and anticancer [9] have been recorded for the 5-A-TZD and proved as a versatile scaffold [10]. Therefore, the preparation of 5-A-TZDs has become increasingly important. Several synthetic methods have been developed to obtain these derivatives, but Knoevenagel condensation (KC) is one of the most widely used synthetic protocols in medicinal chemistry research. KC of aromatic aldehydes with TZD mainly yield 5-A-TZD [11].

KC reaction is a reliable, efficient, versatile, and convenient method for carbon-carbon bond formation, and it is widely used in both industry and academic institutions. The end product is an α,β-unsaturated compound that builds naturally occurring compounds [12]. KC has been used for the synthesis of several organic molecules like coumarin derivatives [13, 14], arylidinemalononitrile derivatives [15], pharmaceutical chemicals [16], antibiotics [17], and chemosensors [18]. KC is also valuable for developing clinical drugs and their derivatives, such as pioglitazone and rosiglitazone, epalrestat, sulindac, nifedipine, and atorvastatin [19]. Because of such exceptional features of KC, medicinal chemists have always shown keen interest in using this simple, easy, and effective tool for producing 5-A-TZD. In the literature, several bases, organic catalysts, inorganic catalysts, heterogeneous solid catalysts, ionic liquids (ILs), and bio-catalysts, have been explored under specific reaction conditions to accelerate the KC for synthesizing 5-A-TZD derivatives. However, some researchers also developed microwave (MW), ultrasound, and grinding-assisted synthetic

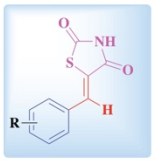

Fig. (1). General structure of 5-A-TZD.

*Address correspondence to this author at the Department of Pharmaceutical Technology, Synthetic and Natural Product Research Laboratory, Jadavpur University, Kolkata-700032, West Bengal, India;
E-mail: jutkmaity@yahoo.com

1875-6298/23 $65.00+.00

CHAPTER

18

Potential application of secondary metabolites in diabetes

Abhik Paul[1,2], *Arnab Sarkar*[2], *Ajeya Samanta*[2], *Akash De*[2], *Sai Satyaprakash Mishra*[2], *Rinki Prasad Bhagat*[2], *Ankita Sadhukhan*[2], *Enjamul Hoque*[2], *Avik Maji*[2], *Sanmoy Karmakar*[2], *and Tapan Kumar Maity*[2]

[1]Department of Pharmaceutical Technology, NSHM Knowledge Campus, Kolkata-Group of Institutions, Kolkata, West Bengal, India [2]Department of Pharmaceutical Technology, Jadavpur University, Kolkata, West Bengal,India

18.1 Introduction

Diabetes mellitus (DM) is a metabolic illness causing hyperglycemia due to impaired glucose metabolism and reduced insulin secretion. It affects around 400 million people globally and is a major public health concern (Kerru et al., 2018; Padhi et al., 2020). Type 2 diabetes mellitus (T2DM) is more prevalent and is primarily caused by dietary and social factors. The worldwide rate of diabetes is projected to attain 366 million by 2030 among those aged 65 and older, with a propensity for inactivity serving as a significant factor (Paul et al., 2023; Wild et al., 2004). It is characterized by insulin resistance or diminished sensitivity, leading to a reduction in the cell's capacity to uptake glucose from the bloodstream due to an impaired insulin signal (Fig. 18.1). Fig. 18.2 illustrates the potential involvement of many "ominous octet" pathways in the pathophysiology of T2DM. Conventional treatments for T2DM include sulfonylureas, biguanides, peroxisome proliferator-activated receptor gamma (PPARγ) agonists, and α-glucosidase inhibitors. However, these drugs have disadvantages such as severe hypoglycemia, increased body weight, reduced therapeutic efficacy, and low potency. Managing T2DM requires a patient-dependent strategy that optimizes glycemic management with current pharmaceutical choices. Early and appropriate treatment is crucial, as patients with newly diagnosed T2DM have lower risks of microvascular complications. Prompt therapy escalation is essential to avoid long-term consequences, but it is often not done, leading to inadequate glycemic

Secondary Metabolites in Stress and Disease Management
DOI: https://doi.org/10.1016/B978-0-443-33959-2.00020-4

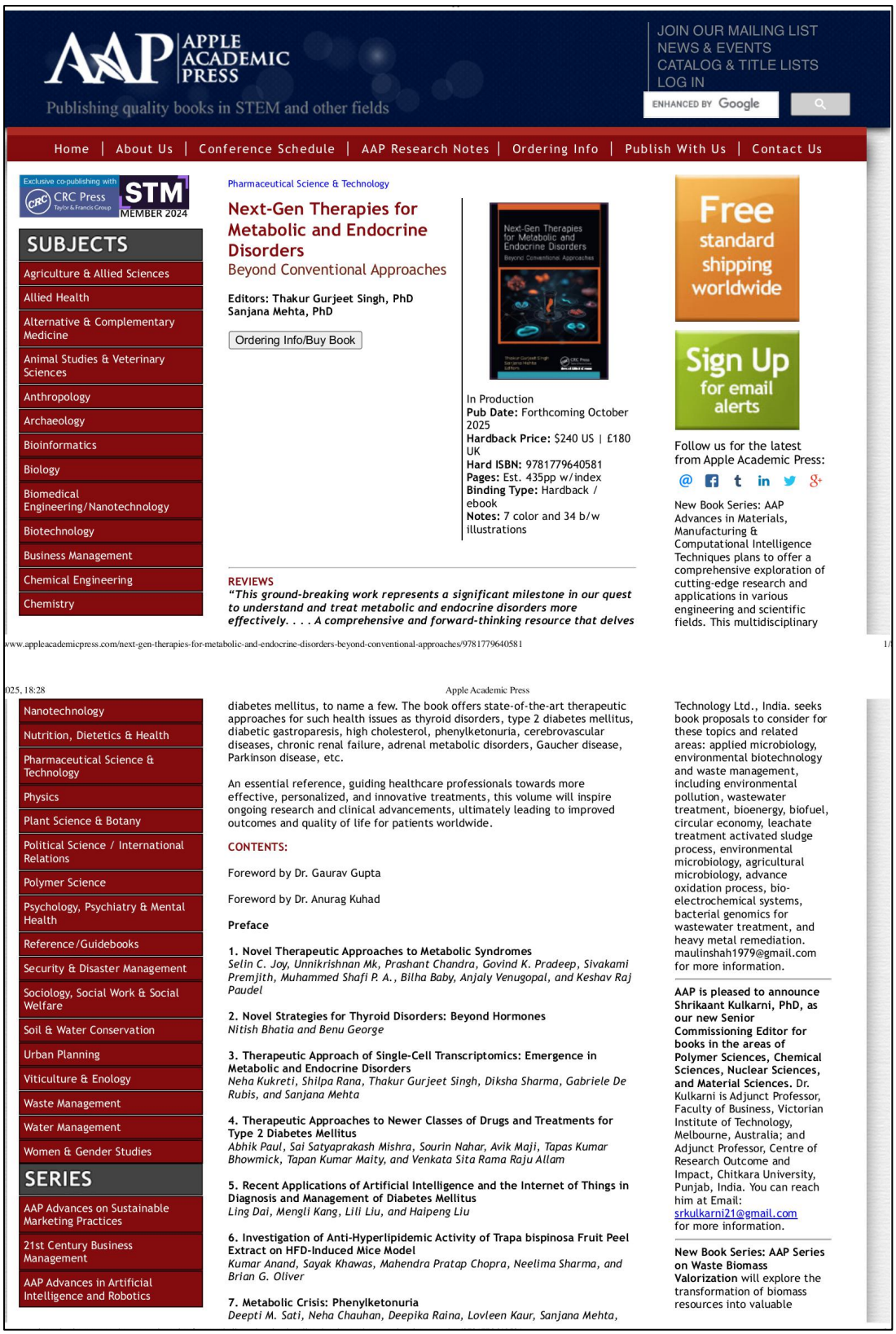

AAP APPLE ACADEMIC PRESS
Publishing quality books in STEM and other fields

JOIN OUR MAILING LIST
NEWS & EVENTS
CATALOG & TITLE LISTS
LOG IN
ENHANCED BY Google

Home | About Us | Conference Schedule | AAP Research Notes | Ordering Info | Publish With Us | Contact Us

Exclusive co-publishing with CRC Press Taylor & Francis Group STM MEMBER 2024

SUBJECTS
- Agriculture & Allied Sciences
- Allied Health
- Alternative & Complementary Medicine
- Animal Studies & Veterinary Sciences
- Anthropology
- Archaeology
- Bioinformatics
- Biology
- Biomedical Engineering/Nanotechnology
- Biotechnology
- Business Management
- Chemical Engineering
- Chemistry
- Nanotechnology
- Nutrition, Dietetics & Health
- Pharmaceutical Science & Technology
- Physics
- Plant Science & Botany
- Political Science / International Relations
- Polymer Science
- Psychology, Psychiatry & Mental Health
- Reference/Guidebooks
- Security & Disaster Management
- Sociology, Social Work & Social Welfare
- Soil & Water Conservation
- Urban Planning
- Viticulture & Enology
- Waste Management
- Water Management
- Women & Gender Studies

SERIES
- AAP Advances on Sustainable Marketing Practices
- 21st Century Business Management
- AAP Advances in Artificial Intelligence and Robotics

Pharmaceutical Science & Technology

Next-Gen Therapies for Metabolic and Endocrine Disorders
Beyond Conventional Approaches

Editors: Thakur Gurjeet Singh, PhD
Sanjana Mehta, PhD

Ordering Info/Buy Book

In Production
Pub Date: Forthcoming October 2025
Hardback Price: $240 US | £180 UK
Hard ISBN: 9781779640581
Pages: Est. 435pp w/index
Binding Type: Hardback / ebook
Notes: 7 color and 34 b/w illustrations

REVIEWS
"This ground-breaking work represents a significant milestone in our quest to understand and treat metabolic and endocrine disorders more effectively. . . . A comprehensive and forward-thinking resource that delves

New Book Series: AAP Advances in Materials, Manufacturing & Computational Intelligence Techniques plans to offer a comprehensive exploration of cutting-edge research and applications in various engineering and scientific fields. This multidisciplinary

diabetes mellitus, to name a few. The book offers state-of-the-art therapeutic approaches for such health issues as thyroid disorders, type 2 diabetes mellitus, diabetic gastroparesis, high cholesterol, phenylketonuria, cerebrovascular diseases, chronic renal failure, adrenal metabolic disorders, Gaucher disease, Parkinson disease, etc.

An essential reference, guiding healthcare professionals towards more effective, personalized, and innovative treatments, this volume will inspire ongoing research and clinical advancements, ultimately leading to improved outcomes and quality of life for patients worldwide.

CONTENTS:

Foreword by Dr. Gaurav Gupta

Foreword by Dr. Anurag Kuhad

Preface

1. Novel Therapeutic Approaches to Metabolic Syndromes
Selin C. Joy, Unnikrishnan Mk, Prashant Chandra, Govind K. Pradeep, Sivakami Premjith, Muhammed Shafi P. A., Bilha Baby, Anjaly Venugopal, and Keshav Raj Paudel

2. Novel Strategies for Thyroid Disorders: Beyond Hormones
Nitish Bhatia and Benu George

3. Therapeutic Approach of Single-Cell Transcriptomics: Emergence in Metabolic and Endocrine Disorders
Neha Kukreti, Shilpa Rana, Thakur Gurjeet Singh, Diksha Sharma, Gabriele De Rubis, and Sanjana Mehta

4. Therapeutic Approaches to Newer Classes of Drugs and Treatments for Type 2 Diabetes Mellitus
Abhik Paul, Sai Satyaprakash Mishra, Sourin Nahar, Avik Maji, Tapas Kumar Bhowmick, Tapan Kumar Maity, and Venkata Sita Rama Raju Allam

5. Recent Applications of Artificial Intelligence and the Internet of Things in Diagnosis and Management of Diabetes Mellitus
Ling Dai, Mengli Kang, Lili Liu, and Haipeng Liu

6. Investigation of Anti-Hyperlipidemic Activity of Trapa bispinosa Fruit Peel Extract on HFD-Induced Mice Model
Kumar Anand, Sayak Khawas, Mahendra Pratap Chopra, Neelima Sharma, and Brian G. Oliver

7. Metabolic Crisis: Phenylketonuria
Deepti M. Sati, Neha Chauhan, Deepika Raina, Lovleen Kaur, Sanjana Mehta,

Technology Ltd., India. seeks book proposals to consider for these topics and related areas: applied microbiology, environmental biotechnology and waste management, including environmental pollution, wastewater treatment, bioenergy, biofuel, circular economy, leachate treatment activated sludge process, environmental microbiology, agricultural microbiology, advance oxidation process, bio-electrochemical systems, bacterial genomics for wastewater treatment, and heavy metal remediation. maulinshah1979@gmail.com for more information.

AAP is pleased to announce Shrikaant Kulkarni, PhD, as our new Senior Commissioning Editor for books in the areas of Polymer Sciences, Chemical Sciences, Nuclear Sciences, and Material Sciences. Dr. Kulkarni is Adjunct Professor, Faculty of Business, Victorian Institute of Technology, Melbourne, Australia; and Adjunct Professor, Centre of Research Outcome and Impact, Chitkara University, Punjab, India. You can reach him at Email: srkulkarni21@gmail.com for more information.

New Book Series: AAP Series on Waste Biomass Valorization will explore the transformation of biomass resources into valuable

(https://www.appleacademicpress.com/next-gen-therapies-for-metabolic-and-endocrine-disorders-beyond-conventional-approaches/9781779640581)

ACS Chemistry for Life®

AMERICAN CHEMICAL SOCIETY

CERTIFICATE OF PRESENTATION

This is to certify that

Abhik Paul

presented research titled

Synthesis, single crystal XRD, in vitro evaluation, and molecular docking studies of dimethylamine containing thiazolidine-2,4-dione derivatives as α-glucosidase inhibitors

at

ACS Spring 2025
San Diego, CA & Virtual
March 23 - 27, 2025

Liz Huh

Liz Huh
Sr. Director, Meetings and Events

Program Area: MEDI
Session Type: Poster - In-person
Abstract Number: 4180521

Certificate No.:DDDLO/ORAL/AWARD/2024/02

CRKC

CIPET

CERTIFICATE OF PRESENTATION

This is to certify that,

Abhik Paul

of ***Department of pharmaceutical technology***

Jadavpur University, Kolkata

has been awarded ***Second position*** *in* ***Poster Presentation*** *on paper entitled*

Structural and molecular insights of protein tyrosine phosphatase 1B (PTP1B) and its inhibitors as antidiabetic agents

In International Conference on

"DRUG DISCOVERY, DEVELOPMENT AND LEAD OPTIMIZATION

Organized By

School of Pharmacy and Emerging Sciences,

Baddi University of Emerging Sciences & Technology, Baddi,

Himachal Pradesh, India

05-06 APRIL, 2024

Prof. (Dr) Tejvir Singh Professor Emeritus	Prof. (Dr) V. K. Kapoor Professor Emeritus	Prof. (Dr) T. R. Bhardwaj Advisor to Chancellor	Prof. (Dr) Ravinesh Mishra Chairperson

No. DBT/BIC/350
Department of Biotechnology, Government of India
Certificate
OF PARTICIPATION
Alkik Paul
Computer-Assisted Formulation Development and Toxicity Prediction: Notion and Significance in Drug Discovery and Development
DBT-SPONSORED BIOINFORMATICS CENTRE
Department of Pharmaceutical Sciences and Drug Research
Punjabi University, Patiala, Punjab 147002
3rd – 5th June, 2024
Dr. Gulshan Bansal
Head, DPSDR
Dr. Om Silakari
Principal Investigator, BIC
(Workshop Coordinator)
Dr. Bharti Sapra
Co-PI, BIC
(Organizing Secretary)
MML
Molecular Modeling Lab
PUNJABI UNIVERSITY PATIALA

CERTIFICATE

OF APPRECIATION

AWARDED TO

Prof./Dr./Mr./Ms. Abhik Paul

FOR HIS/HER ORAL/POSTER PRESENTATION IN THE

14TH INTERNATIONAL CONFERENCE ON

"NAVIGATING THE FUTURE OF HEALTHCARE: Trends, Challenges and Innovations"

ORGANISED BY

NSHM INSTITUTE OF HEALTH SCIENCES

NSHM KNOWLEDGE CAMPUS, KOLKATA ON 27TH AND 28TH SEPTEMBER, 2024

PROF. (DR.) SOUMENDRA NATH BANDYOPADHYAY
CHAIRPERSON,
iNATCONPH 2024

DR. APARNA DATTA
CONVENER,
iNATCONPH 2024

UGC SPONSORED TWO-DAY INTERNATIONAL CONFERENCE ON

COMMUNITY & MENTAL HEALTH:
CONNECT, COMMUNICATE AND CARE

Department of Education
Jadavpur University

Mental Health Foundation Kolkata

CERTIFICATE OF PARTICIPATION

THIS IS AWARDED TO

ABHIK PAUL

in recognition of fully **participating** in the two-day international conference held at Jadavpur University, Kolkata on 3rd & 4th January, 2020

Suranjan Das
Vice-Chancellor
Jadavpur University
Kolkata-700032

DR. MUKTIPADA SINHA
COORDINATOR
DEPT. OF EDUCATION, JU

PROF. SURANJAN DAS
VICE CHANCELLOR
JADAVPUR UNIVERSITY

DR. JAI RANJAN RAM
JOINT DIRECTOR
MENTAL HEALTH FOUNDATION

PROF. BISHNUPADA NANDA
HEAD
DEPT. OF EDUCATION, JU

Certificate of Participation

awarded to

Mr. Abhik Paul

(Jadavpur University)

UGC-SAP Sponsored National Seminar on "Advances in Nanoscience and Nanotechnology Applications" organized by Chemical Engineering Department, Jadavpur University on 10th January, 2020.

Prof. Debashis Roy
Head
Chemical Engg. Dept., JU

Prof. Avijit Bhowal
UGC-SAP Coordinator
Chemical Engg. Dept., JU

Dr. Mehabub Rahaman
Seminar Coordinator
Chemical Engg. Dept., JU

Dr. Saswata Bose
Seminar Coordinator
Chemical Engg. Dept., JU

Centre for Sustainable Development and Resource Efficiency Management,

(Formerly, Centre for Quality Management System)

Faculty of Engineering and Technology,

Jadavpur University

This is to certify that

Abhik Paul

has participated and completed the

Workshop on

"Writing Quality Research Article for Publication"

held at Gandhi Bhavan, Jadavpur University, Kolkata 700032, India during January 13-14, 2020 funded by

Twining Plan of World Bank Assisted TEQIP (TEQIP III), Government of India.

Prof. Dr. Sadhan K Ghosh
Dean, Faculty of Engineering and Technology,
Chief Coordinator, Centre for Sustainable Development and Resource Efficiency Management,
Professor, Mechanical Engineering, Jadavpur University, India

Abhik Paul

Signature of the candidate

Date: 04.02.2025